[AMERICAN JOURNAL OF SCIENCE, VOL. 281, DECEMBER, 1981, P. 1249-1516]

American Journal of Science

DECEMBER 1981

THEORETICAL PREDICTION OF THE THERMODYNAMIC BEHAVIOR OF AQUEOUS ELECTROLYTES AT HIGH PRESSURES AND TEMPERATURES: IV. CALCULATION OF ACTIVITY COEFFICIENTS, OSMOTIC COEFFICIENTS, AND APPARENT MOLAL AND STANDARD AND RELATIVE PARTIAL MOLAL PROPERTIES TO 600°C AND 5 KB

HAROLD C. HELGESON, DAVID H. KIRKHAM,* and GEORGE C. FLOWERS**

Department of Geology and Geophysics, University of California, Berkeley, California 94720

ABSTRACT. Extrapolation to infinite dilution of the apparent molal properties of aqueous electrolytes reported in the literature with the aid of a one-parameter extension of the Debye-Hückel equation corresponding in form to that proposed by Hückel (1925) affords a comprehensive and internally consistent set of standard partial molal heat capacities ($\bar{C}^\circ_P$), volumes ($\bar{V}^\circ$), and compressibilities ($\bar{\kappa}^\circ$), as well as the extended term parameters and their partial derivatives at temperatures $\leqslant$ 200°C and pressures corresponding to liquid-vapor equilibrium. The extrapolation equations, which yield close approximation of the thermodynamic properties of concentrated electrolytes, take into account both long- and short-range ionic interaction, electrostriction solvation of aqueous species, the concentration dependence of the dielectric constant of electrolyte solutions, and the effect of ion association on ionic strength. The Debye-Hückel term incorporates values of å computed independently from the effective electrostatic radii of ions generated by Helgeson and Kirkham (1976) from consideration of ion-solvent interaction at infinite dilution. Contrary to assumptions commonly made in the literature, the *reciprocal* of the dielectric constant of electrolyte solutions can be regarded as a linear function of (1) ionic strength at constant pressure and temperature, and (2) the reciprocal of the dielectric constant of the solvent as a function of temperature and pressure at constant ionic strength. Regression of the extended term parameters for $\bar{C}_P - \bar{C}^\circ_P$, $\bar{V} - \bar{V}^\circ$, and $\bar{\kappa} - \bar{\kappa}^\circ$, as well as the extrapolated values of $\bar{C}^\circ_P$, $\bar{V}^\circ$, and $\bar{\kappa}^\circ$ using equations derived from a theoretical model providing simultaneously for the intrinsic properties of aqueous species and the extent to which ion solvation, cavity formation, and collapse (or expansion) of the local solvent structure in the vicinity of the species affect their thermodynamic behavior permits prediction of ionic activity coefficients and the standard partial molal properties of aqueous species at high pressures and temperatures. Taking account of dissociation constants (K) and their partial derivatives affords corresponding calculation of osmotic and stoichiometric mean activity coefficients, as well as the apparent molal and relative partial molal properties of aqueous electrolytes. Calculations of this kind indicate that activity coefficients of aqueous electrolytes become monotonic functions of ionic strength at high temperatures and low pressures, where ion association contributes significantly to the thermodynamic behavior of electrolyte solutions. The extrema in $\bar{C}^\circ_P$, $\bar{V}^\circ$, $\bar{\kappa}^\circ$, and their extended term analogs as a function of temperature at low pressures move toward higher temperatures with increasing pressure and disappear at pressures above 1 to 3 kb, depending on the property and the electrolyte. The extrema are an additive consequence of opposing contributions

* Present address: Vinalhaven, Maine 04863

** Present address: Department of Earth Sciences, Tulane University, New Orleans, Louisiana 90118

by an asymptotic function of temperature describing the calorimetric consequences of short-range ionic interaction and/or solvent collapse (or expansion) and an exponential function representing the electrostatic influence of ion solvation on the thermodynamic behavior of electrolytes. Owing to dramatic changes in these relative contributions to the standard partial molal volumes of aqueous electrolytes with increasing temperature, $\bar{C}^\circ_P$ and its extended term analog also exhibit extrema with increasing pressure at (constant) high temperatures. The strong dependence of the thermodynamic properties of the solute on the electrostatic properties of the solvent causes the standard partial molal heat capacities, entropies, enthalpies, and volumes of aqueous electrolytes to approach negative infinity at the critical point of H_2O. In contrast, the extended term analogs of these properties approach infinity at the critical point. The thermodynamic properties of aqueous electrolytes are thus highly sensitive to slight changes in pressure, temperature, and concentration in the critical region, where they may exhibit extrema and/or range from large negative values for dilute solutions to large positive values at high ionic strengths. As a consequence, the heats of solution of electrolytes at high temperatures and low pressures may be more than a million cal mole^{-1}. Experimental dissociation constants and calculated values of the activity coefficient of molecular $NaCl_{(aq)}$ as a function of temperature at low pressures suggests the occurrence of maxima in the degrees of association of electrolytes as a function of concentration at high temperatures and pressures.

INTRODUCTION

Calculation of the thermodynamic properties of aqueous species at high pressures and temperatures is a requisite for quantitative description of chemical equilibrium in hydrothermal systems, as well as prediction of the extent to which components are redistributed among minerals and aqueous solutions in geochemical processes. The purpose of the present communication is threefold: (1) to derive from theoretical considerations and experimental data a comprehensive and internally consistent set of equations and coefficients for such calculations, (2) to facilitate application of the calculations to geochemical problems by tabulating and depicting activity coefficients and partial molal properties of aqueous species at temperatures and pressures to 600°C and 5 kb, and (3) to examine and critique the causes and consequences of the thermodynamic behavior of aqueous electrolytes at high pressures and temperatures.

Aqueous solutions involved in geochemical processes range from nearly pure H_2O/CO_2 fluids to concentrated electrolyte solutions. The thermodynamic components of aqueous electrolytes in geologic systems consist primarily of alkali and alkaline earth chlorides with lesser concentrations of bicarbonates and sulfates or bisulfates, together with minor H_2S, SiO_2, $AlCl_3$, $FeCl_3$, $FeCl_2$, $ZnCl_2$, $PbCl_2$, CuCl, AgCl, et cetera. These components are distributed among a host of ionic and neutral species, most of which associate to an increasing but differential degree as the density and dielectric constant of the solvent decrease with increasing temperature and/or decreasing pressure. At a given pressure and temperature, the distribution of species may vary from simple solvated ions at infinite dilution to polyligand complexes at high ionic strengths. Because the temperatures and pressures at which reactions among minerals and aqueous solutions take place in geochemical processes range from 0°C and 1 bar at the surface of the Earth to the melting temperatures of rocks at pressures ranging up to 30 kb or more (Delany and Helgeson, 1978), all such species must be taken into account in computing the thermodynamic properties of these solutions.

Definitive equilibrium and mass transfer calculations for geochemical processes require a general set of predictive equations for the thermodynamic properties of aqueous species which are applicable to the wide variety of temperatures, pressures, and chemical perturbations encountered in geologic systems. Although the approach must be based on sound theoretical concepts, it must also be practical, comprehensive in scope, and yield internally consistent results for both the solvent and solute that afford close approximations of geologic reality. Because the thermodynamic properties of the solvent control to a large extent the thermodynamic behavior of the solute, and because H_2O is the only common denominator for all electrolyte solutions encountered in nature, the first two papers in this series (Helgeson and Kirkham, 1974a and b) were devoted to calculation of the thermodynamic/electrostatic properties of H_2O at high pressures and temperatures.[1] Certain of these properties were used in the third contribution (Helgeson and Kirkham, 1976) to formulate and evaluate an equation of state for aqueous electrolytes at infinite dilution. The present communication extends the theoretical approach to include standard partial molal heat capacities (and thus all standard partial molal properties), activity and osmotic coefficients, and the apparent molal and relative partial molal properties of aqueous electrolytes as a function of pressure, temperature, and ionic strength to 5 kb and 600°C.

CONVENTIONS, UNITS, AND NOTATION

The standard state for aqueous species (other than H_2O) adopted in the present study is one of unit activity of the species in a hypothetical one molal solution referenced to infinite dilution at any pressure and temperature. The standard state for the solvent calls for unit activity of pure H_2O at any pressure and temperature. Accordingly, regardless of

[1] Typographical errors in a number of the equations given by Helgeson and Kirkham (1974a and b, 1976) are corrected in footnote 1 of Helgeson and Kirkham (1976), footnotes 1 and 2 of Walther and Helgeson (1977), and footnote 1 of Delany and Helgeson (1978). In addition, the heading of table 35 in Helgeson and Kirkham (1974a) should read bars instead of kb, and $C_s(\ln T)_T$ in footnote 1 of Delany and Helgeson (1978) should read $C_s(\ln T)/\tau$. Footnote *l* of table 1 in Walther and Helgeson (1977) also contains a typographical error which should be corrected. Instead of 49.003 and 31.208 cal mole^{-1}(°K)$^{-1}$, the values shown in the footnote for the standard molal entropies of $Si_{(c)}$ and $O_{2(g)}$ should read 4.5 and 49.003 cal mole^{-1} (°K)$^{-1}$, respectively. In addition, eq (10) in the sentences preceding eqs (15) and (25) should read eq (13), the second left parenthesis in the third term on the right side of eq (25) should be deleted, and the units of a_i and c_i on page 1330 should be corrected to read cal mole^{-1} bar^{-1} and cal mole^{-1} (°K)$^{-1}$, respectively. The value given for the electronic charge (e) on page 1204 of Helgeson and Kirkham (1974b) and pages 99 and 119 of Helgeson and Kirkham (1976) should read 4.80298×10^{-10} esu, rather than 4.80298 esu. Also, the value of Y given in footnote *n* of table 7 on page 151 of Helgeson and Kirkham (1976) should appear as -5.8021×10^{-5} (°K)$^{-1}$, rather than 5.8021×10^{-6} (°K)$^{-1}$, and the first two terms on the right side of the second identity in eq (126) should be multiplied by Z_i. The following corrections should be made in table 18 of Helgeson and Kirkham (1974b): the multipliers shown at the top of columns 3, 7, and 8 should read 10^{-1}, 10^{-5}, and 10^{-6}, respectively, and footnote *c* in the table should appear as kg$^{1/2}$ cm^{-1} mole$^{-1/2}$, rather than kg$^{1/2}$ cm^{-1} mole$^{-3/2}$. In addition, $\nu b_\gamma I/2$ in the line preceding eq (66) of Helgeson and Kirkham (1974b) should be positive, 2(2.303)RT in the equation should be replaced with a minus sign, and 2(2.303)RT should be deleted from the right side of the first equality in eq (80). Finally, the T immediately preceding the second integral sign in eq (18) of Helgeson and others (1978) should be deleted.

the pressure and temperature, the activity coefficients of all solute species approach unity at infinite dilution, as does the activity of the solvent.

Standard Gibbs free energies and enthalpies of formation from the elements at high pressures and temperatures are expressed below as apparent molal (ΔG° or ΔH°) or apparent partial molal ($\Delta \overline{G}^\circ$ or $\Delta \overline{H}^\circ$) quantities, which are defined by (Benson, 1968; Helgeson, 1969; Helgeson and Kirkham, 1974a, 1976)

$$\Delta G^\circ_{j,P,T} = \Delta \overline{G}^\circ_{j,P,T} \equiv \Delta \overline{G}^\circ_{f,j} + (\overline{G}^\circ_{j,P,T} - \overline{G}^\circ_{j,P_r,T_r}) \quad (1)$$

and

$$\Delta H^\circ_{j,P,T} = \Delta \overline{H}^\circ_{j,P,T} \equiv \Delta \overline{H}^\circ_{f,j} + (\overline{H}^\circ_{j,P,T} - \overline{H}^\circ_{j,P_r,T_r}) \quad (2)$$

where $\Delta G^\circ_{j,P,T}$, $\Delta H^\circ_{j,P,T}$, $\Delta \overline{G}^\circ_{j,P,T}$, and $\Delta \overline{H}^\circ_{j,P,T}$ stand for the conventional apparent standard molal and partial molal Gibbs free energy and enthalpy of formation of the jth aqueous species at the subscripted pressure (P) and temperature (T), $\Delta \overline{G}^\circ_{f,j}$ and $\Delta \overline{H}^\circ_{f,j}$ denote the conventional standard partial molal Gibbs free energy and enthalpy of formation from the elements of the species at a reference pressure (P_r) and temperature (T_r) of 1 bar and 298.15°K, and the two parenthetical terms correspond, respectively, to the difference in the conventional standard partial molal Gibbs free energy and enthalpy of the species at the pressure and temperature of interest and those at P_r, T_r. The apparent molal Gibbs free energy and enthalpy of formation of an electrolyte solution at a given pressure and temperature ($\Delta G_{P,T}$ and $\Delta H_{P,T}$, respectively) are then given by

$$\Delta G_{P,T} \equiv \Delta G^\circ_{P,T} + 55.51\,(\overline{G}_{w,P,T} - \overline{G}^\circ_{w,P,T}) + \sum_k m_k\,(\overline{G}_{k,P,T} - \overline{G}^\circ_{k,P,T}) \quad (3)$$

and

$$\Delta H_{P,T} \equiv \Delta H^\circ_{P,T} + 55.51\,(\overline{H}_{w,P,T} - \overline{H}^\circ_{w,P,T}) + \sum_k m_k\,(\overline{H}_{k,P,T} - \overline{H}^\circ_{k,P,T}) \quad (4)$$

which are consistent with

$$G_{solution,P,T} - G^\circ_{solution,P,T} = \Delta G_{P,T} - \Delta G^\circ_{P,T} \quad (5)$$

and

$$H_{solution,P,T} - H^\circ_{solution,P,T} = \Delta H_{P,T} - \Delta H^\circ_{P,T} \quad (6)$$

where $G^\circ_{solution,P,T}$, $H^\circ_{solution,P,T}$, $G_{solution,P,T}$, and $H_{solution,P,T}$ denote the molal Gibbs free energy and enthalpy of the solution in the standard state and the state of interest, respectively, 55.51[2] corresponds to the number of moles of H_2O (kg H_2O)$^{-1}$, m_k stands for the molality of the kth thermodynamic component of the solute,[3] the parenthetical quantities

[2] For the sake of brevity, 55.51 is used in eq (3) and subsequent equations to represent 55.50837, which is the value used in the calculations summarized below.

[3] The term component is used in the present communication in its strict thermodynamic sense; that is, the term refers to a chemical formula unit representing one of the minimum number of independent compositional variables in the system.

represent the relative partial molal Gibbs free energy and enthalpy of the solvent and solute components, which are designated by the subscripts w and k, respectively, and

$$\Delta G^\circ_{P,T} = 55.51\ \Delta\overline{G}^\circ_{w,P,T} + \sum_k m_k\ \Delta\overline{G}^\circ_{k,P,T} \tag{7}$$

and

$$\Delta H^\circ_{P,T} = 55.51\ \Delta\overline{H}^\circ_{w,P,T} + \sum_k m_k\ \Delta\overline{H}^\circ_{k,P,T} \tag{8}$$

where $\Delta\overline{G}^\circ_{w,P,T}$ and $\Delta\overline{H}^\circ_{w,P,T}$ are defined by appropriate statements of eqs (1) and (2) with j representing H_2O and

$$\Delta\overline{G}^\circ_{k,P,T} = \Delta G^\circ_{k,P,T} = \sum_j \nu_{j,k}\ \Delta\overline{G}^\circ_{j,P,T} \tag{9}$$

and

$$\Delta\overline{H}^\circ_{k,P,T} = \Delta H^\circ_{k,P,T} = \sum_j \nu_{j,k}\ \Delta\overline{H}^\circ_{j,P,T} \tag{10}$$

where $\nu_{j,k}$ refers to the number of moles of the jth aqueous species (mole of the kth solute component)$^{-1}$. Eqs (1) through (10) are consistent with

$$\Delta G_{P,T} = \Delta G_{solvent,P,T} + \Delta G_{solute,P,T} \tag{11}$$

and

$$\Delta H_{P,T} = \Delta H_{solvent,P,T} + \Delta H_{solute,P,T} \tag{12}$$

where

$$\Delta G_{solvent,P,T} = 55.51\ \Delta\overline{G}^\circ_{w,P,T} + 55.51\ (\overline{G}_{w,P,T} - \overline{G}^\circ_{w,P,T}), \tag{13}$$

$$\Delta H_{solvent,P,T} = 55.51\ \Delta\overline{H}^\circ_{w,P,T} + 55.51\ (\overline{H}_{w,P,T} - \overline{H}^\circ_{w,P,T}), \tag{14}$$

$$\Delta G_{solute,P,T} = \sum_k m_k\ \Delta\overline{G}^\circ_{k,P,T} + \sum_k m_k\ (\overline{G}_{k,P,T} - \overline{G}^\circ_{k,P,T}), \tag{15}$$

and

$$\Delta H_{solute,P,T} = \sum_k m_k\ \Delta\overline{H}^\circ_{k,P,T} + \sum_k m_k\ (\overline{H}_{k,P,T} - \overline{H}^\circ_{k,P,T}). \tag{16}$$

Because few completely dissociated two or three-component electrolyte solutions exist in nature, the major part of the discussion below is devoted to thermodynamic relations and predictive equations which apply to individual aqueous species. Similarly, to afford maximum flexibility in geochemical calculations and provide adequately for the diversity and highly variable extent of ion association in natural electrolyte solutions, all relative partial molal properties are expressed in terms of the concentrations of these species, rather than the stoichiometric concentrations of the thermodynamic components of the solutions. The standard state thermodynamic properties of individual aqueous species correspond to conventional properties consistent with

$$\tilde{\Xi}^\circ_j \equiv \tilde{\Xi}^{\circ\,abs}_j - Z_j\ \tilde{\Xi}^{abs}_{H^+} = \Xi^\circ_j \equiv \Xi^{\circ\,abs}_j - Z_j\ \Xi^{\circ\,abs}_{H^+} \tag{17}$$

and

$$\Delta\tilde{\Xi}^\circ_j \equiv \Delta\tilde{\Xi}^\circ_j{}^{abs} - Z_j\Delta\tilde{\Xi}^\circ_{H^+}{}^{abs} = \Delta\Xi^\circ_j \equiv \Delta\Xi^\circ_j{}^{abs} - Z_j\,\Delta\Xi^\circ_{H^+}{}^{abs} \qquad (18)$$

where Ξ°_j stands for the conventional standard molal entropy, heat capacity, volume, expansibility, or compressibility of the jth aqueous species, $\Delta\Xi^\circ_j$ represents the conventional apparent standard molal Gibbs free energy or enthalpy of the subscripted species, $\Xi^\circ_j{}^{abs}$ and $\Delta\Xi^\circ_j{}^{abs}$ denote the absolute counterparts of Ξ°_j and $\Delta\Xi^\circ_j$, and $\tilde{\Xi}^\circ_j$, $\tilde{\Xi}^\circ_j{}^{abs}$, $\Delta\tilde{\Xi}^\circ_j$, and $\Delta\tilde{\Xi}^\circ_j{}^{abs}$ correspond to the partial molal equivalents of Ξ°_j, $\Xi^\circ_j{}^{abs}$, $\Delta\Xi^\circ_j$, and $\Delta\Xi^\circ_j{}^{abs}$. It thus follows that $\Xi^\circ_{H^+} = \tilde{\Xi}^\circ_{H^+} = \Delta\Xi^\circ_{H^+} = \Delta\tilde{\Xi}^\circ_{H^+} = 0$, and the standard partial molal and apparent standard partial molal thermodynamic properties of acid solutes designated by $H_{\nu_H}L$ (where ν_H represents the number of moles of H^+ (mole of $H_{\nu_H}L)^{-1}$ are equal to $\tilde{\Xi}^\circ_L$ and $\Delta\tilde{\Xi}^\circ_L$, respectively. Although eqs (17) and (18) are written for the jth ion, analogous expressions can be written for charged complexes. All symbols representing standard thermodynamic properties of individual aqueous species in the pages that follow refer to the conventional properties unless indicated otherwise by the superscript *abs* or *absolute*. In contrast, all symbols representing nonstandard state properties refer to the absolute properties of the species.

Enthalpies and Gibbs free energies are expressed below in thermochemical calories (4.184 joules) or kilocalories mole $^{-1}$ (cal mole^{-1} or kcal mole^{-1}), entropies and heat capacities in cal mole^{-1} (°K)$^{-1}$, and volumes in cm^3 mole^{-1} (which can be converted to cal mole^{-1} bar^{-1} by multiplying by 0.0239 cal cm^{-3} bar^{-1}). The activity of the ith species (a_i) and equilibrium constants (K) are dimensionless, which requires activity coefficients to have reciprocal units of concentration. All thermodynamic properties of H_2O are consistent with those given by Helgeson and Kirkham (1974a) for a molecular weight of 18.0153 gm mole^{-1}. Pressure is expressed in bars (b) or kilobars (kb) and temperature in °C or °K.

GLOSSARY OF SYMBOLS

a	— coefficient in eqs (151) and (152).
å, $\mathring{a}_k$	— ion size parameters (eqs 124 and 125).
a_1, a_2, a_3, a_4, θ, ω	— equation of state coefficients for computing the standard state thermodynamic properties of aqueous species at high pressures and temperatures (eqs 253 and 273-276).
$\hat{a}_1$, $\hat{a}_2$, $\hat{a}_3$, $\hat{a}_4$, $\hat{a}_5$, θ, ω	— equation of state coefficients for computing extended term parameters for aqueous electrolytes at high pressures and temperatures (eqs 288-295).
$\hat{a}_5$, $\hat{a}_6$	— electrostatic parameters for predicting values of $\hat{b}_k$ and the dielectric constant of electrolyte solutions at high temperatures and pressures (eqs 286 and 287).

a_i, a_j, $a_{\hat{j}}$, a_k, a_l, a_q, a_n — activity of the subscripted aqueous species.

a, b — coefficients in eqs (182) through (184), (281), and (282).

$\mathbf{a}_1$, $\mathbf{b}_1$ — coefficients in eq (245).

$\mathbf{a}_2$, $\mathbf{b}_2$ — coefficients in eq (246).

$\mathbf{a}_3$, $\mathbf{b}_3$ — coefficients in eq (247).

abs, absolute — superscripts designating absolute thermodynamic properties of aqueous species.

anions, — — subscripts or superscripts designating anions.

aq, aqueous — subscripts designating the aqueous state.

aqueous disordered — subscript designating a hypothetical unsolvated aqueous state in schematic diagram (126).

aqueous ordered — subscript designating a solvated aqueous state in schematic diagram (126).

a_w — activity of H_2O.

A+ — representation of a monovalent cation.

A_γ, A_G, A_H, A_J, A_V, A_κ, A_{E_x} — electrostatic Debye-Hückel parameters defined by eqs (C-1) and (C-3) through (C-8) in app. C.

$b_{\gamma,\,k}$, $b_{\gamma,n}$ — extended term parameters (eqs 174 and 176) for computing mean ionic activity coefficients of the kth "completely" dissociated electrolyte and the nth neutral aqueous species from eqs (173) and (175).

$b_{H,k}$, $b_{J,k}$, $b_{V,k}$, $b_{\kappa,k}$, $b_{E_x,k}$, $b_{H,q}$, $b_{J,q}$, $b_{V,q}$ — extended term parameters for the kth "completely" dissociated electrolyte and qth aqueous complex defined by eqs (C-26) through (C-30) in app. C and (214K) through (214M).

$b_{\gamma,NaCl}$, $b_{\gamma,NaCl^\circ}$ — extended term parameters for computing activity coefficients of dissociated and associated $NaCl_{(aq)}$, respectively.

b_{ij}, b_{jl}, $b_{H,ij}$, $b_{H,jl}$, $b_{J,ij}$, $b_{J,jl}$, $b_{V,ij}$, $b_{V,jl}$, $b_{H,qi}$, $b_{H,ql}$, $b_{J,qi}$, $b_{J,ql}$, $b_{V,qi}$, $b_{V,ql}$ — short-range interaction parameters for the ith, jth, lth, and qth aqueous species in eqs (196) through (199) and (214K) through (214M) defined by equations analogous to eqs (C-19) through (C-22) in app. C.

b_{il}, b_{ni}, b_{nl}, $b_{j\hat{j}}$ — short-range interaction parameters for computing activity coefficients of the ith, lth, nth, jth, and $\hat{j}$th aqueous species defined by eqs (170) through (172) and (C-19) in app. C.

$\hat{b}_{il}$, $\hat{b}_{ni}$, $\hat{b}_{nl}$, $\hat{b}_{j\hat{j}}$ — short-range interaction parameters for computing relative partial molal Gibbs free energies of the ith, lth, nth, jth, and $\hat{j}$th aqueous species.

$b_{j\hat{j}}$, $b_{H,j\hat{j}}$, $b_{J,j\hat{j}}$, $b_{V,j\hat{j}}$, $b_{\kappa,j\hat{j}}$, $b_{E_x j\hat{j}}$ — short-range interaction parameters for the jth and $\hat{j}$th aqueous species defined by eqs (C-19) through (C-24) in app. C.

b_k, $b_{H,k}$, $b_{J,k}$, $b_{V,k}$, — electrostatic solvation parameters for the kth

$b_{\kappa,k}$, $b_{E_x,k}$ — electrolyte defined by eqs (149) and (C-14) through (C-18a) in app. C.

$\hat{b}_k$ — electrostatic parameter for computing the dielectric constant of the kth electrolyte from eq (143).

B_γ, B_H, B_J, B_V, B_κ, B_{E_x} — electrostatic Debye-Hückel parameters defined by eqs (C-2) and (C-9) through (C-13) in app. C.

c_1, c_2, θ, ω — heat capacity coefficients for computing thermodynamic properties of aqueous species at infinite dilution from eqs (273) through (276).

$\hat{c}_1$, $\hat{c}_2$, $\hat{a}_5$, θ, ω — heat capacity coefficients for computing extended term parameters for aqueous electrolytes from eqs (288) through (295).

cations, + — subscripts or superscripts designating cations.

C_P — isobaric heat capacity.

C°_P — standard molal isobaric heat capacity.

$C^\circ_{P,j}$, $C^\circ_{P,j}{}^{abs}$ — conventional and absolute standard molal isobaric heat capacity of the jth aqueous species.

$\bar{C}_P$ — partial molal isobaric heat capacity.

$\bar{C}_P - \bar{C}^\circ_P$ — relative partial molal isobaric heat capacity.

$\bar{C}^\circ_P$ — standard partial molal isobaric heat capacity.

$\bar{C}^\circ_{P,j}$, $\bar{C}^\circ_{P,j}{}^{abs}$ — conventional and absolute standard partial molal isobaric heat capacity of the jth aqueous species.

$\bar{C}^\circ_{P,i,j}$, $\bar{C}^\circ_{P_r,i,j}$ — conventional standard partial molal intrinsic heat capacity of the jth aqueous species at the pressures specified by P and P_r, respectively (eq 271).

$\bar{C}^\circ_{P_r,j}$ — conventional standard partial molal heat capacity of the jth aqueous species at the reference pressure specified by P_r (eq 270).

$\Delta\bar{C}^\circ_{P,c,j}$, $\Delta\bar{C}^\circ_{P_r,c,j}$ — contribution by collapse of the local solvent structure to the conventional standard partial molal heat capacity of the jth aqueous species at the pressures specified by P and P_r, respectively (eq 268).

$\Delta\bar{C}^\circ_{P,n,j}$, $\Delta\bar{C}^\circ_{P_r,n,j}$ — sum of the intrinsic and collapse contributions to the conventional standard partial molal heat capacity of the jth aqueous species ($\Delta\bar{C}^\circ_{P,n,j} = \bar{C}^\circ_{P,i,j} + \Delta\bar{C}^\circ_{P,c,j}$) at the pressures specified by P and P_r, respectively (eq 269).

$\Delta\bar{C}^\circ_{P,n,k}$ — sum of the intrinsic and collapse contributions to the standard partial molal isobaric heat capacity of the kth electrolyte.

$\Delta\bar{C}^\circ_{P,r,q}$ — standard partial molal isobaric heat capacity of overall dissociation for the qth aqueous complex.

$\Delta\bar{C}^{\circ}_{P,s,j}$ — conventional standard partial molal isobaric heat capacity of solvation of the jth aqueous species (eq 264).

$\bar{C}_{sat,k}$, $\bar{C}^{\circ}_{sat,k}$ — partial molal and standard partial molal heat capacity of the kth electrolyte along the liquid-vapor equilibrium curve for the electrolyte solution and H_2O, respectively.

e — electronic charge (4.80298×10^{-10} esu).

excess — subscript designation of nonideal contributions to the thermodynamic properties of mixing.

E_x — isobaric expansibility ($E_x \equiv (\partial V/\partial T)_P$).

E°_x — standard molal isobaric expansibility ($E^{\circ}_x \equiv (\partial V^{\circ}/\partial T)_P$).

$E^{\circ}_{x,j}$ — conventional standard molal isobaric expansibility of the jth aqueous species ($E^{\circ}_{x,j} \equiv (\partial V^{\circ}_j/\partial T)_P$).

$E^{\circ}_{x,j}{}^{abs}$ — absolute standard molal isobaric expansibility of the jth aqueous species ($E^{\circ}_{x,j}{}^{abs} \equiv (\partial V^{\circ}_j{}^{abs}/\partial T)_P$).

$\bar{E}_x$ — partial molal isobaric expansibility ($\bar{E}_x \equiv (\partial \bar{V}/\partial T)_P$).

$\bar{E}_x - \bar{E}^{\circ}_x$ — relative partial molal isobaric expansibility ($\bar{E}_x - \bar{E}^{\circ}_x \equiv (\partial \bar{V}/\partial T)_P - (\partial \bar{V}^{\circ}/\partial T)_P$).

$\bar{E}^{\circ}_x$ — standard partial molal isobaric expansibility ($\bar{E}^{\circ}_x \equiv (\partial \bar{V}^{\circ}/\partial T)_P$).

$\bar{E}^{\circ}_{x,i,j}$ — conventional standard intrinsic partial molal isobaric expansibility of the jth aqueous species ($\bar{E}^{\circ}_{x,i,j} = (\partial \bar{V}^{\circ}_{i,j}/\partial T)_P$).

$\bar{E}^{\circ}_{x,j}$ — conventional standard partial molal isobaric expansibility of the jth aqueous species ($\bar{E}^{\circ}_{x,j} \equiv (\partial \bar{V}^{\circ}_j/\partial T)_P$).

$\bar{E}^{\circ}_{x,j}{}^{abs}$ — absolute standard partial molal isobaric expansibility of the jth aqueous species ($\bar{E}^{\circ}_{x,j}{}^{abs} \equiv (\partial \bar{V}^{\circ}_j{}^{abs}/\partial T)_P$).

$\Delta\bar{E}^{\circ}_{x,c,j}$ — contribution by collapse of the local solvent structure to the conventional standard partial molal isobaric expansibility of the jth aqueous species ($\Delta\bar{E}^{\circ}_{x,c,j} = (\partial \Delta\bar{V}^{\circ}_{c,j}/\partial T)_P$).

$\Delta\bar{E}^{\circ}_{x,n,j}$ — sum of the intrinsic and collapse contributions to the conventional standard partial molal isobaric expansibility of the jth aqueous species ($\Delta\bar{E}^{\circ}_{x,n,j} = \bar{E}^{\circ}_{x,i,j} + \Delta\bar{E}^{\circ}_{x,c,j} = (\partial \Delta\bar{V}^{\circ}_{n,j}/\partial T)_P$).

$\Delta\bar{E}^{\circ}_{x,s,j}$ — conventional standard partial molal isobaric expansibility of solvation of the jth aqueous species ($\Delta\bar{E}^{\circ}_{x,s,j} = (\partial \Delta\bar{V}^{\circ}_{s,j}/\partial T)_P$).

f — subscript designating final state in eqs (236) and (237).

G — Gibbs free energy.

G° — standard molal Gibbs free energy.

$\overline{G}$ — partial molal Gibbs free energy.

$\overline{G}_{d,j}$ — long-range ionic interaction contribution to the relative partial molal Gibbs free energy of the jth aqueous species (eq 120).

G_{excess} — excess molal Gibbs free energy of mixing.

$\overline{G}_{ideal}$ — ideal partial molal Gibbs free energy of mixing.

$\overline{G}_{r,i}$, $\overline{G}_{r,j}$, $\overline{G}_{r,l}$, $\overline{G}_{r,n}$ — sum of the intrinsic, collapse, and short-range interaction contributions to the relative partial molal Gibbs free energies of the ith, jth, lth and nth aqueous species (eqs 156-158 and footnote 14).

$\overline{G} - \overline{G}^\circ$ — relative partial molal Gibbs free energy.

$\overline{G}^\circ$ — standard partial molal Gibbs free energy.

$\overline{G}^\circ_{i,j}$ — conventional standard partial molal intrinsic Gibbs free energy of the jth aqueous species.

$\overline{G}^\circ_j$, $\overline{G}^{\circ\,abs}_j$ — conventional and absolute standard partial molal Gibbs free energy of the jth aqueous species.

$\overline{G}^\circ_{(X)}$ — rational standard partial molal Gibbs free energy defined for the ith species by eq (164A).

$\overline{G}^\circ_{ideal\ (X)}$ — ideal rational partial molal Gibbs free energy of mixing defined for the ith species by eq (164B).

ΔG — apparent molal Gibbs free energy of formation defined by eq (3).

ΔG° — apparent standard molal Gibbs free energy of formation defined by eq (1).

ΔG_1, ΔG_2 — Gibbs free energy change accompanying transfer of unsolvated and solvated ions to and from a vacuum as shown in schematic diagram (126).

ΔG°_j, $\Delta G^{\circ\,abs}_j$ — conventional and absolute standard molal Gibbs free energy of formation of the jth aqueous species.

ΔG_s — Gibbs free energy of solvation within an aqueous phase (eq 127).

$\Delta\overline{G}_k$ — apparent partial molal Gibbs free energy of formation of the kth electrolyte ($\Delta\overline{G}_k = \Delta\overline{G}^\circ_k + RT \ln a_k$).

$\Delta\overline{G}_{h,i}$, $\Delta\overline{G}_{h,l}$, $\Delta\overline{G}_{h,n}$ — solvation contributions to the relative partial molal Gibbs free energy of the ith, lth, nth, and nth aqueous species (eqs 153-155).

$\Delta\overline{G}_{n,j}$ — sum of the intrinsic and collapse contributions to the relative partial molal Gibbs free energy of the jth aqueous species.

$\Delta\overline{G}_{s,j}$, $\Delta\overline{G}_{s,k}$ — partial molal Gibbs free energy of solvation of the jth aqueous species and the kth electrolyte, respectively (eqs 128 and 131).

$\Delta\overline{G}°$ — apparent standard partial molal Gibbs free energy of formation defined by eq (1).

$\Delta\overline{G}°_{c,j}$ — contribution by collapse of the local solvent structure to the conventional standard partial molal Gibbs free energy of the jth aqueous species.

$\Delta\overline{G}°_{f}$ — standard partial molal Gibbs free energy of formation from the elements in their stable form at 298.15°K and 1 bar.

$\Delta\overline{G}°_{f,j}$, $\Delta\overline{G}°_{f,j}{}^{abs}$ — conventional and absolute standard partial molal Gibbs free energy of formation of the jth aqueous species from its elements in their stable form at 298.15°K and 1 bar.

$\Delta\overline{G}°_{j}$, $\Delta\overline{G}°_{j}{}^{abs}$ — conventional and absolute apparent standard partial molal Gibbs free energy of formation of the jth aqueous species.

$\Delta\overline{G}°_{n,j}$ — sum of the intrinsic and collapse contributions to the conventional standard partial molal Gibbs free energy of the jth aqueous species ($\Delta\overline{G}°_{n,j} = \overline{G}°_{i,j} + \Delta\overline{G}°_{c,j}$).

$\Delta\overline{G}°_{r}$ — standard partial molal Gibbs free energy of reaction.

$\Delta\overline{G}°_{s,j}$, $\Delta\overline{G}°_{s,j}{}^{abs}$, $\Delta\overline{G}°_{s,n}$, $\Delta\overline{G}°_{s,n}{}^{abs}$ — conventional and absolute standard partial molal Gibbs free energies of solvation of the jth and nth aqueous species.

$\Delta\overline{G}°_{s,k}$ — standard partial molal Gibbs free energy of solvation of the kth electrolyte (eq 134).

H — enthalpy.

$H°$ — standard molal enthalpy.

$\overline{H}$ — partial molal enthalpy.

$\overline{H} - \overline{H}°$ — relative partial molal enthalpy.

$\overline{H}°$ — standard partial molal enthalpy.

$\overline{H}°_{j}$, $\overline{H}°_{j}{}^{abs}$ — conventional and absolute standard partial molal enthalpy of the jth aqueous species.

ΔH — apparent molal enthalpy of formation defined by eq (4).

$\Delta H°$ — apparent standard molal enthalpy of formation defined by eq (2).

ΔH_d — heat of dilution (eq 236).

ΔH°_j, $\Delta H^\circ_j{}^{abs}$ — conventional and absolute standard molal enthalpy of formation of the jth aqueous species.

ΔH_s — heat of solution.

$\Delta \bar{H}_k$ — apparent partial molal enthalpy of formation of the kth electrolyte.

$\Delta \bar{H}^\circ$ — apparent standard partial molal enthalpy of formation defined by eq (2).

$\Delta \bar{H}^\circ_f$ — standard partial molal enthalpy of formation from the elements in their stable form at 298.15°K and 1 bar.

$\Delta \bar{H}^\circ_{f,j}$, $\Delta \bar{H}^\circ_{f,j}{}^{abs}$ — conventional and absolute standard partial molal enthalpy of formation of the jth aqueous species from its elements in their stable form at 298.15°K and 1 bar.

$\Delta \bar{H}^\circ_j$, $\Delta \bar{H}^\circ_j{}^{abs}$ — conventional and absolute apparent standard partial molal enthalpy of formation of the jth aqueous species.

$\Delta \bar{H}^\circ_{r,q}$ — standard partial molal enthalpy of overall dissociation for the qth aqueous complex.

i — index designating aqueous cations ($i = 1, 2, \ldots \hat{\imath}$) or a subscript designating an intrinsic property or an initial state.

ideal — subscript designating ideal contributions to the thermodynamic properties of mixing.

I — stoichiometric ionic strength of an electrolyte solution defined by eq (85).

$\bar{I}$ — "true" ionic strength of an electrolyte solution defined by eq (83).

$\bar{I}'_P$, $\bar{I}''_P$, $\bar{I}'_T$ — ionic strength derivative functions defined by eqs (203) through (205).

j — index designating aqueous ions ($j = 1, 2, \ldots \hat{\jmath}$).

$\bar{J}$ — relative partial molal heat capacity.

k — Boltzman's constant (1.38054×10^{-16} erg $(°K)^{-1}$).

k — subscript representing a single electrolyte or an index designating the thermodynamic components of the solute of a mixed electrolyte solution ($k = 1, 2, \ldots \hat{k}$).

$\hat{k}$ — proportionality constant in eq (284) defined by eq (285).

K_{NaCl°, K_{NaCl} — standard molal dissociation constant for the NaCl molecule.

K_q, K_n — stepwise standard molal dissociation constant for the qth aqueous complex and nth neutral species.

l — index designating aqueous anions ($l = 1, 2, \ldots \hat{l}$).

$\bar{L}$ — relative partial molal enthalpy.

$LiCl^\circ$ — designation of the aqueous LiCl molecule.

m — molality.

m^* — sum of the molalities of all solute species in an electrolyte solution (eq 107).

$m'_{j,P}$, $m'_{q,P}$, $m'_{i,P}$, $m'_{l,P}$ — molality derivative functions defined by eq (207) and its analog for the qth aqueous complex and ith and lth cation and anion, respectively.

$m''_{j,P}$, $m''_{q,P}$, $m''_{i,P}$, $m''_{l,P}$ — molality derivative functions defined by eq (208) and its analog for the qth aqueous complex and ith and lth cation and anion, respectively.

$m'_{j,T}$, $m'_{q,T}$, $m'_{i,T}$, $m'_{l,T}$ — molality derivative functions defined by eq (206) and its analog for the qth aqueous complex and ith and lth cation and anion, respectively.

$\hat{m}(k)$, $\hat{m}(j,q)$ — subscript constraint stipulating that the number of moles of H_2O and each thermodynamic component indexed by k or the number of moles of H_2O and each aqueous species indexed by j and q are held constant.

$\hat{m}_q$, $\hat{m}_j$, $\hat{m}_k$ — subscript constraints stipulating constant molalities of all aqueous species or thermodynamic components other than the qth, jth, or kth.

$m_{t,j}$ — total molality of the jth ion defined by eq (23).

M — molarity.

$\hat{M}$ — molecular weight.

n — index designating neutral aqueous species ($n = 1, 2, \ldots \hat{n}$) or a subscript designating the sum of the intrinsic and collapse properties of aqueous species.

n_w — number of moles of H_2O in solution.

n^*_w — number of moles of H_2O liter^{-1} of solution (eq 243).

$\hat{n}(k)$ — subscript constraint stipulating that the number of moles of each solute component is held constant.

N — electrostatic Born function defined by eq (260).

N° — Avogadro's number (6.02252×10^{23} molecules mole^{-1}).

$NaCl^\circ$ — designation of the aqueous NaCl molecule.

P — pressure in bars or kilobars.

P_r — reference pressure (1 bar).

q — index designating aqueous complexes ($q = 1, 2, \ldots \hat{q}$).

Q — electrostatic Born function defined by eq (256).

$r_{e,j}$, $r_{e,n}$ — effective electrostatic radius of the jth and nth aqueous species.

$r_{i,j}$ — intrinsic radius of the jth aqueous species.

$r_{x,j}$ — crystallographic radius of the jth aqueous species.
R — gas constant (1.9872 cal mole^{-1}(°K)$^{-1}$).
S — entropy.
S_{excess} — excess molal entropy of mixing.
$S°$ — standard molal entropy.
$S°_j$, $S°_j{}^{abs}$ — conventional and absolute standard molal entropy of the jth aqueous species.
$\bar{S}$ — partial molal entropy.
$\bar{S}_{r,j}$ — sum of the intrinsic, collapse, and short-range interaction contributions to the relative partial molal entropy of the jth aqueous ion.
$\bar{S} - \bar{S}°$ — relative partial molal entropy.
$\bar{S}°$ — standard partial molal entropy.
$\bar{S}°_{i,j}$ — conventional standard partial molal intrinsic entropy of the jth aqueous species $(-(\partial \overline{G}°_{i,j}/\partial T)_P)$.
$\bar{S}°_j$, $\bar{S}°_j{}^{abs}$ — conventional and absolute standard partial molal entropy of the jth aqueous species.
$\Delta\bar{S}°_{c,j}$ — contribution by collapse of the local solvent structure to the conventional standard partial molal entropy of the jth aqueous species $(\Delta\bar{S}°_{c,j} = -(\partial\Delta\overline{G}°_{c,j}/\partial T)_P)$.
$\Delta\bar{S}°_{n,j}$ — sum of the intrinsic and collapse contributions to the conventional standard partial molal entropy of the jth aqueous species $(\Delta\bar{S}°_{n,j} = \bar{S}°_{i,j} + \Delta\bar{S}°_{c,j} = -(\partial\Delta\overline{G}°_{n,j}/\partial T)_P)$.
$\Delta\bar{S}°_{s,j}$, $\Delta\bar{S}°_{s,j}{}^{abs}$ — conventional and absolute standard partial molal entropy of solvation of the jth aqueous species.
SAT, *sat*, *saturation* — designations of liquid-vapor equilibrium for aqueous systems.
SAT (H_2O), *Sat* (H_2O), Saturation (H_2O) — designation of the liquid-vapor equilibrium curve for H_2O.
solute — subscript designating the solute of an electrolyte solution.
solution — subscript designating an electrolyte solution.
solvent — subscript designating the solvent of an electrolyte solution.
T — temperature in °C or °K.
T_r — reference temperature (298.15°K).
U — electrostatic Born function defined by eq (259).
u^* — ionic strength parameter defined by eq (192).
V — volume.
$V°$ — standard molal volume.
$V°_j$, $V°_j{}^{abs}$ — conventional and absolute standard molal volume of the jth aqueous species.
$\bar{V}$ — partial molal volume.
$\bar{V} - \bar{V}°$ — relative partial molal volume.

$\bar{V}^\circ$ — standard partial molal volume.

$\bar{V}^\circ_{i,j}$ — conventional standard intrinsic partial molal volume of the jth aqueous species.

$\bar{V}^\circ_j$, $\bar{V}^\circ_j{}^{abs}$ — conventional and absolute standard partial molal volume of the jth aqueous species.

$\bar{V}^\circ_w$ — standard partial molal volume of H_2O.

$\Delta\bar{V}^\circ_{c,j}$ — contribution by collapse of the local solvent structure to the conventional standard partial molal volume of the jth aqueous species.

$\Delta\bar{V}^\circ_{n,j}$ — sum of the intrinsic and collapse contributions to the conventional standard partial molal volume of the jth aqueous species ($\Delta\bar{V}^\circ_{n,j} = \bar{V}^\circ_{i,j} + \Delta\bar{V}^\circ_{c,j} = (\partial\Delta\bar{G}^\circ_{n,j}/\partial P)_T$).

$\Delta\bar{V}^\circ_{r,q}$ — standard partial molal volume of overall dissociation for the qth aqueous complex.

$\Delta\bar{V}^\circ_{s,j}$, $\Delta\bar{V}^\circ_{s,j}{}^{abs}$ — conventional and absolute standard partial molal volume of solvation of the jth aqueous species.

vacuum — subscript designating a vacuum.

w — subscript designating H_2O.

X — mole fraction.

X — electrostatic Born function defined by eq (266).

$\hat{y}$ — subscript constraint stipulating constant $\bar{y}_k$ for all values of k.

y_j, y_k — stoichiometric ionic strength fractions defined by eqs (86) and (89).

$\bar{y}_j$, $\bar{y}_k$, $\bar{y}_q$ — "true" ionic strength fractions defined by eqs (81), (88), and the analog of eq (81) for the qth aqueous complex.

$\bar{y}_{t,j}$ — total "true" ionic strength fraction defined by eq (93).

Y — electrostatic Born function defined by eq (265).

Z — ionic charge.

$Z_{e,n}$ — effective local charge on a neutral polar molecule.

$Z_{P,T}$, Z_{P_r,T_r} — negative reciprocal of the dielectric constant of H_2O (at the subscripted pressures and temperatures) in eqs (276), (277), and (293).

α — coefficient of isobaric thermal expansion ($\alpha = (\partial \ln V/\partial T)_P$).

α_j — degree of formation of the jth aqueous species defined by eq (70A).

α^* — Debye-Hückel function defined by eq (232).

β — coefficient of isothermal compressibility ($\beta = (\partial \ln \rho/\partial P)_T$).

β_q — overall standard molal dissociation constant for the qth aqueous complex.

$\bar{\beta}(\mathring{A}B_\gamma I^{1/2})$ — Debye-Hückel ionic strength function defined by eq (233).

β°_w — coefficient of isothermal compressibility of H_2O ($\beta^\circ_w = (\partial \ ln \ \rho^\circ_w/\partial P)_T$).

$\gamma_{\pm,k}$ — stoichiometric mean activity coefficient of the kth electrolyte.

$\gamma_i, \gamma_j, \gamma_l$ — stoichiometric activity coefficients of the ith, jth, and lth ions.

$\bar{\gamma}_{\pm,k}$ — mean ionic activity coefficient of the kth electrolyte.

$\bar{\gamma}_i, \bar{\gamma}_j, \bar{\gamma}_l$ — individual ion activity coefficients of the subscripted species.

$\bar{\gamma}_n$ — activity coefficient of the nth neutral aqueous species.

$\bar{\gamma}_q$ — activity coefficient of the qth aqueous complex.

$\bar{\gamma}_{\pm,k}, \bar{\gamma}^\circ_{\pm,k}$ — mean ionic activity coefficients of the kth electrolyte (eq 188).

$\Gamma_G, \Gamma_Y, \Gamma_H, \Gamma_J, \Gamma_V$ — mole fraction/molality conversion functions defined by eqs (122), (169), and (209) through (211).

δ_k, δ°_k — activity coefficient difference functions defined by eqs (188) and (189).

$\delta_{\phi_J,k}, \delta_{C_P,solution}$ — finite difference uncertainties in eq (239).

ϵ, ϵ° — dielectric constant of an electrolyte solution and H_2O, respectively.

$\bar{\zeta}(\mathring{A}B_\gamma I^{1/2})$ — Debye-Hückel ionic strength function defined by eq (234).

η — electrostatic parameter defined by eq (129).

θ — "structural" temperature parameter.

κ — isothermal compressibility ($\kappa \equiv -(\partial V/\partial P)_T$).

κ° — standard molal isothermal compressibility ($\kappa^\circ \equiv -(\partial V^\circ/\partial P)_T$).

κ°_j — conventional standard molal isothermal compressibility of the jth aqueous species ($\kappa^\circ_j \equiv -(\partial V^\circ_j/\partial P)_T$).

$\kappa^{\circ\,abs}_j$ — absolute standard molal isothermal compressibility of the jth aqueous species ($\kappa^{\circ\,abs}_j \equiv -(\partial V^{\circ\,abs}_j/\partial P)_T$).

$\bar{\kappa}$ — partial molal isothermal compressibility ($\bar{\kappa} \equiv -(\partial \bar{V}/\partial P)_T$).

$\bar{\kappa} - \bar{\kappa}^\circ$ — relative partial molal isothermal compressibility ($\bar{\kappa} - \bar{\kappa}^\circ \equiv -((\partial \bar{V}/\partial P)_T - (\partial \bar{V}^\circ/\partial P)_T$).

$\bar{\kappa}^\circ$ — standard partial molal isothermal compressibility ($\kappa^\circ \equiv -(\partial \bar{V}^\circ/\partial P)_T$).

$\bar{\kappa}^\circ_{i,j}$ — conventional standard intrinsic partial molal isothermal compressibility of the jth aqueous species ($\bar{\kappa}^\circ_{i,j} = -(\partial \bar{V}^\circ_{i,j}/\partial P)_T$).

$\bar{\kappa}^\circ_j$ — conventional standard partial molal isothermal compressibility of the jth aqueous species ($\bar{\kappa}^\circ_j \equiv -(\partial \bar{V}^\circ_j/\partial P)_T$).

$\bar{\kappa}^{\circ\,abs}_j$ — absolute standard partial molal isothermal compressibility of the jth aqueous species ($\bar{\kappa}^{\circ\,abs}_j \equiv -(\partial \bar{V}^{\circ\,abs}_j/\partial P)_T$).

$\Delta\bar{\kappa}^\circ_{c,j}$ — contribution by collapse of the local solvent structure to the conventional standard partial molal isothermal compressibility of the jth aqueous species ($\Delta\bar{\kappa}^\circ_{c,j} = -(\partial \Delta\bar{V}^\circ_{c,j}/\partial P)_T$).

$\Delta\bar{\kappa}^\circ_{n,j}$ — sum of the intrinsic and collapse contributions to the standard partial molal isothermal compressibility of the jth aqueous species.

$\Delta\bar{\kappa}^\circ_{s,j}$ — conventional standard partial molal isothermal compressibility of solvation of the jth aqueous species ($\Delta\bar{\kappa}^\circ_{s,j} = -(\partial \Delta\bar{V}^\circ_{s\,j}/\partial P)_T$).

Λ, Λ_k — Debye-Hückel function defined by eq (121) and its analog for the kth electrolyte.

Λ'_P, Λ''_P, Λ'_T — Debye-Hückel derivative functions defined by eqs (200) through (202).

μ_i, μ_j, μ_k, μ_l, μ_n, μ_q — chemical potential of the subscripted species.

ν — stoichiometric number of moles of ions (mole of solute)$^{-1}$ in an electrolyte solution.

$\nu_{i,k}$, $\nu_{j,k}$, $\nu_{j,k}$, $\nu_{l,k}$ — stoichiometric number of moles of the subscripted ion (mole of the kth component of an electrolyte solution)$^{-1}$.

$\nu_{j,q}$, $\nu_{j,n}$ — stoichiometric number of moles of the jth ion in one mole of the qth or nth aqueous complex.

ν_k — stoichiometric number of moles of ions in one mole of the kth thermodynamic component of an electrolyte solution (eq 58).

Ξ — designation of an extensive or molal property.

Ξ° — designation of a standard molal property.

Ξ°_j, $\Xi^{\circ\,abs}_j$ — conventional and absolute standard molal properties of the jth aqueous species.

Ξ°_w — standard molal property of H_2O.

$\bar{\Xi}$ — designation of a partial molal property.

$\bar{\Xi}_d$ — long-range ionic interaction (Debye-Hückel) contribution to a relative partial molal property.

$\bar{\Xi}_{ideal}$ — ideal mixing contribution to a relative partial molal property.

$\bar{\Xi}_j$ — partial molal property of the jth aqueous species (eq 21).

$\bar{\Xi}_q$ — partial molal property of the qth aqueous complex (eq 20).

$\bar{\Xi}_r$ — sum of the intrinsic, collapse, and short-range interaction contributions to a relative partial molal property.

$\bar{\Xi}_w$ — partial molal property of H_2O defined by eq (25).

$\bar{\Xi} - \bar{\Xi}^\circ$, $\Delta\bar{\Xi}$ — relative partial molal property.

$\bar{\Xi}^\circ$ — designation of a standard partial molal property.

$\bar{\Xi}^\circ_{i,j}$ — conventional standard intrinsic partial molal property of the jth aqueous species.

$\bar{\Xi}^\circ_j$, $\bar{\Xi}_j^{abs}$ — conventional and absolute standard partial molal property of the jth aqueous species.

$\Delta\bar{\Xi}_h$ — solvation contribution to a relative partial molal property (eq 119).

$\Delta\bar{\Xi}^\circ_{c,j}$ — contribution by local collapse of the solvent structure to a conventional standard partial molal property of the jth aqueous species.

$\Delta\bar{\Xi}^\circ_{e,j}$ — electrostriction contribution to a conventional standard partial molal property of the jth aqueous species (eq 114).

$\Delta\bar{\Xi}^\circ_{f,j}$, $\Delta\bar{\Xi}^\circ_{f,j}{}^{abs}$ — conventional and absolute standard partial molal property of formation of the jth aqueous species from its elements in their stable form at 298.15°K and 1 bar.

$\Delta\bar{\Xi}^\circ_j$, $\Delta\bar{\Xi}^\circ_j{}^{abs}$ — conventional and absolute apparent standard partial molal property of formation of the jth aqueous species.

$\Delta\bar{\Xi}^\circ_{n,j}$ — sum of the intrinsic and collapse contributions to a conventional standard partial molal property of the jth aqueous species (eq 115).

$\Delta\bar{\Xi}^\circ_{s,j}$ — conventional standard partial molal property of solvation of the jth aqueous species.

ρ — density.

ρ°_w — density of H_2O.

ρ^*_γ — activity coefficient difference function defined by eq (177).

ρ^*_H — apparent molal enthalpy difference function defined by eq (235).

$\rho^*_{\Delta H_d}$ — heat of dilution difference function defined by eq (237).

$\rho^*_{\Delta H_s}$ — heat of solution difference function plotted in figures 60 through 64.

ρ^*_J — apparent molal heat capacity difference function defined by eq (238).

ρ^*_κ — apparent molal compressibility difference function defined by eq (241).

ρ^*_ϕ — osmotic coefficient difference function defined by eq (194).

ρ^*_V — apparent molal volume difference function defined by eq (240).

$\sigma(\mathring{a}B_\gamma\bar{I}^{1/2})$ — Debye-Hückel ionic strength function defined by eq (191).

ϕ — osmotic coefficient defined by eq (106).

ϕ_{C_P} — apparent molal heat capacity.

ϕ_{E_x} — apparent molal expansibility.

ϕ_G — apparent molal Gibbs free energy.

ϕ_H — apparent molal enthalpy.

ϕ_κ — apparent molal compressibility.

ϕ_Ξ — apparent molal property defined by eq (77).

ϕ_V — apparent molal volume.

ψ_j, ψ_q, ψ_k — ionic charge parameters defined by eqs (82), (84), and (87).

$\omega_j, \omega_j^{abs}, \omega_n, \omega_n^{abs}$ — conventional and absolute Born coefficients for the jth and nth aqueous species (eqs 130, 135, 138, and $\omega_n = \omega_n^{abs}$).

ω_k — Born coefficient for the kth electrolyte (eqs 132 and 136).

RESUMÉ OF PREVIOUS WORK

Experimental observations of the thermodynamic behavior of aqueous electrolytes at high pressures and temperatures have increased exponentially since the turn of the century when Noyes (1907) pioneered systematic conductance measurements of electrolyte solutions at temperatures ranging up to 305°C. With a few notable exceptions (Noyes, Kato, and Sosman, 1910; Spillner, 1940; Swinnerton and Owen, 1948; Fogo, Benson, and Copeland, 1954) little was done over the next 50 years to augment substantially these high-temperature measurements. Attention was focused instead on extending early experimental studies of the conductance of electrolytes as a function of pressure at low temperatures (Colladon and Sturm, 1827; Herwig, 1877; Fink, 1885; Fanjung, 1894) to higher pressures (Adams, 1931; Adams and Hall, 1931; Zisman, 1932; Buchanan and Hamann, 1953; Hamann and Strauss, 1955, 1956). The relative hiatus in high-temperature conductance measurements in the first half of the century was brought to an end by Franck's (1956a, b, and c) outstanding advances in experimental technology, which sparked a myriad of systematic and comprehensive high pressure/temperature conductance studies. As a result, extensive conductance data (and in many cases derived dissociation constants) are now available for H_2O (for example, see Marshall and Franck, 1981) and a large number of electrolytes at temperatures and pressures to 1000°C and 12 kb.[4] The systems studied include aqueous solutions of HCl, HF, HBr, NaCl, NaI, NaBr, NaF, KCl,

[4] In the case of H_2O, conductance measurements and derived values of K_w, the activity product of H_2O, have been published for temperatures and pressures to 1000°C and > 130 kb (Holzapfel and Franck, 1966; Hamann, 1974).

KBr, KI, RbF, RbCl, RbBr, RbI, CsCl, CsBr, CsI, LiCl, KOH, NH_4Cl, NH_4OH, $MgCl_2$, $CaCl_2$, $SrCl_2$, $BaCl_2$, H_2SO_4, $KHSO_4$, K_2SO_4, Na_2SO_4, Li_2SO_4, Rb_2SO_4, Cs_2SO_4, $(NH_4)_2SO_4$, $FeCl_3$, LiOH, $Fe(OH)_3$, KNO_3, $Ba(OH)_2$, $MgSO_4$, $CaSO_4$, $MnSO_4$, $CoSO_4$, $NiSO_4$, $ZnSO_4$, $CdSO_4$, H_2SO_3, H_2CO_3, H_3PO_4, H_2S, sea salt, and a large number of rare earth electrolytes and organic acids, bases, polyelectrolytes, and micelles (Franck, 1956a, b, and c, 1961; Hensel and Franck, 1964; Franck, Hartmann, and Hensel, 1965; Ritzert and Franck, 1968; Mangold and Franck, 1969; Hartmann and Franck, 1969; Hwang, Lüdemann, and Hartmann, 1970; Renkert and Franck, 1969; Wright, Lindsay, and Druga, 1961; Ellis, 1959b, 1963; Ellis and Anderson, 1961; Clark and Ellis, 1960; Fisher, 1962, 1978; Fisher and Fox, 1975, 1977, 1978, 1979a and b; Fisher and Davis, 1965, 1967; Hamann, 1963, 1974; Hamann and Strauss, 1955, 1956; Hamann and Linton, 1969; Buchanan and Hamann, 1953; Ryzhenko, 1963, 1964, 1967; Pearson, Copeland, and Benson, 1963a and b; Kondrat'ev and Nikich, 1963; Quist, 1970; Quist and others, 1963, 1970; Quist, Marshall, and Jolley, 1965; Quist and Marshall, 1966, 1968a, b, c, and d, 1969, 1970; Dunn and Marshall, 1969a and b; Yeatts and Marshall, 1972a; Leong and Dunn, 1972; Horne and Young, 1967; Fisher and Barnes, 1972; Gancy and Brummer, 1969, 1971; Lown, Thirsk, and Lord Wynne-Jones, 1968, 1970; Kester and Pytkowicz, 1970; Inada, Shimizu, and Osugi, 1971, 1972; Broadwater and Evans, 1974; Read, 1975; Millero, Chetirkin, and Culkin, 1977; Katayama, 1976; Jost, 1976; Hasinoff, 1976; Asano and le Noble, 1978; Ueno, Nakahara, and Osugi, 1979; Corti, Crovetto, and Fernândez-Prini, 1979; Frantz and Marshall, 1982).

The conductance measurements summarized above have been complemented over the past 40 yrs by numerous high pressure/temperature equilibrium studies of aqueous CO_2, KI, LiF, KCl, NaCl, $PbCl_2$, Li_2SO_4, and K_2CO_3 solutions, as well as a large number of other aqueous systems (Kracek, 1931; Gibson, 1934; Benedict, 1939; Keevil, 1942; Booth and Bidwell, 1950; Morey and Hesselgesser, 1951, 1952; Morey and Chen, 1956; Feodotyev and Shlepov, 1958; Tödheide and Franck, 1963; Takenouchi and Kennedy, 1964; Gehrig, Lentz, and Franck, 1979). In addition, over the past decade or so systematic and extensive solubility measurements have been carried out in systems involving H_2O and NaCl, KCl, HCl, CO_2, $CaCO_3$, NaOH, $PbCl_2$, $CaSO_4$, $CaSO_4 \cdot 2H_2O$, $MgSO_4$, $MgSO_4 \cdot H_2O$, $BaSO_4$, AgCl and NaCl, $AgSO_4$, Fe_3O_4, UO_2, SiO_2, copper and iron sulfides, calcium and magnesian silicates, and/or other components, many of which are definitive with respect to ion association at high pressures and/or temperatures (Sourirajan and Kennedy, 1962; Urosova and Ravick, 1971; Ellis, 1959a; Ellis and Golding, 1963; Barnes and Ernst, 1963; Nriagu and Anderson, 1971; Marshall, 1967, 1980a and b; Marshall, Slusher, and Jones, 1964; Marshall and Jones, 1966; Marshall and Slusher, 1966, 1968, 1973, 1975a and b; Yeatts and Marshall, 1972b; Kalyanaraman, Yeatts, and Marshall, 1973a and b; Stoughton and Lietzke, 1960; Lietzke and Stoughton, 1959a, b, c, d, and e, 1962 a, b, and c, 1963a; Templeton, 1960; Templeton and Rodgers, 1967; Sweeton and Baes, 1970; Chou and

Eugster, 1977; Crerar and Anderson, 1971; Crerar and Barnes, 1976; Crerar and others, 1978; Seward, 1973, 1974, 1976, 1977; Frantz and Eugster, 1973; Frantz and Popp, 1979; Popp and Frantz, 1979; Hemley and others, 1971, 1977a and b; Potter and Clynne, 1980; Tremaine and LeBlanc, 1980; Tremaine and others, 1981). Ion association in high pressure-temperature electrolyte solutions has also been the object of many spectral and potentiometric investigations, most of which are concerned with H_2S, H_2O, KCl, NaCl, $CuCl_2$, $Cu(ClO_4)_2$, $MgSO_4$, $Al(OH)_3$, NH_4OH, H_3PO_4, $Mg(OH)_2$, and $B(OH)_3$ (Ellis and Giggenbach, 1971; Scholz, Lüdemann, and Franck, 1972; Chatterjee, Adams, and Davis, 1974; Dzidić and Kebarle, 1970; Arhsadi, Yandagni, and Kebarle, 1970; Arshadi and Kebarle, 1970; Whitfield, 1972; Chatterjee, Adams, and Davis, 1974; Mesmer, Baes, and Sweeton, 1970, 1972; Sweeton, Mesmer, and Baes, 1973, 1974; Mesmer and Baes, 1971, 1974; McGee and Hostetler, 1975; Crerar and Barnes, 1976; Hitch and Mesmer, 1976; Busey and Mesmer, 1976, 1978; Nesbitt, 1981).

With few exceptions, high-temperature osmotic and activity coefficients, as well as relative partial molal enthalpies and heat capacities derived from vapor pressure measurements, emf studies, isopiestic data, or mineral solubilities are available only at temperatures $\leqslant$ 300°C at pressures corresponding to those along the vapor-liquid or vapor-liquid-solid equilibrium curves for aqueous electrolyte systems. A large number of electrolytes have been considered in these studies, including HCl, NaCl, HCl-NaCl, $CaCl_2$-NaCl, HBr, DCl, KCl-HCl, HBr-NaBr, LiCl, CsCl, KCl, RbCl, $NiCl_2$, $CoCl_2$, LiBr, $LiNO_3$, $LiNO_3$-KNO_3, $LiNO_3$-$CsNO_3$, $Ca(NO_3)_2$, $Ca(NO_3)_2$-$CsNO_3$, $CaSO_4$-Na_2SO_4-$NaNO_3$, $MgCl_2$, $CaCl_2$, $BaCl_2$, $MgSO_4$, Na_2SO_4, $Ca(OH)_2$, HCl-NaCl, and sea salt solutions (Bates and Bower, 1954; Harned, 1959, 1960; Harned and Geary, 1937; Harned and Paxton, 1953; Patterson, Gilpatrick, and Soldano, 1960; Soldano and Patterson, 1962; Humphries, Kohrt, and Patterson, 1968; Moore, Humphries, and Patterson, 1972; Soldano and Meek, 1963; Soldano and Bien, 1966; Greeley and others, 1960a and b; Towns, Greeley, and Lietzke, 1960; Gardner, Jones, and De Nordwall, 1963; Gardner, 1969; Faita, Mussini, and Oggioni, 1966; Fabuss and Korosi, 1966; Cerquetti, Longhi, and Mussini, 1968; Yeatts and Marshall, 1967, 1969; Liu and Lindsay, 1970, 1971, 1972; Lindsay and Liu, 1968, 1971; Braunstein and Braunstein, 1971; Gibbard and Scatchard, 1972, 1973; Urusova, 1971, 1974; Gibbard and others, 1974; Lietzke, Hupf, and Stoughton, 1965; Stoughton and Lietzke, 1965, 1967; Lietzke and Stoughton, 1962a, b, and c, 1963b, 1964a and b, 1974; Mashovets, Zarembo, and Federov, 1973; Holmes and Mesmer, 1981; Holmes, Baes, and Mesmer, 1978, 1979, 1981). Emphasis in calorimetric investigation of electrolyte solutions has been placed on heat capacities and heats of mixing, dilution, and solution, but for the most part only at temperatures $\leqslant$ 300°C along the vapor-liquid equilibrium curves for the various solutions. Data of this kind are available for H_2O, NaCl, LiBr, $CaCl_2$, $SrCl_2$, $MgCl_2$, HCl, NaOH, NaF, NaI, NaBr, LiCl, KCl, KF, CsCl, CsI, KBr, KI, LiI, LiF, RbCl, NH_4Cl,

NH_4NO_3, RbF, RbI, RbBr, CsBr, CsF, $BaCl_2$, $CuCl_2$, $CoCl_2$, $FeCl_2$, $Cd(NO_3)_2$, $NiCl_2$, $Cu(ClO_4)_2$, $Mg(ClO_4)_2$, $Mn(ClO_4)_2$, H_3PO_4, $NaClO_4$, H_2SO_4, K_2SO_4, Li_2SO_4, $MgSO_4$, Na_2SO_4, Na_2CO_3, $NaHSO_4$, $NaHCO_3$, $NaReO_4$, $HReO_4$, CsI, $GdCl_3$, $K_2S_4O_6$, KHS, $Na_2S_2O_3$, $Na_2S_2O_8$, $K_2S_2O_8$, K_2CrO_4, Na_2MoO_4, Na_2WO_4, $NaClO_3$, $NaNO_3$, $NaBrO_3$, $NaIO_3$, $KClO_3$, $KBrO_3$, KIO_3, NH_4ClO_4, $AgNO_3$, $AgClO_4$, $KMnO_4$, $MnCl_2$, CH_3COOH, and sea salt solutions (Eigen and Wicke, 1951, 1954; Wicke, Eigen, and Ackermann, 1954; Ackermann, 1958; Ackermann and Schreiner, 1958; Egan, Luff, and Wakefield, 1958; Wakefield, Luff, and Reed, 1972; Mastroianni, ms; Readnour and Cobble, 1969; Ahluwalia and Cobble, 1964a and b; Mitchell and Cobble, 1964; Jekel, Criss, and Cobble, 1964; Cobble and others, 1972; Criss and Cobble, 1961; Gardner, Mitchell, and Cobble, 1969a and b; Stephens and Cobble, 1971; Gardner, Jekel, and Cobble, 1969; Sen, Murray, and Cobble, ms; Cobble and Murray, 1977; Rüterjans and others, 1969; Leung and Grunwald, 1970; Likke, ms; Likke and Bromley, 1973; Bromley, 1968, 1972; Bromley and others, 1970; Singh and Bromley, 1973; Ensor and Anderson, 1973; Snipes, Manly, and Ensor, 1975; Millero, 1973a; Millero, Hansen, and Hoff, 1973; Millero, Perron, and Desnoyers, 1973; Fortier, Leduc, and Desnoyers, 1974; Fortier, Philip, and Desnoyers, 1974; Leung and Millero, 1975a and b; Borodenko and Galinker, 1975, 1976; Puchkov, Styazhkin, and Feodorov, 1976, 1978; Puchkov and Zarembo, 1978; Messikomer and Wood, 1975; Desnoyers and others, 1976; Perron, Fortier, and Desnoyers, 1975; Perron, Desnoyers, and Millero, 1974, 1975; Olofsson, G., 1975; Olofsson, I. V., 1979; Olofsson and Hepler, 1975; Olofsson and Olofsson, 1973, 1977; Olofsson and Sunner, 1979; Olofsson, Spitzer, and Hepler, 1978; Singh and others, 1976, 1977, 1978; Roux and others, 1978; Liphard, Jost, and Schneider, 1977; Spitzer and others, 1978a and b, 1979a and b; Tanner and Lamb, 1978; Bernarducci, Morss, and Mikszial, 1979; Kasper, Holloway, and Navrotsky, 1979; Rogers, ms; Allred and Wooley, 1981a and b). Densities, sound speeds, compressibilities, and expansibilities of electrolyte solutions have also been measured at temperatures $\leqslant 200°C$ along vapor-liquid equilibrium curves or at 20 bars, but relatively few such studies have been carried out at higher temperatures and/or pressures. Data of this kind are available for aqueous solutions of NaCl, NaBr, NaF, HCl, LiCl, KCl, CsCl, RbCl, NH_4Cl, NaBr, NH_4Br, LiBr, KBr, KF, LiI, NaI, NH_4I, KI, $NaHCO_3$, KNO_3, $AgNO_3$, $LiNO_3$, $NaNO_3$, NH_4NO_3, NaHS, NH_4ClO_4, H_2O, D_2O, $MgCl_2$, $CaCl_2$, $SrCl_2$, $BaCl_2$, Na_2SO_4, $MgSO_4$, K_2SO_4, NaOH, and Na_2SO_4 (Adams, 1931; Adams and Hall, 1931; Gibson, 1934, 1935, 1938; Gibson and Loeffler, 1941; Copeland, Silverman, and Benson, 1953; Allam, ms; Allam and Lee, 1964, 1966; Ellis, 1966, 1967, 1968; Ellis and McFadden, 1968, 1972; Desnoyers and others, 1969; Rowe and Chou, 1970; Haas, 1970; Bell, Helton, and Rogers, 1970; Dunn, 1966, 1968, 1974; Millero, 1968, 1970, 1972a and b, 1973b and c, 1977; Millero, ms; Millero, Hoff, and Kahn, 1972; Millero, Knox, and Emmet, 1972; Millero and Drost-Hansen, 1968a and b; Millero and Lepple, 1973; Millero and Masterton, 1974; Millero and Kubinski, 1975; Millero, Gon-

zalez, and Ward, 1976; Ward and Millero, 1974a and b; Millero and others, 1974; Chen and Millero, 1976, 1977, 1981; Chen, Chen, and Millero, 1978; Chen, Emmet, and Millero, 1977; Chen, Fine, and Millero, 1977; Wang and Millero, 1973; Fine and Millero, 1975; Millero, Kembro, and Lo Surdo, 1980; Lo Surdo and Millero, 1980a and b; Mathieson and Conway, 1974; Owen and Simons, 1957; Owen and Kronick, 1961; Ravich and Borovaya, 1971; Dibrov, Mashovets, and Matveeva, 1964; Ostapenko and Samoilovich, 1971; Zarembo and Federov, 1975; Tham, Gubbins, and Walker, 1967; Fisher, 1975; Potter, Babcock, and Czamanske, 1976; Hilbert, ms).

Perhaps because of the phenomenal increase over the past two decades in the incidence, diversity, scope, and reliability of experimental investigations in the field of high pressure/temperature solution chemistry, theoretical interpretation of the myriad of data resulting from these studies has yet to be integrated into a unified, rigorous, and comprehensive frame of reference. Most equations advanced to account for observed changes in one or another thermodynamic property of electrolytes are based to a large extent on extrathermodynamic assumptions and/or semiempirical arguments, many of which fail to take account of related changes in other properties that are inconsistent with the equations. For example, the Guggenheim (1935) and Redlich-Meyer (Redlich and Meyer, 1964) equations have been used extensively to extrapolate experimental calorimetric and volumetric data to infinite dilution, despite the fact that the two equations are incompatible with one another. Few of the equations so far proposed provide adequately for both electrostatic and nonelectrostatic contributions to the thermodynamic behavior of electrolytes as a function of temperature, pressure, and composition. As a consequence, most such equations are restricted to a given property and/or region of pressure/temperature/composition space.

Activity coefficients, osmotic coefficients, and the relative partial molal properties of aqueous electrolytes at low pressures and temperatures have been represented over the past 50 yrs by a myriad of empirical and theoretical modifications and extensions of Debye-Hückel theory. Among these, the first-degree extension of the Debye-Hückel equation proposed originally by Hückel (1925), the Guntelberg (1926), Guggenheim (Guggenheim, 1935; Guggenheim and Turgeon, 1955), Davies (1938), and Scatchard (1936) equations (which are modifications of the equation proposed by Hückel), and the empirical power functions of stoichiometric ionic strength adopted by Lietzke and Stoughton (1962c, 1974) have received the most attention. These equations, as well as various modifications proposed by Meissner and Tester (1972), Meissner, Kusik, and Tester (1972), Meissner and Kusik (1972), and Bromley (1972, 1973) have been used extensively to represent activity and osmotic coefficients in solutions of various ionic strengths at temperatures to 300°C (Robinson and Stokes, 1959; Harned and Owen, 1958; Lewis and Randall, 1961; Lietzke and Stoughton, 1959a, b, c, d, and e, 1962a, b, and c, 1974; Greeley and others, 1960a and b; Towns, Greeley, and Lietzke, 1960; Marshall, Slusher, and

Jones, 1964; Marshall and Slusher, 1966; Marshall, 1967; Mesmer, Baes, and Sweeton, 1970; Guggenheim and Stokes, 1969; Helgeson and James, 1968; Helgeson, 1969; Wood, 1972, 1975, 1976). Owing to differences in the concentration and temperature dependence of ion association, solvation, and long- and short-range interaction in different electrolytes, various truncations of the Lietzke-Stoughton power function were used in many of these studies. The fallibility of this approach is manifested by the fact that in certain cases, one, or more, of the empirical parameters in the truncated expressions varies with concentration and/or temperature, but not in others.

Solvation models such as those adopted by Stokes and Robinson (1948, 1973) and Gluekauf (1955) afford close approximation of activity coefficients in concentrated electrolytes, but the equations are not generally applicable, nor are they as easy to use as their empirical counterparts. This is especially true of many of the more recent theoretical equations that have been advanced, most of which are comprehensive and accurate, but also intricate, complicated, and unwieldy. The more elaborate of these models include the statistical mechanical approaches taken by Friedman (1962, 1972a, b, and c), Justice and Justice (1976, 1977), Justice (1978), and Justice and Ebeling (1979), the series of equations proposed by Scatchard (1961, 1968, 1969, 1976), Wu, Rush, and Scatchard (1968, 1969), and Scatchard, Rush, and Johnson (1970), who include third and fourth virial coefficients to account for short-range interaction among all ions in solution, and those adopted by Reilly and Wood (1969), Reilly, Wood, and Robinson (1971), Robinson, Wood, and Reilly (1971), Pitzer (1973, 1975, 1977, 1979), Pitzer and Mayorga (1973, 1974), Pitzer and Kim (1974), Pitzer, Roy, and Silvester (1977), Pitzer and Silvester (1976), Silvester and Pitzer (1977, 1978), Pitzer, Peterson, and Silvester (1978), and Pitzer and others (1979). Of these, the equations derived by Pitzer and his co-workers, which include modification of the second virial coefficient to provide for changes in short-range interaction as a function of ionic strength, are the simplest and most practical. Nevertheless, even these equations impose a considerable computational burden, involve two or more adjustable parameters which must be obtained by regression of experimental data, and (like most other empirical and theoretical extensions and/or revisions of Debye-Hückel theory) fail to take *explicit* account of ion association. As a consequence, they are not suitable for extrapolation of low-temperature/pressure data to higher pressures and temperatures, which restricts their practical application to reproducing and interpolating experimental data.

Many semiempirical equations have been proposed to describe the temperature and pressure dependence of the thermodynamic properties of aqueous species and dissociational reactions in the standard state. One of the more prominent of these takes advantage of the principle of corresponding states (Criss and Cobble, 1964a and b; Cobble, 1964, 1966a and b; Khodakovskiy, 1969; Ellis, 1968; Helgeson, 1967, 1969) by representing the absolute standard partial molal entropies, volumes, and heat

capacities of aqueous species at a given temperature and pressure as linear functions of the corresponding property at another temperature and pressure. Despite its success and obvious generality, the requirement for extensive experimental data at the temperature and pressure of interest to establish values of correlation coefficients restricts severely the utilitarian value of the corresponding states approach.

The disadvantages of the corresponding states algorithm have to some extent been overcome by application of semiempirical electrostatic/nonelectrostatic models and continuum theory to describe standard partial molal properties of ionization and hydration at high temperatures (Helgeson, 1967; Goldman and Bates, 1972; Goldman and Morss, 1975; Tremaine and Goldman, 1978; Cobble and Murray, 1977; Sen, Murray, and Cobble, ms). However, provision in these models for nonelectrostatic contributions to the thermodynamic properties of aqueous species is largely empirical and commonly inadequate and inconsistent with experimental data. For example, Cobble and Murray (1977) and Sen, Murray, and Cobble (ms) consider the nonelectrostatic statistical and structural contributions to the standard partial molal entropy of ion hydration to be independent of temperature, which requires the standard partial molal heat capacities of aqueous species to be entirely electrostatic. Although experimental heat capacity data indicate clearly that this is not the case, the model nevertheless affords reasonably close approximations of apparent standard partial molal Gibbs free energies of formation at temperatures $\leqslant$ 200°C. Similar observations apply to the other models adduced above.

Despite their shortcomings, approaches of the kind proposed by Cobble and Murray (1977) and Sen, Murray, and Cobble (ms), as well as other models which take explicit account of electrostatic, structural, and statistical contributions to the thermodynamic properties of aqueous electrolytes offer considerable improvement over the consequences of many assumptions commonly made in high temperature solution chemistry. One of the more widely adopted of these is that the standard partial molal heat capacities of reactions involving aqueous species can be regarded as zero or taken to be independent of temperature, which in more cases than not leads to serious error in thermodynamic predictions (Helgeson, 1964, 1967, 1969; Naumov, Ryzhenko, and Khodakovskiy, 1968; Ryzhenko, 1981). Khodakovskiy, Ryzhenko, and Naumov (1968) attempted to improve on these assumptions by assuming instead that the conventional standard partial molal heat capacities of aqueous ions are proportional to temperature, which contravenes electrostatic theory and is clearly inconsistent with experimental heat capacity data. Errors in apparent standard partial molal Gibbs free energies of formation computed on the basis of this assumption are claimed by Khodakovskiy, Ryzhenko, and Naumov to be $\leqslant$ 1 kcal mole^{-1} at temperatures $\leqslant$300°C. It is interesting to note in this regard that the standard partial molal Gibbs free energies of reaction for many equilibria in hydrothermal systems are also of this order of magnitude.

As a rule, least squares fits of Gibbs free energies are insensitive to the form of the temperature function used to represent the heat capacity, which corresponds to the negative product of temperature and the second partial derivative of the regression equation with respect to temperature at constant pressure and composition. As a consequence, many models with fundamental flaws suffice to represent Gibbs free energy data. In a relatively recent publication, Naumov, Ryzhenko, and Khodakovskiy (1971) adopted for aqueous species the standard partial molal heat capacity power function employed by Maier and Kelley (1932) for solids. Although the Maier-Kelley power function is empirical, it closely approximates the temperature dependence of the heat capacities of many minerals at temperatures $> 25°C$, and its success can be justified at least in part on theoretical grounds. In contrast, there is no theoretical justification for application of the Maier-Kelley power function to aqueous species, and the form of the function is glaringly inconsistent with experimental observations of the standard partial molal heat capacities of aqueous electrolytes as a function of temperature.

A number of theoretical, empirical, and semiempirical equations have been proposed to represent the pressure dependence of various thermodynamic properties of aqueous electrolytes. One of the oldest and most successful of these is the Gibson-Tait equation (Gibson, 1934, 1935, 1938), which is based on Tamman's internal pressure theory (Tamman, 1893, 1895) and Tait's empirical observations on the H.M.S. Challenger (Tait, 1889). Owen and Brinkley (1941) employed the Gibson-Tait approach to formulate an equation representing the pressure dependence of dissociation constants. Various modifications of the Tait (1889) equation have been used extensively to represent pressure-volume-temperature data for aqueous solutions (for example, Li, 1967; Hayward, 1967; Wang and Millero, 1973; Emmet and Millero, 1974; Chen and Millero, 1976). An alternative to the Gibson-Tait/Owen-Brinkley equation, which is unwieldy, has been proposed by Lown, Thirsk, and Lord Wynne-Jones (1968, 1970) and adopted by Millero, Hoff, and Kahn (1972), Ward and Millero (1974b) and others. Lown, Thirsk, and Lord Wynne-Jones assume the standard partial molal compressibility of dissociation to be independent of pressure, which, at least in the case of acetic acid, introduces only slight errors in computed equilibrium constants at high pressures and low temperatures. Another approach, and one that has received considerable attention in recent years, has been taken by Quist and Marshall (1968a and e), Marshall (1968, 1969, 1970, 1972, 1975), Marshall and Mesmer (1981), Dunn and Marshall (1969), North (1973), and others who advocate the concept of a "complete" dissociation constant, which takes explicit account of ion solvation. The model is based on Franck's (1956a, b, and c, 1961) early observation of the isothermal quasilinear relation between the logarithm of the density of H_2O and the logarithm of the dissociation constants of aqueous species at high pressures and temperatures. Like the Gibson-Tait/Owen-Brinkley equation and the model adopted by Lown, Thirsk, and Lord Wynne-Jones, the "complete" equi-

librium constant approach advocated by Marshall and his co-workers reproduces experimental dissociation constant data over reasonably wide ranges of pressure and temperature. However, all three approaches suffer from extrathermodynamic assumptions which contravene electrostatic theory and cannot be generalized (see discussions by Hamann, 1974; Matheson, 1969; Gilkerson, 1970; Helgeson and Kirkham, 1976).

Strictly electrostatic models of ion dissociation fail to represent adequately the thermodynamics of dissociational reactions over wide ranges of pressure and temperature. Nevertheless, with the aid of judicious assumptions they can be used to approximate the apparent standard partial molal Gibbs free energies of formation of aqueous electrolytes over restricted temperature ranges. Various attempts (for example, Ryzhenko, ms and 1981) have been made to fit high pressure/temperature standard partial molal Gibbs free energies of dissociation to the Born (1920) equation (as corrected by Bjerrum, 1929), which affords satisfactory representation of dissociation constants only at high temperatures and low pressures where the dielectric constant of H_2O is small. In other regions of pressure/temperature space, nonelectrostatic statistical and structural contributions to the ionization process lead to serious discrepancies between standard partial molal Gibbs free energies of dissociation computed from the Born-Bjerrum equation and those obtained experimentally (Helgeson and Kirkham, 1976).

Numerous extensive reviews, data compilations, critiques, bibliographies, and discussions of high temperature/pressure solution chemistry and related topics have appeared in recent years (Ellis and Fyfe, 1957, Kavanau, 1964; Parker, 1965; Whalley, 1966; Helgeson, 1964, 1969, and in press; Barnes, Helgeson, and Ellis, 1966; Marshall, 1968, 1969; Millero, 1971, 1972a and b, 1979; Tödheide, 1966, 1972; Franck, 1968, 1973, 1980; Sillén and Martell, 1964, 1971; Smith and Martell, 1976; Harned and Robinson, 1968; Guggenheim and Stokes, 1969; Milero, 1971, 1972a and b, 1979;Brummer and Gancy, 1972; Gancy, 1972; Hamann, 1963, 1974, and in press; Khitarov, 1965; Hamer, 1968; Franks, 1972, 1973; Friedman and Krishnan, 1973; Anderson and Wood, 1973; Potter, Shaw, and Haas, 1975; Potter and Brown, 1977; Haas, 1976a and b; Kebarle, 1977; Scatchard, 1976; Hepler and Wooley, 1973; Pottel, 1973; Horne, 1969, 1972; Pitzer, 1977; Baes and Mesmer, 1976, 1981; Conway, 1978, 1979; Asano and le Noble, 1978; Eugster, in press; Seward, in press; Akitt, 1980; Ryzhenko, 1981; Hogfeldt, in press). Many of the experimental data and theoretical and empirical equations discussed in the preceding pages are considered in detail in these and other similar contributions, which afford a frame of reference for the thermodynamic relations and theoretical concepts discussed below.

REVIEW OF THERMODYNAMIC RELATIONS

The extensive thermodynamic properties of electrolyte solutions are expressed in classical thermodynamics as the sum of the products of the concentrations and corresponding partial molal properties of the thermodynamic components of the solution (see footnote 3). The classical ap-

proach thus provides implicitly rather than explicitly for the thermodynamic consequences of ion association.

Experimental data for dissociational equilibria in electrolyte solutions suggest that cations and anions in these solutions associate to an increasing degree with increasing temperature and decreasing pressure. Although most electrolytes are almost completely dissociated at 25°C and 1 bar, they may thus become highly associated under supercritical conditions. As a consequence, unless explicit provision is made for ion association, regression parameters obtained by fitting theoretical equations to low-pressure/temperature data cannot be used with confidence to predict the thermodynamic behavior of electrolyte solutions at high pressures and temperatures. Such provision can be incorporated in the framework of classical solution chemistry by first expressing the Gibbs free energies of electrolytes in terms of the chemical potentials of the cations and anions in solution.

Partial molal properties of aqueous species.—Homogeneous equilibrium in an electrolyte solution at constant pressure and temperature requires

$$\bar{\Xi}_q = \sum_j \nu_{j,q} \bar{\Xi}_j \tag{19}$$

where $\nu_{j,q}$ refers to the number of moles of the jth cation or anion in one mole of the qth complex in solution, and $\bar{\Xi}_q$ and $\bar{\Xi}_j$ represent a given partial molal property of the subscripted complex and ion, respectively, which are defined by[5]

$$\bar{\Xi}_q = \left(\frac{\partial \Xi}{\partial m_q}\right)_{P,T,\hat{m}_q,n_w} \tag{20}$$

and

$$\bar{\Xi}_j = \left(\frac{\partial \Xi}{\partial m_j}\right)_{P,T,\hat{m}_j,n_w} \tag{21}$$

where m_q and m_j stand for the molalities of the qth and jth aqueous species, the subscripts $\hat{m}_q$ and $\hat{m}_j$ designate constant molalities of all aqueous species other than the qth or jth, respectively, n_w refers to the number of moles of H_2O in solution, and Ξ corresponds to the extensive analog for the solution of the partial molal property represented by $\bar{\Xi}_q$ and $\bar{\Xi}_j$. It thus follows that

$$\sum_j m_j \bar{\Xi}_j + \sum_q m_q \bar{\Xi}_q = \sum_j m_{t,j} \bar{\Xi}_j \tag{22}$$

where $m_{t,j}$ stands for the total molality of the jth ion, which is given by

$$m_{t,j} = m_j + \sum_q \nu_{j,q} m_q = \sum_k \nu_{j,k} m_k \tag{23}$$

[5] Note that specifying $\hat{m}_j$, $\hat{m}_q$, or $\hat{m}_k$ does not necessarily require n_w to be constant, and that the subscripts j and q refer to solvated species.

where $\nu_{j,k}$ refers to the number of moles of the jth cation or anion in one mole of the kth solute component, and m_k represents the molality of the component in solution. Any extensive thermodynamic property of an electrolyte solution containing 1 kg of H_2O can thus be expressed as

$$\Xi = 55.51\,\bar{\Xi}_w + \sum_j m_{t,j}\,\bar{\Xi}_j = 55.51\,\bar{\Xi}_w + \sum_j \sum_k \nu_{j,k}\,m_k\,\bar{\Xi}_j \qquad (24)$$

where 55.51 corresponds to the number of moles of H_2O (kg H_2O)$^{-1}$ in solution, and $\bar{\Xi}_w$ denotes the partial molal counterpart of Ξ for the solvent; that is,

$$\bar{\Xi}_w = \left(\frac{\partial \Xi}{\partial n_w}\right)_{P,T,\hat{n}(k)}, \qquad (25)$$

where n_w again refers to the number of moles of H_2O in solution, and the subscript $\hat{n}(k)$ signifies that the number of moles of each of the thermodynamic components of the solute is held constant. The classical analog of eq (24) can be written as

$$\Xi = 55.51\,\bar{\Xi}_w + \sum_k m_k\,\bar{\Xi}_k \qquad (26)$$

where

$$\bar{\Xi}_k \equiv \left(\frac{\partial \Xi}{\partial m_k}\right)_{P,T,\hat{m}_k,n_w} \qquad (27)$$

where the subscript $\hat{m}_k$ refers to constant molalities of all components of the solute other than the kth. Eqs (24) and (26) can now be combined to give

$$\sum_k m_k\,\bar{\Xi}_k = \sum_j \sum_k \nu_{j,k}\,m_k\,\bar{\Xi}_j = \sum_j m_{t,j}\,\bar{\Xi}_j \qquad (28)$$

which relates explicitly the partial molal properties of thermodynamic components to those of their dissociated counterparts. Note that because eq (28) is independent of the number of components, it also follows that

$$\bar{\Xi}_k = \sum_j \nu_{j,k}\,\bar{\Xi}_j \qquad (29)$$

and

$$d\bar{\Xi}_k = \sum_j \nu_{j,k}\,d\bar{\Xi}_j \qquad (30)$$

The partial molal properties of individual aqueous species can be expressed in terms of pressure (P) and temperature (T) by taking explicit account of constraints imposed by homogeneous equilibrium on changes in Ξ. For example, the change in the Gibbs free energy of an electrolyte solution accompanying changes in pressure, temperature, and/or composition at constant n_w is given by

$$dG = -SdT + VdP + \sum_k \overline{G}_k \, dm_k \tag{31}$$

where G, S, and V stand for the Gibbs free energy, entropy, and volume of the solution, and $\overline{G}_k$ represents the partial molal Gibbs free energy (chemical potential) of the kth solute component, which is defined by an appropriate statement of eq (27). Because eq (31) is an exact differential, it follows that eq (27) can also be written for $\bar{V}_k$ and $\bar{S}_k$ as

$$\bar{V}_k \equiv \left(\frac{\partial V}{\partial m_k}\right)_{P,T,\hat{m}_k,n_w} = \left(\frac{\partial \overline{G}_k}{\partial P}\right)_{T,\hat{m}(k)} \tag{32}$$

and

$$\bar{S}_k \equiv \left(\frac{\partial S}{\partial m_k}\right)_{P,T,\hat{m}_k,n_w} = -\left(\frac{\partial \overline{G}_k}{\partial T}\right)_{T,\hat{m}(k)} \tag{33}$$

where $\bar{V}_k$ and $\bar{S}_k$ stand for the partial molal volume and entropy of the kth solute component and the subscript $\hat{m}(k)$ stipulates that the number of moles of H_2O and each of the thermodynamic components of the solution is held constant. It follows from eq (29) that

$$\overline{G}_k = \sum_j \nu_{j,k} \overline{G}_j \, , \tag{34}$$

which can be differentiated to give

$$\left(\frac{\partial \overline{G}_k}{\partial P}\right)_{T,\hat{m}(k)} = \sum_j \nu_{j,k} \left(\frac{\partial \overline{G}_j}{\partial P}\right)_{T,\hat{m}(k)} \tag{35}$$

and

$$\left(\frac{\partial \overline{G}_k}{\partial T}\right)_{P,\hat{m}(k)} = \sum_j \nu_{j,k} \left(\frac{\partial \overline{G}_j}{\partial T}\right)_{P,\hat{m}(k)} \, . \tag{36}$$

Combining eqs (32) and (33), respectively, with eqs (35) and (36) then leads to

$$\bar{V}_k = \sum_j \nu_{j,k} \left(\frac{\partial \overline{G}_j}{\partial P}\right)_{T,\hat{m}(k)} \tag{37}$$

and

$$\bar{S}_k = -\sum_j \nu_{j,k} \left(\frac{\partial \overline{G}_j}{\partial T}\right)_{P,\hat{m}(k)} \, . \tag{38}$$

If we now write statements of eq (29) as

$$\bar{V}_k = \sum_j \nu_{j,k} \bar{V}_j \tag{39}$$

and

$$\bar{S}_k = \sum_j \nu_{j,k} \bar{S}_j \, , \tag{40}$$

it follows from eqs (21) and (37) through (40), together with the fact that all these equations are independent of the number of aqueous species present in solution that

$$\bar{V}_j \equiv \left(\frac{\partial V}{\partial m_j}\right)_{P,T,\hat{m}_j,n_w} = \left(\frac{\partial \bar{G}_j}{\partial P}\right)_{T,\hat{m}(k)} \tag{41}$$

and

$$\bar{S}_j \equiv \left(\frac{\partial S}{\partial m_j}\right)_{P,T,\hat{m}_j,n_w} = -\left(\frac{\partial \bar{G}_j}{\partial T}\right)_{P,\hat{m}(k)} , \tag{42}$$

which describe the relation between the partial molal volume and entropy of the jth aqueous ion and the partial derivatives of the partial molal Gibbs free energy of the ion with respect to pressure and temperature, respectively, *at constant composition*. Note that by taking account of eqs (19), (20), (41), and (42) we can also write

$$\bar{V}_q \equiv \left(\frac{\partial V}{\partial m_q}\right)_{P,T,\hat{m}_q,n_w} = \sum_j \nu_{j,q} \left(\frac{\partial \bar{G}_j}{\partial P}\right)_{T,\hat{m}(k)} \tag{43}$$

and

$$\bar{S}_q \equiv \left(\frac{\partial S}{\partial m_q}\right)_{P,T,\hat{m}_q,n_w} = -\sum_j \nu_{j,q} \left(\frac{\partial \bar{G}_j}{\partial T}\right)_{P,\hat{m}(k)} . \tag{44}$$

These equations, together with many other relations among partial molal properties of individual aqueous species and thermodynamic components are summarized in app. A. All the equations given in app. A can be generated from the expressions derived above.

The stipulation represented by the subscript $\hat{m}(k)$ in eqs (41) through (44) arises from constraints imposed by homogeneous equilibrium. It should perhaps be emphasized that these constraints are not inherent in

$$dG = -SdT + VdP + \sum_j \bar{G}_j dm_j + \sum_q \bar{G}_q dm_q , \tag{45}$$

which expresses the change in the Gibbs free energy of the solution at constant n_w as an explicit function of the changes in the molalities of all the aqueous species in solution. In contrast to eq (31), eq (45) is an exact differential only if homogeneous equilibrium is *not* maintained. Otherwise, m_j and m_q are not independent variables, and the cross partial derivatives of eq (45) are not necessarily equal. For example, if the jth ion occurs in the qth complex, and homogeneous equilibrium is maintained, it follows that

$$\bar{S}_j \equiv \left(\frac{\partial S}{\partial m_j}\right)_{P,T,\hat{m}_j,n_w} \neq -\left(\frac{\partial \bar{G}_j}{\partial T}\right)_{P,\hat{m}(j,q)} = 0 \tag{46}$$

and

$$\bar{V}_j \equiv \left(\frac{\partial V}{\partial m_j}\right)_{P,T,\hat{m}_j,n_w} \neq \left(\frac{\partial \bar{G}_j}{\partial P}\right)_{T,\hat{m}(j,q)} = 0 \tag{47}$$

where the subscript $\hat{m}(j,q)$ stipulates that the number of moles of H_2O and each of the jth and qth aqueous species are held constant.[6] The inequalities in these expressions arise from the fact that $(\partial\overline{G}_j/\partial T)_{P,\hat{m}(k)}$ and $(\partial\overline{G}_j/\partial P)_{T,\hat{m}(k)}$ are not necessarily equal to $(\partial\overline{G}_j/\partial T)_{P,\hat{m}(j,q)}$ and $(\partial G_j/\partial P)_{T,\hat{m}(j,q)}$, respectively. However, it follows from eq (19) that we can write

$$\sum_q \bar{\Xi}_q \, dm_q = \sum_j \sum_q \bar{\Xi}_j \, \nu_{j,q} \, dm_q \ . \tag{48}$$

Hence

$$\sum_j \bar{\Xi}_j \, dm_j + \sum_q \bar{\Xi}_q \, dm_q = \sum_j \bar{\Xi}_j \, dm_{t,j} \tag{49}$$

where $dm_{t,j}$ is given by the derivative of eq (23), which can be written as

$$dm_{t,j} = dm_j + \sum_q \nu_{j,q} \, dm_q = \sum_k \nu_{j,k} \, dm_k \ . \tag{50}$$

Consequently, eq (45) can be expressed as

$$dG = -SdT + VdP + \sum_j \overline{G}_j \, dm_{t,j} \tag{51}$$

or

$$dG = -SdT + VdP + \sum_j \sum_k \nu_{j,k} \, \overline{G}_j \, dm_k \ , \tag{52}$$

which can be combined with an appropriate statement of eq (29) to give eq (31). Hence, in contrast to the effect of homogeneous equilibrium on eq (45), eq (51) and (52) are exact differentials under all conditions.

Eqs (51) and (52), which correspond to analogs of eq (31), take explicit account of constraints imposed by homogeneous equilibrium. Note that the three equations can be combined with eq (45) to give

$$\sum_k \overline{G}_k \, dm_k = \sum_j \overline{G}_j \, dm_{t,j} = \sum_j \sum_k \nu_{j,k} \, \overline{G}_j \, dm_k$$

$$= \sum_j \overline{G}_j \, dm_j + \sum_q \overline{G}_q \, dm_q \tag{53}$$

in which the right side of the last identity is inexact if homogeneous equilibrium is maintained.

Activity/concentration relations.—The activity of the kth solute component (a_k) of an electrolyte solution is related to the chemical potential of the component ($\overline{G}_k$) by

$$\overline{G}_k = \overline{G}^\circ_k + RT \ln a_k \tag{54}$$

[6] Note that stipulating $\hat{m}(j,q)$ also imposes implicitly the constraint represented by $\hat{m}(k)$ but not vice versa.

where R stands for the gas constant and T the temperature in °K. However, we can also write

$$\overline{G}_j = \overline{G}^{\circ}{}_j^{abs} + RT \ln a_j \tag{55}$$

where a_j represents the activity of the jth ion in solution, which is related to the total concentration of the ion ($m_{t,j}$) by

$$a_j = \gamma_j m_{t,j} = \gamma_j \sum_k \nu_{j,k} m_k \tag{56}$$

where γ_j stands for the *stoichiometric* activity coefficient of the subscripted ion. The *stoichiometric* mean activity coefficient of the kth component ($\gamma_{\pm,k}$) is defined by

$$\gamma_{\pm,k} \equiv \left(\prod_j \gamma_j{}^{\nu_{j,k}} \right)^{1/\nu_k} \tag{57}$$

where

$$\nu_k = \sum_j \nu_{j,k} \ . \tag{58}$$

Combining eqs (54) through (57) with alternate statements of eq (29) for $\overline{G}_k$ and $\overline{G}^{\circ}{}_k$ leads to

$$a_k = \prod_j a_j{}^{\nu_{j,k}} = \prod_j (\gamma_j m_{t,j})^{\nu_{j,k}} = \prod_j \gamma_j{}^{\nu_{j,k}} \left(\sum_k \nu_{j,k} m_k \right)^{\nu_{j,k}}$$

$$= \gamma_{\pm,k}{}^{\nu_k} \prod_j m_{t,j}{}^{\nu_{j,k}} = \gamma_{\pm,k}{}^{\nu_k} \prod_j \left(\sum_k \nu_{j,k} m_k \right)^{\nu_{j,k}} \ . \tag{59}$$

Hence, eqs (54) and (55) can also be written as

$$\overline{G}_k = \overline{G}^{\circ}{}_k + RT \left(\nu_k \ln \gamma_{\pm,k} + \sum_j \nu_{j,k} \ln \left(\sum_k \nu_{j,k} m_k \right) \right) \tag{60}$$

and

$$\overline{G}_j = \overline{G}^{\circ}{}_j^{abs} + RT \left(\ln \gamma_j + \ln m_{t,j} \right) \ . \tag{61}$$

For single electrolytes, or mixed electrolytes in which none of the solute components shares a common ion, eqs (59) and (60) reduce to

$$a_k = (\gamma_{\pm,k} m_k)^{\nu_k} \prod_j \nu_{j,k}{}^{\nu_{j,k}} \tag{61A}$$

and

$$\overline{G}_k = \overline{G}^{\circ}{}_k + RT \left(\nu_k \ln(\gamma_{\pm,k} m_k) + \sum_j \nu_{j,k} \ln \nu_{j,k} \right) . \tag{62}$$

The nonstoichiometric analogs of eqs (56) and (57) appear as

$$a_j = \bar{\gamma}_j\, m_j \tag{63}$$

and

$$\bar{\gamma}_{\pm,k} = \left(\prod_j \bar{\gamma}_j^{\nu_{j,k}} \right)^{1/\nu_k} \tag{64}$$

where $\bar{\gamma}_j$ stands for the individual ion activity coefficient of the jth ion and $\bar{\gamma}_{\pm,k}$ represents the mean ionic activity coefficient of the kth component. The overbar appears in these symbols to distinguish the individual ion and mean ionic activity coefficients from their stoichiometric counterparts. The activity of the qth complex in solution can be expressed as

$$a_q = \bar{\gamma}_q\, m_q \tag{65}$$

where $\bar{\gamma}_q$ refers to the activity coefficient of the complex.

Eq (63) permits the partial molal Gibbs free energy of the jth ion to be expressed as

$$\overline{G}_j = \overline{G}^\circ_j{}^{abs} + RT\, ln\, (\bar{\gamma}_j\, m_j)\ , \tag{66}$$

which can be combined with eq (61) to give

$$\bar{\gamma}_j\, m_j = \gamma_j\, m_{t,j} = \gamma_j \sum_k \nu_{j,k}\, m_k\ . \tag{67}$$

Note that it also follows from eqs (57), (59), (64), and (67) that

$$\gamma_{\pm,k}{}^{\nu_k} = \prod_j (\bar{\gamma}_j\, \alpha_j)^{\nu_{j,k}} = \bar{\gamma}_{\pm,k}{}^{\nu_k} \prod_j \alpha_j{}^{\nu_{j,k}}\ , \tag{68}$$

$$\gamma_j = \alpha_j \bar{\gamma}_j\ , \tag{68A}$$

and

$$a_k = \prod_j a_j{}^{\nu_{j,k}} = \prod_j (\bar{\gamma}_j\, m_j)^{\nu_{j,k}} = \bar{\gamma}_{\pm,k}{}^{\nu_k} \prod_j m_j{}^{\nu_{j,k}}$$

$$= \bar{\gamma}_{\pm,k}{}^{\nu_k} \prod_j \left(\alpha_j \sum_k \nu_{j,k}\, m_k \right)^{\nu_{j,k}}\ , \tag{69}$$

which permit eq (60) to be written as

$$\overline{G}_k = \overline{G}^\circ_k + RT \left(\nu_k\, ln\, \bar{\gamma}_{\pm,k} + \sum_j \nu_{j,k}\, ln\, m_j \right)$$

$$= \overline{G}^\circ_k + RT \left(\nu_k\, ln\, \bar{\gamma}_{\pm,k} + \sum_j \nu_{j,k} \left(ln\, \alpha_j + ln \left(\sum_k \nu_{j,k}\, m_k \right) \right) \right)\ , \tag{70}$$

where α_j (the degree of formation of the jth ion) is given by

$$\alpha_j \equiv m_j / m_{t,j}\ . \tag{70A}$$

Hence, as $\alpha_j \rightarrow 1$, $\bar{\gamma}_j \rightarrow \gamma_j$, which requires $\bar{\gamma}_{\pm,k} \rightarrow \gamma_{\pm,k}$ if $\alpha_j \rightarrow 1$ for all finite values of $\nu_{j,k}$. Note that eqs (69) and (70) can be written for single electrolytes or mixed electrolytes in which none of the solute components shares a common ion as

$$a_k = \bar{\gamma}_{\pm,k}{}^{\nu_k} \; m_k{}^{\nu_k} \prod_j \left(\nu_{j,k} \, \alpha_j \right)^{\nu_{j,k}} \tag{71}$$

and

$$\overline{G}_k = \overline{G}^\circ{}_k + \nu_k \, RT \, ln \, (\bar{\gamma}_{\pm,k} \, m_k) + RT \sum_j \nu_{j,k} \, ln \, (\nu_{j,k} \, \alpha_j) \; . \tag{72}$$

Relative partial molal properties.—The equations summarized above permit calculation of the relative partial molal Gibbs free energies and stoichiometric mean activity coefficients of the thermodynamic components of electrolyte solutions from expressions of $\bar{\gamma}_j$ as a function of the concentrations of the aqueous species in solution. All other partial molal properties of the components can be computed by taking the partial derivatives of $ln \, \gamma_j$ or $ln \, \bar{\gamma}_j$ with respect to temperature or pressure, holding n_w and all m_k constant. Note that it follows from eq (50) that[7]

$$\left(\frac{\partial m_j}{\partial P} \right)_{T,\hat{m}(k)} = - \sum_q \nu_{j,q} \left(\frac{\partial m_q}{\partial P} \right)_{T,\hat{m}(k)} \tag{73}$$

and

$$\left(\frac{\partial m_j}{\partial T} \right)_{P,\hat{m}(k)} = - \sum_q \nu_{j,q} \left(\frac{\partial m_q}{\partial T} \right)_{P,\hat{m}(k)} \; . \tag{74}$$

Similarly, taking account of eq (49) we can write

$$\sum_j \Xi_j \left(\frac{\partial m_j}{\partial P} \right)_{T,\hat{m}(k)} = - \sum_q \Xi_q \left(\frac{\partial m_q}{\partial P} \right)_{T,\hat{m}(k)} \tag{75}$$

and

$$\sum_j \Xi_q \left(\frac{\partial m_j}{\partial T} \right)_{P,\hat{m}(k)} = - \sum_q \Xi_j \left(\frac{\partial m_q}{\partial T} \right)_{P,\hat{m}(k)} \; . \tag{76}$$

Equations relating the relative partial molal properties of thermodynamic components and ions to changes in activity coefficients and the distribution of species in solution are summarized in app. B. Calculation of the partial derivatives of m_j in these equations requires dissociation constants and standard partial molal properties of dissociation for the complexes in solution. Partial derivatives of the law of mass action, material balance, and activity coefficient equations can then be combined to compute $(\partial \; ln \; m_j/\partial P)_{T,\hat{m}(k)}$, $(\partial^2 ln \; m_j/\partial P^2)_{T,\hat{m}(k)}$, $(\partial(\partial \; ln \; m_j/\partial P)_{T,m(k)}/\partial T)_{P,\hat{m}(k)}$, $(\partial \; ln \; m_j/\partial T)_{P,\hat{m}(k)}$, and $(\partial^2 \; ln \; {}_{mj}\partial T^2)_{P,m(k)}$ (see below).

[7] Note that the constraint imposed by specifying n_w and all m_k constant ($\hat{m}(k)$) requires all $m_{i,j}$ to be constant but not necessarily all m_j and m_q.

Apparent molal properties and the partial molal properties of the solvent.—Apparent molal properties of electrolytes are given by

$$\phi_\Xi = \frac{\Xi - 55.51\,\bar{\Xi}^\circ_w}{\sum_k m_k} \tag{77}$$

where ϕ_Ξ stands for a given apparent molal property, and $\bar{\Xi}^\circ_w$ represents the corresponding standard partial molal property of the solvent. Combining eqs (24), (26), and (77) leads to

$$55.51\,(\bar{\Xi}_w - \bar{\Xi}^\circ_w) = \phi_\Xi \sum_k m_k - \sum_k m_k\,\bar{\Xi}_k = \phi_\Xi \sum_k m_k$$

$$- \sum_j \sum_k \nu_{j,k}\, m_k\,\bar{\Xi}_j = \phi_\Xi \sum_k m_k - \sum_j m_{t,j}\,\bar{\Xi}_j\ , \tag{78}$$

which relates the relative partial molal property of the solvent, the corresponding apparent molal property of the solute, and the partial molal properties of the components of the solute to those of the cations and anions in solution. Note that it also follows from eq (77) that eq (29) can be written as

$$\bar{\Xi}_k = \sum_j \nu_{j,k}\,\bar{\Xi}_j = \phi_\Xi + \left(\frac{\partial \phi_\Xi}{\partial m_k}\right)_{P,T,\hat{m}_k,n_w} \sum_k m_k = \left(\frac{\partial(\phi_\Xi \sum_k m_k)}{\partial m_k}\right)_{P,T,\hat{m}_k,n_w} \tag{79}$$

Hence, at constant pressure and temperature

$$\phi_\Xi = \frac{1}{\sum_k m_k} \int_0^{m_k} \bar{\Xi}_k\, \mathrm{d}m_k\ . \tag{80}$$

For convenience in later discussion, the "true" (or effective (Johnson and Pytkowicz, 1979)) ionic strength fraction of the jth ion ($\bar{y}_j$) can be defined as

$$\bar{y}_j \equiv \frac{\psi_j\, m_j}{\bar{\mathrm{I}}} \tag{81}$$

where

$$\psi_j \equiv \frac{Z_j^2}{2} \tag{82}$$

and

$$\bar{\mathrm{I}} \equiv \sum_j \psi_j\, m_j + \sum_q \psi_q\, m_q \tag{83}$$

where Z_j denotes the charge on the jth cation or anion and

$$\psi_q \equiv \frac{Z_q^2}{2} \tag{84}$$

where Z_q stands for the charge on the qth complex in solution. The overbars on the symbols $\bar{I}$ and $\bar{y}_j$ serve to distinguish "true" ionic strength and "true" ionic strength fractions from their stoichiometric counterparts (I and y_j), which are given by

$$I = \sum_j \psi_j m_{t,j} = \sum_k \psi_k m_k \tag{85}$$

and

$$y_j = \frac{\psi_j m_{t,j}}{I} = \frac{\psi_j \sum_k \nu_{j,k} m_k}{I} \tag{86}$$

where

$$\psi_k \equiv \frac{\sum_j \nu_{j,k} Z_j^2}{2} = \sum_j \nu_{j,k} \psi_j \quad . \tag{87}$$

The "true" and stoichiometric ionic strength fractions of the kth solute component ($\bar{y}_k$ and y_k, respectively) are given by

$$\bar{y}_k = \frac{\sum_j \nu_{j,k} \psi_j m_k}{\bar{I}} = \frac{\psi_k m_k}{\bar{I}} \tag{88}$$

and

$$y_k = \frac{\psi_k m_k}{I} \, . \tag{89}$$

It thus follows from eqs (86) and (89) that

$$y_j = \psi_j \sum_k \frac{\nu_{j,k} y_k}{\psi_k} \tag{90}$$

and we can write

$$\sum_j y_j = \sum_k y_k = \sum_j \bar{y}_j + \sum_q \bar{y}_q = 1 \tag{91}$$

where $\bar{y}_q$ is the analog of $\bar{y}_j$ for the qth complex in solution. In contrast,

$$\sum_k \bar{y}_k = \frac{I}{\bar{I}} \, . \tag{92}$$

Another convenient fraction, $\bar{y}_{t,j}$, can be defined as

$$\bar{y}_{t,j} \equiv \frac{\psi_j m_{t,j}}{\mathrm{I}} = \frac{\psi_j \sum_k \nu_{j,k} m_k}{\mathrm{I}} = \psi_j \sum_k \frac{\nu_{j,k} \bar{y}_k}{\psi_k} = \frac{y_j \mathrm{I}}{\mathrm{I}} = y_j \sum_k \bar{y}_k \tag{93}$$

so that

$$\sum_j \bar{y}_{t,j} = \sum_k \bar{y}_k = \frac{\mathrm{I}}{\mathrm{I}} . \tag{94}$$

Note that holding all $\bar{y}_j$ and $\bar{y}_q$ constant (indicated below by the subscript $\hat{y}$) implicitly requires all $\bar{y}_{t,j}$ and $\bar{y}_k$ to be constant as well, which is not true in reverse.

Taking account of the definitions summarized above, eqs (24), (77), and (78) can be expressed as

$$\Xi = 55.51\, \bar{\Xi}_w + \sum_j \frac{\bar{y}_{t,j} \bar{\Xi}_j \mathrm{I}}{\psi_j} = 55.51\, \Xi_w + \sum_j \sum_k \frac{\nu_{j,k} \bar{y}_k \bar{\Xi}_j \mathrm{I}}{\psi_k} , \tag{95}$$

$$\phi_\Xi = \frac{\Xi - 55.51\, \Xi^\circ_w}{\sum_k (\bar{y}_k \mathrm{I}/\psi_k)} , \tag{96}$$

and

$$55.51\, (\bar{\Xi}_w - \bar{\Xi}^\circ_w) = \phi_\Xi \sum_k \frac{\bar{y}_k \mathrm{I}}{\psi_k} - \sum_k \frac{\bar{y}_k \bar{\Xi}_k \mathrm{I}}{\psi_k} = \phi_\Xi \sum_k \frac{\bar{y}_k \mathrm{I}}{\psi_k}$$

$$- \sum_j \sum_k \frac{\nu_{j,k} \bar{y}_k \bar{\Xi}_j \mathrm{I}}{\psi_k} = \phi_\Xi \sum_k \frac{\bar{y}_k \mathrm{I}}{\psi_k} - \sum_j \frac{\bar{y}_{t,j} \bar{\Xi}_j \mathrm{I}}{\psi_j} . \tag{97}$$

Let us now employ the subscript $\hat{y}$ to indicate constant $\bar{y}_k$ for all values of k and differentiate eq (96) with respect to I at constant temperature, pressure, and $\bar{y}_k$, which leads to

$$\left(\frac{\partial \Xi}{\partial \mathrm{I}}\right)_{\mathrm{P,T},\hat{y}} = \left(\phi_\Xi + \mathrm{I} \left(\frac{\partial \phi_\Xi}{\partial \mathrm{I}}\right)_{\mathrm{P,T},\hat{y}} \right) \sum_k \frac{\bar{y}_k}{\psi_k} . \tag{98}$$

Note that eq (77) can also be written as

$$\left(\frac{\partial \Xi}{\partial \mathrm{I}}\right)_{\mathrm{P,T},\hat{y}} = \left(\frac{\partial (\phi_\Xi \mathrm{I})}{\partial \mathrm{I}}\right)_{\mathrm{P,T},\hat{y}} \sum_k \frac{\bar{y}_k}{\psi_k} \tag{99}$$

and expressed in terms of $\bar{\Xi}_j$ by taking account of the following isothermal-isobaric identity for constant n_w:

$$\mathrm{d}\Xi = \sum_k \bar{\Xi}_k \,\mathrm{d}m_k = \sum_j \sum_k \nu_{j,k} \bar{\Xi}_j \,\mathrm{d}m_k = \sum_j \Xi_j \,\mathrm{d}m_{t,j} = \sum_j \bar{\Xi}_j \,\mathrm{d}m_j + \sum_q \bar{\Xi}_q \,\mathrm{d}m_q \tag{100}$$

Dividing eq (100) by $d\bar{I}$ and imposing constant pressure, temperature, and the constraint represented by $\hat{y}$ leads to

$$\left(\frac{\partial \Xi}{\partial \bar{I}}\right)_{P,T,\hat{y}} = \sum_j \sum_k \frac{\nu_{j,k}\bar{y}_k \bar{\Xi}_j}{\psi_k} = \sum_j \frac{\bar{y}_{t,j}\bar{\Xi}_j}{\psi_j} \tag{101}$$

which can be combined with eq (99) to give

$$\left(\frac{\partial(\phi_\Xi \bar{I})}{\partial \bar{I}}\right)_{P,T,\hat{y}} = \frac{1}{\sum_k (\bar{y}_k/\psi_k)} \sum_j \sum_k \frac{\nu_{j,k}\bar{y}_k\bar{\Xi}_j}{\psi_k} = \frac{1}{\sum_k \bar{y}_k/\psi_k} \sum_j \frac{\bar{y}_{t,j}\bar{\Xi}_j}{\psi_j} \tag{102}$$

Integrating eq (102) at constant pressure, temperature, and $\bar{y}_k$ for all values of k then leads to

$$\phi_\Xi = \frac{1}{\bar{I} \sum_k (\bar{y}_k/\psi_k)} \sum_j \sum_k \int_0^{\bar{I}} \frac{\nu_{j,k}\bar{y}_k\bar{\Xi}_j}{\psi_k}\, d\bar{I} = \frac{1}{\bar{I} \sum_k (\bar{y}_k/\psi_k)} \sum_j \int_0^{\bar{I}} \frac{\bar{y}_{t,j}\bar{\Xi}_j}{\psi_j}\, d\bar{I} \tag{103}$$

If we now substitute eq (103) in eq (97) we can write

$$\bar{\Xi}_w - \bar{\Xi}^\circ_w = \frac{1}{55.51} \sum_j \sum_k \left(\left(\int_0^{\bar{I}} \frac{\nu_{j,k}\bar{y}_k\bar{\Xi}_j}{\psi_k}\, d\bar{I}\right) - \frac{\nu_{j,k}\bar{y}_k\bar{\Xi}_j\bar{I}}{\psi_k}\right)$$

$$= \frac{1}{55.51} \sum_j \left(\left(\int_0^{\bar{I}} \frac{\bar{y}_{t,j}\bar{\Xi}_j}{\psi_j}\, d\bar{I}\right) - \frac{\bar{y}_{t,j}\bar{\Xi}_j\bar{I}}{\psi_j}\right) \tag{104}$$

which corresponds to the integrated Gibbs-Duhem equation at constant pressure, temperature, and $\bar{y}_k$. Eq (104) permits calculation of the relative partial molal properties of the solvent from those of the ions in solution, expressed as functions of "true" ionic strength. Note that if y_k and I are substituted for $\bar{y}_k$ and $\bar{I}$ in eq (104), the expression reduces to

$$\bar{\Xi}_w - \bar{\Xi}^\circ_w = \frac{1}{55.51} \sum_k \left(\left(\int_0^{I} \frac{y_k\bar{\Xi}_k}{\psi_k}\, dI\right) - \frac{y_k\bar{\Xi}_k I}{\psi_k}\right) \tag{105}$$

The osmotic coefficient of an electrolyte solution (ϕ) is related to the activity of the solvent (a_w) by

$$\phi = -\frac{55.51 \ln a_w}{m^*} \tag{106}$$

where m^* stands for the sum of the molalities of all the aqueous species in solution: that is,

$$m^* = \sum_j m_j + \sum_q m_q \,. \tag{107}$$

For completely dissociated single electrolytes, eq (107) reduces to

$$m^* = \nu_k m_k \quad . \tag{108}$$

Because,

$$\overline{G}_w - \overline{G}^\circ_w = \mathrm{RT}\, ln\, a_w \tag{109}$$

it follows that

$$\phi = -\frac{55.51\,(\overline{G}_w - \overline{G}^\circ_w)}{\mathrm{RT}\, m^*} \,. \tag{110}$$

Taking account of eqs (77), (97), (104), and (110), we can thus write

$$\begin{aligned}
\phi &= -\frac{1}{\mathrm{RT}\, m^*}\ \phi_G\ \sum_k \frac{\bar{y}_k \bar{I}}{\psi_k} \ - \ \sum_j \sum_k \frac{\nu_{j,k} \bar{y}_k \overline{G}_j \bar{I}}{\psi_k} \\
&= -\frac{1}{\mathrm{RT}\, m^*}\ \phi_G\ \sum_k \frac{\bar{y}_k \bar{I}}{\psi_k} \ - \ \sum_j \frac{\bar{y}_{t,j} \overline{G}_j \bar{I}}{\psi_j} \\
&= -\frac{1}{\mathrm{RT}\, m^*} \sum_j \sum_k \left(\left(\int_0^{\bar{I}} \frac{\nu_{j,k} \bar{y}_k \overline{G}_j}{\psi_k} \ \mathrm{d}\bar{I} \right) \ - \ \frac{\nu_{j,k} \bar{y}_k \overline{G}_j \bar{I}}{\psi_k} \right) \\
&= -\frac{1}{\mathrm{RT}\, m^*} \sum_j \left(\left(\int_0^{\bar{I}} \frac{\bar{y}_{t,j} \overline{G}_j}{\psi_j} \ \mathrm{d}\bar{I} \right) \ - \ \frac{\bar{y}_{t,j} \overline{G}_j \bar{I}}{\psi_j} \right)
\end{aligned} \tag{111}$$

which defines the relation between the osmotic coefficient, the apparent molal Gibbs free energy of the solute (ϕ_G), and the partial molal Gibbs free energies of the cations and anions in solution as a function of "true" ionic strength. Note that by taking account of eq (105) we can also write

$$\phi = -\frac{1}{\mathrm{RT}\, m^*} \sum_k \left(\left(\int_0^{I} \frac{y_k \overline{G}_k}{\psi_k} \ \mathrm{d}I \right) \ - \ \frac{y_k \overline{G}_k I}{\psi_k} \right). \tag{112}$$

By expressing $\bar{\Xi}_j$ as a function of $\bar{I}$ and computing values of $\bar{y}_k$ or $\bar{y}_{t,j}$ (see below), all apparent molal properties of the solute as well as the osmotic coefficient and the partial molal properties of the solvent can be computed from the equations summarized above.

THEORETICAL CONCEPTS

The thermodynamic properties of an aqueous electrolyte solution can be expressed in terms of the structural and electrostatic consequences of dissolving an electrolyte in H_2O. In addition to ideal mixing and contributions by the solvent, the conceptual model adopted in the present study takes account of (1) the intrinsic properties of the electrolyte itself, which are independent of the solvent, (2) cavity formation, electrostriction collapse, and local disruption of the solvent structure by the solute, (3) orientation of the disordered H_2O dipoles to form primary and (more

loosely held) secondary solvation shells about the ions, (4) long and short-range interaction of the solvated ions with one another, and (5) ion association. Although all these processes are interdependent and none is strictly separable in either a physical or thermodynamic sense, regression calculations (Helgeson and Kirkham, 1976) together with theoretical and empirical considerations discussed below indicate that each can be represented adequately by separate functions of pressure, temperature, and concentration.

Because contributions by ionic interaction to the thermodynamic properties of an electrolyte are negligible at infinite dilution, the standard partial molal properties of aqueous species depend only on their intrinsic characteristics and the calorimetric and volumetric consequences of cavity formation, electrostriction collapse, and ion solvation. Accordingly, if we regard cavity formation as part of the electrostriction process we can write

$$\bar{\Xi}^\circ_j = \bar{\Xi}^\circ_{i,j} + \Delta\bar{\Xi}^\circ_{e,j} \ , \tag{113}$$

where $\bar{\Xi}^\circ_j$ represents the conventional standard partial molal heat capacity, entropy, enthalpy, internal energy, Gibbs free energy, Helmholtz free energy, volume, expansibility, or compressibility of the jth aqueous ion, and the subscripts i and e denote the *intrinsic* and *electrostriction* contributions to these properties. The *electrostriction* term in eq (113) is given by

$$\Delta\bar{\Xi}^\circ_{e,j} = \Delta\bar{\Xi}^\circ_{c,j} + \Delta\bar{\Xi}^\circ_{s,j} \tag{114}$$

and for convenience in later discussion let us define

$$\Delta\bar{\Xi}^\circ_{n,j} \equiv \bar{\Xi}^\circ_{i,j} + \Delta\bar{\Xi}^\circ_{c,j} \tag{115}$$

where the subscripts c, s, and n refer to the *collapse, solvation,* and the sum of the *intrinsic* and *collapse* contributions to the standard partial molal property, respectively. Note that cavity formation is included implicitly in $\Delta\Xi^\circ_{c,j}$. Combining eqs (113) through (115) leads to

$$\bar{\Xi}^\circ_j = \bar{\Xi}^\circ_{i,j} + \Delta\bar{\Xi}^\circ_{c,j} + \Delta\bar{\Xi}^\circ_{s,j} = \Delta\bar{\Xi}^\circ_{n,j} + \Delta\bar{\Xi}^\circ_{s,j} \ . \tag{116}$$

Analogous statements of eqs (113) through (115) can be written for the standard partial molal properties of electrolytes as well as for the absolute standard partial molal properties of aqueous species, which are related to their conventional counterparts by appropriate statements of eq (17) and its analogs for $\bar{\Xi}^\circ_{i,j}$, $\Delta\bar{\Xi}^\circ_{e,j}$, $\Delta\bar{\Xi}^\circ_{c,j}$, $\Delta\bar{\Xi}^\circ_{n,j}$, and $\Delta\bar{\Xi}^\circ_{s,j}$.

Before considering the pressure and temperature dependence of the intrinsic, collapse, and solvation contributions to the standard partial molal properties of aqueous electrolytes, let us first examine the relative partial molal properties of aqueous species in terms of the theoretical model summarized above.

Any relative partial molal property of the jth ion at a given pressure and temperature ($\Delta\bar{\Xi}_j$) can be expressed as the sum of (1) an ideal mixing term ($\bar{\Xi}_{ideal,j}$), (2) an electrostatic contribution representing long-range

ionic interaction described by Debye-Hückel theory ($\bar{\Xi}_{d,j}$), (3) a nonstandard state analog of the electrostatic and nonelectrostatic terms in eq (116) to provide for the concentration dependence of ion solvation ($\Delta\bar{\Xi}_{h,j}$) and the sum of the intrinsic and collapse contributions to the thermodynamic behavior of the solute, and (4) a short-range interaction term to account for the consequences of collisions among solvated ions. If we let $\bar{\Xi}_{r,j}$ represent the intrinsic, collapse, and short-range interaction contributions to $\Delta\bar{\Xi}_j$, we can thus write

$$\Delta\bar{\Xi}_j = \bar{\Xi}_{ideal,j} + \bar{\Xi}_{d,j} + \Delta\bar{\Xi}_{h,j} + \bar{\Xi}_{r,j} \tag{117}$$

which is consistent with

$$\Delta\bar{\Xi}_j = \bar{\Xi}_j - \bar{\Xi}^\circ{}_j^{abs} \tag{118}$$

and

$$\Delta\bar{\Xi}_{h,j} = \Delta\bar{\Xi}_{s,j} - \Delta\bar{\Xi}^\circ{}_{s\,j}^{abs} \tag{119}$$

where $\Delta\bar{\Xi}_{s,j}$ represents the contribution by electrostriction solvation to the partial molal property of the subscripted ion, and $\Delta\bar{\Xi}^\circ{}_{s,j}^{abs}$ stands for the corresponding contribution in the standard state.[8] The short-range interaction term ($\bar{\Xi}_{r,j}$) in eq (117) modifies the solvation term ($\Delta\bar{\Xi}_{h,j}$), and together they are intended to provide for all departures from ideality which are not accounted for by Debye-Hückel theory. These include changes in the dielectric constant of the solution with increasing ionic strength, polarization of solvated ions, differences in the bulk dielectric constant of the solution and that in the immediate vicinity of the ions, discontinuities in the dielectric medium arising from void spaces and disorder in the solvation shells, changes in solvation with increasing ionic strength, and short-range interaction of the solvated ions. These factors contribute negligibly to departures from ideality in dilute solutions. However, at high ionic strengths they dominate the thermodynamic behavior of electrolytes.

The Debye-Hückel term in eq (117) can be taken to represent electrostatic long-range interaction among idealized solvated ions (Robinson and Stokes, 1959). Consequently, it dominates the thermodynamic behavior of electrolytes only at low concentrations. To ensure adequate provision in the model for the major contributions by ion solvation and short-range interaction to departures from ideality at high concentrations, equations representing $\Delta\bar{\Xi}_{h,j}$ and $\bar{\Xi}_{r,j}$ as functions of temperature, pressure, and composition are derived below from theoretical and semiempirical considerations. Other less important factors contributing to the thermodynamic behavior of electrolytes at high concentrations (see above) are then incorporated implicitly in the coefficients of the equations by regression of experimental data.

Relative Partial Molal Gibbs Free Energy

Because abundant, accurate, and precise experimental data for aqueous electrolytes are available at low pressures and temperatures where

[8] Although eqs (113) through (119) are written for the *j*th ion, analogous expressions can be written for any aqueous species.

most alkali and alkaline earth halides, as well as many other dissolved salts are "completely" dissociated, the dependence of activity coefficients, osmotic coefficients, and the relative partial molal properties of electrolytes on "true" ionic strength is well known at 25°C and 1 bar. Nevertheless, general agreement has yet to be reached on a satisfactory *theoretical* equation to represent these data beyond the range of concentration where Debye-Hückel theory suffices to describe departures from ideality.

Despite Bjerrum's (1926, 1929) early consideration of the effects of ion association on the thermodynamic behavior of electrolytes, few of the many extensions of the Debye-Hückel equation that have been proposed over the past 50 years contain explicit provision for complexing. The importance of including such provision is underscored by the fact that electrostatic theory requires $\bar{I}$ and not I to be used in the Debye-Hückel equation, which is almost certainly responsible for the observation (Guggenheim and Stokes, 1969) that the thermodynamic behavior of electrolytes consisting of divalent cations and anions that associate to a high degree to form species such as $MgSO_4$, $ZnSO_4$, $CuSO_4$, $CaSO_4$, and other similar complexes *apparently* contravenes the Debye-Hückel limiting law.

The effect of ion association on stoichiometric activity coefficients reinforces negative contributions by ionic interaction and opposes the positive consequences of ion solvation. Because complexing in electrolyte solutions increases dramatically with increasing temperature, failure to provide explicitly for its consequences may lead to calculated stoichiometric activity coefficients at high temperatures which are several order of magnitude larger than the actual values. Attempts to take account implicitly of ion association by including provision for its effects solely in short-range interaction terms leads to second, third, or even higher degree extensions of the Debye-Hückel equation (for example, see Pitzer and Mayorga, 1974) and a series of regression parameters (virial coefficients) which cannot be generalized or used with confidence to extrapolate the data from which they are generated. Regardless of the theoretical arguments responsible for the extended terms in such equations, the functional form of the expressions is sufficiently flexible, and they commonly contain enough parameters to fit almost any configuration of activity coefficient data. In such cases, "best fit" criteria are no more meaningful with respect to the validity of the theoretical origin of the equations or the physical significance of the fit parameters than they are in regression calculations with strictly empirical power functions. For example, equations derived by (1) Stokes and Robinson (1948) from hydration theory, (2) Ruff (1977, 1979) and Pytkowicz and Johnson (1979) from a lattice-like model of electrolyte solutions, (3) Panckhurst and Macaskill (1976a and b) from provision for interaction of like-charged ions in Guggenheim's theory of specific interaction, and (4) Pytkowicz and Kester (1969) and Johnson and Pytkowicz (1978, 1979) from an ion association model all yield adequate fits of experimental data. Consequently, none of the fits neither supports nor contravenes the theoretical basis for any of the equations, all of which are capable of overfitting the data. The latter observa-

tion underscores the fact that all the models yield derivative functions which fail to account adequately for all pertinent calorimetric and volumetric data with parameters obtained by regression of activity coefficients.

Virial expansions and second and third-degree extensions of Debye-Hückel theory are commonly employed in solution chemistry to represent departures from ideality in "completely" dissociated electrolytes, notwithstanding the fact that a first-degree extension affords close approximation of experimental activity coefficients for many such electrolytes at high ionic strengths (Helgeson and James, 1968; Helgeson, 1969; Wood, ms and 1975). In most cases, higher order extensions of the Debye-Hückel equation yield improved accuracy over their first-degree counterparts only to the extent of a few percent or less at "true" ionic strengths ranging up to ~ 6 m, depending on the electrolyte (see below). It can be argued from a pragmatic point of view that such a small increase in accuracy hardly justifies practical application of complicated theoretical equations, such as those derived by Mayer (1950), Scatchard (1961, 1968, 1969), Scatchard, Rush, and Johnson (1970), Wu, Rush, and Scatchard (1968, 1969), Friedman (1972a, b, and c), Reilly, Wood, and Robinson (1971), Robinson, Wood, and Reilly (1971), Pitzer (1973, 1975, 1979), Pitzer and Mayorga (1973, 1974), Pitzer and Kim (1974), Justice and Justice (1976, 1977), Justice (1978), and Justice and Ebeling (1979). This certainly is the case in geochemistry, where refinements of the order of 0.1 or less in the logarithm of an activity coefficient are much smaller than uncertainties in the logarithms of most equilibrium constants employed in geochemical calculations.

Regression of apparent molal heat capacities, enthalpies, and volumes of electrolytes with appropriate equations derived from second and third-degree extensions of the Debye-Hückel equation almost invariably lead to overfits of the data. Owing to the interdependence of the fit parameters in extended forms of the Debye-Hückel equation and the relatively large magnification of experimental uncertainties in apparent molal properties, most calorimetric and density data are incapable of yielding "unique" values for more than one adjustable parameter in regression calculations. The interdependence of the fit parameters in these extensions (Helgeson and James, 1968) also commonly leads to close fits of activity coefficients, regardless of whether the electrolytes are "completely" or incompletely dissociated. Ambiguities in the physical significance of the fit parameters or virial coefficients generated by such calculations preclude extrapolation of the parameters to higher temperatures or general application of the regression functions, despite the validity of any or all of the theoretical concepts responsible for the extended terms in the equations.

As a consequence of the observations summarized above, a first degree extension of Debye-Hückel theory was chosen in the present study to represent activity coefficients, osmotic coefficients, and the partial molal properties of aqueous species as a function of "true" ionic strength. The theoretical concepts, assumptions, and approximations involved in the derivation of the equations are summarized below, beginning with the

Debye-Hückel term representing the thermodynamic consequences of long-range electrostatic interaction among solvated ions.

Long-range ionic interaction.—Despite the fact that aqueous electrolytes are not actually composed of hard, spherical, unpolarizable, and incompressible ions in a homogeneous dielectric continuum, the Debye-Hückel equation closely represents activity coefficients in many dilute (< 0.01 m) electrolyte solutions. Although the various assumptions and approximations implicit in the Debye-Hückel equation are clearly invalid at high ionic strengths, the equation is nevertheless invoked to account for long-range interaction among solvated ions in nearly all semi-empirical and theoretical expressions describing the dependence of activity and osmotic coefficients on ionic strength at high concentrations.[9]

The Debye-Hückel equation for $\overline{G}_{\dot{a},j}$ can be written for the molality scale of concentration as[10]

$$\overline{G}_{\dot{a},j} = \frac{\psi_j A_G \bar{I}^{1/2}}{\Lambda} + \Gamma_G \tag{120}$$

where ψ_j is defined by eq (82) and

$$\Lambda \equiv 1 + \mathring{a} B_\gamma \bar{I}^{1/2} \tag{121}$$

where å corresponds to the ion size parameter (see below), $\bar{I}$ designates the "true" ionic strength of the solution in molality units of concentration (eq 83), Γ_G denotes the mole fraction to molality conversion factor given by[11]

$$\Gamma_G \equiv -2.303RT \log(1 + 0.0180153m^*) \tag{122}$$

where m^* stands for the sum of the molalities of all solute species (eq 107) and

$$A_G = -2(2.303)RT\, A_\gamma \tag{123}$$

where A_γ (and B_γ in eq 121) refer to the Debye-Hückel activity coefficient parameters in $kg^{1/2}\ mole^{-1/2}$ and $kg^{1/2}\ mole^{-1/2}\ cm^{-1}$, respectively, which are defined by eqs (C-1) and (C-2) in app. C. Note that a statement of eq (120) can be written for any charged species in solution and that eqs (C-1) and (C-2) in app. C require å in eq (121) to be expressed in centimeters. Values of A_γ, B_γ, and other Debye-Hückel parameters defined below are

[9] Several alternatives to this approach have been suggested recently (Pitzer, 1973, 1977; Pytkowicz, Johnson, and Curtis, 1977). For example, Pitzer's alternate form of the Debye-Hückel equation takes account of hardcore kinetic effects on departures from ideality. Activity coefficients computed from Pitzer's function differ slightly from those predicted by the Debye-Hückel equation, but both reduce to the same limiting law.

[10] Eq (120) and related equations are written above in terms of $\bar{I}$ instead of I because Debye-Hückel theory strictly applies only to completely dissociated electrolytes, many of which become highly associated at high concentrations and/or temperature. Note also that although eq (120) is written for the jth ion, an analogous expression can be written for any charged aqueous species.

[11] The activity coefficient analog of $\Gamma_G(\Gamma_G/(2.303RT))$ in eq (120), which provides for conversion of the rational activity coefficient to its molal counterpart, is commonly omitted from molality expressions of the Debye-Hückel equation because $\Gamma_G/(2.303RT)$ is insignificant in dilute solutions (Harned and Owen, 1958). However, it can be shown that the term becomes important at higher concentrations if eq (120) is used to describe long-range ionic interaction in extensions of Debye-Hückel theory.

TABLE 1

Debye-Hückel parameters computed from equations summarized in app. C by Helgeson and Kirkham (1974b) for 1 bar at temperatures < 100°C and pressures corresponding to those along the liquid-vapor equilibrium curve for H_2O at temperatures > 100°C

T[a]	P[b]	A_γ[c]	B_γ[d] $\times 10^{-8}$	A_V[e]	B_V[f] $\times 10^{-6}$	A_κ[g] $\times 10^{3}$	B_κ[h] $\times 10^{-4}$	A_H[i]	B_H[j] $\times 10^{-9}$	A_J[k]	B_J[l] $\times 10^{-8}$
0	1	0.4913	0.3247	2.34	5.95	-0.56	-0.36	0.392	9.04	10.27	1.25
5	1	0.4943	0.3254	2.41	4.27	-0.73	-0.32	0.446	9.68	11.18	1.32
10	1	0.4976	0.3261	2.48	2.64	-0.83	-0.26	0.503	10.35	11.84	1.39
15	1	0.5012	0.3268	2.56	1.05	-0.91	-0.19	0.564	11.07	12.36	1.46
20	1	0.5050	0.3276	2.65	-0.52	-0.97	-0.12	0.627	11.81	12.80	1.53
25	1	0.5091	0.3283	2.75	-2.07	-1.02	-0.05	0.692	12.60	13.22	1.59
30	1	0.5135	0.3291	2.86	-3.64	-1.07	0.02	0.759	13.41	13.63	1.65
35	1	0.5182	0.3299	2.98	-5.24	-1.12	0.09	0.828	14.24	14.05	1.70
40	1	0.5231	0.3307	3.11	-6.87	-1.18	0.16	0.900	15.10	14.43	1.74
45	1	0.5282	0.3316	3.26	-8.56	-1.25	0.24	0.973	15.99	14.95	1.79
50	1	0.5336	0.3325	3.42	-10.32	-1.33	0.31	1.049	16.89	15.44	1.82
55	1	0.5392	0.3334	3.60	-12.15	-1.41	0.39	1.128	17.81	15.96	1.86
60	1	0.5450	0.3343	3.79	-14.07	-1.52	0.48	1.209	18.75	16.52	1.89
65	1	0.5511	0.3352	4.00	-16.09	-1.63	0.57	1.293	19.70	17.12	1.92
70	1	0.5573	0.3362	4.23	-18.22	-1.76	0.67	1.380	20.67	17.76	1.95
75	1	0.5639	0.3371	4.48	-20.47	-1.91	0.78	1.471	21.65	18.44	1.98
80	1	0.5706	0.3381	4.74	-22.85	-2.07	0.91	1.565	22.65	19.17	2.01
85	1	0.5776	0.3391	5.03	-25.38	-2.26	1.04	1.662	23.66	19.94	2.04
90	1	0.5848	0.3401	5.34	-28.05	-2.46	1.19	1.764	24.68	20.77	2.06
95	1	0.5922	0.3411	5.67	-30.90	-2.70	1.36	1.870	25.72	21.64	2.09
100	1.013	0.5998	0.3422	6.03	-33.92	-2.95	1.54	1.980	26.77	22.57	2.12
105	1.208	0.6077	0.3432	6.41	-37.14	-3.25	1.75	2.095	27.84	23.56	2.15
110	1.433	0.6158	0.3443	6.83	-40.56	-3.57	1.97	2.215	28.93	24.61	2.19
115	1.691	0.6242	0.3454	7.28	-44.21	-3.93	2.23	2.341	30.03	25.73	2.22
120	1.985	0.6328	0.3465	7.76	-48.10	-4.34	2.51	2.472	31.14	26.91	2.26
125	2.321	0.6416	0.3476	8.29	-52.24	-4.80	2.82	2.610	32.28	28.17	2.29
130	2.701	0.6507	0.3487	8.85	-56.66	-5.31	3.17	2.754	33.43	29.52	2.33
135	3.130	0.6601	0.3498	9.46	-61.39	-5.89	3.57	2.904	34.61	30.96	2.38
140	3.613	0.6697	0.3510	10.12	-66.43	-6.53	4.00	3.063	35.80	32.50	2.42
145	4.154	0.6796	0.3521	10.83	-71.83	-7.26	4.49	3.228	37.02	34.15	2.48
150	4.758	0.6898	0.3533	11.60	-77.61	-8.08	5.04	3.403	38.27	35.93	2.53
155	5.431	0.7003	0.3545	12.43	-83.79	-9.01	5.65	3.586	39.54	37.85	2.59
160	6.178	0.7111	0.3556	13.34	-90.42	-10.06	6.34	3.779	40.85	39.94	2.66
165	7.004	0.7222	0.3568	14.32	-97.53	-11.25	7.11	3.983	42.19	42.21	2.74
170	7.916	0.7336	0.3580	15.39	-105.17	-12.60	7.97	4.199	43.57	44.69	2.82
175	8.920	0.7454	0.3592	16.56	-113.39	-14.13	8.95	4.427	44.99	47.41	2.92

T[a]	P[b]	A_γ[c]	B_γ[d] $\times 10^{-8}$	A_V[e]	B_V[f] $\times 10^{-6}$	A_K[g] $\times 10^{3}$	B_K[h] $\times 10^{-4}$	A_H[i]	B_H[j] $\times 10^{-9}$	A_J[k]	B_J[ℓ] $\times 10^{-8}$
180	10.021	0.7575	0.3605	17.82	-122.23	-15.88	10.06	4.669	46.46	50.40	3.03
185	11.226	0.7700	0.3617	19.21	-131.76	-17.89	11.31	4.926	47.98	53.71	3.15
190	12.543	0.7829	0.3629	20.72	-142.05	-20.18	12.73	5.199	49.56	57.37	3.29
195	13.978	0.7962	0.3642	22.38	-153.17	-22.82	14.34	5.491	51.22	61.45	3.45
200	15.537	0.8099	0.3655	24.21	-165.21	-25.86	16.19	5.804	52.95	66.01	3.63
205	17.229	0.8241	0.3668	26.21	-178.27	-29.38	18.29	6.140	54.77	71.12	3.84
210	19.061	0.8387	0.3681	28.42	-192.46	-33.47	20.70	6.501	56.70	76.87	4.07
215	21.041	0.8539	0.3694	30.86	-207.91	-38.23	23.48	6.892	58.74	83.35	4.34
220	23.177	0.8697	0.3707	33.56	-224.76	-43.79	26.69	7.314	60.91	90.70	4.65
225	25.476	0.8860	0.3721	36.56	-243.18	-50.34	30.40	7.773	63.23	99.05	5.00
230	27.947	0.9030	0.3734	39.90	-263.37	-58.06	34.72	8.273	65.72	108.57	5.40
235	30.599	0.9207	0.3748	43.63	-285.55	-67.21	39.77	8.821	68.40	119.48	5.86
240	33.440	0.9391	0.3762	47.81	-309.99	-78.13	45.69	9.421	71.30	132.00	6.39
245	36.480	0.9584	0.3777	52.51	-336.99	-91.21	52.67	10.083	74.46	146.46	7.00
250	29.728	0.9785	0.3792	57.81	-366.91	-106.98	60.96	10.814	77.90	163.21	7.69
255	43.192	0.9996	0.3807	63.82	-400.19	-126.13	70.84	11.628	81.66	182.71	8.50
260	46.883	1.0218	0.3822	70.65	-437.32	-149.54	82.69	12.533	85.80	205.53	9.43
265	50.810	1.0452	0.3838	78.47	-478.92	-178.38	97.02	13.549	90.37	232.39	10.51
270	54.984	1.0699	0.3855	87.45	-525.73	-214.19	114.46	14.690	95.43	264.21	11.77
275	59.415	1.0960	0.3871	97.83	-578.63	-259.08	135.88	15.980	101.06	302.15	13.25
280	64.113	1.1238	0.3889	109.89	-638.73	-315.93	162.40	17.447	107.34	347.77	14.99
285	69.089	1.1534	0.3907	124.01	-707.37	-388.69	195.57	19.125	114.40	403.12	17.06
290	74.356	1.1850	0.3926	140.65	-786.27	-483.00	237.54	21.053	122.35	470.95	19.55
295	79.923	1.2190	0.3945	160.43	-877.59	-606.90	291.28	23.287	131.36	555.07	22.55
300	85.805	1.2555	0.3965	184.17	-984.09	-772.23	361.08	25.893	141.64	660.79	26.23
305	92.012	1.2951	0.3987	212.95	-1,109.4	-996.70	453.17	28.965	153.44	795.73	30.82
310	98.560	1.3381	0.4009	248.28	-1,258.4	-1,307.6	576.88	32.619	167.10	971.09	36.61
315	105.461	1.3851	0.4033	292.23	-1,437.5	-1,748.2	746.61	37.020	183.07	1,203.8	44.08
320	112.732	1.4369	0.4058	347.81	-1,655.9	-2,389.7	985.24	42.395	201.95	1,520.5	53.94
325	120.387	1.4943	0.4085	419.46	-1,926.6	-3,353.7	1,330.6	49.072	224.59	1,964.4	67.34
330	128.446	1.5584	0.4114	513.99	-2,268.9	-4,858.9	1,848.2	57.543	252.22	2,609.2	86.17
335	136.927	1.6309	0.4145	642.27	-2,712.3	-7,321.6	2,658.0	68.567	286.70	3,588.2	113.74
340	145.850	1.7138	0.4178	822.68	-3,304.6	-11,595.	3,995.2	83.394	330.94	5,159.1	156.27
345	155.241	1.8104	0.4215	1,088.4	-4,128.2	-19,600.	6,363.4	104.21	389.89	7,868.4	226.44
350	165.125	1.9252	0.4256	1,504.8	-5,337.0	-36,221.	10,974.	135.18	472.54	13,018.	353.14

[a] °C. [b] bars. [c] $kg^{1/2}\ mole^{-1/2}$. [d] $kg^{1/2}\ mole^{-1}\ cm^{-1}$. [e] $cm^3\ kg^{1/2}\ mole^{-3/2}$. [f] $cm^2\ kg^{1/2}\ mole^{-3/2}$. [g] $cm^3\ kg^{1/2}\ mole^{-3/2}\ bar^{-1}$. [h] $cm^2\ kg^{1/2}\ mole^{-3/2}\ bar^{-1}$. [i] $kcal\ kg^{1/2}\ mole^{-3/2}$. [j] $cal\ kg^{1/2}\ cm^{-1}\ mole^{-3/2}$. [k] $cal\ kg^{1/2}\ mole^{-3/2}(K°)^{-1}$. [ℓ] $cal\ kg^{1/2}\ cm^{-1}\ mole^{-3/2}(K°)^{-1}$.

given in table 1 for temperatures $\leqslant$ 95°C at 1 bar and 100° to 350°C at pressures corresponding to those along the vapor-liquid equilibrium curve for H_2O.

Although å is commonly referred to as the distance of closest approach of ions in solution, it is an electrostatic parameter representing the minimum distance of charge separation among solvated ions, which does not correspond to the sum of their intrinsic radii. Considerable evidence indicates that the effective electrostatic radii of solvated cations are substantially greater than their intrinsic counterparts (Helgeson and Kirkham, 1976). The ion size parameter is defined by Robinson and Stokes (1959) as "the distance from the center of an ion within which no other ion can penetrate," which corresponds to the distance at which the electrostatic fields of the solvated ions interfere with each other to a great enough extent to cause repulsion. The extent of this interference is a function of the effective electrostatic radii of the ions (Helgeson and Kirkham, 1976).

In principle, values of å can be computed from the Debye-Hückel equation with the aid of activity coefficients for dilute aqueous solutions. However, the experimental values of log $\bar{\gamma}_{\pm}$ must be accurate to at least the fourth decimal in order for the calculations to be definitive. Approximations of å were computed from crystal radii and ionic mobilities many years ago by Kielland (1937), but most values generated since the advent of high speed computers have been obtained by regression of stoichiometric activity coefficients with extended forms of the Debye-Hückel equation (Guggenheim and Stokes, 1969; Helgeson and James, 1968; Helgeson, 1969; Hamer and Wu, 1972; Wood, ms and 1975). Although this approach commonly yields acceptable fits of the data, it is not diagnostic with respect to the relative contributions by ionic interaction, solvation, and ion association to the regression parameters, which are interdependent and commonly vary with the range of concentration considered in the fit. Values of å generated in this manner are thus neither unique nor physically significant, despite the fact that they may be of the right order of magnitude. Depending on the degree of the extended Debye-Hückel equation employed, and the range of concentration represented by the data, any value of å of the order of 1 to 6 A may result from regression of activity coefficients.

Although å should in principle be a function of solution composition at constant ionic strength, the algebraic form of eq (120) precludes any such provision for mixed electrolytes. Introduction of the ion size parameter in the derivation of the Debye-Hückel equation is responsible for the appearance of A in the denominator of the expression. As a consequence, the requirements for $dG_{solution}$ to be an exact differential cannot be satisfied without modification of the Debye-Hückel equation (Scatchard, Rush, and Johnson, 1970), unless å is the same for all the solute components of a mixed electrolyte solution. However, the calculations described below, together with theoretical considerations, indicate that å is not the same for all electrolytes. It thus appears that the form of the Debye-Hückel

equation is congenitally flawed for application to mixed electrolytes. This observation has led to the somewhat lame but almost universal decision by solution chemists to assign a single value of å to all electrolytes and make up for errors arising from this procedure by regression of experimental data with extended forms of the Debye-Hückel equation (Robinson and Stokes, 1959; Lewis and Randall, 1961; Harned and Robinson, 1968). In contrast, the approach taken in the present study is to calculate a characteristic but different value of å for each electrolyte solution. As a consequence, provision is included in eq (102) for long-range interaction among all the abundant ions in solution. However, it also means that $\Lambda \neq \Lambda_k$ in the limit as $y_k \rightarrow 1$ in mixed electrolytes, which introduces slight errors in computed values of $\log \bar{\gamma}_{\pm,k}$ in multicomponent solutions (see below). Nevertheless, from a geochemical point of view it seems preferable to accept these small errors rather than introduce an empirical correction function in an attempt to resolve the dichotomy generated by the form of the Debye-Hückel equation applied to mixed electrolytes.

The values of å adopted in the present study were computed from the effective electrostatic radii of aqueous ions ($r_{e,j}$) given by Helgeson and Kirkham (1976) and the relation,

$$\text{å} = 2\sum_k \sum_j \nu_{j,k} r_{ej} \Big/ \sum \nu_k = \frac{\sum_k \nu_k \text{å}_k}{\sum_k \nu_k} \tag{124}$$

where

$$\text{å}_k = 2 \sum_j \nu_{j,k}\, r_{e,j}/\nu_k \tag{125}$$

where j ($j = 1, 2, \ldots \hat{j}$) and k ($k = 1, 2, \ldots \hat{k}$) in this case refer to the *predominant* ions and components of the solute, respectively.

Eq (124) represents a weighted arithmetic mean of the å values for the major components of the solute. As such it takes no account of complexing. The ambiguous and moot significance of the ion size parameter in concentrated solutions precludes explicit provision for the effects of ion association on å. Calculated values of å_k are given in table 2 for a large number of electrolytes. The values of $r_{e,j}$ used to evaluate eq (125) are listed in table 3 and discussed below.

Long-range interaction of polar neutral species with each other and with cations, anions, and charged complexes almost certainly occurs in electrolyte solutions. However, experimental evidence (Randall and Failey, 1927a, b, and c) suggests that the effects of such interaction on the thermodynamic behavior of the species is negligible compared to contributions by solvation and short-range interaction. Accordingly, for most practical purposes $\overline{G}_d$ for neutral species. ($\overline{G}_{d,n}$) can be approximated as

$$\overline{G}_{d,n} = \Gamma_G\,. \tag{125A}$$

Ion-solvent interaction.—The solvation contribution to the thermodynamic behavior of an electrolyte can be described in terms of the Born (1920) transfer process, which, like the Debye-Hückel theory and the Drude-Nernst equation (Drude and Nernst, 1894), is strictly applicable only to idealized incompressible, unpolarizable, spherical ions in a homogeneous dielectric continuum. Owing to structural discontinuities, asymmetric solvation shells, dielectric saturation, and the finite compressibility of solvated ions (which are not necessarily spherical and nonpolar), aqueous electrolytes fail to meet these conditions. Nevertheless, the success of

TABLE 2

"Distance of closed approach" ($\mathring{a}_k$) of ions in various electrolyte solutions (designated by the subscript k) — see text

Solute	$\mathring{a}_k$[a,b]	Solute	$\mathring{a}_k$[a,b]	Solute	$\mathring{a}_k$[a,b]	Solute	$\mathring{a}_k$[a,b]
HCl	4.89	HBr	5.04	HI	5.28	HF	4.41
NaCl	3.72	NaBr	3.87	NaI	4.11	NaF	3.24
LiCl	3.43	LiBr	3.58	KI	4.47	LiF	2.95
RbCl	4.22	RbBr	4.37	CsI	4.81	KF	3.60
CsCl	4.42	CsBr	4.57	MgI_2	4.74	$NaHSO_4$	4.28
NH_4Cl	4.12	$MgBr_2$	4.31	CaI_2	4.85	$KHSO_4$	4.64
$CdCl_2$	4.31	$CaBr_2$	4.53	SrI_2	4.93	$MgSO_4$	5.69
$FeCl_2$	4.16	$SrBr_2$	4.61	BaI_2	5.08	$ZnSO_4$	5.77
$MgCl_2$	4.11	$BaBr_2$	4.76	ZnI_2	4.68	K_2SO_4	5.13
$SrCl_2$	4.41	$ZnBr_2$	4.36	CdI_2	4.83	Na_2SO_4	4.65
$CaCl_2$	4.32	$CdBr_2$	4.51	NaHS	3.75	Li_2SO_4	4.26
$BaCl_2$	4.56	$MnBr_2$	4.40	$NaHCO_3$	4.01	$HClO_4$	6.67
$PbCl_2$	4.47	$FeBr_2$	4.36	$KHCO_3$	4.37	NH_4ClO_4	5.90
$CuCl_2$	4.15	HNO_3	5.89	$LiHCO_3$	3.72	$NaClO_4$	5.50
$MnCl_2$	4.20	KNO_3	5.08	$RbHCO_3$	4.51	NaOH	3.31
$ZnCl_2$	4.16	$NaNO_3$	4.72	$CsHCO_3$	4.71	KOH	3.67
$AlCl_3$	4.38	$LiNO_3$	4.43	$HReO_4$	7.31	NH_4OH	3.71
$FeCl_3$	4.45	NH_4NO_3	5.12	$NaReO_4$	6.14	LiOH	3.02
$GdCl_3$	4.61	$RbNO_3$	5.22	$KReO_4$	6.50	CsOH	4.01

[a]Angstroms. [b]Calculated from equation (125) and values of $r_{e,j}$ given in table 3.

the equation of state proposed recently by Helgeson and Kirkham (1976) for aqueous electrolytes at infinite dilution suggests that the Born-Bjerrum theory affords close approximation of the thermodynamics of ion solvation, provided that separate provision is made for electrostriction collapse of the local solvent structure.

The applicability of the Born equation (as corrected by Bjerrum, 1929) to the solvation process in an aqueous solution can be demonstrated by taking account of

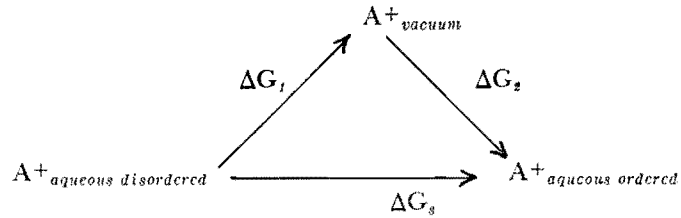

(126)

where $A^+_{aqueous\ disordered}$ refers to the unsolvated ion represented by A^+ in an aqueous state of disorder immediately after collapse of the solvent structure, $A^+_{aqueous\ ordered}$ designates the solvated ion with oriented H_2O dipoles in primary and secondary coordination, A^+_{vacuum} stands for the ion in a vacuum, ΔG_1 and ΔG_2 denote the Gibbs free energy changes attending transfer of the ion from an aqueous disordered state to a vacuum and from a vacuum to an aqueous solvated state, respectively, and ΔG_s corresponds to the Gibbs free energy of solvation within the aqueous phase, which can be expressed as

$$\Delta G_s = \Delta G_1 + \Delta G_2 \ . \tag{127}$$

The solvation process is commonly identified in classical solution chemistry with transfer of an ion from a vaccum (or gas state) to an aqueous solvated state without regard for local collapse of the solvent structure. Consequently, the Born theory alone, which contains no provision for electrostriction collapse, fails to describe adequately the hydration process.[12] However, because the effects of solvent collapse cancel in the transfer of an ion both to and from a vacuum (as depicted in schematic diagram 126), the Born theory is directly applicable to the process of ion solvation within an aqueous phase. Separate provision must then be made for the statistical and structural consequences of electrostriction collapse.

The Born (1920) equation as corrected by Bjerrum (1929) can be written for solvation of one mole of the jth ion as

$$\Delta\overline{G}_{s,j} = \frac{N^\circ Z_j^2 e^2}{2r_{e,j}}\left(\frac{1}{\epsilon} - 1\right) = \frac{\eta Z_j^2}{r_{e,j}}\left(\frac{1}{\epsilon} - 1\right) = \omega_j^{abs}\left(\frac{1}{\epsilon} - 1\right) \tag{128}$$

[12] The terms "ion hydration" and "ion solvation" are used in the present communication to distinguish two different processes. The first denotes transfer of an ion from a vacuum or a gas state to an aqueous solvated state, as in step 2 of schematic diagram (126). In contrast, ion solvation refers to the process of assembly and orientation of H_2O dipoles about an aqueous ion which is already in solution.

where $\Delta\overline{G}_{s,j}$ represents the partial molal Gibbs free energy of solvation of the ion, N° stands for Avogadro's number (6.02252×10^{23} molecules $mole^{-1}$), e designates the electronic charge (4.80298×10^{-10} esu), Z_j and $r_{e,j}$ correspond to the charge and effective electrostatic radius of the subscripted ion, ϵ denotes the dielectric constant of the solution, η refers to a constant defined by

$$\eta \equiv \frac{N^\circ e^2}{2} = 1.66027 \times 10^5 \text{ A cal mole}^{-1} \tag{129}$$

and ω_j^{abs} refers to the absolute Born coefficient for the subscripted ion, which can be expressed as

$$\omega_j^{abs} = \frac{\eta Z_j^2}{r_{e,j}}. \tag{130}$$

The fact that the dielectric constant of the bulk solution is used in eq (128) should not be interpreted as an assumption that ϵ represents a close approximation of the dielectric constant of the medium in the immediate vicinity of the ion. Instead, it means simply that the values of $r_{e,j}$ employed in eq (128) must be consistent with the electrostatic behavior of the bulk solution. For example, evaluation of the Born equation using the dielectric constant of H_2O to generate effective electrostatic radii (Helgeson and Kirkham, 1976) assigns implicitly the effects of dielectric saturation and reduced orientational polarizability of solvated H_2O dipoles to $r_{e,j}$. Nevertheless, because the dielectric constant is always multiplied by $r_{e,j}$ in calculating the thermodynamic consequences of ion solvation, no inconsistencies are introduced by this procedure.

For the kth completely dissociated component of an electrolyte solution, eq (128) becomes

$$\Delta\overline{G}_{s,k} = \omega_k\left(\frac{1}{\epsilon} - 1\right) \tag{131}$$

where

$$\omega_k = \eta \sum_j (\nu_{j,k} Z_j^2 / r_{e,j}) = \sum_j \nu_{j,k}\omega_j^{abs} \ . \tag{132}$$

If $r_{e,j}$ is taken to be independent of concentration (see below), the standard state counterpart of eq (128) can be written for the conventional analog of $\Delta\overline{G}^\circ_{s,j}{}^{abs}$ as

$$\Delta\overline{G}^\circ_{s,j} = \omega_j\left(\frac{1}{\epsilon^\circ} - 1\right), \tag{133}$$

and the standard partial molal Gibbs free energy of solvation of the kth electrolyte can be expressed as

$$\Delta\overline{G}_{s,k} = \omega_k\left(\frac{1}{\epsilon^\circ} - 1\right) \tag{134}$$

where ϵ° stands for the dielectric constant of H_2O and ω_j corresponds to the conventional Born coefficient defined by

$$\omega_j \equiv \omega_j^{abs} - Z_j\omega_{H^+}{}^{abs} \tag{135}$$

which is consistent with

$$\omega_k = \sum_j \nu_{j,k}\, \omega_j \ . \tag{136}$$

Similarly, the absolute analog of $\Delta\overline{G}^\circ_{s,j}$ is given by

$$\Delta\overline{G}^\circ_{s,j}{}^{abs} = \omega_j{}^{abs}\left(\frac{1}{\epsilon^\circ} - 1\right) . \tag{137}$$

Although eqs (128), (130), (133), (135), and (137) apply to the jth ion, analogous expressions can be written for the qth complex.

Representing the thermodynamic consequences of ion solvation with the Born equation is not meant to imply that neutral species fail to solvate. On the contrary, ample evidence indicates that polar neutral complexes solvate to a significant degree. The formal charge of zero on a neutral species can be regarded as an additive consequence of positive and negative vector charges distributed over the polar molecule. If we designate the sum of either the positive or negative contributions to the formal charge of zero as the *effective* local charge (Z_e) of the complex, we can define the Born coefficient for the nth neutral species ($n = 1, 2, \ldots, \hat{n}$) as

$$\omega_n{}^{abs} = \frac{\eta Z_{e,n}{}^2}{r_{e,n}} \tag{138}$$

where $r_{e,n}$ represents the effective electrostatic radius of the complex. The partial molal Gibbs free energy of solvation of the nth neutral species is then given by

$$\Delta\overline{G}_{s,n} = \omega_n{}^{abs}\left(\frac{1}{\epsilon} - 1\right) \tag{139}$$

which is consistent with

$$\Delta\overline{G}_{s,n}{}^{abs} = \omega_n{}^{abs}\left(\frac{1}{\epsilon^\circ} - 1\right) . \tag{140}$$

Because $Z_n = 0$,

$$\omega_n = \omega_n{}^{abs} \tag{140A}$$

and

$$\Delta\overline{G}^\circ_{s,n} = \Delta\overline{G}^\circ_{s,n}{}^{abs} \ . \tag{141}$$

The effective electrostatic radius of an aqueous ion ($r_{e,j}$) differs from its intrinsic counterpart ($r_{i,j}$), and neither (except for $r_{e,anions}$ — see below) is equivalent to its crystallographic radius ($r_{x,j}$). Despite arguments to the contrary (Glueckauf, 1965), $r_{e,j}$ does not necessarily correspond to the physical radius of a solvated ion, nor does the word radius in the term imply that the ion and its solvation shell are actually spherical in symmetry. The effective electrostatic radius of a solvated ion is an idealized parameter representing the net contribution by the ion to the equilibrium distance of charge separation in solution. Although $r_{e,j}$ is referred to a spherical idealization of the ion and its solvation shell, the actual solvated ion may

have a different shape and its contribution to charge separation may be a vector quantity. Nevertheless, the average contribution by the ion to charge separation in solution can be expressed as an equivalent contribution by a hypothetical ion with a spherical configuration. Hence the term "effective" electrostatic radius.

The dependence of $r_{e,j}$ on void space in the solvation shell is an electrostatic function of discontinuities in the dielectric medium, but the dependence of $r_{i,j}$ on void space is a configurational function of the geometry of the solvation shell. Both the intrinsic and effective electrostatic radii of an ion have physical significance only in a statistical context related to the residence time for nearest neighbor configurations of solvent dipoles about the ion (Samoilov, 1972). As a consequence, neither $r_{i,j}$ nor $r_{e,j}$ is strictly independent of short-range ionic interaction, which perturbs the solvation shells about the ions in solution (see below). Nevertheless, empirical considerations suggest that both can be regarded as concentration-independent parameters.

Regression analysis (Helgeson and Kirkham, 1976) indicates that $r_{e,j}$ for anions can be taken to be equivalent to their crystallographic radii

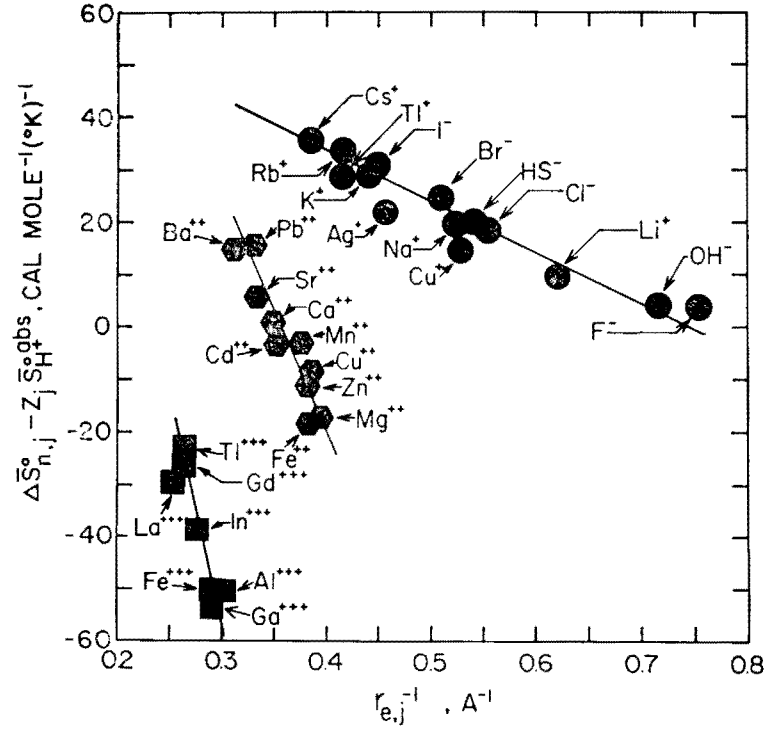

Fig. 1. Correlation of $\Delta\bar{S}^\circ_{n,j}$ ($\Delta\bar{S}^\circ_{n,j} \equiv \bar{S}^\circ_{t,j} + \Delta\bar{S}^\circ_{e,j}$) with the reciprocal of the effective electrostatic radii ($r_{e,j}$) of aqueous ions at 25°C and 1 bar (Helgeson and Kirkham, 1976).

($r_{x,j}$), but that the effective electrostatic radii of cations ($r_{e,+}$) are related to their crystallographic counterparts ($r_{x,+}$) by

$$r_{e,+} = r_{x,+} + 0.94\,Z_+ \tag{142}$$

where Z_+ represents the charge on the cation. Values of $r_{e,j}$ can be computed from eq (142) or estimated from entropy correlations such as those illustrated in figures 1 and 2. The diagrams in these figures depict the difference in the conventional standard partial molal third law entropy of the jth aqueous ion and the corresponding absolute standard partial molal entropy of solvation ($\Delta\bar{S}^\circ_{s,j}{}^{abs}$) as a function of $r_{e,j}{}^{-1}$ and $|Z_j|$ ($r_{e,j}{}^{-1}$), respectively (Helgeson and Kirkham, 1976). Values of both $r_{e,j}$ and $r_{x,j}$ for aqueous species are given in table 3.

Various attempts have been made to improve the applicability of the Born theory to ion hydration (see footnote 12) by regarding $r_{e,j}$ as a function of temperature and/or pressure (Latimer, 1955; Hamann and Strauss, 1955; Benson and Copeland, 1963). Despite the fact that the effective electrostatic radius of an ion might be expected to change as a consequence of changes in the extent to which the ion solvates with increasing pressure and temperature, calculation of the standard partial molal properties of aqueous species at high pressures and temperatures with the aid of continuum theory (Cobble and Murray, 1977; Sen, Murray, and Cobble, ms; Helgeson and Kirkham, 1976) leaves little doubt that $r_{e,j}$ can be taken to be independent of pressure and temperature. Regression analysis of high pressure/temperature data to define values

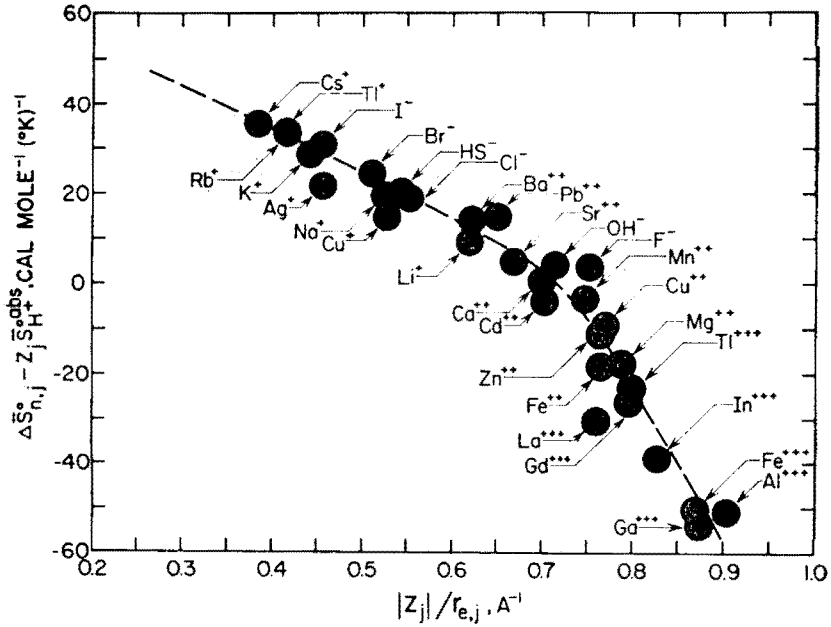

Fig. 2. Correlation of $\Delta\bar{S}^\circ_{n,j}$ ($\Delta\bar{S}^\circ_{n,j} \equiv \bar{S}^\circ_{t,j} + \Delta\bar{S}^\circ_{r,j}$) with the absolute ionic potential of aqueous ions at 25°C and 1 bar (Helgeson and Kirkham, 1976).

TABLE 3

Effective electrostatic ($r_{e,j}$) and crystal ($r_{x,j}$) radii, absolute (ω_j^{abs}) and conventional (ω_j) Born parameters, and conventional standard partial molal entropies ($\bar{S}°_j$) of aqueous ions (designated by the subscript j) at 25°C and 1 bar

Species	$r_{x,j}$ [a]	$r_{e,j}$ [a]	ω_j^{abs} [h] × 10^{-5}	ω_j [h,i] × 10^{-5}	$\bar{S}°_j$ [i,u]	Species	$r_{x,j}$ [a]	$r_{e,j}$ [a]	ω_j^{abs} [h] × 10^{-5}	ω_j [h,i] × 10^{-5}	$\bar{S}°_j$ [i,u]
H^+	2.14[b]	3.08[e]	0.5387[e]	0.0	0.0	Fe^{+++}	0.64[c]	3.46[e]	4.3186[e]	2.7025	-75.5[m]
Li^+	0.68[c]	1.64[e]	1.0249[e]	0.4862	2.7[k]	Al^{+++}	0.51[c]	3.33[e]	4.4872[e]	2.8711	-73.6[p]
Na^+	0.97[c]	1.91[e]	0.8692[e]	0.3305	14.0[k]	Au^{+++}	0.90[c]	3.72[j]	4.0168[g]	2.4007	-51.2[f]
K^+	1.33[c]	2.27[e]	0.7314[e]	0.1927	24.2[k]	La^{+++}	1.14[c]	3.96[e]	3.7733[e]	2.1572	-52.2[q]
Rb^+	1.47[c]	2.41[e]	0.6889[e]	0.1502	28.8[k]	Gd^{+++}	0.97[c]	3.79[e]	3.9426[e]	2.3265	-53.4[q]
Cs^+	1.67[c]	2.61[e]	0.6361[e]	0.0974	31.8[k]	In^{+++}	0.81[c]	3.63[e]	4.1164[e]	2.5003	-53.0[m,n]
NH_4^+	1.37[b]	2.31[e]	0.7170[e]	0.1791	26.6[k]	Ga^{+++}	0.62[c]	3.44[e]	4.3437[e]	2.7276	-79.0[m]
Tl^+	1.47[c]	2.41[e]	0.6889[e]	0.1502	30.0[m]	Tl^{+++}	0.95[c]	3.77[e]	3.9635[e]	2.3474	-46.0[m]
Ag^+	1.26[c]	2.20[e]	0.7547[e]	0.2160	17.5[k]	F^-	1.33[c]	1.33[e]	1.2483[e]	1.7879	-3.2[k]
Au^+	1.37[c]	2.31[j]	0.7187[g]	0.1800	26.5[f]	Cl^-	1.81[c]	1.81[e]	0.9173[e]	1.4569	13.6[k]
Cu^+	0.96[c]	1.90[e]	0.8738[e]	0.3351	9.7[m]	Br^-	1.96[c]	1.96[e]	0.8471[e]	1.3853	19.8[k]
Mg^{++}	0.66[c]	2.54[e]	2.6146[e]	1.5372	-33.0[m]	I^-	2.20[c]	2.20[e]	0.7547[e]	1.2934	25.5[k]
Sr^{++}	1.12[c]	3.00[e]	2.2137[e]	1.1363	-7.8[m]	OH^-	1.40[d]	1.40[e]	1.1859[e]	1.7246	-2.6[k]
Ca^{++}	0.99[c]	2.87[e]	2.3140[e]	1.2366	-13.5[k]	HS^-	1.84[b]	1.84[e]	0.9023[e]	1.4410	15.0[m]
Ba^{++}	1.34[c]	3.22[e]	2.0625[e]	0.9851	2.3[m]	NO_3^-	2.81[b]	2.81[e]	0.5908[e]	1.1295	35.1[k]
Pb^{++}	1.20[c]	3.08[e]	2.1562[e]	1.0788	4.2[k]	HCO_3^-	2.10[b]	2.10[e]	0.7906[e]	1.3293	23.5[s]
Zn^{++}	0.74[c]	2.62[e]	2.5340[e]	1.4574	-26.2[k]	HSO_4^-	2.37[b]	2.37[e]	0.7005[e]	1.2392	27.4[r]
Cu^{++}	0.72[c]	2.60[e]	2.5543[e]	1.4769	-23.2[k]	ClO_4^-	3.59[b]	3.59[e]	0.4625[e]	1.0012	43.5[m]
Cd^{++}	0.97[c]	2.85[e]	2.3302[e]	1.2528	-17.4[k]	ReO_4^-	4.23[b]	4.23[e]	0.3925[e]	0.9312	48.1[m]
Hg^{++}	1.10[c]	2.98[j]	2.2286[g]	1.1512	-8.7[k]	SO_4^{--}	3.15[b]	3.15[e]	2.1083[e]	3.1857	4.5[k]
Fe^{++}	0.74[c]	2.62[e]	2.5348[e]	1.4574	-32.9[m]	CO_3^{--}	2.81[b]	2.81[e]	2.3634[e]	3.4408	-12.0[s]
Mn^{++}	0.80[c]	2.68[e]	2.4780[e]	1.4006	-17.6[n]						

[a]Angstroms. [b]Hypothetical crystal radii computed by Helgeson and Kirkham (1976). [c]Sienko and Plane (1963). [d]Computed assuming $r_{x,OH^-} = r_{x,O^{--}}$ (Helgeson and Kirkham, 1976) [e]Helgeson and Kirkham (1976). [f]Computed from the entropy correlation shown in figure 1 with the aid of equation (74) in Helgeson and Kirkham (1976). [g]Computed from equation (130). [h]Cal $mole^{-1}$. [i]Computed from equation (135). [j]Computed from equation (142). [k]CODATA (1978). [l]Hinchey and Cobble (1970). [m]Wagman and others (1968, 1969); Parker, Wagman, and Evans (1971). [n]Corrected typographical error in Wagman and others (1968). [p]Hemingway and Robie (1977). [q]Computed from data reported by Readnour and Cobble (1969). [s]Berg and Vanderzee (1978). [t]Cal $mole^{-1}$ $(°K)^{-1}$. [u]Other values of $\bar{S}°_j$ (in cal $mole^{-1}$ $(°K)^{-1}$) adopted in the present study include -49.4[q] for Pr^{+++}, -49.4[q] for Nd^{+++}, -52.5[q] for Sm^{+++}, 45.7[m] for MnO_4^-, 33.5[x] for NO_2^-, 28.3[m] for IO_3^-, 39.0[m] for BrO_3^-, -7.0[m] for SO_3^{--}, -53.0[m] for PO_4^{---}, 21.6[m] for $H_2PO_4^-$, and 22.0[m] for $HCOO^-$.

of ω_n^{abs} (see below) indicates that $r_{e,n}$ can also be regarded as a pressure/temperature-independent parameter. Values of ω_j^{abs} together with its conventional analog (ω_j) are given in table 3 for a number of aqueous ions.

If $r_{e,j}$ is regarded as a concentration-independent parameter, $\Delta\overline{G}_{h,j}$ as a function of ionic strength is controlled by the concentration dependence of ϵ^{-1}. The distribution of experimental data shown in figures 3 through 5 suggests that the *reciprocals* of the dielectric constants of electrolyte solutions are linearly related to ionic strength at 25°C and 1 bar, which is consistent with the observed behavior of activity coefficients at high ionic strengths (see below). Few comparable data are available at other temperatures and pressures, but it can be seen in figure 6 that the same behavior is exhibited by electrolytes at 1.5°, 3°, and 10°C. The linear dependence of ϵ^{-1} on ionic strength in figures 3 through 5 contradicts conclusions reached by Hasted, Ritson, and Collie (1948), who represented their data as a linear function of molarity (M) to $\sim 2M$ (fig. 5). Comparative calculations demonstrate that the latter correlation is a fortuitous consequence of the near-proportionality of $(\epsilon^{-1} - \epsilon^{\circ -1})$ to $(\epsilon - \epsilon^{\circ})$ and M to m for $70 \lesssim \epsilon \lesssim 90$ and $M \lesssim 2$.

It can be deduced from figures 3 through 6 that increasing ionic strength affects dramatically the dielectric constant of electrolyte solutions. For example, increasing the concentration of an NaCl solution from 0.1 to ~ 6 m at 1.5°C and 1 bar causes the dielectric constant of the solution to decrease by ~ 45 (fig. 5), which is equal to the decrease in the dielectric constant of H_2O accompanying a temperature increase from 25° to $\sim$ 200°C at pressures corresponding to the liquid-vapor equilibrium curve

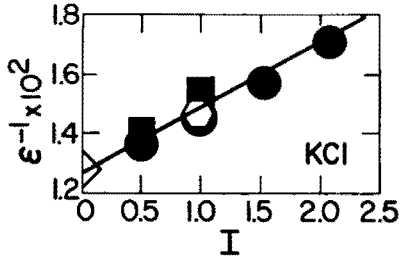

Fig. 3. Reciprocal of the dielectric constant of KCl solutions as a function of stoichiometric ionic strength at 25°C and 1 bar. The symbols in figures 3 through 10, 13, 14, and 131 represent values taken from the following sources: open and closed circles, Hasted, Ritson, and Collie (1948); open and closed hexagons, Pottel (1973) and Giese, Kaatze, and Pottel (1970); striped circles, Hasted and Roderick (1958); striped hexagons, Hasted and El Sabeh (1953); open and closed squares, Haggis, Hasted, and Buchanan (1952); triangles, Helgeson and Kirkham (1976); cross-hatched circles, Harris and O'Konski (1957). The solid curves in these figures are consistent with one another and with the electrostatic parameters and equations summarized in the tables and text. The dashed curves merely connect data points (see text).

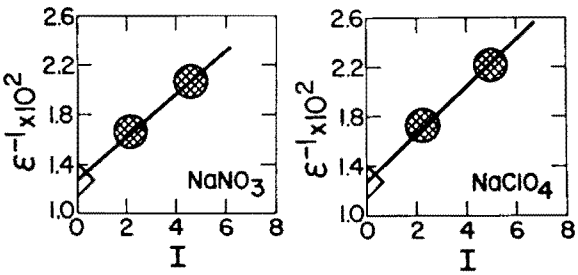

Fig. 4. Reciprocal of the dielectric constant of $NaNO_3$ and $NaClO_4$ solutions as a function of stoichiometric ionic strength at 25°C and 1 bar (see caption of fig. 3).

for H_2O. The disruptive effect of short-range ionic interaction on dipole alignment in the bulk solvent also promotes ion association. The effect of complexing on the dielectric constant of electrolyte solutions can be assessed in figure 7. The increasing departures of the dashed curves in this figure from their solid counterparts with increasing ionic strength is consistent with increasing ion association with increasing concentration.

It has been observed repeatedly (Hasted, Ritson, and Collie, 1948; Haggis, Hasted, and Buchanan, 1952; Hasted and El Sabeh, 1953; Hasted and Roderick, 1958; Harris and O'Konski, 1957; Giese, Kaatze, and Pottel, 1970; Pottel, 1973) that the extent to which the dielectric constant of an electrolyte solution decreases with increasing concentration is highly sensitive to the size and charge of the cation, but essentially independent of the identity of the anion. In contrast to the strong forces of attraction between cations and H_2O dipoles, the solvation shells about anions are loosely held and easily perturbed. The relatively weak forces of attraction between anions and H_2O molecules are apparently of the same order of magnitude as the hydrogen bonds among solvent dipoles, which are oriented about anions with their focus of negative charge outward. Owing to the opposite orientation of H_2O dipoles about cations, few hydrogen bonds are broken by cation solvation. The smaller the cation and the greater its charge, the stronger its influence on the electrostatic behavior of H_2O dipoles in its solvation shell. Because the orientational polarizability of H_2O dipoles about anions is not reduced significantly by coordination, anions contribute only slightly to the electrostatic properties of electrolyte solutions. The solid curves shown in figures 3, 4, 6, and 7 are consistent with this

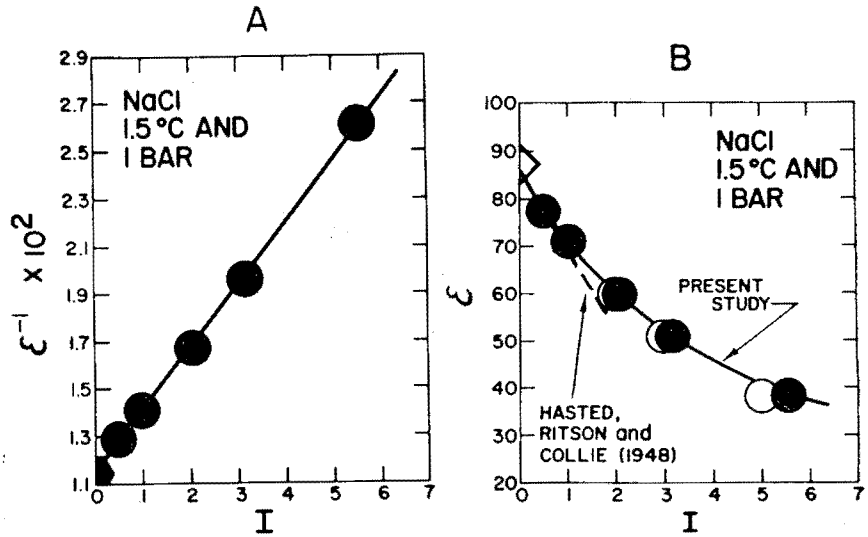

Fig. 5. Reciprocal of the dielectric constant of NaCl solutions as a function of stoichiometric ionic strength at 1.5°C and 1 bar (see caption of fig. 3). The filled and open circles correspond to the same experimental data plotted against molal and molar ionic strength, respectively.

observation; that is, the slopes of the curves for electrolytes consisting of a given cation and different anions (KCl and KF, $NaNO_3$, $NaClO_4$, Na_2SO_4, NaF, and NaI, and $CaCl_2$ and $CaBr_2$) are nearly (but not exactly) identical.

Considerable uncertainty and many assumptions and approximations are involved in extracting static dielectric constants from measurements of the permittivities of electrolyte solutions as a function of frequency. It

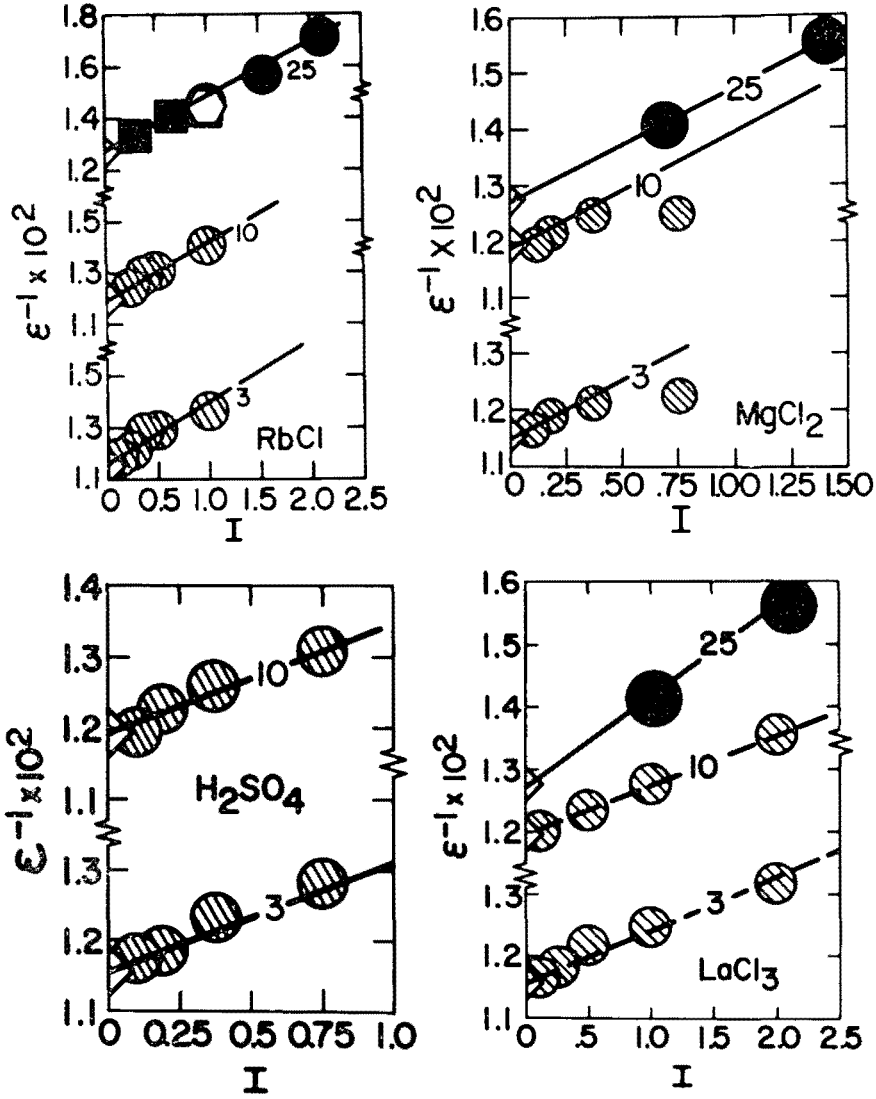

Fig. 6. Reciprocal of the dielectric constant of electrolyte solutions as a function of stoichiometric ionic strength at 3°, 10°, and 25°C and 1 bar (see text and caption of fig. 3).

is thus not surprising that many dielectric constant data reported by different investigators (or the same investigator at different times) contradict one another. For example, all the data reported by Harris and O'Konski (1957) in figure 9 are internally consistent, and the dashed curves drawn through the data points are linear with nearly the same slopes for electrolytes with a common cation. However, none of the dashed curves in figures 8 and 9 has the same slope as the corresponding solid curves for the same electrolytes in figures 3, 7, 8, and 9, which are consistent with data reported by other investigators.

Many dielectric constant data reported for temperatures above and below 25°C are also inconsistent with one another. For example, it can be seen in figure 10 that the data for NaCl at 0°, 10°, 15°, 20°, 25°, 30°, 35°, 40°, and 50°C reported by Pottel (1973) and Hasted, Ritson, and Collie (1948) are incompatible with those obtained at 3°, 25°, and 40°C by Haggis, Hasted, and Buchanan (1952) and Hasted and Roderick (1958). The solid curves in figures 6 and 10 for temperatures other than 25°C are based on consideration of the relation of ϵ^{-1} to $\epsilon^{\circ -1}$ as a function of temperature (see below).

If inconsistencies and departures from linearity in the distribution of data shown in figures 3 through 10 can be attributed to experimental

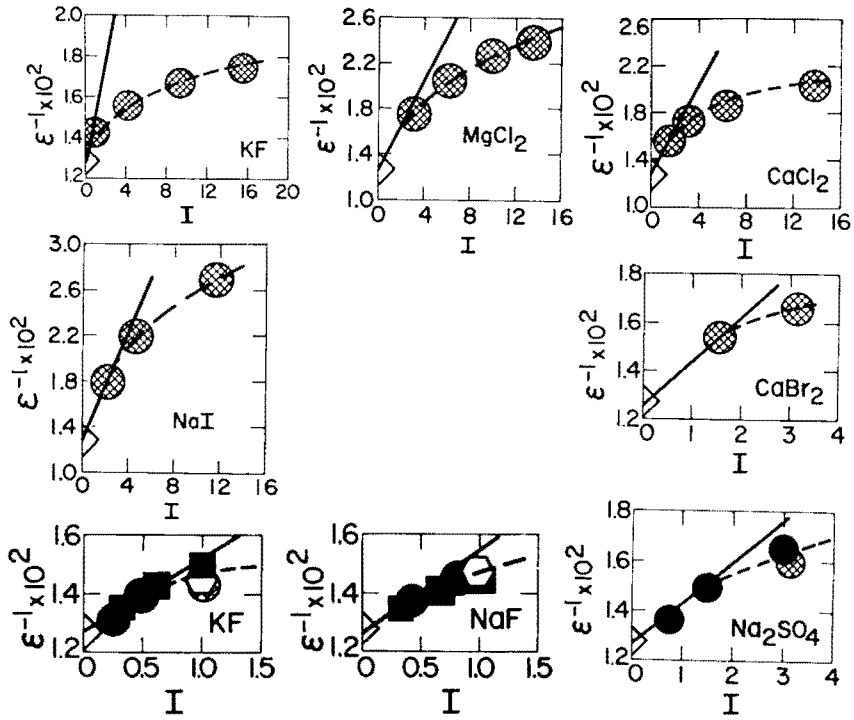

Fig. 7. Reciprocal of the dielectric constant of electrolyte solutions as a function of stoichiometric ionic strength at 25°C and 1 bar (see text and caption of fig. 3).

error and/or ion association (which seems likely) all the data shown in the figures are consistent with

$$\epsilon_k^{-1} - \epsilon^{o-1} = \hat{b}_k \bar{I} \ , \tag{143}$$

where $\hat{b}_k$ corresponds to the slopes of the solid curves in figures 3 through 10. Although eq (143) applies only to single electrolytes, consideration of osmotic coefficient data for mixed electrolytes (see below) suggests that it can be generalized to

$$\epsilon^{-1} - \epsilon^{o-1} = \sum_k \hat{b}_k \, y_k \bar{I} \ , \tag{144}$$

which for "complete" dissociation reduces to

$$\epsilon^{-1} - \epsilon^{o-1} = \sum_k \hat{b}_k \, \psi_k \, m_k \ . \tag{145}$$

At least in principle, the separation of variables represented by eq (117), together with eq (29) and constraints imposed by the fact that $dG_{solution}$ is an exact differential requires

$$\left(\frac{\partial(\Delta\overline{G}_{s,\hat{k}})}{\partial m_k}\right)_{P,T,\hat{m}_k,n_w} = \left(\frac{\partial(\Delta\overline{G}_{s,k})}{\partial m_{\hat{k}}}\right)_{P,T,\hat{m}_{\hat{k}},n_w} \tag{146}$$

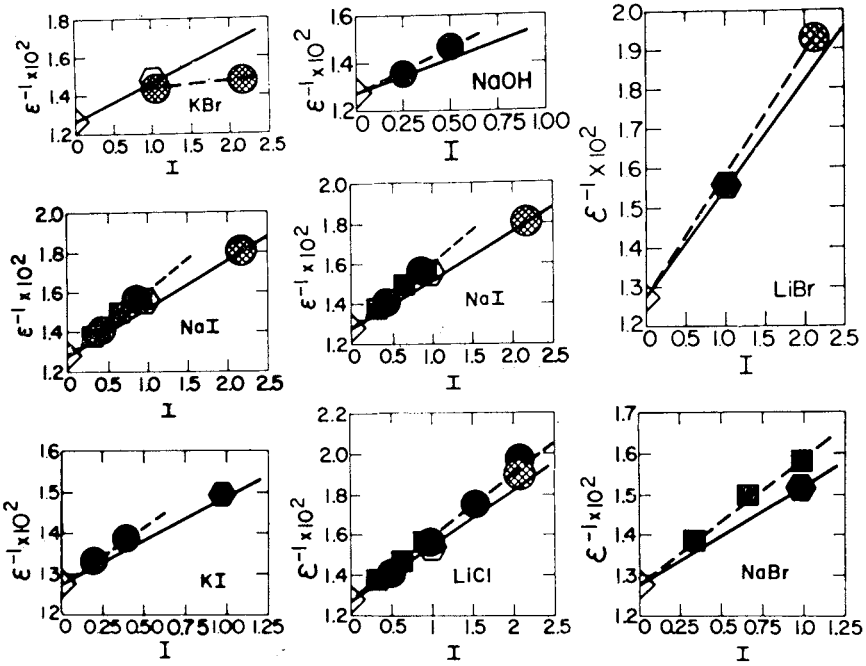

Fig. 8. Reciprocal of the dielectric constant of electrolyte solutions as a function of stoichiometric ionic strength at 25°C and 1 bar (see text and caption of fig. 3).

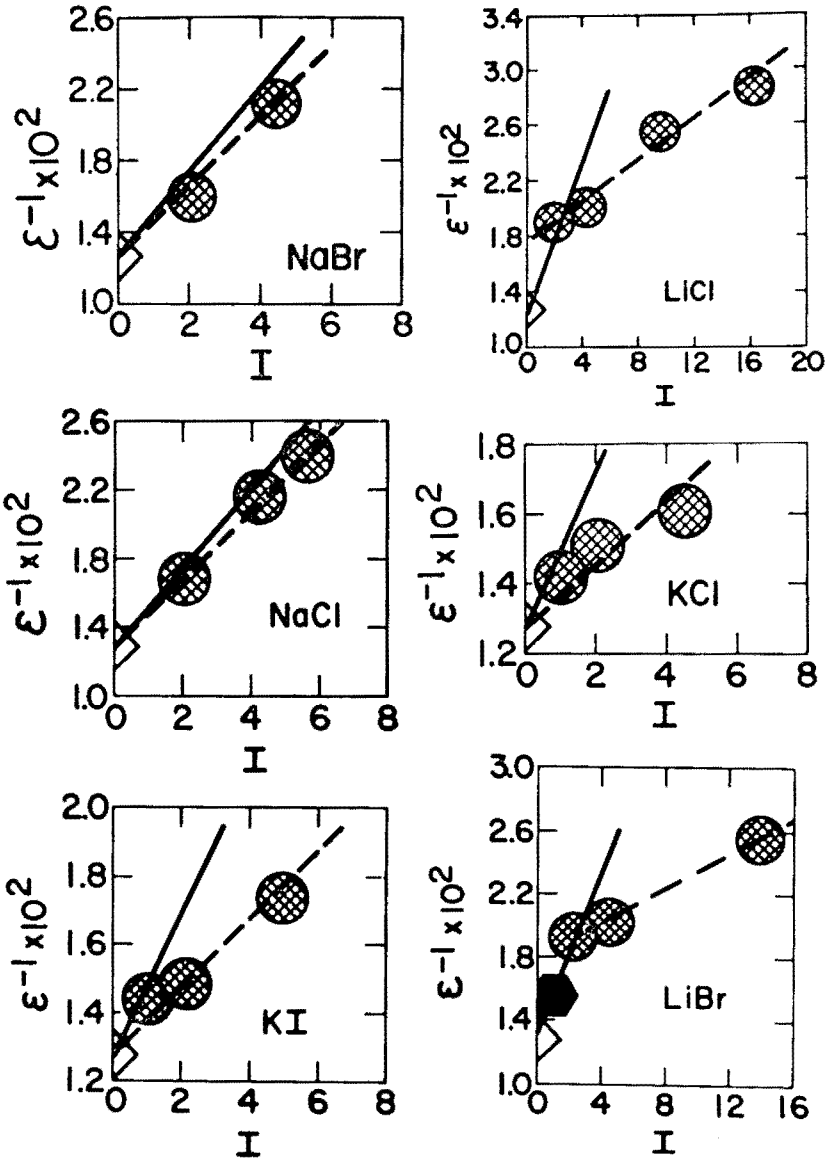

Fig. 9. Reciprocal of the dielectric constant of electrolyte solutions as a function of stoichiometric ionic strength at 25°C and 1 bar (see text and caption of fig. 3).

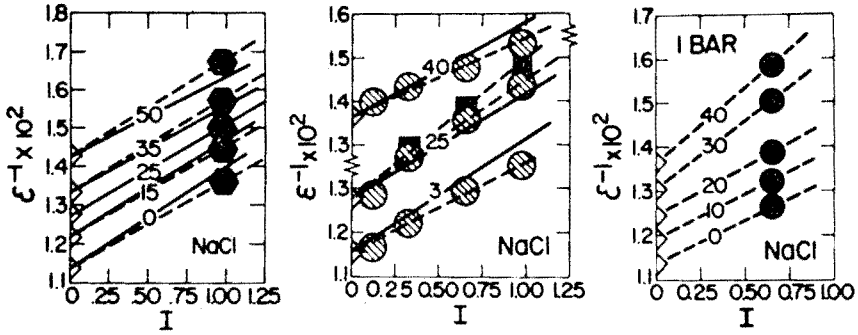

Fig. 10. Reciprocal of the dielectric constant of NaCl solutions as a function of stoichiometric ionic strength at various temperatures (labeled in °C) and 1 bar (see text and caption of fig. 3).

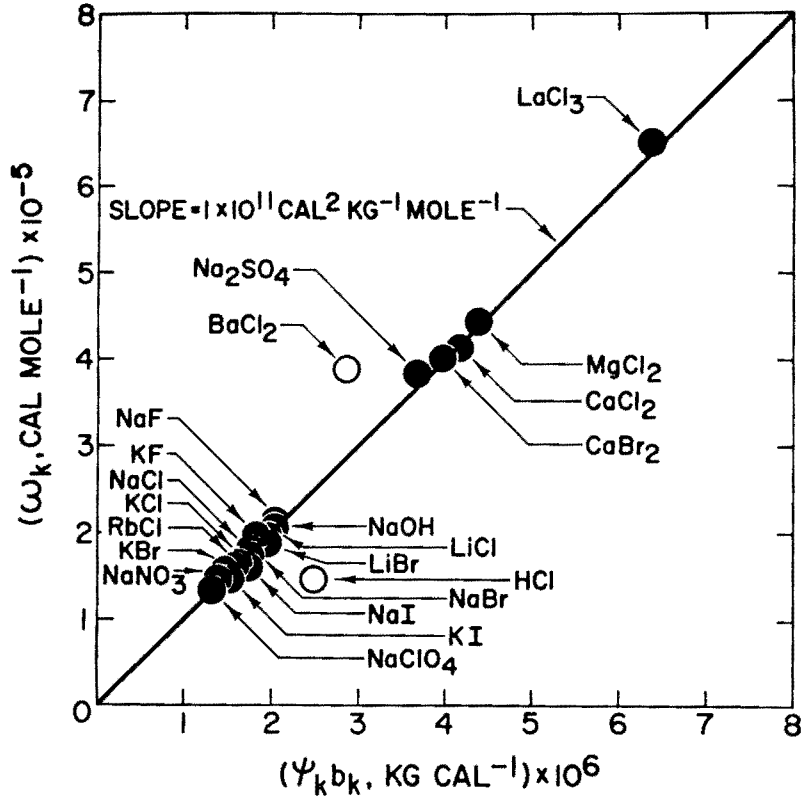

Fig. 11. Correlation of the Born coefficient (ω_k) calculated by Helgeson and Kirkham (1976) with the electrostatic parameter $\psi_k b_k$ computed from the slopes of the solid curves for 25 °C and 1 bar in figures 3, 4, and 6 through 10 (see eq 149 and fig. 12).

where $\hat{m}_k$ and $\hat{m}_{\hat{k}}$ ($k = 1, 2, \ldots \hat{k}$) refer to constant molalities of all components other than the kth and $\hat{k}$th, respectively. Taking account of eq (131), it follows that

$$\omega_{\hat{k}} \left(\frac{\partial \epsilon}{\partial m_k}\right)_{P,T,\hat{m}_k,n_w} = \omega_k \left(\frac{\partial \epsilon}{\partial m_{\hat{k}}}\right)_{P,T,\hat{m}_{\hat{k}},n_w} \tag{147}$$

which can be combined with appropriate partial derivatives of eq (145) to give

$$\omega_{\hat{k}} \psi_k \hat{b}_k = \omega_k \psi_{\hat{k}} \hat{b}_{\hat{k}} \ . \tag{148}$$

Eq (148) is satisfied if ω_k is proportional to $\psi_k \hat{b}_k$ for all values of k. It can be deduced from figures 11 and 12, together with the identity

$$b_k = \hat{b}_k / 2.303RT \tag{149}$$

that this is indeed the case. The solid symbols plotted in figures 11 and 12 correspond to values of b_k computed from the slopes of the solid curves for 25°C in figures 3, 4, and 6 through 10. Because these curves represent (within experimental uncertainty) the bulk of the dielectric constant measurements for "completely" dissociated electrolyte solutions, figures 11 and 12 strongly support the validity of eq (144). The differences between the slopes of the dashed curves (which merely connect data points) in figures 8 through 10 and the solid curves probably arise from experimental error.

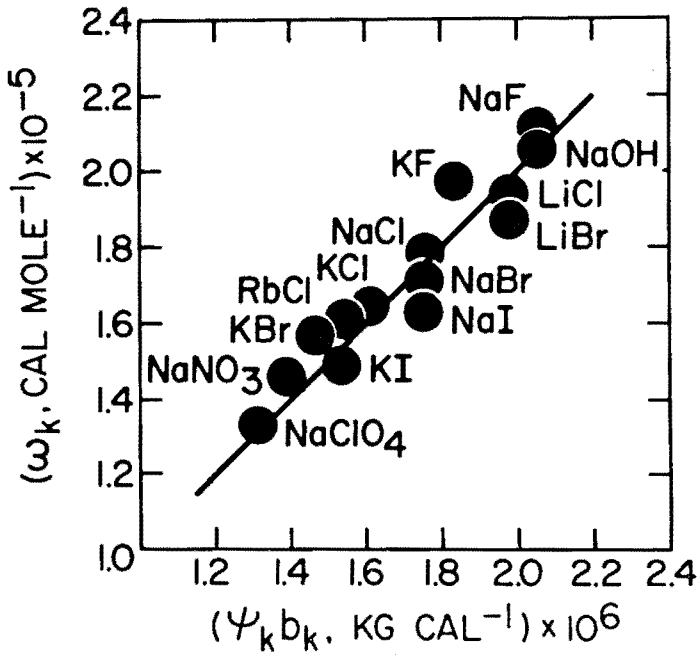

Fig. 12. Enlargement of the lower left corner of figure 11.

TABLE 4

Electrostatic parameters for aqueous electrolytes (designated by the subscript k) at 25°C and 1 bar (see text)

Solute	$\hat{b}_k^{a,b} \times 10^3$	$b_k^{c,d} \times 10^6$	Solute	$\hat{b}_k^{a,b} \times 10^3$	$b_k^{c,d} \times 10^6$	Solute	$\hat{b}_k^{a,b} \times 10^3$	$b_k^{c,d} \times 10^6$
HCl	1.9863	1.4560	CaF_2	2.1876	1.6035	CsI	1.8974	1.3908
NaCl	2.4372	1.7865	SrF_2	2.1420	1.5701	NH_4I	2.0088	1.4725
LiCl	2.6495	1.9421	BaF_2	2.0732	1.5197	AgI	2.0592	1.5094
KCl	2.2492	1.6487	FeF_2	2.2743	1.6671	AuI	2.0101	1.4734
RbCl	2.1912	1.6062	MnF_2	2.2622	1.6582	CuI	2.2217	1.6285
CsCl	2.1192	1.5534	PbF_2	2.1158	1.5509	MgI_2	1.8754	1.3747
NH_4Cl	2.2307	1.6351	ZnF_2	2.2880	1.6771	CaI_2	1.7387	1.2745
AgCl	2.2810	1.6720	CuF_2	2.2968	1.6836	SrI_2	1.6930	1.2410
AuCl	2.2319	1.6360	CdF_2	2.1949	1.6089	BaI_2	1.6243	1.1906
CuCl	2.4435	1.7911	HgF_2	2.1488	1.5751	FeI_2	1.8391	1.3481
$MgCl_2$	2.0233	1.4831	HBr	1.8906	1.3858	MnI_2	1.8132	1.3291
$CaCl_2$	1.8866	1.3829	NaBr	2.3783	1.7433	PbI_2	1.6670	1.2219
$SrCl_2$	1.8409	1.3494	LiBr	2.5907	1.8990	ZnI_2	1.8391	1.3481
$BaCl_2$	1.7721	1.2990	KBr	2.1903	1.6055	CuI_2	1.8480	1.3546
$FeCl_2$	1.9870	1.4565	RbBr	2.1323	1.5630	CdI_2	1.7461	1.2799
$MnCl_2$	1.9611	1.4375	CsBr	2.0234	1.4832	HgI_2	1.6998	1.2460
$PbCl_2$	1.8148	1.3303	NH_4Br	2.1349	1.5649	KOH	2.6157	1.9173
$ZnCl_2$	1.9870	1.4565	AgBr	2.1852	1.6018	NaOH	2.8037	2.0551
$CuCl_2$	1.9959	1.4630	AuBr	2.1361	1.5658	HNO_3	1.5409	1.1295
$CdCl_2$	1.8940	1.3883	CuBr	2.3477	1.7209	$NaNO_3$	1.9918	1.4600
$HgCl_2$	1.8477	1.3544	$MgBr_2$	1.9595	1.4363	$LiNO_3$	2.2042	1.6157
$AlCl_3$	1.6460	1.2065	$CaBr_2$	1.8228	1.3361	KNO_3	1.8038	1.3222
$FeCl_3$	1.6086	1.1792	$SrBr_2$	1.7771	1.3026	NH_4ClO_4	1.6102	1.1803
$GdCl_3$	1.5222	1.1158	$BaBr_2$	1.7083	1.2522	$NaClO_4$	1.8168	1.3317
$LaCl_3$	1.4836	1.0875	$FeBr_2$	1.9232	1.4097	$NaHCO_3$	2.2644	1.6598
HF	2.4379	1.7870	$MnBr_2$	1.8973	1.3907	NaHS	2.4168	1.7715
NaF	2.8888	2.1175	$PbBr_2$	1.8056	1.2835	H_2SO_4	1.4487	1.0619
LiF	3.1012	2.2732	$ZnBr_2$	1.9232	1.4097	Na_2SO_4	1.7492	1.2822
KF	2.7008	1.9797	$CuBr_2$	1.9320	1.4162	K_2SO_4	1.6240	1.1904
RbF	2.6428	1.9372	$CdBr_2$	1.8301	1.3415	Li_2SO_4	1.8908	1.3860
CsF	2.5708	1.8844	$HgBr_2$	1.7839	1.3076	$MgSO_4$	1.6108	1.1807
NH_4F	2.6822	1.9661	HI	1.7645	1.2934	$ZnSO_4$	1.5836	1.1608
AgF	2.7326	2.0030	NaI	2.2154	1.6239	$NaHSO_4$	2.1414	1.5697
AuF	2.6835	1.9670	LiI	2.4278	1.7796	$KHSO_4$	1.9535	1.4319
CuF	2.8951	2.1221	KI	2.0274	1.4861	$HReO_4$	1.2704	0.9312
MgF_2	2.3243	1.7037	RbI	1.9894	1.4436	$NaReO_4$	1.7213	1.2617

[a] Computed from equation (149). [b] kg mole^{-1}. [c] Computed from equation (150). [d] kg cal^{-1}.

In any event, the dashed curves are not all consistent with one another. The equation of the curve in figures 11 and 12 can be written as

$$b_k = (\omega_k/\psi_k) \times 10^{-11} , \qquad (150)$$

which ensures internal consistency among the slopes of the solid curves in figures 3, 4, and 6 through 10.

Values of b_k and $\hat{b}_k$ computed from eqs (136), (149), and (150) using values of ω_j taken from table 3 are given in table 4. It can be deduced from figure 13 that the value of $\hat{b}_{RbI}$ generated in this way is exactly consistent with data reported by Pottel (1973). However, corresponding values for RbF, RBr, and the cesium halides in table 4 are slightly larger than those consistent with the dashed curves for these electrolytes in figure 13, which simply connect $\epsilon^{\circ -1}$ and the single data point for each of the solutions. This observation is consistent with the fact that RbF, RbBr, CsCl, CsI, CsBr, and CsF are all associated to a significant degree at 1 *m* (see below). In contrast, the discrepancy between the calculated slopes of the solid curves in figure 14 and those of the dashed curves (which are dictated by the distribution of the data points) is probably due primarily to systematic experimental error. This conclusion is supported by the fact that the values of $\hat{b}_k$ corresponding to the slopes of the dashed curves for HCl and $BaCl_2$ at 25°C in figure 14 fall well off the curve in figure 11, where they are plotted as open symbols. Regression of apparent molal heat capacity and volume data for electrolytes (see below) indicates similar contradictions in the data reported for HCl and $BaCl_2$ at 3°, 10°, and 40°C (fig. 14).

Because ion solvation contributes significantly to the standard partial molal entropies of aqueous ions, it would be reasonable to expect $\hat{b}_k$ to exhibit a close correlation with $\bar{S}^\circ$ of cations in electrolytes with a common anion. It can be seen in figure 15 that this is indeed the case for the slopes of the solid curves representing chlorides in figures 3 and 6 through 10. However, in contrast to the conclusion reached by Harris and O'Konski (1957), the correlation in figure 15 is linear, and all the curves are parallel

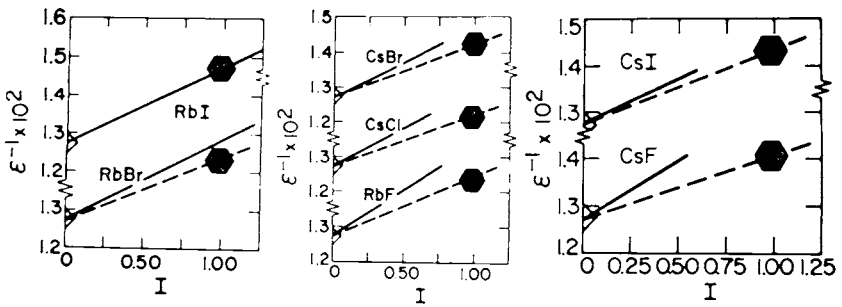

Fig. 13. Reciprocal of the dielectric constant of electrolyte solutions as a function of stoichiometric ionic strength at 25°C and 1 bar (see text and caption of fig. 3).

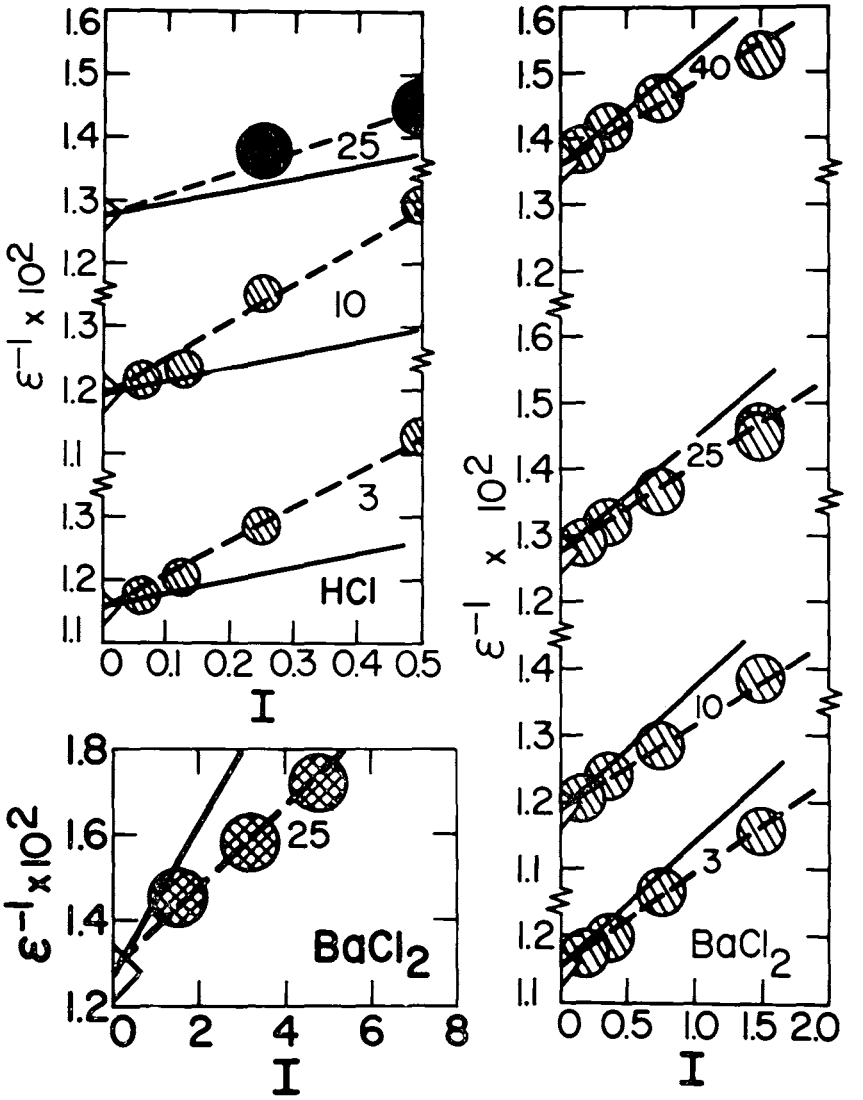

Fig. 14. Reciprocal of the dielectric constant of electrolyte solutions as a function of stoichiometric ionic strength at 3°, 10°, 25°, and 40°C and 1 bar (see text and caption of fig. 3).

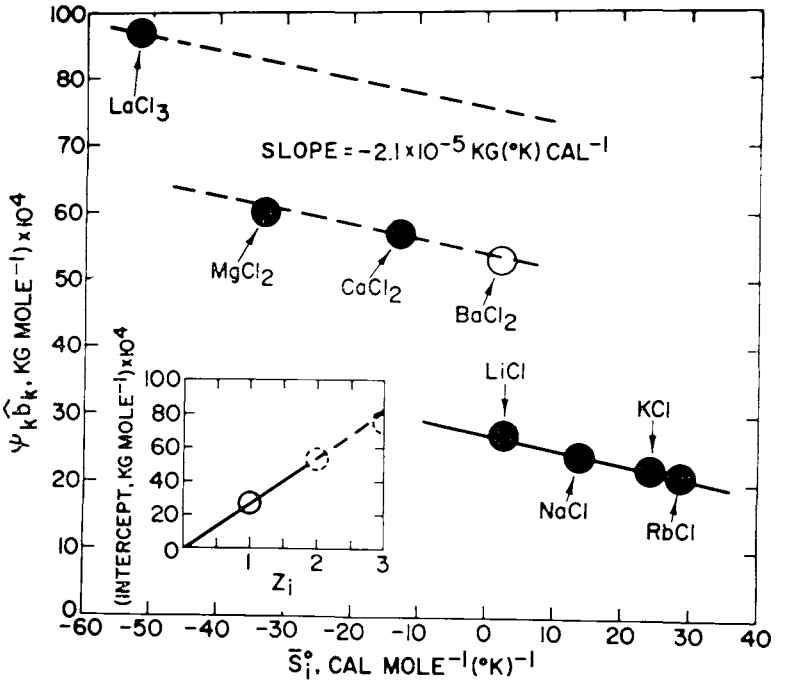

Fig. 15. Correlation of $\psi_k \hat{b}_k$ for chlorides with the conventional standard partial molal entropies of the cations (indicated by the subscript i) in the chloride components at 25°C and 1 bar (see text).

with intercepts that are linearly related to Z_i (the charge on the cations in the electrolytes). The equation of the curves in figure 15 is given by

$$\psi_k \hat{b}_k = \mathbf{a} - 2.1\,\bar{S}^\circ_i \times 10^{-5} \tag{151}$$

where

$$\mathbf{a} = 2.7\,Z_i \times 10^{-3} \tag{152}$$

which apply to 25°C and 1 bar. It can be seen in figure 15 that the value of $\hat{b}_k$ for $BaCl_2$ computed from eq (150) and given in table 4 (which is represented by the open symbol) is consistent with eq (152), but similar agreement cannot be demonstrated for HCl.

Taking account of eqs (119), (128), (137), (139) through (141), and (144), the relative partial molal Gibbs free energy of solvation of aqueous species can be expressed as

$$\Delta\bar{G}_{h,i} = \omega_i \sum_k \hat{b}_k\, y_k \bar{I} \tag{153}$$

$$\Delta\bar{G}_{h,l} = \omega_l^{abs} \sum_k \hat{b}_k\, y_k \bar{I} \tag{154}$$

and

$$\Delta\bar{G}_{h,n} = \omega_n \sum_k \hat{b}_k\, y_k \bar{I} \tag{155}$$

where the subscripts i and l denote positively and negatively charged species, respectively, and the index n again designates neutral complexes.[13] Let us now consider the extent to which contributions by long-range ionic interaction and ion solvation to the relative partial molal Gibbs free energy of an electrolyte are modified by short-range interaction.

Short-range ionic interaction.—Following in part the approach taken by Guggenheim (1935), Scatchard (1936), Harned and Robinson (1968), and others, $\overline{G}_{r,j}$ in a Gibbs free energy statement of eq (117) can be represented in a first approximation by regular solution theory.[14] Adopting Brønsted's (1922) principle of specific interaction and taking account of differences in the forces of attraction among species in solution then leads to

$$\overline{G}_{r,i} = \sum_l \hat{b}_{il}\, m_l = \sum_l \frac{\hat{b}_{il}\bar{y}_l \mathbf{I}}{\psi_l} \tag{156}$$

and

$$\overline{G}_{r,l} = \sum_i \hat{b}_{il}\, m_i = \sum_i \frac{\hat{b}_{il}\bar{y}_i \mathbf{I}}{\psi_i} \tag{157}$$

where $\hat{b}_{il}$ represents the short-range interaction parameter for the ith positively charged species interacting with the lth negatively charged species.[15] Because the forces of attraction among polar neutral complexes are much smaller than those among charged and neutral species, we can also write as a close approximation,

$$\overline{G}_{r,n} = \sum_i \hat{b}_{ni}\, m_i + \sum_l \hat{b}_{nl}\, m_l = \sum_i \frac{\hat{b}_{ni}\bar{y}_i \mathbf{I}}{\psi_i} + \sum_l \frac{\hat{b}_{nl}\bar{y}_l \mathbf{I}}{\psi_l} \tag{158}$$

where $\hat{b}_{ni}$ and $\hat{b}_{nl}$ stand for short-range interaction parameters for the nth

[13] Note that the charged species designated by the subscripts i and l include charged complexes as well as individual cations and anions.

[14] In a strict sense, the term regular solution employed in this context is a misnomer. A regular solution is defined as one for which $S_{excess} = 0$, which is not true of the contribution by $\bar{S}_{r,j}$ to S_{excess} for electrolyte solutions. The term is employed above to indicate that the representation of $\overline{G}_{r,j}$ as a function of molality is consistent with a regular solution dependence of G_{excess} on composition, which is parabolic in mole fraction space. Harned's rule (Harned, 1935; Harned and Owen, 1958), Young's rule (Young, 1951; Young and Smith, 1954; Young, Wu, and Krawetz, 1957; Wu, Smith, and Young, 1965; Wu, 1970) and several other similar algorithms employed in solution chemistry are also consistent with this dependence of G_{excess} on mole fraction.

[15] Brønsted's principle of specific interaction states that short-range interaction among like-charged species can be considered insignificant compared to interaction among species of unlike charge. It simply recognizes that the mutual attraction of oppositely charged species makes them far more likely to come into close proximity to one another than species of like charge, which repel each other. With a few notable exceptions, Brønsted's principle of specific interaction is consistent with the observed thermodynamic behavior of aqueous electrolytes. For this reason, terms accounting for interaction among species of like charge have been omitted from eqs (156) and (157). Similarly, because short-range interaction among charged and neutral species is negligible compared to that among cations and anions, no provision was included in eqs (156) and (157) for interaction of charged and neutral species. Although most neutral complexes are polar, the forces of attraction among neutral molecules are small compared to those among neutral molecules and charged species. Accordingly, analogous terms representing interaction of neutral species were omitted from eq (158).

neutral species interacting with the ith and lth charged species, respectively. The physical significance of the interaction parameters in eqs (156) through (158) is discussed below.

Combined equations.—Substituting the subscript i for j in appropriate statements of eqs (117) and (120) and combining the resulting expressions with eqs (153), (156), and

$$\overline{G}_{ideal,i} = 2.303\ RT \log m_i \tag{159}$$

leads to (see footnote 13)

$$\overline{G}_i - \overline{G}^\circ{}_i^{abs} = \frac{\psi_i A_G I^{1/2}}{\Lambda} + \Gamma_G + \omega_i^{abs} \sum_k \hat{b}_k y_k I + \sum_l \hat{b}_{il} m_l + 2.303\ RT \log m_i \ . \tag{160}$$

Similarly, from statements of eqs (117) and (159) written for the lth and nth species, together with appropriate statements of eqs (120), (125A), (154), (155), (157), and (158) it follows that

$$\overline{G}_l - \overline{G}^\circ{}_l^{abs} = \frac{\psi_l A_G I^{1/2}}{\Lambda} + \Gamma_G + \omega_l^{abs} \sum_k \hat{b}_k y_k I + \sum_i \hat{b}_{il} m_i + 2.303\ RT \log m_l \tag{161}$$

and

$$\overline{G}_n - \overline{G}^\circ{}_n = \Gamma_G + \omega_n \sum_k \hat{b}_k y_k I + \sum_i \hat{b}_{ni} m_i + \sum_l \hat{b}_{nl} m_l + 2.303\ RT \log m_n \ . \tag{162}$$

We can thus write a combined statement of eq (29) and its standard state analog for the kth "completely" dissociated single electrolyte consisting of the ith and lth cation and anion, or the kth 1:1 or 2:2 electrolyte in which only a single ion pair forms to a significant degree as

$$\overline{G}_k - \overline{G}^\circ{}_k = \frac{\psi_k A_G I^{1/2}}{\Lambda} + \nu_k \Gamma_G + \frac{(\omega_k \psi_k \hat{b}_k + 2\nu_{i,k}\nu_{l,k}\hat{b}_{il})I}{\psi_k} + 2.303\ RT \log(\nu_{i,k}^{\nu_{i,k}} \nu_{l,k}^{\nu_{l,k}}) + 2.303\ \nu_k\ RT \log (I/\psi_k) \tag{163}$$

which corresponds to eq (60). Note that if we alternatively define an ideal solution as one in which all activity coefficients on the mole fraction scale of concentration are unity, eq (159) becomes

$$\overline{G}_{ideal,i} = RT\ ln\ m_i + \Gamma_G \tag{164}$$

Eq (164) is consistent with

$$\overline{G}^\circ{}_{i(X)} = \overline{G}^\circ{}_i + RT\ ln(55.51) \tag{164A}$$

and

$$\overline{G}_{i,ideal(X)} = \overline{G}_{i,ideal} - RT\ ln(55.51) = RT\ ln\ X_i \tag{164B}$$

where $\overline{G}^\circ_i$ and $\overline{G}_{i,ideal}$ refer to the molality scale of concentration, $G^\circ_{i(X)}$ and $\overline{G}_{i,ideal(X)}$ represent their mole fraction analogs, and X_i stands for the mole fraction of the subscripted species. Note that if eq (164) is adopted in lieu of eq (159), Γ_G must be removed from eqs (120) and (125A), but eqs (160) through (162) are not affected. Other definitions of ideality such as the one adopted by Harned and Robinson (1968) in which the activity of the solvent in an ideal solution is taken to be equal to its mole fraction yield somewhat different expressions analogous to eq (164).

Eqs (160) through (162) describe the compositional dependence of the partial molal Gibbs free energies of all species in solution in terms of the theoretical model described above. The relative extent to which the solvation and ionic interaction parameters in these expressions affect the chemical and thermodynamic behavior of aqueous electrolytes can be assessed by comparing the consequences of differences and similarities in the sign and magnitude of $\omega_k b_k$ and $2\nu_{i,k}\nu_{l,k}\hat{b}_{il}$ in eq (163).

The effect of increasing concentration on the solvation process in electrolyte solutions is manifested by a positive change in Gibbs free energy at low temperatures, but a negative change at high temperatures. In contrast, the corresponding changes in entropy and volume are positive at all temperatures $\leqslant 500°C$ (see below). Changes in Gibbs free energy and volume caused by the effect of increasing concentration on ion solvation may be either reinforced or opposed by short-range ionic interaction, depending on the temperature. For example, at low temperatures where $\hat{b}_k$ is positive, $\hat{b}_{il}$ is commonly negative, but at high temperatures where $\hat{b}_k$ is negative, $\hat{b}_{il}$ becomes positive (see below). In contrast, the entropy contribution by short-range ionic interaction opposes the corresponding contribution by ion solvation to $\overline{G}_i - \overline{G}^\circ{}_i^{abs}$ and $\overline{G}_l - \overline{G}^\circ{}_l^{abs}$ at all temperatures. Although long-range electrostatic interaction is always accompanied by a positive change in entropy and a negative change in Gibbs free energy, the sum of all three contributions by ion solvation and short- and long-range ionic interaction may either oppose or reinforce the negative contribution by the solvent to the Gibbs free energy of the solution.

In addition to contributions by $\Delta\overline{G}_{n,j}$ (the sum of the intrinsic Gibbs free energy of the jth ion and that associated with collapse of the local solvent structure), $\hat{b}_{il}$ takes into account implicitly the effect of short-range ionic interaction on the extent to which H_2O dipoles are partitioned between solvation shells and the bulk solvent. As observed by Friedman and Krishnan (1973), H_2O dipoles may be "captured" or "liberated" by collisions of solvated ions. Temporary "capture" of solvent dipoles is accompanied by positive contributions to $\overline{G}_i - \overline{G}_i^{abs}$ and $\overline{G}_l - \overline{G}^\circ{}_l^{abs}$, which oppose the Gibbs free energy change associated with collision of the ions. To facilitate conceptual appreciation for the consequences of short-range ionic interaction with respect to the distribution of H_2O dipoles in solution, four of the many possible types of collisions that might occur in an electrolyte solution are depicted schematically in figure 16, where a hypothetical cation with five H_2O dipoles in its primary solvation shell is

shown colliding with a solvated anion, which has six H_2O dipoles in primary coordination. For the sake of clarity, pre-collision secondary solvation shells and H_2O dipoles in the bulk solvent have been omitted from the diagram, which portrays idealized encounters among solvated ions without provision for asymmetry, interpenetration of electron clouds, or transitory perturbation of the solvation shells.

In the case labeled *a* in figure 16, the attractive forces between the solvated cation and anion are too weak for the collision to expel two intervening solvent dipoles. The intervening dipoles are then no longer part of the bulk solvent but are temporarily "captured" in secondary coordination shells about the ions. In contrast, collision *b* results in expulsion of all intervening H_2O dipoles. However, in case *c*, collision of the solvated ions results in a net loss of two H_2O dipoles from the solvation shells of the ions, and in collision *d* the attractive forces between the ions are strong enough to cause exclusion of all intervening H_2O dipoles between the cation and anion, with a net loss of four H_2O dipoles to the bulk solvent.

The distinction between ion association and short-range interaction of the type illustrated in figure 16 is largely statistical. The central configurations in collisions *c* and *d* correspond to outer sphere and inner sphere complexes, respectively. If the dissociation constants for such complexes are small, interactions of type *c* and *d* may predominate in solution. Under these circumstances, ion association dominates departures from ideality, and $\hat{b}_{il}$ is negative and varies with total concentration. In contrast, if the dissociation constants for the collisions depicted in the lower two diagrams of figure 16 are large, ion association contributes negligibly to the thermodynamic behavior of electrolytes. The consequences of in-

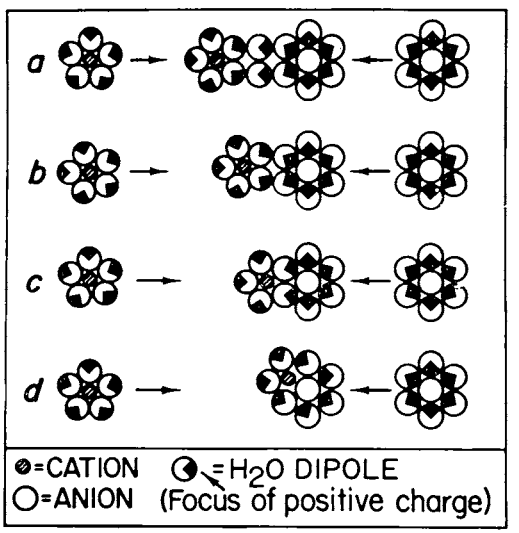

Fig. 16. Schematic illustration of four hypothetical cases of short-range interaction among solvated cations and anions in electrolyte solutions (see text).

termediate cases between these two extremes depends on the magnitude of $\omega_i{}^{abs}\hat{b}_k$ and $\omega_l{}^{abs}\hat{b}_k$. If these parameters are large, ion association may affect the thermodynamic behavior of an electrolyte only at high concentrations. *However, if the forces of attraction among the solvated cations and anions are weak and of the same order of magnitude as those between the ions and their solvated H_2O dipoles, the effects of ion association may be manifest only at low concentrations. Both kinds of behavior are exhibited by aqueous electrolytes at both low and high temperatures and pressures* (Davies, 1962; Hwang, Ludemann, and Hartmann, 1970; Helgeson and Kirkham, 1976; Pitzer, in press).

The short-range interaction parameter ($\hat{b}_{il}$) for the collision depicted in figure 16A may be either positive or negative, depending on whether the energetic consequence of "capturing" two solvent dipoles is greater or less than the loss of energy caused by the collision. In contrast, $\hat{b}_{il}$ is always negative and opposes $\omega_i{}^{abs}\hat{b}_k$ and $\omega_l{}^{abs}\hat{b}_k$ for type b collisions. Because in both cases the forces of attraction between the solvated ions at low temperatures are relatively weak compared to those among the ions and the H_2O dipoles in their solvation shells, the net contribution by the solvation and short-range interaction terms to $\overline{G}_i - \overline{G}^\circ{}_i{}^{abs}$ and $\overline{G}_l - \overline{G}^\circ{}_l{}^{abs}$ for type a and b collisions in figure 16 is positive at low temperatures. However, the opposite is true at high temperatures where the forces of attraction among ions and H_2O dipoles are small compared to those among cations and anions (see below).

ACTIVITY COEFFICIENTS

It follows from eqs (66), (123), (149), and (160) through (162) that the activity coefficients of aqueous species can be expressed as

$$\log \tilde{\gamma}_i = -\frac{A_\gamma Z_i{}^2 \bar{I}^{1/2}}{\Lambda} + \Gamma_\gamma + \omega_i{}^{abs} \sum_k b_k y_k \bar{I} + \sum_l (b_{il}\tilde{y}_l \bar{I}/\psi_l) \quad (165)$$

$$\log \tilde{\gamma}_l = -\frac{A_\gamma Z_l{}^2 \bar{I}^{1/2}}{\Lambda} + \Gamma_\gamma + \omega_l{}^{abs} \sum_k b_k y_k \bar{I} + \sum_i (b_{il}\tilde{y}_i \bar{I}/\psi_i) \quad (166)$$

$$\log \tilde{\gamma}_n = \Gamma_\gamma + \omega_n \sum_k b_k y_k \bar{I} + \sum_i (b_{ni}\tilde{y}_i \bar{I}/\psi_i) + \sum_l (b_{nl}\tilde{y}_l \bar{I}/\psi_l) \quad (167)$$

and for the kth component consisting of the ith and lth ions we can write

$$\log \tilde{\gamma}_{\pm,k} = -\frac{A_\gamma |Z_i Z_l| \bar{I}^{1/2}}{\Lambda} + \Gamma_\gamma + \frac{\omega_k}{\nu_k} \sum_k b_k y_k \bar{I}$$

$$+ \frac{\nu_{i,k}}{\nu_k} \sum_l \left((b_{il}\tilde{y}\bar{I}/\psi_l) \right) + \frac{\nu_{l,k}}{\nu_k} \sum_i (b_{il}\tilde{y}_i \bar{I}/\psi_i) \quad (168)$$

where Λ and A_γ are defined by eqs (121) and (C-1) in app. C and

$$\Gamma_\gamma = \frac{\Gamma_G}{2.303RT} , \tag{169}$$

$$b_{il} = \frac{\hat{b}_{il}}{2.303RT} , \tag{170}$$

$$b_{ni} = \frac{\hat{b}_{ni}}{2.303RT} , \tag{171}$$

and

$$b_{nl} = \frac{\hat{b}_{nl}}{2.303RT} . \tag{172}$$

For an electrolyte solution in which the solute is composed of the kth "completely" dissociated component consisting of the ith and lth cation and anion, or a 1:1 or 2:2 electrolyte in which only a single ion pair forms to a significant degree, eq (168) reduces to

$$\log \bar{\gamma}_{\pm,k} = -\frac{A_\gamma |Z_i Z_l| \bar{I}^{1/2}}{\Lambda} + \Gamma_\gamma + b_{\gamma,k}\bar{I} \tag{173}$$

where

$$b_{\gamma,k} = \frac{\omega_k \psi_k b_k + 2\nu_{i,k}\nu_{l,k} b_{il}}{\nu_k \psi_k} . \tag{174}$$

Similarly, for a two-component solute consisting of an undissociated component corresponding to the nth neutral species (for which $b_n = 0$) and the kth "completely" dissociated component consisting of the ith and lth cation and anion, respectively, eq (167) can be written as

$$\log \bar{\gamma}_n = \Gamma_\gamma + b_{\gamma,n}\bar{I} \tag{175}$$

where

$$b_{\gamma,n} = \frac{\omega_n \psi_k b_k + \nu_{i,k} b_{ni} + \nu_{l,k} b_{nl}}{\psi_k} . \tag{176}$$

Eq (173) is identical to that proposed over 50 years ago by Hückel (1925). Although Hückel derived his equation assuming that the dielectric constant of an electrolyte solution is a linear function of ionic strength (which has since been shown to be incorrect — see above), he nevertheless arrived at an expression that closely approximates the activity coefficients of "completely" dissociated electrolytes at high concentrations (see below). Similarly, eq (175) corresponds in form to the modification of the empirical Setchénow (1892) equation adopted over 50 years ago by Randall and Failey (1927a, b, and c), who demonstrated that the logarithms of the activity coefficients of neutral species in electrolyte solutions are essentially proportional to ionic strength.

The close approximation of activity coefficients afforded by eq (173) is apparent in figures 17 through 21, which depict differences in the values of log $\gamma_\pm$ reported in the literature and those computed from the Debye-

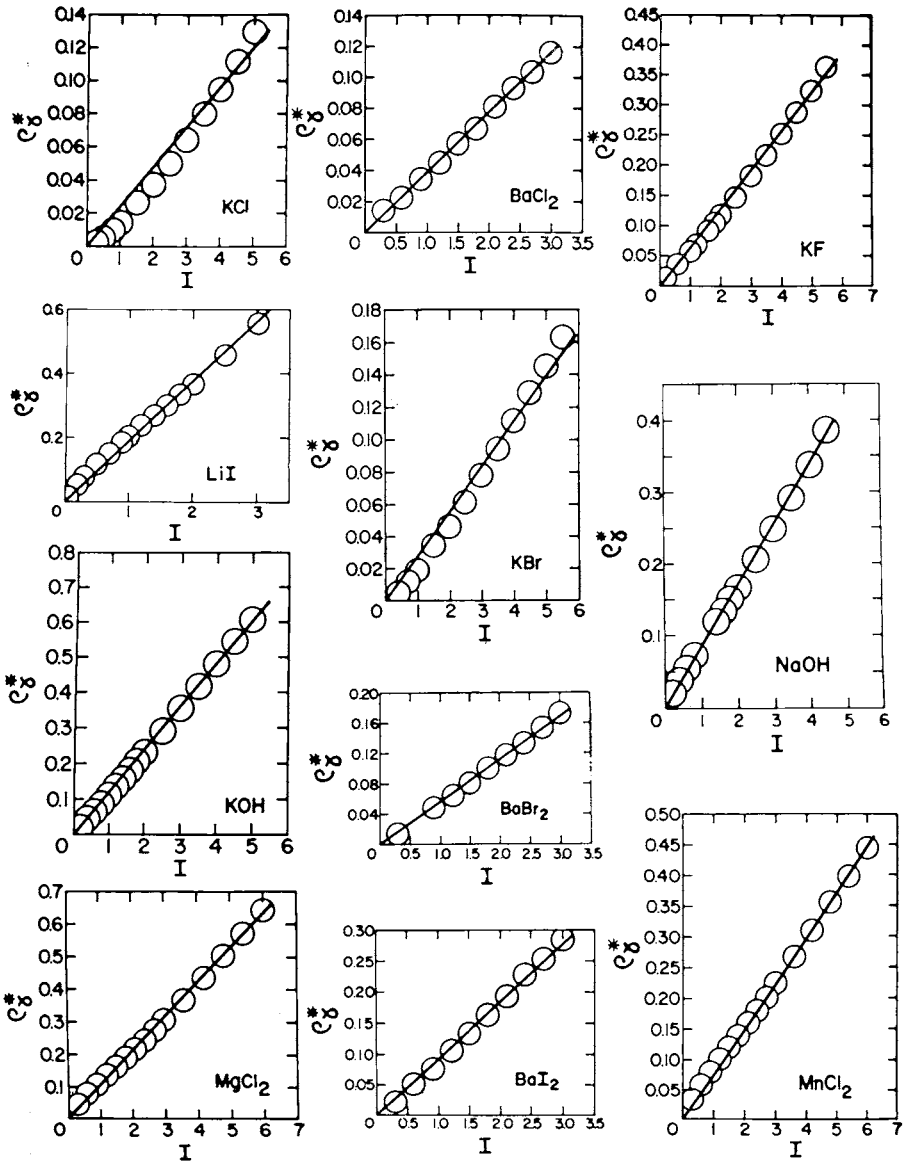

Fig. 17. ρ^*_γ (eqs 177 and 178) as a function of stoichiometric ionic strength at 25°C and 1 bar (see text). The symbols shown above and those plotted in figures 18 through 21, 23 through 34, and 45 through 47 represent experimental data taken from Hamer and Wu (1972) and/or Harned and Owen (1958), Robinson and Stokes (1959), Goldberg and Nuttal (1978), Faita, Mussini, and Oggioni (1966), Holmes, Baes, and Mesmer (1978), Towns, Greeley, and Lietzke (1960), and Greeley and others (1960a and b).

Hückel equation as a function of stoichiometric ionic strength at 25°C and 1 bar. This difference, denoted by the symbol ρ^*_γ, is given by

$$\rho^*_\gamma \equiv \log \gamma_\pm + \frac{A_\gamma |Z_+ Z_-| I^{1/2}}{\Lambda} - \Gamma_\gamma \quad . \tag{177}$$

For a "completely" dissociated single electrolyte designated by the index, k,

$$\rho^*_{\gamma,k} = b_{\gamma,k} I \quad . \tag{178}$$

The values of A_γ, B_γ, and å used to calculate p^*_γ were taken from tables 1 and 2. The experimental activity coefficients used in the calculations are those reported by Hamer and Wu (1972) and Robinson and Stokes (1959). Comparative values of $\rho^*_{\gamma,k}$ generated from activity coefficients given by Goldberg and Nuttall (1978) for $CaCl_2$ and $MgCl_2$ are shown in figure 21.

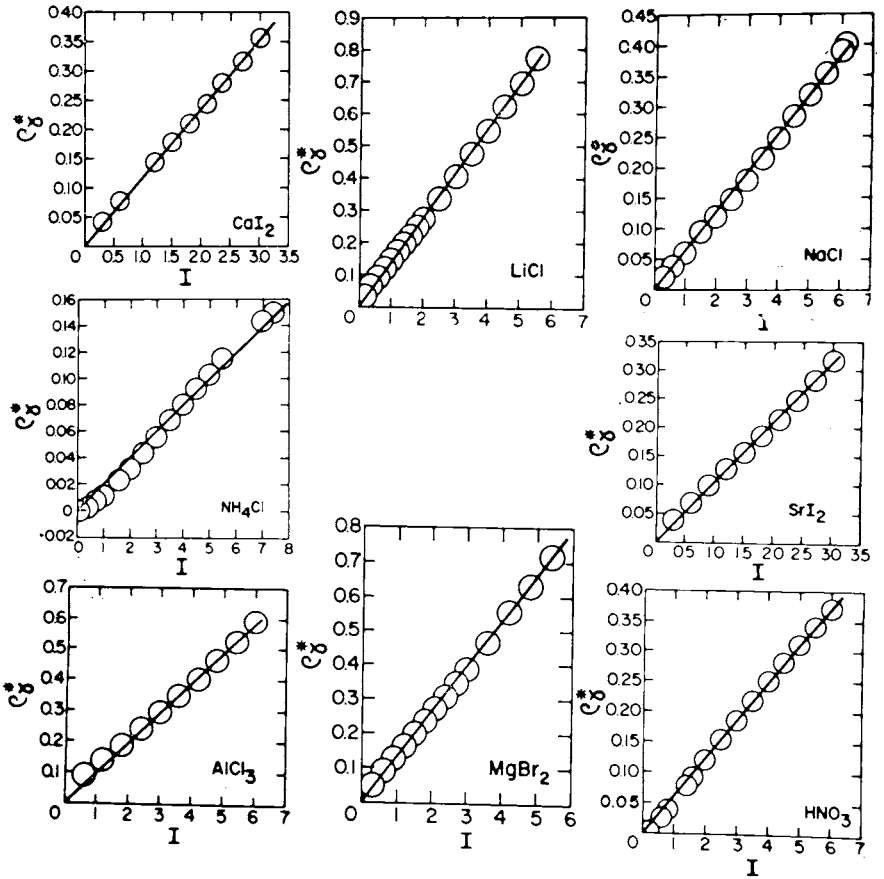

Fig. 18. ρ^*_γ (eqs 177 and 178) as a function of stoichiometric ionic strength at 25°C and 1 bar (see caption of fig. 17).

It can be seen in figures 17 through 21 that the linear curves approximate closely all the values of ρ^*_γ computed from the experimental data. However, it is also apparent that the distribution of data points for all the electrolytes is not strictly linear. For example, in the case of NH_4Cl (fig. 18) the configuration of the data points is slightly sigmoid. In contrast, those for KCl, KBr, and KF exhibit a slight but systematically increasing departure from linearity toward higher values of ρ^*_γ with increasing ionic strength. It can also be seen that some of the data points for many of the electrolytes (notably $SrBr_2$, $MgCl_2$, HNO_3, KCl, KBr, KI, $FeCl_2$, and BaI_2) fall slightly above or below the linear curves in the dilute region of concentration. These observations underscore the fact that eq (173) affords no more than a close approximation of the dependence of

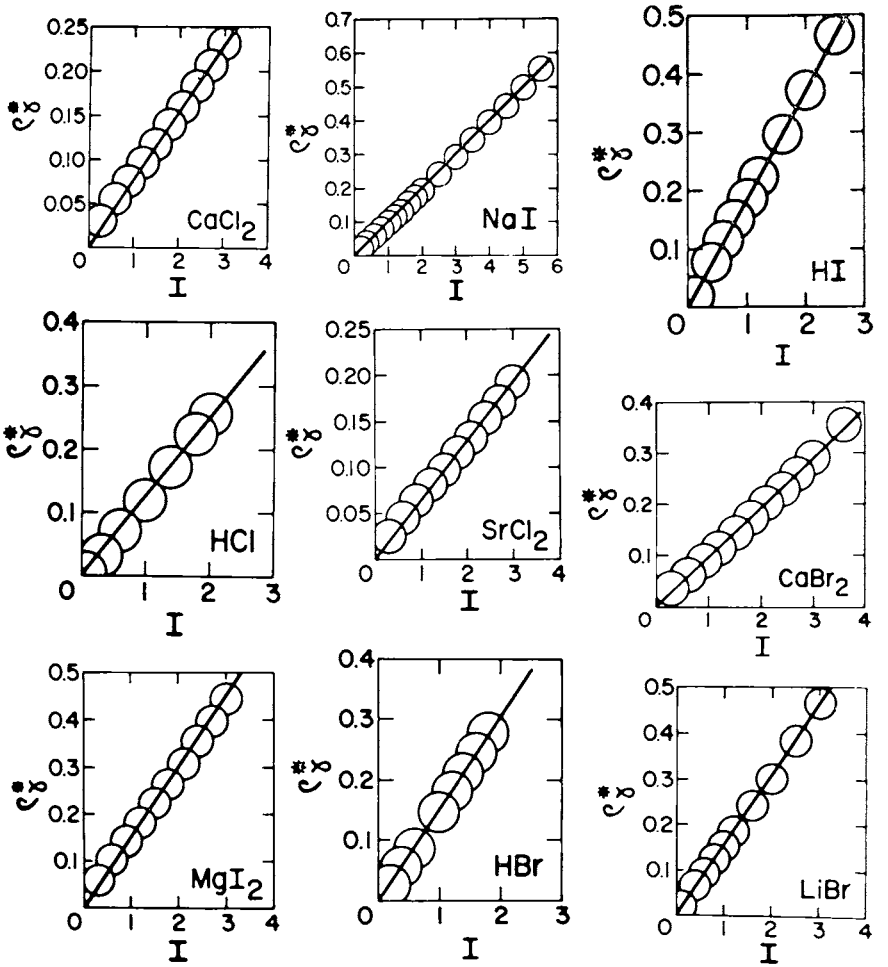

Fig. 19. ρ^*_γ (eqs 177 and 178) as a function of stoichiometric ionic strength at 25°C and 1 bar (see caption of fig. 17).

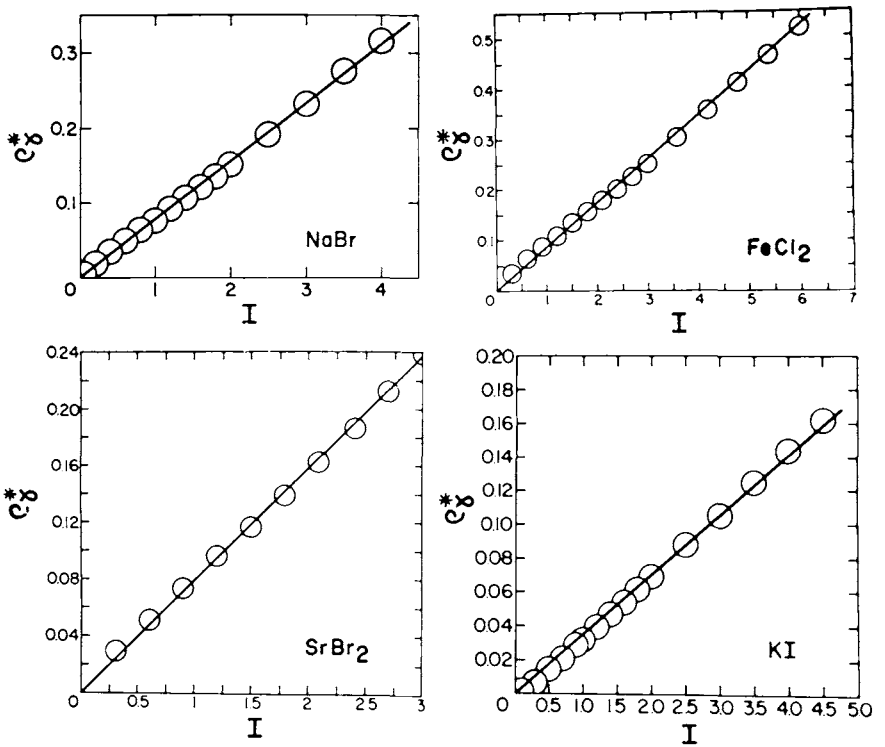

Fig. 20. ρ^*_γ (eqs 177 and 178) as a function of stoichiometric ionic strength at 25°C and 1 bar (see caption of fig. 17).

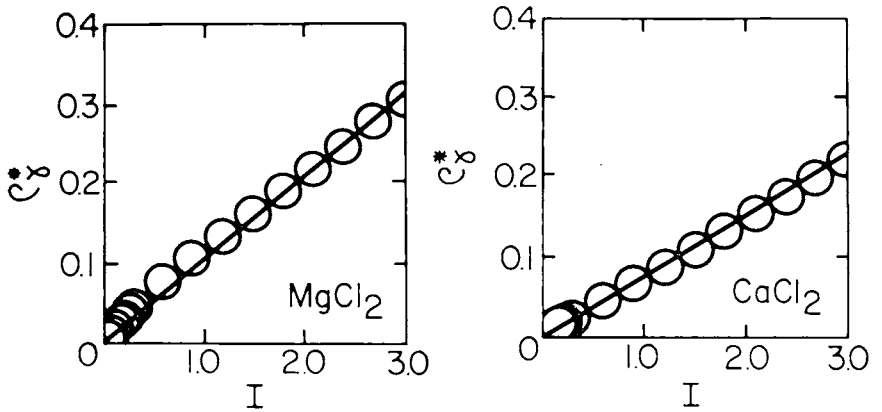

Fig. 21. ρ^*_γ (eqs 177 and 178) as a function of stoichiometric ionic strength at 25°C and 1 bar (see caption of fig. 17).

TABLE 5

Extended term parameters (b_γ) for computing osmotic and mean ionic activity coefficients of aqueous electrolytes at 25°C and 1 bar from eqs (173) and (193)[a]

Solute	b_γ[b]	I Limit[c]	Max. Resid.[d]	Solute	b_γ[b]	I Limit[c]	Max. Resid.[d]
HCl	0.125	2.0	0.006	$MgBr_2$	0.132	5.4	0.011
LiCl	0.140	5.5	0.014	$SrBr_2$	0.079	3.0	0.005
NH_4Cl	0.020	7.4	0.009	$CaBr_2$	0.097	3.6	0.007
KCl	0.024	5.0	0.012	$BaBr_2$	0.056	3.0	0.006
NaCl	0.064	5.0	0.011	HI	0.187	2.5	0.003
$MgCl_2$	0.106	6.0	0.015	LiI	0.190	3.0	0.020
$SrCl_2$	0.064	3.6	0.006	KI	0.035	4.5	0.005
$CaCl_2$	0.077	3.0	0.008	NaI	0.100	5.5	0.008
$BaCl_2$	0.039	3.0	0.003	MgI_2	0.151	3.0	0.015
$FeCl_2$	0.087	6.0	0.012	SrI_2	0.104	3.0	0.006
$MnCl_2$	0.074	6.0	0.015	CaI_2	0.118	3.0	0.007
$AlCl_3$	0.098	6.0	0.032	BaI_2	0.092	3.0	0.008
HBr	0.152	1.8	0.005	KF	0.064	5.5	0.010
LiBr	0.156	3.0	0.006	KOH	0.120	4.5	0.010
KBr	0.023	5.5	0.010	NaOH	0.085	4.5	0.004
NaBr	0.077	4.0	0.008	HNO_3	0.062	6.0	0.011
				$LiNO_3$	0.093	3.0	0.003

[a] The values of b_γ given in this table correspond to the slopes of the linear curves in figures 17 through 21. [b] kg $mole^{-1}$. [c] The I limit designates the maximum stoichiometric ionic strength for which the values of b_γ are applicable. [d] The maximum residual denotes the largest discrepancy between the linear curves and data points shown in figures 17 through 21.

activity coefficients on ionic strength at high concentrations, partly because it contains no provision for short-range interaction among ions of like charge. Similarly, because eq (142) is an empirical approximation, uncertainties in the values of å employed in the calculations are not uniform. *Nevertheless, in all but two of the cases shown in figures 17 through 21, the linear curves correspond to values of ρ^*_γ that are within 0.015 log units of the experimental values at ionic strengths ranging up to ~ 8, depending on the electrolyte.* The two exceptions are $AlCl_3$ and LiI, which exhibit discrepancies of 0.032 and 0.020 log units at low ionic strengths. In contrast, the discrepancies for more than two thirds of the electrolytes shown in figures 17 through 21 are $\leqslant 0.010$, and in most cases the corresponding error in $\bar{\gamma}_\pm$ is less than 1 to 2 percent. Differences in ρ^*_γ of 0.010 to 0.015 log units correspond to differences in $\bar{\gamma}_\pm$ of the order of 0.04 or less, which as a rule introduce insignificant error in geochemical calculations.

Because contributions by ion association to departures from ideality are apparently negligible for the electrolytes depicted in figures 17 through 21, $I = \bar{I}$ and the slopes of the curves correspond to $b_{\gamma,k}$ in eqs (173) and (178). These values of $b_{\gamma,k}$ are given in table 5, together with the maximum uncertainty and range of ionic strength represented by the experimental data from which they were derived.

The close agreement between the linear curves and symbols at both high and low ionic strengths in figures 17 through 21 strongly supports the validity of the values of å *computed independently* from electrostatic considerations and the standard state properties of aqueous ions. It can be deduced from figure 22B that slight errors in å result in a non-linear

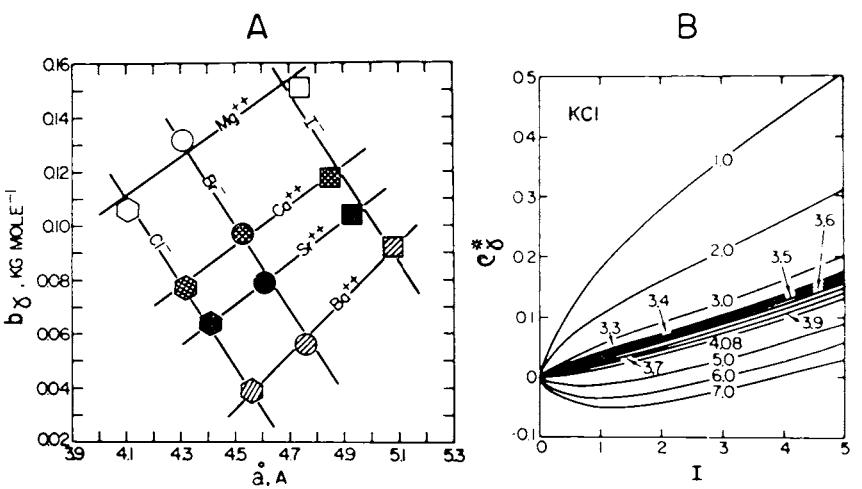

Fig. 22. Diagram A: Correlation of b_γ with å for alkaline earth halides at 25°C and 1 bar. The values represented by the symbols correspond to those given in tables 2 and 5. Diagram B: Hypothetical values of ρ^*_γ for KCl at 25°C and 1 bar generated assuming $I = \bar{I}$ from data tabulated by Hamer and Wu (1972) using alternate values of å (labeled in angstroms) to demonstrate the sensitivity of eq (178) to errors in å.

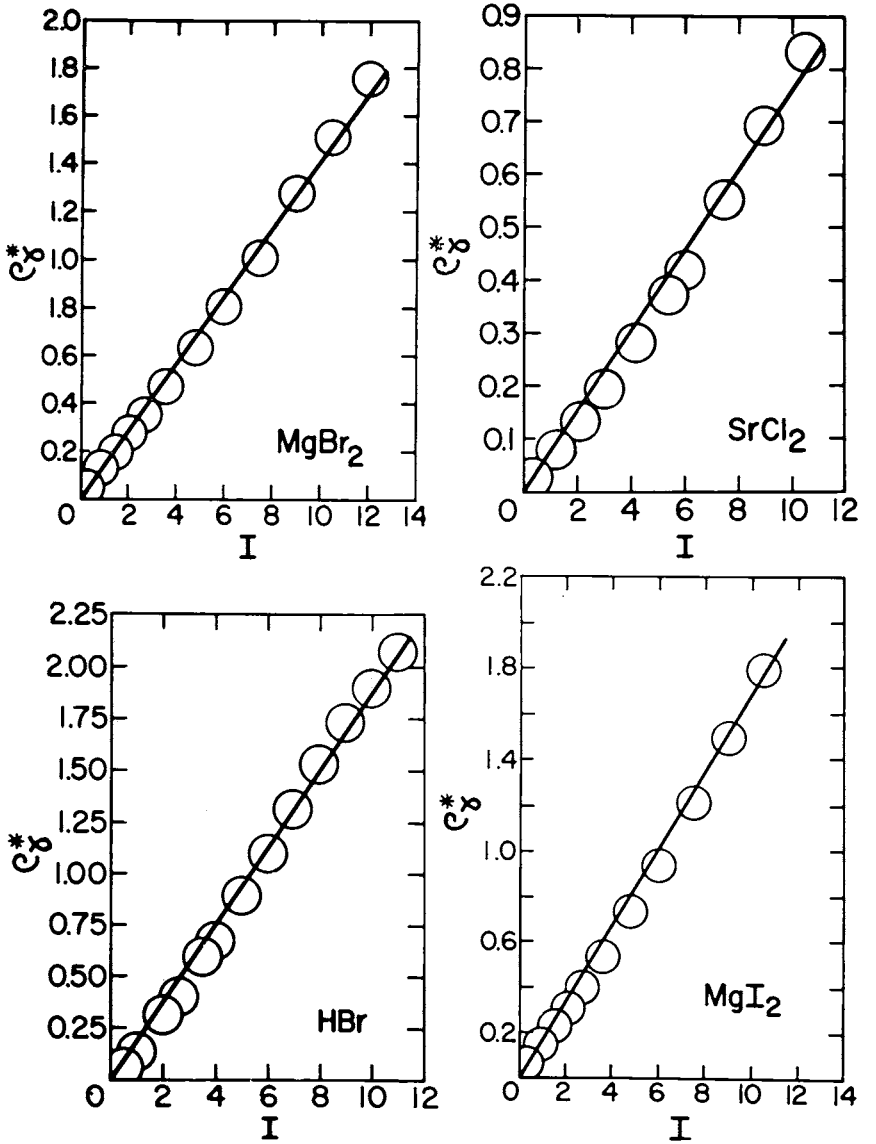

Fig. 23. ρ^*_γ (eqs 177 and 178) as a function of stoichiometric ionic strength (see caption of fig. 17).

TABLE 6

Alternate extended term parameters (b_γ) for computing osmotic and mean ionic activity coefficients of highly concentrated aqueous electrolytes at 25°C and 1 bar from eqs (173) and (193) — see text[a]

Solute	b_γ[b]	I Limit[c]	Max. Resid.[d]	Solute	b_γ[b]	I Limit[c]	Max. Resid.[d]
HCl	0.139	12.0	0.030	$CaBr_2$	0.115	12.0	0.076
LiCl	0.146	12.0	0.036	$BaBr_2$	0.061	6.0	0.015
$MgCl_2$	0.117	12.0	0.058	HI	0.202	8.0	0.041
$SrCl_2$	0.076	10.5	0.039	NaI	0.101	12.0	0.033
$CaCl_2$	0.093	12.0	0.058	MgI_2	0.168	12.0	0.077
$BaCl_2$	0.041	5.4	0.008	SrI_2	0.112	6.0	0.020
$AlCl_3$	0.104	10.8	0.066	CaI_2	0.123	6.0	0.024
HBr	0.187	11.0	0.066	BaI_2	0.099	6.0	0.023
LiBr	0.178	10.0	0.074	KF	0.070	14.0	0.029
NaBr	0.080	9.0	0.013	KOH	0.123	12.0	0.026
$MgBr_2$	0.141	12.0	0.070	NaOH	0.098	11.0	0.054
$SrBr_2$	0.086	6.0	0.020				

[a]The values of b_γ shown in this table correspond to the slopes of the curves for the corresponding electrolytes in figures 23 through 25 and 27. [b]kg $mole^{-1}$ [c]The I limit designates the maximum stoichiometric ionic strength for which the values of b_γ are applicable. [d]The maximum residual denotes the largest discrepancy between the linear curves and data points shown in figures 23 through 25 and 27.

dependence of ρ^*_γ on $\bar{I}$. In addition, it can be seen that an error of only a few tenths of an angstrom in å may introduce a sigmoid distribution of ρ^*_γ as a function of I. The sensitivity of ρ^*_γ to such errors is largely responsible for difficulties encountered in deriving values of both å and b_γ by two-parameter regression of activity coefficient data with eq (173), which commonly leads to non unique values of the fit coefficients (see above). The latter observation is consistent with the correlation of b_γ with å in figure 22A, where it can be seen that b_γ for electrolytes sharing a common anion or cation can be expressed as a linear function of å at 25°C and 1 bar. A similar (but not necessarily linear) correlation of b_γ with å is apparent in values of these coefficients obtained by successive two-parameter regression of activity coefficient data over different ranges of concentration using eq (173) with Γ_γ set to zero (Helgeson and James, 1968; Guggenheim and Stokes, 1969; Wood, ms and 1975).

The dependence of ρ^*_γ on ionic strength at $\bar{I} > 6m$ is shown in figures 23 through 25, where it can be seen that the data points for $AlCl_3$ and

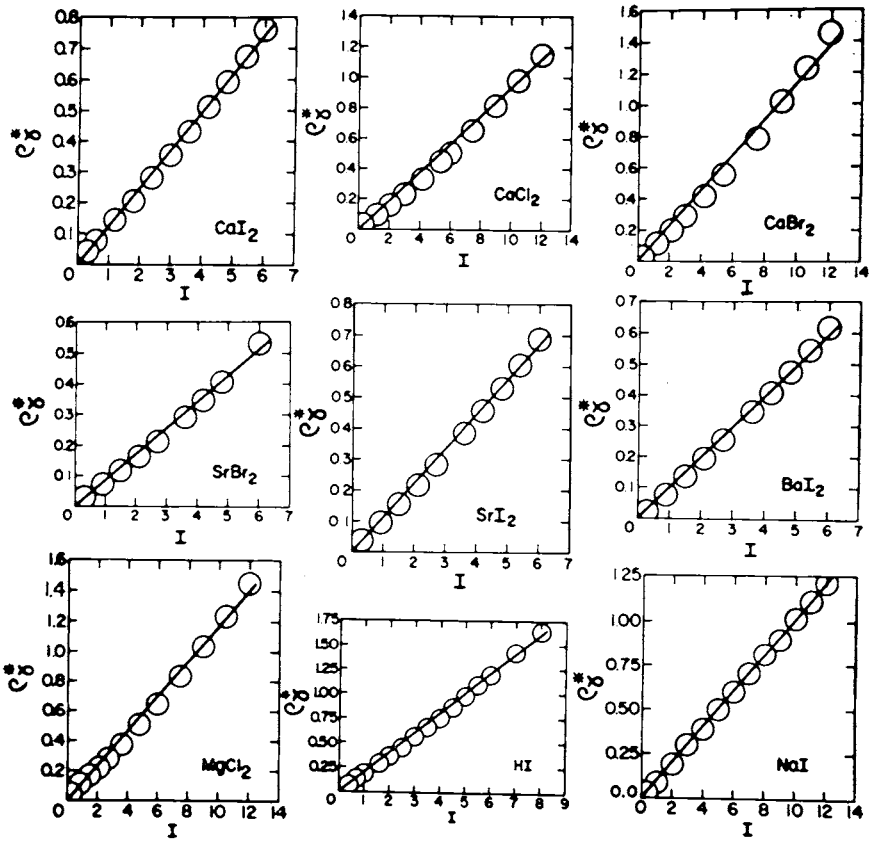

Fig. 24. ρ^*_γ (eqs 177 and 178) as a function of stoichiometric ionic strength at 25°C and 1 bar (see caption of fig. 17).

the alkaline earth halides at high ionic strengths depart to a slight but increasing extent from a linear configuration toward higher values of ρ^*_γ with increasing ionic strength. The opposite behavior is exhibited by $MnCl_2$, HNO_3, LiCl, NaOH, KF, KOH, LiBr, $LiNO_3$, and HCl, which depart from linearity toward lower values of ρ^*_γ at high ionic strengths (see below). The contrasting behavior of these two groups of electrolytes can be attributed to different relative contributions by ion solvation and association to the short range interaction of species responsible for non-Debye-Hückel departures from ideality. Where the linear curves approximate closely the distribution of data points in figures 23 through 25, the behavior of the electrolytes is consistent with "complete" dissociation *up to ionic strengths as high as 14 m.*

Because the deviations from linearity in the distribution of the data points in figures 23 through 25 are greater at high ionic strengths, the differences between the linear curves and the experimental data plotted in these figures are greater than the corresponding differences in figures 17 through 21. Nevertheless, all the linear curves afford close approximation of the data. It can be seen in table 6 that the values of $b_{\gamma,k}$ corresponding to the slopes of the curves in figures 23 through 25 yield corresponding values of ρ^*_γ within 0.077 log units of their experimental counterparts at

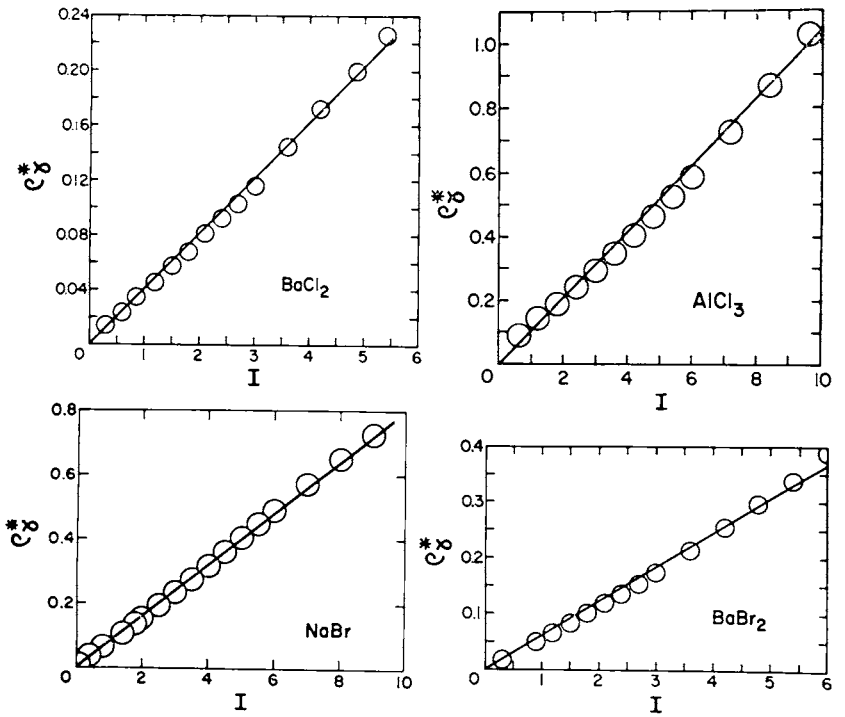

Fig. 25. ρ^*_γ (eqs 177 and 178) as a function of stoichiometric ionic strength at 25°C and 1 bar (see caption of fig. 17).

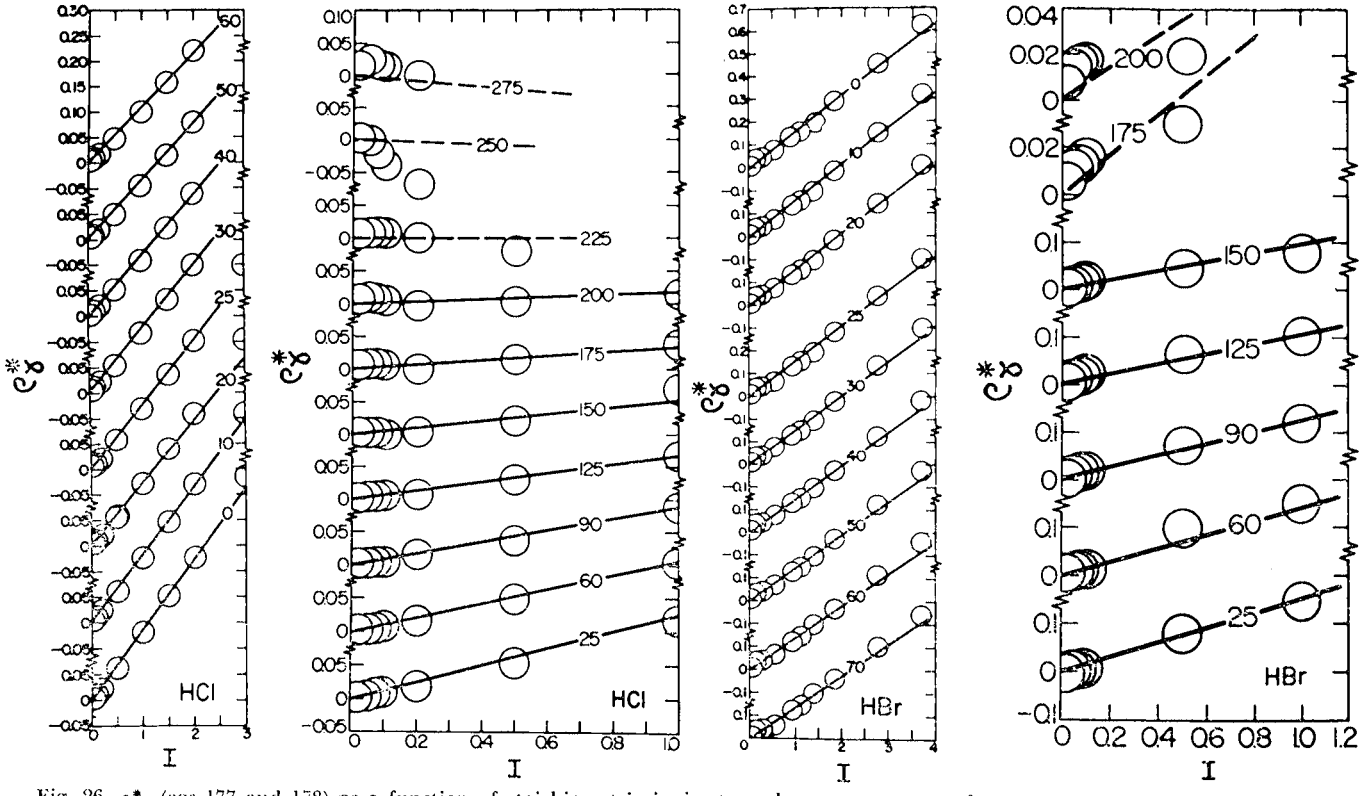

Fig. 26. ρ^*_γ (eqs 177 and 178) as a function of stoichiometric ionic strength at temperatures from 0° to 100°C at 1 bar and 100° to 275°C at pressures corresponding to liquid-vapor equilibrium.

ionic strengths ranging up to 14. Even discrepancies of this order of magnitude are acceptable for many equilibrium and mass transfer calculations in geochemistry. However, few such calculations are concerned with such concentrated electrolytes. For this reason, as well as for the sake of accuracy, the values of $b_{\gamma,k}$ given in table 5 were used in the calculations reported below in preference to those in table 6.

It can be seen in figure 26 that with the exception of HCl at temperatures $> \sim 225$°C and HBr at temperatures > 150°C, the linear dependence of ρ^*_γ on I for these electrolytes at 25°C and 1 bar is manifested also at high temperatures. In addition to experimental uncertainties, the apparent discrepancies above 150° and 225°C in figure 26 almost certainly

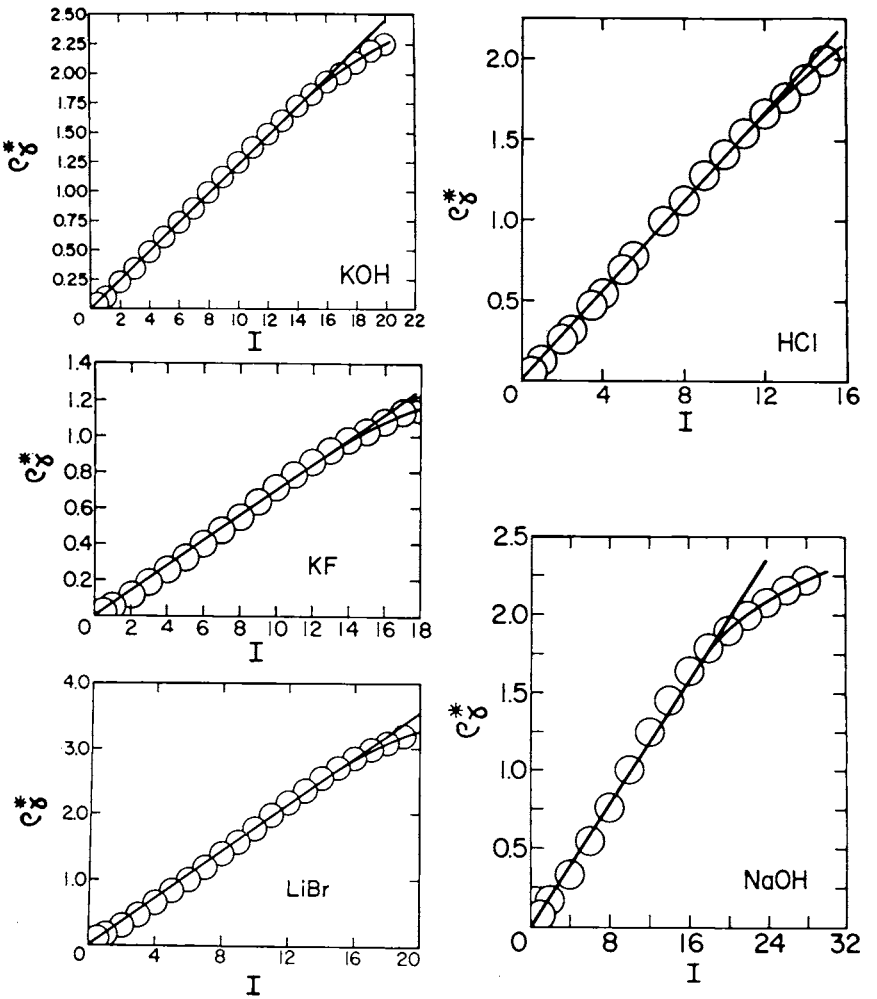

Fig. 27. ρ^*_γ (eqs 177 and 178) as a function of stoichiometric ionic strength at 25°C and 1 bar (see caption of fig. 17).

arise in part from ion association, which also affects significantly the behavior of $\rho^*_{\gamma,NaCl}$ at high temperatures and pressures (see below).

Effects of ion association on ρ^*_γ.—Although contributions by ion association to departures from ideality are apparently negligible (except as noted above) for the electrolytes depicted in figures 12 through 26, those shown in figures 27 and 28 exhibit behavior consistent with increasing ion association with increasing ionic strength at $I > 8$ to 17, depending on the electrolyte. At lower concentrations, ion association is apparently negligible. Dissociation constants at low temperatures and pressures are not available for most of the electrolytes shown in figures 27 and 28, but log K values of 1.53 (25°C), −0.1 (25°C), 0.57 to 0.77 (20°C), 1.45 (30°C), and 1.51 (20°C) have been reported for $HNO_3 \leftrightharpoons H^+ + NO_3^-$, $MnCl^+ \rightleftharpoons Mn^{++} + Cl^-$, $NaOH \rightleftharpoons Na^+ + OH^-$, $LiNO_3 \rightleftharpoons Li^+ + NO_3^-$, and $HCl \rightleftharpoons H^+ + Cl^-$, respectively, at 1 bar and infinite dilution (Haase, Ducker, and Küppers, 1965; Masterton and Berka, 1966; Gimblett and Monk, 1954; von Halban and Eisenbrand, 1928; Posner, 1953). Dissocia-

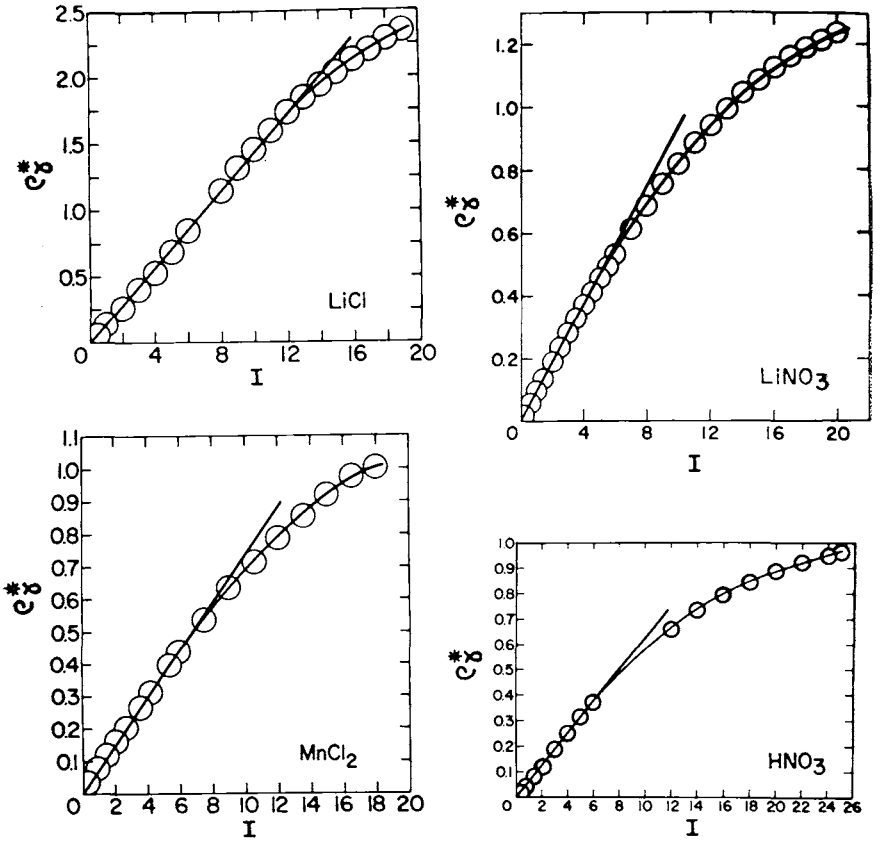

Fig. 28. ρ^*_γ (eqs 177 and 178) as a function of stoichiometric ionic strength at 25°C and 1 bar (see caption of fig. 17).

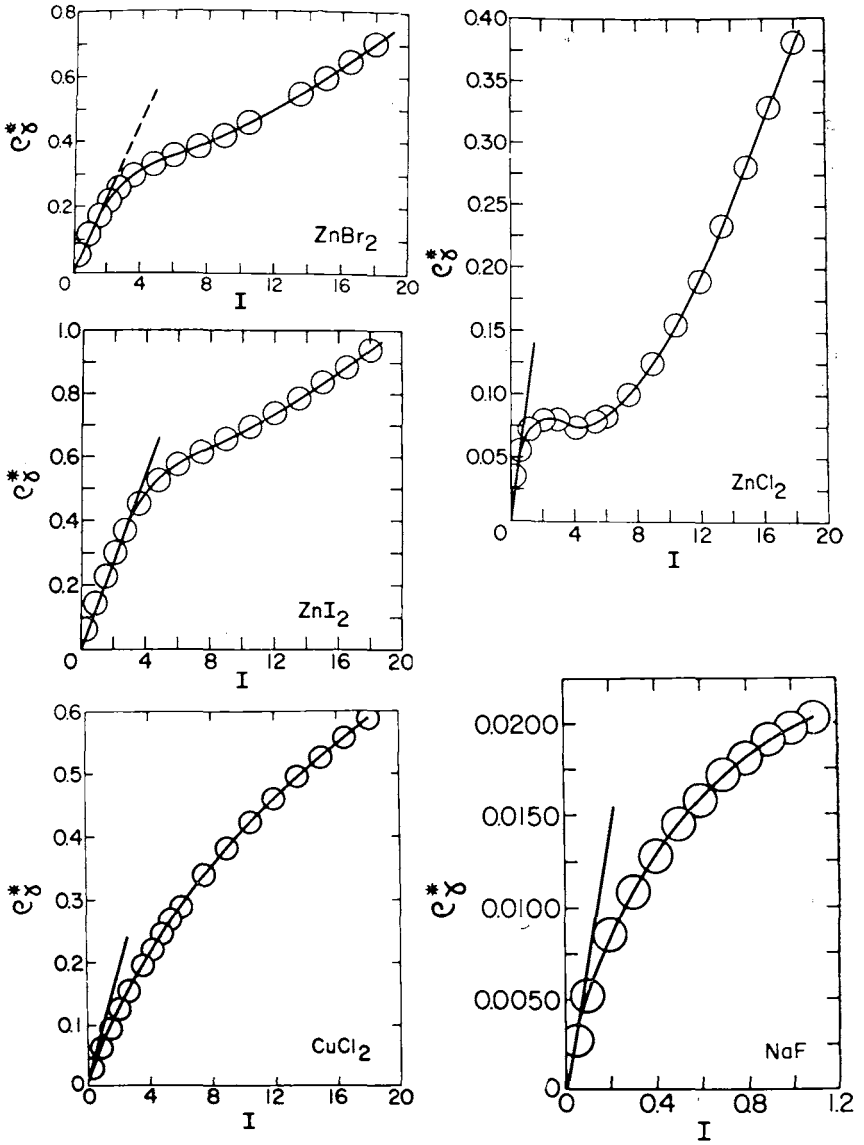

Fig. 29. ρ^*_γ (eqs 177 and 178) as a function of stoichiometric ionic strength at 25°C and 1 bar (see caption of fig. 17).

tion constants of this order of magnitude are consistent with formation of appreciable activities of ion pairs only at relatively high concentrations.

It can be seen in figure 29 that behavior similar to that shown in figures 27 and 28 occurs at much lower ionic strengths in the case of NaF, ZnI_2, $ZnBr_2$, $CuCl_2$, and $ZnCl_2$. Reliable dissociation constants are not available for NaF and ZnI_2 at 25°C and 1 bar, but log K values given in the literature for $CuCl^+ \rightleftharpoons Cu^{++} + Cl^-$, $CuCl_2 \rightleftharpoons Cu^{++} + 2\ Cl^-$, $ZnCl^+ \rightleftharpoons Zn^{++} + Cl^-$, $ZnCl_2 \rightleftharpoons Zn^{++} + 2\ Cl^-$, $ZnCl_3 \rightleftharpoons Zn^{++} + 3\ Cl^-$, $ZnCl_4^{--} \rightleftharpoons Zn^{++} + 4\ Cl^-$, $ZnBr^+ \rightleftharpoons Zn^{++} + Br^-$, $ZnBr_2 \rightleftharpoons ZnBr^+ + Br^-$, $ZnBr_3^- \rightleftharpoons ZnBr_2 + Br^-$, and $ZnBr_4^{--} \rightleftharpoons ZnBr_3^- + Br^-$ at infinite dilution are −0.01, 0.69, −0.43, −0.61, −0.53, −0.20, and (at various concentrations) 0.0, 0.15, 0.30, and 0.52, respectively (Helgeson, 1969; Horne, Holm, and Meyers, 1957). Dissociation constants of this order of magnitude lead to higher degrees of formation of complexes at lower concentrations than those attained in the solutions depicted in figures 27 and 28. The several inflections in the curves for $ZnBr_2$, ZnI_2, and $ZnCl_2$ in figure 29 almost certainly result in part from stepwise formation of polyligand complexes. The linear tangents to the curves in figure 29 are explained in later discussion.

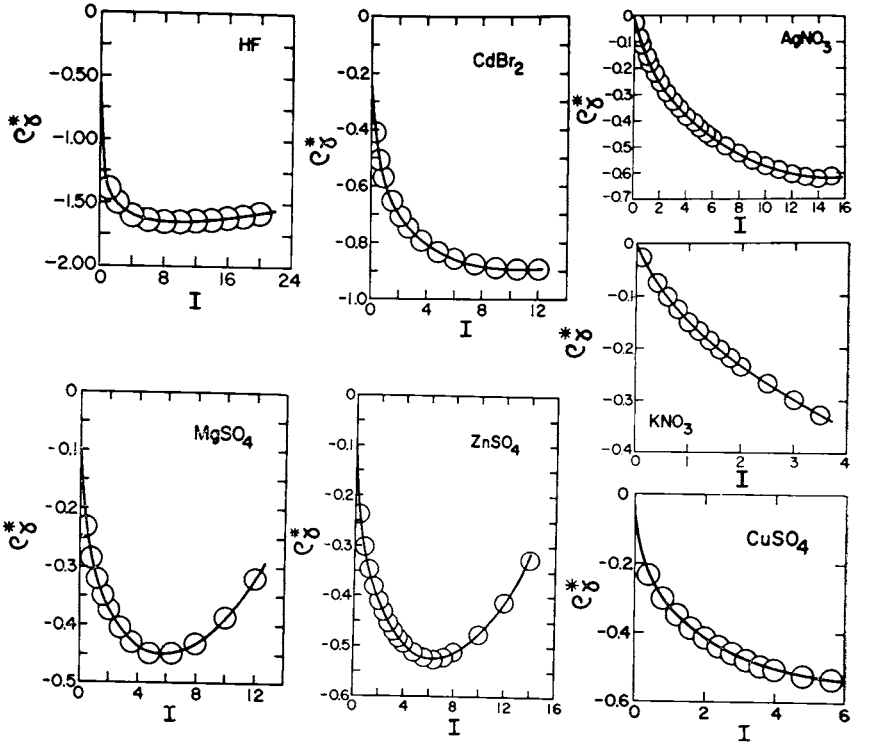

Fig. 30. ρ^*_γ (eqs 177 and 178) as a function of stoichiometric ionic strength at 25°C and 1 bar (see caption of fig. 17).

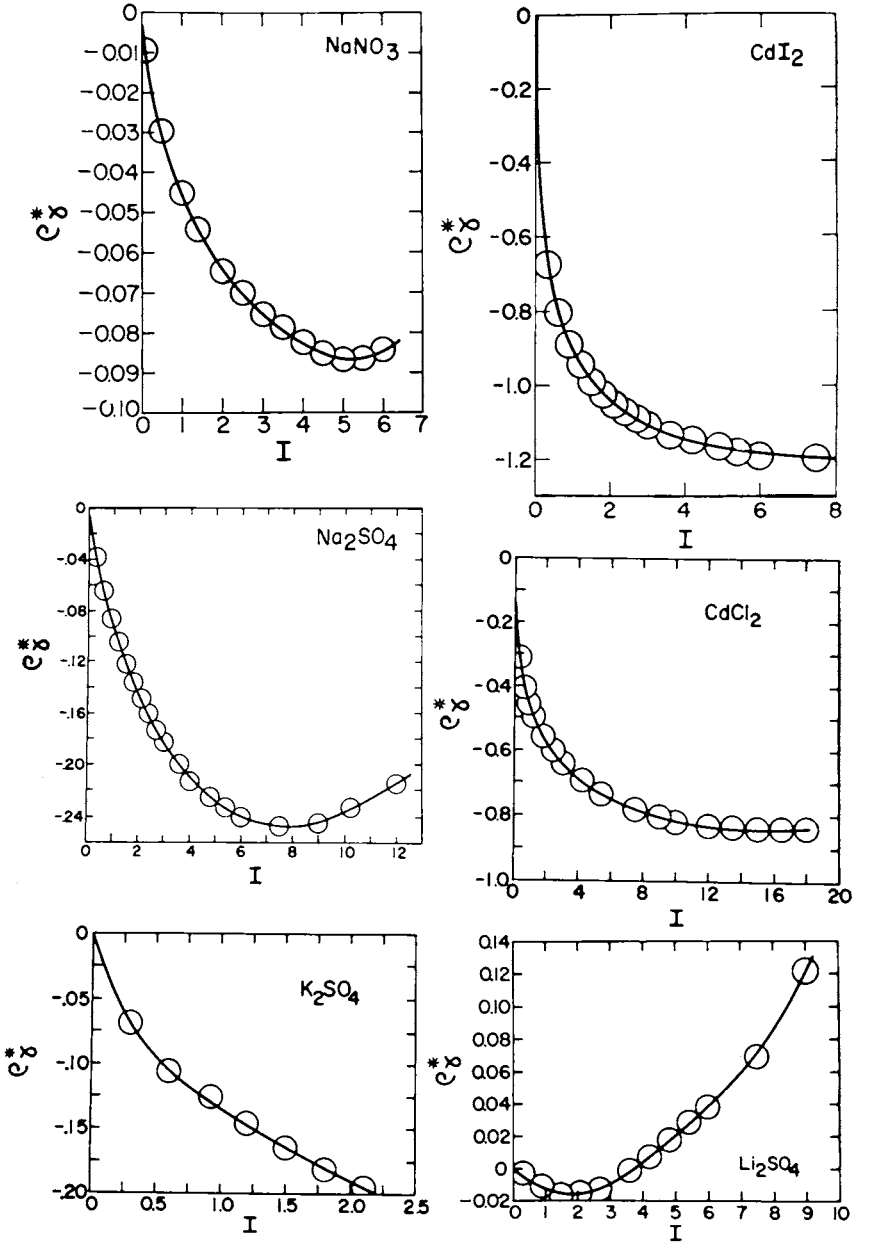

Fig. 31. ρ^*_γ (eqs 177 and 178) as a function of stoichiometric ionic strength at 25°C and 1 bar (see caption of fig. 17).

Even smaller dissociation constants than those adduced above result in negative values of ρ^*_γ, which decrease (and in certain cases minimize) with increasing ionic strength. It can be seen in figures 30 through 32 that (among others) this behavior is exhibited by HF, $ZnSO_4$, Li_2SO_4, $CuSO_4$, Na_2SO_4, K_2SO_4, $MgSO_4$, $CdBr_2$, CdI_2, and $CdCl_2$, for which the first dissociation constants are $10^{-3.18}$, $10^{-2.38}$, $10^{-1.02}$, $10^{-2.33}$, $10^{-1.00}$, $10^{-1.03}$, $10^{-2.25}$, $10^{-2.23}$, $10^{-2.17}$, and $10^{-2.0}$, respectively, at 25°C, 1 bar, and infinite dilution (Ellis, 1963; Nair and Nancollas, 1958; Fisher and Fox, 1977, 1978; Bale, Davies, and Monk, 1956; Nancollas, 1960; Kivalo and Ekari, 1957; Vasilev and Grechina, 1964; Prasad, 1968; Helgeson, 1967, 1969). Because most of these dissociation constants are $< 10^{-2}$, the bulk of the solute is complexed in all but dilute solutions of HF, $ZnSO_4$, $CuSO_4$, $MgSO_4$, $CdBr_2$, CdI_2, and $CdCl_2$. In the case of $CdBr_2$, CdI_2, and $CdCl_2$,

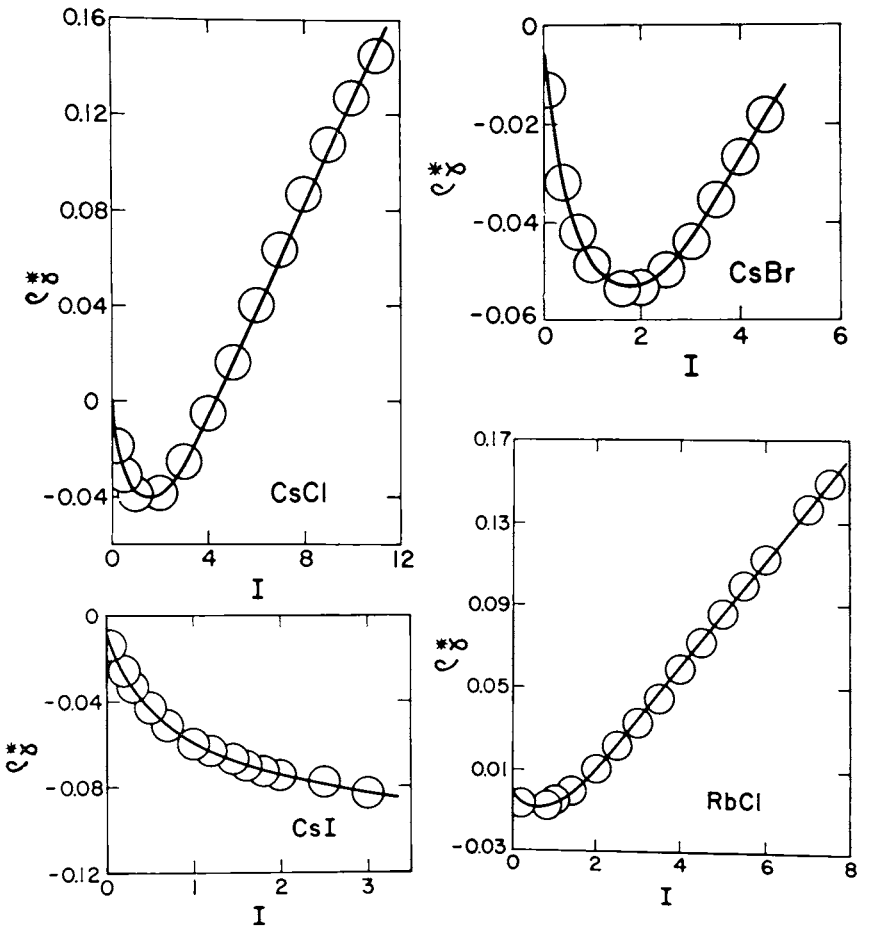

Fig. 32. ρ^*_γ (eqs 177 and 178) as a function of stoichiometric ionic strength at 25°C and 1 bar (see caption of fig. 17).

additional dissociation constant data suggest significant formation of polyligand complexes at high concentration.

Contributions by ion association to the behavior of ρ^*_γ for $AgNO_3$, KNO_3, $NaNO_3$, CsI, and CsBr can also be assessed in figures 30 through 32. The standard state dissociation constants for these species are reported to be $10^{-0.2}$, $10^{0.15}$, $10^{0.3}$ to $10^{0.5}$, $10^{0.03}$, and $10^{-0.03}$, respectively, at 25°C and 1 bar (Masterton and Berka, 1966; Chlebek and Lister, 1966; Robinson, 1937; Hsia and Fuoss, 1968). Corresponding values for RbCl and CsCl are $10^{0.55}$ and $10^{0.39}$ at 25°C, respectively (Smith and Martell, 1976; Dunsmore, Jalota, and Patterson, 1972; Patterson, Jalota, and Dunsmore, 1971). In all seven of these cases, relatively weak ion association appears to be coupled with weak ion solvation, which leads to negative departures from Debye-Hückel theory at low concentrations but positive departures at high. As a consequence, the degree of ion association maximizes with increasing concentration in relatively dilute solutions. In contrast, the degree of ion association as a function of ionic strength at high temperatures apparently maximizes at high concentrations (see below). Differences in the positions of the minima in the curves shown in figures 30 through 32 are a function of the relative size of the dissociation constants and the solvation and short-range interaction parameters for the various aqueous species.

The validity of attributing departures from linearity in ρ^*_γ as a function of I to ion association can be demonstrated by first combining

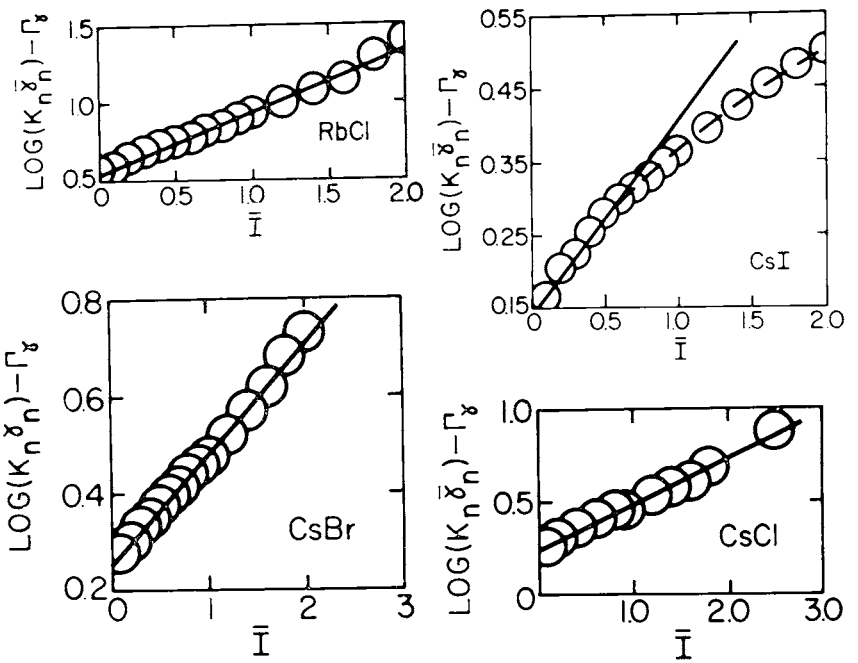

Fig. 33. Graphic representation of eq (181) for electrolytes at 25°C and 1 bar (see text and caption of fig. 17).

eq (68) with appropriate material balance expressions and statements of the law of mass action representing the dissociation of complexes in solution. For example, in the case of 1:1 or 2:2 electrolytes in which only a single ion pair forms, we can write eq (68) as

$$\bar{\gamma}_{\pm}\bar{I} = \gamma_{\pm}I \ , \tag{179}$$

which can be combined with eq (173) and values of A_γ, B_γ, å, and b_γ to compute $\bar{I}$ as a function of I from experimental values of $\gamma_{\pm}I$ and the relation, $m^* = I + \bar{I}$. The resulting values of $\bar{I}$ can then be used to calculate corresponding values of $K_n\bar{\gamma}_n$ from the law of mass action representing the dissociation of the nth neutral complex, which can be written as

$$K_n\bar{\gamma}_n = \frac{\gamma_{\pm}{}^2 I^2}{(I - \bar{I})\psi_k} \tag{180}$$

where K_n and $\bar{\gamma}_n$ refer to the dissociation constant and activity coefficient of the subscripted species. Taking account of eq (175) it follows that

$$\log (K_n\bar{\gamma}_n) - \Gamma_\gamma = \log K_n + b_{\gamma,n}\bar{I} \ . \tag{181}$$

Eq (181) describes the linear curves shown in figures 33 and 34, which were generated from eq (180) in the manner described above using values

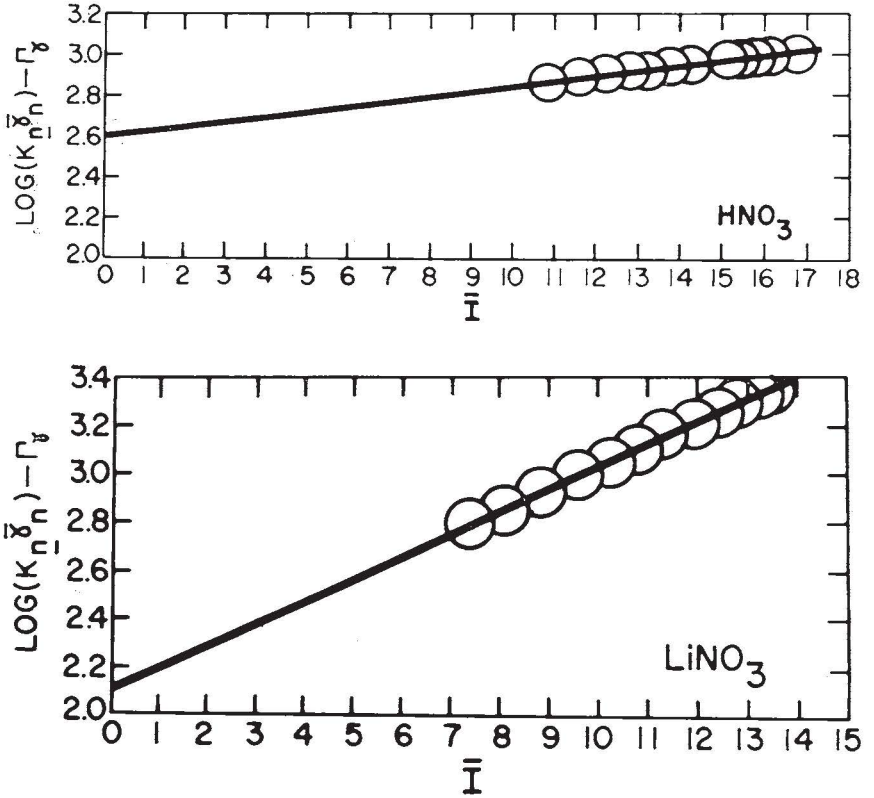

Fig. 34. Graphic representation of eq (181) for electrolytes at 25°C and 1 bar (see text and caption of fig. 17).

TABLE 7

Short-range interaction parameters (b_{ij})[a] for computing activity and osmotic coefficients at 25°C and 1 bar — see text

Cation	Anion				Cation	Anion			
	F^-	Cl^-	Br^-	I^-		F^-	Cl^-	Br^-	I^-
H^+	-0.083[c]	0.019[b]	0.056[b]	0.103[b]	Ca^{++}	-0.493[c]	-0.257[b]	-0.183[b]	-0.100[b]
Li^+	-0.182[c]	-0.049[b]	-0.024[b]	0.032[b]	Sr^{++}	-0.503[c]	-0.266[b]	-0.204[b]	-0.113[b]
Na^+	-0.155[c]	-0.096[b]	-0.075[b]	-0.032[b]	Ba^{++}	-0.529[c]	-0.292[b]	-0.227[b]	-0.112[b]
K^+	-0.132[b]	-0.112[b]	-0.101[b]	-0.075[b]	Pb^{++}	-0.554[c]	-0.324[c]	-0.238[c]	-0.140[c]
Rb^+	-0.127[c]	-0.119[c]	-0.118[c]	-0.097[c]	Zn^{++}	-0.462[c]	-0.259[c]	-0.186[c]	-0.098[c]
Cs^+	-0.119[c]	-0.122[c]	-0.121[c]	-0.108[c]	Cu^{++}	-0.485[c]	-0.277[c]	-0.202[c]	-0.114[c]
NH_4^+	-0.131[c]	-0.114[b]	-0.107[c]	-0.087[c]	Cd^{++}	-0.463[c]	-0.256[c]	-0.180[c]	-0.092[c]
Ag^+	-0.134[c]	-0.086[c]	-0.067[c]	-0.037[c]	Hg^{++}	-0.491[c]	-0.278[c]	-0.198[c]	-0.104[c]
Au^+	-0.131[c]	-0.115[c]	-0.107[c]	-0.087[c]	Fe^{++}	-0.414[c]	-0.282[b]	-0.157[c]	-0.071[c]
Cu^+	-0.153[c]	-0.076[c]	-0.047[c]	-0.007[c]	Mn^{++}	-0.499[c]	-0.298[b]	-0.210[c]	-0.118[c]
Mg^{++}	-0.451[c]	-0.256[b]	-0.167[b]	-0.085[b]	Al^{+++}		-0.481[b]		

[a] kg mole^{-1}. [b] Computed from equation (136) and (174) using the values of ω_j, b_k, and b_γ given in tables 3 through 5, which also yield -0.002, -0.038, -0.126, and -0.064 for b_{HNO_3}, b_{LiNO_3}, b_{NaOH}, and b_{KOH}, respectively. [c] Calculated from equations (136) and (174) using values of ω_j and b_k taken from tables 3 and 4, together with estimated values of b_γ taken from table 8.

of $b_{\gamma,k}$ taken from table 5 or calculated from correlation algorithms (see below). The distribution of the symbols in these figures is a sensitive test of the effect of ion association on stoichiometric activity coefficients. The linear curves shown in figures 33 and 34 are consistent with the nonlinear stoichiometric ionic strength dependence of ρ^*_γ for $LiNO_3$, HNO_3, CsCl, RbCl, CsBr, and CsI in figures 28 and 32.

The departure from linearity of log $(K_n\bar{\gamma}_n)$ for CsI as a function of $\bar{I}$ at high ionic strengths in figure 33 is almost certainly a manifestation of the formation of CsI_2^- with increasing $\bar{I}$. It should perhaps be emphasized that the intercepts of the curves in figures 33 and 34 are in close agreement with the experimental values of log K_n cited above, and the slopes of the curves are similar to those for other neutral species determined experimentally by Randall and Failey (1927a, b, and c). The same observations hold for corresponding curves representing log $(K_n\bar{\gamma}_n)$ for $CaSO_4$, $MgSO_4$, $CuSO_4$, and many other electrolytes in which ion pairs form to a significant degree at 25°C and 1 bar.

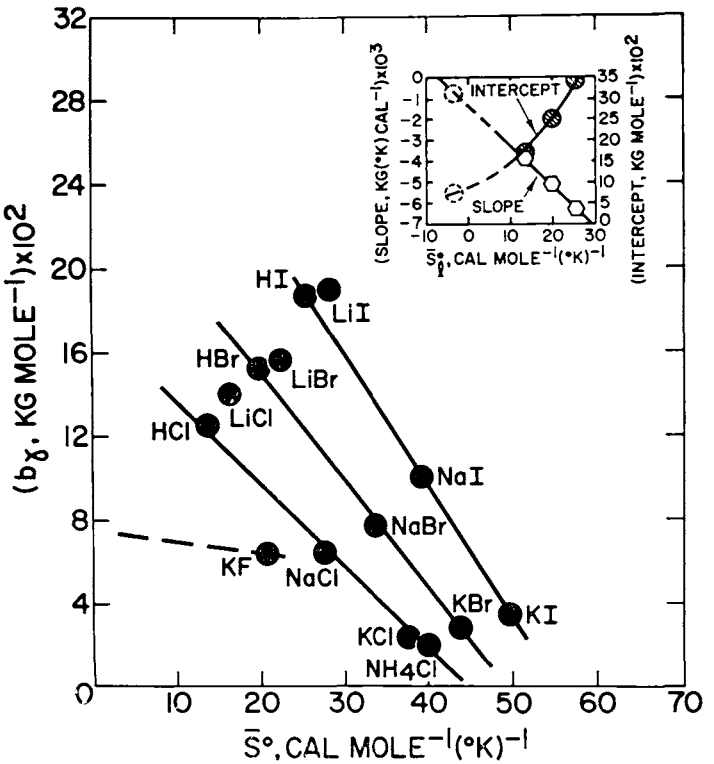

Fig. 35. Correlation of the extended term parameter b_γ with the standard partial molal entropies of electrolytes at 25°C and 1 bar. The symbols represent values of b_γ taken from table 5 and those for $\bar{S}°$ generated from the conventional standard partial molal entropies of aqueous ions given in table 3. $\bar{S}°_l$ stands for the conventional standard partial molal entropy of the lth anion.

Correlation and calculation of b_γ and b_{il}.—The values of $b_{\gamma,k}$ in table 5 permit calculation of b_{il} at 25°C and 1 bar from eq (174) and the values of b_k given in table 4. The results of these calculations are shown in table 7. The other values of b_{il} shown in table 7 were generated from the estimates of $b_{\gamma,k}$ in table 8, which are consistent with the curves shown in figures 35 and 36. It should perhaps be emphasized in this regard that the estimates in table 7 for the lithium and ferrous halides are more uncertain than the others, owing to discrepancies between the curves and the symbols shown for LiCl, LiBr, LiI, and $FeCl_2$ in figures 35 and 36. Similarly, the paucity of data for fluorides in figure 35 reduces the estimates of b_{il} for these electrolytes to the status of first approximations.

The correlation of $b_{\gamma,k}$ with $\bar{S}°_k$ in figures 35 and 36 is similar to that demonstrated by Burns (1964), who correlated the extended term parameter in the Guggenheim equation with the standard molal entropies of electrolytes at 25°C and 1 bar. The equation of the linear curves in figures 35 and 36 can be expressed as

$$b_{\gamma,k} = \mathbf{a} + \mathbf{b}\bar{S}°_k \tag{182}$$

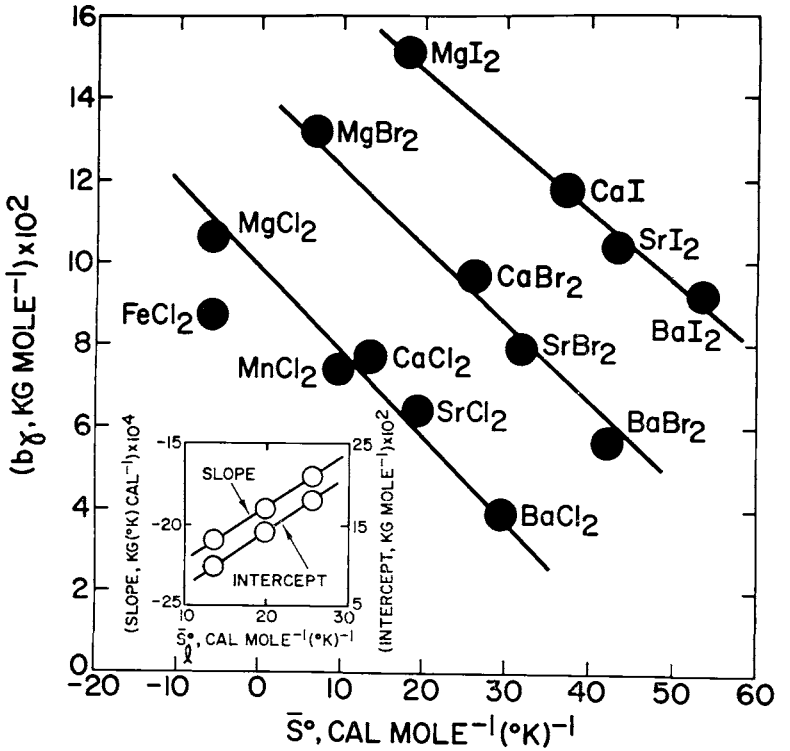

Fig. 36. Correlation of the extended term parameter b_γ with the standard partial molal entropies of electrolytes at 25°C and 1 bar. The symbols represent values of b_γ taken from table 5 and those for $\bar{S}°$ generated from the conventional standard partial molal entropies of aqueous ions given in table 3. $\bar{S}°_l$ stands for the conventional standard partial molal entropy of the lth anion.

where **a** = 0.0755 for 1:1 fluorides, 0.1741 for 1:1 chlorides, 0.2518 for 1:1 bromides, and 0.3453 for 1:1 iodides. In contrast, the **b** parameter for all 1:1 halides is given by

$$\mathbf{b} = -12 \times 10^{-4} - 19.7 \times 10^{-5}\,\bar{S}^{\circ}_{l} \qquad (182A)$$

where $\bar{S}^{\circ}_{l}$ refers to the standard molal entropy of the lth halide ligand at 25°C and 1 bar. The values of **a** and **b** for halides with the stoichiometry of $MgCl_2$ in figure 36 are given by

$$\mathbf{a} = 6.75 \times 10^{-4} + 68.1 \times 10^{-4}\,\bar{S}^{\circ}_{l} \qquad (183)$$

and

$$\mathbf{b} = -25.5 \times 10^{-4} + 33.5 \times 10^{-6}\,\bar{S}^{\circ}_{l} \quad . \qquad (184)$$

Despite the fact that the estimates of $b_{\gamma,k}$ for the fluorides in table 8 were generated by extrapolation of the slopes and intercepts of the curves in figures 35 and 36, it can be seen in figure 29 that the value of $b_{\gamma,NaF}$ (which corresponds to the slope of the linear curve for NaF in the figure) is closely consistent with the experimental data used to calculate $\rho^{*}_{\gamma,NaF}$.

TABLE 8

Estimated extended term parameters (b_γ) for computing osmotic and mean ionic activity coefficients of aqueous electrolytes at 25°C and 1 bar from eqs (173) and (193) and the standard partial molal entropies ($\bar{S}^{\circ}$) used in the calculations — see text

Solute	$\bar{S}^{\circ}$ [a,b]	b_γ [c,d]	Solute	$\bar{S}^{\circ}$ [a,b]	b_γ [c,d]	Solute	$\bar{S}^{\circ}$ [a,b]	b_γ [c,d]
RbCl	42.4	0.010	$ZnBr_2$	13.4	0.116	LiF	-0.5	0.076
CsCl	45.31	-0.001	$CuBr_2$	16.4	0.111	RbF	25.6	0.061
AgCl	31.10	0.054	$CdBr_2$	22.2	0.100	CsF	28.6	0.059
AuCl	40.1	0.019	$HgBr_2$	30.9	0.083	AgF	14.3	0.067
CuCl	23.3	0.084	RbI	54.3	0.007	AuF	23.3	0.062
$PbCl_2$	31.4	0.033	CsI	57.25	-0.011	CuF	6.5	0.072
$ZnCl_2$	1.0	0.097	AgI	43.04	0.077	NH_4F	23.4	0.062
$CuCl_2$	4.0	0.091	AuI	52.0	0.022	FeF_2	-39.3	0.094
$CdCl_2$	9.8	0.079	CuI	35.2	0.126	MnF_2	-24.0	0.053
$HgCl_2$	18.5	0.060	NH_4I	52.1	0.021	MgF_2	-39.4	0.090
RbBr	48.6	0.004	FeI_2	18.1	0.150	CaF_2	-19.9	0.038
CsBr	51.55	-0.011	MnI_2	33.4	0.124	SrF_2	-14.2	0.023
AgBr	37.34	0.061	PbI_2	55.2	0.087	BaF_2	-4.1	-0.004
AuBr	46.3	0.016	ZnI_2	24.8	0.138	PbF_2	-2.2	-0.005
CuBr	29.5	0.101	CuI_2	27.8	0.133	ZnF_2	-32.6	0.076
NH_4Br	46.4	0.015	CdI_2	33.6	0.123	CuF_2	-29.6	0.068
$FeBr_2$	6.7	0.129	HgI_2	42.3	0.109	CdF_2	-23.8	0.053
$MnBr_2$	22.0	0.100	HF	-3.2	0.077	HgF_2	-15.1	0.039
$PbBr_2$	43.8	0.059	NaF	10.8	0.069			

[a] Calculated from the conventional standard partial molal entropies of ionic species given in table 3. [b] Cal $mole^{-1}$ $(°K)^{-1}$. [c] Calculated from equations (182) through (184) and the standard partial molal entropies given above. [d] kg $mole^{-1}$

Even more convincing agreement is apparent in figure 29 between experimental values of ρ^*_γ for $CuCl_2$, $ZnCl_2$, $ZnBr_2$, and ZnI_2 and the linear curves in the dilute range of concentration, which were generated from the estimates of $b_{\gamma,k}$ for these electrolytes in table 8. It thus appears that short-range interaction parameters computed from estimated values of $b_{\gamma,k}$ can be used with confidence to predict the thermodynamic behavior of partially associated electrolyte solutions.

It can be seen in table 7 that all the short-range interaction parameters are negative, except those for HCl, HBr, HI, and LiI. Note also that the values of b_{il} for certain cations (such as Rb^+ and Cs^+) interacting with F^-, Cl^-, Br^-, and I^- differ only slightly from one another. In others, b_{il} increases substantially for successive interaction of a given cation with F^-, Cl^-, Br^-, and I^-. *In general, the values of b_{il} for divalent and trivalent cations interacting with Cl^- are two to three times more negative than those for monovalent interactions.*

Mixed electrolytes.—The equations and parameters summarized above permit calculation of activity coefficients in mixed as well as single electrolytes at 25°C and 1 bar. For example, the mean ionic activity coefficient of the kth component of a mixture of "completely" dissociated electrolytes can be expressed in terms of the ionic strength fractions of the components by combining the identities, $\bar{y}_j = y_j$, $\bar{I} = I$, and $\bar{\gamma}_{\pm,k} = \gamma_{\pm,k}$ with eqs (69) and (144) to give

$$\log \gamma_{\pm,k} = -\frac{A_\gamma |Z_i Z_l| I^{1/2}}{\Lambda} + \Gamma_\gamma + \frac{\omega_k}{\nu_k} \sum_k b_k y_k I + \frac{\nu_{i,k}}{\nu_k} \sum_l b_{il} \left(\sum_k \frac{\nu_{l,k} y_k I}{\psi_k} \right) + \frac{\nu_{l,k}}{\nu_k} \sum_i b_{il} \left(\sum_k \frac{\nu_{i,k} y_k I}{\psi_k} \right) \quad (185)$$

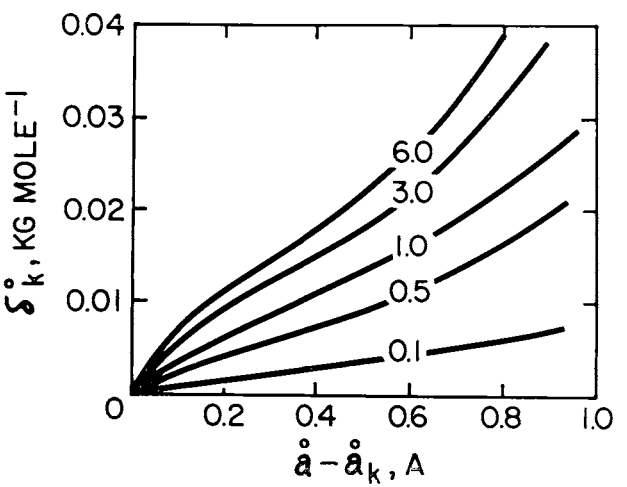

Fig. 37. δ°_k at 25°C and 1 bar computed from eq (189) as a function of $\mathring{a} - \mathring{a}_k$ at constant I (indicated by the numbers on the curves) (see text).

where the subscripts i and l again designate the cation and anion in the kth component. Similarly, we can write eq (107) for a "completely" dissociated electrolyte solution as

$$m^* = \sum_j \sum_k \frac{\nu_{j,k} y_k \mathrm{I}}{\psi_k} \tag{186}$$

which permits eqs (122) and (169) to be combined to give

$$\Gamma_\gamma = -\log\left(1 + 0.0180153 \sum_j \sum_k \frac{\nu_{j,k} y_k \mathrm{I}}{\psi_k}\right) \tag{187}$$

where the subscript j designates both cations and anions.

The difference between the logarithm of the mean ionic activity coefficient of the kth component of a mixed electrolyte ($\log \bar{\gamma}_{\pm,k}$) and that of the component in a single electrolyte solution with the same ionic strength ($\log \bar{\gamma}^\circ_{\pm,k}$) can be expressed as

$$\delta_k \equiv \log \bar{\gamma}_{\pm,k} - \log \bar{\gamma}^\circ_{\pm,k} \tag{188}$$

which at $y_k = 1$ reduces to

$$\delta^\circ_k = -|\mathrm{Z}_i \mathrm{Z}_l| \mathrm{A}_\gamma \mathrm{I}^{1/2} \left(\frac{1}{\Lambda} - \frac{1}{\Lambda_k}\right) \tag{189}$$

where Λ and Λ_k stand for $(1 + \mathring{a}\mathrm{B}_\gamma \mathrm{I}^{1/2})$ and $(1 + \mathring{a}_k \mathrm{B}_\gamma \mathrm{I}^{1/2})$, respectively. It follows that δ°_k represents the error in $\log \bar{\gamma}_{\pm,k}$ resulting from the approximation represented by eq (124) for mixed electrolytes (see above). The magnitude of this error can be assessed in figure 37, where δ°_k is plotted as a function of $\mathring{a} - \mathring{a}_k$. Consideration of the range of $\mathring{a}$ values shown in table 2 suggests that in most cases $|\delta^\circ_k|$ for 1:1 components of mixed electrolyte solutions is $\leqslant 0.02$ at $\mathrm{I} \leqslant 3$. The corresponding error for electrolytes with the stoichiometry of $MgCl_2$ is $\leqslant 0.04$. As a rule, errors of this order of magnitude are insignificant compared to other uncertainties attending calculation of equilibrium and mass transfer in geochemical processes.

Values of $\log \bar{\gamma}_{\pm,k}$ computed from eqs (124), (132), and (185) through (187) using values of A_γ, B_γ, $\mathring{a}_k$, ω_j, b_i, and b_{il} given in tables 1 through 4 and 7 are shown in figures 38 through 43 as a function of ionic strength fraction at 25°C, 1 bar, and various ionic strengths. It should perhaps be emphasized that the symbols in these figures represent experimental data which were *not* used to produce the curves. It can be seen in figures 38 through 43 that in a number of instances the curves generated from the calculations are in close agreement with the experimental data represented by the symbols, but in others the slopes and/or intercepts of the curves differ significantly from those consistent with the trend of the symbols. Nevertheless, all the predicted values of $\log \bar{\gamma}_\pm$ in figures 38 and 39 fall within ~ 0.02 log units of the independent experimental values, and those in figure 40 differ from their experimental counterparts by < 0.04 log units. As noted above, errors of this order of magnitude are insignificant

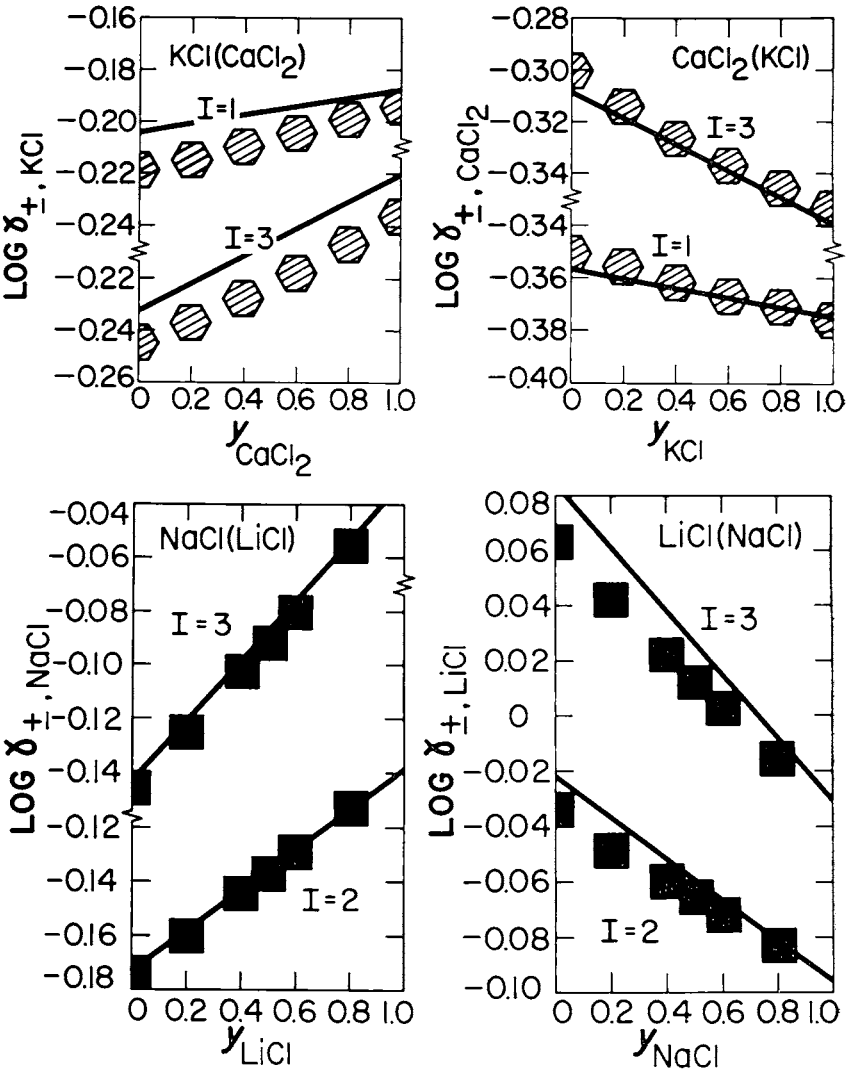

Fig. 38. Predicted (curves) and experimental (symbols) stoichiometric mean activity coefficients of the components of mixed electrolytes at 25°C, 1 bar, and constant ionic strength as a function of the stoichiometric ionic strength fractions of the components (see text). The experimental data represented by the symbols shown above and those in figures 39 through 43 were taken from: cross-hatched circles, Harned (1959, 1960); half-filled circles, Lietzke and Stoughton (1964b); filled squares, Stakhanova, Vasilev, and Epikhin (1963); filled circles, Robinson and Bower (1965, 1966a and b); filled hexagons, Robinson (1961); striped circles, Wu, Rush, and Scatchard (1968); open circles, Lanier (1965); open diamonds, Platford (1968); striped hexagons, Robinson and Covington (1968); circles enclosing dot, Harned and Mason (1931); striped triangles, Harned and Gary (1955a and b). The curves were generated assuming complete dissociation.

in most geochemical calculations. In fact, even the larger discrepancies apparent in figures 41 through 43 have a negligible effect on many equilibrium calculations for natural systems.

The configuration of the curves in figures 38 through 43 is consistent with Harned's rule (Harned, 1935; Harned and Owen, 1958). The fact that in many cases the predicted curves are in remarkable agreement with independent experimental data taken from the literature strongly supports the theoretical basis for eq (185). However, the discrepancies in figures 41 through 43 similarly underscore the fact that (owing in part to

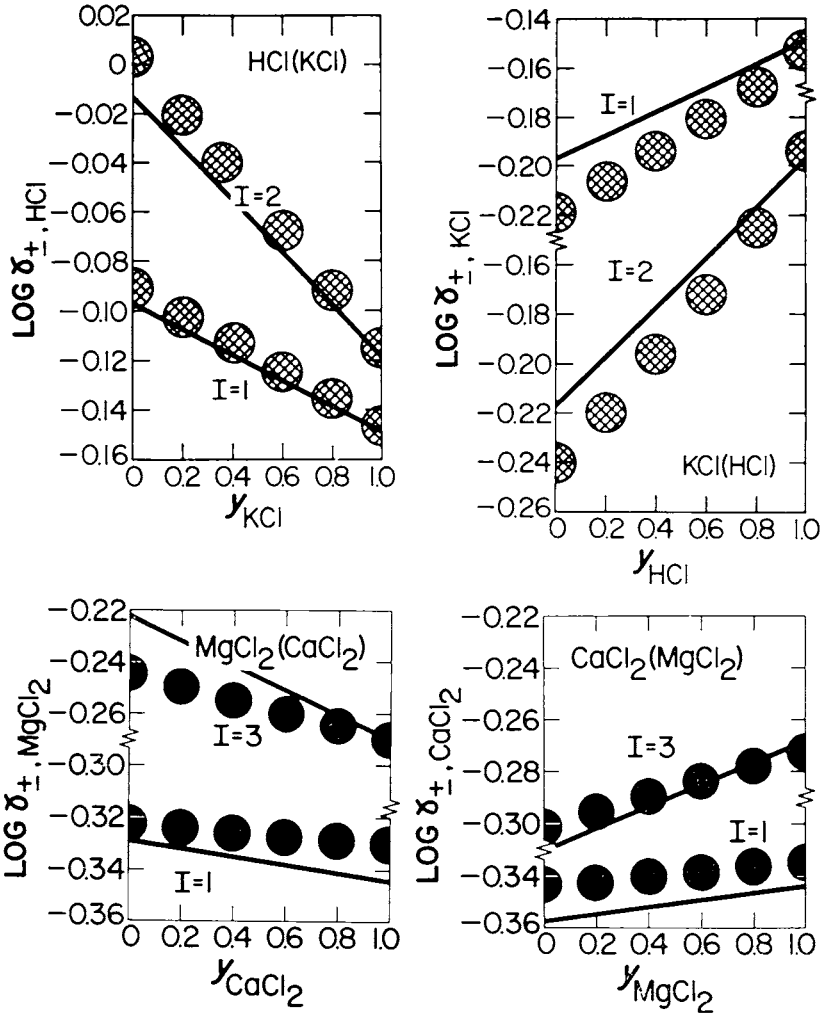

Fig. 39. Predicted (curves) and experimental (symbols) stoichiometric mean activity coefficients of the components of mixed electrolytes at 25 °C, 1 bar, and constant ionic strength as a function of the stoichiometric ionic strength fractions of the components (see text and caption of fig. 38).

the oversimplification represented by eq 142) the predictive equations afford no more than a close approximation of non-ideality in electrolyte solutions. At the same time it can be shown that where large differences occur between the curves and symbols, the theoretical calculations are not necessarily responsible for all the error. Relatively large experimental uncertainties attend extraction of activity coefficients from vapor pressure data for mixed electrolytes, and contradictions in values of $\gamma_{\pm}$ reported by different investigators for the components of the same system are not uncommon. One such example is apparent in figure 43, where the values of log $\gamma_{\pm,\mathrm{NaCl}}$ in NaCl-$CaCl_2$ solutions at $y_{CaCl_2} = 1$ and I = 3 reported by Lanier (1965) and Robinson and Bower (1966b) differ by 0.04 log units.

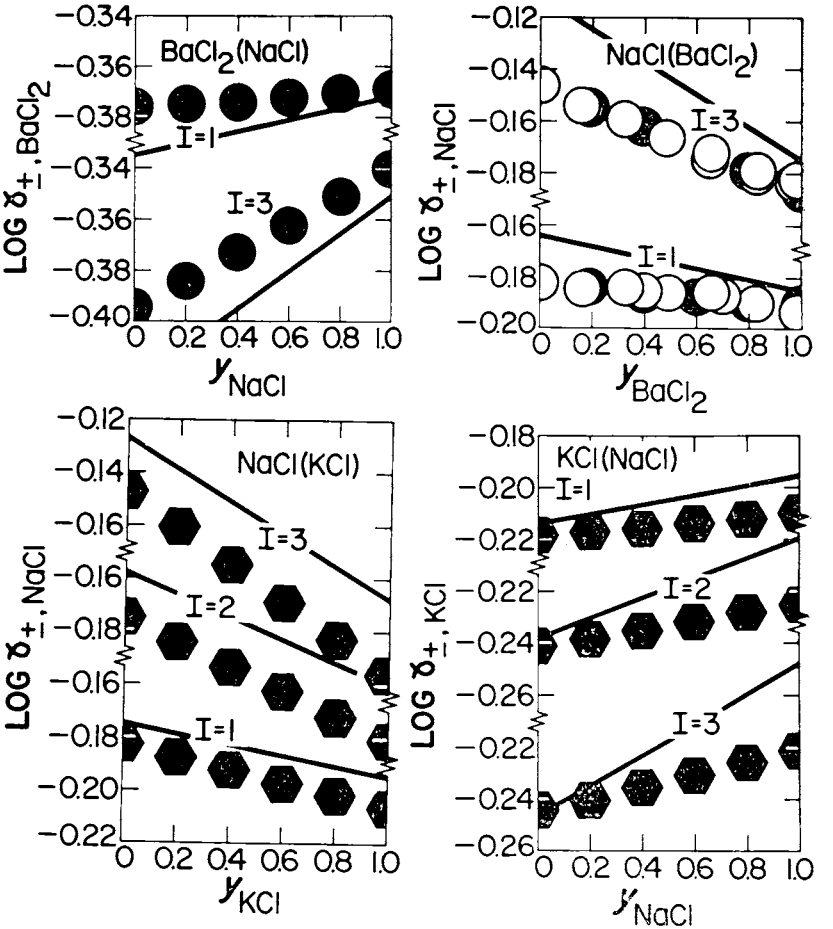

Fig. 40. Predicted (curves) and experimental (symbols) stoichiometric mean activity coefficients of the components of mixed electrolytes at 25°C, 1 bar, and constant ionic strength as a function of the stoichiometric ionic strength fractions of the components (see text and caption of fig. 38).

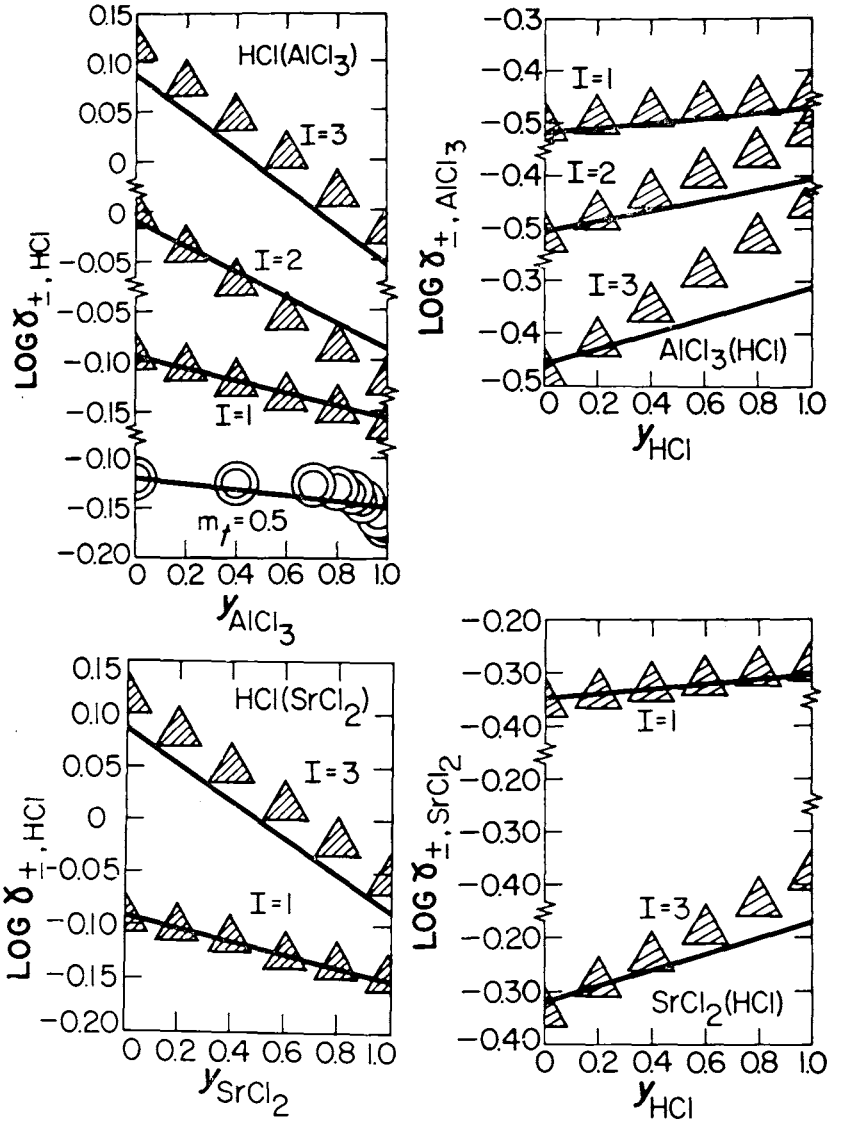

Fig. 41. Predicted (curves) and experimental (symbols) stoichiometric mean activity coefficients of the components of mixed electrolytes at 25°C, 1 bar, and constant ionic strength as a function of the stoichiometric ionic strength fractions of the components (see text and caption of fig. 38).

It can be deduced from figures 38 through 43 that in many cases the errors in the predicted values of log $\gamma_{\pm,k}$ shown in the figures arise solely from $\delta°_k$, which is independent of the composition of the solution. It thus appears (at least in those instances) that eqs (153), (154), (156), and (157) afford accurate representation of the compositional dependence of log $\tilde{\gamma}_{\pm,k}$ at constant $\bar{I} = I$. In other cases, the discrepancies between the trend of the predicted curves and that of the experimental data suggest significant ion association and/or interaction among ions of like charge.

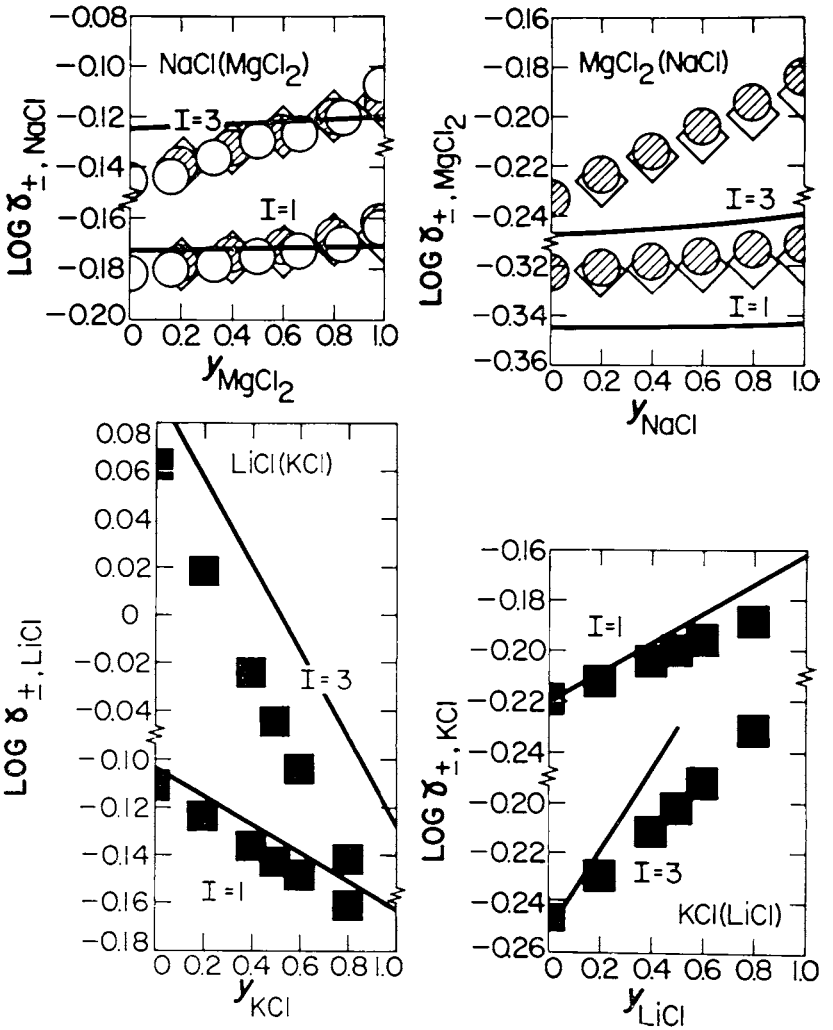

Fig. 42. Predicted (curves) and experimental (symbols) stoichiometric mean activity coefficients of the components of mixed electrolytes at 25°C, 1 bar, and constant ionic strength as a function of the stoichiometric ionic strength fractions of the components (see text and caption of fig. 38).

However, as noted above, the extent to which compositional variation affects $\bar{\gamma}_{\pm,k}$ is for many electrolytes insignificant compared to uncertainties in dissociation constants used in geochemical calculations.

The relative contributions by Γ_γ and the solvation and short-range interaction contributions to log $\bar{\gamma}_{\pm,k}$ at constant $\bar{I} = I$ for a number of mixed electrolytes are depicted in figure 44, where it can be seen that the latter two terms are comparable in magnitude but of opposite sign. Note also that in certain cases at high ionic strength, Γ_γ contributes significantly to log $\bar{\gamma}_{\pm,k}$ by reinforcing the negative contribution by short-range ionic interaction.

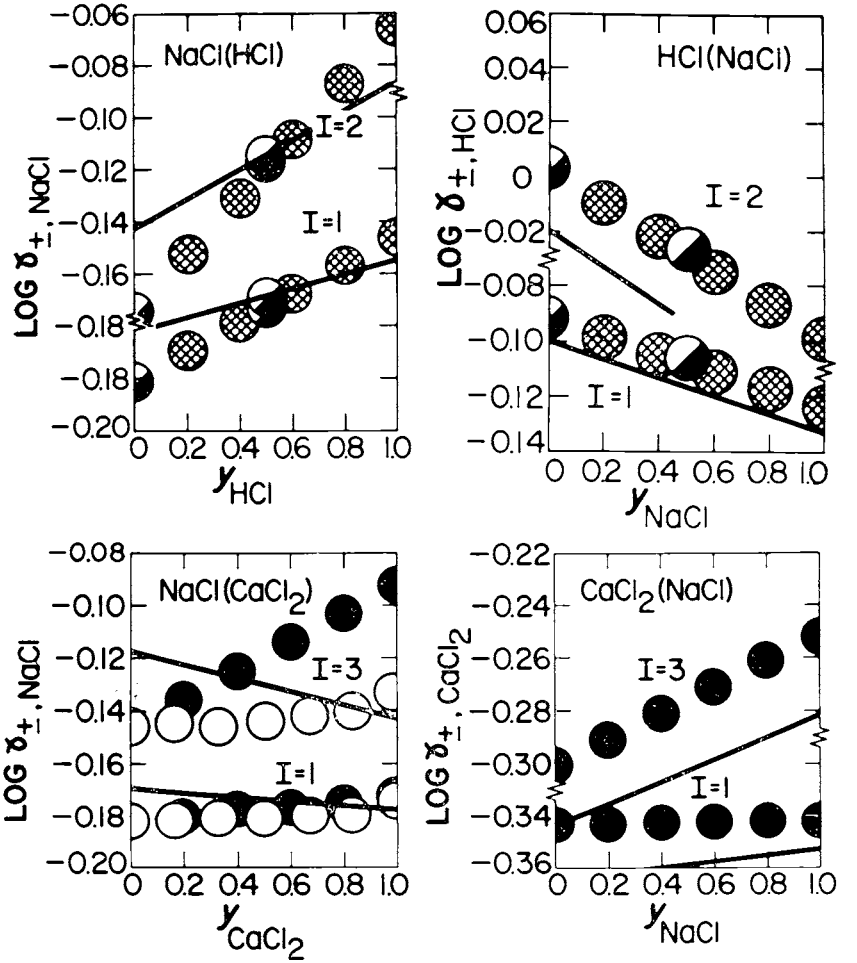

Fig. 43. Predicted (curves) and experimental (symbols) stoichiometric mean activity coefficients of the components of mixed electrolytes at 25°C, 1 bar, and constant ionic strength as a function of the stoichiometric ionic strength fractions of the components (see text and caption of fig. 38).

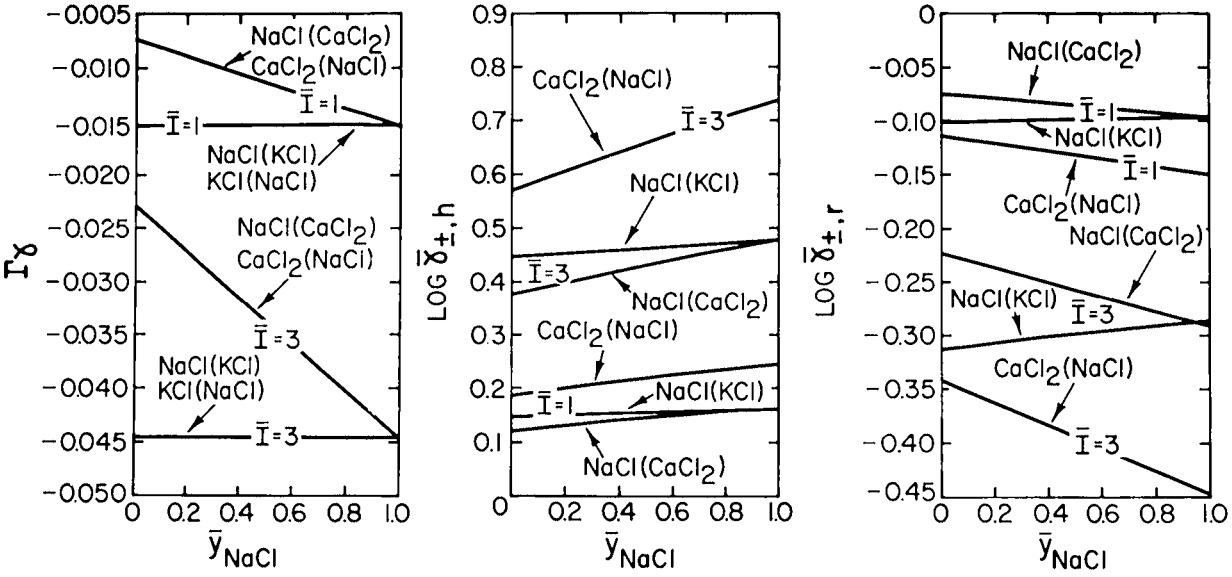

Fig. 44. Calculated contributions by Γ_γ, $\bar{\gamma}_{\pm,h}$, and $\bar{\gamma}_{\pm,r}$ to $\bar{\gamma}_\pm$ of the components of mixed electrolyte solutions at 25°C, 1 bar, and constant "true" ionic strength as a function of the "true" ionic strength fraction of the components. The curves were generated from equations given in the text using parameters taken from tables 3, 4, and 7.

OSMOTIC COEFFICIENTS

Recalling that the subscript j designates only "free" cations and anions, it follows from eqs (111), (160), and (161) that we can write

$$\phi = -\frac{2.303}{m^*}\sum_j m_{t,j}\left(\frac{A_\gamma Z_j^2 I^{1/2}\sigma(\text{å}B_\gamma I^{1/2})}{3} + \frac{\Gamma_\gamma}{0.0180153m^*} - \frac{1}{2}\left(\omega_j\sum_k b_k y_k I + \sum_i b_{ij}m_i + \sum_l b_{jl}m_l\right)\right)$$

$$= -\frac{2.303}{u^*}\sum_j\left(\sum_k \frac{\nu_{j,k}\bar{y}_k}{\psi_k}\right)\left(\frac{A_\gamma Z_j^2 I^{1/2}\sigma(\text{å}B_\gamma I^{1/2})}{3} + \frac{\Gamma_\gamma}{0.0180153m^*} - \frac{I}{2}\left(\omega_j\sum_k b_k y_k + \sum_i \frac{b_{ij}\bar{y}_i}{\psi_i} + \sum_l \frac{b_{jl}\bar{y}_l}{\psi_l}\right)\right) \tag{190}$$

where b_{ij} and b_{jl} correspond to b_{il} above with the stipulation that $b_{ij} = 0$ if j designates a cation but $b_{jl} = 0$ if j designates an anion, and

$$\sigma(\text{å}B_\gamma I^{1/2}) \equiv \frac{3}{\text{å}^3 B_\gamma^3 I^{3/2}}\left(\Lambda - \frac{1}{\Lambda} - 2\ln\Lambda\right) \tag{191}$$

where m^*, Λ, å, and Γ_γ are defined by eqs (107), (121), (124), and (169), and

$$u^* \equiv \sum_j \frac{\bar{y}_j}{\psi_j} + \sum_q \frac{\bar{y}_q}{\psi_q} = \frac{m^*}{I} \tag{192}$$

where the subscript q again designates complexes in solution. Eq (190) can be written for a "completely" dissociated electrolyte or a 1:1 or 2:2 electrolyte in which only a single ion pair forms to a significant degree as

$$\phi = -2.303\left(\frac{|Z_+Z_-|A_\gamma I^{1/2}\sigma(\text{å}B_\gamma I^{1/2})}{3} + \frac{\psi_k\Gamma_\gamma}{0.0180153\nu_k I} - \frac{b_\gamma I}{2}\right). \tag{193}$$

The osmotic coefficient analog of eq (177) for ρ^*_ϕ can now be expressed in terms of eq (193) as

$$\rho^*_\phi \equiv \frac{\phi}{2.303} + \frac{|Z_+Z_-|A_\gamma I^{1/2}\sigma(\text{å}B_\gamma I^{1/2})}{3} + \frac{\psi_k\Gamma_\gamma}{0.0180153\nu_k I}. \tag{194}$$

For the kth completely dissociated single electrolyte solution,

$$\rho^*_\phi = \frac{b_{\gamma,k}I}{2}. \tag{195}$$

Values of ρ^*_ϕ computed from experimental osmotic coefficients at 25°C and 1 bar are plotted against I in figures 45 through 47. As expected,

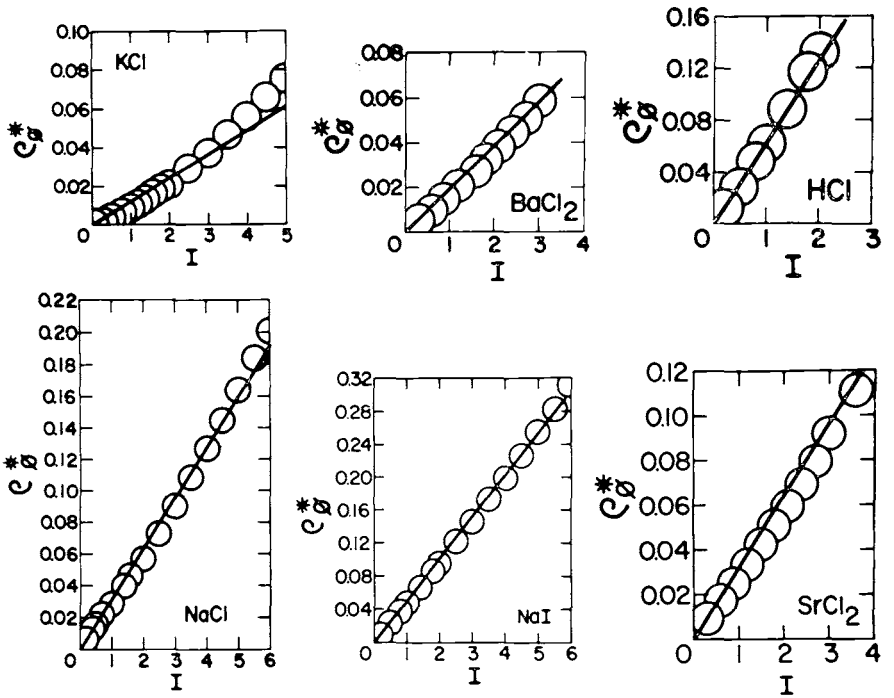

Fig. 45. ρ^*_ϕ (eqs 194 and 195) as a function of stoichiometric ionic strength at 25 °C and 1 bar (see caption of fig. 17.)

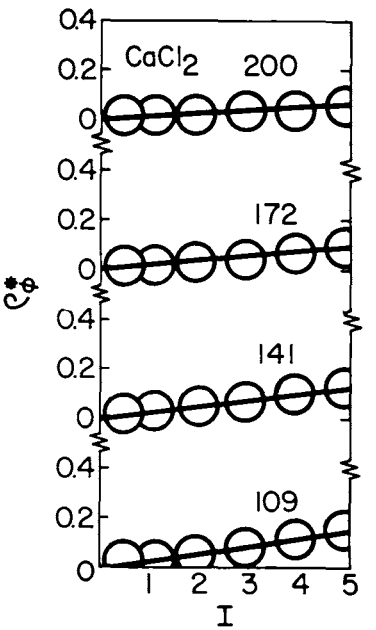

Fig. 46. ρ^*_ϕ (eqs 194 and 195) as a function of stoichiometric ionic strength at pressures corresponding to liquid-vapor equilibrium at the temperatures in °C shown in the figure (see caption of fig. 17).

the slopes of the curves in these figures are consistent with those of the curves representing ρ^*_γ for the same electrolytes in figures 17 through 32. However, the apparent discrepancies between the curves and symbols representing ρ^*_γ are magnified by a factor of 2 in ρ^*_ϕ. The nonlinear distribution of the symbols in figure 47 can be attributed to increasing ion association with increasing concentration (see above). Note in figure 46 that eq (195) is closely consistent with the recent isopiestic measurements reported by Holmes, Baes, and Mesmer (1978) for $CaCl_2$ at temperatures to 200°C. Similarly, experimental osmotic coefficients for NaCl-$BaCl_2$ solutions in figure 48 compare favorably with those predicted independently from eq (190).

RELATIVE PARTIAL MOLAL AND APPARENT MOLAL ENTHALPY, HEAT CAPACITY, VOLUME, COMPRESSIBILITY, AND EXPANSIBILITY

Combining appropriate partial derivatives of eqs (165) and (166) with eqs (B-9) through (B-14) in app. B yields expressions for the relative partial molal volumes, enthalpies, entropies, heat capacities, expansi-

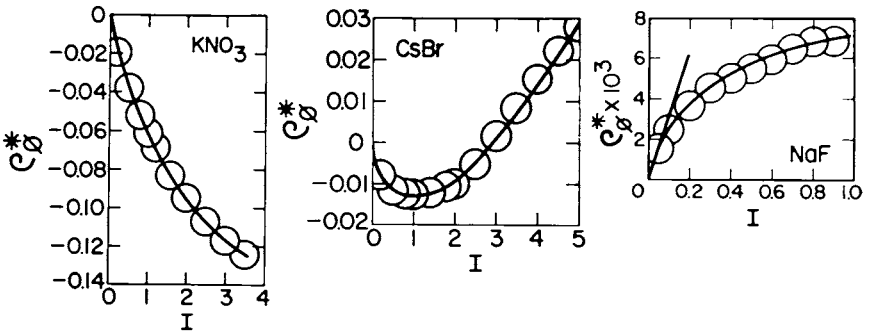

Fig. 47. ρ^*_ϕ (eqs 194 and 195) as a function of stoichiometric ionic strength at 25°C and 1 bar (see caption of fig. 17).

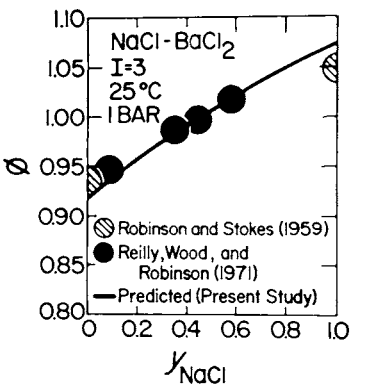

Fig. 48. Calculated (assuming I = I) and experimental osmotic coefficients of NaCl-$BaCl_2$ solutions as a function of the stoichiometric ionic strength fraction of NaCl at 25°C, 1 bar, and I = 3.

bilities, and compressibilities of aqueous ions. Before writing these equations, let us again adopt the index j to designate "free" cations and anions and represent eqs (165) and (166) with the general expression,

$$\log \bar{\gamma}_j = -\frac{A_\gamma Z_j^2 I^{1/2}}{\Lambda} + \Gamma_\gamma + \omega_j \sum_k b_k y_k I + \sum_i \upsilon_{ij} m_i + \sum_l b_{jl} m_l \ , \tag{196}$$

where the subscripts i and l designate cations and anions, respectively, and b_{ij} and b_{jl} correspond to b_{il} in eqs (165) and (166) with the stipulation that $b_{ij} = 0$, if j refers to a cations, but $b_{jl} = 0$ if j designates an anion. If $r_{e,j}$ is independent of temperature and pressure (see above), it follows from eq (196) and those given in app. A, B, and C that we can write,

$$\begin{aligned}\bar{V}_j - \bar{V}^\circ_j{}^{abs} = \psi_j \Big((2\,A_v\,\Lambda I + A_G\,\Lambda I'_T - 2\,A_G\,\Lambda'_T I)/2\,I^{1/2}\,\Lambda^2 \Big) + \Gamma_V \\ + \omega_j{}^{abs} \sum_k (b_{V,k} y_k I + 2\,\hat{b}_k y_k I'_T)/2 + \sum_i (b_{V,ij}\, m_i + 2\hat{b}_{ij}\, m'_{i,T})/2 \\ + \sum_l (b_{V,jl}\, m_l + 2\hat{b}_{jl}\, m'_{l,T})/2 + RT\, m'_{j,T}/m_j \ , \end{aligned} \tag{197}$$

$$\begin{aligned}\bar{L}_j \equiv \bar{H}_j - \bar{H}^\circ_j{}^{abs} = \psi_j \Big((2A_H \Lambda I - A_G T \Lambda I'_P + 2A_G T \Lambda'_P I)/2I^{1/2}\Lambda^2 \Big) - \Gamma_H \\ - \omega_j{}^{abs} \sum_k (b_{H,k} y_k I + 2\hat{b}_k y_k I'_P)/2 - \sum_i (b_{H,ij}\, m_i + 2\hat{b}_{ij}\, m'_{i,P})/2 \\ - \sum_l (b_{H,jl}\, m_l + 2\hat{b}_{jl}\, m'_{l,P})/2 - RT^2\, m'_{j,P}/m_j \ , \end{aligned} \tag{198}$$

and

$$\begin{aligned}\bar{J}_j \equiv \bar{C}_{P,j} - \bar{C}^\circ_{P,j}{}^{abs} = \psi_j \big(((I^{1/2}\Lambda\,(2A_J \Lambda I + 3A_H \Lambda I'_P - 2A_G \Lambda I'_P - A_G T \Lambda I''_P \\ + 4A_G \Lambda'_P I + 2A_G T \Lambda''_P I + A_G T \Lambda'_P I'_P) - (2I^{1/2}\Lambda'_P + (\Lambda I'_P/2I^{1/2}))\,(2A_H \Lambda I \\ - A_G\,T\Lambda I'_P + 2A_G T \Lambda'_P I))/2I\Lambda^3) - \Gamma_J - \omega_j{}^{abs} \sum_k (b_{J,k} y_k I + b_{H,k} y_k I'_P + \\ (((b_{H,k} + 2\hat{b}_k)\, y_k I'_P)/T) + 2\hat{b}_k y_k I''_P)/2 - \sum_i (b_{J,ij}\, m_i + \\ b_{H,ij}\, m'_{i,P} + (((b_{H,ij} + 2\hat{b}_{ij})\, m'_{i,P})/T) + 2\hat{b}_{ij}\, m''_{i,P})/2 \\ - \sum_l (b_{J,jl}\, m_l + b_{H,jl}\, m'_{l,P} + (((b_{H,jl} + 2\hat{b}_{jl})\, m'_{l,P})/T) \\ + 2\hat{b}_{jl}\, m''_{l,P}/2 - 2RT\, m'_{j,P}/m_j - RT^2\, m''_{j,P}/m_j + RT^2\, (m'_{j,P})^2/m_j^2 \end{aligned} \tag{199}$$

where $\hat{b}_k$, $\hat{b}_{ij}$, $\hat{b}_{jl}$, A_G, A_V, $b_{V,k}$, $b_{V,ij}$ $b_{V,jl}$, A_H, $b_{H,k}$, $b_{H,ij}$, $b_{H,jl}$, A_J, $b_{J,k}$, $b_{J,ij}$, and $b_{J,jl}$ are defined in the text and app. C and

$$\Lambda'_T \equiv \left(\frac{\partial \Lambda}{\partial P}\right)_{T,\hat{m}(k)} = \frac{\mathring{a}B_\gamma \bar{I}'_T}{2\bar{I}^{1/2}} + \mathring{a}\bar{I}^{1/2}\left(\frac{\partial B_\gamma}{\partial P}\right)_T , \quad (200)$$

$$\Lambda'_P \equiv \left(\frac{\partial \Lambda}{\partial T}\right)_{P,m(k)} = \frac{\mathring{a}B_\gamma \bar{I}'_P}{2\bar{I}^{1/2}} + \mathring{a}\bar{I}^{1/2}\left(\frac{\partial B_\gamma}{\partial T}\right)_P , \quad (201)$$

and

$$\Lambda''_P \equiv \left(\frac{\partial \Lambda'_P}{\partial T}\right)_P = \frac{\mathring{a}}{2\bar{I}^{1/2}}\left(B_\gamma \bar{I}''_P + \bar{I}'_P\left(\frac{\partial B_\gamma}{\partial T}\right)_P\right) - \frac{\mathring{a}B_\gamma(\bar{I}'_P)^2}{4\bar{I}^{3/2}} + \mathring{a}\bar{I}^{1/2}\left(\frac{\partial^2 B_\gamma}{\partial T^2}\right)_P + \frac{\mathring{a}\bar{I}'_P}{2\bar{I}^{3/2}}\left(\frac{\partial B_\gamma}{\partial T}\right)_P , \quad (202)$$

where $(\partial B_\gamma/\partial P)_T$, $(\partial B_\gamma/\partial T)_P$, and $(\partial^2 B_\gamma/\partial T^2)_P$ correspond to partial derivatives of eq (C-2) in app. C, which can be computed from the values of B_V, B_H, and B_J given by Helgeson and Kirkham (1974b) with the aid of eqs (C-9) through (C-11) in app. C, and

$$\bar{I}'_T \equiv \left(\frac{\partial \bar{I}}{\partial P}\right)_{T,\hat{m}(k)} , \quad (203)$$

$$\bar{I}'_P \equiv \left(\frac{\partial \bar{I}}{\partial T}\right)_{P,\hat{m}(k)} , \quad (204)$$

$$\bar{I}''_P \equiv \left(\frac{\partial \bar{I}'_P}{\partial T}\right)_{P,\hat{m}(k)} , \quad (205)$$

$$m'_{j,T} \equiv \left(\frac{\partial m_j}{\partial P}\right)_{T,\hat{m}(k)} , \quad (206)$$

$$m'_{j,P} \equiv \left(\frac{\partial m_j}{\partial T}\right)_{P,\hat{m}(k)} , \quad (207)$$

and

$$m''_{j,P} \equiv \left(\frac{\partial m'_{j,P}}{\partial T}\right)_{P,\hat{m}(k)} , \quad (208)$$

where the subscript j represents j, i, and l in eqs (197) through (199) and

$$\Gamma_V \equiv -\frac{0.0180153RT}{1 + 0.0180153\, m^*}\left(\frac{\partial m^*}{\partial P}\right)_{T,\hat{m}(k)} , \quad (209)$$

$$\Gamma_H \equiv \frac{0.0180153RT^2}{1 + 0.0180153\, m^*}\left(\frac{\partial m^*}{\partial T}\right)_{P,\hat{m}(k)} , \quad (210)$$

and

$$\Gamma_J = \frac{0.0180153RT^2}{1 + 0.0180153\, m^*}\left(\frac{\partial^2 m^*}{\partial T^2}\right)_{P,\hat{m}(k)} + \frac{0.0180153RT}{1 + 0.0180153\, m^*}\left(\frac{\partial m^*}{\partial T}\right)_{P,\hat{m}(k)}$$

$$-\frac{0.0180153^2 RT^2}{(1+0.0180153\,m^*)^2}\left(\frac{\partial m^*}{\partial T}\right)^2_{P,\hat{m}(k)} \tag{211}$$

where

$$\left(\frac{\partial m^*}{\partial P}\right)_{T,\hat{m}(k)} = \sum_j m'_{j,T} + \sum_q m'_{q,T} \tag{212}$$

$$\left(\frac{\partial m^*}{\partial T}\right)_{P,\hat{m}(k)} = \sum_j m'_{j,P} + \sum_q m'_{q,P} \tag{213}$$

and

$$\left(\frac{\partial^2 m^*}{\partial T^2}\right)_{P,\hat{m}(k)} = \sum_j m''_{j,P} + \sum_q m''_{q,P} \tag{214}$$

where $m'_{q,T}$, $m'_{q,P}$, and $m''_{q,P}$ correspond to the analogs for the qth complex of $m'_{j,T}$, $m'_{j,P}$, and $m''_{j,P}$ for the jth ion in eqs (206) through (208). Similar equations can be written for the relative partial molal expansibility and compressibility of the jth ion.

Eqs (197) through (199) permit calculation of the relative partial molal properties of all the components of an electrolyte solution from conservation of mass constraints and the partial derivatives of the law of mass action for the dissociation of complexes in solution. The law of mass action for dissociation of the qth aqueous complex can be written as

$$\frac{\prod_j m_j^{\nu_{j,q}} \bar{\gamma}_j^{\nu_{j,q}}}{m_q \bar{\gamma}_q} = \beta_q\ , \tag{214A}$$

which is consistent with

$$\sum_j \frac{\nu_{j,q}(\bar{V}_j - \bar{V}^\circ_j{}^{abs})}{RT} - \frac{\bar{V}_q - \bar{V}^\circ_q{}^{abs}}{RT} = \frac{\Delta\bar{V}^\circ_{r,q}}{RT}\ , \tag{214B}$$

$$\frac{\bar{L}_q}{RT^2} - \sum_j \frac{\nu_{j,q}\bar{L}_j}{RT^2} = \frac{\Delta\bar{H}^\circ_{r,q}}{RT^2}\ , \tag{214C}$$

and

$$\sum_j \left(\frac{2\nu_{j,q}\bar{L}_j}{RT^3} - \frac{\nu_{j,q}\bar{J}_j}{RT^2}\right) + \frac{\bar{J}_q}{RT^2} - \frac{2\bar{L}_q}{RT^3} = \frac{\Delta\bar{C}^\circ_{P,r,q}}{RT^2} - \frac{2\Delta\bar{H}^\circ_{r,q}}{RT^3} \tag{214D}$$

where β_q, $\Delta\bar{V}^\circ_{r,q}$, $\Delta\bar{H}^\circ_{r,q}$, and $\Delta\bar{C}^\circ_{P,r,q}$ stand for the overall standard molal dissociation constant and standard partial molal volume, enthalpy, and isobaric heat capacity of dissociation for the qth aqueous complex, and

$$\bar{V}_q - \bar{V}^\circ_q{}^{abs} = RT\left(\left(\frac{\partial\, ln\, \bar{\gamma}_q}{\partial P}\right)_{T,\hat{m}(k)} + \frac{m'_{q,T}}{m_q}\right)\ , \tag{214E}$$

$$\bar{L}_q \equiv \bar{H}_q - \bar{H}^{\circ}{}_q{}^{abs} = -RT^2\left(\left(\frac{\partial \ln \bar{\gamma}_q}{\partial T}\right)_{P,\hat{m}(k)} + \frac{m'_{q,P}}{m_q}\right), \tag{214F}$$

and

$$\bar{J}_q \equiv \bar{C}_{P,q} - \bar{C}^{\circ}{}_{P,q}{}^{abs} = -R\left(2T\left(\left(\frac{\partial \ln \bar{\gamma}_q}{\partial T}\right)_{P,\hat{m}(k)} + \frac{m'_{q,P}}{m_q}\right) + T^2\left(\left(\frac{\partial^2 \ln \bar{\gamma}_q}{\partial T^2}\right)_{P,\hat{m}(k)} + \frac{m''_{qP}}{m_q} - \frac{m'_{q,P}{}^2}{m_q{}^2}\right)\right) \tag{214G}$$

where $m'_{q,T}$, $m'_{q,P}$, and $m''_{q,P}$ represent the analogs for the qth aqueous complex of $m'_{j,T}$, $m'_{j,P}$, and $m''_{j,P}$ defined by eqs (206) through (208), and $(\partial \ln \bar{\gamma}_q/\partial P)_{T,\hat{m}(k)}$, $(\partial \ln \bar{\gamma}_q/\partial T)_{P,\hat{m}(k)}$, and $(\partial^2 \ln \bar{\gamma}_q/\partial T^2)_{P,\hat{m}(k)}$ correspond to partial derivatives (multiplied by 2.303) of eqs (165), (166), or (167), depending on the charge (or lack thereof) on the qth aqueous species. For example, in the case of a single 1:1 or 2:2 electrolyte denoted by the subscript k in which only one ion pair forms to a significant degree, it follows that we can substitute q for n in eq (175) and write

$$\left(\frac{\partial \ln \bar{\gamma}_q}{\partial P}\right)_{T,\hat{m}(k)} = \frac{\Gamma_V}{RT} + \frac{b_{V,q}\bar{I}}{2RT} + b_{\gamma,q}\bar{I}'_T, \tag{214H}$$

$$\left(\frac{\partial \ln \bar{\gamma}_q}{\partial T}\right)_{P,\hat{m}(k)} = -\frac{\Gamma_H}{RT^2} + \frac{b_{H,q}\bar{I}}{2RT^2} + b_{\gamma,q}\bar{I}'_P, \tag{214I}$$

and

$$\left(\frac{\partial^2 \ln \bar{\gamma}_q}{\partial T^2}\right)_{P,\hat{m}(k)} = \frac{T\Gamma_J - 2\Gamma_H}{RT^3} + \frac{b_{J,q}\bar{I}}{2RT^2} - \frac{b_{H,q}\bar{I}}{RT^3} + \frac{b_{H,q}\bar{I}'_P}{2RT^2} + b_{\gamma,q}\bar{I}''_P \tag{214J}$$

where $\bar{I}'_T$, $\bar{I}'_P$, and $\bar{I}''_P$ are defined by eqs (203) through (205) and

$$b_{V,q} \equiv 2(2.303)RT\left(\frac{\partial b_{\gamma,q}}{\partial P}\right)_T = \frac{\omega_q{}^{abs}\psi_k b_{V,k} + \nu_{i,k}b_{V,qi} + \nu_{l,k}b_{V,ql}}{\psi_k}, \tag{214K}$$

$$b_{H,q} \equiv 2(2.303)RT^2\left(\frac{\partial b_{\gamma,q}}{\partial T}\right)_P = \frac{\omega_q{}^{abs}\psi_k b_{H,k} + \nu_{i,k}b_{H,qi} + \nu_{l,k}b_{V,ql}}{\psi_k} \tag{214L}$$

and

$$b_{J,q} \equiv \left(\frac{\partial b_{H,q}}{\partial T}\right)_P = \frac{\omega_q{}^{abs}\psi_k b_{J,k} + \nu_{i,k}b_{J,qi} + \nu_{l,k}b_{J,ql}}{\psi_k} \tag{214M}$$

where $b_{V,k}$, $b_{H,k}$, and $b_{J,k}$ are defined by eqs (C-15) through (C-17) in app. C, $\omega_q{}^{abs}$ stands for the analog of $\omega_n{}^{abs}$ for the qth aqueous complex, ν_i and ν_l refer to the number of moles of the cation and anion, respectively (mole of the kth electrolyte)$^{-1}$, and $b_{V,qi}$, $b_{V,ql}$, $b_{H,qi}$, $b_{H,ql}$, $b_{J,qi}$, and $b_{J,ql}$ correspond to short-range interaction parameters for the qth, ith, and lth aqueous species analogous to those defined for the jth and $\hat{j}$th species by eqs (C-20) through (C-22) in app. C.

Note that in addition to eqs (214H) through (214M), we can also write for the kth 1:1 or 2:2 electrolyte in which a single ion pair forms to a significant degree,

$$\bar{\mathrm{I}} = \psi_k m_i = \psi_k m_l \ , \tag{215}$$

$$\mathrm{I} = \psi_k m_k = \psi_k m_i + \psi_k m_q \ , \tag{216}$$

$$m^* = (\mathrm{I} + \bar{\mathrm{I}})/\psi_k \tag{217}$$

and

$$m_q = (\mathrm{I} - \bar{\mathrm{I}})/\psi_k \tag{218}$$

where i, l, and q again refer to the cation, anion, and ion pair, respectively, in the kth electrolyte. Hence,

$$\bar{\mathrm{I}}'_{\mathrm{T}}/\psi_k = m'_{i,\mathrm{T}} = m'_{l,\mathrm{T}} = -m'_{q,\mathrm{T}} = \left(\frac{\partial m^*}{\partial \mathrm{P}}\right)_{\mathrm{T},\hat{m}(k)} \ , \tag{219}$$

$$\bar{\mathrm{I}}'_{\mathrm{P}}/\psi_k = m'_{i,\mathrm{P}} = m'_{l,\mathrm{P}} = -m'_{q,\mathrm{P}} = \left(\frac{\partial m^*}{\partial \mathrm{T}}\right)_{\mathrm{P},\hat{m}(k)} \ , \tag{220}$$

and

$$\bar{\mathrm{I}}''_{\mathrm{P}}/\psi_k = m''_{i,\mathrm{P}} = m''_{l,\mathrm{P}} = -m''_{q,\mathrm{P}} = \left(\frac{\partial^2 m^*}{\partial \mathrm{T}^2}\right)_{\mathrm{P},\hat{m}(k)} \ . \tag{221}$$

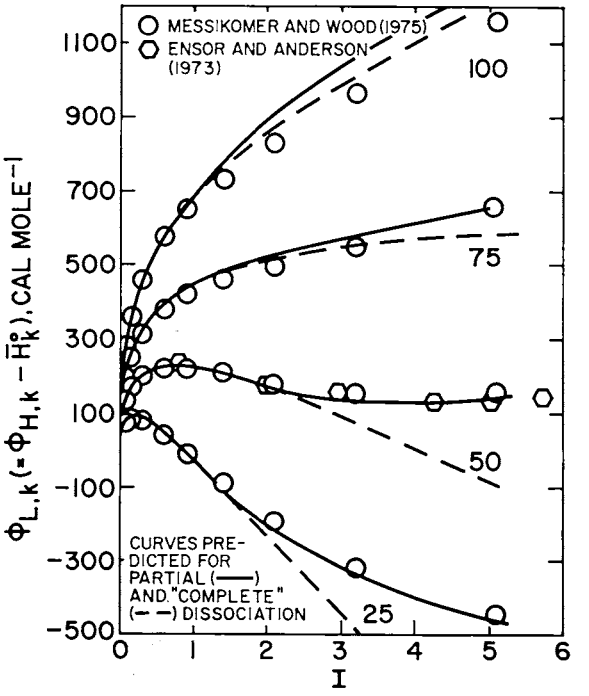

Fig. 49. Relative apparent molal enthalpy of NaCl as a function of stoichiometric ionic strength at 1 bar and 25°, 50°, 75°, and 100°C. The solid and dashed curves, respectively, were generated with and without provision for ion association from equations given in the text.

The equations summarized above permit calculation of the relative partial molal properties of aqueous electrolytes from standard partial molal properties of dissociation and the regression parameters summarized below. Integration of eqs (197) through (199) with respect to $\bar{I}$ at constant pressure, temperature, and $\bar{y}_k$ permits calculation of the apparent molal properties of the solute and the relative partial molal properties of the solvent from eqs (103) and (104). Values of ϕ_L computed in this way for NaCl can be compared with their experimental counterparts in figure 49, where it can be seen that the calculated relative apparent molal enthalpies are in close agreement with those reported by Messikomer and Wood (1975) at temperatures to 100°C. It is also apparent in figure 49 that ϕ_L for NaCl is affected dramatically by ion association as a function of concentration and temperature. The parameters used to generate the curves shown in figure 49 are derived below, together with equations for extending the calculations to 5 kb and 600°C. The latter equations together with eq (96) permit comprehensive prediction of the densities and heat capacities of NaCl solutions at high pressures and temperatures (Helgeson, 1981).

The relative partial molal properties of the kth "completely" dissociated single electrolyte for which å is independent of pressure and temperature can be computed from

$$\bar{V}_k - \bar{V}^\circ_k = \frac{\psi_k A_V \bar{I}^{1/2}}{\Lambda} + \frac{\psi_k A_\gamma å B_V \bar{I}}{\Lambda^2} + \frac{\nu_k b_{V,k} \bar{I}}{2}, \tag{222}$$

$$\bar{L}_k \equiv \bar{H}_k - \bar{H}^\circ_k = \frac{\psi_k A_H \bar{I}^{1/2}}{\Lambda} - \frac{\psi_k A_\gamma å B_H \bar{I}}{\Lambda^2} - \frac{\nu_k b_{H,k} \bar{I}}{2}, \tag{223}$$

$$\bar{J}_k \equiv \bar{C}_{P,k} - \bar{C}^\circ_{P,k} = \frac{\psi_k A_J \bar{I}^{1/2}}{\Lambda} - \frac{\psi_k å (2A_H B_H - A_G B_J T)\bar{I}}{2(2.303)RT^2\Lambda^2} + \frac{\psi_k A_\gamma å^2 B_H^2 \bar{I}^{3/2}}{2.303RT^2\Lambda^3} - \frac{\nu_k b_{J,k} \bar{I}}{2} \tag{224}$$

$$\bar{E}_{x,k} - \bar{E}^\circ_{x,k} = \frac{\psi_k A_{E_x} \bar{I}^{1/2}}{\Lambda} - \frac{\psi_k å (A_V B_H - A_H B_V + A_G B_{E_x} T)\bar{I}}{2(2.303)RT^2\Lambda^2} - \frac{\psi_k A_\gamma å^2 B_H B_V \bar{I}^{3/2}}{2.303RT^2\Lambda^3} + \frac{\nu_k b_{E_x,k} \bar{I}}{2} \tag{225}$$

and

$$-(\bar{\kappa}_k - \bar{\kappa}^\circ_k) = \frac{\psi_k A_\kappa \bar{I}^{1/2}}{\Lambda} - \frac{\psi_k å (2A_V B_V + A_G B_\kappa)\bar{I}}{2(2.303)RT\Lambda^2} - \frac{\psi_k A_\gamma å^2 B_V \bar{I}^{3/2}}{2.303RT\Lambda^3} - \frac{\nu_k b_{\kappa,k} \bar{I}}{2} \tag{226}$$

where A_V, B_V, $b_{V,k}$, A_H, B_H, $b_{H,k}$, A_J, B_J, $b_{J,k}$, A_{E_x}, B_{E_x}, $b_{E_x,k}$, A_κ, B_κ, and $b_{\kappa,k}$ are defined by eqs (C-4) through (C-13) and (C-26) through (C-30) in app. C. Eqs (222) through (226) follow from eqs (B-2) through (B-7) in app. B and the partial derivatives of eq (173) at constant $I = \bar{I}$.

Taking account of eqs (103) and (222) through (226), the apparent molal volume, enthalpy, heat capacity, expansibility, and compressibility of the solute in a single "completely" dissociated electrolyte solution can be expressed as

$$\phi_{V,k} = \bar{V}^\circ_k + \psi_k A_V \bar{I}^{1/2} \bar{\alpha}^* + 2\psi_k A_\gamma B_V \overline{\beta}(\mathring{a}B_\gamma \bar{I}^{1/2}) + \frac{\nu_k b_{V,k} \bar{I}}{4} , \quad (227)$$

$$\phi_{H,k} = \bar{H}^\circ_k + \psi_k A_H \bar{I}^{1/2} \bar{\alpha}^* - 2\psi_k A_\gamma B_H \overline{\beta}(\mathring{a}B_\gamma \bar{I}^{1/2}) - \frac{\nu_k b_{H,k} \bar{I}}{4} , \quad (228)$$

$$\phi_{C_P,k} = \bar{C}^\circ_{P,k} + \psi_k A_J \bar{I}^{1/2} \bar{\alpha}^* - \frac{\psi_k (2A_H B_H - A_G B_J T) \overline{\beta}(\mathring{a}B_\gamma \bar{I}^{1/2})}{2.303RT^2}$$

$$+ \frac{2\psi_k A_\gamma B_H^2 \overline{\zeta}(\mathring{a}B_\gamma \bar{I}^{1/2})}{2.303RT^2} - \frac{\nu_k b_{J,k} \bar{I}}{4} , \quad (229)$$

$$\phi_{E_x,k} = \bar{E}^\circ_{x,k} + \psi_k A_{E_x} \bar{I}^{1/2} \bar{\alpha}^* - \frac{\psi_k (A_V B_H - A_H B_V + A_G B_{E_x} T) \overline{\beta}(\mathring{a}B_\gamma \bar{I}^{1/2})}{2.303RT^2}$$

$$- \frac{2\psi_k A_\gamma B_V B_H \overline{\zeta}(\mathring{a}B_\gamma \bar{I}^{1/2})}{2.303RT^2} + \frac{\nu_k b_{E_x,k} \bar{I}}{4} , \quad (230)$$

and

$$-\phi_{\kappa,k} = -\bar{\kappa}^\circ_k + \psi_k A_\kappa \bar{I}^{1/2} \bar{\alpha}^* - \frac{\psi_k (2A_V B_V + A_G B_\kappa) \overline{\beta}(\mathring{a}B_\gamma \bar{I}^{1/2})}{2.303RT}$$

$$- \frac{2\psi_k A_\gamma B_V^2 \overline{\zeta}(\mathring{a}B_\gamma \bar{I}^{1/2})}{2.303RT} - \frac{\nu_k b_{\kappa,k} \bar{I}}{4} \quad (231)$$

where

$$\bar{\alpha}^* \equiv \frac{1}{\Lambda} - \frac{\sigma(\mathring{a}B_\gamma \bar{I}^{1/2})}{3} \quad (232)$$

$$\overline{\beta}(\mathring{a}B_\gamma \bar{I}^{1/2}) \equiv \frac{1}{\mathring{a}^3 B_\gamma^4 \bar{I}} \left(\frac{\Lambda^2}{2} - 3\Lambda + \frac{1}{\Lambda} + 3 \ln \Lambda + 1.5 \right) \quad (233)$$

and

$$\overline{\zeta}(\mathring{a}B_\gamma \bar{I}^{1/2}) \equiv \frac{1}{\mathring{a}^3 B_\gamma^5 \bar{I}} \left(\frac{\Lambda^2}{2} - 4\Lambda + 6 \ln \Lambda + \frac{4}{\Lambda} - \frac{1}{2\Lambda^2} \right) \quad (234)$$

where $\sigma(\mathring{a}B_\gamma \bar{I}^{1/2})$ is defined by eq (191).

Evaluation of Extended Term Parameters

Calculation of activity coefficients at high pressures and temperatures from the theoretical equations derived above requires equations of state to represent A_γ, B_γ, $b_{\gamma,k}$, b_k, b_{il}, and their partial derivatives as a function of pressure and temperature. These equations have already been derived for the Debye-Hückel parameters (table 1) from the thermodynamic/electrostatic properties of H_2O (Helgeson and Kirkham, 1974b). However, because values of $b_{\gamma,k}$, b_k, b_{il}, and their partial derivatives cannot yet be calculated *a priori* from theoretical considerations, derivation of corresponding equations for the extended term parameters (see below) requires

analysis of experimental enthalpy, heat capacity, volume, and compressibility data for a large number of electrolytes to assess the behavior of these parameters as a function of pressure and temperature.

Enthalpy.—The enthalpy analog of ρ^*_γ and ρ^*_ϕ (ρ^*_H) for the kth "completely" dissociated single electrolyte is given by

$$\rho^*_{H,k} \equiv \phi_{H,k} - \psi_k A_H I^{1/2} \bar{\alpha}^* + 2\psi_k A_\gamma B_H \overline{\beta}(\mathring{a}B_\gamma I^{1/2}) = \bar{H}^\circ_k - \frac{\nu_k b_{H,k} I}{4} \quad (235)$$

which can also be expressed in terms of the heat of dilution of the electrolyte ($\Delta H_{d,k}$) by first taking account of the identity,

$$\Delta H_{d,k} = \phi_{H,k,f} - \phi_{H,k,i} \quad (236)$$

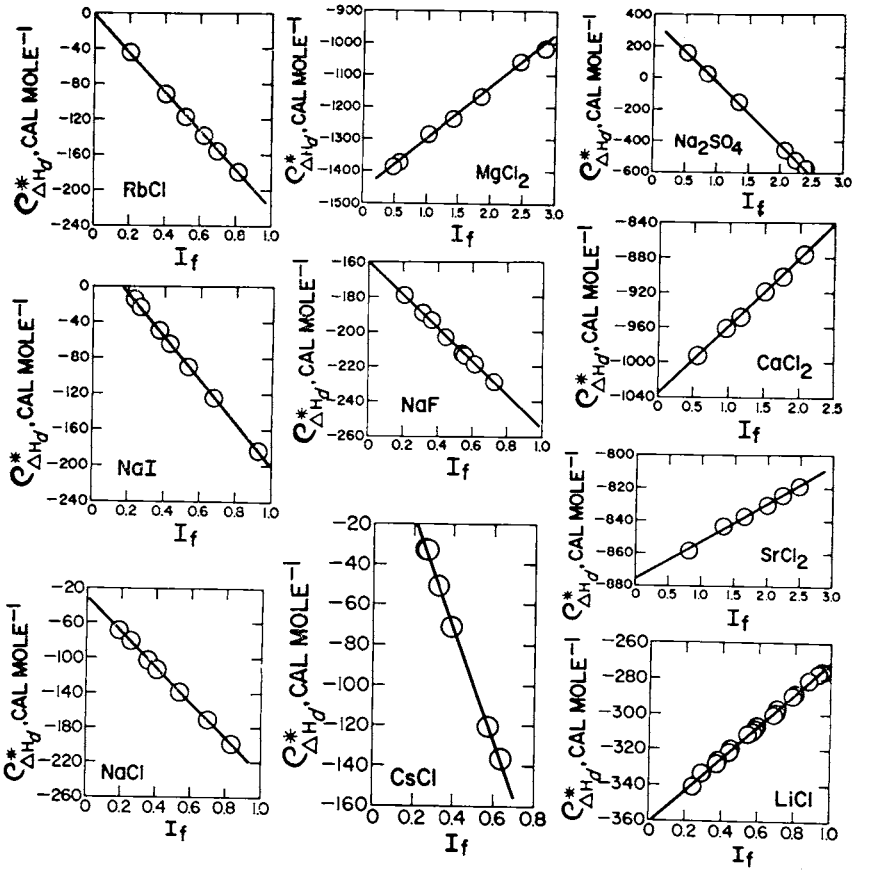

Fig. 50. $\rho^*_{\Delta H_d}$ (eq 237) computed (assuming I = I) from heats of dilution reported by Leung and Millero (1975a and b) as a function of the ionic strength of the solution after dilution from the same initial concentration at 30°C and 1 bar.

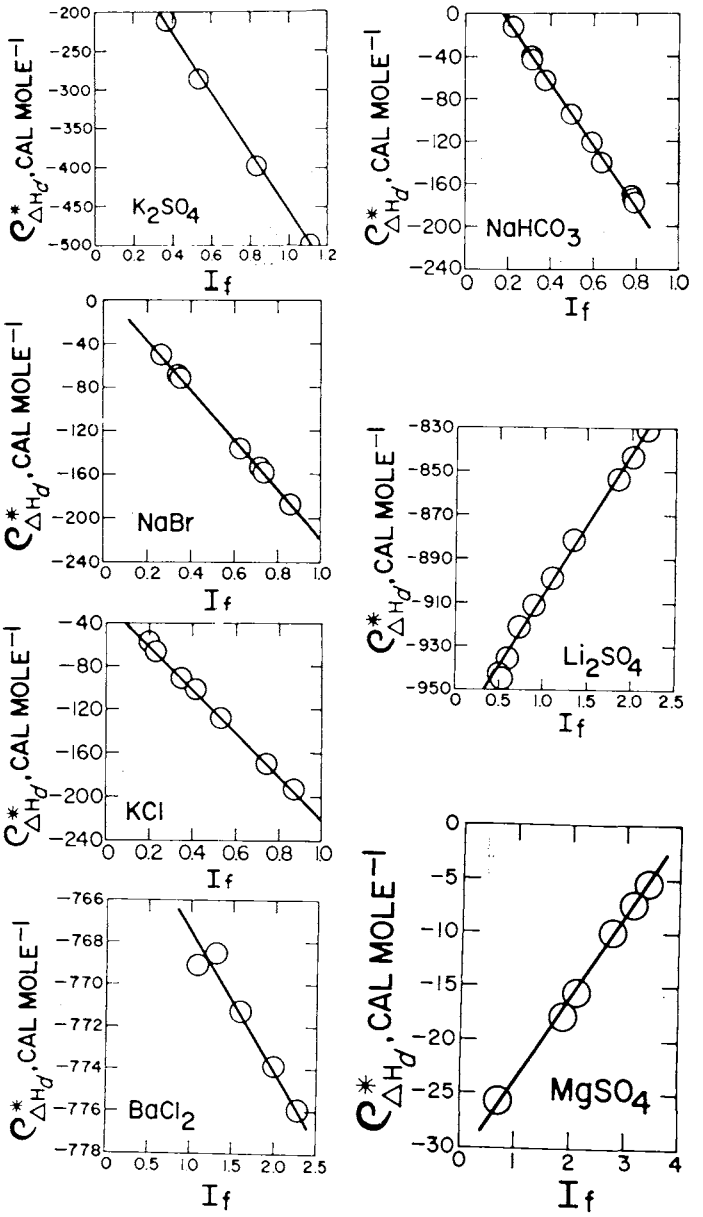

Fig. 51. $\rho^*_{\Delta H_d}$ (eq 237) computed (assuming I = I) from heats of dilution reported by Leung and Millero (1975a and b) as a function of the ionic strength of the solution after dilution from the same initial concentration at 30°C and 1 bar.

where A_H, A_γ, B_H, and b_H are defined in app. C, $\bar{\alpha}^*$ and $\overline{\beta}(\mathring{a}B_\gamma \bar{I}^{1/2})$ are given by eqs (232) and (233), and the subscripts i and f stand for the *initial* and *final* states of the system. It follows from eqs (235) and (236) that

$$\begin{aligned}\rho^*_{\Delta H_d,k} &\equiv \rho^*_{H,k,f} - \rho^*_{H,k,i} \\ &= \Delta H_{d,k} - \psi_k A_H(\bar{I}_f^{1/2}\bar{\alpha}^*_f - \bar{I}_i^{1/2}\bar{\alpha}^*_i) \\ &\quad + 2\psi_k A_\gamma B_H(\overline{\beta}(\mathring{a}B_\gamma \bar{I}^{1/2})_f - \overline{\beta}(\mathring{a}B_\gamma \bar{I}^{1/2})_i) \\ &= \frac{\nu_k b_{H,k}(\bar{I}_i - \bar{I}_f)}{4} . \end{aligned} \tag{237}$$

Hence, for constant $\bar{I}_i$, a plot of $\rho^*_{\Delta H_d,k}$ against $\bar{I}_f$ should yield a straight line with a slope and intercept equal to $-\nu_k b_{H,k}/4$ and $\nu_k b_{H,k}\bar{I}_i/4$, respectively. Curves of this kind are depicted in figures 50 and 51, which were generated assuming $\bar{I} = I$ from heats of dilution at 30°C and 1 bar given by Leung and Millero (1975a and b) using Debye-Hückel parameters taken from table 1. It can be deduced from these figures that eq (237) is closely consistent with the experimental data for all 17 electrolytes. Similar agreement is apparent in figures 52 and 53 between eq (237) and values of $\rho^*_{\Delta H_d,k}$ for $\bar{I}_f \approx 0$ at 25°C and 1 bar reported by Parker (1965) and Lewis and Randall (1961). However, it can be seen in figures 54 and 55 that the heats of dilution given by Fortier, Leduc, and Desnoyers (1974) for NaCl, RbBr, RbCl, RbI, CsBr, LiCl, LiBr, and CsI at 25°C and 1 bar are consistent with eq (237) only at values of $(I_i - I_f) > 0.1$. In contrast, their

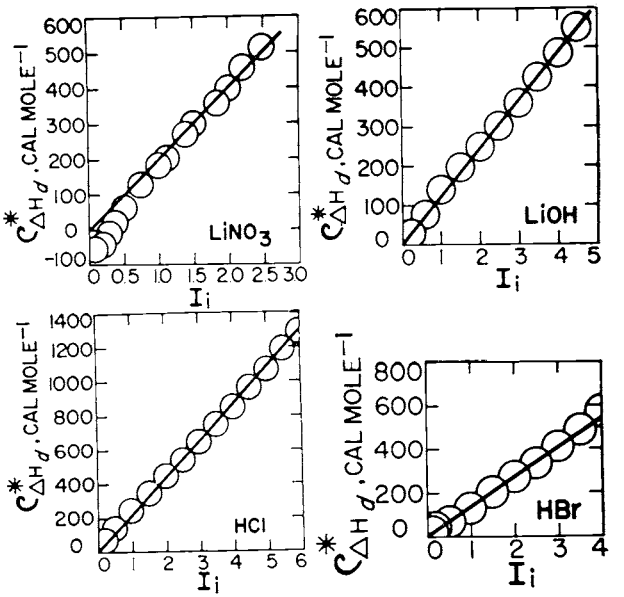

Fig. 52. $\rho^*_{\Delta H_d}$ (eq 237) computed (assuming $I = \bar{I}$) from heats of dilution reported by Parker (1965) as a function of the ionic strength of the solution before diluting to "infinite" dilution at 25°C and 1 bar.

data for NaF, RbF, CsF, and NaI closely represent the values of $\rho^*_{\Delta H_d,k}$ at low values of $I_i - I_f$.

Comparison of figures 50, 51, 54, and 55 indicates that the experimental data reported by Fortier, Leduc, and Desnoyers (1974) for dilute solutions of NaCl, LiCl, and RbCl are inconsistent with the experimental heats of dilution reported by Leung and Millero (1975a and b). Nevertheless, the slopes of all the linear curves in figures 54 and 55 are compatible with those shown for the same electrolytes in figure 50 (see below). However, because $\rho^*_{\Delta H_d}$ is plotted against $I_i - I_f$ in figures 54 and 55, the curves in these figures should pass through the origin. It can be seen that the distribution of the symbols representing the experimental data for NaCl, LiCl, and RbCl in figures 54 and 55 precludes a zero intercept for curves with slopes consistent with those for these electrolytes in figure 50.

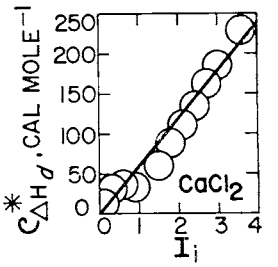

Fig. 53. $\rho^*_{\Delta H_d}$ (eq 237) computed (assuming I = Ī) from heats of dilution taken from Lewis and Randall (1961) as a function of the ionic strength of the solutions before diluting to "infinite" dilution at 25°C and 1 bar.

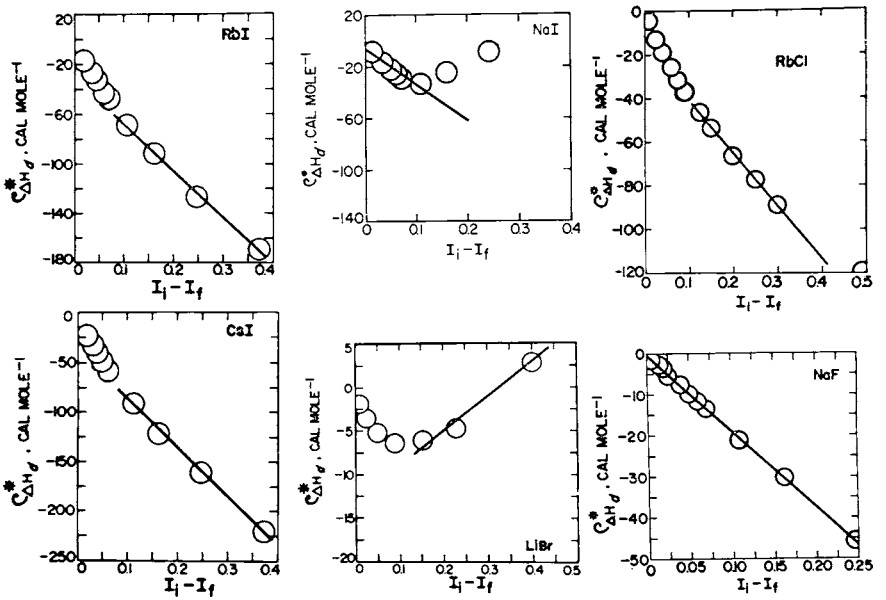

Fig. 54. $\rho^*_{\Delta H_d}$ (eq 237) computed (assuming I = Ī) from heats of dilution reported by Fortier, Leduc, and Desnoyers (1974) as a function of the difference between the initial and final ionic strengths of the solution at 25°C and 1 bar.

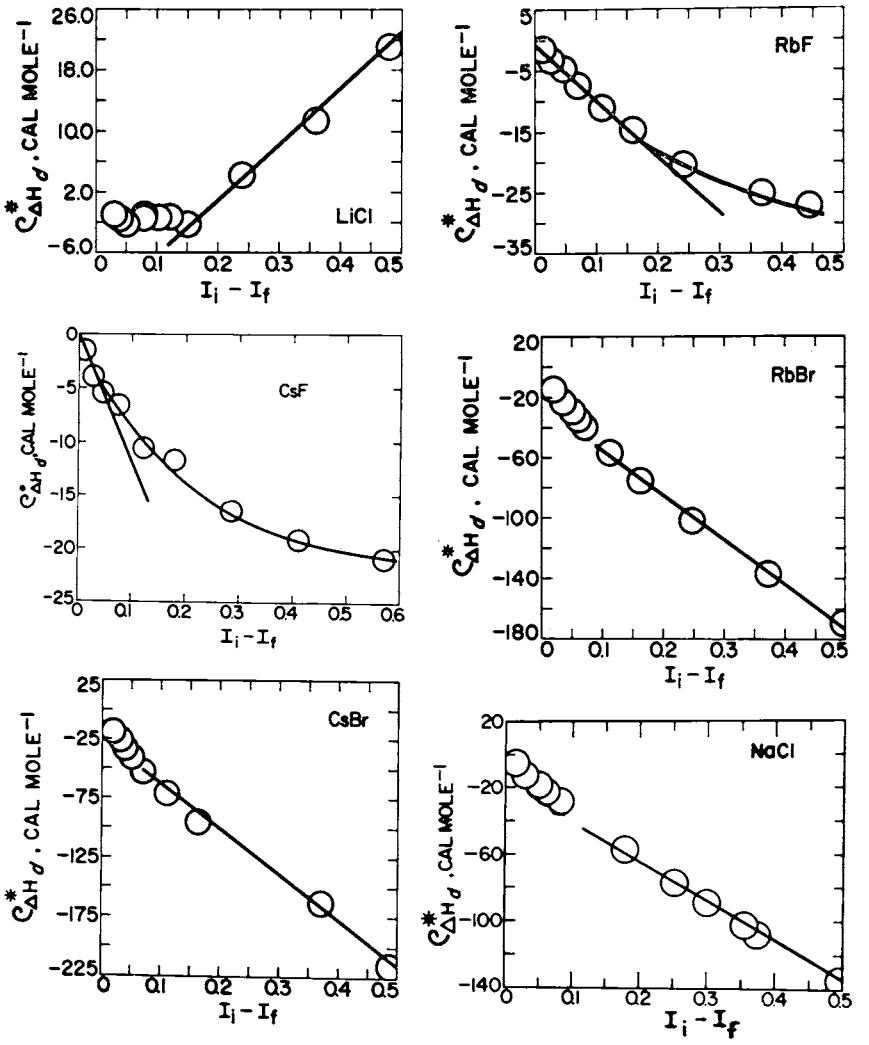

Fig. 55. $\rho^*_{\Delta H_d}$ (eq 237) computed (assuming I = Ī) from heats of dilution reported by Fortier, Leduc, and Desnoyers (1974) as a function of the difference between the initial and final ionic strengths of the solution at 25°C and 1 bar.

It thus appears that in certain cases the curvature in the distribution of data points in figures 54 and 55 is a consequence of *relatively* large uncertainties attending measurement of ΔH_d at small values of $I_i - I_f$. In others (such as RbF and CsF) it almost certainly results from changes in the degree of formation of complexes during the dilution process (see below).

If $\Delta\bar{H}^\circ_{r,q}$ in eq (214C) is positive, dissociation of complexes accompanying dilution commonly causes $\rho^*_{\Delta H_d}$ as a function of I_i to depart from linearity toward less negative values with increasing concentration. This behavior is exhibited by all the electrolytes shown in figures 56 through 60. All the linear curves shown in these figures for a given electrolyte are consistent with one another. Note that in the case of both LiCl and NaCl, the change in the departure from linearity with increasing temperature is consistent with an extremum in the curves representing log K_{LiCl° and log K_{NaCl° as a function of temperature, which leads to negative values of $\Delta\bar{H}^\circ_{r,LiCl^\circ}$ and $\Delta\bar{H}^\circ_{r,NaCl^\circ}$ at high temperatures. In the case of NaCl, the existence of such an extremum can be verified independently (see below). Note also in figures 59 and 60 that the values of $\rho^*_{\Delta H_d}$ for

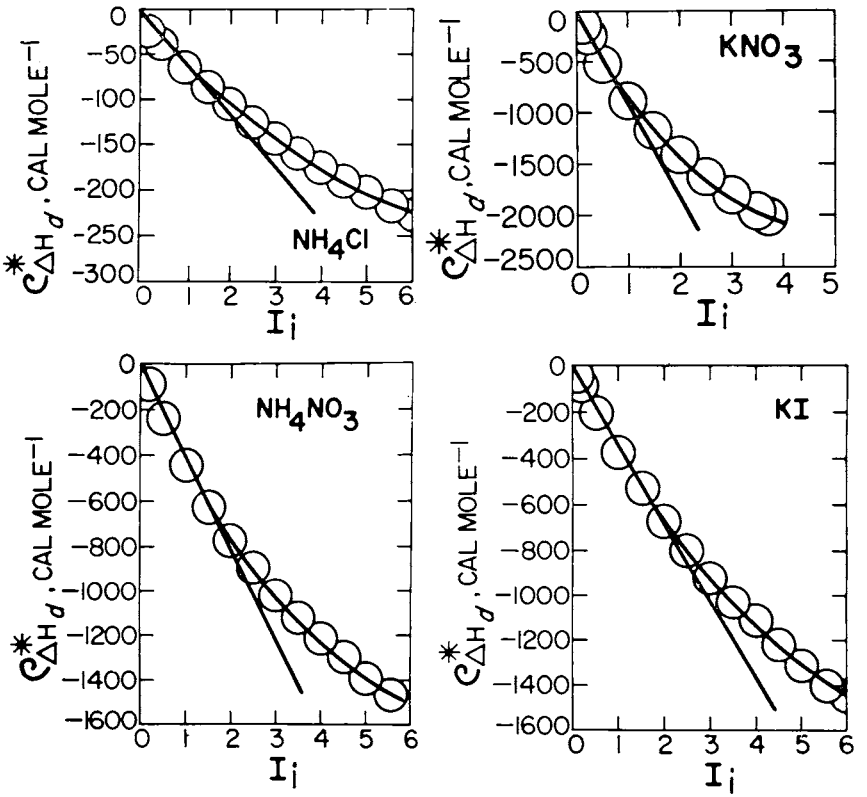

Fig. 56. $\rho^*_{\Delta H_d}$ (eq 237) computed (assuming I = Ī) from heats of dilution reported by Parker (1965) as a function of the ionic strength of the solution before diluting to "infinite" dilution at 25°C and 1 bar.

NaCl at temperatures $\leqslant$ 100°C computed from relative apparent molal enthalpies generated by Gibbard and others (1974) from vapor pressure data are consistent with the calorimetric measurements reported by Messikomer and Wood (1975).

The heat of solution (ΔH_s) analog to ρ^*_H ($\rho^*_{\Delta H_s}$) is defined by an expression analogous to eq (237) in which ΔH_d is replaced by ΔH_s. The values of $\rho^*_{\Delta H_s}$ represented by the symbols in figures 61 through 64 were computed from experimental heats of solution reported in the literature. Because all the data shown in figures 61 through 64 were obtained in dilute solutions (I < 0.01), the ionic strength distribution of the heat of solution data is not definitive with respect to $b_{\Pi,k}$. In fact, analysis of heat capacity data (see below) indicates that the absolute values of $b_{H,k}$ for most electrolytes are < 500 cal mole^{-1} at temperatures < 200°C, which is consistent with essentially horizontal curves representing $\rho^*_{\Delta H_s}$ as a function of I on the scale of figures 60 through 64. It thus appears that in contrast to the assumption made by Cobble and his coworkers (Criss and Cobble, 1961; Mitchell and Cobble, 1964; Ahluwalia and Cobble, 1964a and b; Gardner, Jeckel, and Cobble, 1969; Gardner, Mitchell, and Cobble, 1969b;

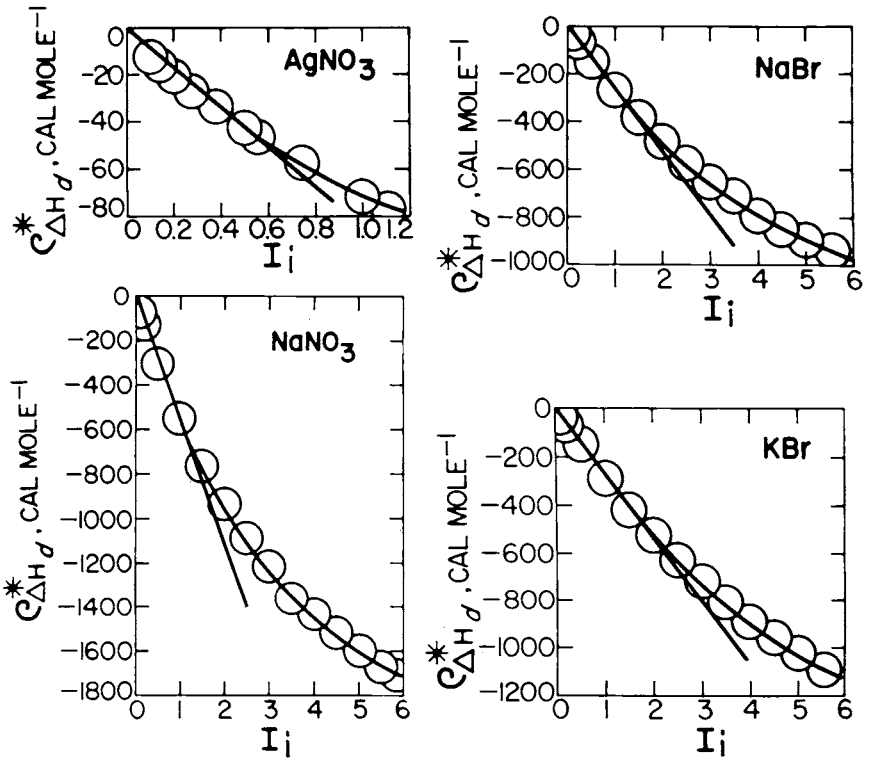

Fig. 57. $\rho^*_{\Delta H_d}$ (eq 237) computed (assuming I = Ī) from heats of dilution reported by Parker (1965) as a function of the ionic strength of the solution before diluting to "infinite" dilution at 25°C and 1 bar.

Jeckel, Criss, and Cobble, 1964), the trends of the data points in the figures are *not* significant. In addition, the accuracy of the data is apparently far less than that implied by the reported experimental uncertainties. These observations lead to the large symbols in the figures, which become larger with increasing dilution to represent increasing uncertainty in $\rho^*_{\Delta H_s}$ with decreasing concentration. The intercepts of the curves were used to calculate standard partial molal heat capacities ($\bar{C}^\circ_P$) from finite difference derivatives of the extrapolated heat of solution data (see below). The constraint that $\bar{C}^\circ_P$ must vary smoothly with temperature, together with the fact that $b_{H,k}$ is too small to affect signicantly the horizontal approximation represented by the linear curves for $BaCl_2$, $GdCl_3$, $NaReO_4$, $HReO_4$, and $NaClO_4$ provided the basis for selecting the relative positions of the intercepts for these electrolytes in figures 61 through 64. In certain instances the scatter in the heat of solution data precluded selection of definitive intercepts. The slopes of the curves shown for NaCl, CsI, and Na_2SO_4 were calculated independently from predicted values of $b_{H,k}$ as a function of temperature (see below).

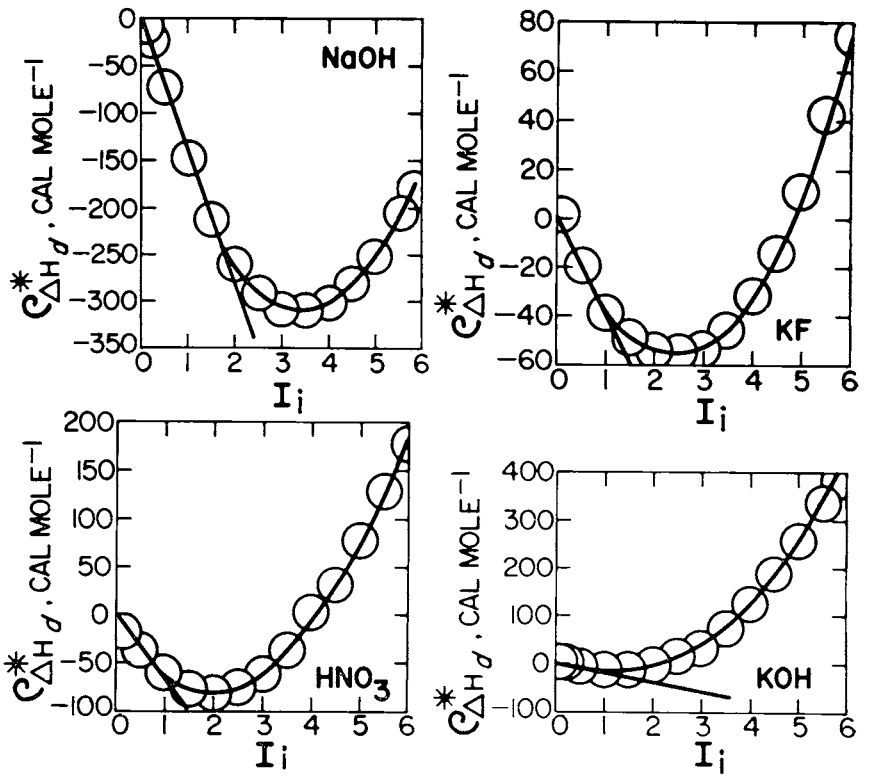

Fig. 58. $\rho^*_{\Delta H_d}$ (eq 237) computed (assuming I = $\bar{\imath}$) from heats of dilution reported by Parker (1965) as a function of the ionic strength of the solution before diluting to "infinite" dilution at 25°C and 1 bar.

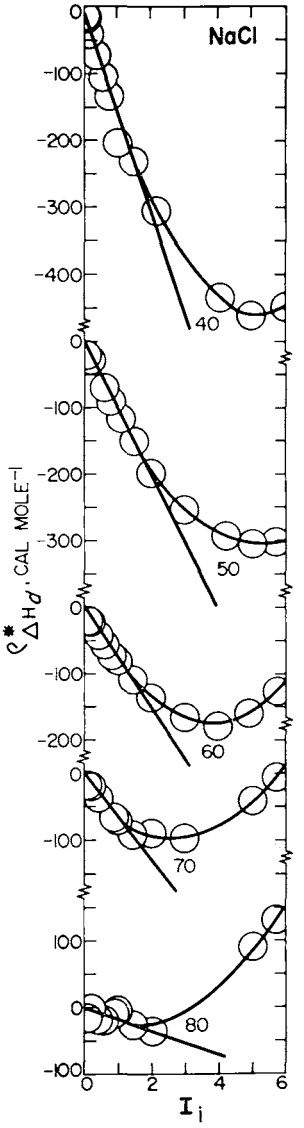

Fig. 59. $\rho^*_{\Delta H_d}$ (eq 237) computed (assuming I = I) from values of $\phi_{L,k}$ ($\phi_{L,k} = \phi_{H,k} - \bar{H}^\circ_k$) reported by Ensor and Anderson (1973) at 1 bar and 40°, 50°, 60°, 70°, and 80°C.

Values of b_H computed from the slopes of the linear curves shown in figures 50 through 58 are given in table 9. Comparative calculations (see below) indicate that the two sets of values at 25° and 30°C are consistent with one another as well as with the apparent molal heat capacity data for the electrolytes.

Heat capacity.—The apparent molal heat capacity function analogous to $\rho^*_{H,k}$ ($\rho^*_{J,k}$) is defined by

$$\rho^*_{J,k} \equiv \phi_{C_P,k} - \psi_k A_J \bar{I}^{1/2}\bar{\alpha}^* + \frac{\psi_k(2A_H B_H - A_G B_J T)\bar{\beta}(\mathring{a}B_\gamma \bar{I}^{1/2})}{2.303RT^2}$$

$$-\frac{2\psi_k A_\gamma B_H{}^2 \bar{\zeta}(\mathring{a}B_\gamma \bar{I}^{1/2})}{2.303RT^2} = \bar{C}^\circ_{P,k} - \frac{\nu_k b_{J,k}\bar{I}}{4} \qquad (238)$$

where $\bar{\zeta}(\mathring{a}B_\gamma \bar{I}^{1/2})$ is given by eq (234). It can be deduced from figures 65 through 69 that eq (238) is closely consistent with experimental values of ϕ_{C_P} for a large number of electrolytes at 25°C and 1 bar. Figures 70 through 78 leave little doubt that this is also true at higher temperatures. The values of ρ^*_J shown in these (and subsequent) figures were calculated assuming $\bar{I} = I$ from eq (238) using values of A_J, A_H, B_H, A_G, B_J, A_γ, and B_γ taken from table 1 and/or computed from equations given in app. C. Although the agreement at high temperatures is to some extent a consequence of the magnification in $\phi_{C_P,k}$ of experimental uncertainties in $C_{P,solution}$ at $m_k < 1$, it can be seen that the bulk of the data is consistent with eq (238). The uncertainty in $\phi_{C_P,k}$ ($\delta_{\phi C_P,k}$) arising from experimental uncertainty in $C_{P,solution}$($\delta_{C_P,solution}$) is given by

$$\delta_{\phi C_P,k} = \delta_{C_P,solution}/m_k \ , \qquad (239)$$

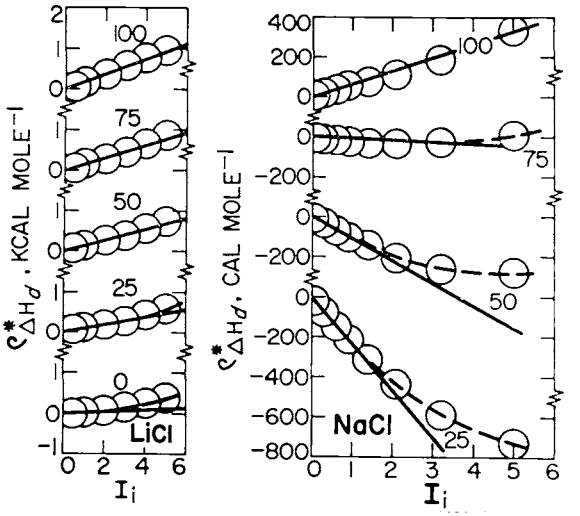

Fig. 60. $\rho^*_{\Delta H_d}$ (eq 237) computed (assuming $I = \bar{I}$) from values of $\phi_{L,k}$ ($\phi_{L,k} = \phi_{H,k} - \bar{H}^\circ_k$) reported by Gibbard and Scatchard (1973) and Messikomer and Wood (1975) at 1 bar and 0°, 25°, 50°, 75°, and 100°C.

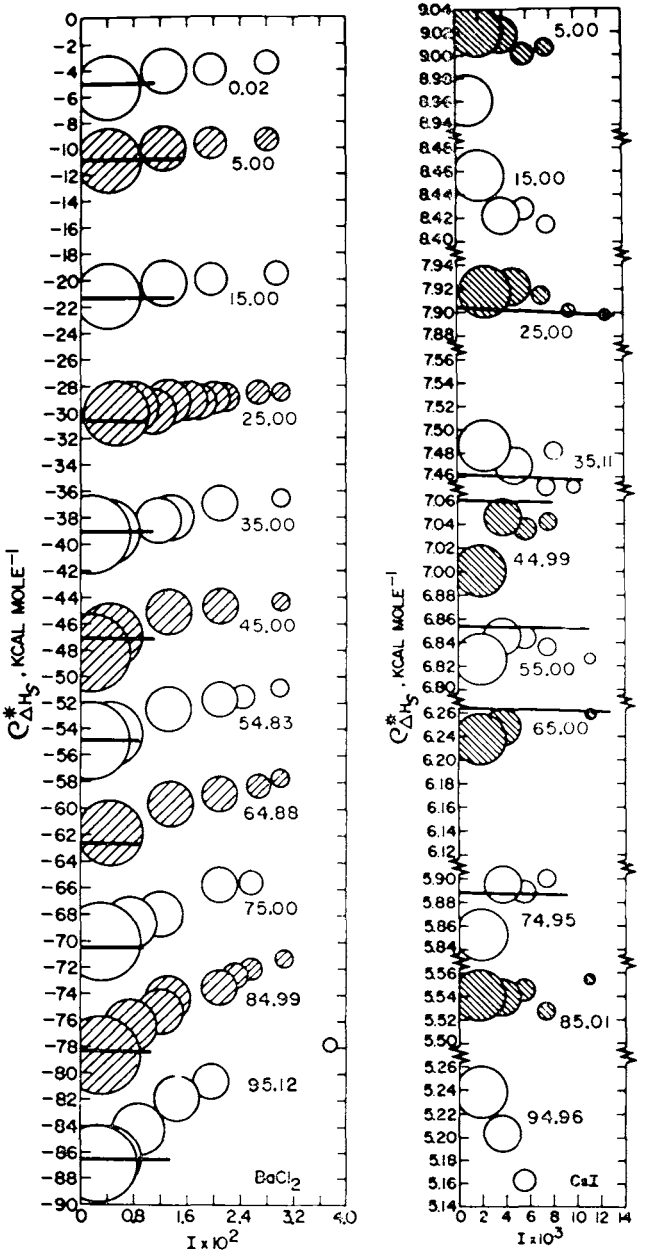

Fig. 61. $\rho^*_{\Delta H_s}$ (see text) computed (assuming I = Ĭ) from heats of solution taken from the literature. The symbols shown above and those in figures 62 through 64 represent experimental data reported by Criss and Cobble (1961), Mitchell and Cobble (1964), Ahluwalia and Cobble (1964a and b), Gardner, Jeckel, and Cobble (1969), Gardner, Mitchell, and Cobble (1969b), and Jeckel, Criss, and Cobble (1964) for 1 bar and the temperatures in °C shown in the figures.

which is responsible for the increasing symbol size with decreasing concentration in figures 74 through 78. The much greater accuracy of the experimental data plotted in figures 65 through 69 led to the decision to represent all the data shown in these figures with symbols of the same size. In certain cases (for example, HCl and LiBr in fig. 77) no curves could be drawn through the data points with slopes and intercepts corresponding to a smooth distribution of $-\nu b_J/4$ and $\bar{C}^\circ_P$ with temperature. The latter constraints were used to control interpretation of the apparent molal heat capacities represented by the linear curves in figures 70 through 78, which led to the conclusion that many of the data points shown for the more dilute concentrations in these figures are unreliable. The slopes of all the curves in figures 70 through 78 that are drawn through data points reported by different investigators for the same electrolyte are equivalent. However, the intercepts are not (see below).

The effect of ion association on ρ^*_J as a function of I is manifested by increasing departures from linearity toward more negative values with increasing I at high ionic strengths. It can be seen in figures 78 through

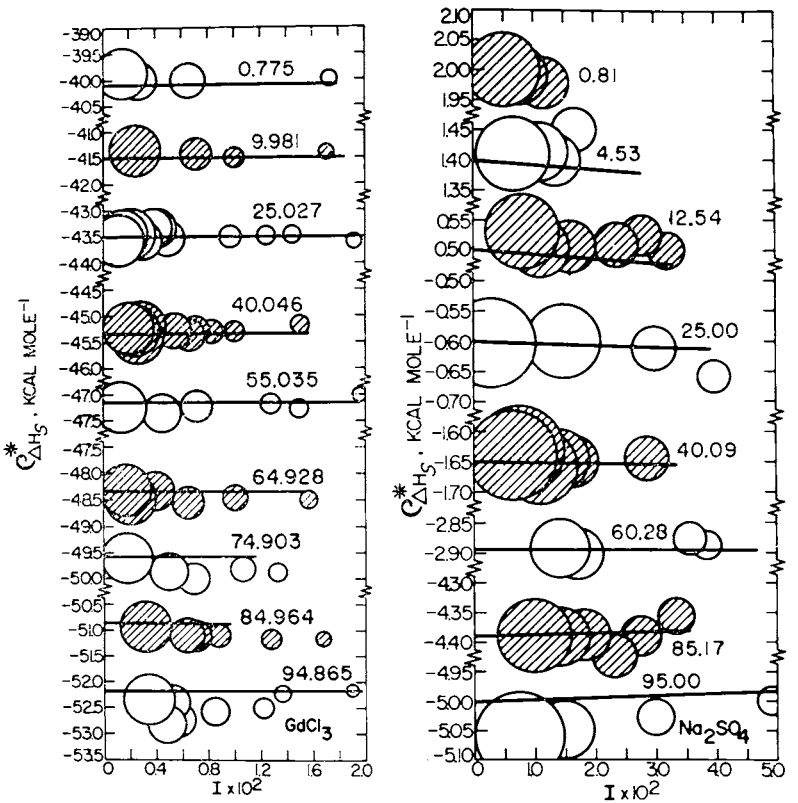

Fig. 62. $\rho^*_{\Delta H_S}$ (see text) computed (assuming I = Ī) from heats of solution taken from the literature (see caption of fig. 61).

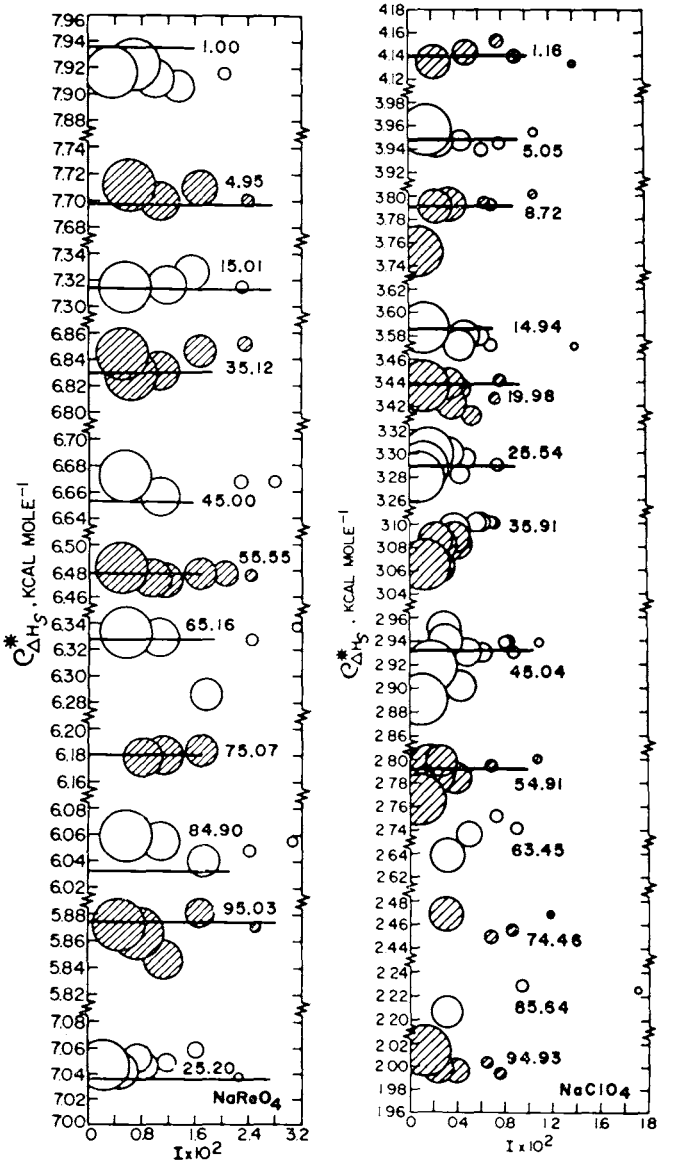

Fig. 63. $\rho^*_{\Delta H_S}$ (see text) computed (assuming I = $\bar{I}$) from heats of solution taken from the literature (see caption of fig. 61).

81 that NaCl as well as many other electrolytes exhibit this behavior at 25°C and 1 bar, which is undoubtedly enhanced (as in the case of Na_2SO_4 in fig. 78) at higher temperatures. Note in figure 82 that ρ^*_J for $MgSO_4$ exhibits considerable scatter and nonlinearity in the distribution of the data points from I = 0.5 to 4. In contrast, $\phi_{C_p,MgSO_4}$ is a linear function of I, which is consistent with theoretical considerations as well as the stoichiometric analog of eq (175) and the high degree of ion association in magnesium sulfate solutions. *For an electrolyte that is "completely" associated in a solvated polar neutral complex, apparent molal properties approximate linear functions of stoichiometric ionic strength.*

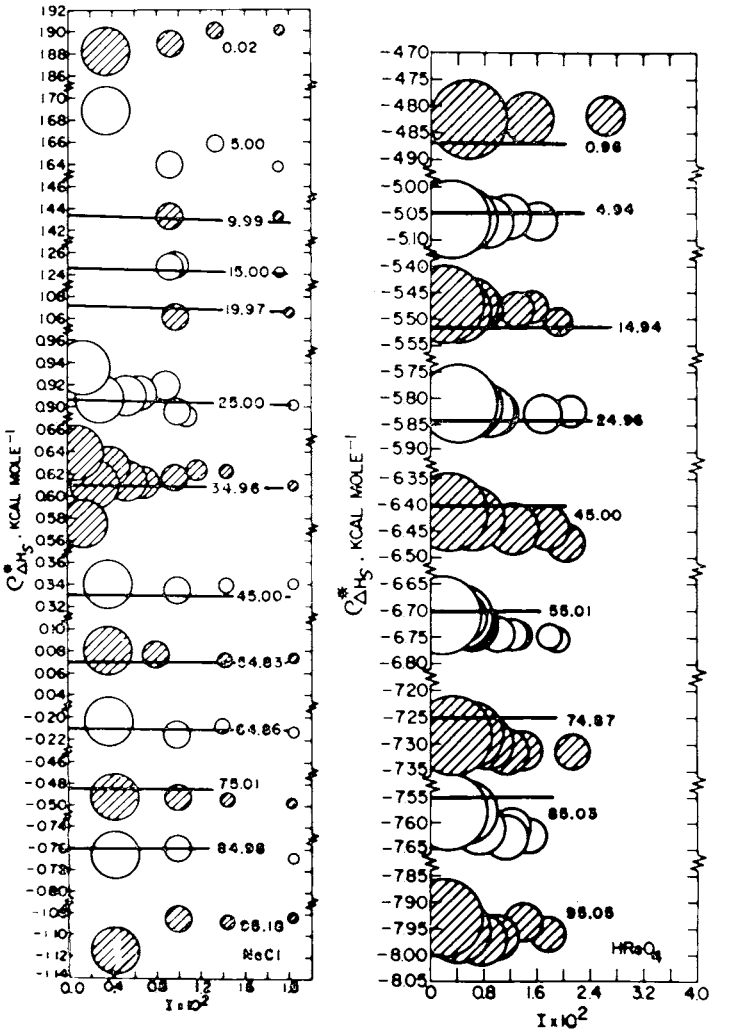

Fig. 64. $\rho^*_{\Delta H_s}$ (see text) computed (assuming I = I) from heats of solution taken from the literature (see caption of fig. 61).

Values of b_J computed from the slopes of the linear curves for 25°C in figures 65 through 70, 72, 73, and 79 through 81 are given in table 10. The slopes of the linear curves for temperatures other than 25°C in figures 70 through 78, together with the intercepts of all the curves in figures 65 through 82 (which correspond to extrapolated values of $\bar{C}^\circ_P$) are considered in later discussion.

Volume and compressibility.—The volume and compressibility analogs of eq (238) can be written as

$$\rho^*_{V,k} \equiv \phi_{V,k} - \psi_k A_V \bar{I}^{1/2} \bar{\alpha}^* - 2\psi_k A_\gamma B_V \overline{\beta}(\mathring{a}B_\gamma \bar{I}^{1/2}) = \bar{V}^\circ_k + \frac{\nu_k b_{V,k} \bar{I}}{4} \quad (240)$$

and

$$-\rho^*_{\kappa,k} \equiv -\phi_{\kappa,k} - \psi_k A_\kappa \bar{I}^{1/2} \bar{\alpha}^* + \frac{\psi_k (2A_V B_V + A_G B_\kappa) \overline{\beta}(\mathring{a}B_\gamma \bar{I}^{1/2})}{2.303RT}$$

$$+ \frac{2\psi_k A_\gamma B_V{}^2 \overline{\xi}(\mathring{a}B_\gamma \bar{I}^{1/2})}{2.303RT} = -\bar{\kappa}^\circ_k - \frac{\nu_k b_{\kappa,k} \bar{I}}{4} \quad . \quad (241)$$

TABLE 9

Extended term parameters (b_H) for computing the relative apparent and partial molal enthalpies of aqueous electrolytes at 25° and 30° C and 1 bar from eqs (223) and (228)

Solute	b_H[a] 25°C	b_H[a] 30°C	Solute	b_H[a] 25°C	b_H[a] 30°C	Solute	b_H[a] 25°C	b_H[a] 30°C
HCl	-430[b]		NaBr	520[b]	454[b]	Na_2SO_4	615[c]	520[b]
LiCl	-148[b]	-180[b]	KBr	540[b]		K_2SO_4		513[b]
NaCl	470[b]	408[b]	RbBr	600[b]		$LiSO_4$		-87[b]
KCl	445[c]	400[b]	CsBr	740[b]		NH_4NO_3	800[b]	
RbCl	490[b]	440[b]	NaI	550[b]	480[b]	$NaNO_3$	1120[b]	
CsCl	620[c]	560[b]	KI	680[b]		HNO_3	134[b]	
NH_4Cl	120[b]		RbI	740[b]		$AgNO_3$	168[b]	
$MgCl_2$	-216[c]	-232[b]	CsI	1000[b]		$LiNO_3$	-400[b]	
$SrCl_2$	-3[d]	-31[b]	NaF	374[b]	192[b]	KNO_3	1820[b]	
$CaCl_2$	-80[b]	-103[b]	KF	80[b]		NaOH	280[b]	
$BaCl_2$	-59[d]	9[b]	RbF	180[b]		KOH	40[b]	
HBr	-274[b]		CsF	240[b]		LiOH	-240[b]	
LiBr	-80[b]		$NaHCO_3$		580[b]			

[a] cal kg mole^{-2}. [b] Computed from the slopes of the linear curves in figures 50 through 57 (see text). [c] Calculated from equation (292) for P = P_r using the values of b_H shown above for 30°C and parameters taken from table 19. [d] Estimated from the value of b_H for 30°C given above and that for b_J at 25°C in table 10, assuming b_J constant from 25° to 30°C.

It can be seen in figures 83 through 85 (which were generated assuming $\bar{I} = I$) that with only a few exceptions, the values of ϕ_V reported by Fortier, Leduc, and Desnoyers (1974) for 1:1 electrolytes at 25°C and 1 bar are closely consistent with eq (240). However, in a number of instances (for example, NaCl, KI, KF, CsF, RbBr, KBr, and KCl), the experimental values of $\rho^*_{V,k}$ depart from the linear curves toward lower values at high ionic strengths, which can be attributed to the effects of increasing ion association with increasing concentration. In contrast, the curvature in the distribution and apparent displacement of the data points for NaBr, CsI, and CsBr in the dilute region of concentration is probably a consequence of experimental error (see below).

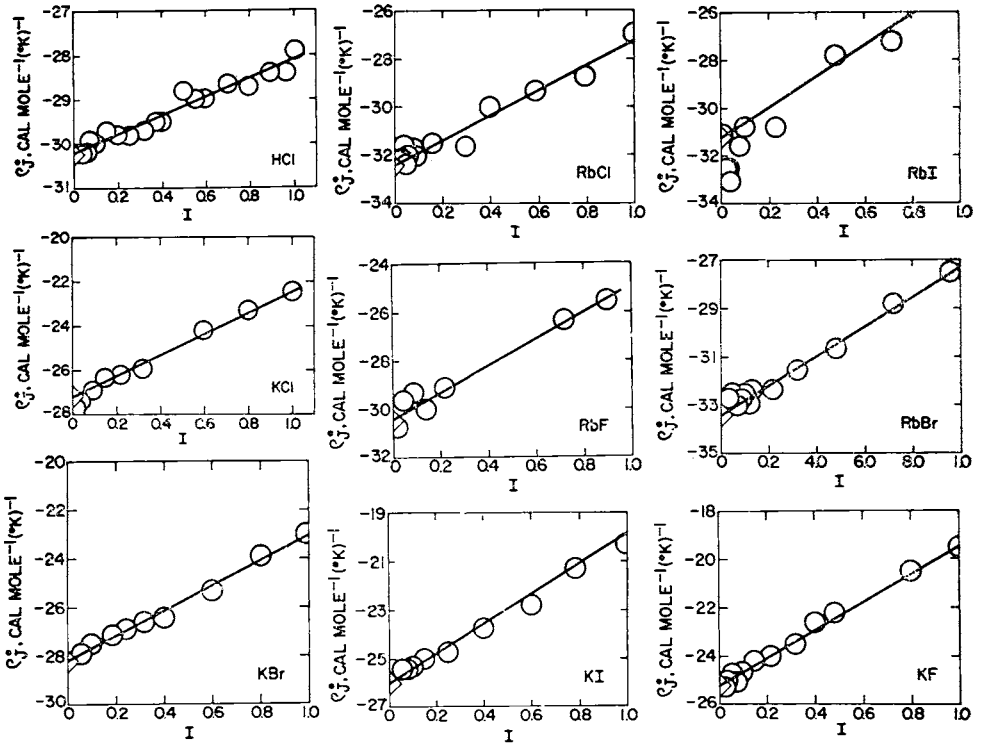

Fig. 65. ρ^*_J (eq 238) computed (assuming $I = \bar{I}$) from apparent molal heat capacities at 25°C and 1 bar taken from the literature. The circles shown above and those in figures 66 through 82 represent experimental data reported by Fortier, Leduc, and Desnoyers (1974), Perron, Desnoyers, and Millero (1974), Perron, Fortier, and Desnoyers (1975), Parker (1965), Lewis and Randall (1961), Tanner and Lamb (1978), Likke and Bromley (1973), Ruterjans and others (1969), Eigen and Wicke (1951, 1954), Wicke, Eigen, and Ackermann (1954), and Ackermann (1958). The apparent molal heat capacities given in the first three of these references were corrected to be consistent with Desnoyers and others (1976). The calculated values of $\bar{C}^\circ_P$ represented by the open triangles on the ordinates of the diagrams correspond to those given in tables 13 and 16. The latter values do not in all instances necessarily correspond to the extrapolated intercepts of the linear curves in the diagrams, which are denoted in figures 74 through 76, 78, and 82B by closed triangles (see text).

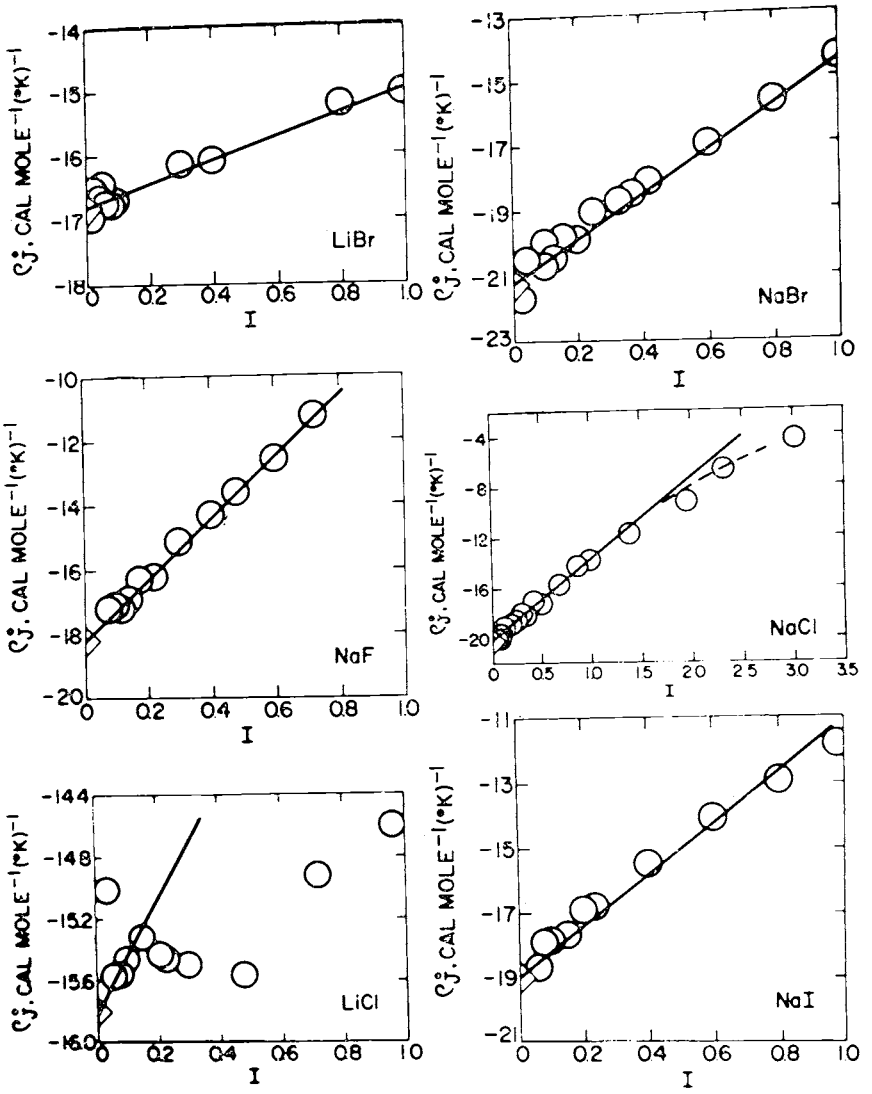

Fig. 66. ρ^*_J (eq 238) computed (assuming I = I) from apparent molal heat capacities at 25 °C and 1 bar (see caption of fig. 65).

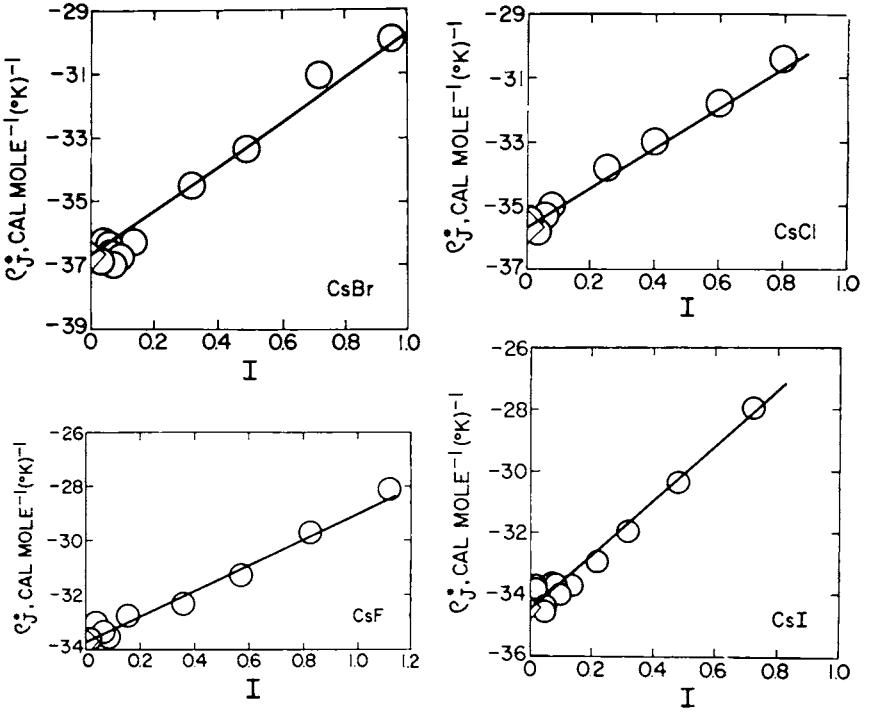

Fig. 67. ρ^*_J (eq 238) computed (assuming I = Ī) from apparent molal heat capacities at 25 °C and 1 bar (see caption of fig. 65).

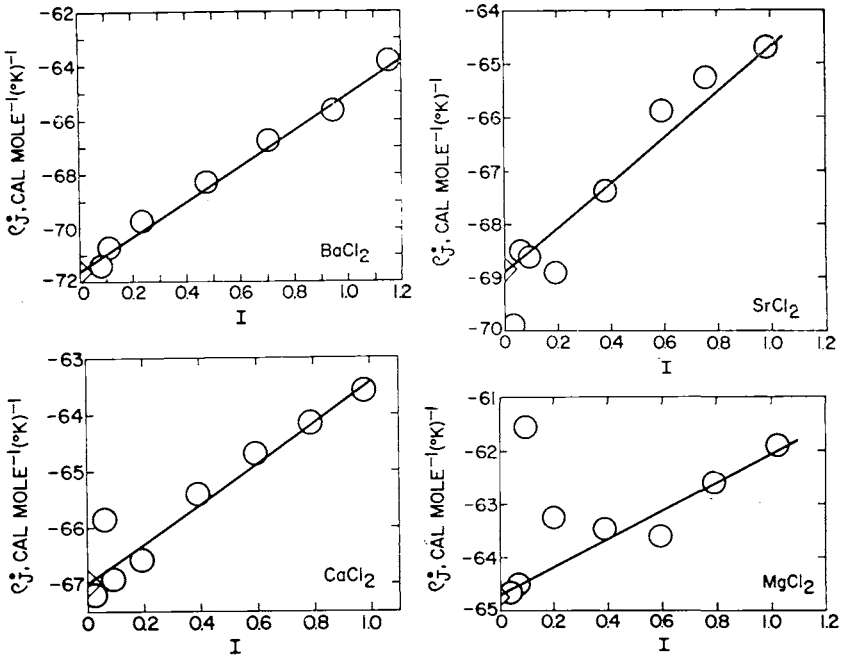

Fig. 68. ρ^*_J (eq 238) computed (assuming I = Ī) from apparent molal heat capacities at 25 °C and 1 bar (see caption of fig. 65).

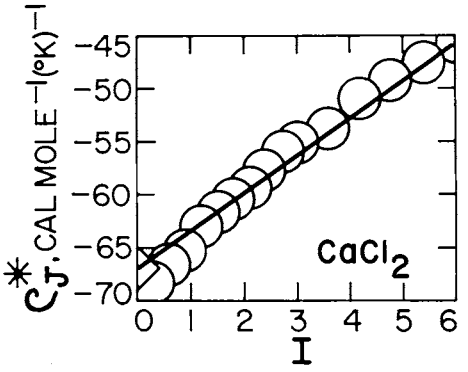

Fig. 69. ρ^*_J (eq 238) computed (assuming I = Ĭ) from apparent molal heat capacities at 25°C and 1 bar (see caption of fig. 65).

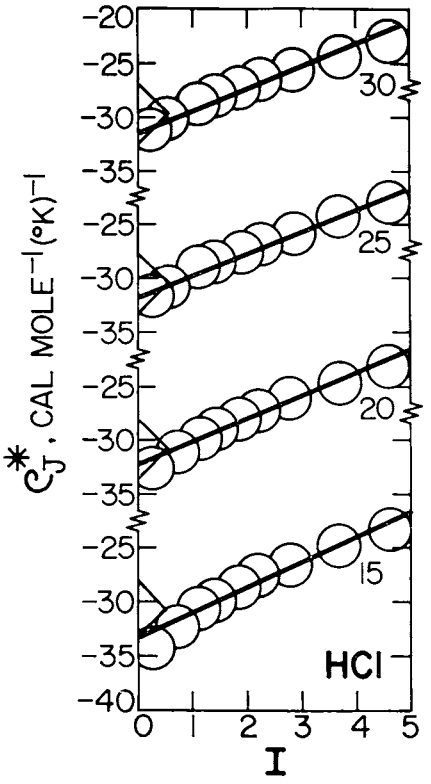

Fig. 70. ρ^*_J (eq 238) computed (assuming I = Ĭ) from apparent molal heat capacities at 1 bar and 15°, 20°, 25°, and 30°C (see caption of fig. 65).

Density data reported by Allam (1963), most of which are for highly concentrated electrolyte solutions, were used to calculate (assuming $\bar{I} = I$) the values of $\rho^*_{V,k}$ shown in figures 86 through 88 from the relation,

$$\phi_{V,k} = \frac{1}{m_k}\left(\frac{1000 + m_k\hat{M}_k}{\rho} - \frac{1000}{\rho^\circ_w}\right) \tag{242}$$

where ρ and ρ°_w stand for the density of the solution and that of pure H_2O, respectively, in g cm^{-3}, and $\hat{M}_k$ represents the molecular weight of the kth electrolyte in g mole^{-1}. Although in certain cases (for example, NaCl, KNO_3, $AgNO_3$, KI, NH_4I, and KOH) the computed values of $\rho^*_{V,k}$ in figures 86 through 88 exhibit considerable scatter, it can be deduced that most of the densities reported by Allam for ionic strengths < 2 to 8 (depending on the electrolyte) are in close agreement with eq (240). At higher ionic strengths, the data points for all the electrolytes except NH_4Cl, LiI, and HNO_3 depart to an increasing degree from the linear curves toward lower values of $\rho^*_{V,k}$ with increasing ionic strength, which is consistent with increasing ion association with increasing concentration.

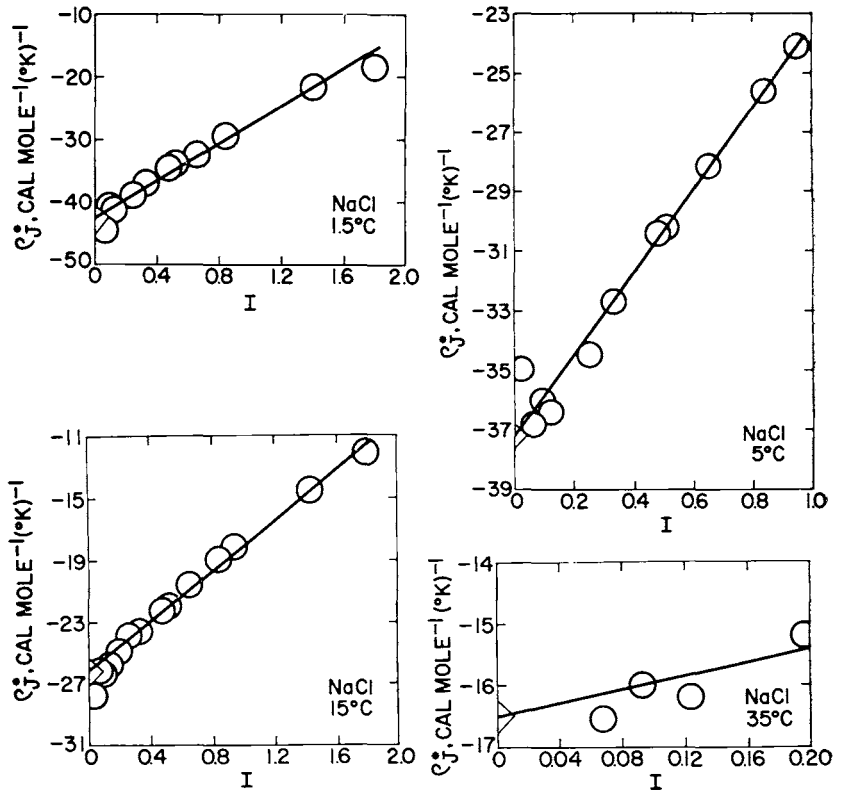

Fig. 71. ρ^*_J (eq 238) computed (assuming $I = I$) from apparent molal heat capacities at 1 bar (see caption of fig. 65).

With the exception of NaCl, NaBr, KBr, and KI, the slopes of the linear curves for the same electrolyte in figures 83 through 88 are identical. Of the two sets of data for these four electrolytes, those reported by Fortier, Leduc, and Desnoyers (1974) were accepted in the present study. In general, the data reported by Allam are more uncertain than those obtained by Fortier, Leduc, and Desnoyers. This observation is consistent with the fact that the intercepts of the curves (which correspond to $\bar{V}^\circ_k$) in figures 86 through 88 differ from the values of $\bar{V}^\circ_k$ represented by the symbols on the ordinate (which correspond to values of $\bar{V}^\circ_k$ calculated by Helgeson and Kirkham, 1976) by as much as 1.5 cm^3 $mole^{-1}$. Although most of these differences are < 0.5 cm^3 $mole^{-1}$, which is not excessive, the discrepancies at $I = 0$ in figures 86 through 88 are considerably larger than those in figures 83 through 85. Note that most of the intercepts of the linear curves in the latter figures are in remarkably close agreement

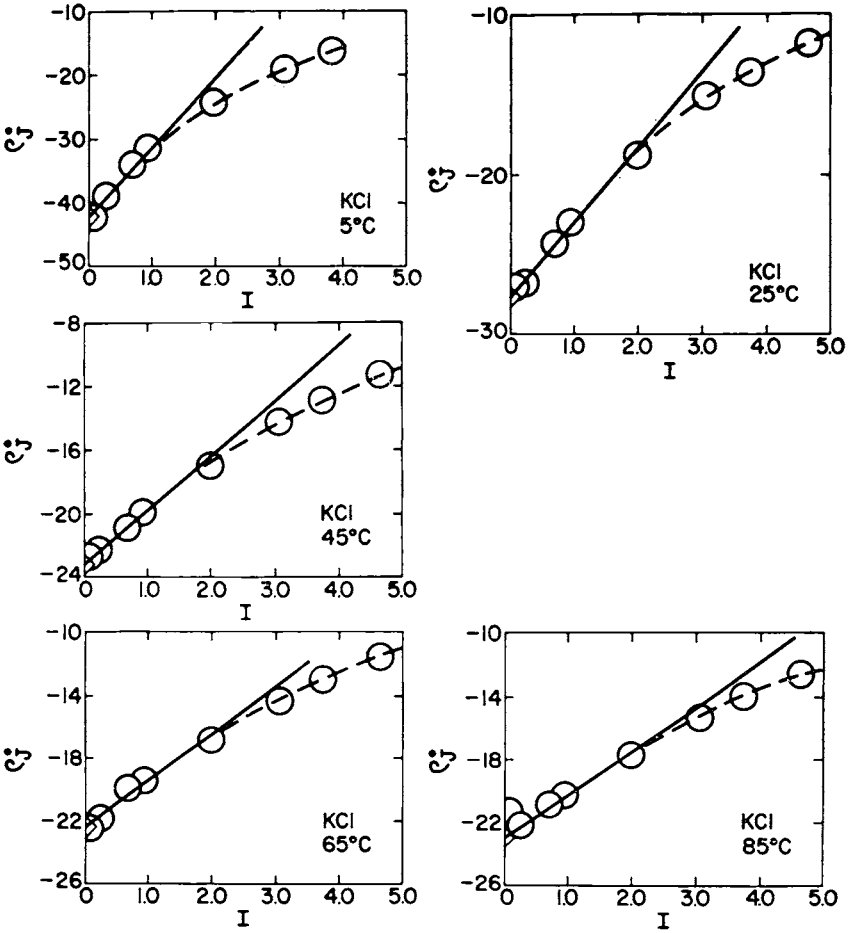

Fig. 72. ρ^*_J (eq 238) computed (assuming I = I) from apparent molal heat capacities at 1 bar (see caption of fig. 65).

with the symbols on the ordinate representing values of $\bar{V}^\circ_k$ computed by Helgeson and Kirkham (1976); the maximum difference (which is exhibited by KCl) is < 0.26 cm^3 mole^{-1}. This observation, together with the fact that Helgeson and Kirkham used the Redlich-Meyer equation (Redlich and Meyer, 1964) to represent ϕ_V as a function of $\bar{I}$ underscores the insensitivity of extrapolated values of $\bar{V}^\circ$ to the equation used to represent ϕ_V as a function of ionic strength. The Redlich-Meyer equation is an improvement over the Masson (1929) equation, but it is nevertheless incompatible with eq (173).

It can be deduced from figures 89 through 93 that eq (240) also represents closely density data for a large number of electrolytes as a function of ionic strength at high temperatures. In most cases, comparison of the extrapolated and computed values of $\bar{V}^\circ$ reported by Helgeson and Kirkham (1976), which are represented by the solid and open symbols, respec-

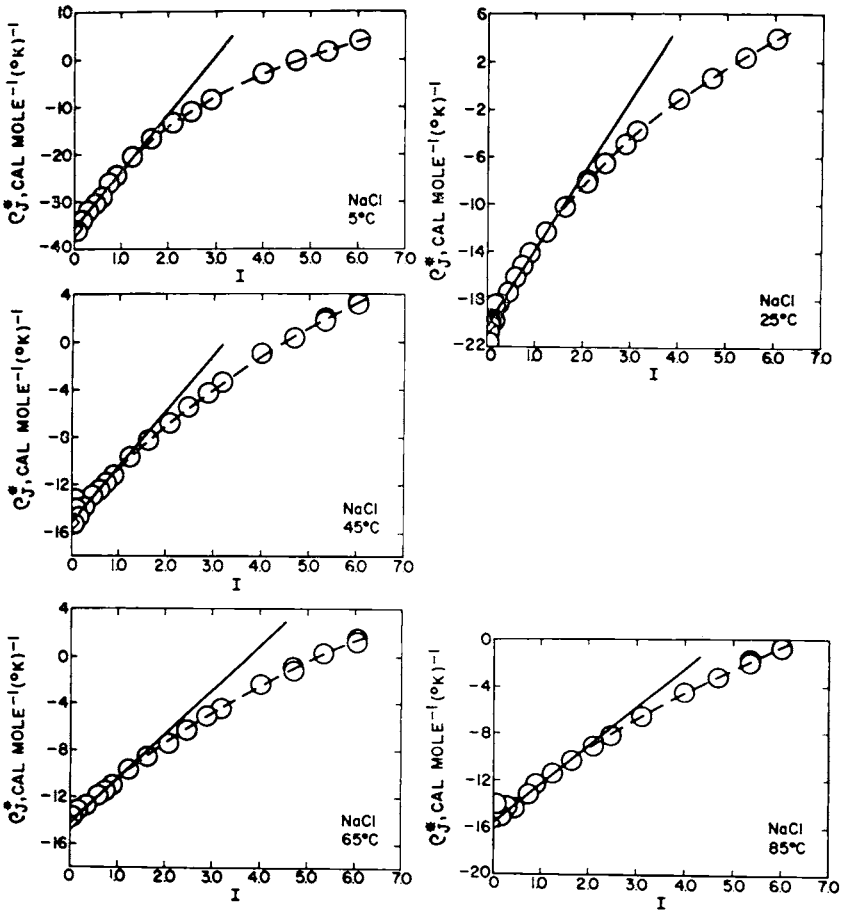

Fig. 73. ρ^*_J (eq 238) computed (assuming I = $\bar{I}$) from apparent molal heat capacities at 1 bar (see caption of fig. 65).

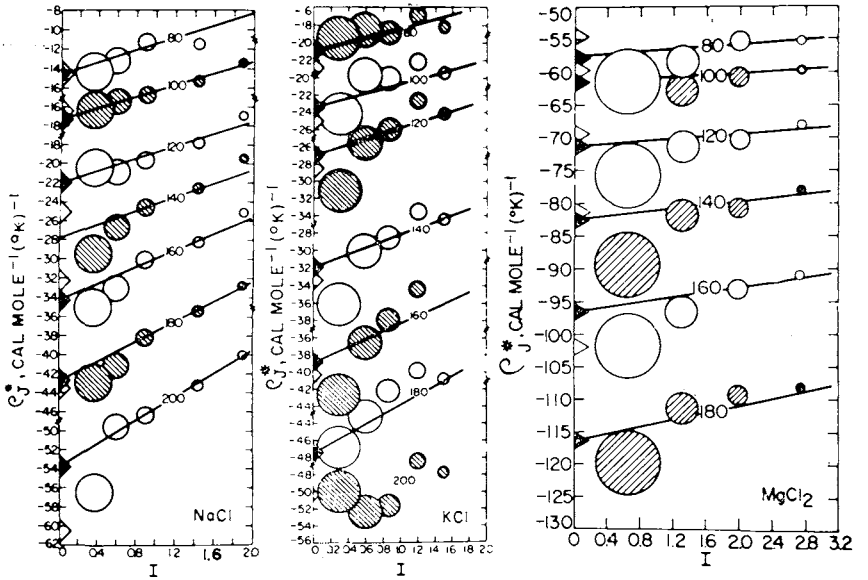

Fig. 74. ρ^*_J (eq 238) computed (assuming I = Ĭ) from apparent molal heat capacities at 1 bar and 80°C, together with those at pressures corresponding to liquid-vapor equilibrium and the temperatures $\geqslant$ 100°C shown in the diagrams (see caption of fig. 65).

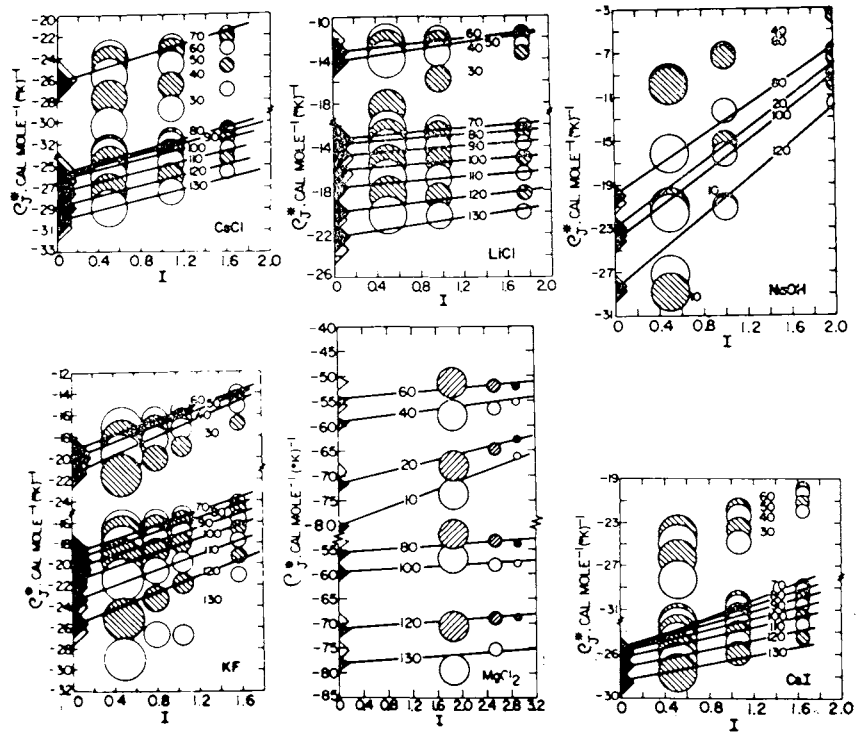

Fig. 75. ρ^*_J (eq 238) computed (assuming I = Ĭ) from apparent molal heat capacities at temperatures from 10° to 100°C at 1 bar, together with those at 100° to 130°C and pressures corresponding to liquid-vapor equilibrium (see caption of fig. 65).

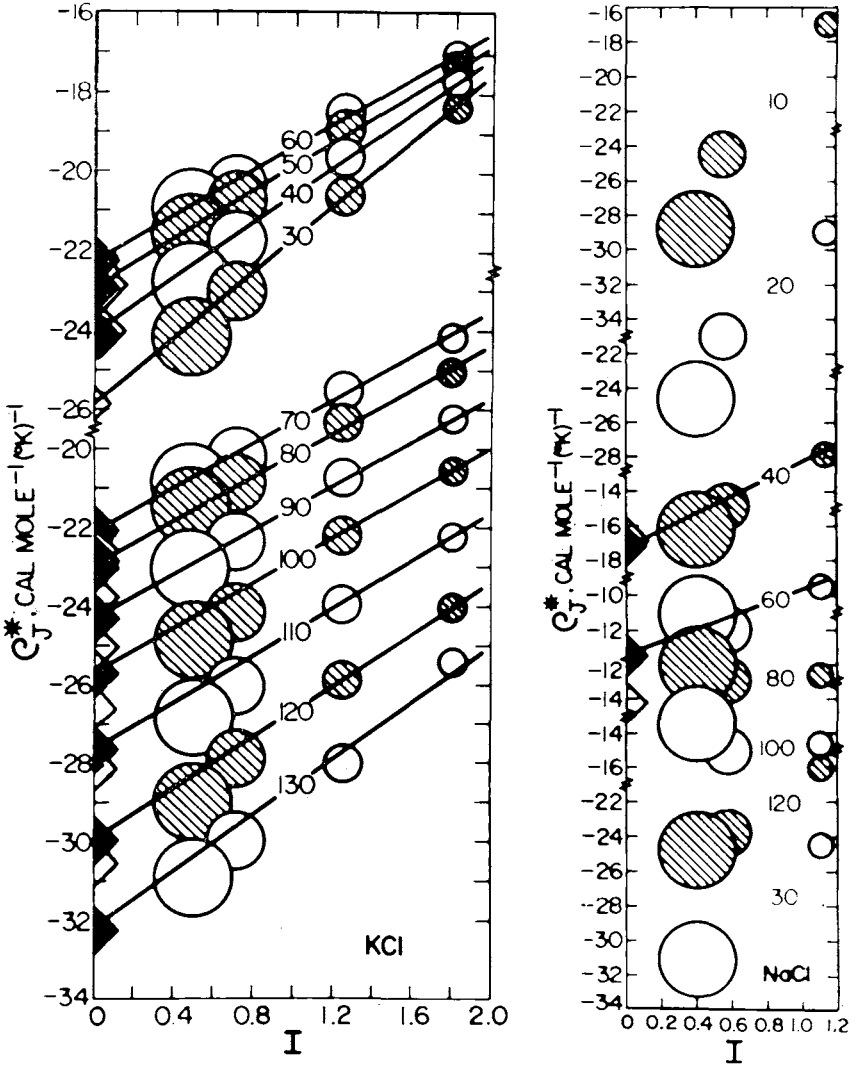

Fig. 76. ρ^*_J (eq 238) computed (assuming I = I) from apparent molal heat capacities at temperatures from 10° to 100°C at 1 bar, together with those at 100° to 130°C and pressures corresponding to liquid-vapor equilibrium (see caption of fig. 65).

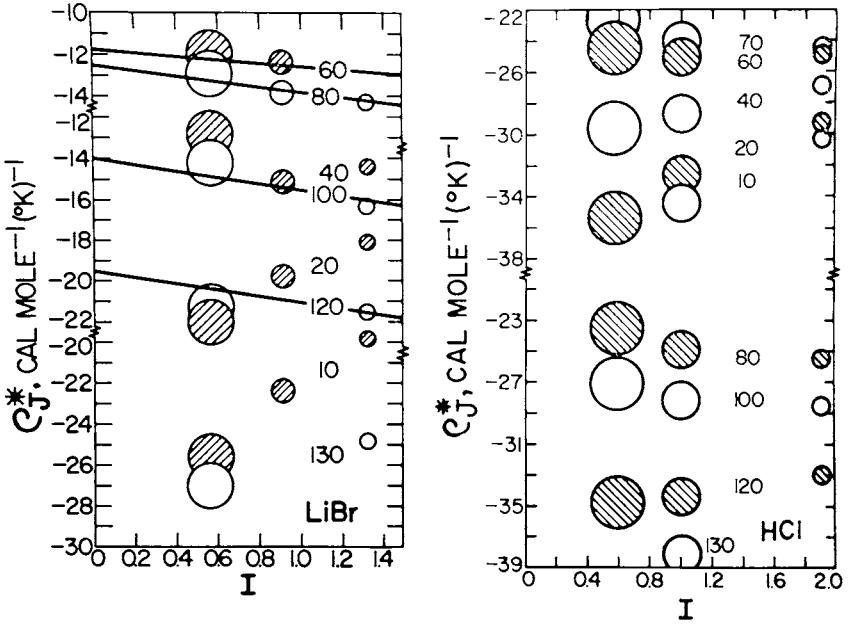

Fig. 77. ρ^*_J (eq 238) computed (assuming I = I) from apparent molal heat capacities at temperatures from 10° to 100°C at 1 bar, together with those at 100° to 130°C and pressures corresponding to liquid-vapor equilibrium (see caption of fig. 65).

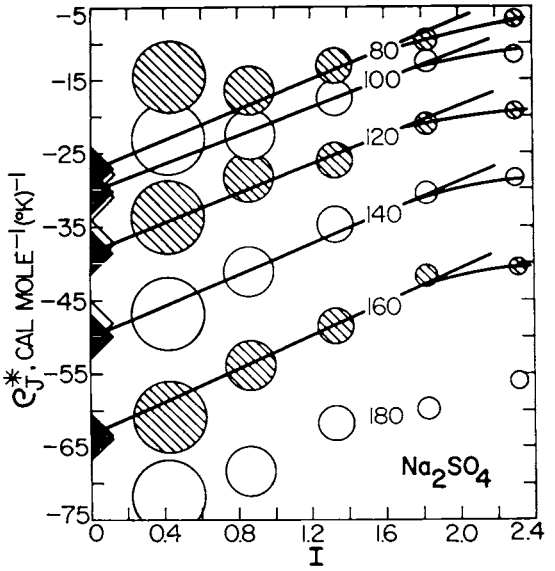

Fig. 78. ρ^*_J (eq 238) computed (assuming I = I) from apparent molal heat capacities at 1 bar and 80°C, together with those at pressures corresponding to liquid-vapor equilibrium and the temperatures $\geqslant$ 100°C shown in the figure (see caption of fig. 65).

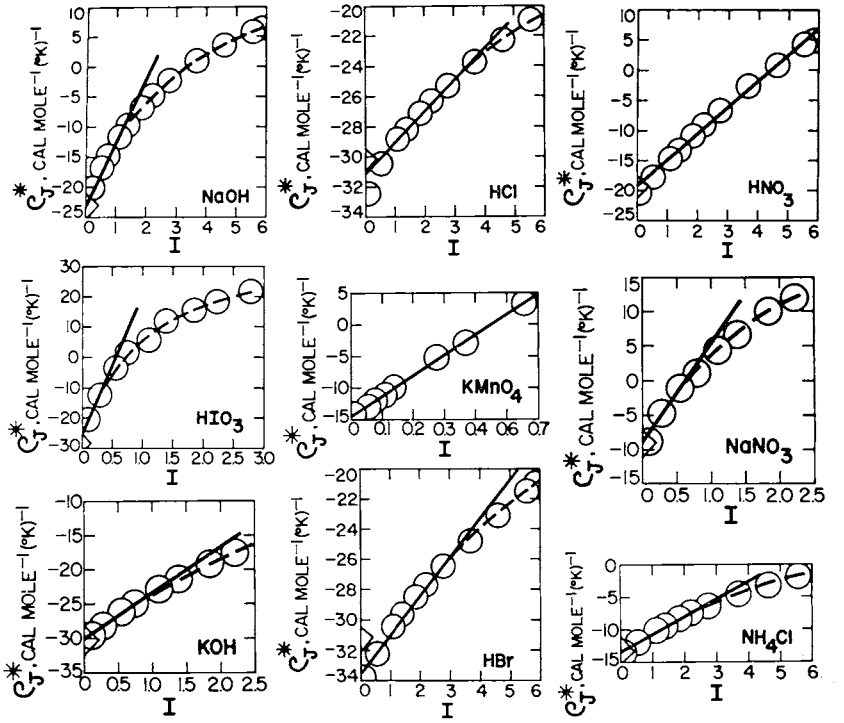

Fig. 79. ρ^*_J (eq 238) computed (assuming I = I) from apparent molal heat capacities at 25°C and 1 bar (see caption of fig. 65).

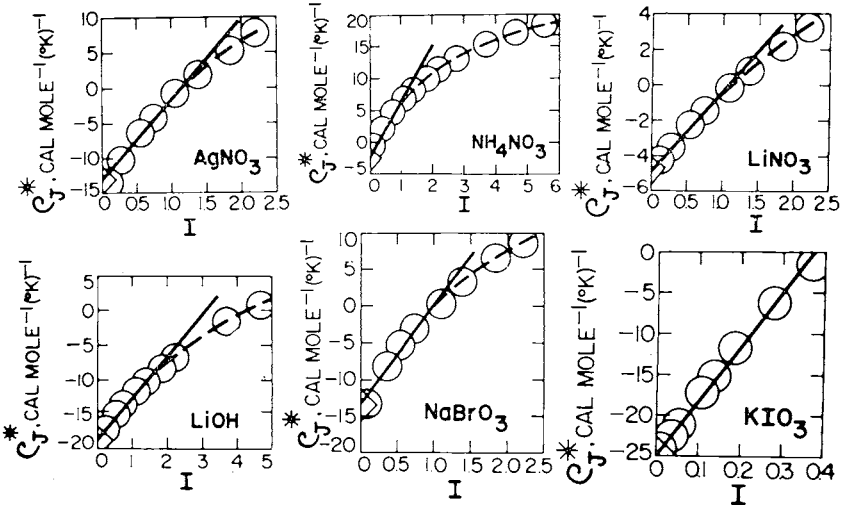

Fig. 80. ρ^*_J (eq 238) computed (assuming I = I) from apparent molal heat capacities at 25°C and 1 bar (see caption of fig. 65).

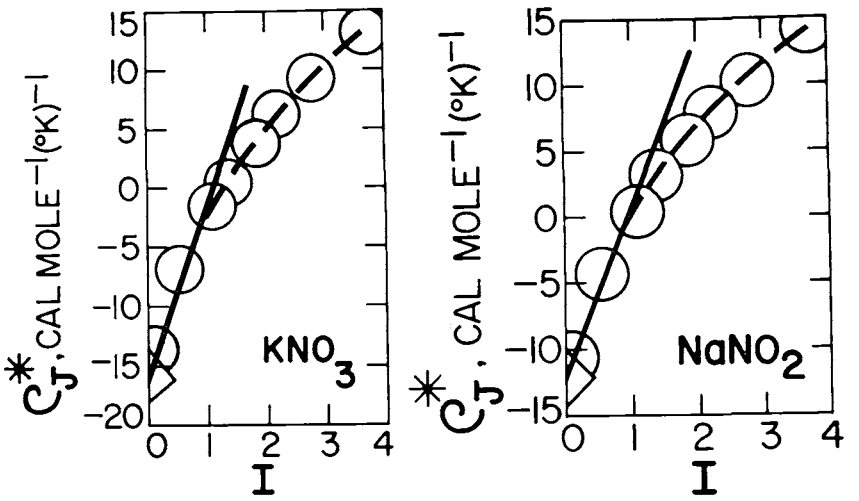

Fig. 81. ρ^*_J (eq 238) computed (assuming I = I) from apparent molal heat capacities at 25 °C and 1 bar (see caption of fig. 65).

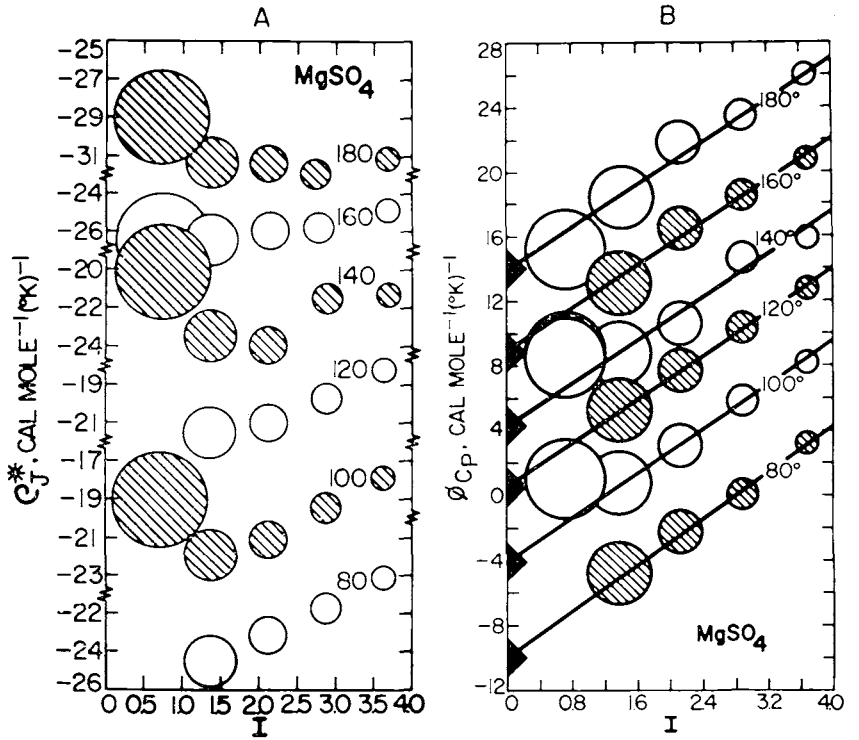

Fig. 82. ρ^*_J and ϕ_{cp} (eqs 229 and 238) for $MgSO_4$ computed (assuming I = I) from experimental data reported in the literature (see caption of fig. 65).

TABLE 10

Extended term parameters (b_j) for computing the relative apparent and partial molal heat capacities of aqueous electrolytes at 25°C and 1 bar from eqs (224) and (229)

Solute	b_J^a	Solute	b_J^a	Solute	b_J^a
HCl	-4.2	NaBr	-13.4	$LiNO_3$	-9.0
LiCl	-7.2	KBr	-10.2	$AgNO_3$	-22.0
NaCl	-12.8	RbBr	-12.2	HNO_3	-8.6
KCl	-9.3	CsBr	-14.0	KNO_3	-30.0
RbCl	-10.4	NaI	-16.0	$NaNO_3$	-31.0
CsCl	-12.6	KI	-12.2	$NaNO_2$	-25.2
NH_4Cl	-5.4	RbI	-12.8	LiOH	-12.0
$CaCl_2$	-4.7	CsI	-18.0	KOH	-13.0
$MgCl_2$	-3.5	NaF	-19.0	NaOH	-21.0
$BaCl_2$	-8.7	KF	-11.4	$NaBrO_3$	-27.0
$SrCl_2$	-5.6	RbF	-11.0	HIO_3	-96.0
HBr	-5.2	CsF	-9.4	KIO_3	-130.0
LiBr	-3.6	NH_4NO_3	-18.0	$KMnO_4$	-64.4

[a] cal kg mole^{-2} (°K)$^{-1}$. [b] Computed from the slopes of the linear curves in figures 65 through 69 and 79 through 81 (see text).

TABLE 11

Extended term parameters (b_V) for computing the relative apparent and partial molal volumes of aqueous electrolytes at 25°C and 1 bar from eqs (222) and (227)

Solute	$b_V^{a,b}$	Solute	$b_V^{a,b}$	Solute	$b_V^{a,b}$
HCl	0.60	RbBr	1.96	RbF	2.80
LiCl	1.00	CsBr	1.92	CsF	2.52
NaCl	1.90	NH_4Br	1.48	HNO_3	0.44
KCl	2.30	LiI	-0.10	$LiNO_3$	0.34
RbCl	2.20	NaI	0.92	$NaNO_3$	1.32
CsCl	2.08	KI	1.64	KNO_3	1.90
NH_4Cl	0.60	RbI	1.62	NH_4NO_3	0.46
$MgCl_2$	0.88	CsI	1.64	$AgNO_3$	1.80
LiBr	0.54	NH_4I	0.36	LiOH	2.24
NaBr	1.52	NaF	2.90	NaOH	3.08
KBr	2.04	KF	2.94	KOH	3.08

[a] cm^3 kg mole^{-2}. [b] Computed from the slopes of the linear curves in figures 83 through 88. In cases where two curves with different slopes are shown for the same electrolyte, those in figures 83 through 85 were accepted in preference to those in figures 86 through 88, which are more uncertain.

TABLE 12

Extended term parameters (b_κ) for computing the relative apparent and partial molal compressibilities of aqueous electrolytes at 25°C and 20 bars from eqs (226) and (231)

Solute	$b_\kappa^{a,b} \times 10^4$	Solute	$b_\kappa^{a,b} \times 10^4$	Solute	$b_\kappa^{a,b} \times 10^4$
HCl	1.6	KBr	6.8	$NaNO_3$	3.0
LiCl	3.2	NH_4Br	2.2	KNO_3	5.6
NaCl	8.0	LiI	1.6	NH_4NO_3	1.2
KCl	8.4	NaI	2.0	$AgNO_3$	4.0
NH_4Cl	3.4	KI	5.0	LiOH	8.4
$MgCl_2$	4.3	NH_4I	0.8	NaOH	15.6
LiBr	2.0	HNO_3	0.8	KOH	13.0
NaBr	5.2	$LiNO_3$	2.0		

[a] cm^3 kg mole^{-2} bar^{-1}. [b] Computed from the slopes of the linear curves in figures 95 through 97.

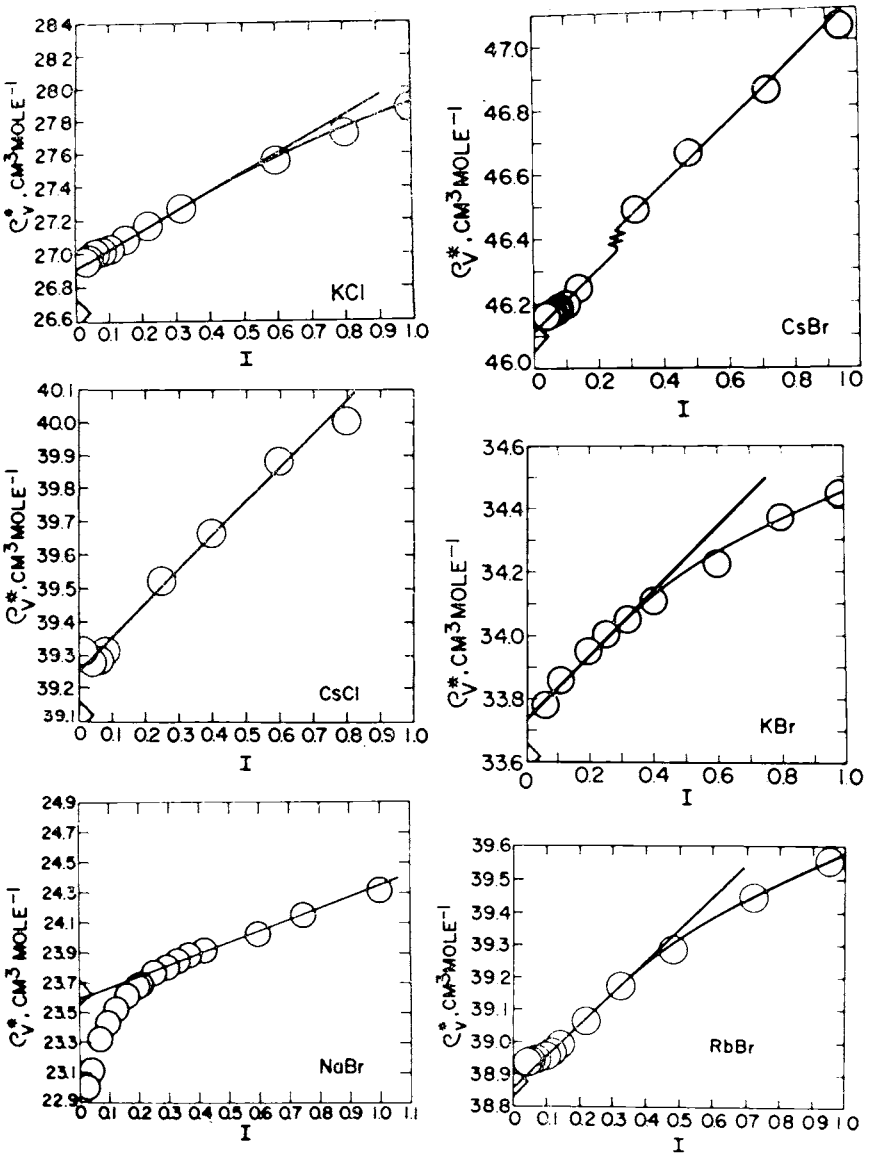

Fig. 83. ρ^*_V (eq 240) at 25°C and 1 bar computed (assuming I = I) from density data taken from the literature. The circles shown above and those in figure 84 through 94 represent experimental data reported by Fortier, Leduc, and Desnoyers (1974), Dunn (1968), Allam (ms), Ellis (1966, 1967, 1968; written commun., 1968) and Ellis and McFadden (1968, 1972). The values of $\bar{V}^\circ$ corresponding to the open triangles on the ordinates of the diagrams represent those computed from regression calculations by Helgeson and Kirkham (1976). The latter values do not in all instances necessarily correspond to the extrapolated intercepts of the linear curves in the diagrams (see text). The values represented by the closed triangles on the ordinates of figures 89 through 92 correspond to extrapolated values of $\bar{V}^\circ$ generated from the Redlich-Meyer equation (Redlich and Meyer, 1964) by Helgeson and Kirkham (1976).

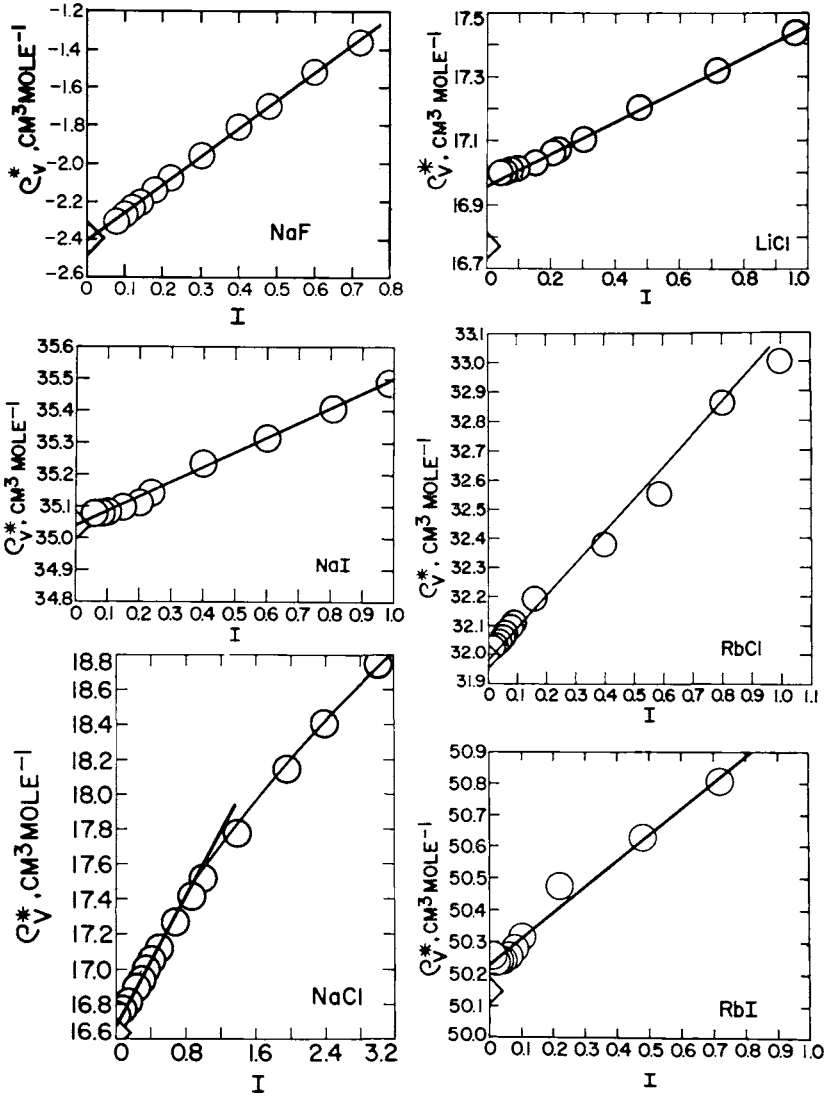

Fig. 84. ρ^*_V (eq 240) at 25°C and 1 bar computed (assuming I = $\hat{I}$) from density data taken from the literature (see caption of fig. 83).

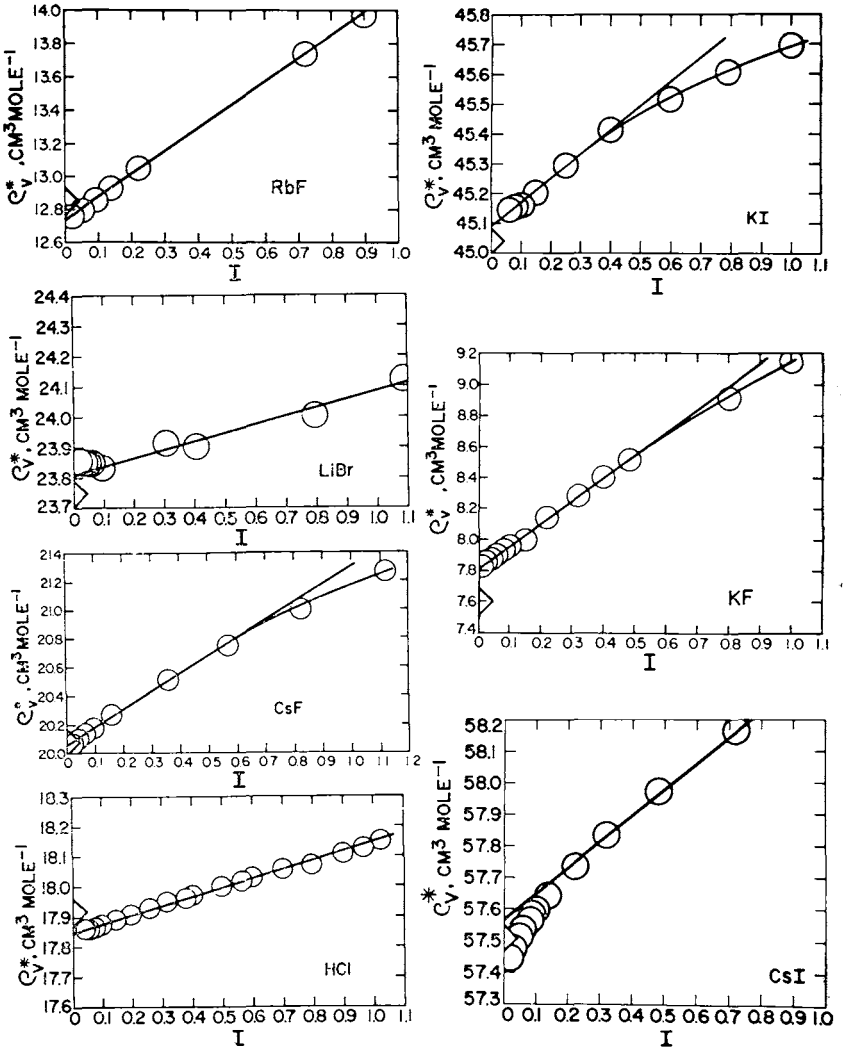

Fig. 85. ρ^*_V (eq 240) at 25°C and 1 bar computed (assuming I = Ī) from density data taken from the literature (see caption of fig. 83).

tively, on the ordinate, with the intercepts of the curves in figures 89 through 93 reveals discrepancies of the order of 1 cm^3 $mole^{-1}$ or less. Uncertainties of this order of magnitude have a negligible effect on most geochemical calculations. Accordingly, values of $b_{V,k}$ computed from the slopes of the linear curves in figures 83 through 93 were accepted without reassessing $\bar{V}°_k$. As a consequence, the conventional standard partial molal volumes of ionic species adopted in the present study correspond to those generated by Helgeson and Kirkham (1976). The values of $b_{V,k}$ at 25°C and 1 bar are given in table 11; those for higher temperatures are discussed in detail below.

The departures from linearity exhibited by ρ^*_V for Na_2SO_4, K_2SO_4, and $BaCl_2$ in figures 89 and 91 are consistent with increasing ion associa-

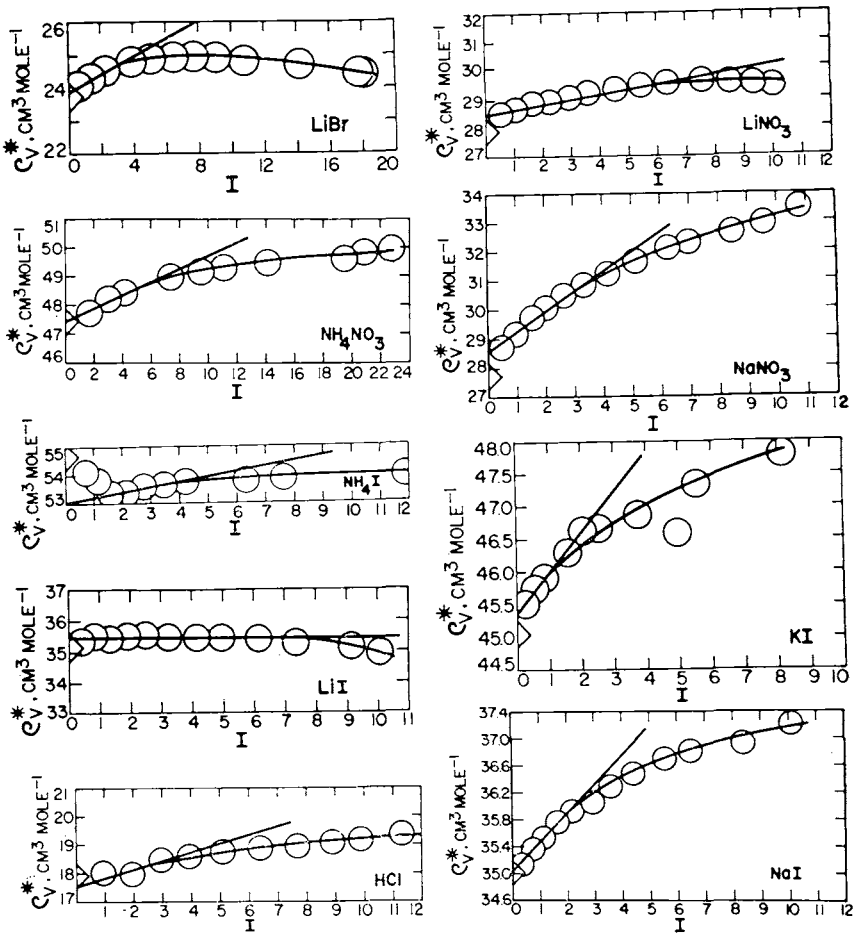

Fig. 86. ρ^*_V (eq 240) at 25°C and 1 bar computed (assuming I = Ī) from density data taken from the literature (see caption of fig. 83).

tion with increasing temperature. Note in figure 94, which corresponds to the volume analog of figure 82B, that $\phi_{V,MgSO_4}$ as a function of I exhibits evidence of polyligand association at high concentrations. However, no such evidence is apparent in the ionic strength dependence of $\phi_{C_P,MgSO_4}$ (fig. 82B). It should perhaps be emphasized in this regard that the effects of ion association on different apparent molal properties may be manifested at different ionic strengths, depending on differences in the standard molal Gibbs free energies, enthalpies, heat capacities, and volumes of dissociation (see below). The fact that ϕ_V and ϕ_{C_P} for $MgSO_4$ are both linear functions of I below I $\approx$ 3 is consistent with predominance of the ion pair at I < 3.

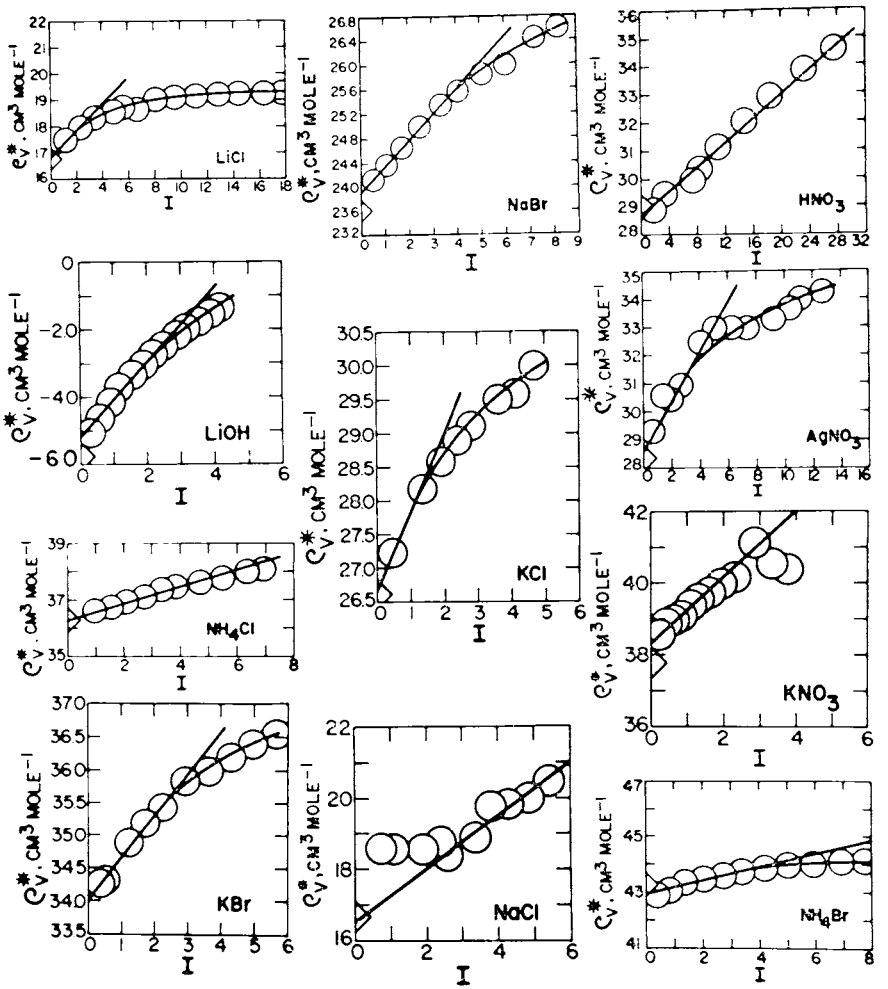

Fig. 87. ρ^*_V (eq 240) at 25°C and 1 bar computed (assuming I = I) from density data taken from the literature (see caption of fig. 83).

Compressibility data reported by Allam (1963) were used to compute the values of $\rho^*_{\kappa,k}$ shown in figures 95 through 97 by taking account of the relation,

$$\phi_{\kappa,k} = \frac{1000\beta - n^*_w \bar{V}^\circ_w \beta^\circ_w}{M_k} , \tag{243}$$

where β stands for the coefficient of isothermal compressibility of the solution ($(\partial \ ln \ \rho/\partial P)_T$), n^*_w denotes the number of moles of H_2O liter^{-1} of solution, $\bar{V}^\circ_w$ and β°_w represent the standard partial molal volume and coefficient of isothermal compressibility of pure H_2O, and M_k refers to the molarity of the kth electrolyte, which is related to the molality of the electrolyte by

$$m_k = \frac{1000M_k}{18.0153n^*_w} . \tag{244}$$

The values of $\bar{V}^\circ_w$ and β°_w employed in the calculations were taken from Helgeson and Kirkham (1974a).

With a few exceptions (for example NaOH and KOH) the computed values of $\rho^*_{\kappa,k}$ shown in figures 95 through 97 for ionic strengths $\leqslant 4$ (depending on the electrolyte) are in close agreement with eq (241). However, at lower ionic strengths the data points for all but a few of the electrolytes depart to an increasing degree from the linear curves toward more negative values of $\rho^*_{\kappa,k}$ with decreasing concentration. It can be deduced from comparison of the intercepts of the linear curves with the symbols on the ordinates representing values of $-\bar{\kappa}^\circ_k$ taken from Mathieson and Conway (1974) and Helgeson and Kirkham (1976) that this trend is inconsistent with values of $\bar{\kappa}^\circ_k$ derived from other experimental studies. The latter observation suggests systematic errors in Allam's compressibility measurements at low ionic strengths. For this reason the conventional standard partial molal compressibilities of aqueous species computed by Helgeson and Kirkham (1976) were accepted in the present study in pref-

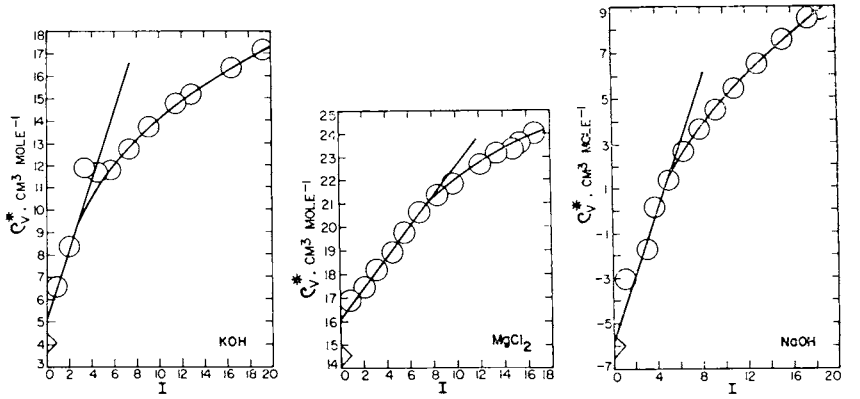

Fig. 88. ρ^*_V (eq 240) at 25°C and 1 bar computed (assuming I = $\bar{I}$) from density data taken from the literature (see caption of fig. 83).

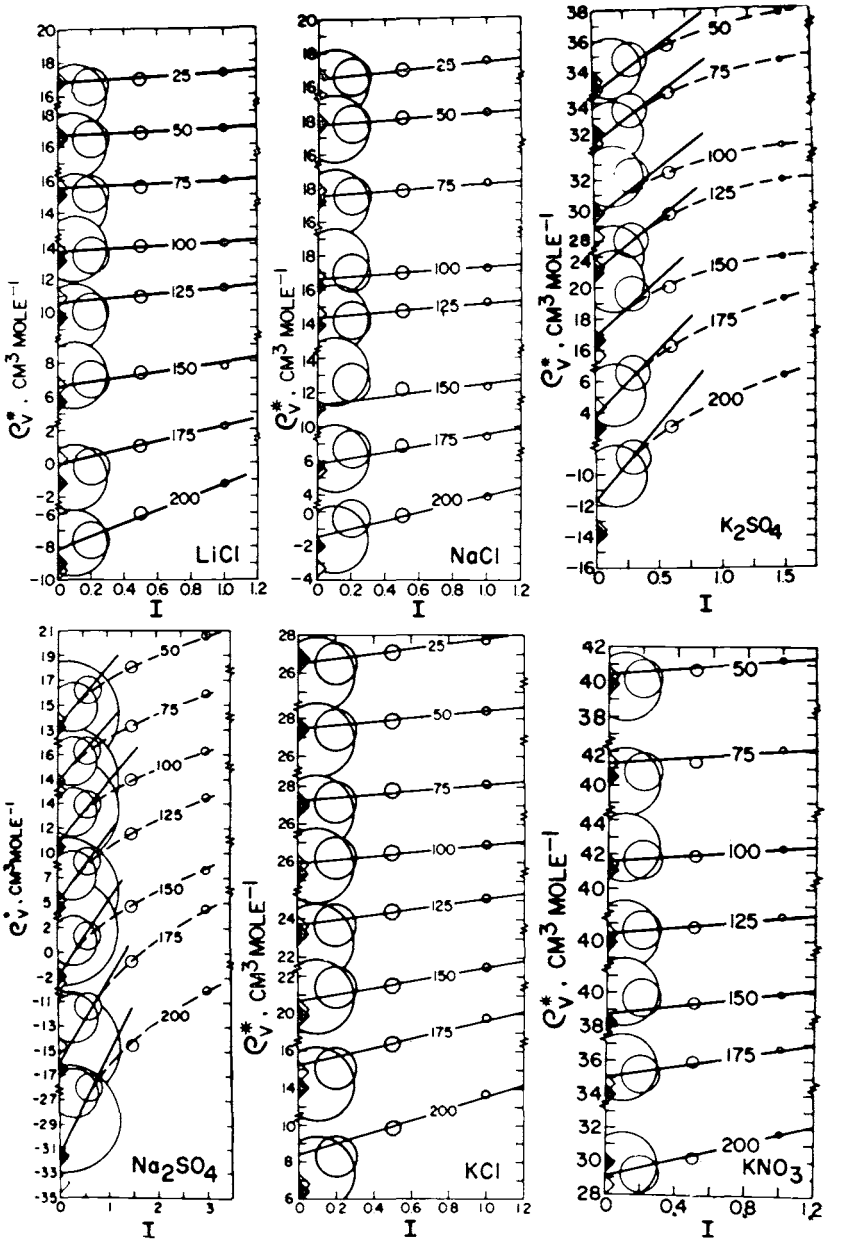

Fig. 89. ρ^*_V (eq 240) at 20 bars and various temperatures (indicated in °C) computed (assuming I = Ī) from density data taken from the literature (see caption of fig. 83).

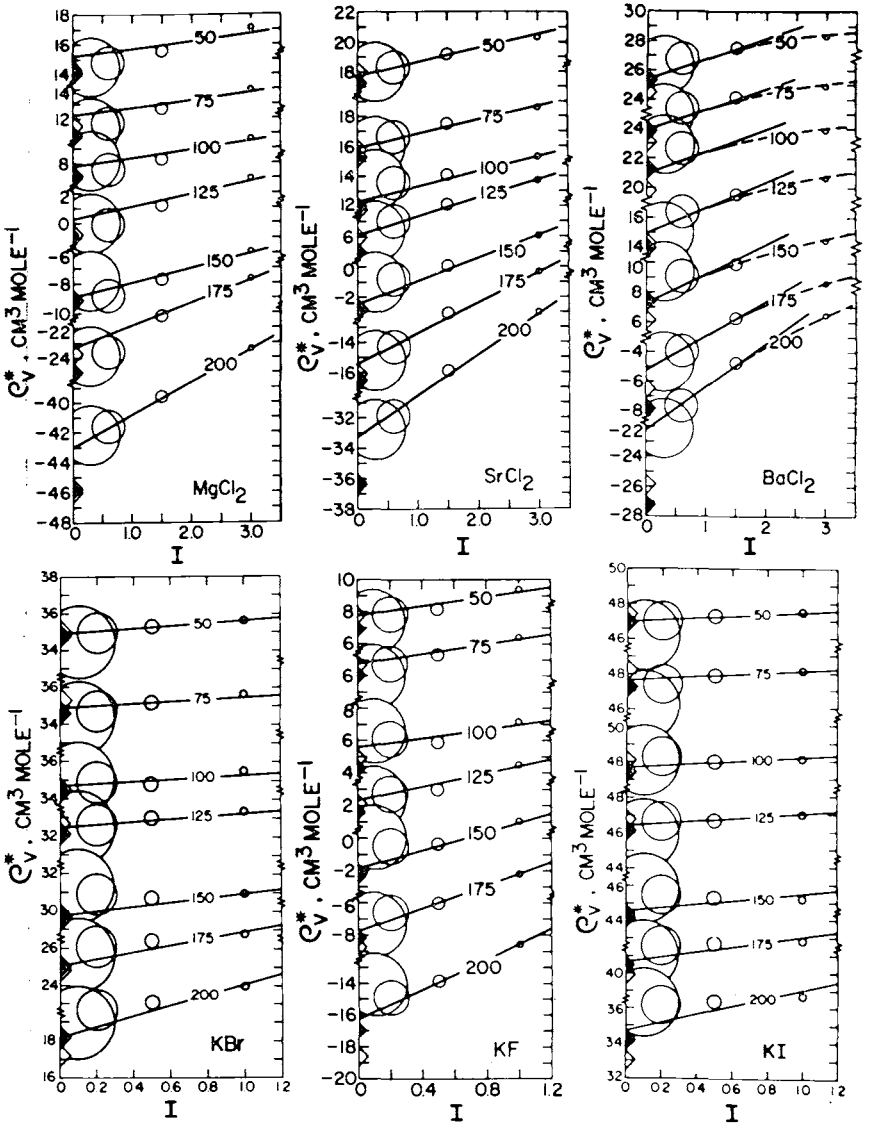

Fig. 90. ρ^*_V (eq 240) at 20 bars and various temperatures (indicated in °C) computed (assuming $I = \bar{I}$) from density data taken from the literature (see caption of fig. 83).

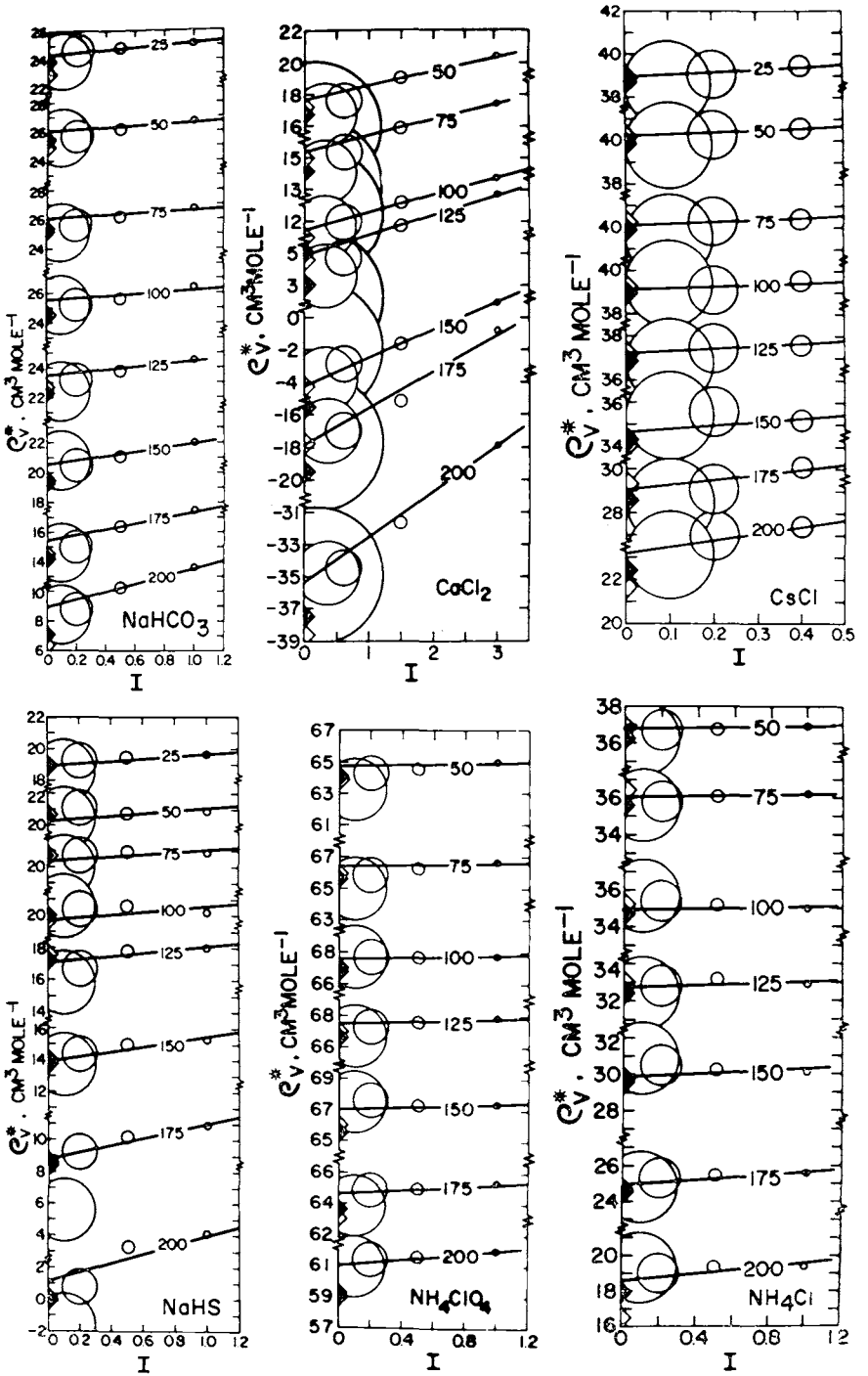

Fig. 91. ρ^*_V (eq 240) at 20 bars and various temperatures (indicated in °C) computed (assuming I = I) from density data taken from the literature (see caption of fig. 83).

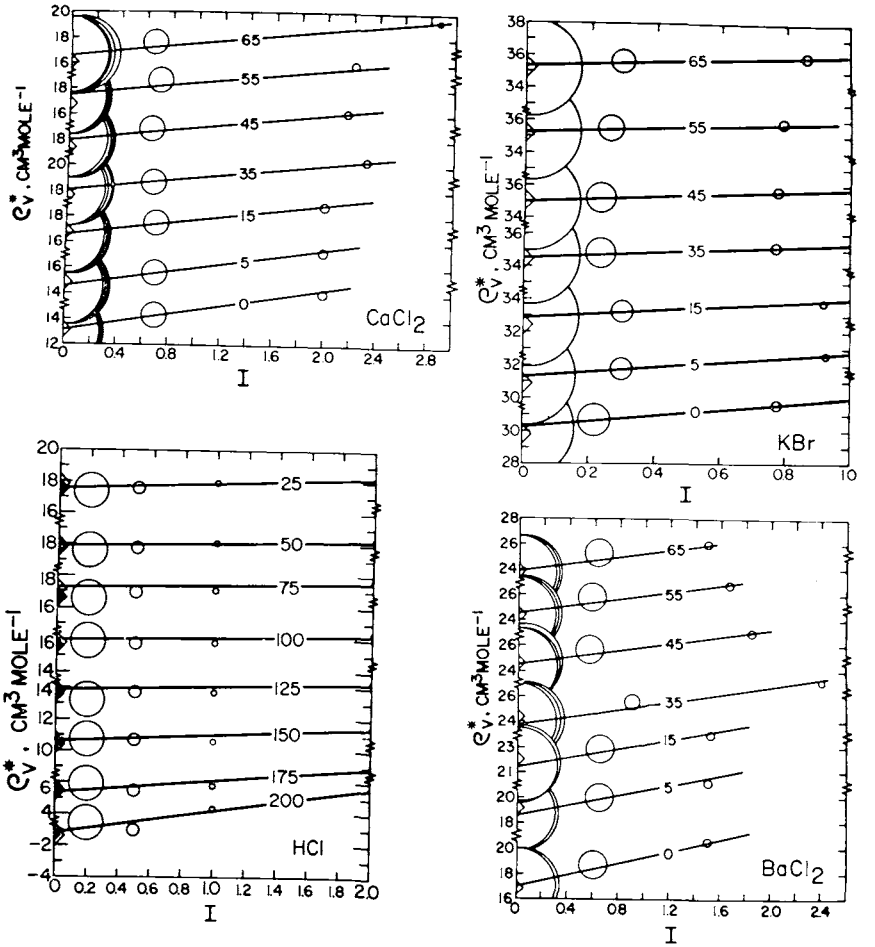

Fig. 92. ρ^*_V (eq 240) at various temperatures (indicated in °C) at 1 ($CaCl_2$, KBr, $BaCl_2$) and 20 (HCl) bars computed (assuming I = i) from density data taken from the literature (see caption of fig. 83).

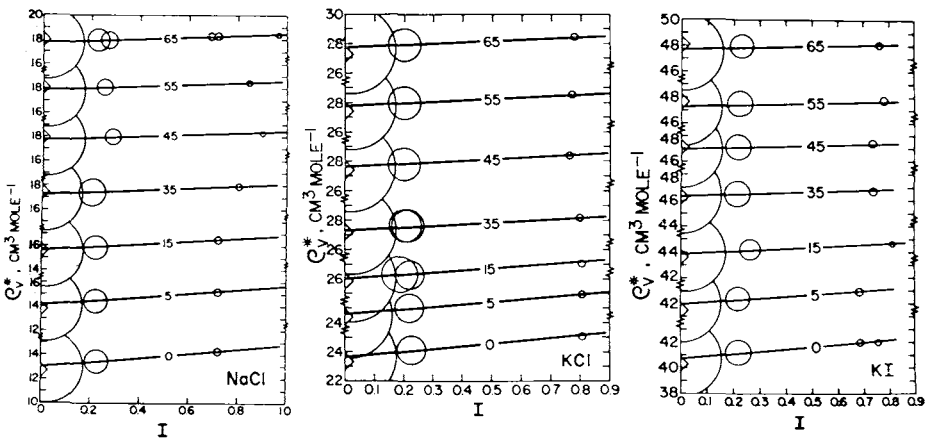

Fig. 93. ρ^*_V (eq 240) at various temperatures (indicated in °C) and 1 bar computed (assuming I = i) from density data taken from the literature (see caption of fig. 83).

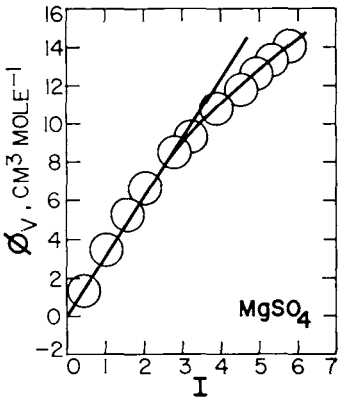

Fig. 94. Apparent molal volume of $MgSO_4$ as a function of stoichiometric ionic strength at 25°C and 1 bar (see text and caption of fig. 83).

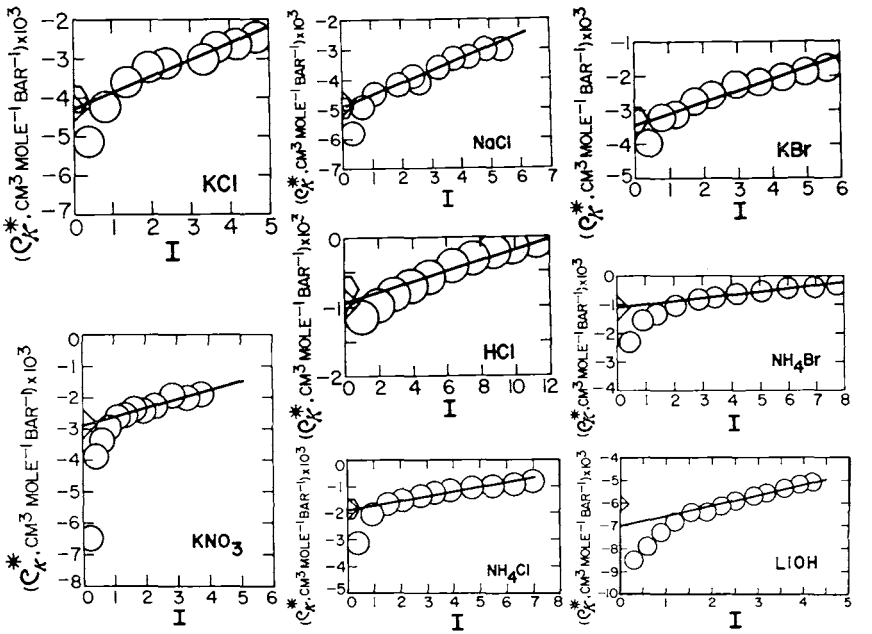

Fig. 95. ρ^*_κ (eq 241) at 25°C and 1 bar computed (assuming I = $\bar{I}$) from compressibility data reported by Allam (ms). The values of $\bar{\kappa}^\circ$ represented by the half-pentagons and triangles on the ordinates of the diagrams shown above and those in figures 96 through 99 correspond to standard partial molal compressibilities given by Mathieson and Conway (1974) and Helgeson and Kirkham (1976), respectively.

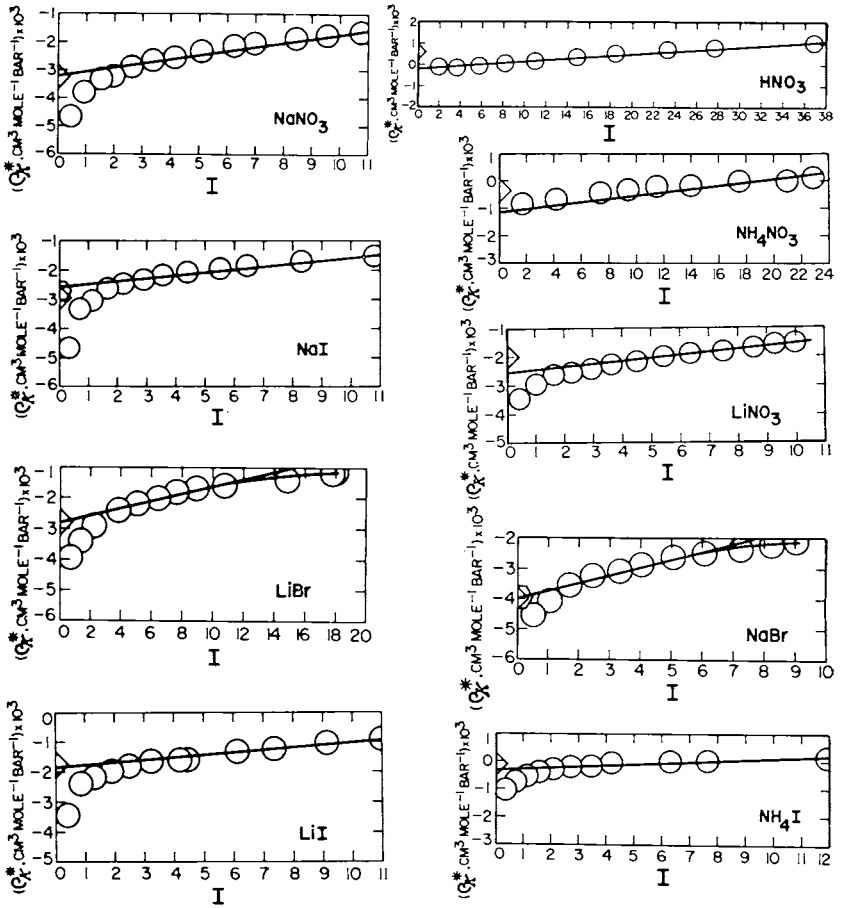

Fig. 96. ρ^*_κ (eq 241) at 25°C and 1 bar computed (assuming I = $\bar{I}$) from compressibility data reported by Allam (ms) (see caption of fig. 95).

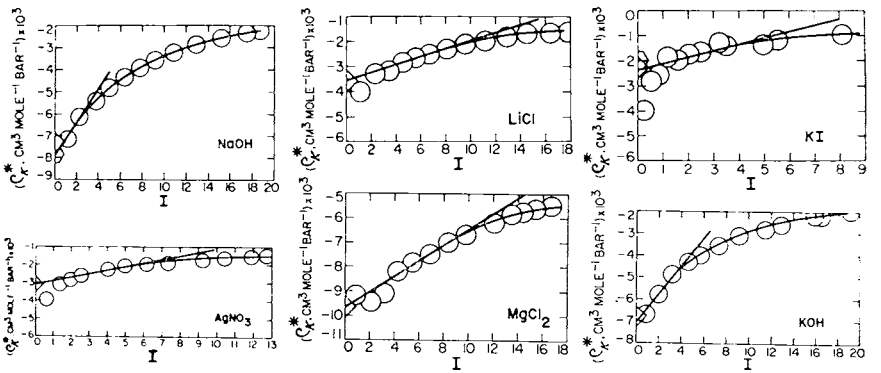

Fig. 97. ρ^*_κ (eq 241) at 25°C and 1 bar computed (assuming I = $\bar{I}$) from compressibility data reported by Allam (ms) (see caption of fig. 95).

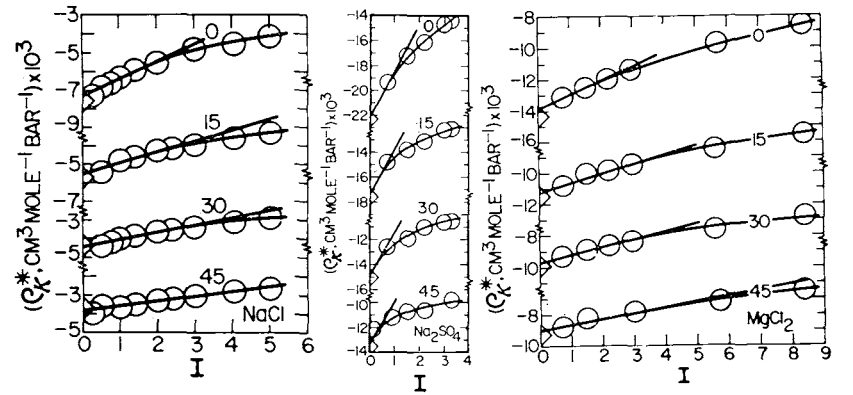

Fig. 98. ρ^*_κ (eq 241) at various temperatures (indicated in °C) and 1 bar computed (assuming I = Ī) from compressibility data reported by Millero and others (1974) (see caption of fig. 95).

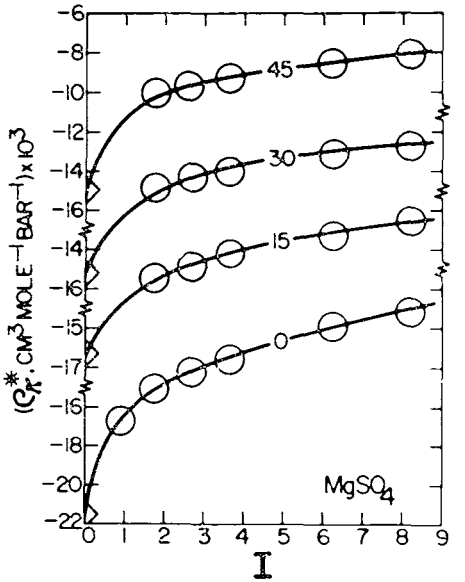

Fig. 99. ρ^*_κ (eq 241) for $MgSO_4$ as a function of stoichiometric ionic strength at various temperatures (indicated in °C) and 1 bar computed (assuming I = Ī) from data reported by Millero and others (1974) (see caption of fig. 95).

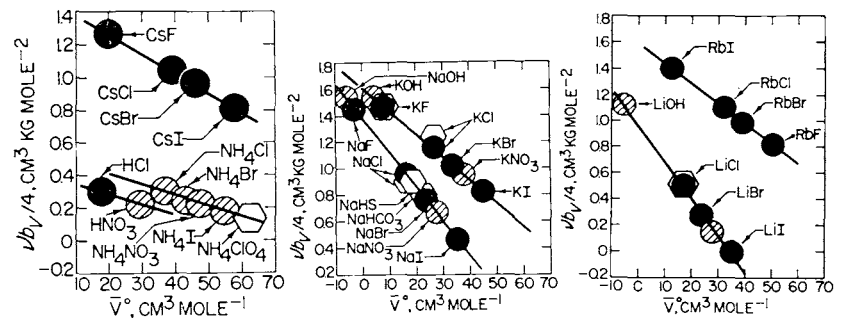

Fig. 100. Correlation of apparent molal volume extended term parameters with the standard partial molal volumes of aqueous electrolytes at 25°C and 1 bar (see text). The various symbols represent the slopes of the linear curves for the electrolytes at 25°C in figures 83 through 97 and corresponding values of V̄° given by Helgeson and Kirkham (1976).

erence to the intercepts of the linear curves shown in figures 95 through 99.

Values of $b_{\kappa,k}$ computed from the slopes of the linear curves shown in figures 95 through 97 are given in table 12. Note in figure 98 that the experimental data for NaCl, Na_2SO_4, and $MgCl_2$ at temperatures above and below 25°C are also consistent with eq (241). However, it can be deduced from figure 98 that $\rho^*_{\kappa,k}$ as a function of I for these three electrolytes, as well as those for NaOH, $AgNO_3$, LiCl, KI, and KOH in figure 97 exhibit departures from linearity consistent with increasing ion association with increasing concentration at high ionic strength. Note in figure 99 that $\rho^*_{\kappa,MgSO_4}$ is a non-linear function of ionic strength at all temperatures $\leqslant 45$°C.

Corresponding states relations.—It can be deduced from figure 100 that b_V is linearly related to $\bar{V}^\circ$ for 1:1 electrolytes with a common cation. The curves in figure 100 are consistent with

$$\nu_k b_{V,k}/4 = a_1 + b_1 \bar{V}^\circ_k \qquad (245)$$

which can be used to estimate values of $b_{V,k}$ in cm^3 kg $mole^{-2}$ from standard partial molal volumes expressed in cm^3 $mole^{-1}$. The requisite coefficients for eq (245) are:

	a_1	$b_1 \times 10^3$
Li — electrolytes	0.96	−28.2
Na — electrolytes	1.38	−25.9
K — electrolytes	1.61	−17.5
Rb — electrolytes	1.59	−15.4
Cs — electrolytes	1.50	−11.9
NH_4 — electrolytes	0.54	−6.6

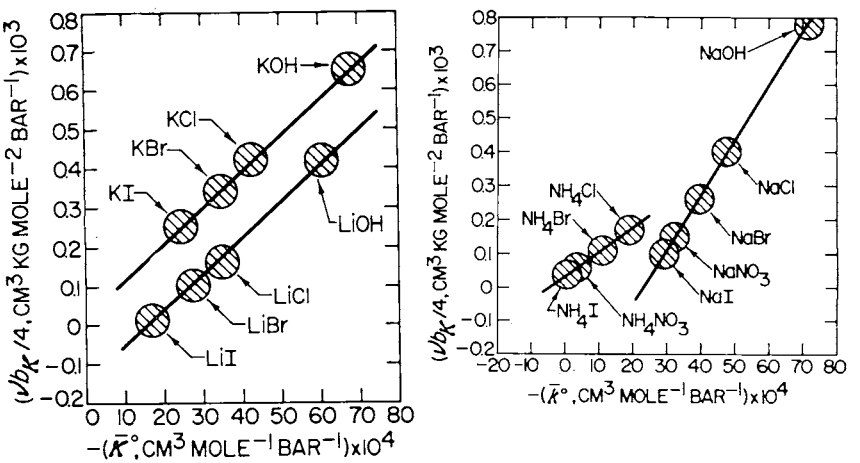

Fig. 101. Correlation of apparent molal compressibility extended term parameters with the standard partial molal compressibilities of aqueous electrolytes at 25°C and 1 bar (see text). The symbols represent the slopes of the linear curves for the electrolytes at 25°C in figures 95 through 97 and corresponding values of $\bar{\kappa}^\circ$ given by Helgeson and Kirkham (1976).

Note that the progression in these coefficients is roughly related to the effective electrostatic radii of the cations in table 3, which is also true of the coefficients in the other algorithms discussed below.

A corresponding states relation for compressibility similar to that for volume in figure 100 is shown in figure 101, where it can be seen that $\nu b_{\kappa,k}/4$ is linearly related to $\bar{\kappa}^\circ_k$ for 1:1 electrolytes with a common cation. Note also in figure 102 that the same "families" of electrolytes exhibit a linear correlation of $\bar{\kappa}^\circ_k$ to $\bar{V}^\circ_k$. Estimation algorithms corresponding to the curves in figures 101 and 102 can be written for $b_{\kappa,k}$ in cm^3 kg mole^{-2} bar^{-1}, $\bar{\kappa}^\circ$ in cm^3 mole^{-1} bar^{-1}, and $\bar{V}^\circ$ in cm^3 mole^{-1} as

$$\nu_k b_{\kappa,k}/4 = a_2 + b_2 \bar{\kappa}^\circ_k \tag{246}$$

and

$$\bar{\kappa}^\circ_k = a_3 + b_3 \bar{V}^\circ_k \tag{247}$$

where $b_3 = 5 \times 10^{-4}$ and

	$a_2 \times 10^5$	$b_2 \times 10^2$	$a_3 \times 10^4$
Li — electrolytes	−16	−9.2	−51
Na — electrolytes	−37	−16.0	−63
K — electrolytes	2	−9.2	−68
Rb — electrolytes			−60
Cs — electrolytes			−74
NH_4 — electrolytes	3	−7.2	−54

Discussion.—The remarkable agreement and internal consistency of the many sets of experimental activity coefficient, osmotic coefficient, enthalpy, heat capacity, volume, and compressibility data represented by the symbols in figures 17 through 21, 23 through 29, 45 through 47, and 50 through 99 strongly support the theoretical model and equations responsible for the linear curves shown in the figures, as well as the å values used in the calculations. The fact that the latter values were derived independently from standard partial molal volumes and entropies of aque-

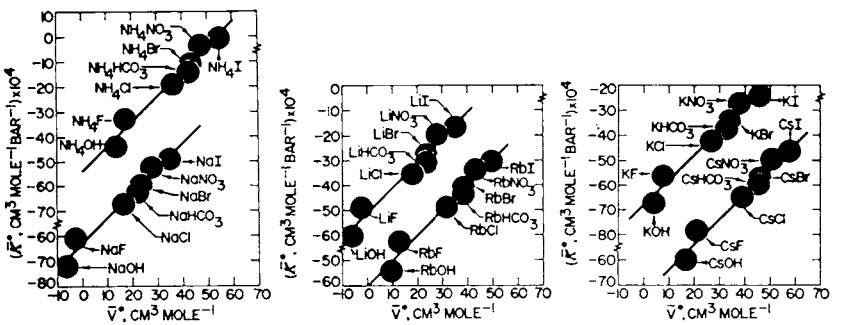

Fig. 102. Correlation of the standard partial molal compressibilities and volumes of aqueous electrolytes at 25°C and 1 bar. The symbols represent values given by Helgeson and Kirkham (1976) and Mathieson and Conway (1974).

ous species underscores the generality of the approach. The agreement is particularly impressive in view of the relatively large uncertainties in apparent molal heat capacities, volumes, and compressibilities that result from experimental measurements of the properties of dilute solutions. Measurements in highly concentrated solutions yield more reliable values of apparent molal properties, but they are subject to significant contributions by ion association. The extent to which complexing affects the different apparent molal properties of an electrolyte at the same ionic strength may be quite different, depending on the electrolyte and the relative magnitude of the property compared to the change in the property attending ion association. For example, $(\partial^2 m_j/\partial T^2)_{P,\hat{m}(k)}$ may be small compared to ϕ_{C_P} and $(\partial m_j/\partial P)_{T,\hat{m}(k)}$ so that ion association might have a significant effect on ρ^*_V but not on ρ^*_J. Similarly, the standard molal enthalpy of dissociation for a given complex may be small (of the order of a few hundred cal mole^{-1}), but the effect on $\rho^*_{\Delta H_d}$ could be dramatic if ϕ_H is also small, despite the fact that the degree of formation of the complex might be no more than a few percent. In other cases, log K for the dissociation of a complex may be substantially negative, causing $\gamma_\pm$ to be affected in dilute as well as concentrated solutions. Nevertheless, the standard partial molal enthalpy, heat capacity, and/or volume of dissociation may have an insignificant effect on $\rho^*_{\Delta H_d}$, ρ^*_J, or ρ^*_V if the degree of formation of the complex is insensitive to changes in temperature and pressure. In still others, the effects of ion association may be significant only in the dilute range of concentration. In general, it appears from the data considered above that $\rho^*_{\Delta H_d}$ is more sensitive to ion association than ρ^*_J or ρ^*_V, but that ρ^*_κ is relatively insensitive to complexing. Similarly, ρ^*_V is affected by ion association to a much greater extent than is ρ^*_J.

PREDICTION OF THERMODYNAMIC PROPERTIES AT HIGH PRESSURES AND TEMPERATURES

Calculation of the thermodynamic behavior of hydrothermal/geothermal systems at high pressures and temperatures requires predictive equations describing the pressure and temperature dependence of the standard partial molal properties of aqueous species as well as corresponding equations for the extended term parameters in the equations summarized above. Equations of this kind can be derived from the theoretical model proposed by Helgeson and Kirkham (1976).

Standard Partial Molal Properties

As noted above any standard partial molal property of an aqueous species can be viewed as the sum of its intrinsic counterpart and contributions by electrostriction collapse of the local solvent structure and solvation of the species in solution (eq 113). Although these contributions are not independent of one another, analysis of the thermodynamic behavior of electrolyte solutions as a function of pressure and temperature indicates that eq (116) affords close approximation of the standard partial molal properties of aqueous species at high as well as low temperatures and pressures.

The standard partial molal properties of aqueous species at high pressures and temperatures can be calculated by combining eq (116) with an equation of state describing the volumetric consequences of electrostriction collapse and ion solvation as a function of pressure and temperature, together with a corresponding equation representing the dependence of the standard partial molal heat capacity of the species on temperature at a reference pressure of 1 bar. The equation of state adopted in the present study corresponds to that derived by Helgeson and Kirkham (1976), which is reviewed briefly below.

Equation of state.—Consideration of standard partial molal volume and compressibility data for aqueous electrolytes as a function of temperature at low pressures indicates that $\bar{V}^\circ_{i,j}$ (the conventional intrinsic standard partial molal volume of the jth ion) can be regarded as a temperature/pressure-independent constant and that $\Delta\bar{V}^\circ_{c,j}$ (the collapse contribution to $\bar{V}^\circ_j$) is an asymptotic function of temperature, which is linearly dependent on pressure (Helgeson and Kirkham, 1976). These observations are consistent with

$$\bar{V}^\circ_{i,j} = a_{1,j} \tag{248}$$

$$-\bar{\kappa}^\circ_{i,j} \equiv \left(\frac{\partial \bar{V}_{i,j}}{\partial P}\right)_T = \bar{E}^\circ_{x,i,j} \equiv \left(\frac{\partial \bar{V}^\circ_{i,j}}{\partial T}\right)_P = \left(\frac{\partial \bar{E}^\circ_{x,i,j}}{\partial T}\right)_P \equiv \left(\frac{\partial^2 \bar{V}^\circ_{i,j}}{\partial T^2}\right)_P = 0 \,, \tag{249}$$

$$\Delta\bar{V}^\circ_{c,j} = a_{2,j}P + \frac{a_{3,j}T + a_{4,j}PT}{T - \theta_j} \,, \tag{250}$$

$$\Delta\bar{E}^\circ_{x,c,j} \equiv \left(\frac{\partial \Delta\bar{V}^\circ_{c,j}}{\partial T}\right)_P = -\left(\frac{\partial \Delta\bar{S}^\circ_{c,j}}{\partial P}\right)_T = \Delta\bar{E}^\circ_{x,n,j} = \left(\frac{\partial \Delta\bar{V}^\circ_{n,j}}{\partial T}\right)_P = -\left(\frac{\partial \Delta\bar{S}^\circ_{n,j}}{\partial P}\right)_T = -\frac{\theta_j(a_{3,j} + a_{4,j}P)}{(T - \theta_j)^2} \,, \tag{251}$$

$$-\Delta\bar{\kappa}^\circ_{c,j} \equiv \left(\frac{\partial \Delta\bar{V}^\circ_{c,j}}{\partial P}\right)_T = -\Delta\bar{\kappa}^\circ_{n,j} \equiv \left(\frac{\partial \bar{V}^\circ_{n,j}}{\partial P}\right)_T = a_{2,j} + \frac{a_{4,j}T}{T - \theta_j} \,, \tag{252}$$

and

$$\Delta\bar{V}^\circ_{n,j} = \bar{V}^\circ_{i,j} + \Delta\bar{V}^\circ_{c,j} = a_{1,j} + a_{2,j}P + \frac{a_{3,j}T + a_{4,j}PT}{T - \theta_j} \tag{253}$$

where $a_{1,j}$, $a_{2,j}$, $a_{3,j}$, $a_{4,j}$, and θ_j (which can be regarded as a "structural" temperature analogous to that introduced by Bernal and Fowler, 1933) correspond to temperature/pressure-independent coefficients characteristic of the jth aqueous species. Note that it follows from eqs (116), (253), and the partial derivative of eq (133) at constant temperature that we can write

$$\bar{V}^\circ_j = a_{1,j} + a_{2,j}P + \frac{a_{3,j}T + a_{4,j}PT}{T - \theta_j} - \omega_j Q \,, \tag{254}$$

which is consistent with

$$\Delta\bar{V}^\circ_{s,j} = -\omega_j Q \tag{255}$$

where ω_j is defined by eq (130) and

$$Q \equiv -\left(\frac{\partial(1/\epsilon^\circ)}{\partial P}\right)_T = \frac{1}{\epsilon^\circ}\left(\frac{\partial \ln \epsilon^\circ}{\partial P}\right)_T \tag{256}$$

where ϵ° denotes the dielectric constant of the solvent. Note that it follows from eq (254) that we can also write

$$\bar{E}^\circ_{x,j} \equiv \left(\frac{\partial \bar{V}^\circ_j}{\partial T}\right)_P = -\left(\frac{\partial \bar{S}^\circ_j}{\partial P}\right)_T = -\frac{\theta_j(a_{3,j} + a_{4,j}P)}{(T-\theta_j)^2} - \omega_j U \tag{257}$$

and

$$-\bar{\kappa}^\circ_j = \left(\frac{\partial \bar{V}^\circ_j}{\partial P}\right)_T = a_{2,j} + \frac{a_{4,j}T}{T-\theta_j} - \omega_j N \tag{258}$$

where

$$U \equiv \left(\frac{\partial Q}{\partial T}\right)_P = \frac{1}{\epsilon^\circ}\left(\left(\frac{\partial(\partial \ln \epsilon^\circ/\partial P)_T}{\partial T}\right)_P - \left(\frac{\partial \ln \epsilon^\circ}{\partial P}\right)_T \left(\frac{\partial \ln \epsilon^\circ}{\partial T}\right)_P\right) \tag{259}$$

and

$$N \equiv \left(\frac{\partial Q}{\partial P}\right)_T = \frac{1}{\epsilon^\circ}\left(\left(\frac{\partial^2 \ln \epsilon^\circ}{\partial P^2}\right)_T - \left(\frac{\partial \ln \epsilon^\circ}{\partial P}\right)^2_T\right) \tag{260}$$

which represent the electrostatic contributions by the solvent to the conventional standard partial molal expansibility and compressibility of solvation. These latter properties are defined by

$$\Delta\bar{E}^\circ_{x,s,j} = -\omega_j U \tag{261}$$

and

$$\Delta\bar{\kappa}^\circ_{s,j} = \omega_j N \quad . \tag{262}$$

The equations summarized above afford close approximation of the pressure dependence of the thermodynamic properties of aqueous species in the standard state at both high and low pressures and temperatures (Helgeson and Kirkham, 1976). In addition, consideration of standard partial molal heat capacity data for aqueous electrolytes as a function of temperature indicates that the calorimetric consequences of electrostriction collapse and ion solvation as a function of temperature can be described in terms of the same theoretical model used to represent the temperature dependence of $\Delta\bar{V}^\circ_j$ in eq (254), which constitutes a general equation of state for aqueous species at infinite dilution.

Calorimetric consequences of electrostriction collapse and ion solvation.—Calculation of $\Delta\bar{C}^\circ_{P,n,k}$ (the sum of the intrinsic and collapse contributions to the standard partial molal heat capacity of the kth electrolyte) from calorimetric data at temperatures from 0° to 200°C along the

liquid-vapor equilibrium curve for H_2O suggests that $\bar{C}^\circ_{P,i,j}$ corresponds to a pressure/temperature-independent constant and that $\Delta\bar{C}^\circ_{P,c,j}$ is essentially proportional to $\Delta\bar{V}^\circ_{c,j}$ as a function of temperature. These calculations were carried out by first taking the partial derivative of eq (133) with respect to temperature at constant pressure, which can be written as

$$\Delta\bar{S}^\circ_{s,j} = -\left(\frac{\partial\Delta\bar{G}^\circ_{s,j}}{\partial T}\right)_P = \omega_j Y \tag{263}$$

which is consistent with

$$\Delta\bar{C}^\circ_{P,s,j} = T\left(\frac{\partial\Delta\bar{S}^\circ_{s,j}}{\partial T}\right)_P = \left(\frac{\partial\Delta\bar{H}^\circ_{s,j}}{\partial T}\right)_P = \omega_j TX \tag{264}$$

where $\Delta\bar{S}^\circ_{s,j}$ and $\Delta\bar{C}^\circ_{P,s,j}$ stand for the conventional standard partial molal entropy and heat capacity of solvation and

$$Y \equiv -\left(\frac{\partial(1/\epsilon^\circ)}{\partial T}\right)_P = \frac{1}{\epsilon^\circ}\left(\frac{\partial \ln \epsilon^\circ}{\partial T}\right)_P \tag{265}$$

and

$$X \equiv \left(\frac{\partial Y}{\partial T}\right)_P = \frac{1}{\epsilon^\circ}\left(\left(\frac{\partial^2 \ln \epsilon^\circ}{\partial T^2}\right)_P - \left(\frac{\partial \ln \epsilon^\circ}{\partial T}\right)_P^2\right) \tag{266}$$

where ϵ° again refers to the dielectric constant of the solvent. The values of $\Delta\bar{C}^\circ_{P,n,k}$ were then computed from eqs (29), (116), and (264) using the experimental standard partial molal heat capacities of electrolytes represented by the intercepts of the linear curves in figures 70 through 78, together with values of ω_j taken from table 3 and those of X given by Helgeson and Kirkham (1974a). Because the effect on $\bar{C}^\circ_{P,k}$ of the 15 bar pressure variation from 0° to 200°C along the liquid-vapor equilibrium curve for H_2O is negligible compared to the consequences of experimental uncertainties on the intercepts of the linear curves in these figures, no correction was made for pressure differences in the experiments at temperatures > 100°C. For the same reason, no correction for changes in vapor pressure as a function of concentration, and no conversion of $\bar{C}^\circ_{sat,k}$ (the standard partial molal heat capacity of the kth electrolyte along the liquid-vapor equilibrium curve for the solvent) to $\bar{C}^\circ_{P,k}$ was necessary. The latter two variables are related by

$$\bar{C}^\circ_{P,k} = \bar{C}^\circ_{sat,k} + T\left(\frac{\partial\bar{V}^\circ_k}{\partial T}\right)_P \left.\frac{dP}{dT}\right|_{sat} \tag{267}$$

where $dP/dT|_{sat}$ stands for the derivative of pressure with respect to temperature along the liquid-vapor equilibrium curve for H_2O. The last term on the right side of eq (267) is insignificant for most electrolytes at temperatures and pressures $\leq$ 200°C and 15 bars, as is the difference between $\bar{C}_{P,k}$ and $\bar{C}_{sat,k}$.

It follows from the observations made above that we can write for the reference pressure (P_r),

$$\Delta\bar{C}^\circ_{P_r,c,j} = \frac{c_{2,j}T}{T-\theta_j} , \tag{268}$$

and

$$\Delta\bar{C}^\circ_{P_r,n,j} = c_{1,j} + \frac{c_{2,j}T}{T-\theta_j} , \tag{269}$$

where $c_{i,j}$ and $c_{2,j}$ stand for temperature/pressure-independent coefficients analogous to a_1 and a_3 in eq (254), and θ_j is again the "structural" temperature for the jth species. Summing eqs (268), (269), and a statement of eq (264) for $P = P_r$ then leads to

$$\bar{C}^\circ_{P_r,j} = c_{1,j} + \frac{c_{2,j}T}{T-\theta_j} + \omega_j TX , \tag{270}$$

which is consistent with

$$\bar{C}^\circ_{P_r,i,j} = \bar{C}^\circ_{P,i,j} = c_{1,j} . \tag{271}$$

Taking account of the partial derivative of eq (257) with respect to temperature at constant pressure and the relation

$$\left(\frac{\partial\bar{C}^\circ_P}{\partial P}\right)_T = -T\left(\frac{\partial\bar{E}^\circ_x}{\partial T}\right)_P \tag{272}$$

leads to

$$\bar{C}^\circ_{P,j} = \left(\frac{\partial\bar{H}^\circ_j}{\partial T}\right)_P = -T\left(\frac{\partial\bar{S}^\circ_j}{\partial T}\right)_P = c_{1,j} + \frac{c_{2,j}T}{T-\theta_j} - \frac{\theta_j T(2a_{3,j}(P-P_r) + a_{4,j}(P^2-P_r^2))}{(T-\theta_j)^3} + \omega_j TX \tag{273}$$

which describes the pressure and temperature dependence of the standard partial molal heat capacities of aqueous species.

Standard partial molal entropy, enthalpy, and Gibbs free energy.— Integration of eq (273) with respect to temperature at constant pressure leads to

$$\bar{S}^\circ_{j,P,T} = \bar{S}^\circ_{j,P_r,T_r} + c_{1,j}\ln(T/T_r) + c_{2,j}\ln\left(\frac{T-\theta_j}{T_r-\theta_j}\right) + \frac{\theta_j(2a_{3,j}(P-P_r) + a_{4,j}(P^2-P_r^2))}{2(T-\theta_j)^2} + \omega_j(Y_{P,T} - Y_{P_r,T_r}) , \tag{274}$$

and

$$\Delta\bar{H}^\circ_{j,P,T} = \Delta\bar{H}^\circ_{f,j} + (c_{1,j} + c_{2,j})(T - T_r) + c_{2,j}\theta_j \ln\left(\frac{T - \theta_j}{T_r - \theta_j}\right) + a_{1,j}(P - P_r) + a_{2,j}(P^2 - P_r^2)/2 + \frac{2a_{3,j}T(P - P_r) + a_{4,j}T(P^2 - P_r^2)}{2(T - \theta_j)} + \frac{2\theta_j a_{3,j}T(P - P_r) + \theta_j a_{4,j}T(P^2 - P_r^2)}{2(T - \theta_j)^2} + \omega_j(TY_{P,T} - T_rY_{P_r,T_r} - Z_{P,T} + Z_{P_r,T_r}) \quad (275)$$

which lead to

$$\Delta\bar{G}^\circ_{j,P,T} = \Delta\bar{G}^\circ_{f,j} - \bar{S}^\circ_{j,P_r,T_r}(T - T_r) - c_{1,j}(T \ln(T/T_r) - T + T_r) + c_{2,j}\left(T - T_r - (T - \theta_j)\ln\left(\frac{T - \theta_j}{T_r - \theta_j}\right)\right) + \frac{2(a_{1,j}(T - \theta_j) + a_{3,j}T)(P - P_r) + (a_{2,j}(T - \theta_j) + a_{4,j}T)(P^2 - P_r^2)}{2(T - \theta_j)} - \omega_j(Z_{P,T} - Z_{P_r,T_r} - Y_{P_r,T_r}(T - T_r)) \quad (276)$$

where $\Delta\bar{H}^\circ_{j,P,T}$ and $\Delta\bar{G}^\circ_{j,P,T}$ refer to the apparent standard partial molal enthalpy and Gibbs free energy of formation of the jth ion at the subscripted pressure and temperature (eqs 1 and 2) and

$$Z_{P,T} \equiv -\frac{1}{\epsilon^\circ_{P,T}} . \quad (277)$$

The reliability of eqs (274) through (276) rests solely on the validity of the equation of state (eq 254) and the corresponding equation for the standard partial molal heat capacity of an electrolyte as a function of temperature at P_r (eq 270). The validity of the equation of state has already been demonstrated in a previous communication (Helgeson and Kirkham, 1976), and the reliability of eq (270) is substantiated by regression calculations summarized below.

Regression calculations.—The intercepts of the linear curves for 25°C in figures 65 through 82, which correspond to $\bar{C}^\circ_{P,k}$, are listed in table 13, together with the conventional standard partial molal heat capacities of aqueous ions. The intercepts for higher and lower temperatures are plotted as symbols in figures 103 through 106, where it can be seen that in every case except $MgSO_4$, $\bar{C}^\circ_{P,k}$ maximizes as a function of temperature at pressures corresponding to those along the liquid-vapor equilibrium curve for H_2O. Other symbols shown in figures 103 through 105 represent values of $\bar{C}^\circ_{P,k}$ computed from finite difference derivatives of the heats of solution at infinite dilution shown in figures 61 through 64.

TABLE 13

Standard partial molal heat capacities of aqueous electrolytes designated by the subscript k and the conventional standard partial molal heat capacities of aqueous ions denoted by the subscript j at 25°C and 1 bar

Elec.	$\bar{C}^\circ_{P,k}$ [a,b]	Elec.	$\bar{C}^\circ_{P,k}$ [a,b]	Elec.	$\bar{C}^\circ_{P,k}$ [a,b]	Ion	$\bar{C}^\circ_{P,j}$ [a]	Ion	$\bar{C}^\circ_{P,j}$ [a]	Ion	$\bar{C}^\circ_{P,j}$ [a]
HCl	-30.2	NaBr	-21.2	$NaNO_3$	-9.2 [l]	H^+	0.0	Zn^{++}	-5.9 [j]	Br^-	-31.2 [c]
LiCl	-15.8	KBr	-28.2	KNO_3	-16.2	Li^+	14.4 [c]	Cu^{++}	-5.7 [j]	I^-	-29.0 [c]
NaCl	-20.2	RbBr	-33.4	NH_4NO_3	-2.5 [l]	Na^+	10.0 [c]	Ni^{++}	-10.3 [d]	ReO_4^-	-1.8 [h]
KCl	-27.2	CsBr	-36.7	$AgNO_3$	-13.0 [l]	K^+	3.0 [c]	Mn^{++}	-3.1 [j]	BrO_3^-	-23.5 [c]
RbCl	-32.4	NaI	-19.0	$NaNO_2$	-12.0	Rb^+	-2.2 [c]	Gd^{+++}	-11.9 [h]	IO_3^-	-28.0 [c]
CsCl	-35.7	KI	-26.0	HIO_3	-28.0	Cs^+	-5.5 [c]	Al^{+++}	3.9 [i]	MnO_4^-	-17.5 [c]
NH_4Cl	-13.5 [l]	RbI	-31.2	KIO_3	-25.0 [l]	Ag^+	6.2 [c]	Fe^{+++}	4.9 [i]	NO_3^-	-19.2 [c]
$MgCl_2$	-64.7	CsI	-34.5	$NaBrO_3$	-13.5 [l]	NH_4^+	16.7 [c]	La^{+++}	-10.4 [e]	NO_2^-	-22.0 [c]
$CaCl_2$	-67.0	NaF	-18.2	$KMnO_4$	-14.5 [l]	Mg^{++}	-4.3 [c]	Sm^{+++}	-12.4 [e]	HCO_3^-	-11.7 [g]
$SrCl_2$	-68.9	KF	-25.2	LiOH	-18.6	Ca^{++}	-6.6 [c]	Pr^{+++}	-14.4 [e]	$HCOO^-$	-21.0 [k]
$BaCl_2$	-71.6	RbF	-30.4	NaOH	-23.0	Sr^{++}	-8.5 [c]	Nd^{+++}	-12.4 [e]	ClO_4^-	-5.8 [d]
HBr	-31.2	HNO_3	-19.2	KOH	-30.0	Ba^{++}	-11.2 [c]	OH^-	-33.0 [c]	HSO_4^-	14.6 [f]
LiBr	-16.8	$LiNO_3$	-4.8			Cd^{++}	-0.1 [d]	F^-	-28.2 [c]	SO_4^{--}	-68.5 [h]
						Co^{++}	-7.0 [d]	Cl^-	-30.2 [c]		

[a] Cal mole^{-1} $(K°)^{-1}$. [b] The values of $\bar{C}^\circ_{P,k}$ shown in these columns correspond to the intercepts of the linear curves in figures 65 through 69 and 79 through 81. [c] Computed from values of $\bar{C}^\circ_{P,k}$ shown above. [d] Calculated from the mean of $\bar{C}^\circ_{P,k}$ for $Ca(ClO_4)_2$ and $Mg(ClO_4)_2$, $CoCl_2$ and $Co(ClO_4)_2$, $NiCl_2$ and $Ni(ClO_4)_2$, and $Cd(ClO_4)_2$ and $Cd(NO_3)_2$, respectively, given by Spitzer and others (1978a and b) using the values of $\bar{C}^\circ_{P,j}$ shown above for ClO_4^-, Cl^-, and NO_3^-. [e] Calculated from data reported by Schumm and others (1973) using the value of $\bar{C}^\circ_{P,Cl^-}$ shown above. [f] Readnour and Cobble (1969). [g] Calculated from the sum of $\bar{C}^\circ_{P,j}$ for Na^+ and HCO_3^- given by Desnoyers and others (1976) using the value of $\bar{C}^\circ_{P,Na^+}$ shown above. [h] Calculated from the values of $\bar{C}^\circ_{P,k}$ for $GdCl_3$, $HReO_4$, and Na_2SO_4 at 25°C in table 16 using the values of $\bar{C}^\circ_{P,j}$ for Gd^{+++} and Na^+ shown above. [i] Estimated from equation (7) of Criss and Cobble (1964b) using values of $\bar{S}^\circ_j$ taken from table 3 and $\bar{C}^\circ_{P,H^+}^{abs}$ = 28 cal mole^{-1} $(°K)^{-1}$ and $\bar{S}^\circ_{H^+}^{abs}$ = = -5 cal mole^{-1} $(°K)^{-1}$ at 25°C and 1 bar (Criss and Cobble, 1964a and b). [j] Calculated from values of $\bar{C}^\circ_{P,k}$ reported by Spitzer and others (1978a and b) for $Cu(ClO_4)_2$, $Zn(ClO_4)_2$, and $Mn(ClO_4)_2$ using the value shown above for $\bar{C}^\circ_{P,ClO_4^-}$. [k] Wagman and others (1968). [l] Owing to vagaries in regression results reported in the literature, these values were accepted in preference to those reported by Roux and others (1978), Singh and others (1978), and Spitzer and others (1979b).

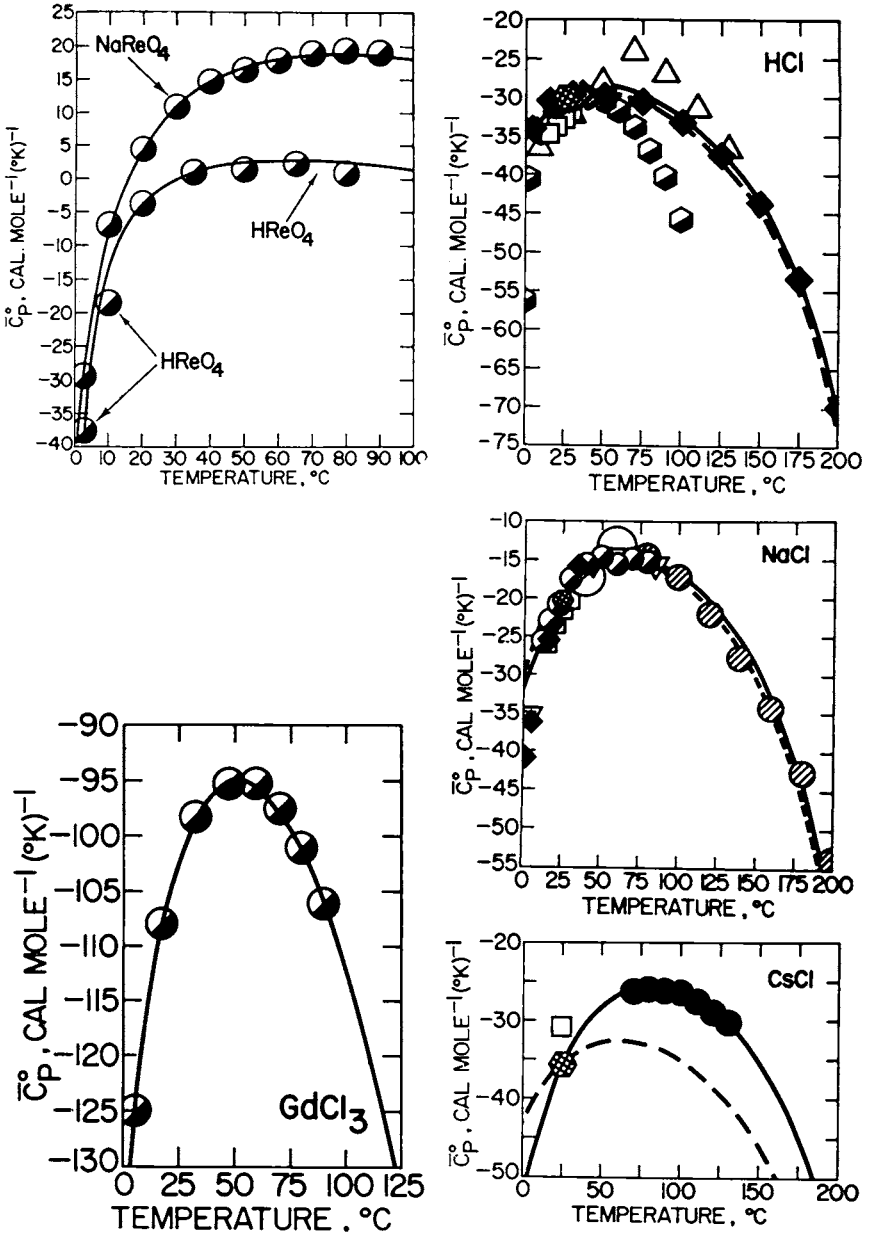

Fig. 103. Calculated (curves) and experimental (symbols) standard partial molal heat capacities of aqueous electrolytes as a function of temperature (T) at 1 bar for T < 100°C and pressures corresponding to those along the liquid-vapor equilibrium curve for H_2O at T $\geqslant$ 100°C. The symbols correspond to the intercepts of the linear curves for the electrolytes in figures 65 through 82 and/or values of $\bar{C}°_P$ computed from finite difference derivatives of the intercepts of the linear curves in figures 61 through 64 using thermodynamic data for the crystalline solids taken from Stull and Prophet (1971). The c_1 and c_2 parameters used to generate the solid curves from eq (273) were obtained by regression of the values represented by the symbols, but those responsible for the dashed curves were estimated (see text). The different symbols represent extrapolation of experimental data taken from the various sources cited in the caption of figure 65.

The values of $\bar{C}^\circ_{P,HCl}$ represented by the solid diamonds in figure 103 were computed from

$$\bar{C}^\circ_{P,HCl} = \bar{C}^\circ_{P,HReO_4} + \bar{C}^\circ_{P,NaCl} - \bar{C}^\circ_{P,NaReO_4} \cdot \qquad (278)$$

Eq (278) was also used by Ahluwalia and Cobble (1964b), who extrapolated their heat of solution data to infinite dilution with the aid of the Guggenheim (1935) equation. It can be deduced from figure 103 that the results of their extrapolation differ considerably from those in the present study.

Two-parameter regression of the data represented by the symbols for HCl, NaCl, KCl, LiCl, $MgCl_2$, $BaCl_2$, LiBr, CsBr, CsI, KF, and Na_2SO_4 in figures 103 through 105 with an appropriate statement of eq (273) generated the solid curves shown for these electrolytes and the corresponding values of $c_{1,k}$, $c_{2,k}$, and $\bar{C}^\circ_{P,k}$ given in tables 14 and 15, respectively. The values of ω_k, θ_k, $a_{3,k}$, $a_{4,k}$, and X used in the calculations were taken from Helgeson and Kirkham (1974a, 1976), which insured consistency of the fit results with the temperature dependence of the standard partial molal volume data represented by the open symbols on the ordinates of figures 89 through 93. The electrostatic properties of H_2O computed by Helgeson

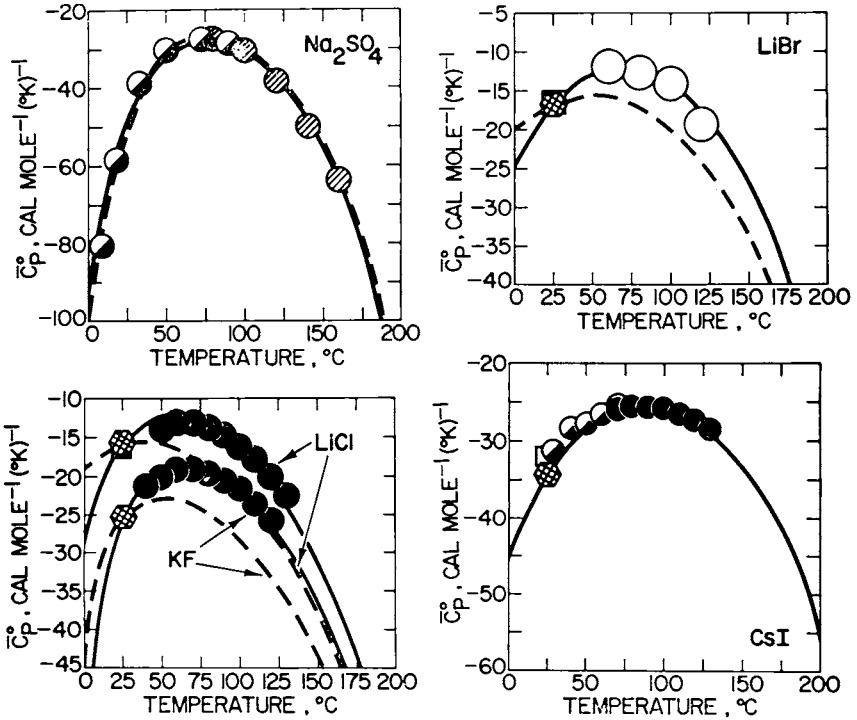

Fig. 104. Calculated (curves) and experimental (symbols) standard partial molal heat capacities of aqueous electrolytes as a function of temperature (T) at 1 bar for $T < 100°C$ and pressures corresponding to those along the liquid-vapor equilibrium curve for H_2O at $T \geqslant 100°C$ (see caption of fig. 103).

and Kirkham (1974a) were adopted for this purpose in preference to those calculated by Silvester and Pitzer (1976) and Bradley and Pitzer (1979), which apply only to pressures and temperatures $\leqslant$ 1 kb and 350°C, because they are consistent with those used below to predict the thermodynamic properties of aqueous species to 5 kb and 600°C. Because no equation of state parameters are available for $HReO_4$, $NaReO_4$, $GdCl_3$, and $NaClO_4$, $a_{3,k}$ and $a_{4,k}$ for these electrolytes were set to zero before regressing the data to obtain values of $c_{1,k}$ and $c_{2,k}$, as well as θ_k. It can be shown that this procedure introduces negligible regression errors at temperatures $\lesssim$ 200°C along the liquid-vapor equilibrium curve for H_2O. The dashed

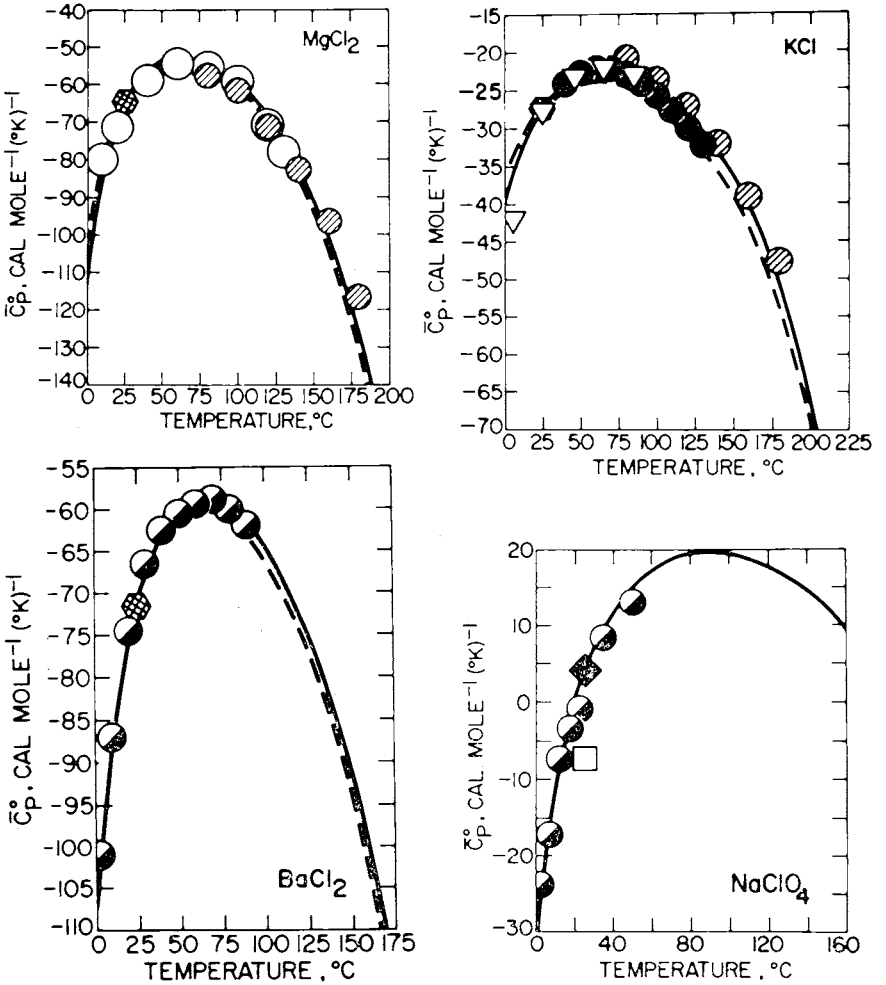

Fig. 105. Calculated (curves) and experimental (symbols) standard partial molal heat capacities of aqueous electrolytes as a function of temperature (T) at 1 bar for T < 100°C and pressures corresponding to those along the liquid-vapor equilibrium curve for H_2O at T $\geqslant$ 100°C (see caption of fig. 103).

TABLE 14

Regression coefficients for calculating the standard partial molal properties of the kth aqueous electrolyte from appropriate statements of eqs (273) through (276)

Solute	$c^a_{1,k}$	$c^a_{2,k}$	θ^b_k	$\omega^c_k \times 10^{-5}$
HCl	-4.8384	-2.0410	246.02	1.4560
LiCl	23.0954	-3.5676	246.49	1.9421
NaCl	30.3726	-7.8764	228.58	1.7865
KCl	13.4374	-4.8696	240.20	1.6487
CsCl	22.5549	-9.8123	231.08	1.5534
$MgCl_2$	36.90252	-10.17292	247.32	4.4492
$BaCl_2$	24.1261	-10.4036	245.52	3.8970
$GdCl_3$	14.5745	-8.8609	249.16	6.6945
LiBr	41.7539	-12.2178	209.09	1.8719
CsI	36.0092	-19.1509	198.67	1.3908
KF	18.0446	-3.1746	259.66	1.9797
Na_2SO_4	73.8864	-16.9270	239.39	3.8468
$NaClO_4$	61.0754	-7.2356	249.45	1.3317
$NaReO_4$	47.8022	-3.3271	262.48	1.2617
$HReO_4$	19.6863	-1.2232	269.45	0.9312

[a] cal mole^{-1} (°K)$^{-1}$. [b] °K. [c] cal mole^{-1}.

TABLE 16

Regression coefficients for calculating the conventional standard partial molal properties of the jth aqueous ion from eqs (273) through (276)

Ion	$c^a_{1,j}$	$c^a_{2,j}$	θ^b_j	$\omega^c_j \times 10^{-5}$
Na^+	35.7153	-6.2856	215.17	0.3306
K^+	18.4682	-2.9265	234.19	0.1927
Cs^+	29.9613	-9.3863	217.04	0.0974
Li^+	27.2981	-1.2342	253.94	0.4862
Ba^{++}	34.2215	-6.4428	245.02	0.9851
Mg^{++}	39.0257	-2.6665	270.56	1.5372
Cl^-	-4.8384	-2.0410	246.02	1.4560
Br^-	6.4161	-7.5141	206.75	1.3858
F^-	0.8814	-1.0551	272.42	1.7870
I^-	1.3667	-6.8157	186.51	1.2934
OH^-	24.7208	-6.2074	253.52	1.7246
SO_4^{--}	1.3418	-4.6940	263.03	3.1857

[a] cal mole^{-1} (°K)$^{-1}$. [b] °K. [c] cal mole^{-1}.

TABLE 15

Standard partial molal heat capacities[a] of aqueous electrolytes computed from an appropriate statement of eq (273) for the kth electrolyte as a function of temperature at 1 bar for temperatures < 100°C and pressures corresponding to those along the liquid-vapor equilibrium curve for H_2O at temperatures ≥ 100°C — see text

Solute	Temperature, °C							
	25	50	75	100	125	150	175	200
HCl	-30.2	-28.8	-29.8	-32.6	-37.1	-43.8	-54.0	-70.8
LiCl	-15.8	-12.5	-13.1	-16.5	-22.2	-30.9	-44.4	-66.6
NaCl	-20.2	-15.5	-14.7	-16.7	-21.2	-28.6	-40.5	-60.5
KCl	-27.2	-23.0	-22.7	-24.9	-29.3	-36.4	-47.6	-66.3
CsCl	-35.7	-28.3	-25.8	-26.5	-29.6	-35.4	-45.3	-67.4
$MgCl_2$	-64.7	-53.5	-53.3	-59.8	-72.3	-91.8	-122.2	-172.9
$BaCl_2$	-71.6	-60.4	-59.4	-64.6	-75.1	-91.9	-118.4	-162.6
$GdCl_3$	-102.5	-95.0	-99.4	-112.2	-133.0	-163.7	-210.7	-287.7
LiBr	-16.8	-12.7	-12.0	-14.0	-18.6	-26.2	-38.6	-59.4
CsI	-34.5	-28.4	-25.8	-25.8	-27.9	-32.7	-41.0	-55.9
KF	-25.2	-19.1	-18.9	-22.0	-27.7	-36.5	-50.2	-72.9
Na_2SO_4	-48.3	-32.1	-27.9	-30.9	-39.7	-55.2	-80.4	-123.3
$NaClO_4$	4.2	15.3	19.1	19.3	17.1	12.3	3.9	-10.6
$NaReO_4$	8.1	16.7	18.7	17.7	14.7	9.5	1.1	-13.1
$HReO_4$	-1.8	2.5	2.8	1.4	-1.3	-5.5	-11.9	-22.6

[a] cal mole^{-} (°K)$^{-1}$

curves in figures 103 through 105 were generated from a correlation algorithm (see below), but that shown in figure 106 merely connects the data points for $MgSO_4$. Insufficient data are available for the latter electrolyte to permit definitive regression of $\bar{C}^\circ_{P,MgSO_4}$ as a function of temperature.

It can be deduced from figures 103 through 105 that the analog of eq (273) for the kth electrolyte represents closely the experimental heat capacity data corresponding to the symbols at temperatures $\gtrsim 15°C$. The discrepancies below $\sim 15°C$ can be attributed to inconsistencies in the calorimetric and volumetric data for the electrolytes at low temperatures. The agreement between the regression curves and symbols in figures 103 through 105 (which correspond to the calculated and observed intercepts of the linear curves in figures 70 through 76 and 78) is particularly impressive in view of the fact that *independent* values of θ and/or ω derived from standard partial molal volume and compressibility data were specified in the calculations. The validity of eqs (254), (270), and (273) are further substantiated by the close correspondence of the curves and symbols in figures 107 and 108, which are consistent with the standard state requirement for unit activity of pure H_2O at all pressures and temperatures. The symbols in these figures represent high-pressure/temperature standard molal activity product constants for H_2O (K_w) derived from conductance data reported in the literature, but the curves were generated from calculated standard partial molal Gibbs free energies of dissociation ($\Delta\bar{G}^\circ_r$) and the relation

$$\log K_w = -\frac{\Delta\bar{G}^\circ_r}{2.303RT} = -\frac{\Delta\bar{G}^\circ_{OH^-} - \Delta\bar{G}^\circ_{H_2O}}{2.303RT} \qquad (279)$$

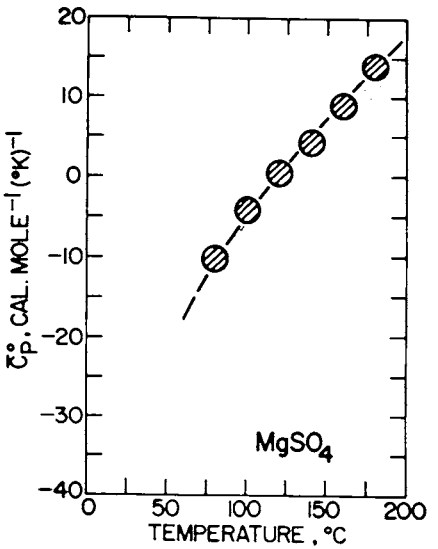

Fig. 106. Standard partial molal heat capacity of $MgSO_4$ as a function of temperature (T) at 1 bar for $T < 100°C$ and pressures corresponding to those along the liquid-vapor equilibrium curve for H_2O at $T \geq 100°C$. The symbols correspond to the intercepts of the curves in figure 82B (see text).

using the heat capacity parameters for OH^- given in table 16, together with revised values of the equation of state parameters for OH^- (which replace those given by Helgeson and Kirkham, 1976) to evaluate eq (276). The value of ω_{OH^-} and the thermodynamic/electrostatic properties of H_2O employed in the calculations were computed from equations summarized elsewhere (Helgeson and Kirkham, 1974a, 1976), but the standard partial molal properties of OH^- at the reference pressure and temperature were taken from CODATA (1978).

The values of c_1, c_2, and θ for OH^- in table 16, as well as the values of a_1, a_2, a_3, and a_4 given below for the hydroxyl ion were generated from a convergent series of regression calculations involving fits of eq (276) to values of $\Delta\overline{G}^\circ_{OH^-}$ computed from the experimental data shown in figures 107 and 108, together with fits of eq (254) to finite difference derivatives of these values. This procedure was adopted in lieu of fitting eq (273) to the low-temperature heat capacity data shown in figure 109 in order to

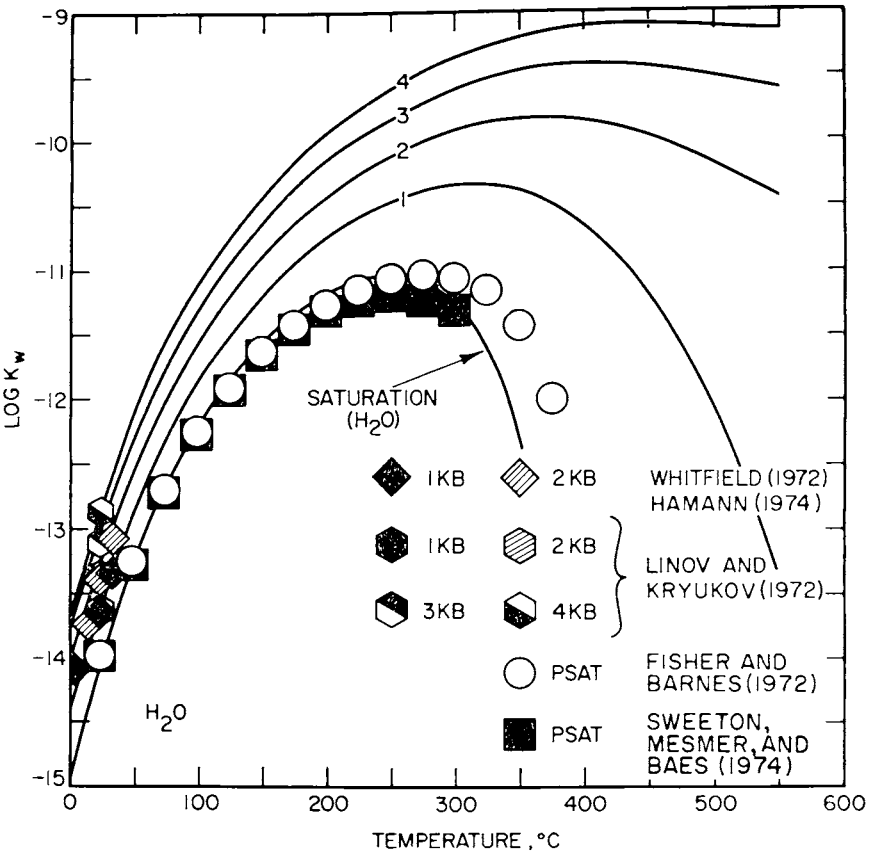

Fig. 107. Calculated (curves) and experimental (symbols) logarithm of the standard molal activity product constant of H_2O (K_w) as a function of temperature at constant pressure (labeled in kb). Saturation (H_2O) refers to the liquid-vapor equilibrium curve for H_2O.

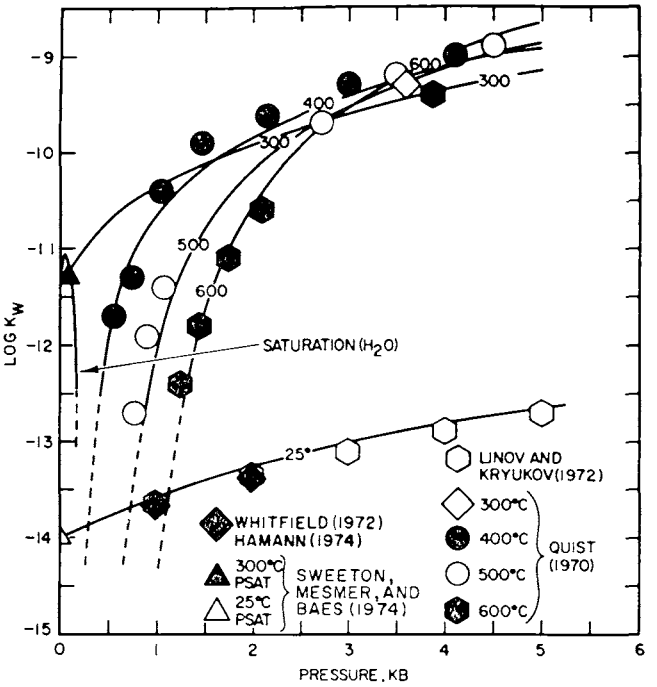

Fig. 108. Calculated (curves) and experimental (symbols) logarithm of the standard molal activity product constant of H_2O (K_w) as a function of pressure at constant temperature (labeled in °C). Saturation (H_2O) refers to the liquid-vapor equilibrium curve for H_2O.

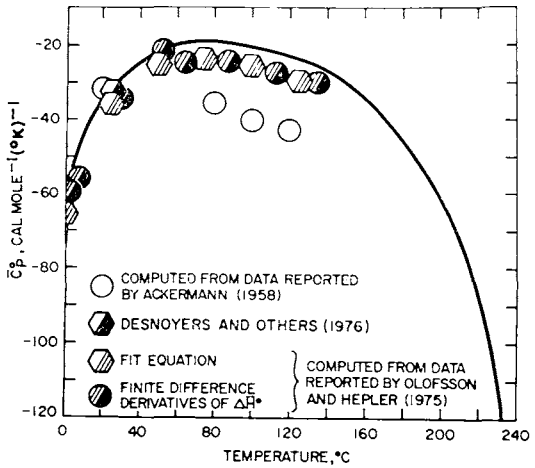

Fig. 109. Calculated (curve) and experimental (symbols) conventional standard partial molal heat capacity of OH^- as a function of temperature at pressures corresponding to those along the liquid-vapor equilibrium curve for H_2O (see text).

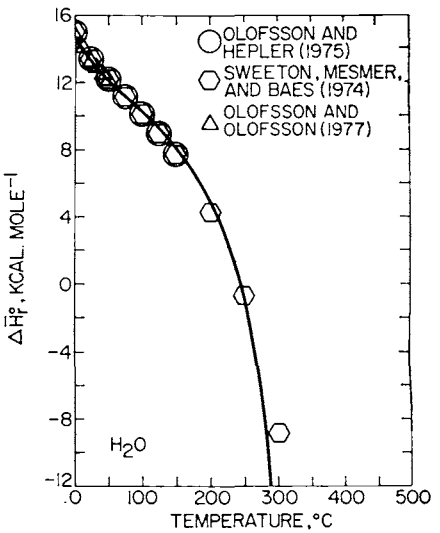

Fig. 110. Calculated (curve) and experimental (symbols) standard partial molal enthalpy of dissociation for H_2O as a function of temperature at pressures corresponding to those along the liquid-vapor equilibrium curve for H_2O (see text).

insure adequate representation of log K_w at high pressures and temperatures. Figures 107 and 108 leave little doubt that the regression calculations afford close approximation of the experimental values of log K_w for H_2O reported by Quist (1970), Sweeton, Mesmer, and Baes (1974), Whitfield (1972), and Linov and Kryukov (1972). In contrast, the regression curve representing log K_w for liquid H_2O in equilibrium with the vapor phase (fig. 107) differs considerably from the experimental values given by Fisher and Barnes (1972) for temperatures $> 250°C$. The latter data appear to be inconsistent also with the other experimental values of log K_w shown in figures 107 and 108. It should perhaps be emphasized in this regard that the apparent discrepancies between the symbols and curves in figure 108 are within the experimental uncertainty reported by Quist (1970), which is ± 0.3 to 0.5 log units. Although the discrepancies at temperatures $\lesssim 150°C$ in figure 107 are greater than the corresponding experimental uncertainties, they are nevertheless small enough to be considered negligible in geochemical calculations.

It can be seen in figure 109 that the values of $\bar{C}°_{P,OH^-}$ computed above are in reasonably close agreement with those generated from experimental data reported in the literature. Similar agreement is apparent in figures 110 and 111A, where $\Delta\bar{H}°_r$ and $\Delta\bar{V}°_r$ for the dissociation of H_2O are plotted as functions of temperature at pressures corresponding to the liquid-vapor equilibrium curve for H_2O. However, the corresponding values of $\Delta\bar{C}°_{P,r}$ computed in the present study for temperatures $> 150°C$ (fig. 111B) differ significantly from those calculated from power function fits of log K_w by Sweeton, Mesmer, and Baes (1974).

The values of c_1 and c_2 for all the ions other than OH^- in table 16 were generated by fitting eq (273) to conventional standard partial molal

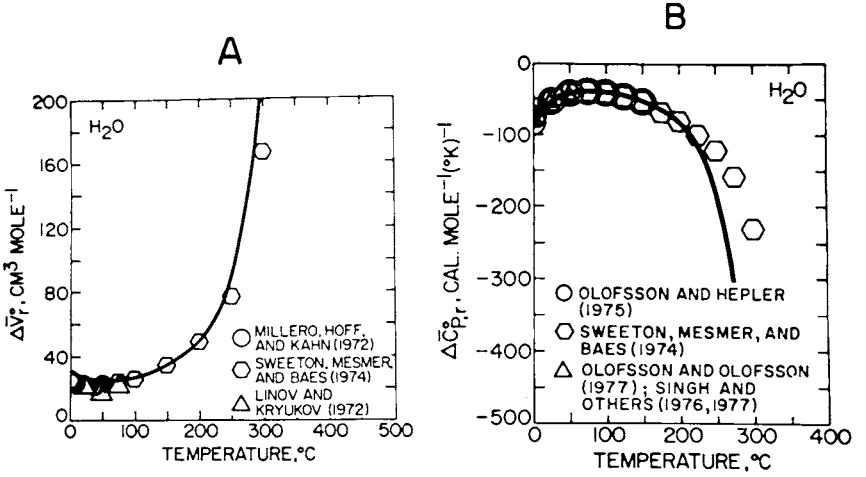

Fig. 111. Calculated (curve) and experimental (symbols) standard partial molal volume and heat capacity of dissociation for H_2O as a function of temperature at pressures corresponding to those along the liquid-vapor equilibrium curve for H_2O.

heat capacities computed from the values of $\bar{C}^\circ_{P,k}$ in table 15 and the relation

$$\bar{C}^\circ_{P,j} = C^\circ_{P,j}{}^{abs} - Z_j \bar{C}^\circ_{P,H^+}{}^{abs} \tag{280}$$

where $\bar{C}^\circ_{P,j}$ refers to the absolute standard partial molal heat capacity of the jth ion. The values of a_3, a_4, θ, ω, and X specified in the calculations were taken from Helgeson and Kirkham (1974a, 1976). In principle, c_1 and c_2 coefficients for ionic species can also be calculated directly from corresponding coefficients obtained by regression of $\bar{C}^\circ_P$ data for electrolytes. However, this procedure may lead to significant errors in computed values of conventional standard partial molal properties, owing to magnification of the consequences of uncertainties inherent in fit parameters obtained by nonlinear regression of experimental data (see discussion by Helgeson and Kirkham, 1976).

Values of $\bar{C}^\circ_P$ computed from eq (273) using the parameters shown in table 16, together with the values of a_3 and a_4 employed in the regression calculations are listed in table 17. The values given in the table are also plotted as curves in figure 112, where it can be seen that $\bar{C}^\circ_P$ for all the ions maximizes as a function of temperature at pressures corresponding to those along the vapor-liquid equilibrium curve for H_2O. Note, however, that the extrema in the curves representing monovalent anions are less pronounced than those exhibited by the curves for cations. Nevertheless,

TABLE 17

Conventional standard partial molal heat capacities[a] of aqueous ions computed from eq (273) for 1 bar at temperatures < 100°C and pressures corresponding to those along the liquid-vapor equilibrium curve for H_2O at temperatures $\geqslant 100$°C — see text

Ion	Temperature, °C							
	25	50	75	100	125	150	175	200
Na^+	10.0	13.4	15.2	15.9	15.9	15.2	13.5	10.2
K^+	3.0	5.8	7.1	7.7	7.8	7.4	6.4	4.5
Cs^+	-5.5	0.3	3.8	6.1	7.5	8.4	8.8	8.5
Li^+	14.4	16.4	16.7	16.2	14.9	12.8	9.5	4.0
Ba^{++}	-11.2	-2.9	0.3	0.7	-0.8	-4.1	-10.2	-20.9
Mg^{++}	-4.3	6.4	8.0	6.3	2.3	-4.4	-15.8	-32.3
Cl^-	-30.2	-28.8	-29.8	-32.6	-37.1	-43.8	-54.0	-70.8
Br^-	-31.2	-29.1	-29.2	-31.2	-34.9	-40.7	-50.0	-65.6
F^-	-28.2	-24.8	-26.1	-29.8	-35.5	-43.9	-56.6	-77.3
I^-	-29.0	-28.4	-29.3	-31.6	-35.4	-41.1	-50.0	-64.7
OH^-	-33.0	-22.3	-19.5	-20.4	-24.3	-31.2	-42.5	-61.7
SO_4^{--}	-68.5	-57.6	-57.3	-62.2	-71.4	-85.7	-107.7	-144.2

[a] cal $mole^{-1}$ $(°K)^{-1}$.

all the curves are similar in configuration to those for the electrolytes in figures 103 through 105. Additivity values of $\bar{C}^\circ_P$ for NaBr computed from eq (270) and the regression parameters for Na^+ and Br^- are plotted on the ordinate of figure 113, where it can be seen that (except at 5°C) they are closely consistent with independent calorimetric data reported by Tanner and Lamb (1978). The slopes of the linear curves in figure 113 (which correspond to $\nu b_J/4$ for NaBr) are plotted as a function of temperature in figure 114. Values of $\bar{C}^\circ_{P,NaCl}$ computed in the present study can be compared in figure 115 with those calculated by Silvester and Pitzer (1977) and Pitzer and others (1979) for temperatures to 275°C along the liquid-vapor equilibrium curve for H_2O, all of which are significantly less negative than the corresponding values of $\bar{C}^\circ_P$ generated below from calorimetric data reported by Puchokov, Styazhkin, and Federov (1976). The 25°C values of $\bar{C}^\circ_{P,j}$ in table 17 compare favorably with those calculated by Desnoyers and others (1976).

Although in certain instances the conventional standard partial molal heat capacities in table 17 yield additivity values of $\bar{C}^\circ_{P,k}$ that differ (as a result of regression vagaries) by as much as 1.8 cal $mole^{-1}$ $(°K)^{-1}$ from

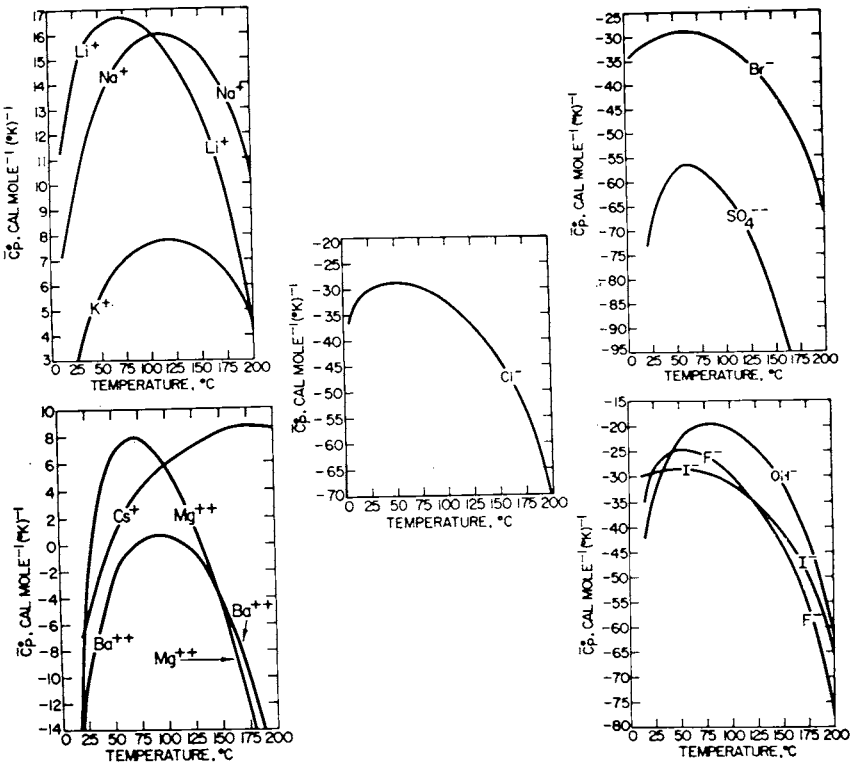

Fig. 112. Calculated conventional standard partial molal heat capacities of aqueous ions as a function of temperature at pressures corresponding to those along the liquid-vapor equilibrium curve for H_2O (see text and table 17).

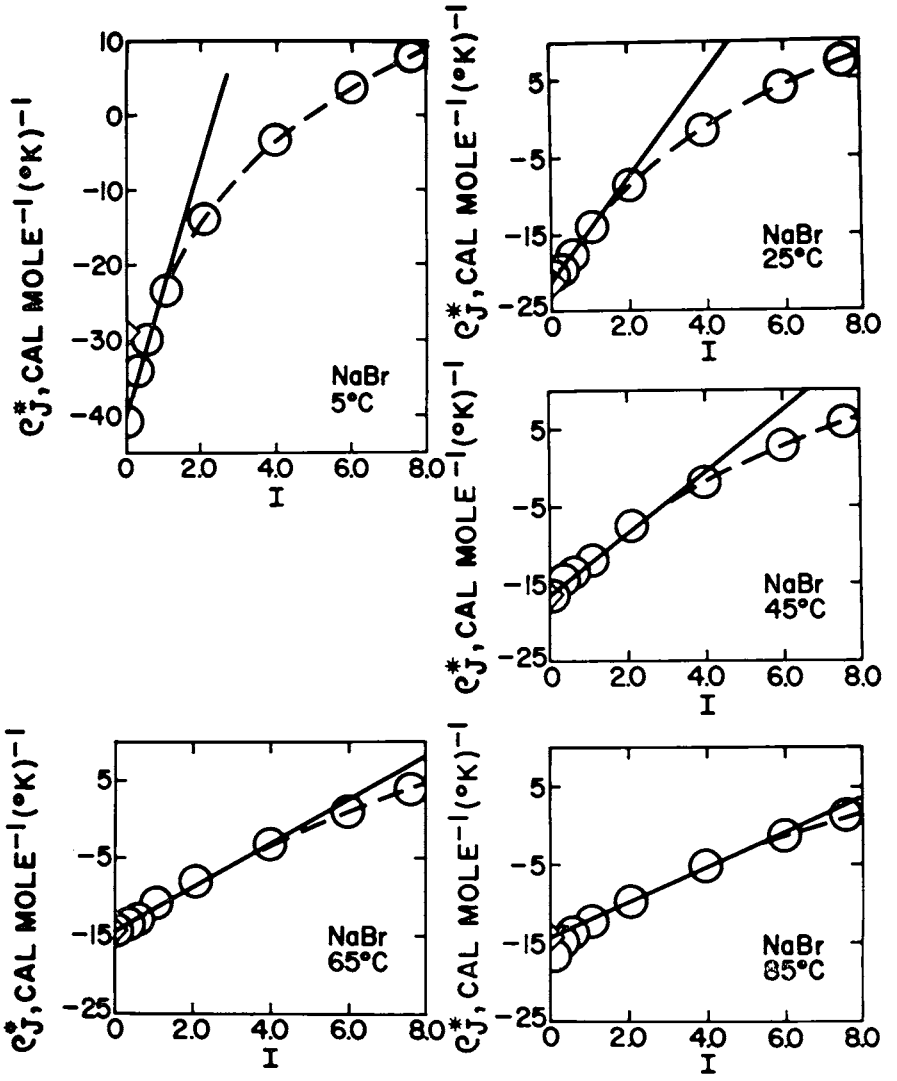

Fig. 113. ρ^*_J (eq 238) computed (assuming I = $\bar{I}$) from apparent molal heat capacities at 1 bar reported by Tanner and Lamb (1978). The values represented by the open triangles on the ordinates of the diagrams correspond to values of $\bar{C}^\circ_P$ generated independently in the present study (see text).

those of corresponding electrolytes in table 15, the bulk of the discrepancies are $\lesssim 0.1$ cal mole^{-1} (°K)$^{-1}$. Differences of this order of magnitude are small enough to be considered insignificant in most geochemical calculations.

The equations derived above can also be used to represent the thermodynamic properties of neutral complexes at high pressures and temperatures. The validity of this conclusion has already been demonstrated in the case of aqueous silica (Walther and Helgeson, 1977, 1979), and another example is shown in figures 116 and 117 where experimental and calculated values of log K_{NaCl° (where NaCl° stands for the aqueous NaCl molecule) are plotted against temperature and pressure. The values of log K represented by the filled circles in figure 116 correspond to the intercepts of the curves shown in figure 118, which were generated from eqs (180) and (181) using experimental osmotic coefficient data reported by Liu and Lindsay (1972). The requirement for both the slopes and intercepts of the curves shown in figure 118 to be smooth functions of temperature led to the interpretation of the data represented by the curves in the figures and the values of $b_{\gamma,NaCl^\circ}$ and log K_{NaCl° represented by the filled circles in figures 116 and 119. The open symbols in figure 119 represent values of $b_{\gamma,NaCl^\circ}$ generated by fitting a combined statement of eqs (29), (103), and (198) to the experimental data represented by the symbols in figure 49 (see above). It can be deduced from figure 119 that the latter values are consistent with those derived from the high-temperature vapor pressure data represented by the symbols in figure 118. The minimum in the curve shown in figure 119 is similar to, but more pronounced than, that exhibited by $b_{\gamma,CO_2(aq)}$ in NaCl solutions as a function of temperature at pressures corresponding to liquid-vapor equilibrium (Helgeson

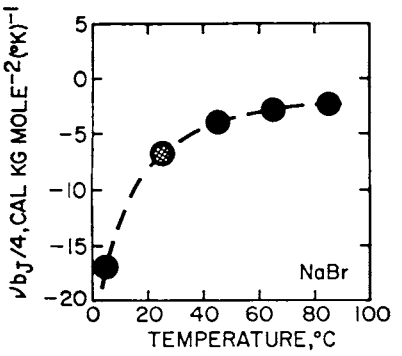

Fig. 114. Temperature dependence (at 1 bar) of the negative equivalents of the slopes of the linear curves for NaBr in figures 66 and 113 (see text and eq 238).

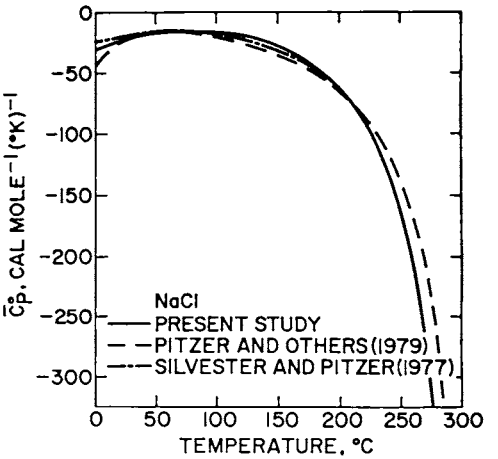

Fig. 115. Comparative plot of various computed values of the standard partial molal heat capacity of NaCl as a function of temperature (T) at 1 bar for T < 100°C and pressures corresponding to those along the liquid-vapor equilibrium curve for H_2O at T $\geqslant$ 100°C.

and James, 1968). In contrast, $b_{\gamma,SiO_2(aq)}$ in $NaNO_3$ solutions apparently decreases monotonically with increasing temperature, at least to 300°C (Marshall, 1980b).

The curves shown in figures 116 and 117 were generated using values of a_1, a_2, a_3, a_4, c_1, c_2, ω, and θ for the aqueous NaCl molecule that were obtained by regression of the experimental data shown in the figures using an approach similar to that described above for OH^-. The close agreement of the curves and the bulk of the symbols in figure 117 leaves little doubt that eqs (254) and (273) afford close approximation of the thermodynamic behavior of NaCl° at high temperatures and pressures. The cause of the systematic discrepancies between the calculated and experimental values of log $K_{NaCl°}$ at temperatures and pressures from ~ 400°C and ~ 500 bars to ~ 500°C and 3 kb in figure 117 is not clear. It may well be due to experimental error, but it could also result from errors in the equation of state parameters caused by insufficient regression control at the boundaries of the fit region. In any event, these discrepancies, together with those apparent in figure 116 reduce the status of the parameters given for NaCl° in table 18 to first approximations. *Under no circumstances should they be used for temperatures and pressures outside the fit region in figures 116 and 117.*

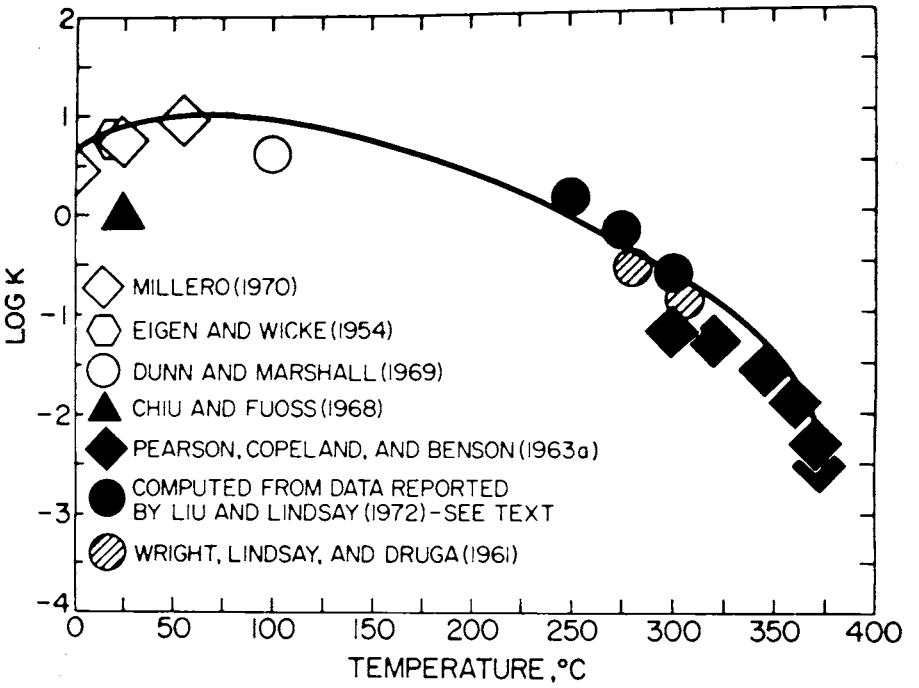

Fig. 116. Calculated (curve) and experimental (symbols) logarithm of the standard molal dissociation constant of NaCl as a function of temperature at pressures corresponding to those along the liquid-vapor equilibrium curve for H_2O.

The opposite configurations of the curves shown in figures 116 and 119 suggest that the degree of ion association in NaCl solutions may maximize as a function of concentration at high temperatures. This behavior is exhibited by $ZnSO_4$ and other electrolytes at 25°C (Davies, 1962; Pitzer, in press), as well as LiCl, LiBr, KCl, and CsCl solutions at high pressures and temperatures (Hwang, Lüdemann, and Hartmann, 1970). The latter electrolytes are "completely" dissociated in both concentrated and dilute solutions. At intermediate concentrations the electrolytes are highly associated. *The fact that the second derivatives of the two curves in figures 116 and 119 are of opposite sign contributes significantly to the high uncertainties attending both theoretical prediction and experimental documentation of the thermodynamic properties of concentrated electrolyte solutions at high temperatures and low pressures (Helgeson, in press).*

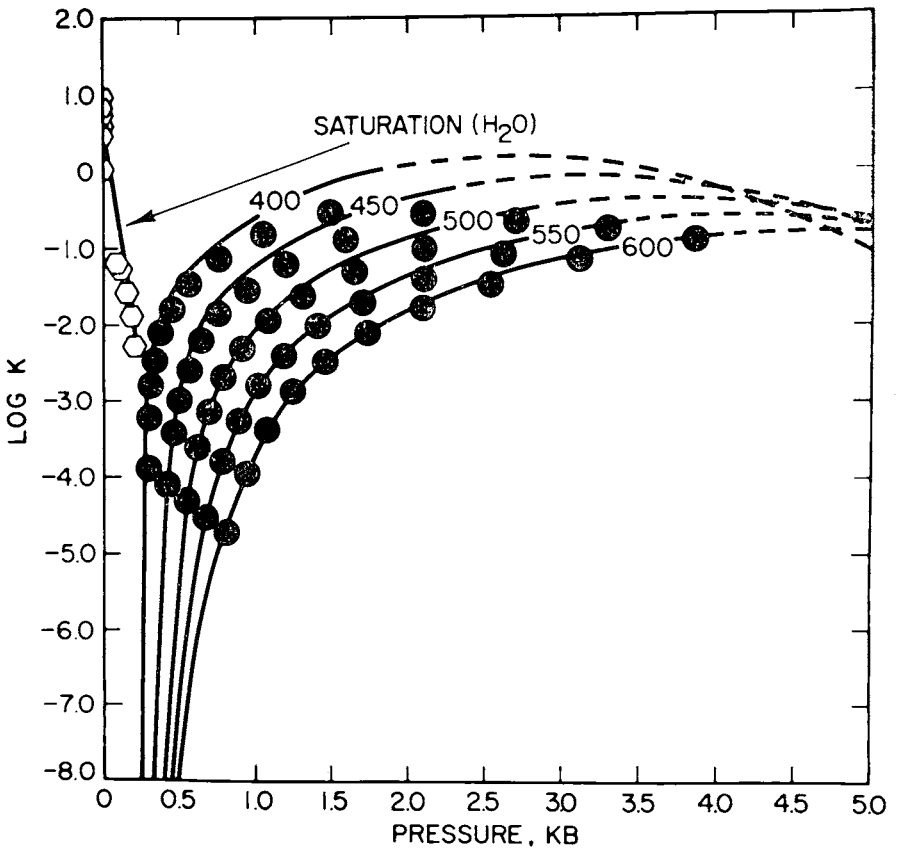

Fig. 117. Calculated (curves) and experimental (symbols) logarithm of the standard molal dissociation constant of NaCl as a function of pressure at constant temperature (labeled in °C). The symbols represent experimental data reported by Eigen and Wicke (1954), Pearson, Copeland, and Benson (1963a), Quist and Marshall (1968a), and Millero (1970). Saturation (H_2O) refers to the liquid-vapor equilibrium curve for H_2O.

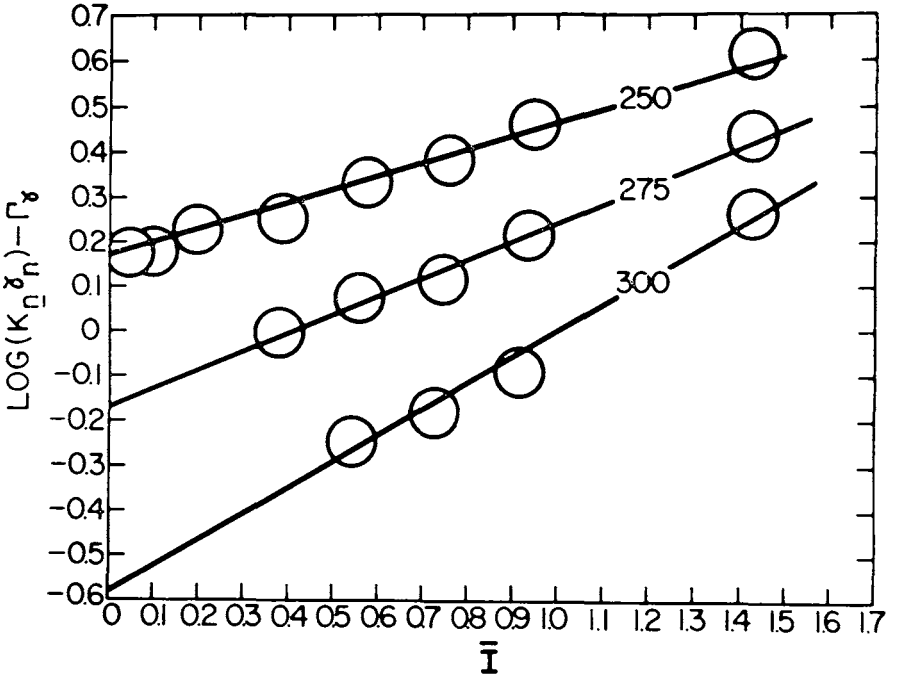

Fig. 118. Graphic representation of eq (181) for NaCl at various temperatures (indicated in °C) and pressures corresponding to those along the liquid-vapor equilibrium curves. The symbols represent experimental data reported by Liu and Lindsay (1972) (see text).

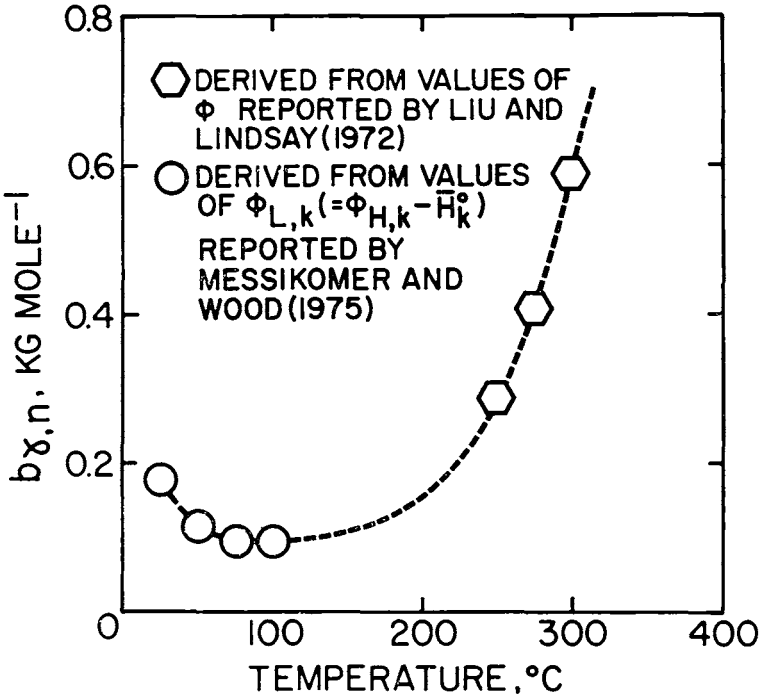

Fig. 119. Extended term parameter for the activity coefficient of NaCl° in NaCl solutions as a function of temperature at pressures corresponding to those along the liquid-vapor equilibrium curve for H_2O.

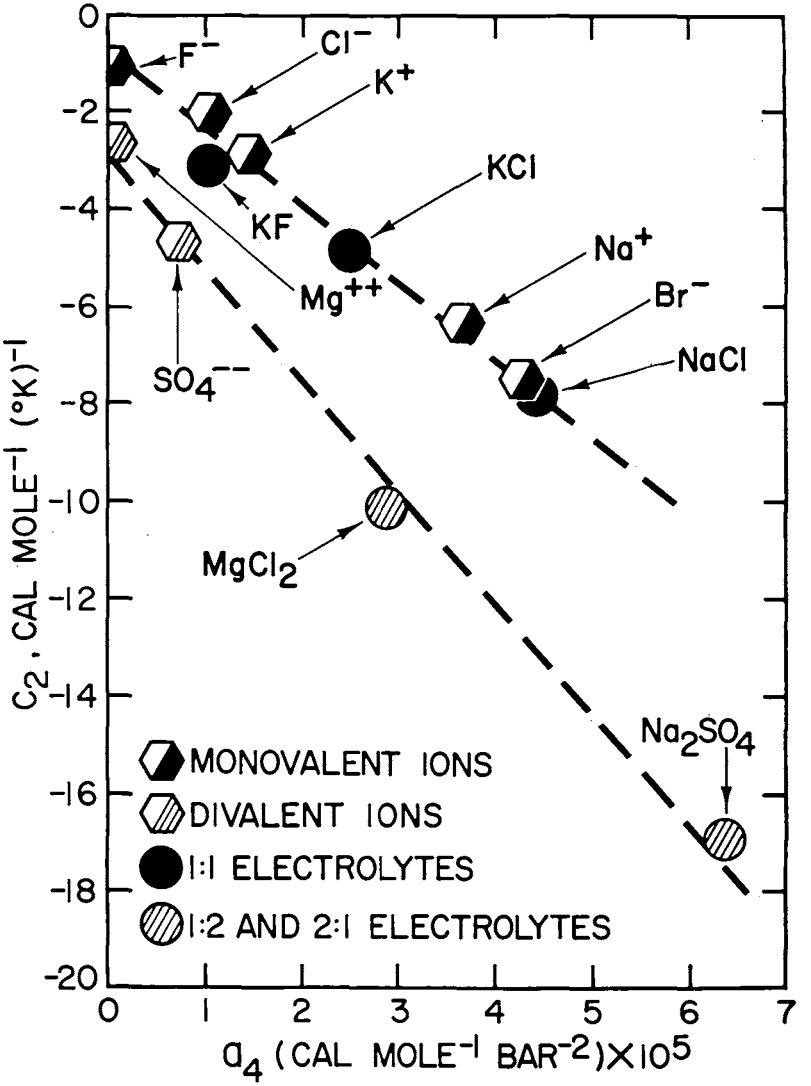

Fig. 120. Correlation of the heat capacity collapse parameter (c_2) with the corresponding compressibility parameter (a_4) in eq (273). The values of c_2 were generated in the present study (see text and tables 14 and 15), but those of a_4 were taken from Helgeson and Kirkham (1976).

Correlation and estimation algorithms.—A number of correlations among thermodynamic properties, effective electrostatic and crystal radii, and equation of state parameters for ionic species have been summarized elsewhere (Helgeson and Kirkham, 1976), which can be used in conjunction with those described below to estimate values of c_1 and c_2 for aqueous species. For example, it can be seen in figures 120 and 121 that c_2 can be regarded as a linear function of a_4, and that a_2 can also be expressed as a function of a_4. These observations permit calculation of c_2 for aqueous species from compressibility data. The equation corresponding to the curves shown in figure 120 can be written as

$$c_2 = \mathbf{a} + \mathbf{b}\, a_4 \tag{281}$$

where $\mathbf{a} = -0.7$ and $\mathbf{b} = -1.60 \times 10^5$ for monovalent ions and 1:1 electrolytes, but $\mathbf{a} = -2.90$ and $\mathbf{b} = -2.30 \times 10^5$ for divalent ions and 1:2 or 2:1 electrolytes. Eq (281) together with data and algorithms given by Helgeson and Kirkham (1976) were used in the present study to estimate values of c_2 for a large number of aqueous species for which insufficient heat capacity data are available to permit retrieval of c_1 and c_2 from regression calculations. These estimates were then combined with eq (270) and values

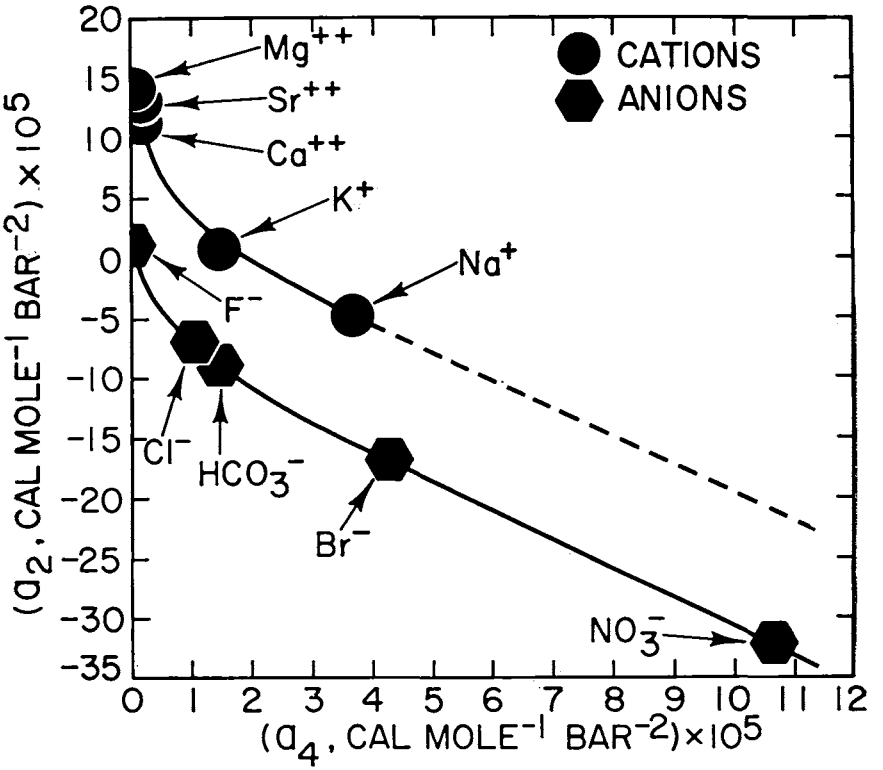

Fig. 121. Correlation of a_2 with a_4 in eq (254). The values of the parameters (table 18) are those given by Helgeson and Kirkham (1976).

of ω, θ, and X to calculate estimates of c_1 from corresponding values of $\bar{C}^\circ_{P_r,T_r}$. In certain instances where no heat capacity data are available, estimates of $\bar{C}_{P_r,T_r}$ were used to calculate c_1. The latter estimates were generated from correlation algorithms represented by the linear curves in figures 122 through 124, which are consistent with

$$\bar{C}^\circ_{P,j} = a + bS^\circ_j \tag{282}$$

where a and b stand for the following parameters:

	a	b
Monovalent cations (curve a, fig. 122):	18	−0.67
Alkaline earth cations (curve b, fig. 122):	−10	−0.2
Transition metal cations (curve d, fig. 122):	7.2	0.55
Trivalent cations (curve c, fig. 122):	−48	−0.7
Monovalent anions (curve e, fig. 122):	−30.5	0
Oxygenated anions (fig. 123):	−76	1.5
Acid oxygenated anions (fig. 124):	−164.5	6.5

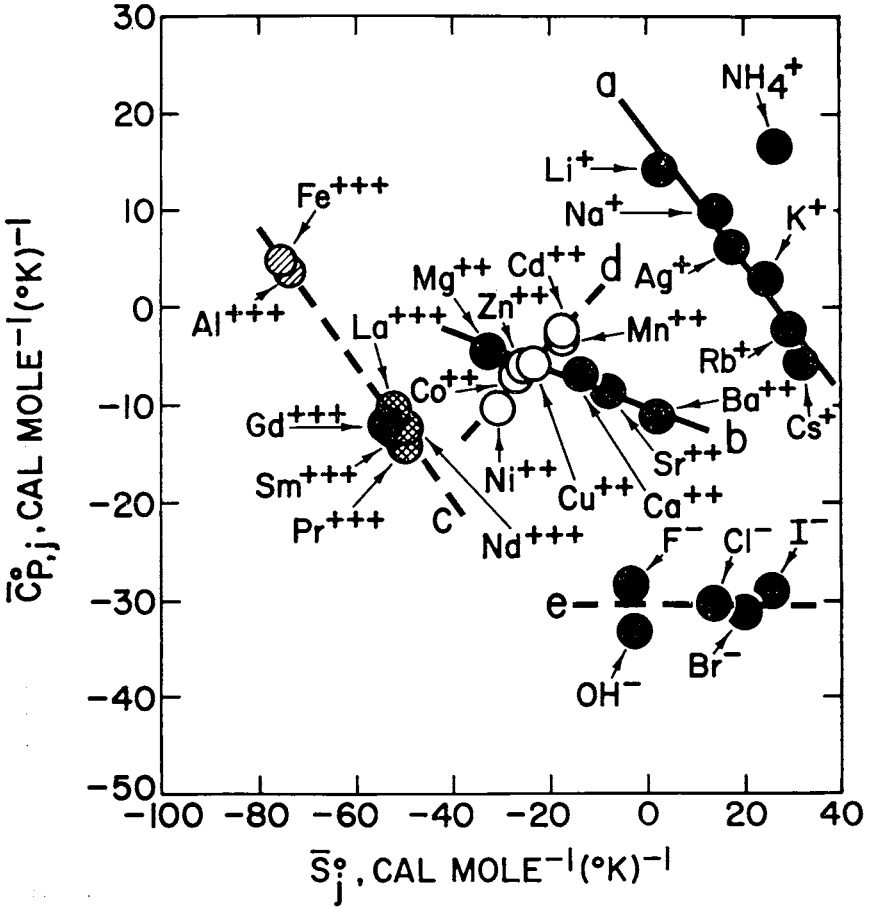

Fig. 122. Correlation of the conventional standard partial molal heat capacities and entropies of aqueous species at 25°C and 1 bar (tables 3, 13, and 18).

Similar estimates can be made for polar neutral species by taking account of other correlations, such as those discussed by Cobble (1953a, b, and c) and Helgeson (1969). One of these is shown in figure 125, which is consistent with

$$\bar{S}^\circ_n = 105 - 205(r_{x,+,n} + r_{x,-,n})^{-1} \tag{283}$$

where $r_{x,+,n}$ and $r_{x,-,n}$ refer to the crystal radii of the cation and anion in the nth neutral molecule.

Although considerable uncertainty attends the estimation procedure described above, it can be seen in figures 103 through 105 that many of the dashed curves generated from such estimates are in close agreement with the solid regression curves. In fact, that for CsI coincides with the solid curve. In other cases, discrepancies of the order of 5 or 6 cal mole^{-1} (°K)$^{-1}$ occur between the dashed and solid curves. Nevertheless, errors in $\bar{C}^\circ_P$ of this order of magnitude commonly introduce corresponding errors in computed values of $\Delta\bar{G}^\circ$ at high pressures and temperatures that are within the overall uncertainty attending geochemical calculations. Consequently even these rough estimates are useful. Estimated values of $\bar{C}^\circ_{P,j}$ as a function of temperature for a number of aqueous species are shown in figure 126.

The equation of state parameters for aqueous species given by Helgeson and Kirkham (1976) and those derived above from regression calculations and estimation algorithms are summarized in table 18, together with thermodynamic data for the species at 298.15°K and 1 bar. It can be seen by comparing figures 103 through 105 and 112 with figure 126 that the curves generated from the estimated parameters given in table 18 exhibit the same configuration as those derived from the regression calculations.

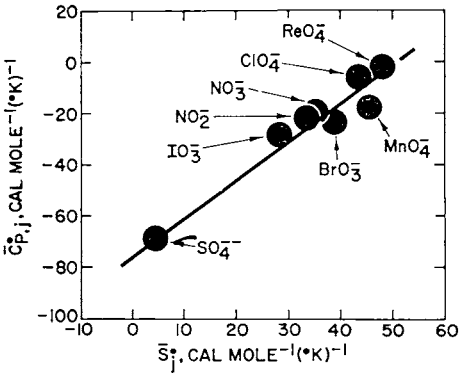

Fig. 123. Correlation of the conventional standard partial molal heat capacities and entropies of aqueous species at 25°C and 1 bar (tables 3, 13, and 18).

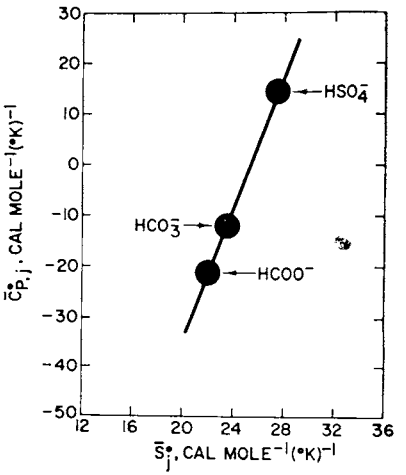

Fig. 124. Correlation of the conventional standard partial molal heat capacities and entropies of aqueous species at 25°C and 1 bar (tables 3, 13, and 18).

TABLE 18

Summary of the conventional standard partial molal thermodynamic properties of aqueous species designated by the subscript j at 25°C and

Species	$\Delta\bar{G}^{\circ}_{f,j}$ [a]	$\Delta\bar{H}^{\circ}_{f,j}$ [a]	$\bar{S}^{\circ}_{j}$ [b,g]	$\bar{C}^{\circ}_{P,j}$ [b,g]	$\bar{V}^{\circ}_{j}$ [c]	$\underline{c}^{\circ}_{1,j}$ [b,g]
H^+	0.0	0.0	0.0	0.0	0.0	0.0
Li^+	-69,946[bb]	-66,552[z]	2.7	14.4	-1.2[k]	27.2981
Na^+	-62,622[bb]	-57,433[z]	14.0	10.0	-1.3[k]	35.7153
K^+	-67,576[bb]	-60,270[z]	24.2	3.0	8.7[k]	18.4682
Cs^+	-69,718[bb]	-61,673[z]	31.8	-5.5	21.2[k]	29.9613
NH_4^+	-18,991[bb]	-31,850[z]	26.6	16.7	17.8[k]	34.04[j]
Ag^+	18,426[z]	25,275[z]	17.5	6.2	-0.7[p]	20.07[j]
Cu^+	11,950[dd]	17,132[aa]	9.7	11.5[h]	-10.5[n]	27.14[j]
Au^+	39,000[ee]	48,175[aa]	26.5	0.2[h]	13.0[n]	16.02[j]
Mg^{++}	-108,700[dd]	-111,563[aa,gg]	-33.0	-4.3	-21.3[k]	39.0257
Ca^{++}	-132,155[bb]	-129,804[z]	-13.5	-6.6	-18.5[k]	35.88[j]
Sr^{++}	-133,710[dd]	-130,458[aa]	-7.8	-8.5	-17.8[k]	33.98[j]
Ba^{++}	-134,020[dd]	-128,502[aa]	2.3	-11.2	-12.5[k]	34.2215
Pb^{++}	-5,742[bb]	220[z]	4.2	9.5[h]	-15.6[l]	55.32[j]
Zn^{++}	-35,331[bb]	-36,661[z]	-26.2	-5.9	-21.8[l]	43.29[j]
Cu^{++}	15,651[bb]	15,700[z]	-23.2	-5.7	-27.8[m]	39.73[j]
Hg^{++}	39,352[bb]	40,669[z]	-8.7	2.4[h]	-19.5[l]	49.81[j]
Fe^{++}	-18,850[dd]	-21,302[aa]	-32.9	-10.9[h,hh]	-24.9[l]	35.32[j]
Mn^{++}	-54,500[dd]	-52,724[aa]	-17.6	-3.1	-18.1[l]	45.59[j]
Fe^{+++}	-1,100[dd]	-11,601[aa]	-75.5	4.9	-43.8[l]	66.02[j]
Al^{+++}	-116,969[cc]	-127,008[cc]	-73.6	3.9	-42.4[l]	65.27[j]
Au^{+++}	103,600[ee]	98,913[aa]	-51.2	-12.2[h]	-41.3[n]	44.73[j]
F^-	-67,323[bb]	-80,151[z]	-3.2	-28.2	-1.1[k]	0.8814
Cl^-	-31,380[bb]	-39,933[z]	13.6	-30.2	17.9[k]	-4.8384
Br^-	-24,866[bb]	-29,039[z]	19.8	-31.2	24.9[k]	6.4161
I^-	-12,412[bb]	-13,599[z]	25.5	-29.0	36.3[k]	1.3667
OH^-	-37,604[bb]	-54,977[z]	-2.6	-33.0	-7.7[k]	24.7208[s]
HS^-	2,880[dd]	-4,218[aa]	15.0	-30.5[h]	20.2[k]	-2.47[j]
NO_3^-	-26,610[dd]	-49,530[aa,gg]	35.1	-19.2	29.0[k]	38.24[j]
HCO_3^-	-140,282[ff]	-164,898[ff]	23.5	-11.7	24.2[k]	15.40[j]
SO_4^{--}	-177,951[bb]	-217,400[z]	4.5	-68.5	14.1[k]	1.3418
$NaCl^\circ$	-92,740[x]	-99,873[x]	15.0[x]	43.8[x]	13.5[x]	63.6309[x]
$SiO_{2(aq)}$	-199,190[y]	-210,726[y]	14.8[y]	-25.0[y]	13.6[y]	48.5169[y]

1 bar and the parameters required to calculate the corresponding properties at high pressures and temperatures from eqs (254) and (273) through (276)*

Species	$c_2^{b,g}$, $\underline{j}$	a_1^{d}, $\underline{j}$	a_2^{e}, $\underline{j}\times10^{5}$	a_3^{d}, $\underline{j}\times10^{2}$	a_4^{e}, $\underline{j}\times10^{5}$	θ^{f} / $\underline{j}$	$\omega^{ag}\times10^{-5}$ / $\underline{j}$
H^+	0.0	0.0	0.0	0.0	0.0	0.0	0.0
Li^+	-1.2342	0.004[r]	3.62[r]	-0.043[r]	0.223[r]	253.94[r]	0.4862
Na^+	-6.2856	0.1914[r]	-4.7852[r]	-5.6282[r]	3.6560[r]	215.17[r]	0.3306
K^+	-2.9265	0.3107[r]	0.7452[r]	-1.9460[r]	1.4504[r]	234.19[r]	0.1927
Cs^+	-9.3863	0.670[r]	-4.41[r]	-4.286[r]	2.806[r]	217.04[r]	0.0974
NH_4^+	-3.83[i]	0.555[r]	-6.08[r]	-2.886[r]	1.954[r]	225.29[r]	0.1791
Ag^+	-1.32[i]	0.02[t]	7.5[w]	-0.31[t]	0.39[u]	264.9[v]	0.2160
Cu^+	-1.12[i]	-0.22[t]	8.5[w]	-0.10[t]	0.26[u]	271.4[v]	0.3351
Au^+	-2.49[i]	0.41[t]	3.0[w]	-1.50[t]	1.12[u]	245.6[v]	0.1800
Mg^{++}	-2.6665	-0.4170[r]	14.0877[r]	-0.0063[r]	0.0704[r]	270.56[r]	1.5372
Ca^{++}	-3.31[i]	-0.3573[r]	11.4034[r]	-0.1252[r]	0.1768[r]	266.14[r]	1.2366
Sr^{++}	-3.11[i]	-0.3447[r]	13.0761[r]	-0.1391[r]	0.0903[r]	268.97[r]	1.1363
Ba^{++}	-6.4428	-0.111[r]	10.39[r]	-2.287[r]	1.589[r]	245.02[r]	0.9851
Pb^{++}	-3.63[i]	-0.29[t]	7.8[w]	-0.20[t]	0.32[u]	267.8[v]	1.0788
Zn^{++}	-3.80[i]	-0.41[t]	7.5[w]	-0.31[t]	0.39[u]	266.2[v]	1.4574
Cu^{++}	-4.35[i]	-0.53[t]	5.5[w]	-0.70[t]	0.63[u]	257.0[v]	1.4769
Hg^{++}	-3.71[i]	-0.37[t]	7.6[w]	-0.25[t]	0.35[u]	267.9[v]	1.1512
Fe^{++}	-4.07[i]	-0.47[t]	6.4[w]	-0.50[t]	0.51[u]	260.8[v]	1.4574
Mn^{++}	-3.57[i]	-0.33[t]	8.3[w]	-0.15[t]	0.29[u]	267.5[v]	1.4006
Fe^{+++}	-8.88[i,q]	-0.729[t]	-2.1[w]	-3.9[t]	2.60[u]	223.9[v]	2.7025
Al^{+++}	-7.89[i,q]	-0.703[t]	-0.9[w]	-3.2[t]	2.17[u]	229.6[v]	2.8711
Au^{+++}	-7.87[i,q]	-0.705[t]	-0.9[w]	-3.2[t]	2.17[u]	229.6[v]	2.4007
F^-	-1.0551	0.0821[r]	1.1184[r]	-0.0219[r]	0.0313[r]	272.42[r]	1.7870
Cl^-	-2.0410	0.5761[r]	-6.9590[r]	-1.0698[r]	1.0365[r]	246.02[r]	1.4560
Br^-	-7.5141	0.8941[r]	-16.7628[r]	-6.6404[r]	4.2899[r]	206.75[r]	1.3858
I^-	-6.8157	1.396[r]	-28.68[r]	-16.863[r]	10.459[r]	186.51[r]	1.2934
OH^-	-6.2074[s]	0.0515[s]	-0.0994[s]	-1.9845[s]	1.0832[s]	253.52[s]	1.7246
HS^-	-2.27[i]	0.651[r]	-6.98[r]	-1.291[r]	0.983[r]	252.19[r]	1.4110
NO_3^-	-17.72[i]	1.2438[r]	-32.0602[r]	-18.2754[r]	10.6342[r]	185.29[r]	1.1295
HCO_3^-	-3.00[i]	0.7887[r]	-8.9225[r]	-2.6787[r]	1.4350[r]	236.87[r]	1.3293
SO_4^{--}	-4.6940	0.5825[r]	4.4576[r]	-0.6501[r]	0.7125[r]	263.03[r]	3.1857
$NaCl^\circ$	-1.00[x]	4.6779[x]	267.2977[x]	-47.1027[x]	-243.5009[x]	265.25[x]	1.1381[x]
$SiO_{2(aq)}$	-15.7891[y]	0.0214[y]	4.9341[y]	6.8259[y]	0.2979[y]	233.00[y]	0.1291[y]

*The c_1 and c_2 parameters shown in the table for NH_4^+, HS^-, NO_3^- and HCO_3^-, together with c_1, c_2, a_1, a_2, a_3, a_4, and θ for Pb^{++}, Zn^{++}, Cu^{++}, Hg^{++}, Fe^{++}, Ag^+, Cu^+, and Au^+ and Mn^{++} correspond to revised estimates of earlier parameters used to generate the curves for these species in figures 7.3 and 7.4 of Helgeson (in press). The revised estimates do not affect the general configurations of the curves, but they alter slightly their positions. As a consequence, the curves in the lower diagram of figure 7.3 of Helgeson (in press) are not the same as the corresponding curves in figure 126 of the present communication.

Table 18 notes continued on p. 1436.

Table 18 and the equations derived in the preceding pages have been combined with thermodynamic data and equations for minerals (Helgeson and others, 1978) and electrostatic/thermodynamic equations and data for H_2O (Helgeson and Kirkham, 1974a; Delany and Helgeson, 1978) in computer program SUPCRT, which can be used to calculate equilibrium phase relations in a wide variety of hydrothermal systems at high pressures and temperatures. Prediction and analysis of the thermodynamic behavior of aqueous species under these conditions affords insight into the causal processes responsible for many of the chemical and mineralogic changes observed in rocks. Copies of the program and data file, together with a program description can be obtained at cost from the senior author before

Notes for table 18 (continued)

[a]Cal mole^{-1}. [b]Cal mole^{-1}(°K)$^{-1}$. [c]Cm^{3}mole^{-1}. [d]Cal mole^{-1}bar^{-1}. [e]Cal mole^{-1}bar^{-2}. [f]°K. [g]Except where indicated otherwise, the values of $\bar{S}^\circ_j$, $\bar{C}^\circ_{P,j}$, $c_{1,j}$, $c_{2,j}$, θ_j, and ω_j in these columns were taken from tables 3, 13 and 15. [h]Estimated from equation (282) using values of $\bar{S}^\circ_j$ shown above and the parameters given in the text for monovalent anions and monovalent, transition metal, and trivalent cations. [i]Estimated from equation (281) and values of $a_{4,j}$ shown above. [j]Calculated from equation (270) using values of $\bar{C}^\circ_{P,j}$, $c_{2,j}$, θ_j, and ω_j given above together with $X_{P_r,T_r} = -3.16 \times 10^{-7}$(°K)$^{-2}$ (Helgeson and Kirkham, 1974a). [k]Calculated from equation (254) using values of $a_{1,j}$, $a_{2,j}$, $a_{3,j}$, $a_{4,j}$, θ_j, and ω_j given above, together with $Q_{P_r,T_r} = 5.95 \times 10^{-7}$ bar^{-1} (Helgeson and Kirkham, 1974a). [l]Calculated from standard partial molal volume data for electrolytes tabulated by Millero (1972b) and values of $\bar{V}^\circ_j$ shown above. [m]Millero (1972a). [n]Estimated from the correlation of $\bar{V}^\circ_j$ with $\bar{S}^\circ_j$ in figure 56 of Helgeson and Kirkham (1976). [p]Computed from the intercept of the linear curve for $AgNO_3$ in figure 87 and the value of $\bar{V}^\circ_{NO_3^-}$ shown above. [q]Estimated from equation (281) assuming the same $c_{2,j}$ dependence on $a_{4,j}$ for trivalent ions as that for divalent ions in figure 120. The validity of this assumption is supported by correlation of $c_{2,GdCl_3}$ in table 14 with an estimated value of $a_{4,GdCl_3}$. [r]Helgeson and Kirkham (1976). [s]Generated in the present study by regression of log K_w (see text). [t]Estimated by first computing $\bar{V}^\circ_{i,j}$ and $\Delta\bar{V}^\circ_{c,j}$ from equations (115), (253) and (255), together with the correlation shown in figure 54 of Helgeson and Kirkham (1976). Values of $a_{1,j}$ and $a_{3,j}$ were then generated from $a_{1,j} = \bar{V}^\circ_{i,j}$ and the correlation of $a_{3,j}$ with $\Delta\bar{V}^\circ_{c,j}$ in figure 59 of Helgeson and Kirkham (1976). [u]Generated from equation (131) in Helgeson and Kirkham (1976) using values of $a_{3,j}$ shown above. [v]Calculated from equation (250) using values of $a_{2,j}$, $a_{3,j}$, and $a_{4,j}$ given above and values of $\Delta V_{c,j}$ generated in the manner described in footnote [t]. [w]Generated from the correlation of $a_{2,j}$ with $a_{4,j}$ in figure 121. [x]Calculated in the present study by regression of log K_{NaCl}° (see text). [y]Walther and Helgeson (1977). [z]CODATA (1978). [aa]Calculated from the values of $\Delta\bar{G}^\circ_{f,j}$ shown above using standard partial molal entropies of the elements taken from the sources shown in footnotes [z] and/or [dd]. [bb]Calculated from the values of $\Delta\bar{H}^\circ_{f,j}$ shown above using standard partial molal entropies of the elements taken from the sources shown in footnotes [z] and/or [dd]. [cc]Hemingway and Robie (1977). [dd]Wagman and others (1968, 1969) and/or Parker, Wagman and Evans (1971). [ee]Latimer (1952). [ff]Berg and Van der Zee (1978). [gg]These values are in close agreement with those reported by Coffy and Olofsson (1979), Shin and Criss (1979), and Cox, Harrop, and Head (1979). [hh]Owing to interpolation vagaries, this value was accepted in preference to that reported by Bernarducci, Morss, and Mikszial (1979).

July 1, 1982. The program description, program (which is written in FORTRAN IV for CDC 6400, 6600, and 7600 computers), and data file are stored on magnetic tape (7 track, 800 binary bits $inch^{-1}$, 132 characters $record^{-1}$, 1 record $block^{-1}$).

High pressure/temperature predictions.—Prediction of the thermodynamic behavior of aqueous species at high pressures and temperatures with eqs (273) through (276) generated the curves shown for Mg^{++}, Na^{+}, Cl^{-}, and SO_4^{--} in figures 127 through 130. The configurations of these curves are representative of those for other monovalent and divalent cations and anions. The electrostatic properties of H_2O employed in the calculations are those given by Helgeson and Kirkham (1974a).

It can be seen in figure 127 that the calculations discussed above indicate that $\bar{C}^\circ_P$ as a function of temperature at constant pressure exhibits a double inflection. The maxima in the isobars arise from opposing contributions by local collapse of the solvent structure and ion solvation to $\bar{C}^\circ_P$, which become less negative and more negative, respectively, with increasing temperature. The high-temperature minima are a consequence of the large negative values of $(\partial \ ln \ \epsilon^\circ/\partial T)_P$ in the critical region, where $(\partial \ ln \ \epsilon^\circ/\partial T)_P$ increases dramatically from $-\infty$ at the critical point with either increasing or decreasing pressure and/or temperature (Helgeson and Kirkham, 1974a). As expected, both extrema tend to dampen with

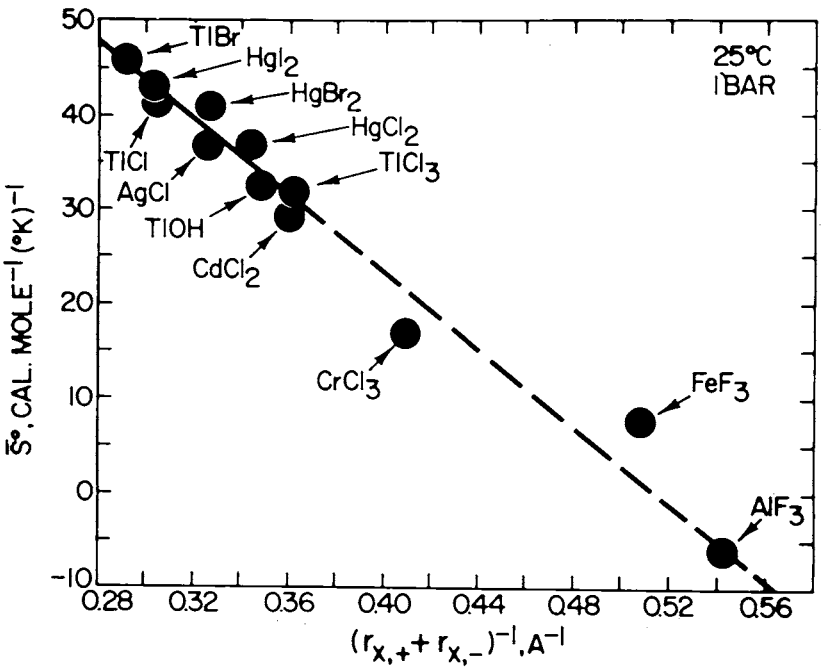

Fig. 125. Correlation of, the standard partial molal entropies of neutral aqueous species at 25°C and 1 bar (Wagman and others, 1968, 1969) with the reciprocal sum of the crystal radii of the ionic constituents of the species taken from Sienko and Plane (1963).

increasing pressure. Note that the calculations indicate that $\bar{C}°_P$ also maximizes with increasing pressure at constant temperature. However, it should be emphasized in this regard that the positions and configurations of the curves shown in figures 127 through 130 are more uncertain for temperatures $\lesssim$ 100°C at pressures $>$ 1 kb, temperatures $\gtrsim$ 500°C at all pressures, and 5 kb at all temperatures. The greater uncertainties in these pressure/temperature regions (which are indicated by the dashed curves in figs. 127 through 130) arise from uncertainties in calculated values of the dielectric constant of H_2O in these regions (Helgeson and Kirkham, 1974a).

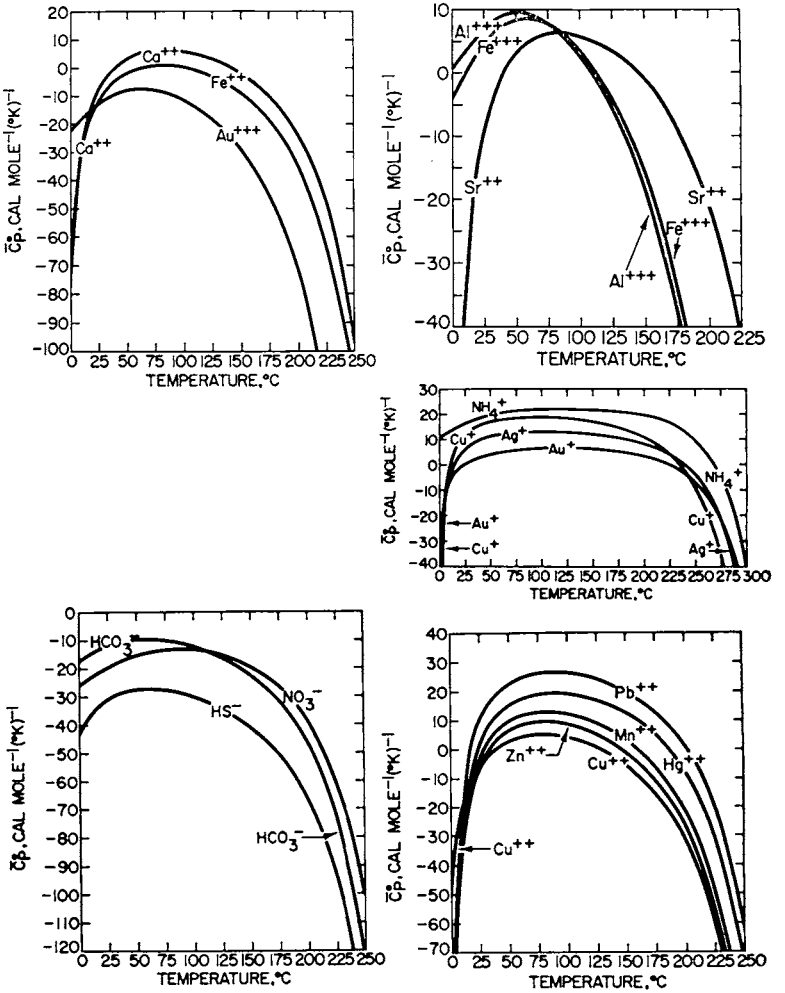

Fig. 126. Estimated conventional standard partial molal heat capacities of aqueous ions as a function of temperature at pressures corresponding to those along the liquid-vapor equilibrium curve for H_2O (see text). The curves were generated from eq (273) using parameters given in table 18.

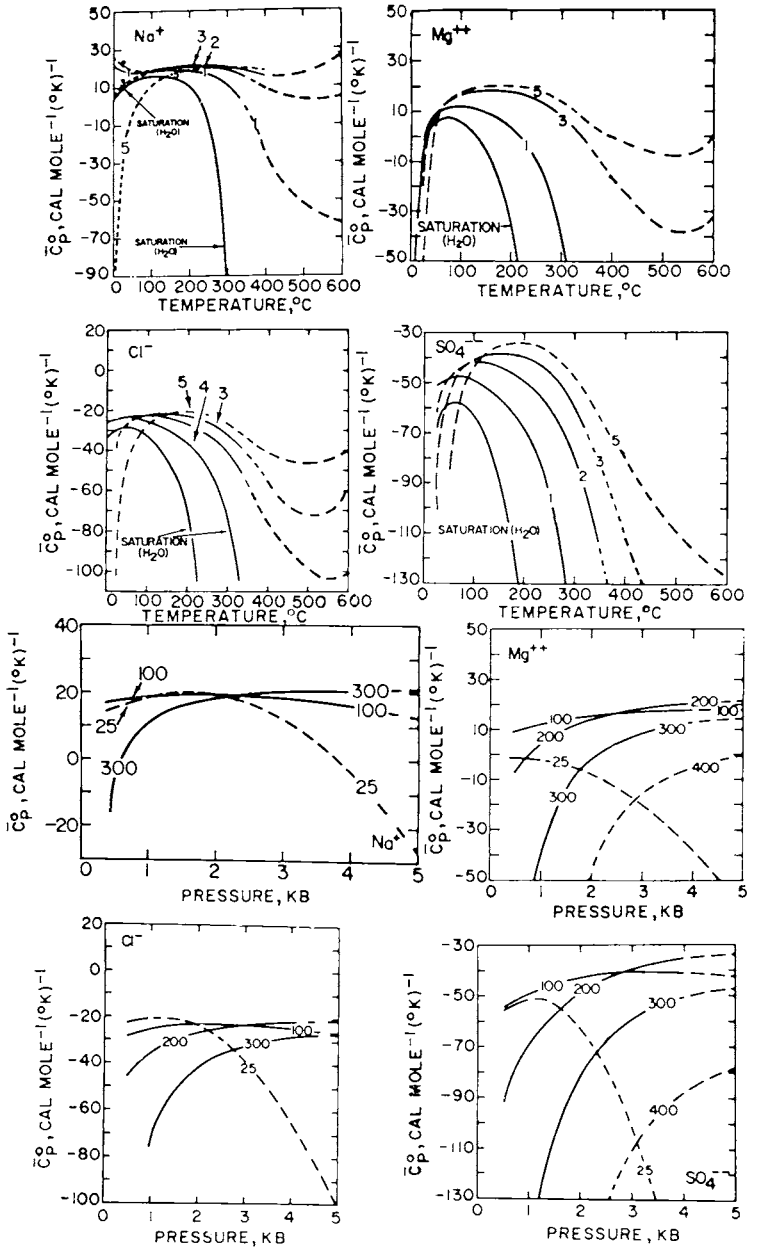

Fig. 127. Conventional standard partial molal heat capacities of aqueous ions at high pressure (labeled in kb) and temperature (labeled in °C) computed from eq (273) using thermodynamic data and parameters taken from table 18 and the electrostatic properties of the solvent given by Helgeson and Kirkham (1974a). The dashed curves are more uncertain than their solid counterparts.

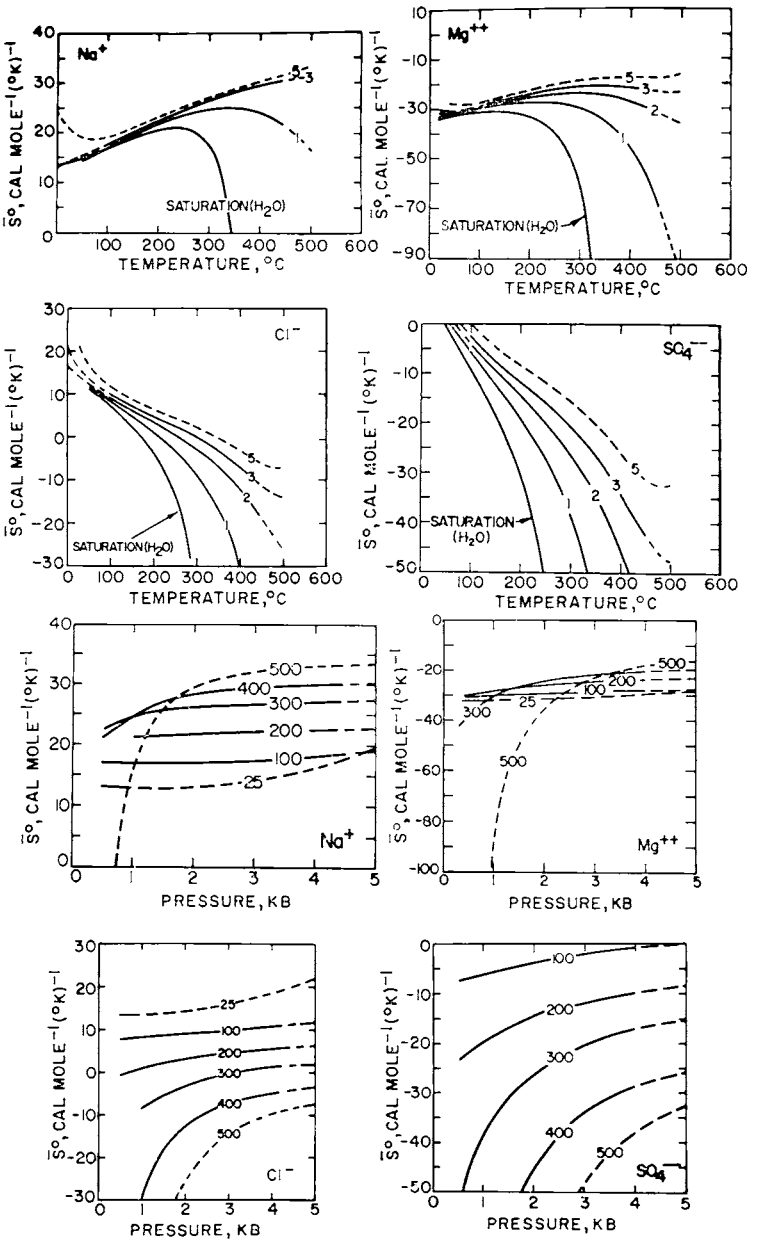

Fig. 128. Conventional standard partial molal entropies of aqueous ions at high pressure (labeled in kb) and temperature (labeled in °C) computed from eq (274) using thermodynamic data and parameters taken from table 18 and the electrostatic properties of the solvent given by Helgeson and Kirkham (1974a). The dashed curves are more uncertain than their solid counterparts.

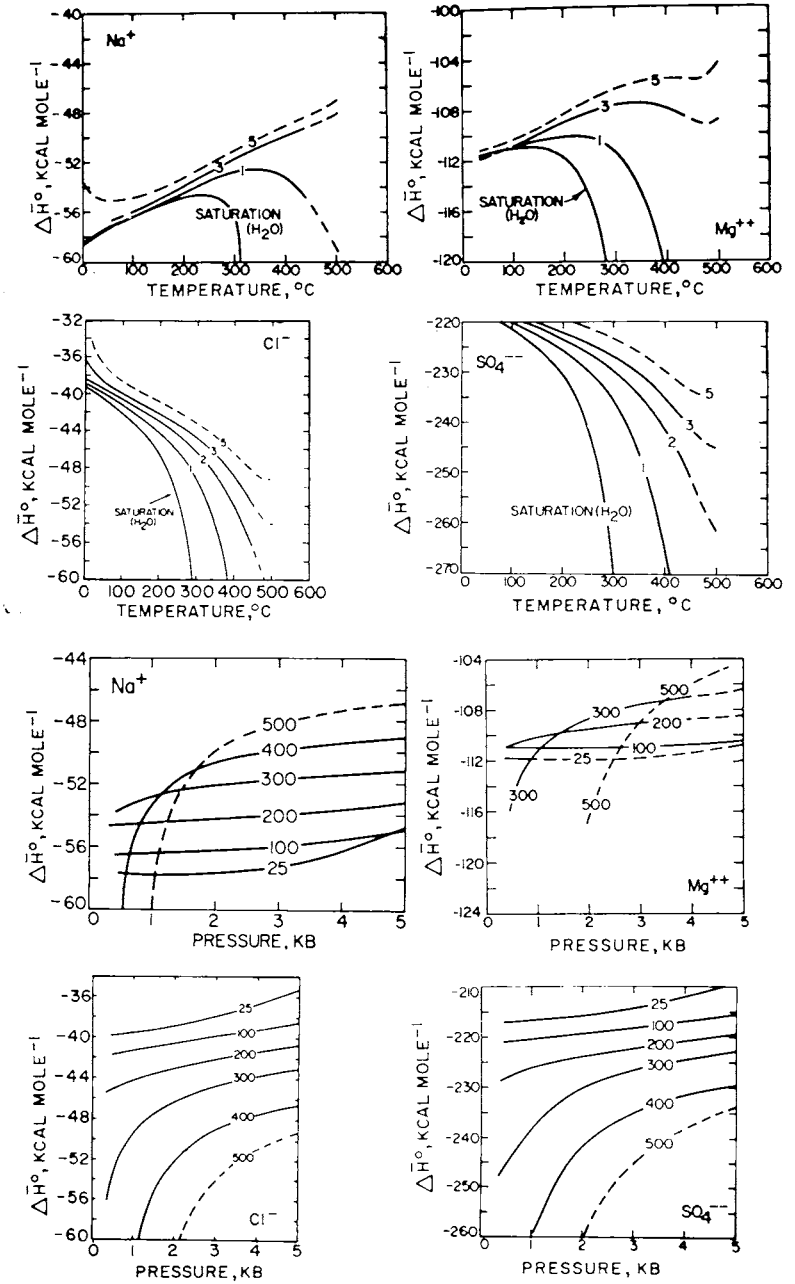

Fig. 129. Conventional apparent standard partial molal enthalpies of formation of aqueous ions at high pressure (labeled in kb) and temperature (labeled in °C) computed from eq (275) using thermodynamic data and parameters taken from table 18 and the electrostatic properties of the solvent given by Helgeson and Kirkham (1974a). The dashed curves are more uncertain than their solid counterparts.

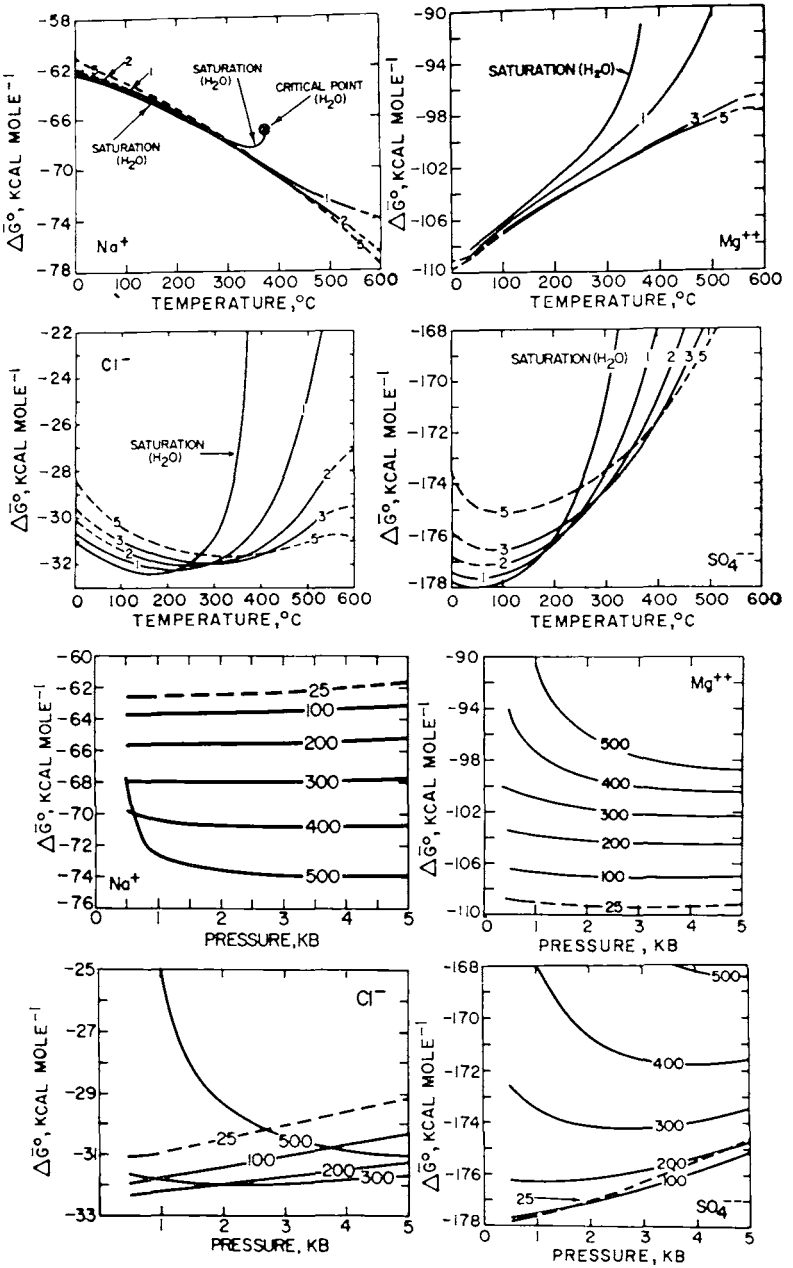

Fig. 130. Conventional apparent standard partial molal Gibbs free energy of formation of aqueous ions at high pressure (labeled in kb) and temperature (labeled in °C) computed from eq (276) using thermodynamic data and parameters taken from table 18 and the electrostatic properties of the solvent given by Helgeson and Kirkham (1974a). The dashed curves are more uncertain than their solid counterparts.

As a consequence of different degrees of influence on $\bar{C}^\circ_{P,j}$ for cations and anions by the electrostatic properties of the solvent in different regions of pressure/temperature space, the curves in figure 128 representing $\bar{S}^\circ$ for Cl^- and SO_4^{--} as a function of temperature at constant pressure exhibit a "synclinal" configuration which is not apparent in the curves representing $\bar{S}^\circ$ for Na^+ and Mg^{++}. Note in figure 129 that the same observation holds for $\Delta\bar{H}^\circ$, which, like $\bar{S}^\circ$ and $\bar{C}^\circ_P$, approaches negative infinity at the critical point of H_2O.

It can be seen in figure 130 that increasing pressure at constant temperature has little effect on $\Delta\bar{G}^\circ$ for Na^+ and Mg^{++} at pressures > 2 kb, which is not true for any pressure and temperature in the case of Cl^- and SO_4^{--}. As a consequence, $\Delta\bar{G}^\circ$ for Cl^- and SO_4^{--} minmizes with increasing temperature at constant pressure, while $\Delta\bar{G}^\circ$ for Na^+ and Mg^{++} changes monotonically. Contributions by ion solvation and local collapse of the solvent structure to $\Delta\bar{G}^\circ$ are both negative. Because $\bar{S}^\circ$ is positive for Na^+ and negative for Mg^{++} throughout the pressure/temperature region considered in figures 127 through 130, $\Delta\bar{G}^\circ_{Mg^{++}}$ increases and $\Delta\bar{G}^\circ_{Na^+}$ decreases with increasing temperature at constant pressure. As a consequence, the solubilities of magnesian compounds would be expected to decrease relative to those of sodium minerals with increasing temperature at all pressures, which is in general agreement with geologic observations.

Standard molal enthalpies of hydration (see footnote 12) of aqueous species at 300°C and 86 bars computed with the aid of the equations and parameters summarized above using thermodynamic data and equations for gaseous species taken from Wagman and others (1969) and Helgeson (1969) compare favorably with those generated from calorimetric measurements by Cobble and Murray (1977). Similarly, activity/composition relations and stability fields for minerals on activity diagrams generated with the aid of the equations and parameters derived in the present study afford close approximation of both experimental and geologic phase relations at high pressures and temperatures (Helgeson and others, 1978; Walther and Helgeson, 1980; Bird and Helgeson, 1981). These observations underscore the general validity and applicability of the theoretical equations, parameters, and standard partial molal properties of aqueous species summarized above.

Extended Term Parameters for Single Electrolytes

Because the short-range interaction contribution to $\log \bar{\gamma}_\pm$ as a function of pressure and temperature incorporates the ionic strength dependence of departures from ideality caused by collapse of the local solvent structure about the ions in solution, it would be reasonable to expect expressions of the form of eqs (254), (258), and (273) to describe the pressure and temperature dependence of $b_{V,k}$, $b_{\kappa,k}$, and $b_{J,k}$, respectively. However, for this to be the case the reciprocals of the dielectric constants of electrolyte solutions (ϵ^{-1}) at a given ionic strength must be linearly related to the reciprocal of the dielectric constant of the solvent ($\epsilon^{\circ -1}$) as a func-

tion of pressure and temperature. Although the paucity of reliable experimental dielectric constant data for electrolyte solutions at high pressures and temperatures precludes a definitive conclusion in this regard, it appears from the correspondence of the curves and symbols in figure 131 that at least at low temperatures, ϵ^{-1} can be regarded as a linear function of $\epsilon^{\circ -1}$ at constant ionic strength. Although obvious discrepancies between the symbols and curves are apparent in figure 131, most of these can be attributed to experimental uncertainty, which increases substantially with increasing temperature. For example, it can be seen that the trend of the experimental values of ϵ^{-1} for NaCl reported by Hasted, Ritson, and

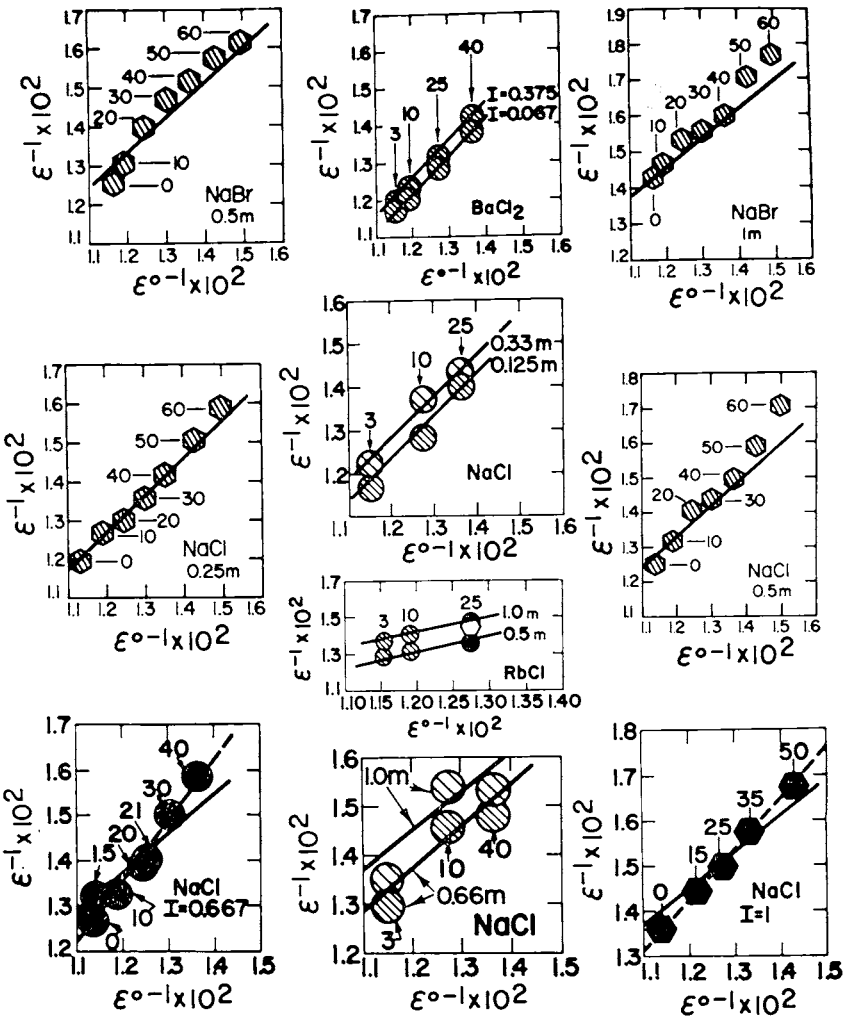

Fig. 131. Correlation of the reciprocal of the dielectric constant of electrolyte solutions (ϵ^{-1}) with that of the solvent ($\epsilon^{\circ -1}$) as a function of temperature at 1 bar and constant composition (see caption of fig. 3).

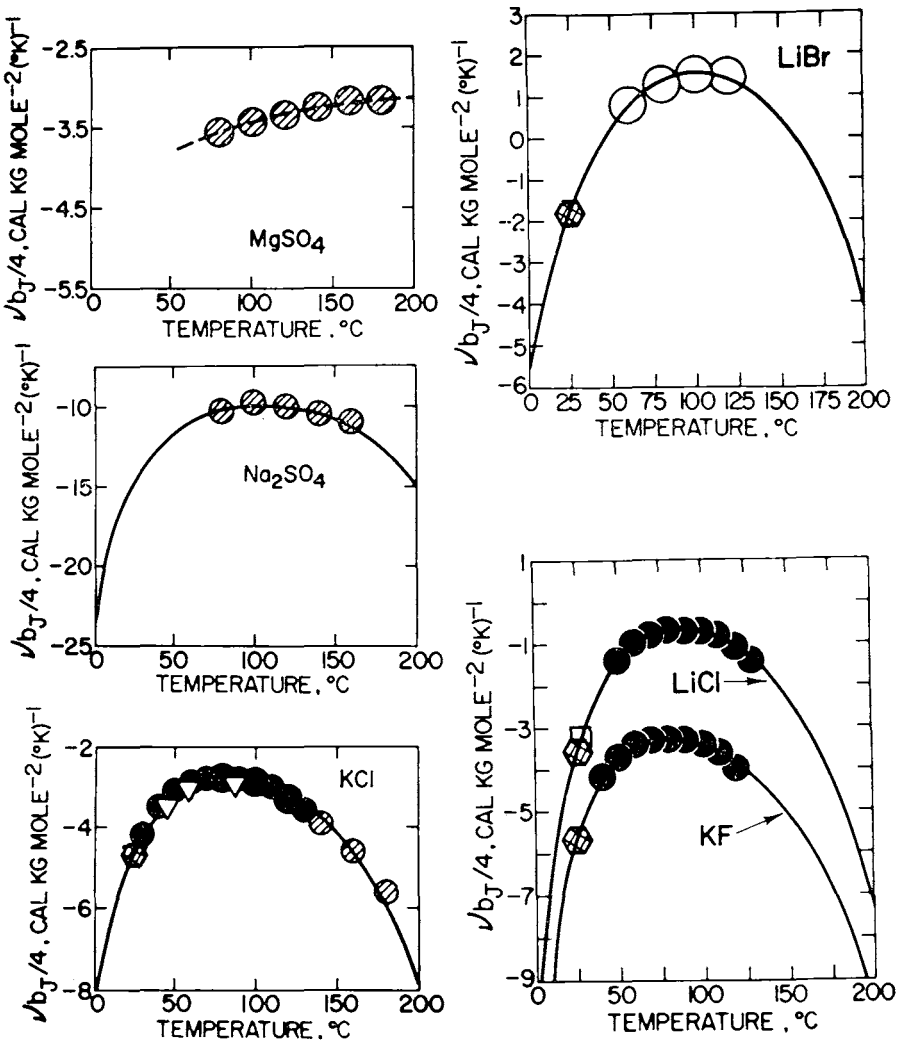

Fig. 132. Calculated (curves) and experimental (symbols) extended term parameters for the apparent molal heat capacities of electrolytes as a function of temperature (T) at 1 bar for $T < 100°C$ and pressures corresponding to liquid-vapor equilibrium at $T \geqslant 100°C$. The symbols represent the negative equivalents of the slopes of the linear curves shown for the electrolytes in figures 65 through 82, but (with the exception of the dashed curve for $MgSO_4$) the curves were generated from eq (291) (see text). The different symbols represent experimental data taken from the various sources cited in the caption of figure 65.

Collie (1948) from 0° to 40°C is inconsistent with the corresponding trend of the data reported by Hasted and Roderick (1958). It should perhaps be emphasized in this regard that the solid curves in figure 131 are consistent with one another and with the equations and parameters derived below. The dashed curves merely connect data points.

The bulk of the experimental data shown in figure 131 can be described by

$$\frac{1}{\epsilon_{P,T}} - \frac{1}{\epsilon_{P_r,T_r}} = \hat{k}\left(\frac{1}{\epsilon^{\circ}_{P,T}} - \frac{1}{\epsilon^{\circ}_{P_r,T_r}}\right) \tag{284}$$

where $\epsilon_{P,T}$ and $\epsilon^{\circ}_{P,T}$ denote the dielectric constant of the electrolyte solution and the solvent, respectively, at the subscripted pressure and temperature, and $\hat{k}$ stands for a pressure/temperature-independent coefficient char-

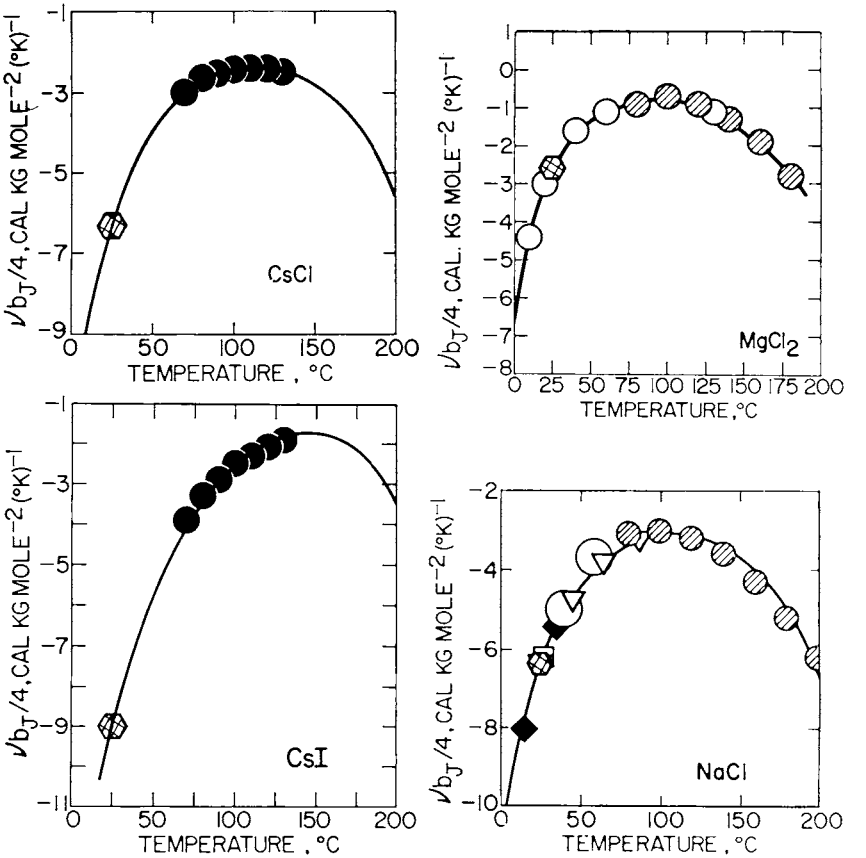

Fig. 133. Calculated (curves) and experimental (symbols) extended term parameters for the apparent molal heat capacities of electrolytes as a function of temperature (T) at 1 bar for T < 100°C and pressures corresponding to liquid-vapor equilibrium at T ⩾ 100°C. The symbols represent the negative equivalents of the slopes of the linear curves shown for the electrolytes in figures 65 through 82, but the curves were generated from equation (291) (see text). The different symbols represent experimental data taken from the various sources cited in the caption of figure 65.

acteristic of both the electrolyte and the ionic strength of the solution. Note that it follows from eqs (144) and (284) that we can write

$$\hat{k} = 1 + \sum_k \hat{a}_{5,k}\, y_k \bar{I} \tag{285}$$

where $\hat{a}_{5,k}$ represents an electrostatic parameter characteristic of the kth electrolyte, which is independent of ionic strength as well as pressure and

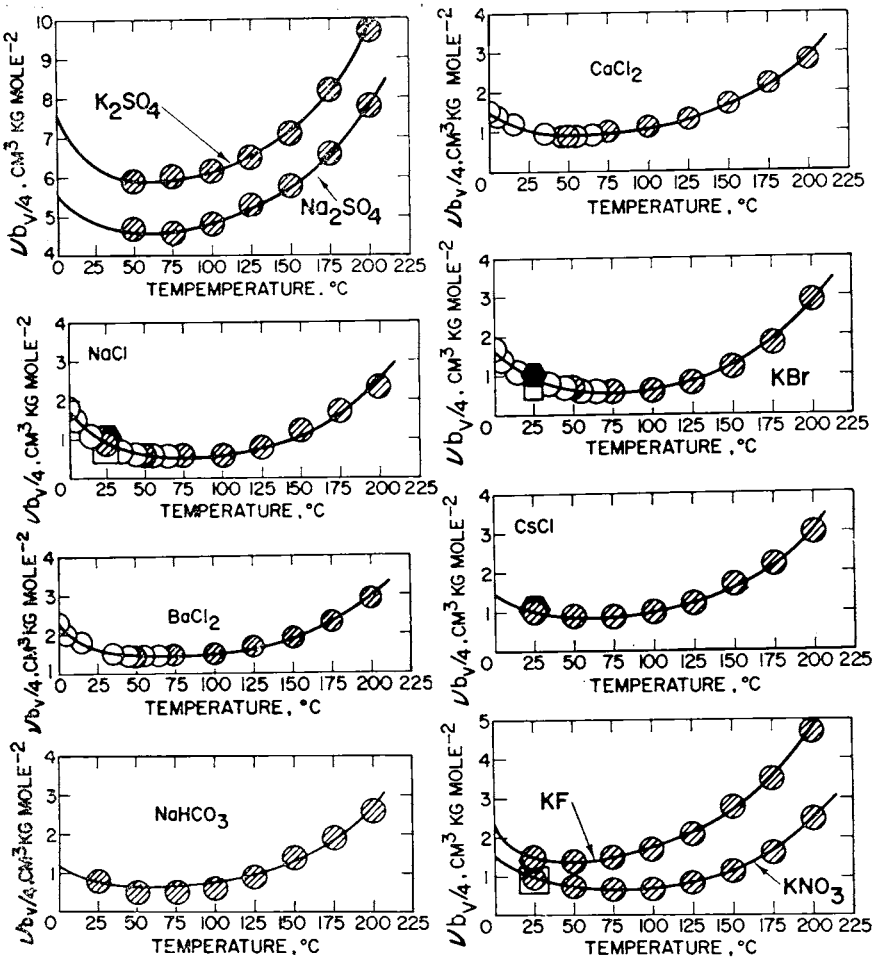

Fig. 134. Calculated (curves) and experimental (symbols) extended term parameters for the apparent molal volumes of electrolytes as a function of temperature (T) at 1 bar for $T < 100$°C and pressures corresponding to liquid-vapor equilibrium at $T \geqslant 100$°C. The symbols represent the slopes of the linear curves shown for the electrolytes at 1 and 20 bars in figures 83 through 93, but the curves were generated from eq (288) (see text). The different symbols represent experimental data taken from the various sources cited in the caption of figure 83.

temperature. Eqs (284) and (285) are consistent with

$$\frac{1}{\epsilon_{P,T}} = \frac{1}{\epsilon^{\circ}_{P,T}} + \frac{\sum_k \hat{a}_{5,k}\, y_k \bar{I}}{\epsilon^{\circ}_{P,T}} + \sum_k \hat{a}_{6,k}\, y_k \bar{I} \qquad (286)$$

where $\hat{a}_{6,k}$ corresponds to an electrostatic parameter analogous to $\hat{a}_{5,k}$. Hence,

$$\hat{b}_k = \hat{a}_{6,k} + \frac{\hat{a}_{5,k}}{\epsilon^{\circ}_{P,T}} . \qquad (287)$$

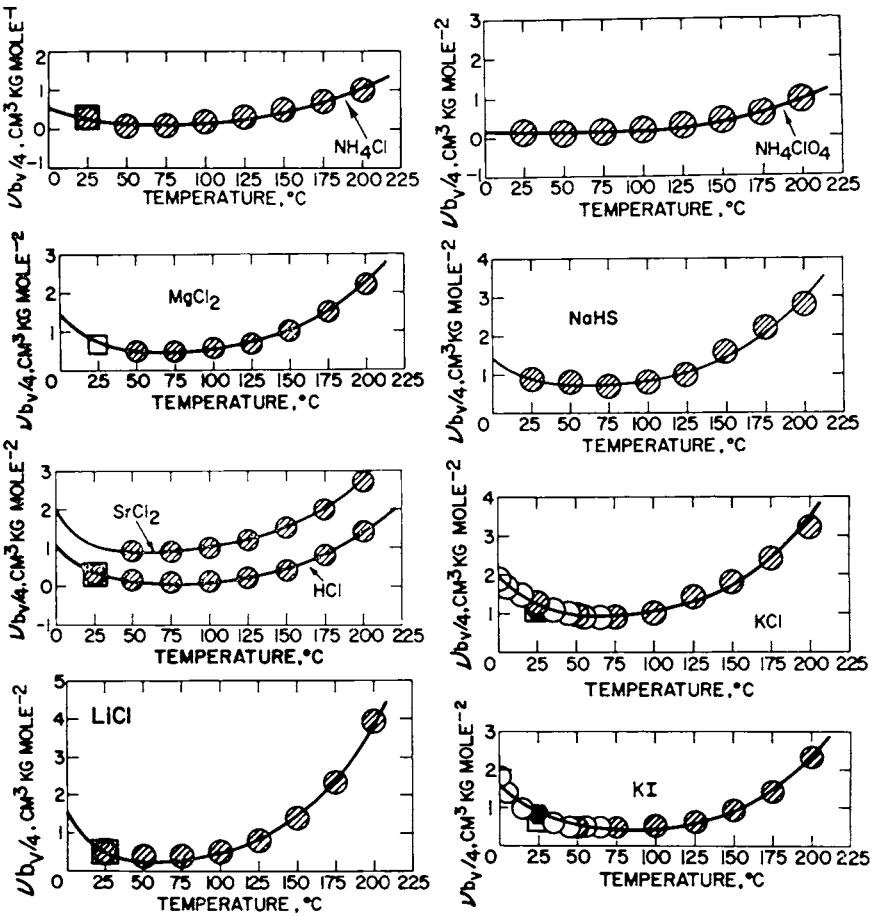

Fig. 135. Calculated (curves) and experimental (symbols) extended term parameters for the apparent molal volumes of elctrolytes as a function of temperature (T) at 1 bar for T < 100°C and pressures corresponding to liquid-vapor equilibrium at T ≥ 100°C. The symbols represent the slopes of the linear curves shown for the electrolytes at 1 and 20 bars in figures 83 through 93, but the curves were generated from eq (288) (see text). The different symbols represent experimental data taken from the various sources cited in the caption of figure 83.

Empirical evidence supporting the validity of the hypothesis that the temperature and pressure dependence of b_γ should be consistent with the functional form of eqs (254) and (273) can be adduced by comparative analysis of the distribution of the symbols shown in figures 132 through 136 with those in analogous figures depicting the standard partial molal properties of electrolytes (see below). The symbols in figures 132 through 136 represent the slopes of the curves shown for the electrolytes in figures 65 through 98.

It can be seen in figures 132 and 133 that the temperature dependence of $b_{J,k}$ is identical in form to that of $\bar{C}_{P,k}$ in figures 103 through 105. Similar comparison of figures 134 through 136 with those representing the

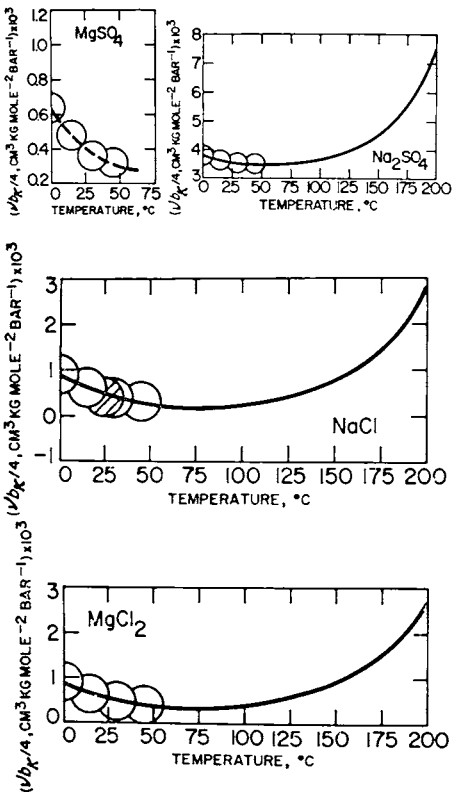

Fig. 136. Calculated (curves) and experimental (symbols) extended term parameters for the apparent molal compressibilities of aqueous electrolytes as a function of temperature (T) at 1 bar for T < 100°C and pressures corresponding to liquid-vapor equilibrium for T ≥ 100°C. The symbols represent the slopes of the linear curves shown for NaCl, Na_2SO_4, $MgCl_2$, and $MgSO_4$ in figures 95, 98, and 99, but the curves were generated from eq (289) (see text). The different symbols represent experimental data reported by Allam (ms) and Millero and others (1974).

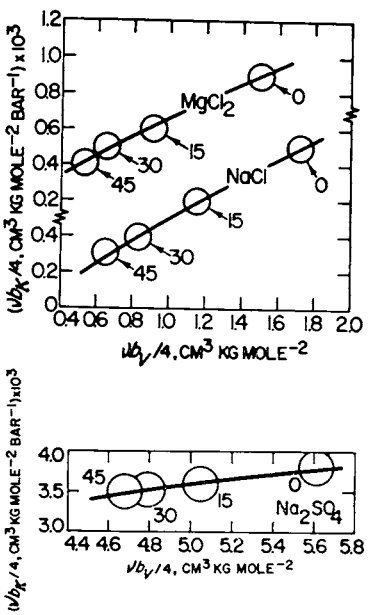

Fig. 137. Correlation of the extended term parameters for the apparent molal volumes and compressibilities of aqueous electrolytes as a function of temperature at 1 bar. The symbols represent experimental data cited in the captions of figures 83 and 98, but the curves were generated from equations given in the text.

temperature dependence of the standard partial molal volumes and compressibilities of electrolytes in figures 17 through 19, 26, 27, and 32 through 36 in Helgeson and Kirkham (1976) leaves little doubt that $b_{V,k}$ and $b_{\kappa,k}$ vary with increasing temperature in the same manner as $-\bar{V}^\circ_k$ and $-\bar{\kappa}^\circ_k$, respectively. In fact, all the curves in these various figures have the same absolute configuration with extrema in the vicinity of $\sim$ 100°C. These observations suggest that the linear correlation of $b_{\kappa,k}$ with $b_{V,k}$ for electrolytes with a common cation at 25°C and 1 bar (which follows from the correlations shown in figs. 100 through 102) also holds at higher temperatures. This conclusion is supported by the fact that the relation of $b_{\kappa,k}$ to $b_{V,k}$ for a given electrolyte as a function of temperature in figure 137 is identical to that of $\bar{\kappa}^\circ_k$ to $\bar{V}^\circ_k$, which has been shown (Helgeson and Kirkham, 1976) to be consistent with eqs (254) and (258).

The observations and equations summarized above suggest that $\nu_k b_{V,k}/2$, $-\nu_k b_{\kappa,k}/2$, and $-\nu_k b_{J,k}/2$ (which correspond to the extended term contributions to $(\bar{V}_k - \bar{V}^\circ_k)/\bar{I}$, $-(\bar{\kappa}_k - \bar{\kappa}^\circ_k)/\bar{I}$, and $\bar{J}_k/\bar{I}$, respectively) for a given electrolyte can be represented by extended terms analogs of eqs (254), (258), and (270). These analogs can be written as

$$\nu_k b_{V,k}/2 = \hat{a}_{1,k} + \hat{a}_{2,k}P + \frac{\hat{a}_{3,k}T + \hat{a}_{4,k}PT}{T - \theta_k} - \omega_k \hat{a}_{5,k} Q \quad , \tag{288}$$

$$-\nu_k b_{\kappa,k}/2 = \hat{a}_{2,k} + \frac{\hat{a}_{4,k}T}{T - \theta_k} - \omega_k \hat{a}_{5,k} N \quad , \tag{289}$$

and

$$-\nu_k b_{J,k,P_r}/2 = \hat{c}_{1,k} + \frac{\hat{c}_{2,k}T}{T - \theta_k} + \omega_k \hat{a}_{5,k} TX \tag{290}$$

where $\hat{a}_{1,k}$, $\hat{a}_{2,k}$, $\hat{a}_{3,k}$, $\hat{a}_{4,k}$, $\hat{c}_{1,k}$, and $\hat{c}_{2,k}$ designate parameters analogous to $a_{1,k}$, $a_{2,k}$, $a_{3,k}$, $a_{4,k}$, $c_{1,k}$, and $c_{2,k}$. The last terms in these equations represent the electrostatic contribution by ion solvation to $\nu_k b_{V,k}/2$, $-\nu_k b_{\kappa,k}/2$ and $-\nu_k b_{J,k,P_r}/2$.

It follows from eqs (288) and (290) that we can now write the extended term analogs of eqs (273), (275), and (276) as

$$-\nu_k b_{J,k,P,T}/2 = \hat{c}_{1,k} + \frac{\hat{c}_{2,k}T}{T - \theta_k} - \frac{\theta_k T(2\hat{a}_{3,k}(P - P_r) + \hat{a}_{4,k}(P^2 - P_r^2))}{(T - \theta_k)^3} + \omega_k \hat{a}_{5,k} TX \tag{291}$$

$$\begin{aligned} -\nu_k b_{H,k,P,T}/2 = &-\nu_k b_{H,k,P_r,T_r}/2 + (\hat{c}_{1,k} + \hat{c}_{2,k})(T - T_r) \\ &+ \hat{c}_{2,k}\theta_k \ln\left(\frac{T - \theta_k}{T_r - \theta_k}\right) \\ &+ \hat{a}_{1,k}(P - P_r) + \hat{a}_{2,k}(P^2 - P^2_r)/2 \\ &+ \frac{2\hat{a}_{3,k}T(P - P_r) + \hat{a}_{4,k}T(P^2 - P_r^2)}{2(T - \theta_k)} \\ &+ \frac{2\theta_k \hat{a}_{3,k}T(P - P_r) + \theta_k \hat{a}_{4,k}T(P^2 - P_r^2)}{2(T - \theta_k)^2} \\ &+ \omega_k \hat{a}_{5,k}(TY_{P,T} - T_r Y_{P_r,T_r} - Z_{P,T} + {}_{P_r,T_r}) \end{aligned} \tag{292}$$

and

$$-\nu_k b_{G,k,P,T}/2 = -\nu_k b_{G,k,P_r,T_r}/2 - \nu_k b_{S,k,P_r,T_r}(T - T_r) - \hat{c}_{1,k}(T\,ln(T\,ln\,(T/T_r) - T + T_r) + \hat{c}_{2,k}\left(T - T_r - (T - \theta_k)\,ln\left(\frac{T - \theta_k}{T_r - \theta_k}\right)\right) + \frac{2(\hat{a}_{1,k}(T - \theta_k) + \hat{a}_{3,k}T)\,(P - P_r) + (\hat{a}_{2,k}(T - \theta_k) + \hat{a}_{4,k}T)\,(P^2 - P_r^2)}{2(T - \theta_k)} - \omega_k \hat{a}_{5,k}\,(Z_{P,T} - Z_{P_r,T_r} - Y_{P_r,T_r}\,(T - T_r)) \quad (293)$$

where

$$b_{G,k,P_r,T_r} = -2(2.303)\,RT_r b_{\gamma,k,P_r,T_r} \quad (294)$$

and

$$b_{S,k,P_r,T_r} = \frac{b_{H,k,P_r,T_r} - b_{G,P_r,T_r}}{T_r} \quad (295)$$

Regression calculations.—Fits of eqs (288) through (290) to the data represented by the symbols in figures 132 through 136 generated most of the values of $\hat{c}_{1,k}$, $\hat{c}_{2,k}$, $\hat{a}_{1,k}$, $\hat{a}_{2,k}$, $\hat{a}_{3,k}$, $\hat{a}_{4,k}$ and $\hat{a}_{5,k}$ given in tables 19 through

TABLE 19

Regression coefficients for calculating extended term parameters for activity and osmotic coefficients and the relative apparent and partial molal properties of the kth aqueous electrolyte from eqs (288) through (295)

Solute	$\hat{c}_{1,k}$ [a]	$\hat{c}_{2,k}$ [a]	θ_k [b]	ω_k [c] x 10^{-5}	$\hat{a}_{5,k}$ [d]
HCl	0.4534	0.2980	246.02	1.4560	-0.162
LiCl	-17.0174	3.2366	246.49	1.9421	-0.303
NaCl	-12.1943	5.0130	228.58	1.7865	-0.206
KCl	-7.6178	2.4973	240.20	1.6487	-0.262
CsCl	-14.5437	5.3483	231.08	1.5534	-0.229
$MgCl_2$	-8.3421	1.8230	247.32	4.4492	-0.068
$CaCl_2$	-0.9301	0.7870	252.00	4.1485	-0.074
HBr	-3.8680	2.0470	206.75	1.3858	-0.162
LiBr	-32.5401	9.1978	209.09	1.8719	-0.303
CsI	-36.1803	17.0634	198.67	1.3908	-0.229
KF	-6.4343	1.6708	259.66	1.9797	-0.262
Na_2SO_4	-3.5235	5.5248	239.39	3.8468	-0.137

[a] cal kg mole^{-2} (°K)$^{-1}$. [b] °K. [c] cal mole^{-1}. [d] kg mole^{-1}.

21 and those of $b_{J,k}$, $b_{V,k}$, and $b_{\kappa,k}$ listed in tables 22 through 24, respectively, which (with the exception of $MgSO_4$) are represented by the curves in figures 132 through 136. Provision for $\bar{C}_P - \bar{C}_{sat}$ and the fact that figures 89 through 91 apply to 20 bars were omitted from the calculations, as were the slight pressure differences attending compositional variation and increasing temperature to 200°C along the liquid-vapor equilibrium curves for the electrolytes. It can be shown that these omissions introduce negligible uncertainties in the fit coefficients obtained from the regression calculations. The values of ω_k, θ_k, Q, N, and X employed in the calculations were taken from Helgeson and Kirkham (1974a, 1976). Owing to

TABLE 20

Regression coefficients for calculating extended term parameters for activity and osmotic coefficients and the relative apparent and partial molal properties of the kth aqueous electrolyte from eqs (288) through (295)

Solute	$\underline{\hat{a}}_{1,k}$[a] × 10^2	$\underline{\hat{a}}_{3,k}$[a] × 10^2	$\underline{\theta}_k$[b]	$\underline{\omega}_k$[c] × 10^{-5}	$\underline{\hat{a}}_{5,k}$[d]
HCl	-4.7746	0.8673	246.02	1.4560	-0.162
LiCl	-7.9087	1.1828	246.49	1.9421	-0.303
NaCl	-7.0809	2.1723	228.58	1.7865	-0.206
KCl	-3.6895	1.3218	240.20	1.6487	-0.262
CsCl	-2.0202	1.0613	231.08	1.5534	-0.229
NH_4Cl	-2.6961	0.6359	234.68	1.6351	-0.099
KBr	-8.4187	2.7757	219.27	1.5785	-0.262
KF	1.1050	0.3766	259.66	1.9797	-0.262
KI	-12.6597	4.5868	204.46	1.4861	-0.262
$NaHCO_3$	-3.2200	1.1594	226.95	1.6599	-0.206
KNO_3	-8.3133	3.4659	203.02	1.3222	-0.262
NaHS	-2.7498	0.9954	237.21	1.7716	-0.206
NH_4ClO_4	-2.2478	1.6117	71.37	1.1803	-0.099
$MgCl_2$	-3.2435	0.8303	247.32	4.4492	-0.068
$CaCl_2$	0.4665	0.4058	252.00	4.1485	-0.074
$SrCl_2$	-0.2140	0.4925	256.90	4.0482	-0.074
$BaCl_2$	2.1425	0.7341	245.52	3.8970	-0.065
Na_2SO_4	13.6043	1.2777	239.39	3.8468	-0.137
K_2SO_4	18.3867	1.2427	250.97	3.5711	-0.175

[a] cal kg mole^{-2} bar^{-1}. [b] °K. [c] cal mole^{-1}. [d] kg mole^{-1}.

insufficient data, the dashed curve for $MgSO_4$ in figure 132 merely connects the data points, which are not distributed over a wide enough temperature range to permit definitive calculation of $\hat{c}_{1,MgSO_4}$ and $\hat{c}_{2,MgSO_4}$ by regression.

It can be deduced from figures 132 through 136 that eqs (288) through (290) afford close representation of all the extended term parameters represented by the symbols. Note in figure 138 that the values of $\psi_k \hat{a}_{5,k}/\nu_{i,k}$ obtained by regression of $\nu b_J/2$ (figs. 132 and 133) with eq (290) are nearly identical to those for the same electrolytes retrieved from the fits of eq (288) to $\nu b_V/2$ (figs. 134 and 135). It can also be seen in figure 138 that $\psi_k \hat{a}_{5,k}/\nu_{i,k}$ is essentially the same for all electrolytes with a common cation. These observations, together with others summarized below, strongly support the theoretical model responsible for eqs (288) through (293).

It follows from the equations, data, and calculations summarized above that the extended term contributions to $\bar{V} - \bar{V}^\circ$, $\bar{\kappa} - \bar{\kappa}^\circ$, and $\bar{C}_P -$

TABLE 21

Regression coefficients for calculating extended term parameters for activity and osmotic coefficients and the relative apparent and partial molal properties of the kth aqueous electrolyte from eqs (288) through (295)

Solute	$\hat{a}^a_{2,k} \times 10^5$	$\hat{a}^a_{4,k} \times 10^5$	θ^f_k	$\omega^g_k \times 10^{-5}$	$\hat{a}^h_{5,k}$
HCl	2.06[d]	-0.334[c]	246.02	1.4560	-0.162
LiCl	3.61[d]	-0.529[c]	246.49	1.9421	-0.303
NaCl	4.3391[b]	-1.3217[b]	228.58	1.7865	-0.206
KCl	2.12[d]	-0.614[c]	240.20	1.6487	-0.262
$MgCl_2$	0.8232[b]	-0.4441[b]	247.32	4.4492	-0.068
$CaCl_2$	-1.46[e]	-0.050[c]	252.00	4.1485	-0.074
Na_2SO_4	-13.1620[b]	-0.5209[b]	239.39	3.8468	-0.137

[a] Cal kg mole^{-2}bar^{-2}. [b] Generated by regression of experimental values of b_K shown in figure 136 with equation (289)--see text. [c] Estimated from equation (296) and values of $\hat{a}_{3,k}$ taken from table 20. [d] Calculated from equation (289) using the values of $\hat{a}_{4,k}$, θ_k, ω_k, and $\hat{a}_{5,k}$ shown above together with values of b_K taken from table 12 and $N = -2.24 \times 10^{-10}$ bar^{-2} (Helgeson and Kirkham, 1974a). [e] Computed as described in footnote d assuming $b_{K,CaCl_2} = b_{K,MgCl_2} = 6.9 \times 10^{-4}$ cm^{3}kg mole^{-2}bar^{-1} at 25°C and 1 bar. [f] °K. [g] Cal mole^{-1}. [h] kg mole^{-1}

$\bar{C}^\circ_P$ as a function of temperature oppose those by $\bar{V}^\circ$, $\bar{\kappa}^\circ$, and $\bar{C}^\circ_P$. In contrast to $(\partial^2 b_V/\partial T^2)_P$, $(\partial^2 b_\kappa/\partial T^2)_P$, and $-(\partial^2 b_J/\partial T^2)_P$, which are positive, $(\partial^2 \bar{V}^\circ/\partial T^2)_P$, $(\partial^2 \bar{\kappa}^\circ/\partial T^2)_P$, and $(\partial^2 \bar{C}^\circ_P/\partial T^2)_P$ are negative. Hence b_V, b_κ, and $-b_J$ approach ∞ at the critical point of H_2O, where $\bar{V}^\circ$, $\bar{\kappa}^\circ$, and $\bar{C}^\circ_P$ approach $-\infty$. Similarly, the various Debye-Hückel and ion association contributions to $\bar{V} - \bar{V}^\circ$, $\bar{\kappa} - \bar{\kappa}^\circ$, and $\bar{C}_P - \bar{C}^\circ_P$ approach ∞ or $-\infty$ (depending on the contribution)at the critical point of H_2O. As a consequence, the densities and heat capacities of aqueous electrolyte solutions (and therefore the apparent molal and partial molal properties of the components of the solutions) at high temperatures and low pressures may exhibit dramatic and multiple inflections and extrema as a function of concentration and/or temperature and pressure.

Because all the regression calculations described above led to essentially the same values of $\psi_k \hat{a}_{5,k}/\nu_{i,k}$ for electrolytes with the same cation (fig. 138), a single optimized value of this parameter was adopted for each such group of electrolytes. These values (tables 19 and 20) were used together with values of $\hat{b}_k$ taken from table 4 to compute corresponding values of $\hat{a}_{6,k}$ from eq (287). The results of these calculations are summarized in table 25, which at least in principle can be used together with

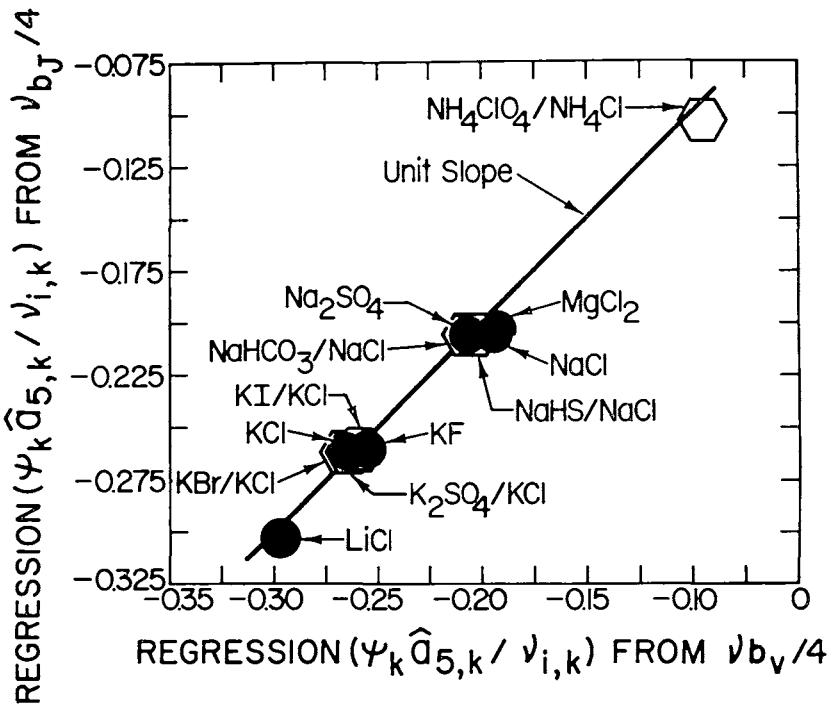

Fig. 138. Correlation of $\hat{a}_i$ values derived by regression of extended term parameters for the apparent molal heat capacities of aqueous electrolytes as a function of temperature in figures 132 and 133 with those generated by regression of the corresponding apparent molal volume parameters in figures 134 and 135 (see text).

eqs (149), (174), (286), and (287) to calculate values of $\hat{b}_k$, b_k, b_{il} and ϵ at high pressures and temperatures from the dielectric constant data for H_2O given by Helgeson and Kirkham (1974a) and calculated values of b_γ like those in table 26 (see below). Estimates of $\hat{b}_k$ computed from eq (287) using values of $\hat{a}_5$ and $\hat{a}_6$ taken from tables 20 and 25 were used to generate the solid linear curves for temperatures other than 25°C in figures 5, 6, 10, 14, and 131. It can be seen that these curves are in close agreement with the bulk of the experimental data shown in the figures for RbCl, NaCl, NaBr, $MgCl_2$, and H_2SO_4, but not with those for other than dilute solutions of $BaCl_2$ and HCl in figure 14. The cause of the discrepancies at higher concentrations in the latter two cases remains unclear.

As might be expected, large uncertainties attend calculation of values of $\hat{b}_k$, b_k, b_{il}, and ϵ at high pressures and temperatures from eqs (149), (174), (286), and (287) using calculated values of $\hat{a}_6$ and b_γ generated by regression of low-temperature data to obtain values of $\hat{a}_1$, $\hat{a}_2$, $\hat{a}_3$, $\hat{a}_4$, $\hat{a}_5$, $\hat{c}_1$, and $\hat{c}_2$. The uncertainties arise in part from the fact that small errors in $\hat{a}_5$ resulting from regression vagaries are magnified in high-temperature values of $\hat{b}_k$ computed from eq (287). As a consequence, calculated values of $\hat{b}_k$ for a series of electrolytes at a given high temperature may be inconsistent with the cross differentiation requirement represented by eq (148).

TABLE 22

Computed values of the extended term parameter[a] for calculating the relative apparent and partial molal heat capacities of aqueous electrolytes from eqs (224) and (229) at 1 bar for temperatures < 100°C and pressures corresponding to liquid-vapor equilibrium at temperatures ≥ 100°C

Solute	Temperature, °C								
	0	25	50	75	100	125	150	175	200
HCl	-5.3	-4.4[b]	-4.2	-4.4	-4.9	-5.6	-6.7	-8.3	-11.1
LiCl	-20.6	-7.2	-2.9	-1.3	-1.3	-2.4	-4.5	-8.2	-14.7
NaCl	-21.3	-12.8	-8.8	-7.0	-6.2	-6.4	-7.3	-9.3	-13.1
KCl	-16.4	-9.3	-6.7	-5.8	-5.8	-6.6	-8.2	-11.0	-15.7
CsCl	-22.9	-12.6	-8.0	-5.8	-4.8	-4.8	-5.6	-7.4	-11.0
$MgCl_2$	-8.9	-3.5	-1.8	-1.1	-1.1	-1.4	-2.1	-3.3	-5.5
$CaCl_2$	-7.7	-4.7	-3.9	-3.8	-4.1	-4.6	-5.5	-6.9	-9.2
HBr	-6.3	-4.9[b]	-4.2	-3.9	-4.1	-4.5	-5.4	-6.8	-9.3
LiBr	-11.0	-3.6	0.5	2.5	3.1	2.7	1.1	-2.1	-8.0
CsI	-28.8	-18.0	-11.5	-7.5	-5.1	-3.8	-3.4	-4.2	-6.7
KF	-31.5	-11.4	-7.6	-6.6	-6.8	-8.0	-10.0	-13.4	-19.2
Na_2SO_4	-30.1	-19.7	-15.6	-13.7	-13.2	-13.4	-14.4	-16.3	-20.0

[a] Cal kg mole^{-2} (°K)$^{-1}$. [b] Owing to derivation of these values by regression of $b_{\gamma,k}$ as a function of temperature, they differ slightly from those generated from $\rho^*_{J,k}$ as a function of $\bar{I}$ in table 10.

For example, it can be shown that such inconsistencies occur among calculated values of $\hat{b}_k$ for HCl, KCl, NaCl, LiCl, $MgCl_2$, and $CaCl_2$ at temperatures $\gtrsim$ 100°C. Errors in computed values of $\hat{b}_k$ and $b_{\gamma,k}$ at high pressures and temperatures are magnified in values of b_{il} generated from eq (174) to the extent of $\omega_k\psi_k/2(2.303)\nu_{i,k}\nu_{l,k}$ and $\nu_k\psi_k/2\nu_{i,k}\nu_{l,k}$, respectively. Similarly, uncertainties in computed values of $\hat{b}_k$ are magnified in calculated estimates of ϵ at high pressures and temperatures by $\epsilon^2\bar{I}$. It follows that computed values of $\hat{b}_k$, b_k, b_{il}, and ϵ at high pressures and temperatures from eqs (149), (174), (286), and (287) should be regarded as provisional approximations.

TABLE 23

Computed values of the extended term parameter[a] for calculating the relative apparent and partial molal volumes of aqueous electrolytes from eqs (222) and (227) at 1 bar for temperatures < 100°C and pressures corresponding to liquid-vapor equilibrium at temperatures ≥ 100°C

Solute	Temperature, °C								
	0	25	50	75	100	125	150	175	200
HCl	2.2	0.7	0.2	0.1	0.2	0.4	0.9	1.6	2.8
LiCl	3.1	1.0	0.5	0.6	1.0	1.7	2.9	4.8	7.7
NaCl	3.4	1.8[b]	1.2	1.0	1.1	1.5	2.2	3.3	5.0
KCl	4.0	2.4[b]	1.9	1.8	2.1	2.6	3.4	4.8	6.9
CsCl	2.8	2.0[b]	1.8	1.8	2.0	2.5	3.2	4.3	6.0
NH_4Cl	1.1	0.5[b]	0.3	0.3	0.4	0.5	0.9	1.4	2.1
$MgCl_2$	2.0	1.0[b]	0.7	0.6	0.7	1.0	1.4	2.0	3.0
$CaCl_2$	2.1	1.4	1.2	1.3	1.5	1.7	2.2	2.8	3.8
$SrCl_2$	2.7	1.4	1.2	1.2	1.3	1.6	2.0	2.6	3.6
$BaCl_2$	3.0	2.2	1.9	1.9	2.0	2.2	2.5	3.1	3.9
KBr	3.3	1.9[b]	1.3	1.1	1.3	1.7	2.4	3.7	5.6
KF	4.8	3.0[b]	2.8	3.0	3.5	4.2	5.3	7.0	9.6
KI	3.2	1.8[b]	1.1	0.8	0.8	1.1	1.8	2.9	4.7
KNO_3	2.9	1.9	1.4	1.3	1.4	1.7	2.3	3.3	4.9
K_2SO_4	10.3	8.4	7.9	7.9	8.2	8.7	9.6	10.9	12.9
Na_2SO_4	7.5	6.5	6.2	6.2	6.5	6.9	7.6	8.8	10.5
$NaHCO_3$	2.3	1.5	1.3	1.3	1.5	1.9	2.6	3.7	5.4
NaHS	2.8	1.8	1.5	1.5	1.7	2.2	2.9	4.1	5.9
NH_4ClO_4	0.2	0.2	0.3	0.3	0.5	0.6	0.9	1.3	1.8

[a] $cm^3 kg\ mole^{-2}$. [b] Owing to the 19 bar difference in pressure, these values differ slightly from those for 25°C and 1 bar in table 11.

TABLE 24

Computed values of the extended term parameter[a] for calculating the relative apparent and partial molal compressibilities of aqueous electrolytes from eqs (226) and (231) at 1 bar for temperatures < 100°C and pressures corresponding to liquid-vapor equilibrium at temperatures ≥ 100°C

Solute	Temperature, °C								
	0	25	50	75	100	125	150	175	200
HCl	6.8	1.6	0.0	-0.2	0.9	3.5	8.4	17.7	35.6
LiCl	10.9	3.2	0.9	1.6	4.9	11.8	24.4	47.8	92.6
NaCl	17.8	9.0[b]	3.3	2.4	3.0	5.3	10.2	19.6	38.0
KCl	14.9	8.4	6.1	6.1	8.3	13.1	22.2	39.2	72.0
$MgCl_2$	12.0	6.9[b]	5.3	5.1	6.0	8.2	12.4	20.3	35.6
$CaCl_2$	7.1	6.9	7.0	7.8	9.2	11.8	16.3	24.6	40.2
Na_2SO_4	50.5	47.4	46.3	46.8	48.8	52.9	60.5	74.4	101.2

[a] $(cm^3 kg\ mole^{-2} bar^{-1}) \times 10^4$. [b] As a consequence of differences in the experimental data reported by Allam (ms) and Millero and others (1974), these values differ slightly from those in table 12.

TABLE 25

Summary of electrostatic parameters for calculating the dielectric constant and short-range interaction parameters for aqueous electrolytes at high temperatures and pressures — see text

Solute	$\hat{a}^a_{\underline{c},k} \times 10^3$	Solute	$\hat{a}^a_{\underline{c},k} \times 10^3$	Solute	$\hat{a}^a_{\underline{c},k} \times 10^3$
HCl	4.1	$SrCl_2$	2.8	KF	6.0
LiCl	6.5	$BaCl_2$	2.6	KNO_3	5.1
NaCl	5.1	HBr	4.0	K_2SO_4	3.9
KCl	5.6	LiBr	6.5	Na_2SO_4	3.5
CsCl	5.0	KBr	5.5	NaHS	5.0
NH_4Cl	3.5	KI	5.4	$NaHCO_3$	4.9
$MgCl_2$	2.9	CsI	4.8	NH_4ClO_4	3.5
$CaCl_2$	2.8				

[a] $kg\ mole^{-1}$.

TABLE 26

Predicted values of the extended term parameter $(b_\gamma)^a$ for computing osmotic and mean ionic activity coefficients of aqueous electrolytes at 1 bar for temperatures < 100°C and pressures corresponding to liquid-vapor equilibrium at temperatures ≥ 100°C — see text

Solute	Temperature, °C						
	0	25	50	75	100	125	150
HCl	13.7	12.5	11.1	9.7	8.2	6.7	5.2
LiCl	14.1	14.0	13.4	12.7	12.0	11.3	10.6
NaCl	4.2	6.4	7.4	7.6	7.5	7.0	6.4
KCl	0.4	2.4	3.4	3.8	3.9	3.6	3.2
$MgCl_2$	11.1	10.6	9.9	9.2	8.5	7.8	7.2
$CaCl_2$	7.7	7.7	7.3	6.8	6.1	5.3	4.4
Solute	175	200	225	250	275	300	325
HCl	3.6	1.8	0.0	-2.1	-4.5	-7.4	-11.5
LiCl	9.9	9.0	7.7	6.0	3.5	-0.5	-7.2
NaCl	5.6	4.6	3.3	1.7	-0.5	-3.6	-8.4
KCl	2.5	1.5	-0.2	-1.6	-4.0	-7.5	-13.1
$MgCl_2$	6.6	5.9	5.2	4.3	3.1	1.5	-1.1
$CaCl_2$	3.4	2.3	1.1	-0.3	-2.1	-4.3	-7.5

[a] $(Kg\ mole^{-1}) \times 10^2$.

Regression of the experimental values of $b_{\gamma,k}$ represented by the symbols for HBr, HCl, and $CaCl_2$ in figure 139 with eqs (293) through (295) after setting $\hat{a}_{1,k}$, $\hat{a}_{2,k}$, $\hat{a}_{3,k}$, and $\hat{a}_{4,k}$ to zero generated the curves shown for these electrolytes in figure 139 and the values of $\hat{a}_{5,k}$ for $CaCl_2$ and $\hat{c}_{1,k}$ and $\hat{c}_{2,k}$ for HCl, HBr, and $CaCl_2$ in table 19. Because only a small pressure variation (< 15 bars) is associated with increasing temperature from 0° to 200°C along the liquid-vapor equilibrium curves for the electrolytes, this procedure yields reliable values of $\hat{a}_{5,k}$, $\hat{c}_{1,k}$, and $\hat{c}_{2,k}$. The values of $\nu b_{S,k}/2$ employed in the calculations were generated from eq (295) using data given in tables 5 and 9. It can be seen in figure 139 that the regression calculations yield values of $\nu b_{J,k}/2$ that are in close agreement with independent calorimetric data at low temperatures.

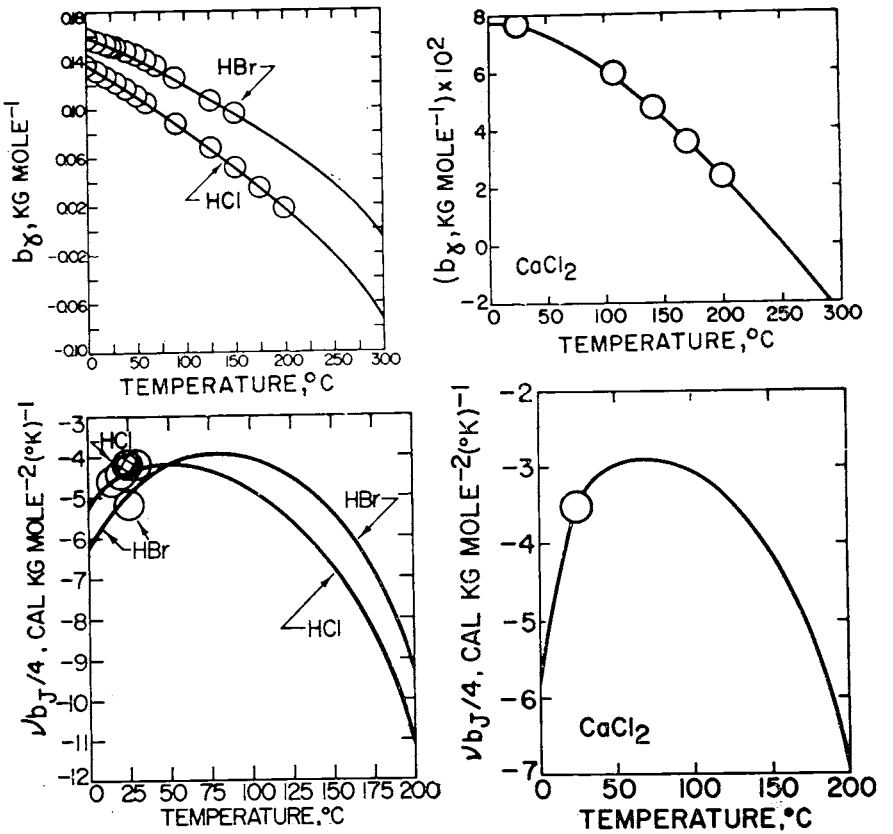

Figure 139. Calculated extended term parameters for activity coefficients and apparent molal heat capacities of electrolytes as a function of temperature (T) at 1 bar for T < 100°C and pressures corresponding to liquid-vapor equilibrium at T ≥ 100°C (see text). The symbols in the upper two diagrams correspond to the slopes of the solid linear curves for HBr, HCl, and $CaCl_2$ in figures 19 and 26 (eq 178) and twice the slopes of the linear curves for $CaCl_2$ in figure 46 (eq 195). The symbols in the lower two diagrams correspond to the negative equivalents of the slopes of the linear curves for HBr, HCl, and $CaCl_2$ in figures 65, 69, 70, and 79 (eq 238). The curves in all four of the diagrams were derived by regression of the b_γ values with eqs (293) through (295) (see text).

Correlation and estimation of compressibility parameters.—It can be seen in figure 140 that *the regression values of* $\hat{a}_{4,k}$ *and* $\hat{a}_{3,k}$ *derived above correlate with each other in the same manner as* $a_{4,k}$ *and* $a_{3,k}$. This observation, together with others adduced above strongly supports the general applicability of the equation of state derived by Helgeson and Kirkham (1976). Because the equation of the curve in figure 140 is identical to that given by Helgeson and Kirkham (1976) for $a_{4,k}$ as a function of $a_{3,k}$, it follows that

$$\hat{a}_{4,k} = 2 \times 10^{-6} - 6.16 \times 10^{-4}\,\hat{a}_{3,k} \tag{296}$$

Eq (296) was used to generate the estimated compressibility parameters shown in table 21. Note that in the absence of experimental compressibility data, values of $\hat{a}_{2,k}$ and $\hat{a}_{4,k}$ can be estimated from $\bar{V}^{\circ}_{k}$ and $\hat{a}_{3,k}$ by simultaneous evaluation of eqs (246), (247), (289), and (296).

Discussion.—In contrast to the close agreement of the symbols and curves in figures 132 and 133, it can be deduced from figure 141 that the values of b_J for NaCl in table 22 are consistent with calorimetric data reported by Puchkov, Styazhkin, and Federov (1976) only at temperatures from 25° to 125°C. In addition, the intercepts of the curves in figure 141 differ significantly from the values of $\bar{C}^{\circ}_{P,NaCl}$ given in table 16 and plotted as symbols on the ordinates of the diagrams in figure 141. The latter discrepancies increase markedly at higher temperatures, and none of the data reported by Puchkov, Styazhkin, and Federov (1976) for 150° to 350°C is compatible with values of $b_{J,NaCl}$ computed from equation (291). In contrast, it can be deduced from figure 142 that predicted values

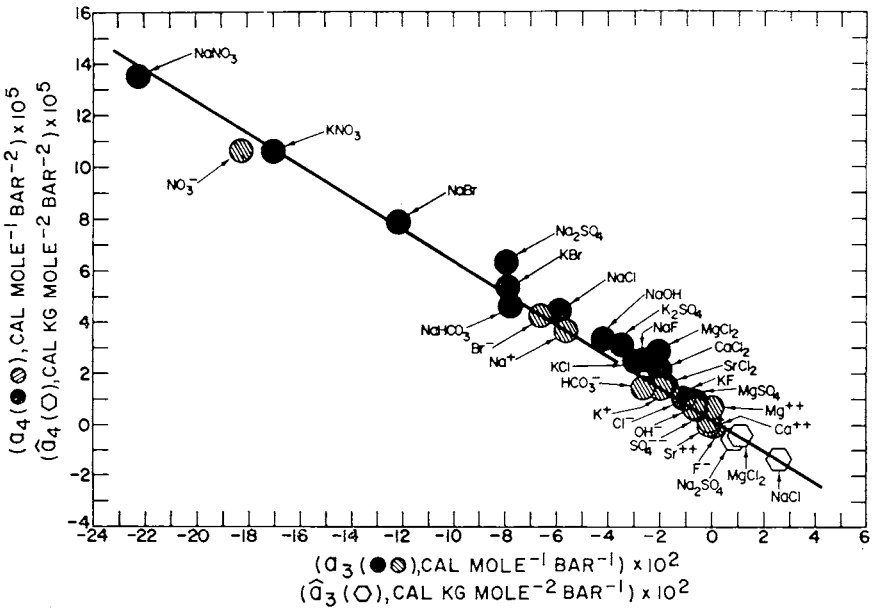

Fig. 140. Correlation of a_4 with a_3 (Helgeson and Kirkham, 1976) and $\hat{a}_4$ with $\hat{a}_3$ (tables 20 and 21) (see text).

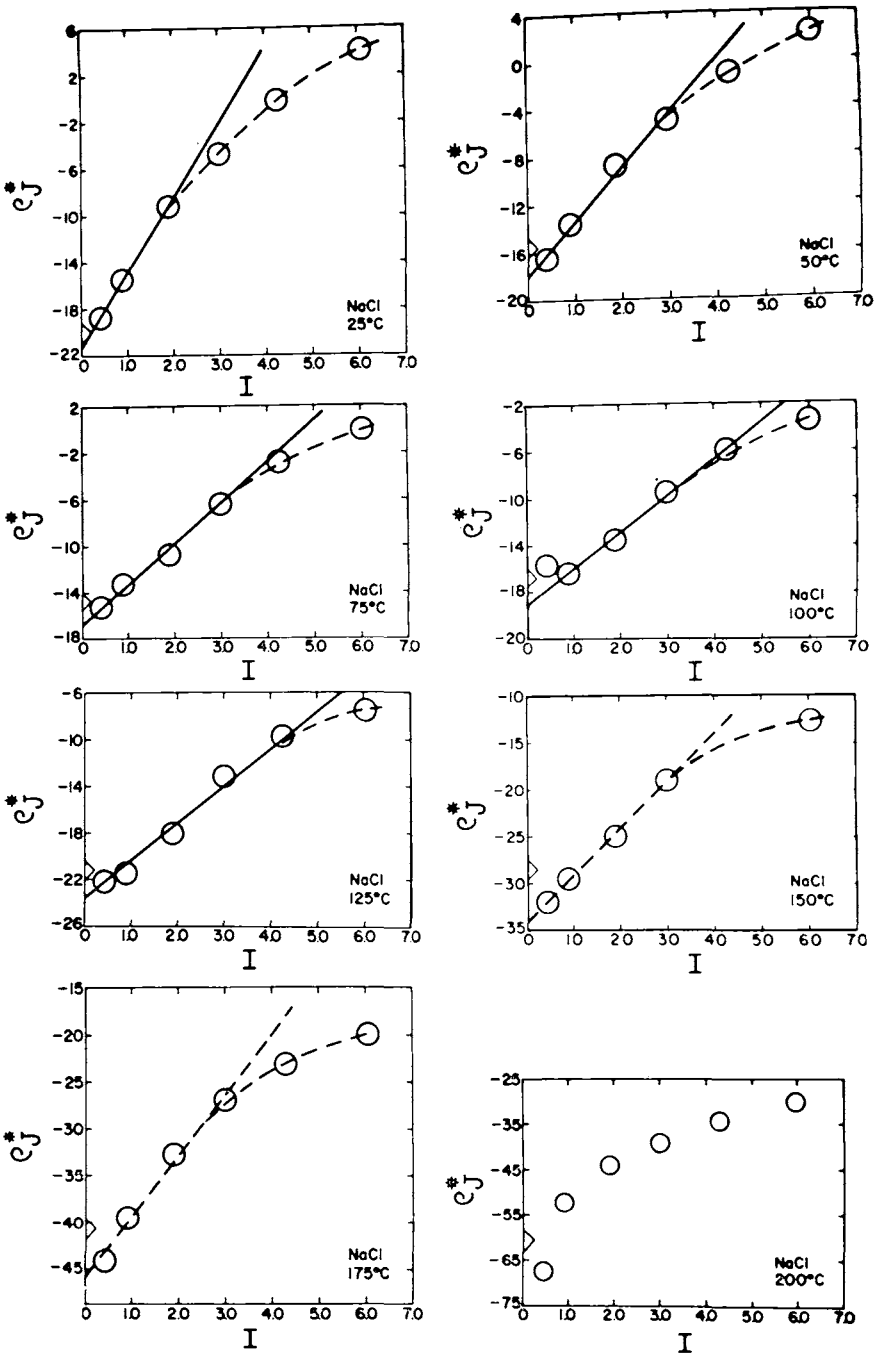

Fig. 141. ρ^*_J (eq 238) for NaCl computed (assuming I = I) from experimental heat capacity data reported by Puchkov, Styazhkin, and Fedorov (1976) for 1 bar at temperatures < 100°C and pressures corresponding to liquid-vapor equilibrium for temperatures ≥ 100°C (circles). The slopes of the solid curves correspond to −1/2 the values of b_J for NaCl at the corresponding temperatures in table 22, which were generated independently from eq (291) using parameters given in tables 19 through 21. The dashed curves merely connect data points, but the symbols on the ordinates of the diagrams correspond to values of $\bar{C}^\circ_P$ taken from table 16 (see text).

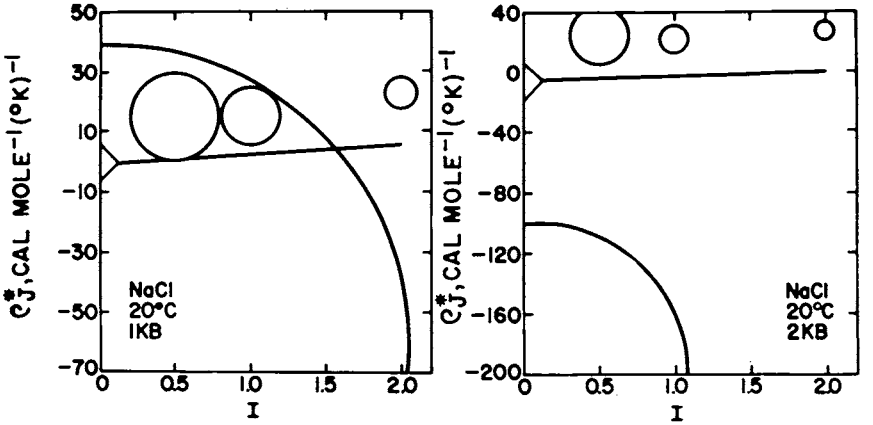

Fig. 142. ρ^*_J (eq 238) for NaCl computed (assuming I = J) from experimental heat capacity data reported by Liphard, Jost, and Schneider (1977) at 20°C and 1 and 2 kb (circles). The symbols on the ordinates and the slopes of the linear curves correspond to values of $\bar{C}^\circ_P$ and $\nu b_J/4$ generated independently from eqs (273) and (291) (see text).

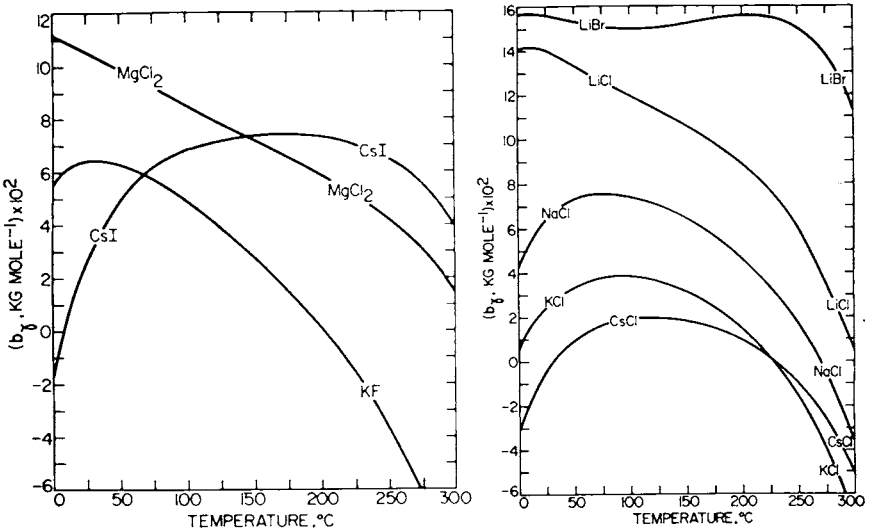

Fig. 143. Predicted values of the extended term parameter for activity coefficients of aqueous electrolytes as a function of temperature (T) at 1 bar for T < 100°C and pressures corresponding to liquid-vapor equilibrium for H_2O at T $\geqslant$ 100°C. The curves were generated from eqs (293) through (295) with $\hat{a}_2 = \hat{a}_4 = 0$ (see text).

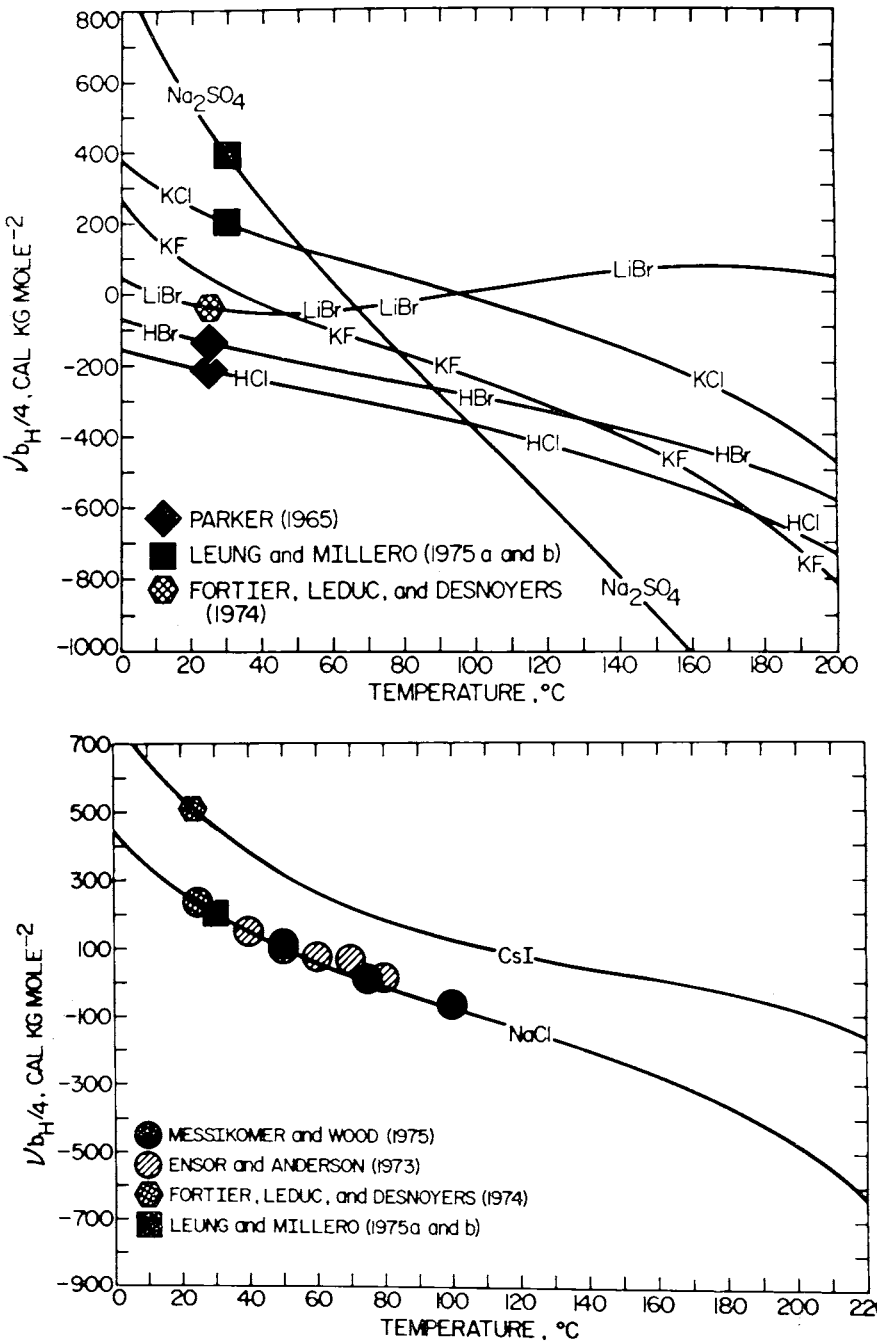

Fig. 144. Extended term parameter for the apparent molal enthalpy of aqueous electrolytes (eq 228) as a function of temperature (T) at 1 bar for $T < 100°C$ and pressures corresponding to liquid-vapor equilibrium for H_2O at $T \geqslant 100°C$. The symbols shown above and those in figure 145 correspond to the negative equivalent of the slopes of the linear curves for the corresponding electrolytes in figures 50, 51, 52, 55, 59, and 60, but the curves were generated independently from eq (292).

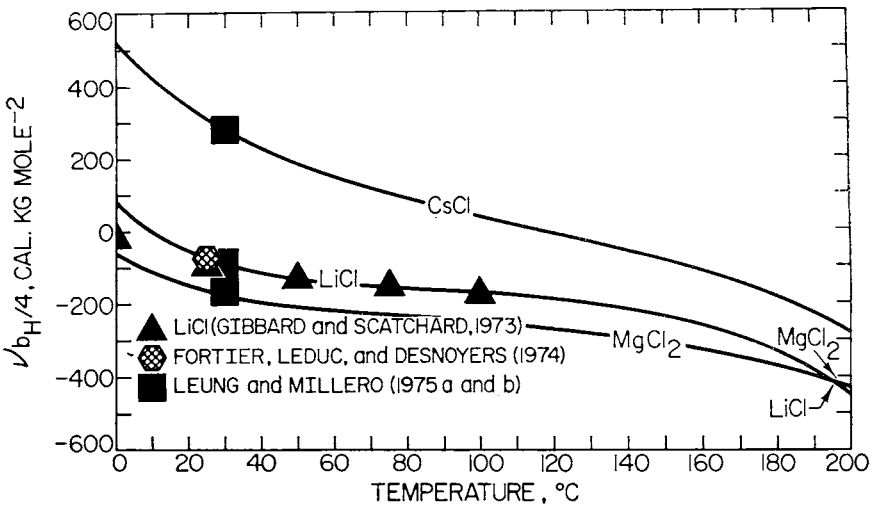

Fig. 145. Extended term parameter for the apparent molal enthalpy of aqueous electrolytes (eq 228) as a function of temperature (T) at 1 bar for $T < 100°C$ and pressures corresponding to liquid-vapor equilibrium for H_2O at $T \geqslant 100°C$ (see caption of fig. 144).

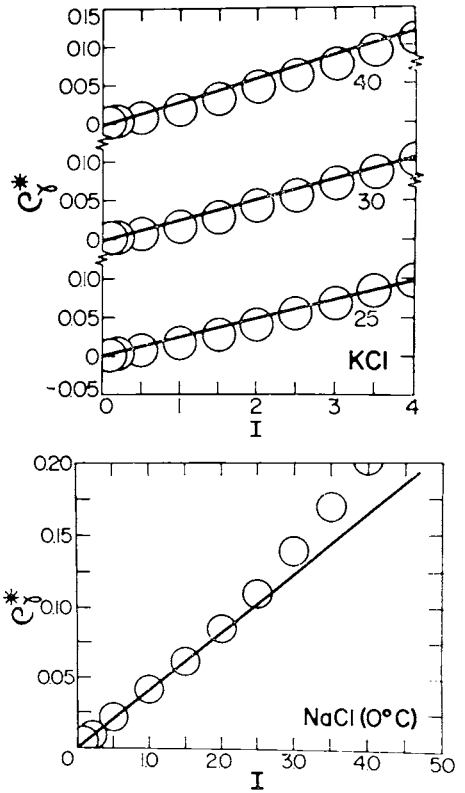

Fig. 146. Experimental (symbols) and independently predicted (linear curves) values of ρ^*_γ (eqs 177 and 178) for $I = \bar{I}$ in NaCl and KCl solutions as a function of stoichiometric ionic strength at various temperatures (indicated in °C) and 1 bar *(see* text). The symbols represent experimental data reported by Scatchard and Prentiss (1933) and Harned and Owen (1958).

of $b_{J,NaCl}$ at 25°C and 1 and 2 kb (which were used to generate the slopes of the curves shown in the figure) are consistent with the relative distribution of the bulk of the data reported by Liphard, Jost, and Schneider (1977). However, the intercepts of the curves in figure 142, which correspond to values of $\bar{C}^\circ_{P,NaCl}$ computed from eq (273), are not. The large experimental uncertainty (represented by the size of the circles in fig. 142) renders the significance of the latter observation somewhat dubious. Similarly, the fact that the experimental data shown in figure 141 are inconsistent with those responsible for the symbols for NaCl in figure 103 casts

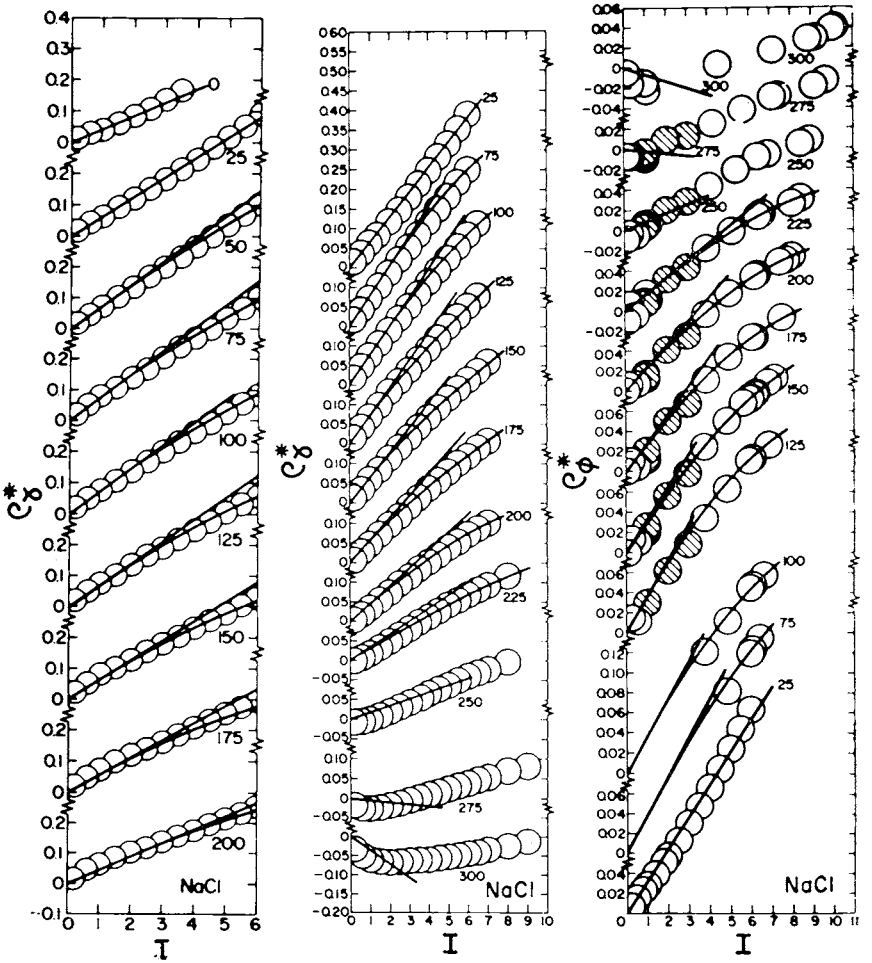

Fig. 147. Experimental (symbols) and independpently predicted (linear curves) values of ρ^*_γ and ρ^*_ϕ (eqs 177, 178, 194, and 195) for I = $\bar{I}$ in NaCl solutions as a function of stoichiometric ionic strength at various temperatures (indicated in °C) and 1 bar for temperatures < 100°C and pressures corresponding to liquid-vapor equilibrium for temperatures ≥ 100°C (see text). The symbols and nonlinear curves represent experimental data reported by Gibbard and others (1974) and Liu and Lindsay (1972).

doubt on the reliability of the higher temperature data reported by Puchkov, Styazhkin, and Federov (1976).

Predicted values of b_γ generated from eq (293) for pressures and temperatures corresponding to liquid-vapor equilibrium are listed in table 26 and plotted as curves in figure 143. It can be seen in this figure that all the curves except that for $MgCl_2$ exhibit extrema, and that in every case b_γ becomes negative at high temperatures. The latter observation is consistent with decreasing ion solvation with increasing temperature above ~ 100°C. Although at first glance it might seem unreasonable for a curve representing b_γ as a function of temperature to exhibit a double inflection like that for LiBr in figure 143, such a configuration is inevitable if $\nu b_J/2$ maximizes as a function of temperature at values > 0. It can be seen in figures 132 and 133 that this is indeed the case for LiBr and nearly so for LiCl and $MgCl_2$, all three of which exhibit seemingly anomalous changes in b_γ with increasing temperature. This behavior is consistent with the curves for these electrolytes in figures 144 and 145, which represent predicted values of $\nu b_H/4$ as a function of temperature at pressures corresponding to liquid-vapor equilibrium. The fact that the values of b_γ and b_H shown in figures 143 through 145 for CsI, CsCl, LiBr, LiCl, KF, HBr, and Na_2SO_4 were generated with $\hat{a}_2 = \hat{a}_4 = 0$ introduces negligible uncertainties in the calculated values at pressures corresponding to liquid-vapor equilibrium at temperatures $\leqslant$ 300°C. The symbols in figures 144 and 145 correspond to values of $\nu b_H/4$ computed from data given in table 9 and the slopes of the linear curves shown in figures 50 through 60. It can be seen in figures 144 and 145 that the curves generated from the equations and parameters derived above for LiCl and NaCl at temperatures $\geqslant$ 25°C

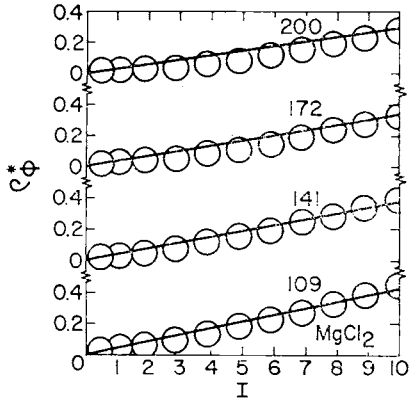

Fig. 148. Experimental (symbols) and independently predicted (curves) values of ρ^*_ϕ (eqs 194 and 195) for $I = \bar{I}$ in $MgCl_2$ solutions as a function of stoichiometric ionic strength at various temperatures (indicated in °C) and pressures corresponding to liquid-vapor equilibrium (see text). The symbols represent experimental data reported by Holmes, Baes, and Mesmer (1978).

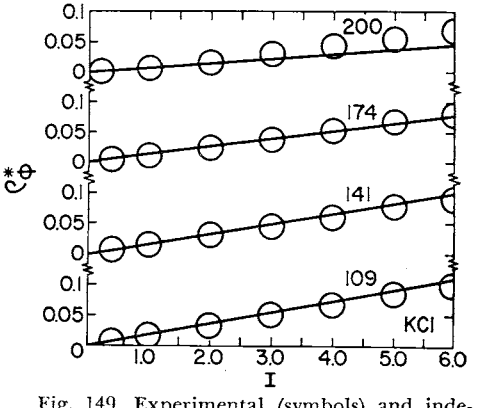

Fig. 149. Experimental (symbols) and independently predicted (curves) values of ρ^*_ϕ (eqs 194 and 195) for $I = \bar{I}$ in KCl solutions as a function of stoichiometric ionic strength at various temperatures (indicated in °C) and pressures corresponding to liquid-vapor equilibrium (see text). The symbols represent experimental data reported by Holmes, Baes, and Mesmer (1978).

are in close agreement with the experimental data represented by the symbols. Similar agreement is apparent between the predicted (curves) and experimental (symbols) values of $\rho^*_{\gamma,NaCl}$ at 0°C and $I \leqslant 3.0$ and $\rho^*_{\gamma,KCl}$ at 30° and 40°C in figure 146. Other predictions of ρ^*_γ and ρ^*_ϕ, which were generated from calculated values of $b_{\gamma,NaCl}$, $b_{\gamma,MgCl_2}$, and $b_{\gamma,KCl}$ in table 26, are represented by the curves in figures 147 through 149. It can be deduced from these figures that the experimental data represented by the symbols are in close agreement with the independently predicted values of b_γ at all temperatures $\lesssim 250$°C. The effect of ion association on ρ^*_γ is manifested in figure 147 by increasing departures from linearity of the distribution of data points toward lower values of ρ^*_γ with increasing stoichiometric ionic strength. Note, however, that at temperatures $>$ 250°C, the trend of Liu and Lindsay's (1972) data departs systematically in the opposite direction from the linear curves. The cause of these departures at high temperatures is not clear, but they cannot be attributed to specific interaction among the species in solution. Although the discrepancies could result from increasing solvation of the NaCl molecule with increasing temperature above ~ 250°C, it seems highly unlikely that this is the case. A more reasonable explanation is probably lurking in the

TABLE 27

Predicted values of the extended term parameter $(b_\gamma)^a$ for computing the osmotic and mean ionic activity coefficients of NaCl at high pressures and temperatures — see text. Values with high uncertainty are shown in parentheses

T,[b]	Pressure, Kb					
	0.5	1	2	3	4	5
0	(5.6)	(6.6)	(7.4)	(6.5)	(4.0)	(0.1)
25	7.1	7.7	(8.3)	(8.3)	(7.7)	(6.7)
50	7.8	8.7	(8.8)	(9.2)	(9.5)	(9.6)
75	8.0	8.3	(8.9)	(9.6)	(10.3)	(11.1)
100	7.8	8.2	8.9	9.7	10.7	(11.8)
125	7.5	7.9	8.7	9.6	10.8	(12.2)
150	7.0	7.5	8.5	9.4	10.8	(12.4)
175	6.4	7.0	8.1	9.3	10.8	(12.4)
200	5.7	6.5	7.8	9.2	10.7	(12.4)
225	4.8	5.9	7.4	9.0	10.6	(12.4)
250	3.8	5.2	7.0	8.8	10.5	(12.4)
275	2.6	4.4	6.6	8.6	10.4	(12.3)
300	1.0	3.5	6.2	8.3	10.3	(12.3)
325	-1.2	2.5	5.8	8.1	10.2	(12.2)
350	-4.1	1.1	5.2	7.8	10.0	(12.1)
375	-8.4	-0.6	4.6	7.5	9.8	(11.9)
400	-15.2	-2.8	3.8	7.1	9.6	(11.8)
425		-5.7	2.9	6.6	9.3	(11.5)
450		-9.3	1.8	6.0	8.9	(11.3)
475		-13.7	0.5	5.4	8.5	(11.0)
500		-19.2	-1.0	4.8	8.2	(10.8)

[a](Kg mole^{-1}) x 10^2. [b]Temperature, °C.

TABLE 28

Predicted values of the extended term parameter $(b_\gamma)^a$ for computing the osmotic and mean ionic activity coefficients of $MgCl_2$ at high pressures and temperatures — see text. Values with high uncertainty are shown in parentheses

T,[b]	Pressure, Kb					
	0.5	1	2	3	4	5
0	(11.9)	(12.5)	(12.7)	(11.8)	(9.8)	(6.8)
25	11.0	11.2	(11.2)	(10.7)	(9.8)	(8.4)
50	10.1	10.3	(10.3)	(10.0)	(9.4)	(8.6)
75	9.4	9.5	(9.5)	(9.4)	(9.0)	(8.4)
100	8.7	8.9	9.0	8.9	8.6	(8.2)
125	8.1	8.3	8.5	8.5	8.3	(8.1)
150	7.6	7.8	8.1	8.2	8.1	(8.0)
175	7.1	7.4	7.7	7.9	8.0	(7.9)
200	6.6	7.0	7.5	7.8	7.9	(7.9)
225	6.0	6.6	7.2	7.6	7.8	(7.9)
250	5.5	6.7	7.0	7.5	7.8	(7.9)
275	4.8	5.8	6.9	7.5	7.8	(8.0)
300	4.0	5.4	6.7	7.5	7.9	(8.1)
325	2.9	4.9	6.5	7.4	7.9	(8.2)
350	1.4	4.3	6.3	7.4	8.0	(8.3)
375	-0.1	3.4	6.1	7.3	8.0	(8.4)
400	-4.4	2.3	5.8	7.2	8.1	(8.5)
425		.9	5.4	7.1	8.1	(8.6)
450		-.9	5.0	7.0	8.0	(8.6)
475		-3.2	4.4	6.8	8.0	(8.7)
500		-6.1	3.8	6.6	8.0	(8.7)

[a](Kg mole^{-1}) x 10^2. [b]Temperature, °C.

questionable validity of a number of the assumptions made by Liu and Lindsay in calculating osmotic coefficients from their high-temperature vapor pressure data.

Calculated values of b_γ for NaCl and $MgCl_2$ at temperatures and pressures to 600°C and 5 kb are given in tables 27 and 28 and plotted together with corresponding predicitions of b_H, b_J, and b_V for these electrolytes in figures 150 and 151. Note in figure 150 that $b_{\gamma,NaCl}$ as a function of temperature at constant pressure exhibits extrema at all pressures $\leqslant 5$ kb, which is not true of $b_{\gamma,MgCl_2}$ in figure 151. Nevertheless, the isothermal pressure dependence of b_γ is nearly identical for the two electrolytes, which is a consequence of the similarity of $b_{V,NaCl}$ and $b_{V,MgCl_2}$ as isobaric functions of temperature. As expected (see above) the configuration of the latter two functions in figures 150 and 151 approximates an inverted image of $\bar{V}^\circ_{NaCl}$ and $\bar{V}^\circ_{MgCl_2}$ as a function of temperature at constant pressure (Helgeson and Kirkham, 1976). Similarly, the isobaric dependence of b_J and b_H in figures 150 and 151 is similar to that of $\bar{C}^\circ_P$ and $\Delta\bar{H}^\circ$ for NaCl and $MgCl_2$. It can be seen in figures 150 and 151 that b_γ changes only slightly with increasing temperature from ~ 100° to 500° C at pressures $\geqslant 3$ kb. However, at high temperatures and low pressures, b_γ is a highly sensitive function of both variables.

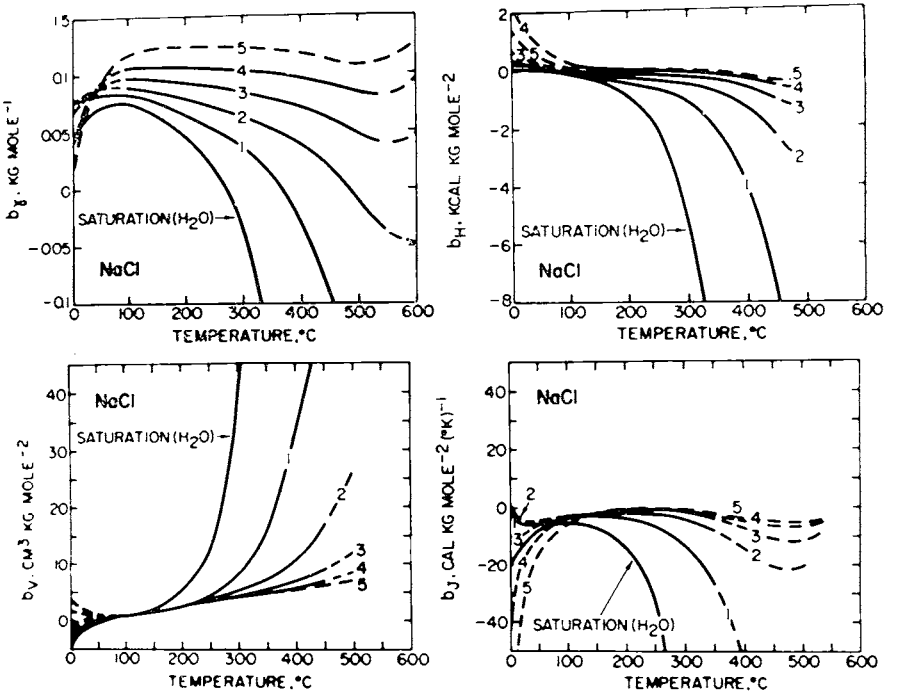

Fig. 150. Predicted (eqs 288 and 291 through 295) values of b_V, b_J, b_H, and b_γ for NaCl as a function of temperature at high pressures (indicated in kb). Saturation (H_2O) refers to the liquid-vapor equilibrium curve for H_2O. The dashed curves are more uncertain than their solid counterparts.

Activity and Osmotic Coefficients

Calculated osmotic and mean ionic activity coefficients generated from the equations and parameters summarized above are represented by the curves plotted against or specified for a given value of $\bar{I}$ in figures 152 through 159 at pressures corresponding to liquid-vapor equilibrium. The symbols in these figures represent experimental osmotic and stoichiometric mean activity coefficients, which are plotted against, or refer to a given value of I.

It can be seen in figures 152 through 159 that the curves generated in the present study are in close agreement with the bulk of the experimental data represented by the symbols. The departures at high temperatures in figure 157 of the predicted curves as a function of $\bar{I}$ from the experimental osmotic coefficients for $MgCl_2$ solutions as a function of I are consistent with increasing ion association with increasing temperature. In contrast, the discrepancies between the curve and symbols for NaCl at 300°C and high ionic strengths in figures 154 and 157 cannot be attributed to ion association (see above). It should perhaps be emphasized in this regard that eq (173), which was used to generate the curves shown in figures 152 through 159, is not applicable to the dissociated fraction of

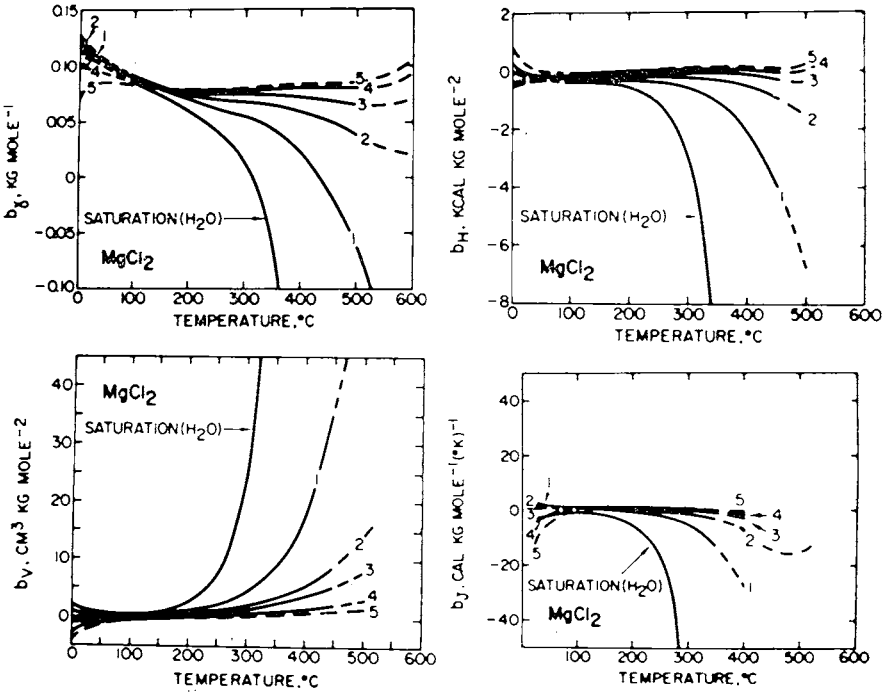

Fig. 151. Predicted (eqs 288 and 291 through 295) values of b_V, b_J, b_H, and b_γ for $MgCl_2$ as a function of temperature at high pressures (indicated in kb). Saturation (H_2O) refers to the liquid-vapor equilibrium curve for H_2O. The dashed curves are more uncertain than their solid counterparts.

partially associated 2:1 or 1:2 electrolytes. Because $m_i \neq \nu_{i,k} m_k$, $m_l \neq \nu_{l,k} m_k$, or $m_i \neq m_l \neq \bar{I}/\psi_k$ in these cases, eq (168) must be used together with dissociation constants to calculate $\bar{\gamma}_\pm$ as a function of $\bar{I}$. In contrast, eq (173) can be used to compute $\bar{\gamma}_\pm$ for the dissociated fraction of 1:1 or 2:2 electrolytes in which significant ion association is limited to a single ion pair. Under these circumstances, dissociation constants are needed only to calculate I as a function of $\bar{I}$.

It can be seen in figures 152 through 159 that increasing temperature decreases $\bar{\gamma}_\pm$ to an increasing degree with increasing ionic strength. Note that the "synclinal" configurations of the curves in figures 152 through 154, 157, and 158 tend to dampen (and disappear if b_γ becomes negative)

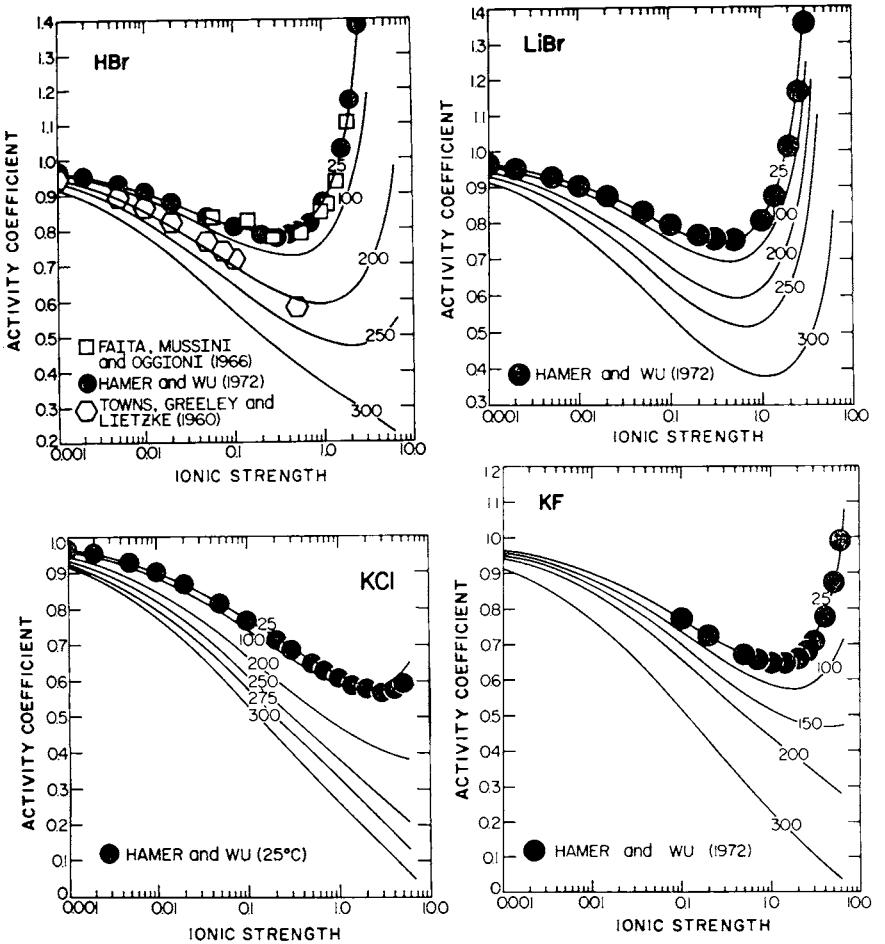

Fig. 152. Experimental stoichiometric mean activity coefficients (symbols) and independently predicted mean ionic activity coefficients (curves) of electrolytes as a function of "true" (curves) and stoichiometric (symbols) ionic strength at various temperatures (indicated in °C) and 1 bar for temperatures < 100°C and pressures corresponding to liquid-vapor equilibrium for temperatures ≥ 100°C (see text).

with increasing temperature. At high temperatures and low pressures, $\bar{\gamma}_{\pm}$ for all electrolytes becomes a monotonic function of $\bar{I}$.

Calculated values of $b_{\gamma,NaCl}$ and $b_{\gamma,MgCl_2}$ at pressures and temperatures to 5 kb and 500°C are given in tables 27 and 28. The parameters shown in table 27 were used to generate the curves shown in figures 160 through 162. Note in figure 160 that the monotonic character of the high-temperature curves in figure 154 disappears with increasing pressure above ~ 2 kb. At higher pressures, all the curves are "synclinal." The pressure dependence of $\bar{\gamma}_{\pm,NaCl}$ at constant $\bar{I}$ and temperature is depicted in figure 161, where it is apparent that $\bar{\gamma}_{\pm,NaCl}$ at high ionic strengths increases sharply with increasing pressure at all temperatures. However, at low temperatures in dilute solutions, $\bar{\gamma}_{\pm,NaCl}$ is hardly affected by increasing pressure.

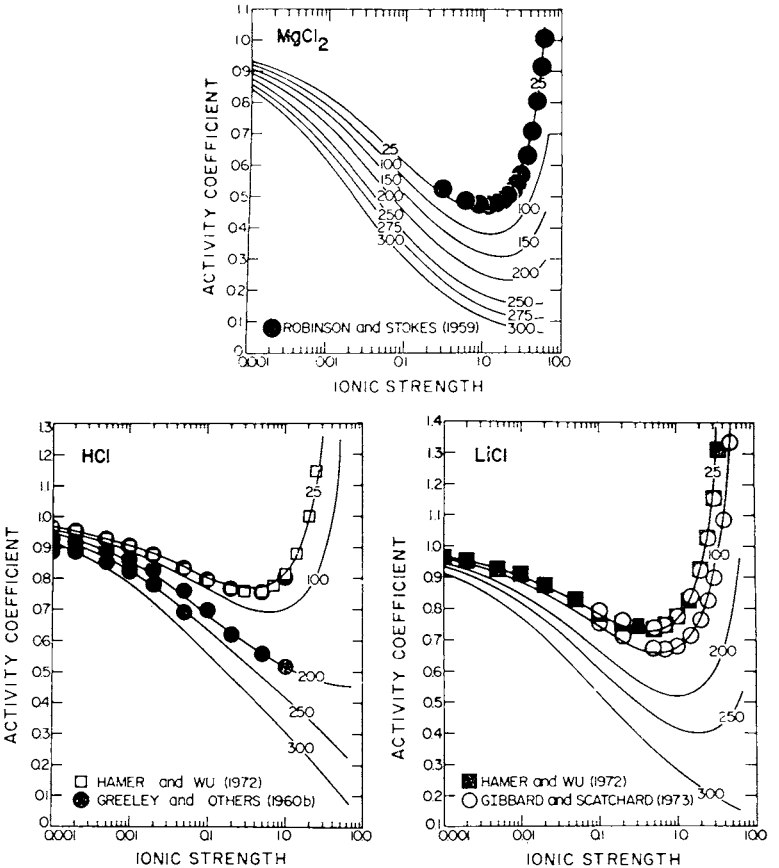

Fig. 153. Experimental stoichiometric mean activity coefficients (symbols) and independently predicted mean ionic activity coefficients (curves) of electrolytes as a function of "true" (curves) and stoichiometric (symbols) ionic strength at various temperatures (indicated in °C) and 1 bar for temperatures < 100°C and pressures corresponding to liquid-vapor equilibrium for temperatures ≥ 100°C (see text).

It can be seen in figure 162 that the calculations suggest that $\bar{\gamma}_{\pm,\mathrm{NaCl}}$ minimizes as a function of temperature at high ionic strengths and constant pressure above ~ 2 kb. However, the fact that the minima occur at the boundary of the dielectric constant fit region (Helgeson and Kirkham, 1974a) renders the significance of this observation somewhat moot. Note in figure 162 that $\bar{\gamma}_{\pm,\mathrm{NaCl}}$ is < 0.1 above ~ 400°C at 1 kb and high ionic strengths. The curves shown in figures 160 through 162 represent the dissociated fraction of the solute, which decreases with increasing temperature, but increases with increasing pressure at constant temperature. At high temperatures and low pressures the "true" ionic strength of NaCl solutions is highly sensitive to changes in either variable. It is in this "supercritical" region that departures from ideality become large and significant in geochemical processes. *It is also in this region where the exothermic heats of solution of buried evaporite deposits may exceed a million cal mole*$^{-1}$.

Geochemical approximations.—Owing to the inaccessibility and complex nature of geochemical processes at high pressures and temperatures,

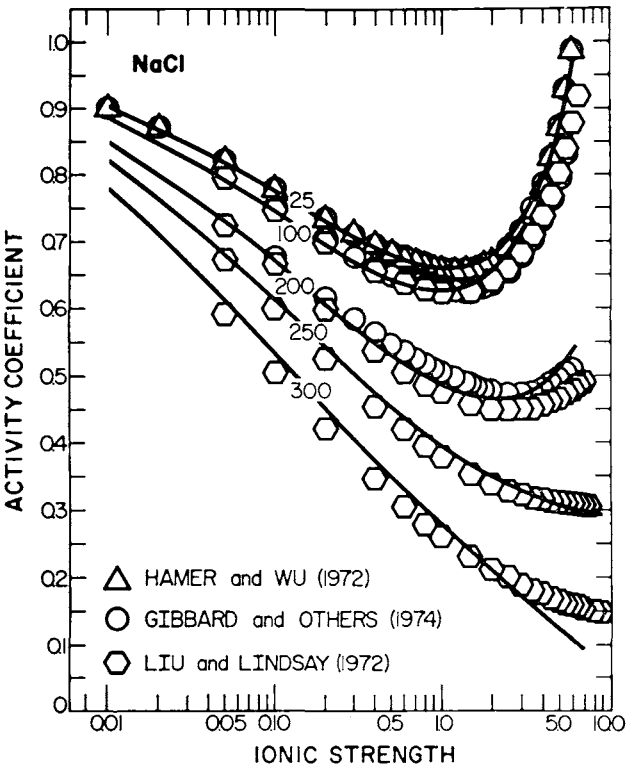

Fig. 154. Experimental stoichiometric mean activity coefficients (symbols) and independently predicted mean ionic activity coefficients (curves) of NaCl as a function of "true" (curves) and stoichiometric (symbols) ionic strength at various temperatures (indicated in °C) and 1 bar for temperatures < 100°C and pressures corresponding to liquid-vapor equilibrium for temperatures ≥ 100°C (see text).

prediction of the thermodynamic behavior of aqueous species involved in the processes necessarily requires simplifying approximations to provide for compositional variation in the aqueous phase. Approximations of this kind can be made without introducing undue uncertainties in calculated activity coefficients by taking account of fluid inclusion data and analyses of the compositions of interstitial fluids in geothermal reservoirs. These data suggest that in many cases the thermodynamic properties of natural hydrothermal solutions are similar to those of NaCl solutions. Consequently, despite the relatively large uncertainties involved (see above), calculated values of $\hat{b}_k$ and b_{il} for NaCl ($\hat{b}_{NaCl}$ and $b_{Na^+Cl^-}$, respectively) at high pressures and temperatures probably afford a reasonable basis for generating estimates of activity coefficients of other aqueous species in geochemical processes. Calculated values of these parameters are shown in tables 29 and 30 and plotted as curves in figure 163. It can be seen in this figure that increasing temperature is accompanied at all pressures by a dramatic decrease in $\hat{b}_{NaCl}$, which becomes negative at $\sim 170°C < T < 240°C$ at $P \lesssim 5$ kb. In contrast, $\hat{b}_{NaCl}$ increases with increasing pressure at constant temperature.

The configuration of the curves shown in figure 163A is consistent with decreasing ion solvation with increasing temperature and/or decreasing pressure. The fact that $\hat{b}_{NaCl}$ is negative at high temperatures is manifested in figure 164A by the negative slopes of the curves for temperatures $\gtrsim 200°C$. The curves in figure 164A indicate that addition of NaCl to

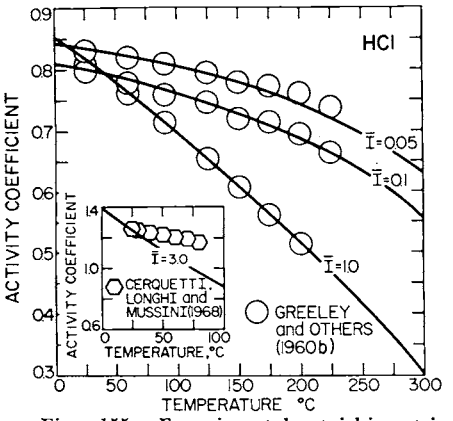

Fig. 155. Experimental stoichiometric mean activity coefficients (symbols) and independently predicted mean ionic activity coefficients (curves) of HCl as a function of temperature at constant "true" (curves) and corresponding stoichiometric (symbols) ionic strengths at 1 bar for temperatures < 100°C and pressures corresponding to liquid-vapor equilibrium at temperatures ≥ 100°C (see text).

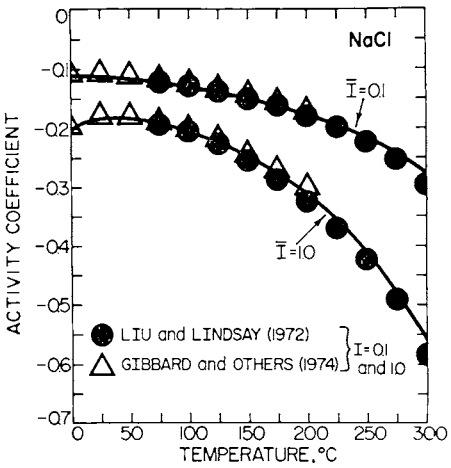

Fig. 156. Experimental stoichiometric mean activity coefficients (symbols) and independently predicted mean ionic activity coefficients (curves) of NaCl as a function of temperature at constant "true" (curves) and corresponding stoichiometric (symbols) ionic strengths at 1 bar for temperatures < 100°C and pressures corresponding to liquid-vapor equilibrium at temperatures ≥ 100°C (see text).

H_2O at high temperatures increases the dielectric constant of the solution, which is the opposite effect to that observed at low temperatures. The configurations of the curves in figures 163A and 164A can be attributed to disruption of the local solvent structure by NaCl only at temperatures $< 170°$ to 240°C, depending on the pressure. At higher temperatures, addition of NaCl apparently stabilizes the local solvent structure and enhances transitory alignment of the H_2O dipoles. As a consequence, the dielectric constant of NaCl solutions varies only slightly as a function of pressure and concentration in the vicinity of 200°C. Note in figure 165 that increasing temperature from 25° to 500°C is accompanied by a decrease in the dielectric constant of a $3m$ NaCl solution of only $\sim$ 30 units, compared to $\sim$ 70 units for H_2O. Note also in figure 165 that addition of

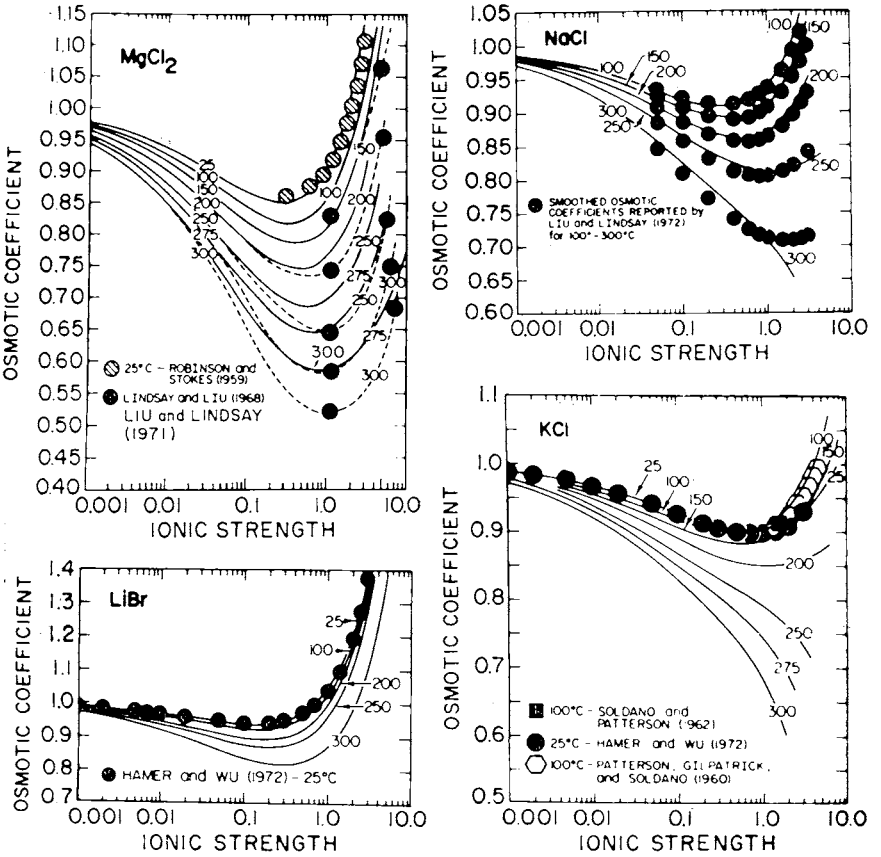

Fig. 157. Experimental (symbols) and independently predicted (solid curves) osmotic coefficients of aqueous electrolytes as a function of "true" (curves) and stoichiometric (symbols) ionic strength at various temperatures (indicated in °C) and 1 bar for temperatures < 100°C and pressures corresponding to liquid-vapor equilibrium for temperatures $\geqslant$ 100°C (see text). The solid curves were generated from equations given in the text (assuming I = I), but the dashed curves merely connect experimental data points.

NaCl to H_2O reduces substantially the pressure dependence of the dielectric constant of the solution.

It can be seen in figure 163B that the short-range interaction parameter for NaCl ($b_{Na^+Cl^-}$) increases dramatically and becomes positive with increasing temperature at all pressures $\leqslant$ 5 kb. Note also that only a slight increase in $b_{Na^+Cl^-}$ accompanies increasing pressure at temperatures above 60°C. At lower temperatures, $b_{Na^+Cl^-}$ decreases slightly with increasing pressure. The positive values of $b_{Na^+Cl^-}$ at high temperatures in figure 163B can be attributed to temporary capture of intervening solvent dipoles during collision of ionic species (as in case *a* of figure 16), which apparently dominates short-range interaction at temperatures $\gtrsim$ 90° to 150°C, depending on the pressure. At lower temperatures, where the ions are highly solvated (and therefore "shielded"), short-range interaction is apparently too weak to cause capture of intervening solvent dipoles. Nevertheless, the collisions result in negative contributions to the relative partial molal Gibbs free energy of NaCl at low temperatures. In contrast, contributions

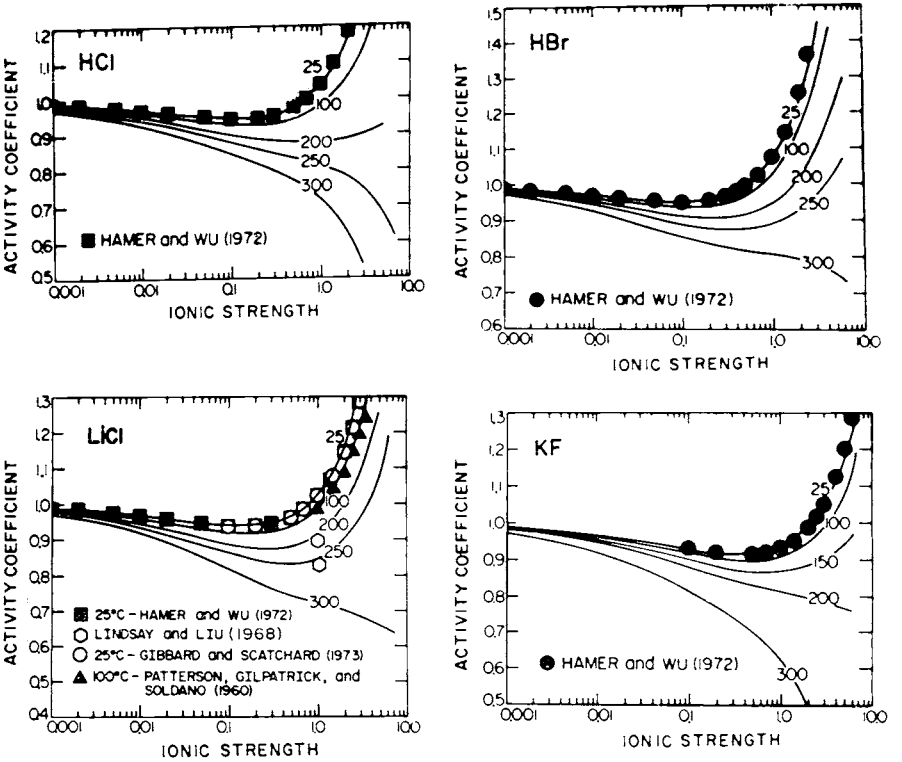

Fig. 158. Experimental (symbols) and independently predicted (solid curves) osmotic coefficients of aqueous electrolytes as a function of "true" (curves) and stoichiometric (symbols) ionic strength at various temperatures (indicated in °C) and 1 bar for temperatures <100°C and pressures corresponding to liquid-vapor equilibrium for temperatures $\geqslant$ 100°C (see text). The curves were generated from equations given in the text assuming I = $\bar{I}$.

by ion solvation to the relative partial molal Gibbs free energy of NaCl are negative only at high temperatures. The effects of short-range interaction and ion solvation on $\bar{\gamma}_{\pm,\mathrm{NaCl}}$ are thus reversed at high and low temperatures. Nevertheless, in both cases the concentration dependence of ion solvation dominates the behavior of b_γ as a function of temperature.

As noted above, calculation of values of b_{il} at high temperatures and pressures from parameters generated by regression of low-temperature data is accompanied by large uncertainties. Accordingly, it seems preferable for most purposes to estimate "average" relative values of these parameters in electrolyte solutions involved in geochemical processes by taking account of the correlation of b_{il} with cation charge in figure 166. The open symbols shown in this figure represent the values of b_{il} for Li^+Cl^-, Na^+Cl^-, K^+Cl^-, Rb^+Cl^-, Cs^+Cl^-, $NH_4^+Cl^-$, Ag^+Cl^-, Au^+Cl^-, Cu^+Cl^-, $Mg^{++}Cl^-$, $Ca^{++}Cl^-$, $Sr^{++}Cl^-$, $Ba^{++}Cl^-$, $Pb^{++}Cl^-$, $Zn^{++}Cl^-$, $Cu^{++}Cl^-$, $Cd^{++}Cl^-$, $Hg^{++}Cl^-$, $Fe^{++}Cl^-$, $Mn^{++}Cl^-$, and $Al^{+++}Cl^-$ at 25°C and 1 bar in table 7. The hatched symbols in figure 166 represent highly uncertain values of b_{il} for Li^+Cl^-, Na^+Cl^-, K^+Cl^-, $Mg^{++}Cl^-$, and $Ca^{++}Cl^-$ at 200°C and 15 bars computed from eqs (149), (174), and (287) using values of $\hat{a}_5$, $\hat{a}_6$, and b_γ taken from tables 21, 25, and 26. It can be deduced from figure 166 that the isothermal distribution of

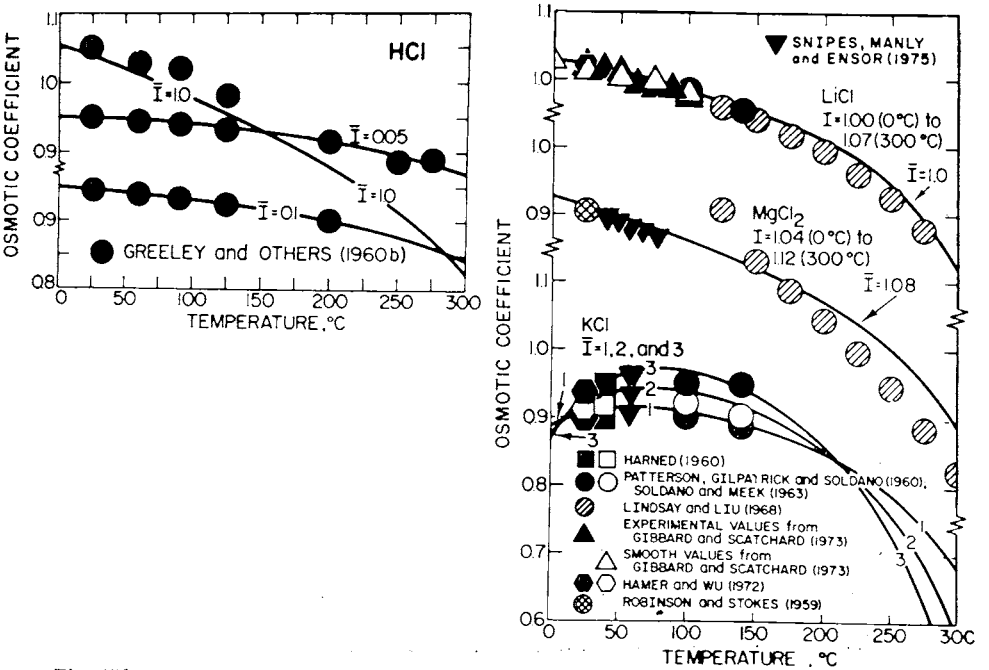

Fig. 159. Experimental (symbols) and independently predicted (curves) osmotic coefficients of aqueous electrolytes as a function of temperature at constant "true" (curves) and stoichiometric (symbols) ionic strength at 1 bar for temperature < 100°C and pressures corresponding to liquid-vapor equilibrium for temperatures ≥ 100°C (see text). The curves were generated assuming I = Ī.

the symbols in the figure is consistent with linear correlation of the mean $b_{il} \pm \sim 0.05$ for cations of the same charge with the charge of the cation. Note also that the slopes of the two curves in figure 166 are the same. The mean of the b_{il} values for monovalent cations at 25°C in figure 166 is −0.099, which is nearly identical to the value of $b_{Na^+Cl^-}$ in table 7 (−0.096).

Because the predominant ligand in most natural hydrothermal solutions is Cl^-, the observations summarized above suggest that values of b_{il} for aqueous species in these solutions can be estimated from

$$b_{il} = b_{Na^+Cl^-} - 0.19(Z_i - 1) \tag{297}$$

Similarly, because the values of $b_{H^+Cl^-}$ and $b_{H^+NO_3^-}$ at 25°C in table 7 are close to zero, which is also true of calculated values of $b_{H^+Cl^-}$ at higher temperatures, b_{il} for short-range interaction of H^+ (or more explicitly, H_3O^+) with anions in hydrothermal solutions can be regarded as zero. Note also in table 7 that $b_{Li^+NO_3^-}$, $b_{Na^+OH^-}$, and $b_{K^+OH^-}$ fall within or just outside the range of values for monovalent cations at 25°C in figure 7. Although the same observation cannot be made for all the fluorides, bromides, and iodides in table 7, these ligands are commonly present in

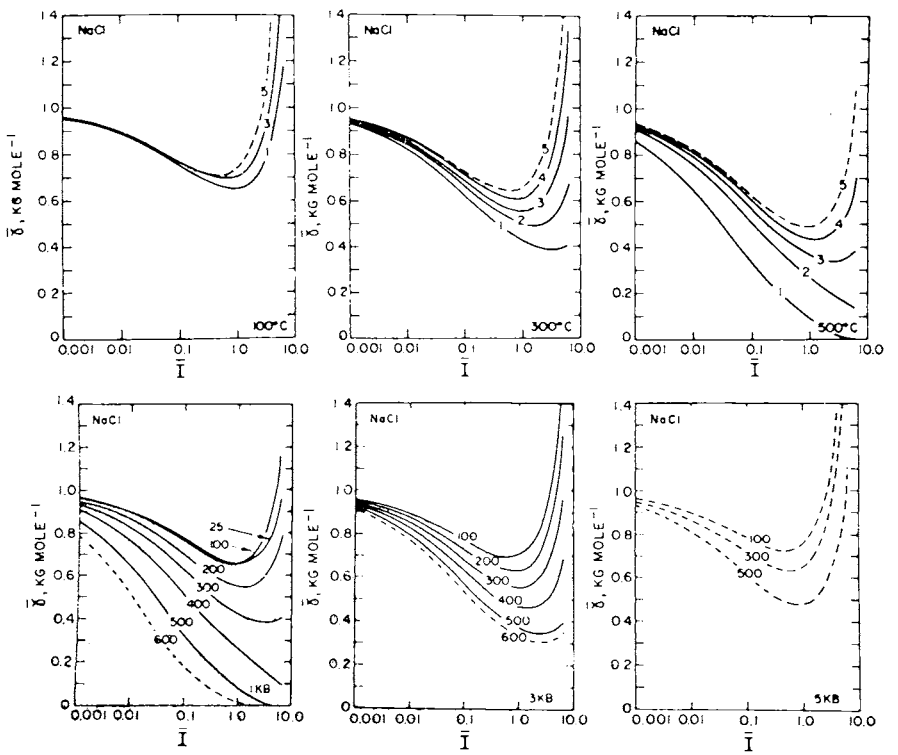

Fig. 160. Predicted values of the mean ionic activity coefficient ($\bar{\gamma}_\pm$) of NaCl at high pressures (labeled in kb) and temperatures (labeled in °C) as a function of "true" ionic strength (see text). The dashed curves are more uncertain than their solid counterparts.

TABLE 29

Predicted values of the solvation parameter for NaCl ($\hat{b}_{NaCl}$)[a] at high pressures and temperatures — see text. Sat refers to liquid-vapor equilibrium, and the parentheses indicate high uncertainty.

T[b]	Pressure, Kb					
	Sat	1	2	3	4	5
25	2.47	(2.58)	(2.66)	(2.72)	(2.77)	(2.82)
50	2.15	(2.28)	(2.37)	(2.45)	(2.51)	(2.56)
75	1.79	(1.95)	(2.06)	(2.15)	(2.22)	(2.28)
100	1.39	1.58	1.72	1.83	1.91	(1.99)
125	0.93	1.18	1.35	1.48	1.58	(1.67)
150	0.41	0.73	0.95	1.11	1.23	(1.33)
175	-0.18	0.25	0.51	0.72	0.86	(0.98)
200	-0.85	-0.28	0.04	0.29	0.47	(0.60)
225	-1.64	-0.86	-0.46	-0.15	0.05	(0.21)
250	-2.57	-1.50	-1.00	-0.63	-0.38	(-0.20)
275	-3.71	-2.20	-1.57	-1.13	-0.84	(-0.63)
300	-5.21	-2.99	-2.19	-1.67	-1.33	(-1.09)
325	-7.32	-3.88	-2.85	-2.24	-1.85	(-1.58)
350		-4.91	-3.58	-2.86	-2.40	(-2.10)
375		-6.11	-4.38	-3.52	-2.99	(-2.65)
400		-7.56	-5.26	-4.24	-3.63	(-3.25)
425		-9.31	-6.24	-5.03	-4.32	(-3.89)
450		-11.43	-7.34	-5.87	-5.06	(-4.57)
475		-14.01	-8.56	-6.78	-5.84	(-5.28)
500		-17.12	-9.88	-7.73	-6.63	(-6.00)

[a](Kg mole^{-1}) x 10^3. [b]Temperature, °C.

TABLE 30

Predicted values of the short-range interaction parameter for NaCl ($b_{Na^+Cl^-}$)[a] at high pressures and temperatures — see text. Sat refers to liquid-vapor equilibrium, and the parentheses indicate high uncertainty

T[b]	Pressure, Kb					
	Sat	1	2	3	4	5
25	-9.77	-9.19	-9.12	-9.51	-10.44	(-11.76)
50	-5.59	(-5.07)	(-5.52)	(-5.60)	(-5.66)	(-5.87)
75	-2.43	(-2.63)	(-2.65)	(-2.46)	(-2.15)	(-1.68)
100	0.23	-0.07	-0.10	0.13	0.71	(1.39)
125	2.44	1.71	1.85	2.14	3.05	(4.21)
150	4.51	4.13	4.12	4.28	5.13	(6.26)
175	6.38	5.91	5.88	6.16	7.05	(8.13)
200	8.11	7.48	7.66	8.18	9.05	(10.30)
225	9.73	9.27	9.30	9.59	10.40	(11.58)
250	11.29	10.80	10.73	11.15	11.92	(13.15)
275	12.71	12.24	12.19	12.62	13.39	(14.54)
300	14.15	13.68	13.66	13.99	14.83	(16.01)
325	15.49	15.16	15.10	15.41	16.23	(17.36)
350		16.48	16.42	16.76	17.52	(18.63)
375		17.90	17.79	18.10	18.81	(19.88)
400		19.12	19.11	19.40	20.13	(21.23)
425		20.33	20.35	20.66	21.38	(22.38)
450		21.55	21.61	21.85	22.56	(23.64)
475		22.86	22.84	23.09	23.74	(24.78)
500		24.03	23.95	24.32	24.94	(25.95)

[a](Kg mole^{-1}) x 10^2. [b]Temperature, °C.

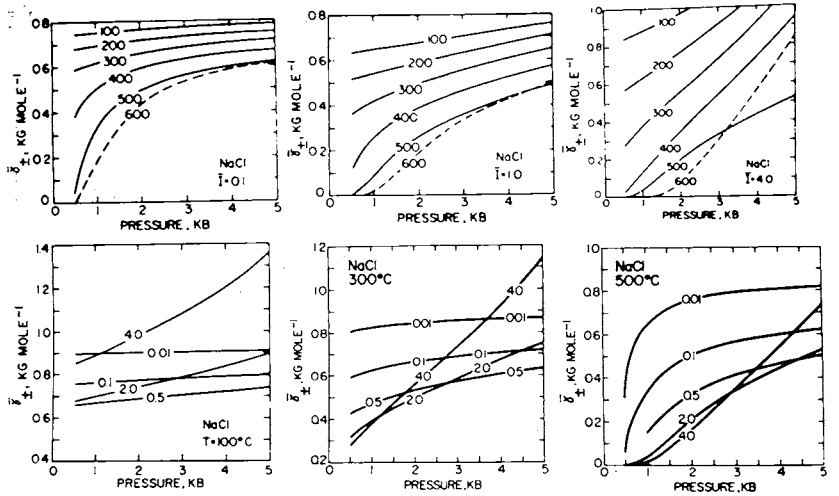

Fig. 161. Predicted values of the mean ionic activity coefficient ($\bar{\gamma}_\pm$) of NaCl at high temperatures (labeled in °C) and "true" ionic strengths of 0.01, 0.1, 0.5, 2, and 4 as a function of pressure (see text). The dashed curves are more uncertain than their solid counterparts.

relatively minor concentrations in natural electrolyte solutions, which is also true of OH^-, NO_3^-, HSO_4^-, SO_4^{--}, HCO_3^-, and CO_3^{--}. It seems likely that b_{il} representing short-range interaction of a monovalent cation with a divalent anion is comparable in magnitude to that representing corresponding interaction of a divalent cation with a monovalent anion. It thus appears that eq (297) can be used in a first approximation to estimate "average" values of b_{il} for short-range interaction of all the cations and anions in electrolyte solutions involved in geochemical processes. In addition, if the curves shown in figure 163A are representative of those for most such solutions (which seems likely), b_k in eqs (165) and (166) for natural hydrothermal solutions can be replaced in a first approximation by b_{NaCl}. Taking account of eqs (165), (166), and (297), it follows from these observations (and the high probability that the bulk of the positively charged species in natural electrolyte solutions are monovalent) that we can write for the jth positively or negatively charged aqueous species,

$$\log \bar{\gamma}_j \approx \frac{-A_\gamma Z_j^2 \bar{I}^{1/2}}{\Lambda} + \Gamma_\gamma + (\omega_j{}^{abs} b_{NaCl} + b_{Na^+Cl^-} - 0.19\,(|Z_j| - 1))\,\bar{I}, \quad (298)$$

which should afford close approximation of individual ion activity coefficients in concentrated as well as dilute electrolyte solutions involved in geochemical processes at high temperatures and pressures. Values of Γ_γ can be approximated from $m^* \approx \bar{I}$. Owing to a dearth of definitive data for neutral species, there is little alternative to assuming for the general case,

$$\bar{\gamma}_n = 1 \quad (299)$$

in these solutions at high pressures and temperatures. Figure 119 notwithstanding, ample evidence suggests that the latter approximation introduces negligible error in geochemical calculations (Orville, 1963; Helgeson, 1969; Marshall, 1980b).

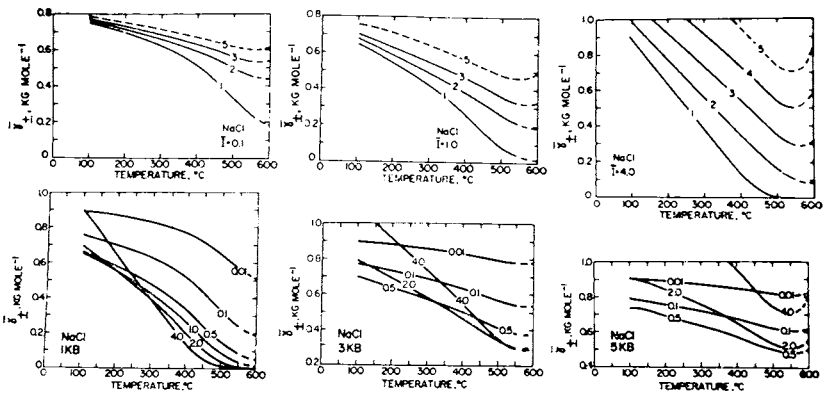

Fig. 162. Predicted values of the mean ionic activity coefficient ($\bar{\gamma}_\pm$) of NaCl at high pressures (labeled in kb) and "true" ionic strengths of 0.01, 0.1, 0.5, 2, and 4 as a function of temperature (see text). The dashed curves are more uncertain than their solid counterparts.

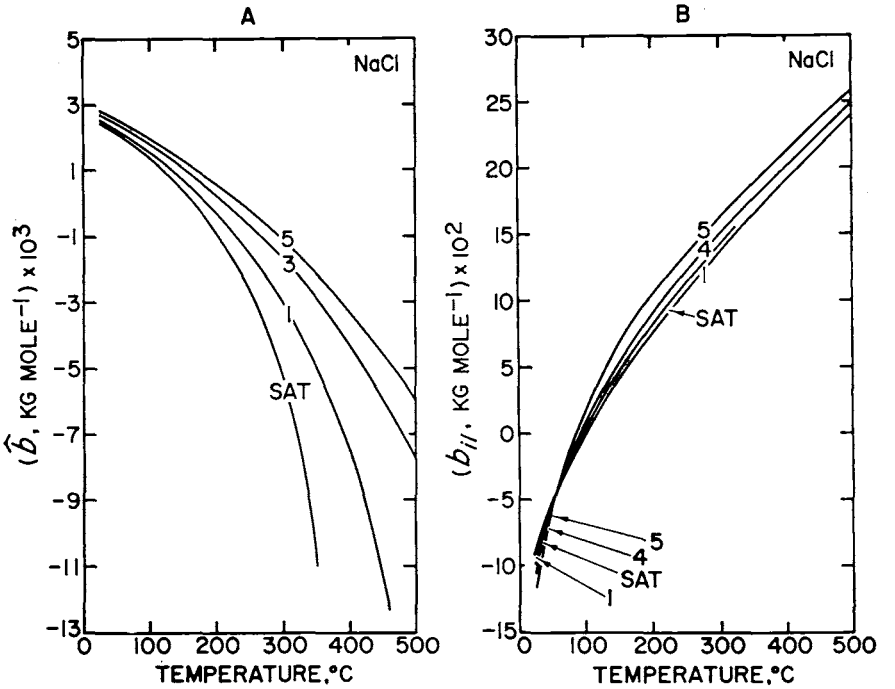

Fig. 163. Predicted (tables 29 and 30) solvation ($\hat{b}$) and short-range interaction parameters (b_{il}) for NaCl as a function of temperature at high pressures (labeled in kb) (see text). SAT refers to liquid-vapor equilibrium.

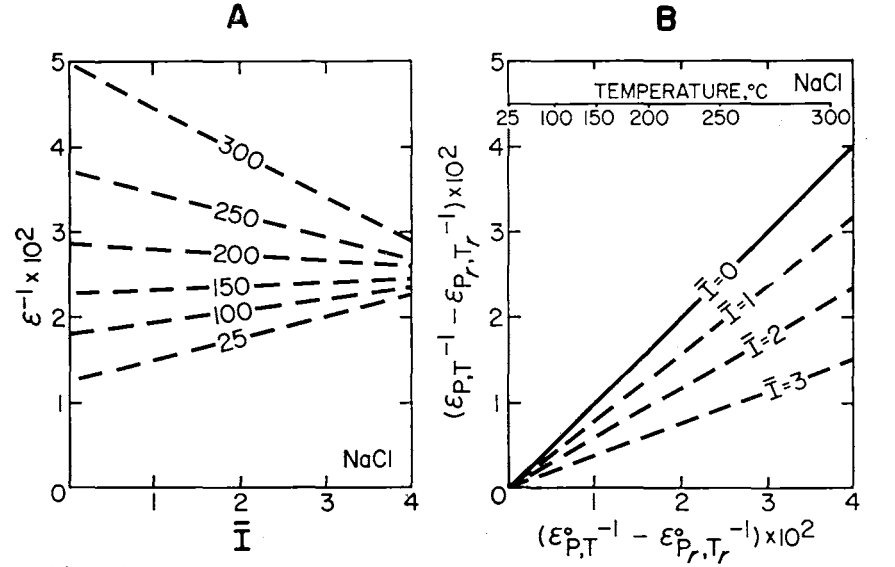

Fig. 164. Predicted (assuming I = $\bar{I}$) reciprocals of the dielectric constant (eqs 284 through 286) of NaCl solutions (ϵ^{-1}) at temperatures and pressures corresponding to liquid-vapor equilibrium as a function of stoichiometric ionic strength and the reciprocal of the dielectric constant of the solvent ($\epsilon^{\circ -1}$).

Eq (298) permits calculation of mineral solubilities in hydrothermal solutions at high pressures and temperatures. Calculations of this kind can be carried out by first specifying trial values of $\bar{I}$ and m^* and then evaluating simultaneously (1) statements of the law of mass action for each homogeneous and heterogeneous reaction in the system, (2) conservation of mass and charge equations for the species in the aqueous phase, and (3) statements of eqs (298) and (299) for all aqueous species. New values of $\bar{I}$ and m^* can then be computed, and the procedure repeated until the successive approximations converge. The requisite equilibrium constants can be calculated using equations, parameters, and thermodynamic data summarized above, together with those of minerals, gases, and aqueous complexes (Helgeson, 1967, 1969; Helgeson and Kirkham, 1974a, 1976; Helgeson and others, 1978; Sillen and Martell, 1964, 1971; Smith and Martell, 1976; Hogfeldt, in press; Seward, in press). The values of A_γ, B_γ, å, ω_j, b_{NaCl}, and $b_{Na^+Cl^-}$ required for the calculations can be obtained from equations and tables given above and/or generated from equations and correlation algorithms (like those in figs. 1 and 2) given by Helgeson and Kirkham (1974b; 1976). Where values of $r_{e,j}$ cannot be computed with

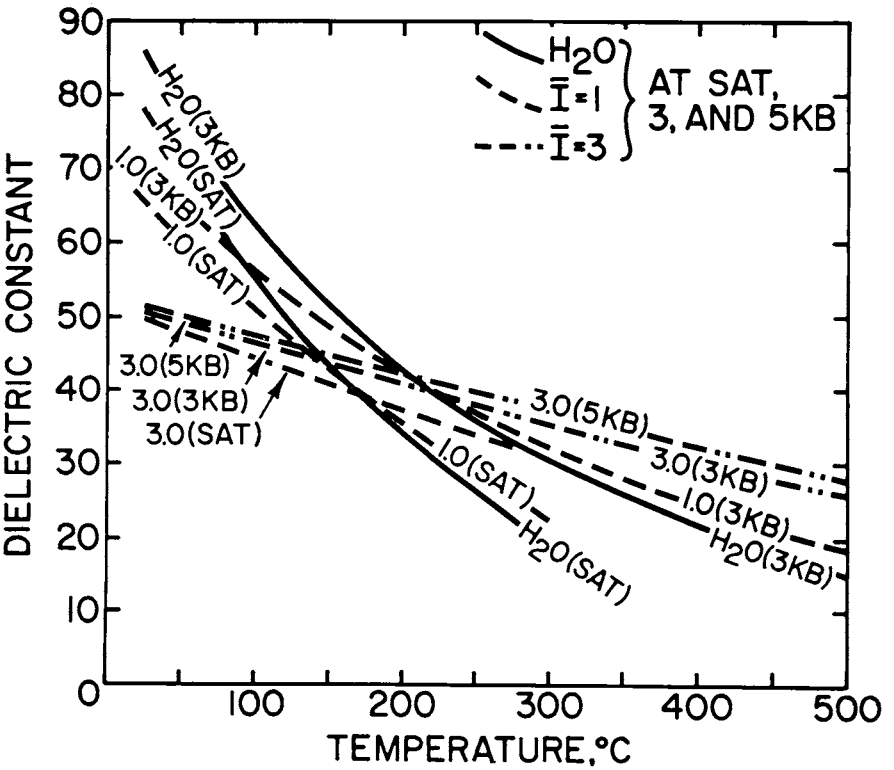

Fig. 165. Predicted (assuming $I = \bar{I}$) values of the dielectric constant of NaCl solutions as a function of temperature at constant pressure and "true" ionic strength corresponding to the labels on the curves. SAT refers to liquid-vapor equilibrium. The curves for H_2O represent values of ϵ° given by Helgeson and Kirkham (1974a), but those for NaCl solutions were generated from eq (286).

confidence, they can be estimated by assuming equalities of $r_{e,j}$ for similar aqueous species.

CONCLUDING REMARKS

Although the approach taken above is based on sound principles, it is also somewhat unconventional; but then, so too is the geologic problem. Much remains to be done to refine and test further the many theoretical concepts, equations, calculations, and extrapolations summarized in the preceding pages. Although they are consistent with a myriad of experimental observations, the predictive equations and fit parameters were generated primarily from consideration of the thermodynamic/electrostatic behavior of electrolytes at low temperatures. Nevertheless, the fact that values of $r_{e,j}$, ω_j, θ_j, and å derived from standard state considerations are consistent with both standard and nonstandard-state properties of aqueous electrolytes insures internal consistency in the equations and lends considerable support to the generality of the approach. As more and better high pressure/temperature data become available, the theoretical concepts, as well as the equations and parameters will no doubt require revision and improvement; particularly the algorithms represented by eqs (124) and (142). In the meantime, the calculations summarized above should afford reasonable approximation of geologic reality

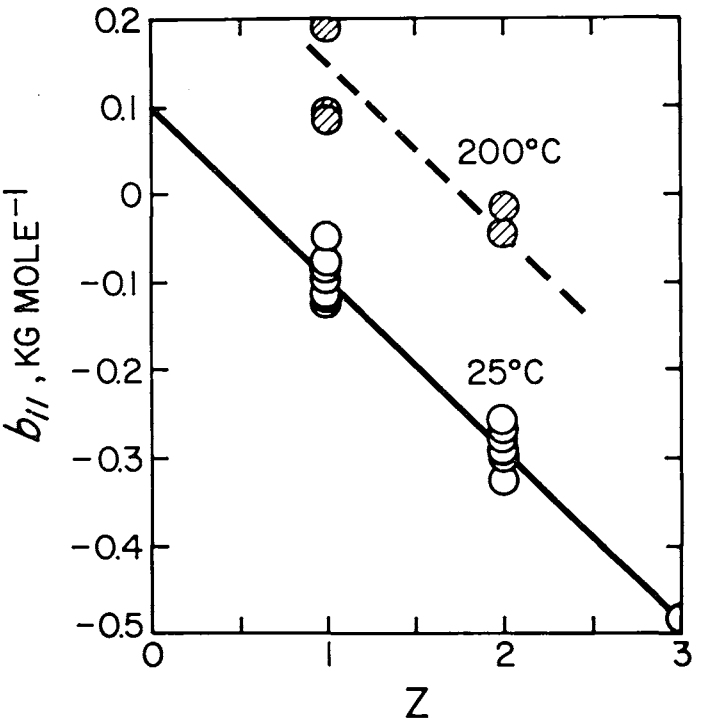

Fig. 166. Short-range interaction parameters (b_{11}) for cation-chloride interaction but the hatched symbols correspond to computed values at 200°C and 15 bars (see as a function of cation charge. The open circles represent values taken from table 7, text).

in applications of high temperature/pressure solution chemistry to the study of geochemical processes.

ACKNOWLEDGMENTS

The research described above has been supported over the past 10 yrs by the National Science Foundation (NSF grants GA 25314, GA 21509, GA 35888, GA 36023, EAR 74-14280, and EAR 77-14492), the donors of the Petroleum Research Fund administered by the American Chemical Society (PRF grants 5356 AC2 and 8927 AC2C), and the Miller Institute and Committee on Research at the University of California, Berkeley. We are indebted to these agencies as well as the Division of Physical Research of the U.S. Energy Research and Development Administration for financial support derived from the Geoscience Programs at the Lawrence Berkeley Laboratory (ERDA Contract UCB-ENG-4288) and the Lawrence Livermore Laboratory (ERDA Contract 7405-ENG-48) of the University of California. The present communication benefited greatly from critical reviews by K. S. Pitzer, G. M. Anderson, F. J. Millero, W. L. Marshall, A. J. Ellis, John C. Tanger IV, and J. R. Wood, who detected important errors in earlier versions of the manuscript and made many suggestions for improvement. Nevertheless we hasten to absolve them of any "guilt by association" that might befall these reviewers as a consequence of the approach taken in the preceding pages, and we exonerate them from all responsibility for any errors or oversights that may have escaped their attention. Thanks are also due K. S. Pitzer, F. J. Millero, L. G. Hepler, E. U. Franck, P. Tremaine, D. Miller, and J. W. Cobble for preprints and experimental data in advance of publication. We are also grateful to our friends and colleagues at Berkeley for many helpful suggestions and willing and repeated assistance with calculations, programming, data analysis, literature search, plotting, drafting, and reproduction. In particular we would like to thank John C. Tanger IV, J. M. Delany, J. V. Walther, D. K. Bird, W. F. McKenzie, B. Russell, K. Jackson, T. Bowers, C. Bruton, C. Frisch, M. Lee, T. Boleslawski, L. Bridges, P. Mullen, S. Tuxen, D. Maskell, M. Ryan, D. Gilbert, L. Goodwin, M. O'Leary, T. Welch, and J. Hampel. We are also indebted to T. Brooks, D. Aoki, S. Genelza, and especially J. Bossart for their outstanding patience, persistence, talent, and skill in typing and retyping the manuscript. Parts of the research described above were presented by HCH at the Fifth International Conference on Chemical Thermodynamics (1977) and the Nobel Symposium on the Chemistry and Geochemistry of Solutions at High Temperatures and Pressures (1979). The critical comments and suggestions made by the participants in these conferences are acknowledged with thanks. Finally, we would like to express our appreciation to the American Journal of Science and in particular Marie Casey and the late Philip M. Orville for their help and cooperation in publishing this series of unusually long papers. Phil Orville's farsight, integrity, staunch support, and encouragement are largely responsible for the appearance of this issue of the American Journal of Science, which we humbly dedicate to his memory.

Note added in proof

Line 14 of footnote 1 in Helgeson (in press) should be amended to read "and the first two terms on the right side of the second identity in eq (126) should be multiplied by Z_j." In addition, $NaHCO_3$ at the bottom of figure 60 in Helgeson and Kirkham (1976) should read $NaNO_3$ and table 55 in the caption of the figure should read table 31.

APPENDIX A

Summary of Identities Among Partial Molal Properties of Components and Aqueous Species

It follows from equations derived in the text that

$$\bar{G}_k = \mu_{\underline{k}} = \left(\frac{\partial G}{\partial m_{\underline{k}}}\right)_{P,T,\hat{m}_{\underline{k}}} = \sum_{\underline{j}} \nu_{\underline{j},\underline{k}} \bar{G}_{\underline{j}} \qquad \text{(A-1)}$$

$$\bar{V}_{\underline{k}} = \left(\frac{\partial V}{\partial m_{\underline{k}}}\right)_{P,T,\hat{m}_{\underline{k}}} = \left(\frac{\partial \bar{G}_{\underline{k}}}{\partial P}\right)_{T,\hat{m}(\underline{k})} = \sum_{\underline{j}} \nu_{\underline{j},\underline{k}} \bar{V}_{\underline{j}} , \qquad \text{(A-2)}$$

$$\bar{S}_{\underline{k}} = \left(\frac{\partial S}{\partial m_{\underline{k}}}\right)_{P,T,\hat{m}_{\underline{k}}} = -\left(\frac{\partial \bar{G}_{\underline{k}}}{\partial T}\right)_{P,\hat{m}(k)} = \sum_{\underline{j}} \nu_{\underline{j},\underline{k}} \bar{S}_{\underline{j}} , \qquad \text{(A-3)}$$

$$\bar{H}_{\underline{k}} = \left(\frac{\partial H}{\partial m_{\underline{k}}}\right)_{P,T,\hat{m}_{\underline{k}}} = \bar{G}_{\underline{k}} + T\bar{S}_{\underline{k}} = \sum_{\underline{j}} \nu_{\underline{j},\underline{k}} \bar{H}_{\underline{j}} , \qquad \text{(A-4)}$$

$$\bar{C}_{P,\underline{k}} = \left(\frac{\partial C_P}{\partial m_{\underline{k}}}\right)_{P,T,\hat{m}_{\underline{k}}} = \left(\frac{\partial \bar{H}_{\underline{k}}}{\partial T}\right)_{P,\hat{m}(\underline{k})} = T\left(\frac{\partial \bar{S}_{\underline{k}}}{\partial T}\right)_{P,\hat{m}(\underline{k})} = \sum_{\underline{j}} \nu_{\underline{j},\underline{k}} \bar{C}_{P,\underline{j}} , \qquad \text{(A-5)}$$

$$\bar{E}_{\underline{x},\underline{k}} = \left(\frac{\partial E_{\underline{x}}}{\partial m_{\underline{k}}}\right)_{P,T,\hat{m}_{\underline{k}}} = \left(\frac{\partial \bar{V}_{\underline{k}}}{\partial T}\right)_{P,\hat{m}(\underline{k})} = \sum_{\underline{j}} \nu_{\underline{j},\underline{k}} \bar{E}_{\underline{x},\underline{j}} , \qquad \text{(A-6)}$$

and

$$\bar{\kappa}_{\underline{k}} = \left(\frac{\partial \kappa}{\partial m_{\underline{k}}}\right)_{P,T,\hat{m}_{\underline{k}}} = -\left(\frac{\partial \bar{V}_{\underline{k}}}{\partial P}\right)_{T,\hat{m}(\underline{k})} = \sum_{\underline{j}} \nu_{\underline{j},\underline{k}} \bar{\kappa}_{\underline{j}} \qquad \text{(A-7)}$$

where $\hat{m}_{\underline{k}}$ stands for constant molalities of all solute components other than the $\underline{k}$th, $m_{\underline{k}}$ represents the molality of the $\underline{k}$th component, $\nu_{\underline{j},\underline{k}}$ denotes the number of moles of the $\underline{j}$th ion in one mole of the $\underline{k}$th component, $\hat{m}(\underline{k})$ refers to constant molalities of all the components of the solute, $\bar{G}_{\underline{k}}$, $\bar{G}_{\underline{j}}$, $\bar{H}_{\underline{k}}$, $\bar{H}_{\underline{j}}$, $\bar{C}_{P,\underline{k}}$, $\bar{C}_{P,\underline{j}}$, $\bar{E}_{\underline{x},\underline{k}}$, $\bar{E}_{\underline{x},\underline{j}}$, $\bar{\kappa}_{\underline{k}}$, and $\bar{\kappa}_{\underline{j}}$ refer to the partial molal Gibbs free energies, enthalpies, heat capacities,

APPENDIX A (continued)

expansibilities, and compressibilities of the $\underline{k}$th solute component and the $\underline{j}$th aqueous ion, respectively, G, H, Cp, $E_{\underline{x}}$, and κ stand for the extensive analogs of these properties for the solution, and

$$\overline{G}_{\underline{j}} = \left(\frac{\partial G}{\partial \underline{m}_{\underline{j}}}\right)_{P,T,\hat{\underline{m}}_{\underline{j}}} , \tag{A-8}$$

$$\overline{V}_{\underline{j}} = \left(\frac{\partial V}{\partial \underline{m}_{\underline{j}}}\right)_{P,T,\hat{\underline{m}}_{\underline{j}}} = \left(\frac{\partial \overline{G}_{\underline{j}}}{\partial P}\right)_{T,\hat{\underline{m}}(\underline{k})} , \tag{A-9}$$

$$\overline{S}_{\underline{j}} = \left(\frac{\partial S}{\partial \underline{m}_{\underline{j}}}\right)_{P,T,\hat{\underline{m}}_{\underline{j}}} = -\left(\frac{\partial \overline{G}_{\underline{j}}}{\partial T}\right)_{P,\hat{\underline{m}}(\underline{k})} , \tag{A-10}$$

$$\overline{H}_{\underline{j}} = \left(\frac{\partial H}{\partial \underline{m}_{\underline{j}}}\right)_{P,T,\hat{\underline{m}}_{\underline{j}}} = \overline{G}_{\underline{j}} + T\overline{S}_{\underline{j}} , \tag{A-11}$$

$$\overline{C}_{P,\underline{j}} = \left(\frac{\partial C_P}{\partial \underline{m}_{\underline{j}}}\right)_{P,T,\hat{\underline{m}}_{\underline{j}}} = \left(\frac{\partial \overline{H}_{\underline{j}}}{\partial T}\right)_{P,\hat{\underline{m}}(\underline{k})} = T\left(\frac{\partial \overline{S}_{\underline{j}}}{\partial T}\right)_{P,\hat{\underline{m}}(k)}, \tag{A-12}$$

$$\overline{E}_{\underline{x},\underline{j}} = \left(\frac{\partial E_{\underline{x}}}{\partial \underline{m}_{\underline{j}}}\right)_{P,T,\hat{\underline{m}}_{\underline{j}}} = \left(\frac{\partial \overline{V}_{\underline{j}}}{\partial T}\right)_{P,\hat{\underline{m}}(\underline{k})} , \tag{A-13}$$

and

$$\overline{\kappa}_{\underline{j}} = \left(\frac{\partial \kappa}{\partial \underline{m}_{\underline{j}}}\right)_{P,T,\hat{\underline{m}}_{\underline{j}}} = -\left(\frac{\partial \overline{V}_{\underline{j}}}{\partial P}\right)_{T,\hat{\underline{m}}(\underline{k})} \tag{A-14}$$

where $\underline{m}_{\underline{j}}$ stands for the molality of the $\underline{j}$th ion and $\hat{\underline{m}}_{\underline{j}}$ refers to constant molalities of all other species in solution. The partial molal properties of the $\underline{j}$th complex in solution are given by

$$\overline{G}_{\underline{q}} = \left(\frac{\partial G}{\partial \underline{m}_{\underline{q}}}\right)_{P,T,\hat{\underline{m}}_{\underline{q}}} = \sum_{\underline{j}} \nu_{\underline{j},\underline{q}} \overline{G}_{\underline{j}} , \tag{A-15}$$

$$\overline{V}_{\underline{q}} = \left(\frac{\partial V}{\partial \underline{m}_{\underline{q}}}\right)_{P,T,\hat{\underline{m}}_{\underline{q}}} = \sum_{j} \nu_{\underline{j},\underline{q}} \overline{V}_{\underline{j}} , \tag{A-16}$$

APPENDIX A (continued)

$$\bar{S}_q = \left(\frac{\partial S}{\partial m_q}\right)_{P,T,\hat{m}_q} = \sum_j \nu_{j,q} \bar{S}_j \qquad \text{(A-17)}$$

$$\bar{H}_q = \left(\frac{\partial H}{\partial m_q}\right)_{P,T,\hat{m}_q} = \bar{G}_q + T\bar{S}_q = \sum_j \nu_{j,q} \bar{H}_j , \qquad \text{(A-18)}$$

$$\bar{C}_{P,q} = \left(\frac{\partial C_P}{\partial m_q}\right)_{P,T,\hat{m}_q} = \sum_j \nu_{j,q} \bar{C}_{P,j} , \qquad \text{(A-19)}$$

$$\bar{E}_{x,q} = \left(\frac{\partial E_x}{\partial m_q}\right)_{P,T,\hat{m}_q} = \sum_j \nu_{j,q} \bar{E}_{x,j} \qquad \text{(A-20)}$$

and

$$\bar{\kappa}_q = \left(\frac{\partial \kappa}{\partial m_q}\right)_{P,T,\hat{m}_q} = \sum_j \nu_{j,q} \bar{\kappa}_j \qquad \text{(A-21)}$$

where m_q stands for the molality of the qth complex, $\hat{m}_q$ designates constant molalities of all aqueous species other than the qth, and $\nu_{j,q}$ corresponds to the number of moles of the jth ion in one mole of the qth complex.

APPENDIX B

Summary of Relations Among Relative Partial Molal Properties of Components and Aqueous Species

Equations derived in the text lead to the following identities:

$$\bar{G}_k - \bar{G}^\circ_k = \nu_k RT \ln (\gamma_{\pm,k}\, m_k) + RT \sum_j \nu_{j,k} \ln \nu_{j,k}$$

$$= \nu_k RT \ln (\bar{\gamma}_{\pm,k}\, m_k) + RT \sum_j \nu_{j,k} \ln\left(\frac{\nu_{j,k}\, m_j}{m_{t,j}}\right)$$

$$= \sum_j \nu_{j,k} (\bar{G}_j - \bar{G}^{\circ\,abs}_j), \qquad \text{(B-1)}$$

$$\bar{V}_k - \bar{V}^\circ_k = \left(\frac{\partial \bar{G}_k}{\partial P}\right)_{T,\hat{m}(k)} - \left(\frac{\partial \bar{G}^\circ_k}{\partial P}\right)_T = \nu_k RT \left(\frac{\partial \ln \gamma_{\pm,k}}{\partial P}\right)_{T,\hat{m}(k)}$$

$$= RT\left(\nu_k \left(\frac{\partial \ln \bar{\gamma}_{\pm,k}}{\partial P}\right)_{T,\hat{m}(k)} + \sum_j \nu_{j,k} \left(\frac{\partial \ln m_j}{\partial P}\right)_{T,\hat{m}(k)}\right)$$

$$= \sum_j \nu_{j,k} (\bar{V}_j - \bar{V}^{\circ\,abs}_j) , \qquad \text{(B-2)}$$

APPENDIX B (continued)

$$\bar{L}_k \equiv \bar{H}_k - \bar{H}^\circ_k = -T^2\left(\left(\frac{\partial(\bar{G}_k/T)}{\partial T}\right)_{P,\hat{m}(k)} - \left(\frac{\partial(\bar{G}^\circ_k/T)}{\partial T}\right)_P\right)$$

$$= -\nu_k RT^2\left(\frac{\partial \ln \gamma_{\pm,k}}{\partial T}\right)_{P,\hat{m}(k)}$$

$$= -RT^2\left(\nu_k\left(\frac{\partial \ln \bar{\gamma}_{\pm,k}}{\partial T}\right)_{P,\hat{m}(k)} + \sum_j \nu_{j,k}\left(\frac{\partial \ln m_j}{\partial T}\right)_{P,\hat{m}(k)}\right)$$

$$= \sum_j \nu_{j,k}\bar{L}_j = \sum_j \nu_{j,k}(\bar{H}_j - \bar{H}^{\circ\,abs}_j), \qquad \text{(B-3)}$$

$$\bar{S}_k - \bar{S}^\circ_k = -\left(\left(\frac{\partial \bar{G}_k}{\partial T}\right)_{P,\hat{m}(k)} - \left(\frac{\partial \bar{G}^\circ_k}{\partial T}\right)_P\right) = \frac{(\bar{H}_k - \bar{H}^\circ_k) - (\bar{G}_k - \bar{G}^\circ_k)}{T}$$

$$= \sum_j \nu_{j,k}(\bar{S}_j - \bar{S}^{\circ\,abs}_j), \qquad \text{(B-4)}$$

$$\bar{J}_k \equiv \bar{C}_{P,k} - \bar{C}^\circ_{P,k} = \left(\frac{\partial \bar{L}_k}{\partial T}\right)_{P,\hat{m}(k)} = T\left(\left(\frac{\partial \bar{S}_k}{\partial T}\right)_{P,\hat{m}(k)} - \left(\frac{\partial \bar{S}^\circ_k}{\partial T}\right)_P\right)$$

$$= -\nu_k R\left(2T\left(\frac{\partial \ln \gamma_{\pm,k}}{\partial T}\right)_{P,\hat{m}(k)} + T^2\left(\frac{\partial^2 \ln \gamma_{\pm,k}}{\partial T^2}\right)_{P,\hat{m}(k)}\right)$$

$$= -R\left(2T\left(\nu_k\left(\frac{\partial \ln \bar{\gamma}_{\pm,k}}{\partial T}\right)_{P,\hat{m}(k)} + \sum_j \nu_{j,k}\left(\frac{\partial \ln m_j}{\partial T}\right)_{P,\hat{m}(k)}\right)\right.$$

$$\left. + T^2\left(\nu_k\left(\frac{\partial^2 \ln \bar{\gamma}_{\pm,k}}{\partial T^2}\right)_{P,\hat{m}(k)} + \sum_j \nu_{j,k}\left(\frac{\partial^2 \ln m_j}{\partial T^2}\right)_{P,\hat{m}(k)}\right)\right)$$

$$= \sum_j \nu_{j,k}\bar{J}_j = \sum_j \nu_{j,k}(\bar{C}_{P,j} - \bar{C}^{\circ\,abs}_{P,j}), \qquad \text{(B-5)}$$

$$\bar{E}_{x,k} - \bar{E}^\circ_{x,k} = \left(\frac{\partial \bar{V}_k}{\partial T}\right)_{P,\hat{m}(k)} - \left(\frac{\partial \bar{V}^\circ_k}{\partial T}\right)_P = \nu_k RT\left(\frac{\partial\left(\frac{\partial \ln \gamma_{\pm,k}}{\partial P}\right)_{T,\hat{m}(k)}}{\partial T}\right)_{P,\hat{m}(k)} + \frac{\bar{V}_k - \bar{V}^\circ_k}{T}$$

$$= RT\left(\nu_k\left(\frac{\partial\left(\frac{\partial \ln \gamma_{\pm,k}}{\partial P}\right)_{T,\hat{m}(k)}}{\partial T}\right)_{P,\hat{m}(k)} + \sum_j \nu_{j,k}\left(\frac{\partial\left(\frac{\partial \ln m_j}{\partial P}\right)_{T,\hat{m}(k)}}{\partial T}\right)_{P,\hat{m}(k)}\right)$$

$$+ \frac{\bar{V}_k - \bar{V}^\circ_k}{T} = \sum_j \nu_{j,k}(\bar{E}_{x,j} - \bar{E}^{\circ\,abs}_{x,j}), \qquad \text{(B-6)}$$

APPENDIX B (continued)

and

$$\bar{\kappa}_{\underline{k}} - \bar{\kappa}^{\circ}_{\underline{k}} = -\left(\left(\frac{\partial \bar{V}_{\underline{k}}}{\partial P}\right)_{T,\hat{\underline{m}}(\underline{k})} - \left(\frac{\partial \bar{V}^{\circ}_{\underline{k}}}{\partial P}\right)_{T}\right) = -\nu_{\underline{k}} RT\left(\frac{\partial^2 \ln \gamma_{\pm,\underline{k}}}{\partial P^2}\right)_{T,\hat{\underline{m}}(\underline{k})}$$

$$= -RT\left(\nu_{\underline{K}}\left(\frac{\partial^2 \ln \bar{\gamma}_{\pm,\underline{k}}}{\partial P^2}\right)_{T,\hat{\underline{m}}(\underline{k})} + \sum_{\underline{j}} \nu_{\underline{j},\underline{k}}\left(\frac{\partial^2 \ln m_{\underline{j}}}{\partial P^2}\right)_{T,\hat{\underline{m}}(\underline{k})}\right)$$

$$= \sum_{\underline{j}} \nu_{\underline{j},\underline{k}} \left(\bar{\kappa}_{\underline{j}} - \bar{\kappa}^{\circ}_{\underline{j}}{}^{\underline{abs}}\right) , \tag{B-7}$$

where $\hat{\underline{m}}(\underline{k})$, $\nu_{\underline{j},\underline{k}}$, $\nu_{\underline{k}}$ and the other symbols are defined in Appendix A and

$$\bar{G}_{\underline{j}} - \bar{G}^{\circ}_{\underline{j}}{}^{\underline{abs}} = RT \ln(\gamma_{\underline{j}} m_{\underline{t},\underline{j}}) = RT \ln(\bar{\gamma}_{\underline{j}} m_{\underline{j}}) \tag{B-8}$$

$$\bar{V}_{\underline{j}} - \bar{V}^{\circ}_{\underline{j}}{}^{\underline{abs}} = \left(\frac{\partial \bar{G}_{\underline{j}}}{\partial P}\right)_{T,\hat{\underline{m}}(\underline{k})} - \left(\frac{\partial \bar{G}^{\circ}_{\underline{j}}{}^{\underline{abs}}}{\partial P}\right)_{T} = RT\left(\frac{\partial \ln \gamma_{\underline{j}}}{\partial P}\right)_{T,\hat{\underline{m}}(\underline{k})}$$

$$= RT\left(\left(\frac{\partial \ln \bar{\gamma}_{\underline{j}}}{\partial P}\right)_{T,\hat{\underline{m}}(\underline{k})} + \left(\frac{\partial \ln m_{\underline{j}}}{\partial P}\right)_{T,\hat{\underline{m}}(\underline{k})}\right) \tag{B-9}$$

$$\bar{L}_{\underline{j}} \equiv \bar{H}_{\underline{j}} - \bar{H}^{\circ}_{\underline{j}}{}^{\underline{abs}} = -RT^2\left(\left(\frac{\partial(\bar{G}_{\underline{j}}/T)}{\partial T}\right)_{P,\hat{\underline{m}}(\underline{k})} - \left(\frac{\partial(\bar{G}^{\circ}_{\underline{j}}{}^{\underline{abs}}/T)}{\partial T}\right)_{P}\right)$$

$$= -RT^2\left(\frac{\partial \ln \gamma_{\underline{j}}}{\partial T}\right)_{P,\hat{\underline{m}}(\underline{k})}$$

$$= -RT^2\left(\left(\frac{\partial \ln \bar{\gamma}_{\underline{j}}}{\partial T}\right)_{P,\hat{\underline{m}}(\underline{k})} + \left(\frac{\partial \ln m_{\underline{j}}}{\partial T}\right)_{P,\hat{\underline{m}}(\underline{k})}\right), \tag{B-10}$$

$$\bar{S}_{\underline{j}} - \bar{S}^{\circ}_{\underline{j}}{}^{\underline{abs}} = -\left(\left(\frac{\partial \bar{G}_{\underline{j}}}{\partial T}\right)_{P,\hat{\underline{m}}(\underline{k})} - \left(\frac{\partial \bar{G}^{\circ}_{\underline{j}}{}^{\underline{abs}}}{\partial T}\right)_{P}\right)$$

$$= \frac{(\bar{H}_{\underline{j}} - \bar{H}^{\circ}_{\underline{j}}) - (\bar{G}_{\underline{j}} - \bar{G}^{\circ}_{\underline{j}})}{T} , \tag{B-11}$$

APPENDIX B (continued)

$$\bar{J}_j \equiv \bar{C}_{P,j} - \bar{C}^{\circ}_{P,j}{}^{\text{abs}} = \left(\frac{\partial \bar{L}_j}{\partial T}\right)_{P,\hat{\underline{m}}(\underline{k})}$$

$$= T\left(\left(\frac{\partial \bar{S}_j}{\partial T}\right)_{P,\hat{\underline{m}}(\underline{k})} - \left(\frac{\partial \bar{S}^{\circ}{}^{\text{abs}}_j}{\partial T}\right)_P\right)$$

$$= -R\left(2T\left(\frac{\partial \ln \gamma_j}{\partial T}\right)_{P,\hat{\underline{m}}(\underline{k})} + T^2\left(\frac{\partial^2 \ln \gamma_j}{\partial T^2}\right)_{P,\hat{\underline{m}}(\underline{k})}\right)$$

$$= -R\left(2T\left(\left(\frac{\partial \ln \bar{\gamma}_j}{\partial T}\right)_{P,\hat{\underline{m}}(\underline{k})} + \left(\frac{\partial \ln m_j}{\partial T}\right)_{P,\hat{\underline{m}}(\underline{k})}\right)\right.$$

$$\left. + T^2\left(\left(\frac{\partial^2 \ln \bar{\gamma}_j}{\partial T^2}\right)_{P,\hat{\underline{m}}(\underline{k})} + \left(\frac{\partial^2 \ln m_j}{\partial T^2}\right)_{P,\hat{\underline{m}}(\underline{k})}\right)\right), \qquad \text{(B-12)}$$

$$\bar{E}_{x,j} - \bar{E}^{\circ}_{x,j}{}^{\text{abs}} = \left(\frac{\partial \bar{V}_j}{\partial T}\right)_{P,\hat{\underline{m}}(\underline{k})} - \left(\frac{\partial \bar{V}^{\circ}{}^{\text{abs}}_j}{\partial T}\right)_P = RT\left(\frac{\left(\frac{\partial \ln \gamma_j}{\partial P}\right)_{T,\hat{\underline{m}}(\underline{k})}}{\partial T}\right)_{P,\hat{\underline{m}}(\underline{k})}$$

$$= RT\left(\left(\frac{\partial\left(\frac{\partial \ln \bar{\gamma}_j}{\partial P}\right)_{T,\hat{\underline{m}}(\underline{k})}}{\partial T}\right)_{P,\hat{\underline{m}}(\underline{k})} + \left(\frac{\partial\left(\frac{\partial \ln m_j}{\partial P}\right)_{T,\hat{\underline{m}}(\underline{k})}}{\partial T}\right)_{P,\hat{\underline{m}}(\underline{k})}\right) \qquad \text{(B-13)}$$

and

$$\bar{\kappa}_j - \bar{\kappa}^{\circ}_j{}^{\text{abs}} = -\left(\left(\frac{\partial \bar{V}_j}{\partial P}\right)_{T,\hat{\underline{m}}(\underline{k})} - \left(\frac{\partial \bar{V}^{\circ}{}^{\text{abs}}_j}{\partial P}\right)_T\right) = -RT\left(\frac{\partial^2 \ln \gamma_j}{\partial P^2}\right)_{T,\hat{\underline{m}}(\underline{k})}$$

$$= -RT\left(\left(\frac{\partial^2 \ln \bar{\gamma}_j}{\partial P^2}\right)_{T,\hat{\underline{m}}(\underline{k})} + \left(\frac{\partial^2 \ln m_j}{\partial P^2}\right)_{T,\hat{\underline{m}}(\underline{k})}\right) \qquad \text{(B-14)}$$

APPENDIX C

The temperature/pressure dependent parameters in equations derived in the text for activity coefficients, osmotic coefficients, and apparent molal and relative partial molal properties are defined by the expressions summarized below.

Debye-Hückel Parameters

The electrostatic parameters in the Debye-Hückel equation are defined by

$$A_\gamma \equiv \frac{(2\pi \underline{N}^\circ)^{1/2} e^3 \rho^{\circ 1/2}}{2.302585(1000)^{1/2}(\varepsilon^\circ kT)^{3/2}}$$

$$= \frac{1.824829238 \times 10^6 \rho^{\circ 1/2}}{(\varepsilon^\circ T)^{3/2}} \qquad (C\text{-}1)$$

and (for å expressed in cm)

$$B_\gamma \equiv \left(\frac{8\pi \underline{N}^\circ \rho^\circ e^2}{1000 \varepsilon^\circ kT}\right)^{1/2}$$

$$= \frac{50.29158649 \times 10^8 \rho^{\circ 1/2}}{(\varepsilon^\circ T)^{1/2}} \qquad (C\text{-}2)$$

where $\pi = 3.14159265$, $\underline{N}^\circ$ corresponds to Avogadro's number (6.02252×10^{23} $mole^{-1}$), e stands for the absolute electronic charge (4.80298×10^{-10} esu), ρ° represents the density in g cm^{-3} and ε° the dielectric constant of H_2O, T designates temperature on the thermodynamic scale in °K, and k denotes Boltzman's constant (1.38054×10^{-16} erg $(°K)^{-1}$). Values of A_γ, B_γ, and other Debye-Hückel parameters defined below are given in table 1 for temperatures up to 350°C at 1 bar and/or pressures corresponding to the vapor-liquid equilibrium curve for H_2O. The remaining Debye-Hückel parameters can be expressed in terms of A_γ, B_γ, or their partial derivatives by writing

APPENDIX C (continued)

$$A_G \equiv -2(2.303)RT\,A_\gamma \tag{C-3}$$

$$A_H \equiv -\left(\frac{\partial(A_G/T)}{\partial T}\right)_P T^2 = 2(2.303)RT^2\left(\frac{\partial A_\gamma}{\partial T}\right)_P \tag{C-4}$$

$$A_J \equiv \left(\frac{\partial A_H}{\partial T}\right)_P = 2(2.303)R\left(2T\left(\frac{\partial A_\gamma}{\partial T}\right)_P + T^2\left(\frac{\partial^2 A_\gamma}{\partial T^2}\right)_P\right) \tag{C-5}$$

$$A_V \equiv \left(\frac{\partial A_G}{\partial P}\right)_T = -2(2.303)RT\left(\frac{\partial A_\gamma}{\partial P}\right)_T \tag{C-6}$$

$$A_K \equiv \left(\frac{\partial A_V}{\partial P}\right)_T = -2(2.303)RT\left(\frac{\partial^2 A_\gamma}{\partial P^2}\right)_T \tag{C-7}$$

$$A_{E_x} \equiv \left(\frac{\partial A_V}{\partial T}\right)_P = \frac{A_V}{T} - \frac{1}{T}\left(\frac{\partial A_H}{\partial P}\right)_T = \frac{A_V}{T} - 2(2.303)RT\left(\frac{\partial\left(\frac{\partial A_\gamma}{\partial P}\right)_T}{\partial T}\right)_P \tag{C-8}$$

$$B_H \equiv 2(2.303)RT^2\left(\frac{\partial B_\gamma}{\partial T}\right)_P \tag{C-9}$$

$$B_J \equiv \left(\frac{\partial B_H}{\partial T}\right)_P = 2(2.303)R\left(2T\left(\frac{\partial B_\gamma}{\partial T}\right)_P + T^2\left(\frac{\partial^2 B_\gamma}{\partial T^2}\right)_P\right) \tag{C-10}$$

$$B_V \equiv 2(2.303)RT\left(\frac{\partial B_\gamma}{\partial P}\right)_T \tag{C-11}$$

$$B_K \equiv \left(\frac{\partial B_V}{\partial P}\right)_T = 2(2.303)RT\left(\frac{\partial^2 B_\gamma}{\partial P^2}\right)_T \tag{C-12}$$

and

$$B_{E_x} \equiv \left(\frac{\partial B_V}{\partial T}\right)_P = \frac{B_V}{T} + \frac{1}{T}\left(\frac{\partial B_H}{\partial P}\right)_T = \frac{B_V}{T} + 2(2.303)RT\left(\frac{\partial\left(\frac{\partial B_\gamma}{\partial P}\right)_T}{\partial T}\right)_P \tag{C-13}$$

APPENDIX C (continued)

Solvation Parameters

$$\underline{b}_{\underline{k}} \equiv \frac{\hat{\underline{b}}_{\underline{k}}}{2.303RT} \tag{C-14}$$

$$\underline{b}_{H,\underline{k}} \equiv 2T^2\left(\frac{\partial(\hat{\underline{b}}_{\underline{k}}/T)}{\partial T}\right)_P = 2(2.303)RT^2\left(\frac{\partial \underline{b}_{\underline{k}}}{\partial T}\right)_P \tag{C-15}$$

$$\underline{b}_{J,\underline{k}} \equiv \left(\frac{\partial \underline{b}_{H,\underline{k}}}{\partial T}\right)_P = 2(2.303)R\left(2T\left(\frac{\partial \underline{b}_{\underline{k}}}{\partial T}\right)_P + T^2\left(\frac{\partial^2 \underline{b}_{\underline{k}}}{\partial T^2}\right)_P\right) \tag{C-16}$$

$$\underline{b}_{V,\underline{k}} \equiv 2\left(\frac{\hat{\underline{b}}_{\underline{k}}}{\partial P}\right)_T = 2(2.303)RT\left(\frac{\partial \underline{b}_{\underline{k}}}{\partial P}\right)_T \tag{C-17}$$

$$\underline{b}_{\underline{K},\underline{k}} \equiv -\left(\frac{\partial \underline{b}_{V,\underline{k}}}{\partial P}\right)_T = -2(2.303)RT\left(\frac{\partial^2 \underline{b}_{\underline{k}}}{\partial P^2}\right)_T \tag{C-18}$$

and

$$\underline{b}_{\underline{E}_{\underline{x},\underline{k}}} \equiv \left(\frac{\partial \underline{b}_{V,\underline{k}}}{\partial T}\right)_P = \frac{\underline{b}_{V,\underline{k}}}{T} + \frac{1}{T}\left(\frac{\partial \underline{b}_{H,\underline{k}}}{\partial P}\right)_T = \frac{\underline{b}_{V,\underline{k}}}{T} + 2(2.303)RT\left(\frac{\partial\left(\frac{\partial \underline{b}_{\underline{k}}}{\partial P}\right)_T}{\partial T}\right)_P \tag{C-18a}$$

where $\underline{k}$ designates a component of the solute and $\hat{\underline{b}}_{\underline{k}}$ is defined in the text.

Short-Range Interaction Parameters

If any two aqueous species are designated by the subscripts $\underline{j}$ and $\hat{\underline{j}}$, short range interaction parameters for both charged and neutral species can be represented by

$$\underline{b}_{\underline{j}\hat{\underline{j}}} \equiv \frac{\hat{\underline{b}}_{\underline{j}\hat{\underline{j}}}}{2.303RT} \tag{C-19}$$

$$\underline{b}_{H,\underline{j}\hat{\underline{j}}} \equiv 2T^2\left(\frac{\partial(\hat{\underline{b}}_{\underline{j}\hat{\underline{j}}}/T)}{\partial T}\right)_P = 2(2.303)RT^2\left(\frac{\partial \underline{b}_{\underline{j}\hat{\underline{j}}}}{\partial T}\right)_P \tag{C-20}$$

$$\underline{b}_{J,\underline{j}\hat{\underline{j}}} \equiv \left(\frac{\partial \underline{b}_{H,\underline{j}\hat{\underline{j}}}}{\partial T}\right)_P = 2(2.303)R\left(2T\left(\frac{\partial \underline{b}_{\underline{j}\hat{\underline{j}}}}{\partial T}\right)_P + T^2\left(\frac{\partial^2 \underline{b}_{\underline{j}\hat{\underline{j}}}}{\partial T^2}\right)_P\right) \tag{C-21}$$

APPENDIX C (continued)

$$\underline{b}_{V,\underline{j}\hat{\underline{j}}} \equiv 2\left(\frac{\partial \hat{\underline{b}}_{\underline{j}\hat{\underline{j}}}}{\partial P}\right)_T = 2(2.303)RT\left(\frac{\partial^2 \underline{b}_{\underline{j}\hat{\underline{j}}}}{\partial P^2}\right)_T \tag{C-22}$$

$$\underline{b}_{\kappa,\underline{j}\hat{\underline{j}}} \equiv -\left(\frac{\partial \underline{b}_{V,\underline{j}\hat{\underline{j}}}}{\partial P}\right)_T = -2(2.303)RT\left(\frac{\partial^2 \underline{b}_{\underline{j}\hat{\underline{j}}}}{\partial P^2}\right)_T \tag{C-23}$$

and

$$\underline{b}_{E_{\underline{x}},\underline{j}\hat{\underline{j}}} \equiv \left(\frac{\partial \underline{b}_{V,\underline{j}\hat{\underline{j}}}}{\partial T}\right)_P = \frac{\underline{b}_{V,\underline{j}\hat{\underline{j}}}}{T} + \frac{1}{T}\left(\frac{\partial \underline{b}_{H,\underline{j}\hat{\underline{j}}}}{\partial P}\right)_T = \frac{\underline{b}_{V,\underline{j}\hat{\underline{j}}}}{T} + 2(2.303)RT\left(\frac{\partial\left(\frac{\partial \underline{b}_{\underline{j}\hat{\underline{j}}}}{\partial P}\right)_T}{\partial T}\right)_P \tag{C-24}$$

where $\hat{\underline{b}}_{\underline{j}\hat{\underline{j}}}$ is defined in the text.

Extended Term Parameters for "Completely" Dissociated Single Electrolytes

It follows from equations derived in the text and those summarized above that we can write for the $\underline{k}$th "completely" dissociated electrolyte consisting of the $\underline{i}$th and $\underline{\ell}$th cation and anion, respectively,

$$\underline{b}_{\gamma,\underline{k}} \equiv -\frac{\underline{b}_{G,\underline{k}}}{2(2.303RT)} = \frac{\psi_{\underline{k}}\omega_{\underline{k}}\underline{b}_{\underline{k}} + 2\nu_{\underline{i},\underline{k}}\nu_{\underline{\ell},\underline{k}}\underline{b}_{\underline{i}\underline{\ell}}}{\nu_{\underline{k}}\psi_{\underline{k}}} \tag{C-25}$$

$$\underline{b}_{H,\underline{k}} \equiv 2(2.303)RT^2\left(\frac{\partial \underline{b}_{\gamma}}{\partial T}\right)_P = \frac{\psi_{\underline{k}}\omega_{\underline{k}}\underline{b}_{H,\underline{k}} + 2\nu_{\underline{i},\underline{k}}\nu_{\underline{\ell},\underline{k}}\underline{b}_{H,\underline{i}\underline{\ell}}}{\nu_{\underline{k}}\psi_{\underline{k}}} \tag{C-26}$$

$$\underline{b}_{J,\underline{k}} \equiv 2(2.303)R\left(2T\left(\frac{\partial \underline{b}_{\gamma}}{\partial T}\right)_P + T^2\left(\frac{\partial^2 \underline{b}_{\gamma}}{\partial T^2}\right)_P\right)$$

$$= \frac{\psi_{\underline{k}}\omega_{\underline{k}}\underline{b}_{J,\underline{k}} + 2\nu_{\underline{i},\underline{k}}\nu_{\underline{\ell},\underline{k}}\underline{b}_{J,\underline{i}\underline{\ell}}}{\nu_{\underline{k}}\psi_{\underline{k}}} \tag{C-27}$$

$$\underline{b}_{V,\underline{k}} \equiv 2(2.303)RT\left(\frac{\partial \underline{b}_{\gamma}}{\partial P}\right)_T = \frac{\psi_{\underline{k}}\omega_{\underline{k}}\underline{b}_{V,\underline{k}} + 2\nu_{\underline{i},\underline{k}}\nu_{\underline{\ell},\underline{k}}\underline{b}_{V,\underline{i}\underline{\ell}}}{\nu_{\underline{k}}\psi_{\underline{k}}} \tag{C-28}$$

$$\underline{b}_{\kappa,\underline{k}} \equiv -2(2.303)RT\left(\frac{\partial^2 \underline{b}_{\gamma}}{\partial P^2}\right)_T = \frac{\psi_{\underline{k}}\omega_{\underline{k}}\underline{b}_{\kappa,\underline{k}} + 2\nu_{\underline{\ell},\underline{k}}\underline{b}_{\kappa,\underline{i}\underline{\ell}}}{\nu_{\underline{k}}\psi_{\underline{k}}} \tag{C-29}$$

and

$$\underline{b}_{E_{\underline{x}},\underline{k}} \equiv 2(2.303)RT\left(\frac{\partial\left(\frac{\partial \underline{b}_{\gamma}}{\partial P}\right)_T}{\partial T}\right)_P + \frac{\underline{b}_{V,\underline{k}}}{T} = \frac{\psi_{\underline{k}}\omega_{\underline{k}}\underline{b}_{E_{\underline{x}},\underline{k}} + 2\nu_{\underline{i},\underline{k}}\nu_{\underline{\ell},\underline{k}}\underline{b}_{E_{\underline{x}},\underline{i}\underline{\ell}}}{\nu_{\underline{k}}\psi_{\underline{k}}} \tag{C-30}$$

where $\psi_{\underline{k}}$, $\nu_{\underline{i},\underline{k}}$, and $\nu_{\underline{\ell},\underline{k}}$, are defined in the text.

REFERENCES

Ackermann, Th., 1958, Aussagen über die Eigendissoziation des Wassers aus Molwärmemessungen gelöster Elektrolyte: Zeitschr. für Elektrochemie, v. 62, p. 411-419.

Ackerman, Th., and Schreiner, F., 1958, Molwärmen und Entropien einiger Fettsäuren und ihrer Anionen in wässriger Lösung: Zeitschr. Elektrochemie; v. 62, p. 1143-1151.

Adams, L. H., 1931, Equilibrium in binary systems under pressure. I. An experimental and thermodynamic investigation of the system, NaCl-H_2O, at 25°: Am. Chem. Soc. Jour., v. 53, p. 3769-3813.

Adams, L. H., and Hall, R. E., 1931, The effect of pressure on the electrical conductivity of solutions of sodium chloride and of other electrolytes: Jour. Phys. Chemistry, v. 35, p. 2145-2163.

Ahluwalia, J. C., and Cobble, J. W., 1964a, The thermodynamic properties of high temperature aqueous solutions. II. Standard partial molal heat capacities of sodium perrhenate and perrhenic acid from 0 to 100°: Am. Chem. Soc. Jour., v. 86, p. 5377-5381.

———— 1964b, The thermodynamic properties of high temperature aqueous solutions. III. The partial molal heat capacities of hydrochloric acid from 0 to 100° and the third-law potentials of the silver-silver chloride and calomel electrodes from 0 to 100°: Am. Chem. Soc. Jour., v. 86, p. 5381-5384.

Akitt, J. W., 1980, Limiting single-ion molar volumes. Intrinsic volume as a function of the solvent parameters: Faraday Soc. Trans., I, v. 76, p. 2259-2284.

Allam, D. S., ms, 1963, Ultrasonic studies in some electrolyte solutions: Ph.D. dissert., Univ. London, 189 p.

Allam, D. S., and Lee, W. H., 1964, Ultrasonic studies of electrolyte solutions. Part I. Ultrasonic velocities in solutions of inorganic salts: Chem. Soc. [London] Jour. (A), p. 6049-6053.

———— 1966, Ultrasonic studies of electrolyte solutions. Part II. Compressibilities of electrolytes: Chem. Soc. [London] Jour. (A), p. 5-9.

Allred, G. C., and Woolley, E. M., 1981a, Heat capacities of aqueous HCl, NaOH, and NaCl at 283.15, 298.15, and 313.15 K: $\Delta C°_p$ for ionization of water: Jour. Chem. Thermodynamics, v. 13, p. 147-154.

———— 1981b, Heat capacities of aqueous acetic acid, sodium acetate, ammonia, and ammonium chloride at 283.15, 298.15, and 313.15K: $\Delta C°_p$ for ionization of acetic acid and for dissociation of ammonium ion: Jour. Chem. Thermodynamics, v. 13, p. 155-164.

Anderson, H. L., and Wood, R. H., 1973, Thermodynamics of aqueous mixed electrolytes, *in* Franks, F., ed., Water, v. 3, Aqueous Solutions of Simple Electrolytes: New York, Plenum Press, p. 119-143.

Arhsadi, M., and Kebarle, P., 1970, Hydration of OH^- and O_2^- in the gas phase. Comparative solvation of OH^- by water and the hydrogen halides. Effects of acidity: Jour. Phys. Chemistry, v. 74, p. 1483-1486.

Arshadi, M., Yamdagui, R., and Kebarle, P., 1970, Hydration of the halide negative ions in the gas phase. II. Comparison of hydration energies for the alkali positive and halide negative ions: Jour. Phys. Chemistry, v. 74, p. 1475-1482.

Asano, T., and le Noble, W. J., 1978, Activation and reaction volumes in solution: Chem. Reviews, v. 78, p. 407-489.

Baes, C. F., Jr., and Mesmer, R. E., 1976, The Hydrolysis of Cations: New York, John Wiley & Sons, 489 p.

———— 1981, The thermodynamics of cation hydrolysis: Am. Jour. Sci., v. 281, p. 935-962.

Bale, W. D., Davies, E. W., and Monk, C. B., 1956, Spectrophotometric studies of electrolytic dissociation. Part 3. Lead nitrate, cupric sulphate, and cobalt hexamine sulphate in water: Faraday Soc. Trans., v. 52, p. 816-823.

Barnes, H. L., and Ernst, W. G., 1963, Ideality and ionization in hydrothermal fluids. The system MgO-H_2O-NaOH: Am. Jour. Sci., v. 261, p. 129-150.

Barnes, H. L., Helgeson, H. C., and Ellis, A. J., 1966, Ionization constants in aqueous solutions, *in* Clark, S. P., Jr., ed., Handbook of Physical Constants: Boulder, Colo., Geol. Soc. America, p. 401-413.

Bates, R. G., and Bower, V. E., 1954, Standard potential of the silver-silver-chloride electrode from 0° to 95° and the thermodynamic properties of dilute hydrochloric acid solutions: Natl. Bur. Standards Jour. Research, v. 53, no. 5, p. 283-290.

Bell, J. T., Helton, D. M., and Rogers, T. G., 1970, Densities of aqueous KCl and UO_2SO_4 from 25° to 374°C.: Jour Chem. Eng. Data, v. 15, p. 44-46.

Benedict, M., 1939, Properties of saturated aqueous solutions of potassium chloride at temperatures above 250°C.: Jour. Geology, v. 67, p. 252-276.

Benson, S. W., 1968, Thermochemical Kinetics: New York, John Wiley & Sons, 223 p.

Benson, S. W., and Copeland, C. S., 1963, The partial molar volumes of ions: Jour. Phys. Chemistry, v. 67, p. 1194-1197.

Berg, R. L., and Vanderzee, C. E., 1978, Thermodynamics of carbon dioxide and carbonic acid: (a) the standard enthalpies of solution of $Na_2CO_3(s)$, $NaHCO_3(s)$, and $CO_2(g)$ in water at 298.15K; (b) the standard enthalpies of formation, standard Gibbs energies of formation and standard entropies of $CO_2(aq)$, $HCO_3^-(aq)$, $CO_3^{2-}(aq)$, $NaHCO_3(s)$, $Na_2CO_3(s)$, $Na_2CO_3 \cdot H_2O(s)$, and $Na_2CO_3 \cdot 10H_2O(s)$: Jour. Chem. Thermodynamics, v. 10, p. 1113-1136.

Bernal, J. D., and Fowler, R. H., 1933, A theory of water and ionic solution with particular reference to hydrogen and hydroxyl ions: Jour. Chem. Physics, v. 1, p. 515-548.

Bernaducci, E. E., Morss, L. R., and Mikszial, A. R., 1979, Partial molal heat capacity of aqueous ferrous chloride from measurements of integral heats of dilution: Jour. Solution Chemistry, v. 8, p. 717-727.

Bird, D. K., and Helgeson, H. C., 1981, Chemical interaction of aqueous solutions with epidote-feldspar mineral assemblages in geologic systems. 2. Equilibrium constraints in metamorphic/geothermal processes: Am. Jour. Sci., v. 281, p. 576-614.

Bjerrum, N., 1926, Untersuchungen über Ionenassoziation. Der Einfluss der Ion Mass auf die Aktivität der Ionen bei mittleren Assoziationsgraden: Kgl. Danske Vidensk., v. 7, p. 1-48.

———— 1929, Neuere Anschauungen über Elektrolyte: Deutsche Chem. Gesell Ber., v. 62, p. 1091-1103.

Booth, H. S., and Bidwell, R. M., 1950, Solubilities of salts in water at high temperatures: Am. Chem. Soc. Jour., v. 72, p. 2567-2575.

Born, Von M., 1920, Volumen und Hydratationswärme der Ionen: Zeitschr. Physik, v. 1, p. 45-48.

Borodenko, V. I., and Galinker, I. S., 1975, Heat capacities and heats of dilution of aqueous solutions of sodium and potassium chlorides at 300 deg.: Izv. Vyssh. Ucheb. Zaved. Khimiya Khim. Tekhnol., v. 18, p. 591-594.

———— 1976, Heat capacities and thermal effects of the dissolution of sodium and potassium chlorides in water at 200, 250, and 300°C: Izv. Vyssh. Ucheb. Zaved. Khimiya Khim. Tekhnol., v. 19, p. 1908-1910.

Bradley, D. J., and Pitzer, K. S., 1979, Thermodynamics of electrolytes. 12. Dielectric properties of water and Debye-Hückel parameters to 350°C and 1 kbar: Jour. Phys. Chemistry, v. 83, p. 1599-1603.

Braunstein, H., and Braunstein, J., 1971, Isopeistic studies of very concentrated aqueous electrolyte solutions of LiCl, LiBr, $LiNO_3$, $Co(NO_3)_2$, $LiNO_3 + KNO_3$, $LiNO_3 \pm CsNO_3$, and $Ca(NO_3)_2 + CsNO_3$ at 100 to 150°C.: Jour. Chem. Thermodynamics, v. 3, p. 419-432.

Broadwater, T. L., and Evans, D. F., 1974, The conductance of divalent ions in H_2O at 10 and 25°C and in D_2O: Jour. Solution Chemistry, v. 3, p. 757-770.

Bromley, L. A., 1968, Heat capacity of sea water solutions. Partial and apparent values for salts and water: Jour. Chem. Eng. Data, v. 13, p. 60-62.

———— 1972, Approximate individual ion values of β (or B) in extended Debye-Hückel theory for uni-univalent aqueous solutions at 298.15K: Jour Chem. Thermodynamics, v. 4, p. 669-673.

———— 1973, Thermodynamic properties of strong electrolytes in aqueous solutions: Am. Inst. Chem. Engineers Jour., v. 19, p. 313-320.

Bromley, L. A., Diamond, A. E., Salami, E., and Wilkins, D. G., 1970, Heat capacities and enthalpies of sea salt solutions to 200°C.: Jour. Chem. Eng. Data, v. 15, p. 246-253.

Brönsted, J. N., 1922, Studies on solubility IV. Principle of the specific interaction of ions: Am. Chem. Soc. Jour., v. 44, p. 877-898.

Brummer, S. B., and Gancy, A. B., 1972, Aqueous solutions under extreme conditions. I. High pressures, *in* Horne, R. A., ed., Water and Aqueous Solutions: New York, Wiley-Intersci., p. 745-770.

Buchanan, J., and Hamann, S. D., 1953, The chemical effects of pressure, Part I: Faraday Soc. Trans., v. 49, p. 1425-1433.

Burns, D., 1964, The activity coefficients of some strong uni-univalent halides in aqueous solution: Electrochim. Acta, v. 9, p. 1545-1547.

Busey, R. H., and Mesmer, R. E., 1976, The ionization of water in NaCl media to 300°C: Jour. Solution Chemistry, v. 5, p. 147-152.

———— 1978, Thermodynamic quantities for the ionization of water in sodium chloride media to 300°C: Jour. Chem. Eng. Data, v. 23, p. 175-176.

Cerquetti, A., Longhi, P., and Mussini, T., 1968, Thermodynamics of aqueous hydrochloric acid from E. M. F.'s of hydrogen-chlorine cells: Jour. Chem. Eng. Data, v. 13, p. 458-461.

Chatterjee, R. M., Adams, W. A., and Davis, A. R., 1974, A high pressure laser Raman spectroscopic investigation of aqueous magnesium sulfate solutions: Jour. Phys. Chemistry, v. 78, p. 246-250.

Chen, C.-T., and Millero, F. J., 1976, The specific volume of seawater at high pressures: Deep-Sea Research, v. 23, p. 595-612.

———— 1977, The volume and compressibility charge for the formation of the $LaSO_4^+$ ion pair at 25°C: Jour. Solution Chemistry, v. 6, p. 589-607.

———— 1981, Equations of state for NaCl, $MgCl_2$, Na_2SO_4, and $MgSO_4$ aqueous solutions at high pressures: Jour. Chem. Eng. Data, v. 26, p. 270-274.

Chen, C.-T., Chen, L.-S., and Millero, F. J., 1978, Speed of sound in NaCl, $MgCl_2$, Na_2SO_4, and $MgSO_4$ aqueous solutions as functions of concentration, temperature, and pressure: Acoustical Soc. America Jour., v. 63, p. 1795-1800.

Chen, C.-T., Emmet, R. T., and Millero, F. J., 1977, The apparent molal volumes of aqueous solutions of NaCl, KCl, $MgCl_2$, Na_2SO_4, and $MgSO_4$ from 0 to 1000 bars at 0, 25, and 50°C: Jour. Chem. Eng. Data, v. 22, p. 201-207.

Chen, C.-T., Fine, R. A., and Millero, F. J., 1977, The equation of state of pure water determined from sound speeds: Jour. Chem. Physics, v. 66, no. 5, p. 2142-2144.

Chiu, Y.-C., and Fuoss, R. M., 1968, Conductance of the alkali halides. XII. Sodium and potassium chlorides in water at 25°C: Jour. Phys. Chemistry, v. 72, p. 4123-4129.

Chlebek, R. W., and Lister, M. W., 1966, Ion pair effects in the reaction between potassium ferrocyanide and potassium persulfate: Canadian Jour. Chemistry, v. 44, p. 437-445.

Chou, I., and Eugster, H. P., 1977, Solubility of magnetite in supercritical chloride solutions: Am. Jour. Sci., v. 277, p. 1296-1314.

Clark, R. H., and Ellis, A. J., 1960, The effect of pressure on the ionization of some benzoic acids: Chem. Soc. Jour., v. 48, p. 247-254.

Cobble, J. W., 1953a, Empirical considerations of entropy. I. The entropies of the oxy-anions and related species: Jour. Chem. Physics, v. 21, p. 1443-1446.

———— 1953b, Empirical considerations of entropy. II. The entropies of inorganic complex ions: Jour. Chem. Physics, v. 21, p. 1446-1450.

———— 1953c, Empirical considerations of entropy. III. A structural approach to the entropies of aqueous organic solutes and complex ions: Jour. Chem. Physics, v. 21, p. 1451-1456.

———— 1964, The thermodynamic properties of high temperature aqueous solutions. VI. Applications of entropy correspondence to thermodynamics and kinetics: Am. Chem. Soc. Jour., v. 86, p. 5394-5401.

———— 1966a, High temperature aqueous solutions: Science, v. 152, p. 1479-1485.

———— 1966b, Thermodynamics, *in* Eyring, H., ed., Annual Review of Physical Chemistry: Palo Alto, Calif., Annual Reviews, Inc., p. 15-36.

Cobble, J. W., and Murray, R. C., Jr., 1977, Unusual ion solvation energies in high temperature water: Faraday Soc. Discussion, v. 64, p. 144-149.

Cobble, J. W., Stephens, H. P., McKinnon, I. R., and Westrum, E. F., Jr., 1972, Thermodynamic properties of oxygenated sulfur complex ions. Heat capacity from 5 to 300°K for $K_2S_4O_6$ (c) and from 273 to 373°K for $S_4O_6^{2-}$ (aq). Revised thermodynamic functions for HSO_3^- (aq), SO_3^{2-} (aq), and $S_4O_6^{2-}$ (aq) at 298°K. Revised potential of the thiosulfate-tetrathionate electrode: Inorganic Chemistry, v. 11, p. 1670-1674.

CODATA, 1978, Recommended key values for thermodynamics, 1977. Report of the CODATA Task Group on key values for thermodynamics, 1977: Jour. Chem. Thermodynamics, v. 10, p. 903-906.

Coffy, G., and Olofsson, G., 1979, The standard enthalpy of formation of aqueous magnesium ion at 298.15°K: Jour. Chem. Thermodynamics, v. 11, p. 141-144.

Colladon, D., and Sturm, C., 1827, Suite du mémoire sur la compression des liquides: Ann. Chimie Physique, Sér. 2, v. 36, p. 225-257.

Conway, B. E., 1978, The evaluation and use of properties of individual ions in solution: Jour. Solution Chemistry, v. 7, p. 727-770.

———— 1979, Activity coefficients and hydration of ions, *in* Pytkowicz, R. M., ed., Activity Coefficients in Electrolyte Solutions, v. 1: Boca Raton, Fla., CRC Press, Inc., p. 95-138.

Copeland, C. S., Silverman, J., and Benson, S. W., 1953, The system NaCl-H_2O at supercritical temperatures and pressures: Jour. Chem. Physics, v. 21, p. 12-16.

Corti, H., Crovetto, R., and Fernández-Prini, R., 1979, Aqueous solutions of lithium hydroxide at various temperatures: conductivity and activity coefficients: Jour. Solution Chemistry, v. 8, p. 897-908.

Cox, J. D., Harrop, D., and Head, A. J., 1979, The standard enthalpy of formation of ammonium nitrate and of the nitrate ion: Jour. Chem. Thermodynamics, v. 11, p. 811-814.

Crerar, D. A., and Anderson, G. M., 1971, Solubility and solvation reactions of quartz in dilute hydrothermal solutions: Chem. Geology, v. 8, p. 107-122.

Crerar, D. A., and Barnes, H. L., 1976, Ore solution chemistry V. Solubilities of chalcopyrite and chalcocite assemblages in hydrothermal solution at 200° to 350°C: Econ. Geology, v. 71, p. 772-794.

Crerar, D. A., Susak, N. J., Borcsik, M., and Schwartz, S., 1978, Solubility of the buffer assemblage pyrite + pyrrhotite + magnetite in NaCl solutions from 200 to 350°C: Geochim. et Cosmochim. Acta, v. 42, p. 1427-1437.

Criss, C. M., and Cobble, J. W., 1961, The thermodynamic properties of high temperature aqueous solutions. I. Standard partial molal heat capacities of sodium chloride and barium chloride from 0 to 100°: Jour. Phys. Chemistry, v. 83, p. 3223-3228.

———— 1964a, The thermodynamic properties of high temperature aqueous solutions. IV. Entropies of the ions up to 200° and the correspondence principle: Am. Chem. Soc. Jour., v. 86, p. 5385-5390.

———— 1964b, The thermodynamic properties of high temperature aqueous solutions. V. The calculation of ionic heat capacities up to 200°. Entropies and heat capacities above 200°: Am. Chem. Soc. Jour., v. 86, p. 5390-5393.

Davies, C. W., 1938, The extent of dissociation of salts in water. Part VIII. An equation for the mean ionic activity coefficient of an electrolyte in water, and a revision of the dissociation constants of some sulphates: Chem. Soc. [London] Jour., p. 2093-2098.

———— 1962, Ion Association: Washington, Butterworths, 190 p.

Delany, J. M., and Helgeson, H. C., 1978, Calculation of the thermodynamic consequences of dehydration in subducting oceanic crust: Am. Jour. Sci., v. 278, p. 638-686.

Desnoyers, J. E., Arel, M., Perron, G., and Jolicoeur, C., 1969, Apparent molal volumes of alkali halides in water at 25°. Influence of structural hydration interactions on the concentration dependence: Jour. Phys. Chemistry, v. 73, p. 3346-3351.

Desnoyers, J. E., de Visser, C., Perron, G., and Picker, P., 1976, Reexamination of the heat capacities obtained by flow microcalorimetry. Recommendation for the use of a chemical standard: Jour. Solution Chemistry, v. 5, p. 605-616.

Desnoyers, J. E., and Jolicoeur, C., 1969, Hydration effects and thermodynamic properties of ions, *in* Bockris, J. O'M., and Conway, B. E., eds., Modern aspects of electrochemistry, no. 5: New York, Plenum Press, p. 1-89.

Dibrov, I. A., Mashovets, V. P., and Mateeva, R. P., 1964, The density and compressibility of aqueous sodium hydroxide solutions at high temperature: Jour. Appl. Chemistry, USSR (translation), v. 37, p. 38-44.

Drude, P., and Nernst, W., 1894, Über electrostriktion durch freie ionen: Zeitschr. Phys. Chemie, v. 15, p. 79-85.

Dunn, L. A., 1966, Apparent molar volumes of electrolytes: Faraday Soc. Trans., v. 62, p. 2348-2354.

———— 1968, Apparent molar volumes of electrolytes: Faraday Soc. Trans., v. 64, p. 1898-1903.

———— 1974, Ion-solvent interactions in aqueous solutions at various temperatures: Jour. Solution Chemistry, v. 3, p. 1-14.

Dunn, L. A., and Marshall, W. L., 1969a, Electrical conductances and ionization behavior of sodium chloride in dioxane-water mixtures at 100°: Jour. Phys. Chemistry, v. 73, p. 2619-2622.

———— 1969b, Electrical conductances of aqueous sodium iodide and the comparative thermodynamic behavior of aqueous sodium halide solutions to 800° and 4000 bars: Jour. Phys. Chemistry, v. 73, p. 723-728.

Dunsmore, H. S., Jalota, S. K., and Paterson, R., 1972, Ion association of rubidum chloride in aqueous solutions at 25°: Faraday Soc. Trans. I, v. 68, p. 1583-1585.

Dzidić, I., and Kebarle, P., 1970, Hydration of the alkali ions in the gas phase. Enthalpies and entropies of reactions $M^+(H_2O)_{n-1} + H_2O = M^+(H_2O)_n$: Jour. Phys. Chemistry, v. 74, p. 1466-1474.

Egan, E. P., Jr., Luff, B. B., and Wakefield, Z. T., 1958, Heat capacity of phosphotic acid solutions, 15 to 80°: Jour. Phys. Chemistry, v. 62, p. 1091-1095.

Eigen, M., and Wicke, E., 1951, Ionenhydration und spezifische wärme wässriger elektrolytlösungen: Zeitschr. Phys. Chemie, v. 55, p. 354-363.

———— 1954, The thermodynamics of electrolytes at higher concentration: Jour. Phys. Chemistry, v. 58, p. 702-714.

Ellis, A. J., 1959a, The system Na_2CO_3-$NaHCO_3$-CO_2-H_2O at temperatures up to 200°: Am. Jour. Sci., v. 257, p. 287-296.

———— 1959b, The effect of pressure on the first dissociation constant of "carbonic acid": Chem. Soc. [London] Jour., p. 3689-3699.

———— 1963, The effect of temperature on the ionization of hydrofluoric acid: Chem. Soc. [London] Jour., p. 4300-4304.

———— 1966, Partial molal volumes of alkali chlorides in aqueous solution to 200°: Chem. Soc. [London] Jour. (A), p. 1579-1584.

———— 1967, Partial molal volumes of $MgCl_2$, $CaCl_2$, $SrCl_2$, and $BaCl_2$ in aqueous solution to 200°: Chem. Soc. [London] Jour. (A), p. 600-664.

———— 1968, Partial molal volumes in high-temperature water. Part III. Halide and oxyanion salts: Chem. Soc. [London] Jour. (A), p. 1138-1143.

Ellis, A. J., and Anderson, D. W., 1961, The first acid dissociation constant of hydrogen sulphide at high pressures: Chem. Soc. [London] Jour., v. 917, p. 4678-4680.

Ellis, A. J., and Fyfe, W. S., 1957, Hydrothermal Chemistry: Rev. Pure Appl. Chemistry [Australia], v. 7, p. 261-316.

Ellis, A. J., and Giggenbach, W., 1971, Hydrogen sulphide ionization and sulphur hydrolysis in high temperature solution: Geochim. et. Cosmochim. Acta, v. 35, p. 247-260.

Ellis, A. J., and Golding, R. M., 1963, The solubility of carbon dioxide above 100°C in water and in sodium chloride solutions: Am. Jour. Sci., v. 261, p. 47-60.

Ellis, A. J., and McFadden, I. M., 1968, The partial molal volume of hydrochloric acid in high-temperature water: Chem. Communications, p. 516.

———— 1972, Partial molal volumes of ions in hydrothermal solutions: Geochim. et Cosmochim. Acta, v. 36, p. 413-426.

Emmet, R. T., and Millero, F. J., 1974, Direct measurement of the specific volume of seawater from −2 to 40°C and from 0 to 1000 bars, preliminary results: Jour. Geophys. Research, v. 79, p. 3463-3472.

Ensor, D. D., and Anderson, H. L., 1973, Heats of dilution of NaCl: temperature dependence: Jour. Chem. Eng. Data, v. 18, p. 205-212.

Eugster, H. P., in press, Metamorphic solutions and reactions, *in* Wickman, F., and Rickard, D., eds., Proceedings, Nobel Symposium on the Chemistry and Geochemistry of Solutions at High Temperatures and Pressures (Stockholm, Royal Swedish Acad. Sci.): New York, Pergamon Press.

Fabuss, B. M., and Korosi, A., 1966, Vapor pressures of binary aqueous solutions of NaCl, KCl, Na_2SO_4 and $MgSO_4$ at concentrations and temperatures of interest in desalination processes: Desalination, v. 1, p. 139-149.

Faita, G., Mussini, T., and Oggioni, R., 1966, Thermodynamic functions of aqueous hydrobromic acid at various concentrations and temperatures: Jour. Chem. Eng. Data, v. 11, p. 162-164.

Fanjung, L., 1894, Über den Einfluss des Druckes auf die Leitfähigkeit von Elektrolyten: Zeitschr. Phys. Chemie, v. 14, p. 673-700.

Feodotyev, K. M., and Shlepov, V. K., 1958, Solubility of salts of some elements in supercritical water vapor: Internat. Geology Rev., v. 1958, p. 114-119.

Fine, R. A., and Millero, F. J., 1975, The high pressure PVT properties of deuterium oxide: Jour. Chem. Physics, v. 63, p. 89-95.

Fink, J., 1885, Über den Einfluss des Druckes auf den electrischen Leitungswiderstand von Electrolyten: Ann. der Physik und Chemie [Leipzig], Neue Folge, v. 26, p. 481-517.

Fisher, F. H., 1962, The effect of pressure on the equilibrium of magnesium sulfate: Jour. Phys. Chemistry, v. 66, p. 1607-1611.

———— 1975, Dissociation of Na_2SO_4 from ultrasonic-absorption reduction in $MgSO_4$-NaCl solutions: Jour. Solution Chemistry, v. 4, p. 237-240.

———— 1978, Ion association and departure from additivity of equivalent conductance as a function of pressure: Jour. Solution Chemistry, v. 7, p. 897-900.

Fisher, F. H., and Davis, D. F., 1965, The effect of pressure on the dissociation of manganese sulfate ion pairs in water: Jour. Phys. Chemistry, v. 69, p. 2595-2598.

———— 1967, Effect of pressure on the dissociation of the $(LaSO_4)^+$ complex ion: Jour. Phys. Chemistry, v. 71, p. 819-822.

Fisher, F. H., and Fox, A. P., 1975, $NaSO_4^-$ ion pairs in aqueous solutions at pressures up to 2000 atm.: Jour. Solution Chemistry, v. 4, p. 225-236.

———— 1977, KSO_4^-, $NaSO_4^-$, and $MgCl^+$ ion pairs in aqueous solutions up to 2000 atm.: Jour. Solution Chemistry, v. 6, p. 641-650.

———— 1978, $LiSO_4^-$, $RbSO_4^-$, $CsSO_4^-$, and $(NH_4)SO_4^-$ ion pairs in aqueous solutions at pressures up to 2000 atm.: Jour. Solution Chemistry, v. 7, p. 561-570.

———— 1979a, Divalent sulfate ion pairs in aqueous solutions at pressures up to 2000 atm.: Jour. Solution Chemistry, v. 8, p. 309-328.

———— 1979b, Electrical conductance of KCl solutions at pressures up to 2000 atm.: Jour. Solution Chemistry, v. 8, p. 627-634.

Fisher, J. R., and Barnes, H. L., 1972, The ion product constant of water to 350°: Jour. Phys. Chemistry, v. 76, p. 90-98.

Fogo, J. K., Benson, S. W., and Copeland, C. W., 1954, The electrical conductivity of supercritical solutions of sodium chloride and water: Jour. Chem. Physics, v. 22, p. 212-216.

Fortier, J.-L., and Desnoyers, J. E., 1976, Thermodynamic properties of alkali halides V. Temperature and pressure dependence of excess free energies in water: Jour. Solution Chemistry, v. 5, p. 297-308.

Fortier, J.-L., Leduc, P.-A., and Desnoyers, J. E., 1974, Thermodynamic properties of alkali halides. II. Enthalpies of dilution and heat capacities in water at 25°C.: Jour. Solution Chemistry, v. 3, p. 323-349.

Fortier, J.-L., Philip, P. R., and Desnoyers, J. E., 1974, Thermodynamic properties of alkali halides. III. Volumes and heat capacities of transfer from H_2O to D_2O at 25°C.: Jour. Solution Chemistry, v. 3, p. 523-538.

Franck, E. U., 1956a, Hochverdichteter Wasserdampf I. Elektrolytische Leitfähigkeit in KCl-H_2O-Lösungen bis 750°C: Zeitschr. Phys. Chemie, v. 8, p. 92-106.

———— 1956b, Hochverdichteter Wasserdampf II. Ionendissoziation von KCl in H_2O bis 750°C: Zeitschr. Phys. Chemie, v. 8, p. 107-126.

———— 1956c, Hochverdichteter Wasserdampf III. Ionendissoziation von KCl, KOH und H_2O in überkritischem Wasser: Zeitschr. Phys. Chemie, v. 8, p. 192-206.

———— 1961, Überkritisches Wasser als electrolytisches Lösungsmittel: Angew. Chemie, v. 73, p. 309-322.

———— 1968, Supercritical Water: Endeavour, v. 27, p. 55-59.

———— 1969, Ions in aqueous solutions at high temperatures and pressures: Jour. Chimie Physique, p. 9-17.

———— 1973, Concentrated electrolyte solutions at high temperatures and pressures: Jour. Solution Chemistry, v. 2, p. 339-353.

———— in press, Survey of selected non-thermodynamic properties and chemical phenomena of fluids and fluid mixtures, *in* Wickman, F., and Rickard, D., eds., Proceedings, Nobel Symposium on the Chemistry and Geochemistry of Solutions at High Temperatures and Pressures (Stockholm, Royal Swedish Acad. Sci.) New York, Pergamon Press.

Franck, E. U., Hartmann, D., and Hensel, F., 1965, Proton mobility in water at high temperatures and pressures: Faraday Soc. Discussion, v. 39, p. 200-206.

Franks, F., 1972, Water, v. 1. The Physics and Physical Chemistry of Water: New York, Plenum Press, 596 p.

———— 1973, Water, v. 3. Aqueous Solutions of Simple Electrolytes: New York, Plenum Press, 472 p.

Frantz, J. D., and Eugster, H. P., 1973, Acid-base buffers: Use of Ag + AgCl in the experimental control of solution equilibria at elevated pressures and temperatures: Am. Jour. Sci., v. 273, p. 268-286.

Frantz, J. D., and Marshall, W. L., 1982, Electrical conductances and ionization constants of calcium chloride and magnesium chloride in aqueous solutions at temperatures to 600°C and pressures to 4000 bars: Am. Jour. Sci., v. 282.

Frantz, J. D., and Popp, R. K., 1979, Mineral-solution equilibria: (1) An experimental study of complexing and thermodynamic properties of aqueous $MgCl_2$ in the system MgO-SiO_2-H_2O-HCl: Geochim. et Cosmochim. Acta, v. 43, p. 1223-1239.

Friedman, H. L., 1962, Ionic Solution Theory Based on Cluster Expansion Methods: New York, Wiley-Intersci., 265 p.

———— 1972a, Lewis-Randall to McMillan-Mayer conversion for the thermodynamic excess functions of solutions. Part I. Partial free energy coefficients: Jour. Solution Chemistry, v. 1, p. 387-412.

———— 1972b, Lewis-Randall to McMillan-Mayer conversion for the thermodynamic excess functions of solutions. Part II. Excess energy and volume: Jour. Solution Chemistry, v. 1, p. 413-417.

———— 1972c, Lewis-Randall to McMillan-Mayer conversion for the thermodynamic excess functions of solutions. Part III. Common-ion mixtures of two electrolytes: Jour. Solution Chemistry, v. 5, p. 419-431.

Friedman, H. L., and Krishnan, C. V., 1973, Thermodynamics of ionic solvation, *in* Franks, F., ed., Water, v. 3, Aqueous solutions of simple electrolytes: New York, Plenum Press, p. 1-118.

Gancy, A. B., 1972, Aqueous solutions under extreme conditions. II. High temperatures, *in* Horne, R. A., ed., Water and aqueous solutions: New York, Wiley-Intersci., p. 771-801.

Gancy, A. B., and Brummer, S. B., 1969, The effect of solution concentration on the high-pressure coefficient of ionic conductance: Jour. Phys. Chemistry, v. 73, p. 2429-2436.

———— 1971, Conductance of aqueous electrolyte solutions at high pressures: Jour. Chem. Eng. Data, v. 16, p. 385-388.

Gardner, E. R., 1969, Osmotic coefficients of some aqueous sodium chloride solutions at high temperatures: Faraday Soc. Trans., v. 65, p. 91-97.

Gardner, E. R., Jones, P. J., and de Nordwall, H. J., 1963, Osmotic coefficients of some aqueous sodium chloride solutions at high temperatures: Faraday Soc. Trans., v. 59, p. 1994-2000.

Gardner, W. L., Jekel, E. C., and Cobble, J. W., 1969, The thermodynamic properties of high-temperature aqueous solutions. IX. Sodium sulfate and sulfuric acid from 0 to 100°: Jour. Phys. Chemistry, v. 73, p. 2017-2020.

Gardner, W. L., Mitchell, R. E., and Cobble, J. W., 1969a, The thermodynamic properties of high-temperature aqueous solutions. X. The electrode potentials of sulfate ion electrodes from 0 to 100°. Activity coefficients and the entropy of aqueous sulfuric acid: Jour. Phys. Chemistry, v. 78, p. 2021-2024.

———— 1969b, The thermodynamic properties of high temperature aqueous solutions. XI. Calorimetric determination of the standard partial molal heat capacity and entropy of sodium chloride solutions from 100 to 200°: Jour Phys. Chemistry, v. 73, p. 2025-2032.

Gehrig, M., Lentz, H., and Franck, E. U., 1979, Thermodynamic properties of water-carbon dioxide-sodium chloride mixtures at high temperatures and pressures, *in* Timmerhaus, K. D., and Barber, M. S., eds., High Pressure Science and Technology, Volume 1, Physical Properties and Material Synthesis: New York, Plenum Press, p. 539-542.

Gibbard, H. F., Jr., and Scatchard, G., 1972, Vapor-liquid equilibria of synthetic seawater solutions from 25-100°C: Jour. Chem. Eng. Data, v. 17, p. 498-501.

———— 1973, Liquid-vapor equilibrium of aqueous lithium chloride, from 25° to 100°C and from 1.0 to 18.5 molal, and related properties: Jour. Chem. Eng. Data, v. 18, p. 293-298.

Gibbard, H. F., Jr., Scatchard, G., Rousseau, R. A., and Creek, J. L., 1974, Liquid-vapor equilibrium of aqueous sodium chloride, from 290 to 373 K and from 1 to 6 mol kg^{-1}, and related properties: Jour. Chem. Eng. Data, v. 19, p. 281-288.

Gibson, R. E., 1934, The influence of concentration on the compressions of aqueous solutions of certain sulphates and a note on the representation of the compressions of aqueous solutions as a function of pressure: Am. Chem. Soc. Jour., v. 56, p. 4-14.

———— 1935, The influence of the concentration and nature of the solute on the compressions of certain aqueous solutions: Am. Chem. Soc. Jour., v. 57, p. 284-293.

———— 1938, On the effect of pressure on the solubility of solids in liquids: Am. Jour. Sci., 5th ser., v. 35A, p. 49-69.

Gibson, R. E., and Loeffler, O. H., 1941, Pressure-volume-temperature relations in solutions. IV. The apparent volumes and thermal expansibilities of sodium chloride and sodium bromide in aqueous solutions between 25 and 95°: Am. Chem. Soc. Jour., v. 63, p. 443-449.

Giese, K., Kaatze, U., and Pottel, R., 1970, Permittivity and dielectric and proton magnetic relaxation of aqueous solutions of the alkali halides: Jour. Phys. Chemistry, v. 74, p. 3718-3725.

Gilkerson, W. R., 1970, The importance of the effect of the solvent dielectric constant on ion-pair formation in water at high temperatures and pressures: Jour. Phys. Chemistry, v. 74, p. 746-750.

Gimblett, F. G. R., and Monk, C. B., 1954, E. M. F. Studies of electrolytic dissociation, Part 7. Some alkali and alkaline earth metal hydroxides in water: Faraday Soc. Trans., v. 50, p. 965-972.

Glueckauf, E., 1955, The influence of ionic hydration on activity coefficients in concentrated electrolyte solutions: Faraday Soc. Trans., v. 51, p. 1235-1244.

———— 1965, Molar volumes of ions: Faraday Soc. Trans., v. 61, p. 914-921.

Goldberg, R. N., and Nuttall, R. L., 1978, Evaluated activity and osmotic coefficients for aqueous solutions: The alkaline earth metal halides: Jour. Phys. Chem. Ref. Data, v. 7, p. 263-310.

Goldman, S., and Bates, R. G., 1972, Calculation of thermodynamic functions for ionic hydration: Am. Chem. Soc. Jour., v. 94, p. 1476-1484.

Goldman, S., and Morss, L. R., 1975, Semi-empirical calculations on the free energy and enthalpy of hydration for the trivalent lanthanides and actinides: Canadian Jour. Chemistry, v. 53, p. 2695-2700.

Greeley, R. S., Smith, W. J., Jr., Stoughton, R. W., and Lietzke, M. H., 1960a, Electromotive force studies in aqueous solutions at elevated temperatures. I. The standard potential of the silver-silver chloride electrode: Jour. Phys. Chemistry, v. 64, p. 652-657.

Greeley, R. S., Smith, W. J., Jr., Lietzke, M. H., and Stoughton, R. W., 1960b, Electromotive force measurements in aqueous solutions at elevated temperatures. II. Thermodynamic properties of hydrochloric acid: Jour. Phys. Chemistry, v. 64, p. 1445-1448.

Guggenheim, E. A., 1935, The specific thermodynamic properties of aqueous solutions of strong electrolytes: Philos. Mag., v. 19, p. 588-643.

Guggenheim, E. A., and Stokes, R. H., 1969, Equilibrium properties of aqueous solutions of single strong electrolytes: New York, Pergamon Press, 148 p.

Guggenheim, E. A., and Turgeon, J. C., 1955, Specific interaction of ions: Faraday Soc. Trans., v. 51, p. 747-761.

Güntelburg, E., 1926, Untersuchungen über Ioneninteraktion: Zeitschr. Phys. Chemie, v. 123, p. 199-247.

Haas, J. L., 1970, An equation for the density of vapor-saturated NaCl-H_2O solutions from 75° to 325°C: Am. Jour. Sci., v. 269, p. 489-493.

———— 1976a, Physical properties of the coexisting phases and thermochemical properties of the H_2O component in boiling NaCl solutions: U. S. Geol. Survey Bull. 1421-A, 73 p.

———— 1976b, Thermodynamic properties of the coexisting phases and thermochemical properties of the NaCl component in boiling NaCl solutions: U. S. Geol. Survey Bull. 1421-B, 71 p.

Haase, R., Dücker, K.-H., and Küppers, H. A., 1965, Aktivitätskoeffizienten und Dissoziationskonstanten wässriger Salpetersäure und Uberchlorsäure: Bunsengesell. für Phys. Chemie Ber., v. 69, p. 97-109.

Haggis, G. H., Hasted, J. B., and Buchanan, T. J., 1952, The dielectric properties of water in solutions: Jour. Chem. Physics, v. 20, p. 1452-1465.

Hamann, S. D., 1963, Chemical equilibria in condensed systems, *in* Bradley, R. S., ed., High pressure physics and chemistry, v. 2: New York, Academic Press, p. 131-162.

———— 1974, Electrolyte solutions at high pressure, *in* Bockris, J. O'M., ed., Modern Aspects of Electrochemistry, no. 9: New York, Plenum Press, p. 47-158.

———— in press, Properties of electrolyte solutions at high pressures and temperatures, *in* Wickman, F., and Rickard, D., eds., Proceedings, Nobel Symposium on the Geochemistry of Solutions at High Temperatures and Pressures (Stockholm, Royal Swedish Acad. Sci.): New York, Pergamon Press.

Hamann S. D., and Linton, M., 1969, Electrical conductivities of aqueous solutions of KCl, KOH and HCl, and the ionization of water at high shock pressures: Faraday Soc. Trans., v. 65, p. 2186-2196.

Hamann, S. C., and Strauss, W., 1955, The chemical effects of pressure, Pt. 3. Ionization constants at pressures to 12,000 atmospheres: Faraday Soc. Trans., v. 51, p. 1684-1690.

———— 1956, Ionization of piperidine in methanol to 12,000 ATM: Faraday Soc. Discussions, v. 22, p. 70-74.

Hamer, W. J., 1968, Theoretical mean activity coefficients of strong electrolytes in aqueous solutions from 0 to 100°C: Natl. Bur. Standards, Natl. Standard Ref. Data Ser., no. 24, 271 p.

Hamer, W. J., and Wu, Y.-C., 1972, Osmotic coefficients and mean activity coefficients of univalent electrolytes in water at 25°C: Jour. Phys. Chem. Ref. Data, v. 1, p. 1047-1100.

Harned, H. S., 1935, The hydrogen- and hydroxyl-ion activities of solutions of hydrochloric acid, sodium and potassium hydroxides in the presence of neutral salts: Am. Chem. Soc. Jour., v. 37, p. 2460-2482.

———— 1959, The thermodynamic properties of the system: hydrochloric acid, sodium chloride and water from 0 to 50°: Jour. Phys. Chemistry, v. 63, p. 1299-1302.

———— 1960, The thermodynamic properties of the system: Hydrochloric acid, potassium chloride and water from 0 to 40°: Jour. Phys. Chemistry, v. 64, p. 112-114.

Harned, H. S., and Gary, R., 1955a, The activity coefficient of hydrochloric acid in concentrated aqueous higher valence type chloride solutions at 25°. II. The system hydrochloric acid-strontium chloride: Am. Chem. Soc. Jour., v. 77, p. 1994-1995.

———— 1955b, The activity coefficient of hydrochloric acid in concentrated aqueous higher valence type chloride solutions at 25°. III. The system hydrochloric acid-aluminum chloride: Am. Chem. Soc. Jour., v. 77, p. 4695-4697.

Harned, H. S., and Geary, C. G., 1937, The ionic activity coefficient product and ionization of water in barium chloride solutions from 0 to 50°: Am. Chem. Soc. Jour., v. 59, p. 2032-2035.

Harned, H. S., and Mason, C. M., 1931, The activity coefficient of hydrochloric acid in aluminum chloride solutions: Am. Chem. Soc. Jour., v. 53, p. 3377-3380.

Harned, H. S., and Owen, B. B., 1958, The physical chemistry of electrolytic solutions: New York, Reinhold Book Corp., 803 p.

Harned, H. S., and Paxton, T. R., 1953, The thermodynamics of ionized water in strontium chloride solutions from electromotive force measurements: Jour. Phys. Chemistry, v. 57, p. 531-535.

Harned, H. S., and Robinson, R. A., 1968, Multicomponent electrolyte solutions: Oxford, Pergamon Press, 110 p.

Harris, F. E., and O'Konski, C. T., 1957, Dielectric properties of aqueous ionic solutions at microwave frequencies: Jour. Phys. Chemistry, v. 61, p. 310-319.

Hartman, D., and Franck, E. U., 1969, Elektrische Leitfähigkeit wasseriges Lösungen bei hohen Temperaturen und Drucken. III: Bunsengesell. für Phys. Chemie Ber., v. 73, p. 514-521.

Hasinoff, B. B., 1976, The kinetic activation volumes for the bendy of chloride to iron (III), studied by means of a high pressure laser temperature jump apparatus: Canadian Jour. Chemistry, v. 54, p. 1820-1826.

Hasted, J. B., Ritson, D. M., and Collie, C. H., 1948, Dielectric properties of aqueous ionic solutions. Parts I and II.: Jour. Chem. Physics, p. 1-21.

Hasted, J. B., and El Sabeh, S. M., 1953, Dielectric properties of water in solutions: Faraday Soc. Trans., v. 49, p. 1003-1011.

Hasted, J. B., and Roderick, G. W., 1958, Dielectric properties of aqueous and alcoholic electrolytic solutions: Jour. Chem. Physics, v. 29, p. 17-26.

Hayward, A. T. J., 1967, Compressibility equations for liquids: a comparative study: British Jour. Appl. Physics, v. 18, p. 965-977.

Heger, K., ms, 1969, Die statische Dielecktrizitätskonstante von Wasser und Methylalkohol im überkritischen Temperatur- und Druckbereich: Ph.D. dissert., Univ. Karlsruhe, Karlsruhe, West Germany, 59 p.

Helgeson, H. C., 1964, Complexing and hydrothermal ore deposition: London, Pergamon Press, 128 p.

Helgeson, H. C., 1967, Thermodynamics of complex dissociation in aqueous solution at elevated temperatures: Jour. Phys. Chemistry, v. 71, p. 3121-3126.

———— 1969, Thermodynamics of hydrothermal systems at elevated temperatures and pressures: Am. Jour. Sci., v. 267, p. 729-804.

———— in press, Prediction of the thermodynamic properties of electrolytes at high pressures and temperatures, *in* Wickman, F., and Rickard, D., eds., Proceedings, Nobel Symposium on the Chemistry and Geochemistry of Solutions at High Temperatures and Pressures (Stockholm, Royal Swedish Acad. Sci.): New York, Pergamon Press.

Helgeson, H. C., and James, W. R., 1968, Activity coefficients in concentrated electrolyte solutions at high temperatures: Am. Chem. Soc., 155th Natl. Mtg., San Francisco, April 1968, Abs. of Papers, p. 5-130.

Helgeson, H. C., and Kirkham, D. H., 1974a, Theoretical prediction of the thermodynamic behavior of aqueous electrolytes at high pressures and temperatures. I. Summary of the thermodynamic/electrostatic properties of the solvent: Am. Jour. Sci., v. 274, p. 1089-1098.

———— 1974b, Theoretical prediction of the thermodynamic behavior of aqueous electrolytes at high pressures and temperatures. II. Debye-Hückel parameters for activity coefficients and relative partial molal properties: Am. Jour. Sci., v. 274, p. 1199-1261.

———— 1976, Theoretical prediction of the thermodynamic properties of aqueous electrolytes at high pressures and temperatures. III. Equation of state for aqueous species at infinite dilution: Am. Jour. Sci., v. 276, p. 97-240.

Hemingway, B. S., and Robie, R. A., 1977, The entropy and Gibbs free energy of formation of the aluminum ion: Geochim. et Cosmochim. Acta, v. 41, p. 1402-1404.

Hemley, J. J., Montoya, J. W., Christ, C. L., and Hostetler, P. B., 1977a, Mineral equilibria in the MgO-SiO_2-H_2O system: I. Talc-chrysotile-forsterite-brucite stability relations: Am. Jour. Sci., v. 277, p. 322-351.

Hemley, J. J., Montoya, J. W., Nigrini, A., and Vincent, H. A., 1971, Some alteration reactions in the system CaO-Al_2O_3-SiO_2-H_2O: Soc. Mining Geology [Japan], Spec. Issue 2, p. 58-63.

Hemley, J. J., Montoya, J. W., Shaw, D. R., and Luce, R. W., 1977b, Mineral equilibria in the MgO-SiO_2-H_2O system: II. Talc-antigorite-forsterite-anthophyllite-enstatite stability relations and some geologic implications in the system: Am. Jour. Sci., v. 277, p. 353-383.

Hensel, F., and Franck, E. U., 1964, Die elektrische Leitfähigkeit wässriger Salzlösungen bis zu 130°C und 8000 bar: Zeitschr. Naturforsch., v. 19a, p. 127-132.

Hepler, L. G., and Wooley, E. M., 1973, Hydration effects and acid-base equilibria, *in* Franks, F., ed., Water, v. 3, Aqueous Solutions of Simple Electrolytes: New York, Plenum Press, p. 145-172.

Herwig, H., 1877, Über den elektrischen Widerstand von Flüssigkeiten under hohem Druck: Ann. Physik und Chemie, v. 160, p. 110-113.

Hilbert, R., ms, 1979, pVT-Daten von Wasser und von wässrigen Natriumchlorid-Lösungen bis 873 K, 4000 Bar und 25 Gewichtsprozent NaCl: Ph.D. dissert., Univ. Karlsruhe, Karlsruhe, West Germany, 212 p.

Hinchey, R. J., and Cobble, J. W., 1970, Standard state entropies for the aqueous trivalent lanthanide and yttrium ions: Inorganic Chemistry, v. 9, p. 917-921.

Hitch, B. F., and Mesmer, R. E., 1976, The ionization of aqueous ammonia to 300°C in KCl media: Jour. Solution Chemistry, v. 5, p. 667-680.

Hogfeldt, E., in press, Stability constants of metal-ion complexes — Part A — Inorganic ligands, IUPAC Chem. Data Ser. 22: Oxford, Pergamon Press.

Holmes, H. F., Baes, C. F., Jr., and Mesmer, R. E., 1978, Isopiestic studies of aqueous solutions at elevated temperatures. I. KCl, $CaCl_2$, and $MgCl_2$: Jour. Chem. Thermodynamics, v. 10, p. 983-996.

———— 1979, Isopiestic studies of aqueous solutions at elevated temperatures. II. NaCl + KCl mixtures: Jour. Solution Chemistry, v. 11, p. 1035-1050.

———— 1981, Isopiestic studies of aqueous solutions at elevated temperatures. III. $\{(1-y)NaCl + yCaCl_2\}$: Jour. Chem. Thermodynamics, v. 13, p. 101-113.

Holmes, H. F., and Mesmer, R. E., 1981, Isopiestic studies of aqueous solutions at elevated temperatures. IV. $NiCl_2$ and $CoCl_2$: Jour. Chem. Thermodynamics, v. 13, p. 131-137.

Holzapfel, W., and Franck, E. U., 1966, Leitfähigkeit und Ionendissoziation des Wassers bis 1000°C und 100 Kbar: Ber. Bunsengesell. für Phys. Chemie, v. 70, p. 1106-1112.

Horne, R. A., 1969, Marine Chemistry: New York, Wiley-Intersci., 568 p.

———— ed., 1972, Water and Aqueous Solutions: New York, Wiley-Intersci., 837 p.

Horne, R. A., Holm, R. H., and Meyers, M. D., 1957, The adsorption of zinc (II) on anion-exchange resins. III. The adsorption from bromide, fluoride, cyanide, oxalate, acetate, nitrate, phosphate, sulfate, and alkaline media; the perchlorate effect and the adsorption from mixed solvent media: Jour. Phys. Chemistry, v. 61, p. 1661-1665.

Horne, R. A., and Young, R. P., 1967, The electrical conductivity of aqueous 0.03 to 4.0 m potassium chloride solutions under hydrostatic pressure: Jour. Phys. Chemistry, v. 71, p. 3824-3832.

Hsia, K.-L., and Fuoss, R. M., 1968, Conductance of the alkali halides, XI. Cesium bromide and iodide in water at 25°: Am. Chem. Soc. Jour., v. 90, p. 3055-3060.

Hückel, E., 1925, Zur Theorie konzentrierterer wässeriger Lösungen starker Elektrolyte: Phys. Zeitschr., v. 26, p. 93-147.

Humphries, W. T., Kohrt, C. F., and Patterson, C. S., 1968, Osmotic properties of some aqueous electrolytes at 60°C: Jour. Chem. Eng. Data, v. 13, p. 327-330.

Hwang, J. U., Ludemann, H. D., and Hartmann, D., 1970, Die elektrische Leitfähigkeit konzentrierter wässriger Alkalihalogenidlösungen bei hohen Drucken und Temperaturen: High Temperatures-High Pressures, v. 2, p. 651-669.

Inada, E., Shimizu, K., and Osugi, J., 1971, Electrical conductance of $CaSO_4$ in aqueous solution under high pressure: Nippon Kagaku Zasshi, v. 92, p. 1096-1101.

———— 1972, Electrical conductivity of $CaSO_4$ in aqueous solution under high pressure: Rev. Phys. Chemistry [Japan], v. 42, p. 1-11.

Jekel, E. C., Criss, C. M., and Cobble, J. W., 1964, The thermodynamic properties of high temperature aqueous solutions. VIII. Standard partial molal heat capacities of gadolinium chloride from 0 to 100°: Am. Chem. Soc. Jour., v. 86, p. 5405-5407.

Johnson, K. S., and Pytkowicz, R. M., 1978, Ion association of Cl^- with H^+, Na^+, K^+, Ca^{++}, and Mg^{++} in aqueous solutions at 25°C: Am. Jour. Sci., v. 278, p. 1428-1447.

———— 1979, Ion association and activity coefficients in multicomponent solutions, *in* Pytkowicz, R. M., ed., Activity Coefficients in Electrolyte Solutions, v. II: Boca Raton, Florida, CRC Press, Inc., p. 1-62.

Jost, A., 1976, Fast reactions in solutions at high pressures (III): The effect of pressure on the reactions of Fe(III)-ions with thiocyanate in water up to 2 KBAR and 25°C: Bunsengesell. Phys. Chemie Ber., v. 80, p. 316-321.

Justice, J., 1978, Ionic interactions in solutions. III. Derivation of the "associated" electrolyte formulation from the Onsager treatment of conductance: Jour. Solution Chemistry, v. 7, p. 859-875.

Justice, J., and Ebeling, W., 1979, Ionic interactions in solutions. IV. Conductance theory of binary electrolytes for Hamiltonian models: Jour. Solution Chemistry, v. 8, p. 809-833.

Justice, M., and Justice, J., 1976, Ionic interactions in solutions. I. The association concepts and the McMillan-Mayer theory: Jour. Solution Chemistry, v. 5, p. 543-561.

———— 1977, Ionic interactions in solutions. II. The theoretical basis of the equilibrium between free and pairwise associated ions: Jour. Solution Chemistry, v. 6, p. 819-826.

Kalyanaraman, R., Yeatts, L. B., and Marshall, W. L., 1973a, High-temperature Debye-Huckel correlated solubilities of calcium sulfate in aqueous sodium perchlorate solutions: Jour. Chem. Thermodynamics, v. 5, p. 891-898.

———— 1973b, Solubility of calcium sulfate and association equilibria in $CaSO_4 + Na_2SO_4 + NaClO_4 + H_2O$ at 273 to 623°K: Jour. Chem. Thermodynamics, v. 5, p. 899-909.

Kasper, R. B., Holloway, J. R., and Naviotski, A., 1979, Direct calorimetric measurements of enthalpies of aqueous sodium chloride solutions at high temperatures and pressures: Jour. Chem. Thermodynamics, v. 11, p. 13-24.

Katayama, S., 1976, Conductimetric determination of ion-association constants for calcium, cobalt, zinc, and cadmium sulfates in aqueous solutions at various temperatures between 0°C and 45°C: Jour. Solution Chemistry, v. 5, p. 241-248.

Kavanau, J. L., 1964, Water and solute-water interactions: San Francisco, Holden-Day, Inc., 101 p.

Kebarle, P., 1977, Ion thermochemistry and solvation from gas phase ion equilibria, *in* Rabinovitch, B. S., ed., Annual Review of Physical Chemistry, Volume 28: Palo Alto, Calif., Ann. Rev., Inc., p. 445-476.

Keevil, N. B., 1942, Vapor pressures of aqueous solutions at high temperature: Am. Chem. Soc. Jour., v. 64, p. 841-849.

Kester, D. R., and Pytkowicz, R. M., 1970, Effect of temperature and pressure on sulphate ion association in sea water: Geochim. et Cosmochim. Acta, v. 34, p. 1039-1051.

Khitarov, N. I., 1965, Geochemical investigation in the field of higher pressures and temperatures (in Russian): Moscow, Nauka Publishing Office, 204 p.

Khodakovskiy, I. L., 1969, Thermodynamics of aqueous solutions of electrolytes at elevated temperatures (entropies of ions in aqueous solutions at elevated temperatures): Geokhimiya, no. 1, p. 57-63.

Khodakovskiy, I. L., Ryzhenko, B. N., and Naumov, G. B., 1968, Thermodynamics of aqueous electrolyte solutions at elevated temperatures (temperature dependence of the heat capacities of ions in aqueous solutions): Geokhimiya, no. 12, p. 1486-1503.

Kielland, J., 1937, Individual activity coefficients of ions in aqueous solutions: Am. Chem. Soc. Jour., v. 59, p. 1675-1678.

Kivalo, P., and Ekari, P., 1957, A polarographic study of the bromo complexes of cadmium. Variation of the stability contents with ionic strength: Suomen Kem., v. 30, B, p. 116-120.

Konrat'ev, V. P., and Nikich, V. I., 1963, Specific conductance of aqueous solutions of alkaline earth metal chlorides at high temperatures: Russian Jour. Phys. Chemistry, v. 37, p. 47-50.

Kracek, F. C., 1931, The solubility of potassium iodide in water to 240°: Jour. Phys. Chemistry, v. 35, p. 947-949.

Lanier, R. D., 1965, Activity coefficients of sodium chloride in aqueous three-component solutions by cation-sensitive glass electrodes: Jour. Phys. Chemistry, v. 69, p. 3992-3998.

Latimer, W. M., 1952, The Oxidation States of the Elements and their Potentials in Aqueous Solutions: Englewood Cliffs, N. J., Prentice-Hall, Inc., 392 p.

———— 1955, Single ion free energies and entropies of aqueous ions: Jour. Chem. Physics, v. 23, p. 90-92.

Leong, T. H., and Dunn, L. A., 1972, Electrical conductances and ionization behavior of sodium chloride in dioxane-water mixtures at 50°: Jour. Phys. Chemistry, v. 76, p. 2294-2298.

Leung, C. S., and Grunwald, E., 1970, Temperature dependence of $\Delta Cp°$ for the self-ionization of methanol and for the acid dissociation of benzoic acid in methanol: Jour. Phys. Chemistry, v. 74, p. 696-699.

Leung, W. H., and Millero, F. J., 1975a, The enthalpy of dilution of some 1-1 and 2-1 electrolytes in aqueous solution: Jour. Chem. Thermodynamics, v. 7, p. 1067-1078.

———— 1975b, The enthalpy of formation of magnesium sulfate ion pairs: Jour. Solution Chemistry, v. 4, p. 145-160.

Lewis, G. N., and Randall, M., 1961, Thermodynamics, 2d ed., revised by Pitzer, K. S., and Brewer, L.: New York, McGraw-Hill, 723 p.

Li, Y. H., 1967, Equation of the state of water and sea water: Jour. Geophys. Research, v. 72, p. 2665-2678.

Lietzke, M. H., and Stoughton, R. W., 1959a, The solubility of silver sulfate in electrolyte solutions. Part 1. Solubility in potassium nitrate solutions: Jour. Phys. Chemistry, v. 63, p. 1183-1186.

———— 1959b, The solubility of silver sulfate in electrolyte solutions. Part 2. Solubility in potassium sulfate solutions: Jour. Phys. Chemistry, v. 63, p. 1186-1187.

———— 1959c, The solubility of silver sulfate in electrolyte solutions. Part 3. Solubility in sulfuric acid solutions: Jour. Phys. Chemistry, v. 63, p. 1188-1189.

———— 1959d, The solubility of silver sulfate in electrolyte solutions. Part 4. Solubility in nitric acid solutions: Jour. Phys. Chemistry, v. 63, p. 1190-1192.

———— 1959e, The solubility of silver sulfate in electrolyte solutions. Part 5. Solubility in magnesium sulfate solutions: Jour. Phys. Chemistry, v. 63, p. 1984-1986.

———— 1962a, The thermodynamic investigation of aqueous electrolytes to 275°C: Jour. Chem. Education, v. 39, p. 230-235.

———— 1962b, The thermodynamics of aqueous electrolyte mixtures at elevated temperatures. The solubility of silver sulfate in KNO_3-K_2SO_4, K_2SO_4-$MgSO_4$, and K_2SO_4-H_2SO_4 mixtures: Jour. Phys. Chemistry, v. 66, p. 2264-2266.

———— 1962c, The calculation of activity coefficients from osmotic coefficient data: Jour. Phys. Chemistry, v. 66, p. 508-509.

———— 1963a, The second dissociation constant of deuteriosufuric acid from 25 to 225°: Jour. Phys. Chemistry, v. 67, p. 652-654.

———— 1963b, Electromotive force studies in aqueous solutions at elevated temperatures. IV. The activity coefficients of hydrogen bromide and potassium bromide in hydrogen bromide-potassium bromide mixtures: Jour. Phys. Chemistry, v. 67, p. 2573-2576.

———— 1964a, Electromotive force studies in aqueous solutions at elevated temperatures. V. The thermodynamic properties of DCl solutions: Jour. Phys. Chemistry, v. 68, p. 3043-3047.

———— 1964b, The activity coefficients of hydrochloric acid and sodium chloride in hydrochloric acid-sodium chloride mixtures: Tennessee Acad. Sci. Jour., v. 39, p. 30-34.

———— 1974, The prediction of osmotic and activity coefficients for electrolyte mixtures at elevated temperatures: Oak Ridge Natl. Lab. Rep. 4999, UC-4, 16 p.

Lietzke, M. H., Hupf, H. B., and Stoughton, R. W., 1965, Electromotive force studies in aqueous solutions at elevated temperatures. VI. The thermodynamic properties of HCl-NaCl mixtures: Jour. Phys. Chemistry, v. 69, p. 2395-2399.

Likke, S., ms, 1967, Heat capacity and some thermodynamic properties of several aqueous salt solutions to 200°C: Ph.D. dissert., Univ. California, Berkeley, 149 p.

Likke, S., and Bromley, L. A., 1973, Heat capacities of aqueous NaCl, KCl, $MgCl_2$, $MgSO_4$, and Na_2SO_4 solutions between 80°C and 200°C: Jour. Chem. Eng. Data, v. 18, p. 189-195.

Lindsay, W. T., Jr., and Liu, C. T., 1968, Vapor pressure lowering of aqueous solutions at elevated temperatures: Final report, Contract #14-01-0001-407: U. S. Dept. Interior, Washington, D. C., Div. Chemistry, Office of Saline Water, 235 p.

———— 1971, Osmotic coefficients of one molal alkali metal chloride solutions over a 300° temperature range: Jour. Phys. Chemistry, v. 75, p. 3723-3727.

Linov, E. D., and Kryukov, P. A., 1972, Ionization of water at pressures up to 8000 kg/cm²: Akad. Nauk. SSSR Izv. Sibirsk. Otd., Ser. Khim, Nauk 4, p. 10-13.

Liphard, K. G., Jost, A., and Schneider, G. M., 1977, Determination of the specific heat capacities of aqueous sodium chloride solutions at high pressure with the temperature jump technique: Jour. Phys. Chemistry, v. 81, p. 547-550.

Liu, C., and Lindsay, W. T., Jr., 1970, Osmotic coefficients of aqueous sodium chloride solutions from 125 to 300°: Jour. Phys. Chemistry, v. 74, p. 341-346.

———— 1971, Thermodynamic properties of aqueous solutions at high temperatures. Final report, Contract No. 14-01-0001-2126: Washington, D. C., Office of Saline Water, Div. Chemistry, U. S. Dept. Interior, 124 p.

———— 1972, Thermodynamics of sodium chloride solutions at high temperatures: Jour. Solution Chemistry, v. 1, p. 45-70.

Lo Surdo, A., and Millero, F. J., 1980a, Apparent molal volumes and adiabatic compressibilities of aqueous transition metal chlorides at 25°C: Jour. Phys. Chemistry, v. 84, p. 710-715.

———— 1980b, The volume and compressibility change for the formation of transition metal sulfate ion pairs at 25°C: Jour. Solution Chemistry, v. 9, p. 163-181.

Lown, D. A., Thirsk, H. R., and Lord Wynne-Jones, 1968, Effect of pressure on ionization equilibria in water at 25°C: Faraday Soc. Trans., v. 64, p. 2073-2080.

———— 1970, Temperature and pressure dependence of the volume of the ionization of acetic acid in water from 25-225°C and 1-3000 bars: Faraday Soc. Trans., v. 66, p. 51-73.

Mangold, K., and Franck, E. U., 1969, Elektrische Leitfähigkeit wässeriger Lösungen bei hohen Temperaturen und Drucken. II: Bunsengesell. für Phys. Chemie Ber., v. 73, p. 21-27.

Maier, C. G., and Kelley, K. K., 1932, An equation for the representation of high temperature heat content data: Am. Chem. Soc. Jour., v. 54, p. 3243-3246.

Marshall, W. L., 1967, Aqueous systems at high temperature. XX. The dissociation constant and thermodynamic functions for magnesium sulphate to 200°: Jour. Phys. Chemistry, v. 71, p. 3584-3588.

———— 1968, Conductances and equilibria of aqueous electrolytes over extreme ranges of temperature and pressure: Rev. Pure Appl. Chemistry, v. 18, p. 167-186.

———— 1969, Correlations in aqueous electrolyte behavior to high temperatures and pressures: Rev. Chem. Progress, v. 30, p. 61-84.

———— 1970, Complete equilibrium constants, electrolyte equilibria, and reaction rates: Jour. Phys. Chemistry, v. 74, p. 346-355.

———— 1972a, Predictions of the geochemical behavior of aqueous electrolytes at high temperatures and pressures: Chem. Geology, p. 59-68.

———— 1972b, A further description of complete equilibrium constants: Jour. Phys. Chemistry, v. 76, p. 720-731.

———— 1975, Water and its solutions at high temperatures and pressures: Chemistry, v. 48, p. 6-12.

———— 1980a, Amorphous silica solubilities I. Behavior in aqueous sodium nitrate solutions; 25-300°C, 0-6 molal: Geochim. et Cosmochim. Acta, v. 44 (in press).

———— 1980b, Amorphous silica solubilities III. Activity coefficient relations and predictions of solubility behavior in salt solutions, 0-350°C: Geochim. et Cosmochim. Acta, v. 44 (in press).

Marshall, W. L., and Franck, E. U., 1981, Ion product of water substance, 0-1000°C, 1-10,000 bars, New international formulation and its background: Jour. Phys. Chem. Ref. Data, v. 10, p. 295-304.

Marshall, W. L., and Jones, E. V., 1966, Second dissociation constant of sulfuric acid from 25 to 350° evaluated from solubilities of calcium sulfate in sulfuric acid solutions: Jour. Phys. Chemistry, v. 70, p. 4028-4040.

Marshall, W. L., and Mesmer, R. E., 1981, On the treatment of pressure effects on ionization constants in aqueous solution: Jour. Solution Chemistry, v. 10, p. 121-127.

Marshall, W. L., and Slusher, R., 1965, Aqueous systems at high temperature. XV. Solubility and hydrolytic instability of magnesium sulfate in sulfuric acid-water and deuterosulfuric acid-deuterium oxide solutions, 200° to 350°C: Jour. Chem. Eng. Data, v. 10, p. 353-359.

———— 1966, Thermodynamics of calcium sulfate dihydrate in aqueous sodium chloride solutions, 0-110°: Jour. Phys. Chemistry, v. 70, p. 4015-4027.

———— 1968, Aqueous systems at high temperature. Solubility to 200° of calcium sulfate and its hydrates in sea water with saline water concentrates, and temperature-concentration limits: Jour. Chem. Eng. Data, v. 13, p. 83-93.

———— 1973, Debye-Hückel correlated solubilities of calcium sulfate in water and in aqueous sodium nitrate and lithium nitrate solutions of molality 0 to 6 mol Kg^{-1} and at temperatures from 398 to 623 K: Jour. Chem. Thermodynamics, v. 5, p. 189-197.

———— 1975a, The ionization constant of nitric acid at high temperatures from solubilities of calcium sulfate in HNO_3-H_2O, 100-350°C; activity coefficients and thermodynamic functions: Jour. Inorganic Nuclear Chemistry, v. 37, p. 1191-1202.

———— 1975b, Experimental and calculated solubilities of magnesium sulfate monohydrate in aqueous nitric acid and related solubilities, 200-350°C; ionization constants of nitric acid at 300-370°C: Jour. Inorganic Nuclear Chemistry, v. 37, p. 2165-2170.

Marshall, W. L., Slusher, R., and Jones, E. V., 1964, Aqueous systems at high temperature. XIV. Solubility and thermodynamic relationships for $CaSO_4$ in NaCl-H_2O solutions from 40° to 220°C, 0 to 4 molal NaCl: Jour. Chem. Eng. Data, v. 9, p. 187-191.

Mashovets, V. P., Zarembo, V. I., and Fedorov, M. K., 1973, Vapor pressures of aqueous solutions of NaCl, NaBr, and NaI at temperatures in the range 150-350°: Zhur. Prikladnoi Khimii, v. 46, p. 650-652.

Masson, D. O., 1929, Solute molecular volumes in relation to solvation and ionization: Philos. Mag., v. 8, p. 218-235.

Masterton, W. L., and Berka, L. H., 1966, Evaluation of ion-pair dissociation constants from osmotic coefficients: Jour. Phys. Chemistry, v. 70, p. 1924-1929.

Mastroianni, M., ms, 1971, The partial molal heat capacities of selected electrolytes in water and methanol at various temperatures: Ph.D. dissert., Univ. Miami, Coral Gables, Fla., 113 p.

Matheson, R. A., 1969, The thermodynamics of electrolyte equilibria in media of variable water composition: Jour. Phys. Chemistry, v. 73, p. 3635-3642.

Mathieson, J. G., and Conway, B. E., 1974, Partial molal compressibilities of salts in aqueous solution and assignment of ionic contributors: Jour. Solution Chemistry, v. 3, p. 455-477.

Mayer, J. E., 1950, The theory of ionic solutions: Jour. Chem. Physics, v. 18, p. 1426-1436.

McGee, K. A., and Hostetler, P. B., 1975, Studies in the system MgO-SiO_2-CO_2-H_2O (IV): The stability of $MgOH^+$ from 10° to 90°C: Am. Jour. Sci., v. 275, p. 305-317.

McKenzie, W. F., and Helgeson, H. C., 1979, Calculation of the dielectric constant of H_2O and the thermodynamic properties of aqueous species to 900°C: Geol. Soc. America Abs. with Programs, v. 11, p. 476.

Meissner, H. P., and Kusik, C. L., 1972, Activity coefficients of strong electrolytes in multicomponent aqueous solutions: Am. Inst. Chem. Eng. Jour., v. 18, p. 294-298.

Meissner, H. P., Kusik, C. L., and Tester, J. W., 1972, Activity coefficients of strong electrolytes in aqueous solution — effect of temperature: Am. Inst. Chem. Eng. Jour., v. 18, p. 661-662.

Meissner, H. P., and Tester, J. W., 1972, Activity coefficients of strong electrolytes in aqueous solutions: Ind. Eng. Chem. Process Design Devel., v. 11, p. 128-133.

Mesmer, R. E., and Baes, C. F., Jr., 1971, Acidity measurements at elevated temperatures. V. Aluminum ion hydrolysis: Inorganic Chemistry, v. 10, p. 2290-2296.

———— 1974, Phosphoric acid dissociation equilibria in aqueous solutions to 300°C: Jour. Solution Chemistry, v. 3, p. 307-322.

Mesmer, R. E., Baes, C. F., Jr., and Sweeton, F. H., 1970, Acidity measurements at elevated temperatures. IV. Apparent dissociation product of water in 1 m potassium chloride up to 292°: Jour. Phys. Chemistry, v. 74, p. 1937-1952.

———— 1972, Acidity measurements at elevated temperatures. VI. Boric acid equilibria: Inorganic Chemistry, v. 11, p. 537-543.

Messikomer, E. E., and Wood, R. H., 1975, The enthalpy of dilution of aqueous sodium chloride at 298.15 to 373.15 K, measured with a flow calorimeter: Jour. Chem. Thermodynamics, v. 7, p. 117-130.

Millero, F. J., 1968, Apparent molal expansibilities of some divalent chlorides in aqueous solution at 25°: Jour. Phys. Chemistry, v. 72, p. 4589-4593.

———— 1970, The apparent and partial molal volume of aqueous sodium chloride solutions at various temperatures: Jour. Phys. Chemistry, v. 74, p. 356-362.

———— 1971, The molal volumes of electrolytes: Chem. Rev., v. 71, p. 147-176.

———— 1972a, The partial molal volume of electrolytes in aqueous solutions, *in* Horne, R. A., ed., Water and aqueous solutions: New York, John Wiley & Sons, Inc., p. 519-564.

———— 1972b, Compilation of the partial molal volumes of electrolytes at infinite dilution, $\bar{V}°$, and the apparent molal volume concentration dependence constants, S_V^* and b_V, at various temperatures, *in* Horne, R. A., ed., Water and aqueous solutions: New York, John Wiley & Sons, Inc., p. 565-595.

———— ms, 1973, Compilation of apparent molal compressibility data for electrolytes: Miami, Fla., Rosentiel School of Marine and Atmospheric Sciences, 12 p.

———— 1973a, Heat capacity of seawater solutions from 5° to 35°C and 0.5 to 22% chlorinity: Jour. Geophys. Research, v. 78, p. 4499-4507.

———— 1973b, Seawater — A test of multicomponent electrolyte solutions theories. I. The apparent equivalent volume, expansibility and compressibility of artificial seawater: Jour. Solution Chemistry, v. 2, p. 1-22.

———— 1973c, Theoretical estimates of the isothermal compressibility of sea water: Deep-Sea Research, v. 20, p. 101-105.

———— 1977, The use of the specific interaction model to estimate the partial molal volumes of electrolytes in seawater: Geochim. et Cosmochim. Acta, v. 41, p. 215-223.

———— 1979, Effects of pressure and temperature on activity coefficients, *in* Pytkowicz, R. M., ed., Activity Coefficients in Electrolyte Solutions, v. 2: Boca Raton, Fla., CRC Press, Inc., p. 63-151.

Millero, F. J., Chetirkin, P., and Culkin, F., 1977, The relative conductivity and density of standard seawaters: Deep-Sea Research, v. 24, p. 315-321.

Millero, F. J., and Drost-Hansen, W., 1968a, Apparent molal volumes of ammonium chloride and some symmetrical tetraalkylammonium chlorides at various temperatures: Jour. Phys. Chemistry, v. 72, p. 1758-1763.

———— 1968b, Apparent molal volumes of aqueous monovalent salt solutions at various temperatures: Jour. Chem. Eng. Data, v. 13, p. 330-333.

Millero, F. J., Gonzalez, A., and Ward, G. K., 1976, The density of seawater solutions at one atmosphere as a function of temperature and salinity: Jour. Marine Research, v. 34, p. 61-93.

Millero, F. J., Hansen, L. D., and Hoff, E. V., 1973, The enthalpy of seawater from 0 to 30°C and from 0 to 40% salinity: Jour. Marine Research, v. 31, p. 21-39.

Millero, F. J., Hoff, E. V., and Kahn, L., 1972, The effect of pressure on the ionization of water at various temperatures from molal-volume data: Jour. Solution Chemistry, v. 1, p. 309-327.

Millero, F. J., Kembro, A., and Lo Surdo, A., 1980, Adiabatic partial molal compressibilities of electrolytes in 0.725 m NaCl solutions at 25°C: Jour. Phys. Chemistry, v. 84, p. 2728-2734.

Millero, F. J., Knox, J. H., and Emmet, R. T., 1972, A high-precision, variable-pressure magnetic float densimeter: Jour. Solution Chemistry, v. 1, p. 173-186.

Millero, F. J., and Kubinski, 1975, The speed of sound in seawater as a function of temperature and salinity at one atmosphere: Acoustical Soc. America Jour., v. 57, p. 312-319.

Millero, F. J., and Lepple, F. K., 1973, The density and expansibility of artificial seawater solutions from 0 to 40°C and 0 to 21% chlorinity: Marine Chemistry, v. 1, p. 89-104.

Millero, F. J., and Masterton, W. L., 1974, Volume change for the formation of magnesium sulfate ion pairs at various temperatures: Jour. Phys. Chemistry, v. 78, p. 1287-1294.

Millero, F. J., Perron, G., and Desnoyers, J. E., 1973, Heat capacity of seawater solutions from 5 to 35°C and 0.5 to 22% chlorinity: Jour. Geophys. Research, v. 78, p. 4499-4507.

Millero, F. J., Ward, G. K., Lepple, F. K., and Hoff, E. V., 1974, Isothermal compressibility of aqueous sodium chloride, magnesium chloride, sodium sulfate, and magnesium sulfate solutions from 0 to 45° at 1 atm: Jour. Phys. Chemistry, v. 78, p. 1636-1643.

Mitchell, R. E., and Cobble, J. W., 1964, The thermodynamic properties of high temperature aqueous solutions. VII. The standard partial molal heat capacities of cesium iodide from 0 to 100°: Am. Chem. Soc. Jour., v. 86, p. 5401-5403.

Moore, J. T., Humphries, W. T., and Patterson, C. S., 1972, Isopiestic studies of some aqueous electrolyte solutions at 80°C: Jour. Chem. Eng. Data, v. 17, p. 180-184.

Morey, G. W., and Chen, W. T., 1956, Pressure-temperature curves in some systems containing water and salt: Am. Chem. Soc. Jour., v. 78, p. 4249-4252.

Morey, G. W., and Hesselgesser, J. M., 1951, The solubility of some minerals in superheated steam at high pressures: Econ. Geology, 46, 821-835.

———— 1952, The system H_2O-Na_2O-SiO_2 at 400°C: Am. Jour. Sci., Bowen Volume, p. 343-358.

Nair, V. S. K., and Nancollas, G. H., 1958, Thermodynamics of ion association. Part IV. Magnesium and zinc sulphates: Chem. Soc. [London] Jour., p. 3706-3710.

Nancollas, G. H., 1960, Thermodynamics of ion association in aqueous solution: Quart. Rev. [London], v. 14, p. 402-426.

Naumov, G. B., Ryzhenko, B. N., and Khodakovskiy, I. L., 1968, Thermodynamics of aqueous electrolyte solutions at elevated temperatures: Geochemistry Internat., v. 5, p. 696-705.

———— 1971, Handbook of Thermodynamic Quantities for Geology (in Russian): Moscow, Atomic Press, 240 p.

Nesbitt, H. W., 1981, pH-electrode measurements of single-ion activity coefficients consistent with a pH convention: Chem. Geology, v. 32, p. 207-219.

North, N. A., 1973, Pressure dependence of equilibrium constants in aqueous solutions: Jour. Phys. Chemistry, v. 77, p. 931-934.

Noyes, A. A., 1907, The electrical conductivity of aqueous solutions: Carnegie Inst. Washington, Pub. 63, 352 p.

Noyes, A. A., Kato, Y., and Sosman, R. B., 1910, The hydrolysis of ammonium acetate and the ionization of water at high temperatures: Am. Chem. Soc. Jour., v. 32, p. 159-178.

Nriagu, J. O., and Anderson, G. M., 1971, Stability of the lead (II) chloride complexes at elevated temperatures: Chem. Geology, v. 7, p. 171-183.

Olofsson, G., 1975, Thermodynamic quantities for the dissociation of the ammonium ion and for the ionization of aqueous ammonia over a wide temperature range: Jour. Chem. Thermodynamics, v. 7, p. 507-514.

Olofsson, G., and Hepler, L. G., 1975, Thermodynamics of ionization of water over wide ranges of temperature and pressure: Jour. Solution Chemistry, v. 4, p. 127-144.

Olofsson, G., and Olofsson, I. V., 1973, A calorimetric determination of the enthalpy of ionization of water from 290 to 418 K: Jour. Chem. Thermodynamics, v. 5, p. 533-540.

———— 1977, The enthalpy of ionization of water between 273 and 323 K: Jour. Chem. Thermodynamics, v. 9, p. 65-69.

Olofsson, I. V., 1979, Apparent molar heat capacities and volumes of aqueous NaCl, KCl, and KNO_3 at 298.15 K. Comparison of Picker flow calorimeter with other calorimeters: Jour. Chem. Thermodynamics, v. 11, p. 1005-1014.

Olofsson, I. V., Spitzer, J. J., and Hepler, L. G., 1978, Apparent molar heat capacities and volumes of aqueous electrolytes at 25°C: Na_2SO_4, K_2SO_4, $Na_2S_2O_3$, $Na_2S_2O_8$, $K_2S_2O_8$, K_2CrO_4, Na_2MoO_4, and Na_2WO_4: Canadian Jour. Chemistry, v. 56, p. 1871-1873.

Olofsson, I. V., and Sunner, S., 1979, A modified reaction-solution rotating bomb calorimeter with air thermostat. The enthalpy of ionization of water at 298.15, 373.65, and 415.15 K: Jour. Chem. Thermodynamics, v. 11, p. 605-611.

Orville, P. M., 1963, Alkali ion exchange between vapor and feldspar phases: Am. Jour. Sci., v. 261, p. 201-237.

Oshry, H. I., ms, 1949, The dielectric constant of saturated water from the boiling point to the critical point: Ph.D. dissert., Univ. Pittsburgh, Pittsburgh, Pa., 13 p.

Ostapenko, G. T., and Samoilovich, L. A., 1971, Partial and apparent molar volumes in aqueous lithium chloride, sodium chloride, and potassium chloride solutions at high temperatures and pressures: Russian Jour. Phys. Chemistry, v. 45, p. 1198-1199.

Owen, B. B., and Brinkley, S. R., Jr., 1941, Calculation of the effect of pressure upon ionic equilibria in pure water and in salt solutions: Chem. Reviews, v. 29, p. 461-474.

Owen, B. B., and Kronick, P. L., 1961, Standard partial molal compressibilities by ultrasonics. II. Sodium and potassium chlorides and bromides from 0 to 30°: Jour. Phys. Chemistry, v. 65, p. 84-87.

Owen, B. B., Miller, R. C., Milner, C. E., and Cogan, H. L., 1961, The dielectric constant of water as a function of temperature and pressure: Jour. Phys. Chemistry, v. 65, p. 2065-2070.

Owen, B. B., and Simons, H. L., 1957, Standard partial molal compressibilities by ultrasonics. I. Sodium chloride and potassium chloride at 25°: Jour. Phys. Chemistry, v. 61, p. 479-482.

Panckhurst, M. H., and Macaskill, J. B., 1976a, Specific interactions and single-ion activity coefficients in mixed electrolyte solutions: Jour. Solution Chemistry, v. 5, p. 469-482.

———— 1976b, Specific interactions in mixed electrolyte solutions from solubility measurements: Jour. Solution Chemistry, v. 5, p. 483-490.

Parker, V. B., 1965, Thermal properties of aqueous uni-valent electrolytes: Natl. Bur. Standards, Natl. Standard Ref. Data ser., NSRDS-NBS 2, 66 p.

Parker, V. B., Wagman, D. D., and Evans, W. H., 1971, Selected values of chemical thermodynamic properties. Tables for the alkaline earth elements: Natl. Bur. Standards Tech. Note 270-6, 106 p.

Paterson, R., Jalota, S. K., and Dunsmore, H. S., 1971, Ion association of caesium chloride solutions and its effect upon the iterionic frictional coefficients of an irreversible thermodynamic analysis: Chem. Soc. [London] Jour. (A), p. 2116-2121.

Patterson, C. S., Gilpatrick, L. O., and Soldano, B. A., 1960, The osmotic behavior of representative aqueous salt solutions at 100°: Chem. Soc. [London] Jour., p. 2730-2734.

Pearson, D., Copeland, C. S., and Benson, S. W., 1963a, The electrical conductance of aqueous sodium chloride in the range 300 to 383°: Am. Chem. Soc. Jour., v. 85, p. 1044-1047.

———— 1963b, The electrical conductance of aqueous hydrochloric acid in the range 300 to 383°: Am. Chem. Soc. Jour., v. 85, p. 1047-1049.

Perron, G., Desnoyers, J. E., and Millero, F. J., 1974, Apparent molal volumes and heat capacities of alkaline earth chlorides in water at 25°C: Canadian Jour. Chemistry, v. 52, p. 3738-3741.

———— 1975, Apparent molal volumes and heat capacities of some sulfates and carbonates in water at 25°C: Canadian Jour. Chemistry, v. 53, p. 1134-1138.

Perron, G., Fortier, J. L., and Desnoyers, J. E., 1975, The apparent molar heat capacities and volumes of aqueous NaCl from 0.01 to 3 mol kg^{-1} in the temperature range 274.65 to 318.15K: Jour. Chem. Thermodynamics, v. 12, p. 1177-1184.

Pitzer, K. S., 1973, Thermodynamics of electrolytes. I. Theoretical basis and general equations: Jour. Phys. Chemistry, v. 77, p. 268-277.

———— 1975, Thermodynamics of electrolytes. V. Effects of higher-order electrostatic terms: Jour. Solution Chemistry, v. 4, p. 249-265.

———— 1977, Electrolyte theory — Improvements since Debye and Hückel: Accounts of Chem. Research, v. 10, p. 371-377.

———— 1979, Theory: Ion interaction approach, *in* Pytkowicz, R. M., ed., Activity Coefficients in Electrolyte Solutions, Volume I: Boca Raton, Fla., CRC Press, Inc., p. 157-208.

———— in press, Characteristics of very concentrated aqueous solutions, *in* Wickman, F., and Rickard, D., eds., Proceedings, Nobel Symposium on the Chemistry and Geochemistry of Solutions at High Temperatures and Pressures (Stockholm, Royal Swedish Acad. Sci.): New York, Pergamon Press.

Pitzer, K. S., Bradley, D. J., Rogers, P. S. Z., and Peiper, C. J., 1979, Thermodynamics of high temperature brines: Interim Rept. to the U. S. Dept. of Energy under Contract No. 8973, Lawrence Berkeley Lab. Preprint No. 8973, 39 p.

Pitzer, K. S., and Kim, J. J., 1974, Thermodynamics of electrolytes. IV. Activity and osmotic coefficients for mixed electrolytes: Am. Chem. Soc. Jour., v. 96, p. 5701-5708.

Pitzer, K. S., and Mayorga, G., 1973, Thermodynamics of electrolytes. II. Activity and osmotic coefficients for strong electrolytes with one or both ions univalent: Jour. Phys. Chemistry, v. 77, p. 2300-2308.

———— 1974, Thermodynamics of electrolytes. III. Activity and osmotic coefficients for 2-2 electrolytes: Jour. Solution Chemistry, v. 3, p. 539-546.

Pitzer, K. S., Peterson, J. R., and Silvester, L. F., 1978, Thermodynamics of electrolytes. IX. Rare earth chlorides, nitrates, and perchlorates: Jour. Solution Chemistry, v. 7, p. 45-56.

Pitzer, K. S., Roy, R. N., and Silvester, L. F., 1977, Thermodynamics of electrolytes. VII. Sulfuric acid: Am. Chem. Soc. Jour., v. 99, p. 4930-4936.

Pitzer, K. S., and Silvester, L. F., 1976, Thermodynamics of electrolytes. VI. Weak electrolytes including H_3PO_4: Jour. Solution Chemistry, v. 5, p. 269-277.

Platford, R. F., 1968, Isopiestic measurements on the system water-sodium chloride-magnesium chloride at 25°C: Jour. Phys. Chemistry, v. 72, p. 4053-4057.

Popp, R. K., and Frantz, J. D., 1979, Mineral-solution equilibria — II. An experimental study of mineral solubilities and the thermodynamic properties of aqueous CaCl in the system CaO-SiO_2-H_2O-HCl: Geochim. et Cosmochim. Acta, v. 43, p. 1777-1790.

Posner, A. M., 1953, Activity data and the association of hydrogen chloride in concentrated solutions: Nature, v. 171, p. 519-521.

Pottel, R., 1973, Dielectric properties, *in* Franks, F., ed., Water, v. 3, Aqueous solutions of simple electrolytes: New York, Plenum Press, p. 401-431.

Potter, R. W., II, Babcock, R. S., and Czamanske, G. K., 1976, An investigation of the critical liquid-vapor properties of dilute KCl solutions: Jour. Solution Chemistry, v. 5, p. 223-230.

Potter, R. W., II, and Brown, D. L., 1977, The volumetric properties of aqueous sodium chloride solutions from 0° to 500°C at pressures up to 2000 bars based on a regression of available data in the literature: U. S. Geol. Survey Bull. 1421-C, 36 p.

Potter, R. W., II, and Clynne, M. A., 1980, Solubility of NaCl and KCl in aqueous HCl from 20 to 85°C: Jour. Chem. Eng. Data, v. 25, p. 50.

Potter, R. W., II, Shaw, D. R., and Haas, J. L., Jr., 1975, Annotated bibliography of studies on the density and other volumetric properties for major components in geothermal waters 1928-74: U. S. Geol. Survey Bull. 1417, 78 p.

Prasad, B., 1968, Incomplete dissociation of salts: Indian Chem. Soc. Jour., v. 45, p. 1037-1046.

Puchkov, L. V., Styazhkin, P. S., and Fedorov, M. K., 1976, Specific heats of aqueous NaCl solutions at temperatures up to 350°C and pressures up to 1000 kg/cm²: Zhur. Prikladnoi Khimii [Leningrad], v. 49, p. 1232-1235.

———— 1978, Effect of temperature to 623 K and pressure to 150 megapascals on integral enthalpies and entropies of lithium, sodium, and potassium chloride dissolution: Zhur. Prikladnoi Khimii [Leningrad], v. 51, p. 2687-2691.

Puchkov, L. V., and Zarembo, V. I., 1978, Standard values of thermodynamic functions of electrolytes in aqueous solutions under high temperatures and pressures: Geokhimiya, p. 1671-1676.

Pytkowicz, R. M., and Johnson, K. S., 1979, Lattice theories and a new lattice concept for ionic solutions, *in* Pytkowicz, R. M., ed., Activity Coefficients in Electrolyte Solutions, v. 1: Boca Raton, Fla., CRC Press, Inc., p. 209-264.

Pytkowicz, R. M., Johnson, K., and Curtis, C., 1977, Long-range order model of aqueous electrolyte solutions: Geochem. Jour., v. 11, p. 1-7.

Pytkowicz, R. M., and Kester, D. R., 1969, Harned's rule behavior of NaCl-Na_2SO_4 solutions explained by an ion association model: Am. Jour. Sci., v. 267, p. 217-229.

Quist, A. S., 1970, The ionization constant of water to 800° and 4000 bars: Jour. Phys. Chemistry, v. 74, p. 3396-3502.

Quist, A. S., Franck, E. U., Jolley, H. R., and Marshall, W. L., 1963, Electrical conductances of aqueous solutions at high temperatures and pressures. I. The conductances of potassium sulphate-water solutions from 25° to 800° and at pressures up to 4000 bars: Jour. Phys Chemistry, v. 67, p. 2453-2459.

Quist, A. S., and Marshall, W. L., 1966, Electrical conductances of aqueous solutions at high temperatures and pressures. III. The conductances of potassium bisulphate solutions from 0 to 700° and at pressures to 4000 bars: Jour. Phys. Chemistry, v. 70, p. 3714-3725.

———— 1968a, Electrical conductances of aqueous sodium chloride solutions from 0-800° and at pressures to 4000 bars: Jour. Phys. Chemistry, v. 72, p. 684-703.

———— 1968b, Electrical conductances of aqueous hydrogen bromide solutions from 0-800°C and at pressures to 4000 bars: Jour. Phys. Chemistry, v. 72, p. 1545-1552.

———— 1968c, Ionization equilibria in ammonia-water solutions to 700° and to 4000 bars of pressure: Jour. Phys. Chemistry, v. 72, p. 3123-3128.

———— 1968d, Electrical conductances of aqueous sodium bromide solutions from 0 to 800° and at pressures to 4000 bars: Jour. Phys. Chemistry, v. 72, p. 2100-2105.

———— 1968e, The independence of isothermal equilibria in electrolyte solutions on changes in dielectric constant: Jour. Phys Chemistry, v. 72, p. 1536-1544.

———— 1969, The electrical conductances of some alkali metal halides in aqueous solutions from 0-800° and at pressures to 4000 bars: Jour. Phys. Chemistry, v. 73, p. 978-985.

———— 1970, Electrical conductance fo aqueous potassium nitrate and tetramethylammonium bromide solutions to 800°C and 4000 bars: Jour. Chem. Eng. Data, v. 15, p. 375-376.

Quist, A. S., Marshall, W. L., Franck, E. U., and von Osten, W., 1970, A reference solution for electrical conductance measurements to 800° and 12,000 bars. Aqueous 0.01 demal potassium chloride: Jour. Phys. Chemistry, v. 74, p. 2241-2243.

Quist, A. S., Marshall, W. L., and Jolley, H. R., 1965, Electrical conductances of aqueous solutions at high temperatures and pressures. II. The conductances and ionization constants of sulphuric acid-water solutions from 0-800° and at pressures up to 4000 bars: Jour. Phys. Chemistry, v. 69, p. 2726-2735.

Randall, M., and Failey, C. F., 1927a, The activity coefficients of gases in aqueous salt solutions: Chem. Rev., v. 4, p. 271-290.

———— 1927b, The activity coefficient of non-electrolytes in aqueous salt solutions from solubility measurements. The salting-out order of the ions: Chem. Reviews, v. 4, p. 285-290.

———— 1927c, The activity coefficient of the undissociated part of weak electrolytes: Chem. Reviews, v. 4, p. 291-318.

Ravich, M. I., and Borovaya, F. E., 1971, Volume properties of aqueous solutions of potassium sulphate at elevated pressures in the temperature range 300-500°C: Russian Jour. Inorganic Chemistry, v. 16, p. 1662-1666.

Read, A. J., 1975, The first ionization constant of carbonic acid from 25 to 250°C and to 2000 bar: Jour. Solution Chemistry, v. 4, p. 53-70.

Readnour, J. M., and Cobble, J. W., 1969, Thermodynamic properties for the dissociation of bisulfate ion and the partial molal heat capacities of bisulfuric acid and sodium bisulfate over an extended temperature range: Inorganic Chemistry, v. 8, p. 2174-2182.

Redlich, O., and Meyer, D., 1964, The molal volumes of electrolytes: Chem. Reviews, v. 64, p. 221-227.

Reilly, P. J., and Wood, R. H., 1969, The prediction of the properties of mixed electrolytes from measurements on common ion mixtures: Jour. Phys. Chemistry, v. 73, p. 4292-4297.

Reilly, P. J., Wood, R. H., and Robinson, B. A., 1971, The prediction of osmotic and activity coefficients in mixed-electrolyte solutions: Jour. Phys. Chemistry, v. 75, p. 1305-1315.

Renkert, H., and Franck, E. U., 1969, Elektrische Leitfähigkeit wässeriger Lösungen bei hohen Temperaturen und hohen Drucken. IV. Kaliumchlorid bis 350°C und 8 Kbar: Bunsengesell. für Phys. Chemie Ber., v. 74, p. 40-42.

Ritzert, G., and Franck, E. U., 1968, Elektrische Leitfähigkeit wässeriger Lösungen bei hohen Temperaturen und Drucken. I. KCl, $BaCl_2$, $Ba(OH)_2$, und $MgSO_4$ bis 750°C und 6 Kbar: Bunsengesell. für Phys. Chemie Ber., v. 72, p. 798-808.

Robinson, R. A., 1937, The osmotic and activity coefficient data of some aqueous salt solutions from vapor pressure measurements: Am. Chem. Soc. Jour., v. 59, p. 84-90.

———— 1961, Activity coefficients of sodium chloride and potassium chloride in mixed aqueous solutions at 25°: Jour. Phys. Chemistry, v. 65, p. 662-667.

Robinson, R. A., and Bower, V. E., 1965, Thermodynamics of the ternary system: water-sodium chloride-barium chloride at 25°C: Natl. Bur. Standards Research Jour., v. 69A, p. 19-27.

———— 1966a, Properties of aqueous mixtures of pure salts. Thermodynamics of the ternary system: water-calcium chloride-magnesium chloride at 25°C: Natl. Bur. Standards Research Jour., v. 70A, p. 305-311.

———— 1966b, Properties of aqueous mixtures of pure salts. Thermodynamics of the ternary system: water-sodium chloride-calcium chloride at 25°C: Natl. Bur. Standards Research Jour., v. 70A, p. 313-318.

Robinson, R. A., and Covington, A. K., 1968, The thermodynamics of the ternary system: water-potassium chloride-calcium chloride at 25°C: Natl. Bur. Standards Research Jour., v. 72A, p. 239-245.

Robinson, R. A., and Stokes, R. H., 1959, Electrolyte Solutions, 2d ed.: London, Butterworths, 559 p.

Robinson, R. A., Wood, R. H., and Reilly, P. J., 1971, Calculation of excess Gibbs energies and activity coefficients from isopiestic measurements on mixtures of lithium and sodium salts: Jour. Chem. Thermodynamics, v. 3, p. 461-471.

Rogers, P. S. Z., ms, 1981, Thermodynamics of geothermal fluids: Ph.D. dissert., Dept. Chemistry, Univ. California, Berkeley, 243 p.

Roux, A., Musbally, G. M., Perron, G., Desnoyers, J. E., Singh, P. P., Wooley, E. M., and Hepler, L. G., 1978, Apparent molal heat capacities and volumes of aqueous electrolytes: $NaClO_3$, $NaClO_4$, $NaNO_3$, $NaBrO_3$, $NaIO_3$, $KClO_3$, $KbrO_3$, KlO_3, NH_4NO_3, NH_4Cl, and NH_4ClO_4: Canadian Jour. Chemistry, v. 56, p. 24-28.

Rowe, A. M., Jr., and Chou, J. C., 1970, Pressure-volume-temperature-concentration relation of aqueous NaCl solutions: Jour. Chem. Eng. Data, v. 15, p. 61-66.

Ruff, I., 1977, Theory of concentrated solutions of strong electrolytes. Part I. — Some thermodynamic quantities of a latticelike network of ions surrounded by a dielectric gradient: Faraday Soc. Trans. 11, v. 73, p. 1858-1877.

———— 1979, Theory of concentrated solutions of strong electrolytes. Part II. — Thermodynamic properties of mixed electrolytes. Theoretical basis of the Harned Rule: Faraday Soc. Trans. 11, v. 75, p. 1-11.

Rüterjans, H., Schreiner, F., Sage, U., and Ackermann, Th., 1969, Apparent molal heat capacities of aqueous solutions of alkali halides and alkylammonium salts: Jour. Phys. Chemistry, v. 73, p. 986-994.

Ryzhenko, B. N., 1963, Determination of dissociation constants of carbonic acid and the degree of hydrolysis of the CO_3^{--} and HCO_3^- ions in solutions of alkali carbonates and bicarbonates at elevated temperatures: Geochemistry, p. 151-164.

———— 1964, Determination of the second dissociation constant of sulfuric acid, and precipitation of salts in the reciprocal system Ca^{2+}, Ba^{2+}, SO_4^{2-}, CO_3^{2-} under hydrothermal conditions: Geochem. Internat., v. 1, p. 8-13.

———— 1967, Determination of hydrolysis of sodium silicate and calculation of dissociation constants of orthosilicic acid at elevated temperatures: Geochim. Internat., v. 4, p. 99-107.

———— ms, 1974, Regularities of the thermodynamic process of electrolyte dissociation of inorganic substances and evaluation of the form of transport of chemical elements in hydrothermal solutions: Ph.D. dissert., Order of Lenin Inst. Geochemistry and Analytic Chemistry, Moscow, 51 p.

———— 1981, Equilibrium Thermodynamics of Hydrothermal Solutions: Moscow, Izd. Nayuka, 192 p.

Samoilov, O. Y., 1972, Residence times of ionic hydration, *in* Horne, R. A., ed., Water and aqueous solutions: New York, Wiley-Intersci., p. 597-610.

Scatchard, G., 1936, Concentrated solutions of strong electrolytes: Chem. Reviews, v. 19, p. 309-327.

———— 1961, Osmotic coefficients and activity coefficients in mixed electrolyte solutions: Am. Chem. Soc. Jour., v. 83, p. 2636-2642.

———— 1968, The excess free energy and related properties of solutions containing electrolytes: Am. Chem. Soc. Jour., v. 90, p. 3124-3127.

———— 1969, Corrections to "The excess free energy and related properties of solutions containing electrolytes": Am. Chem. Soc. Jour., v. 91, p. 2410.

———— 1976, Equilibrium in Solutions: Cambridge, Mass., Harvard Univ. Press, 208 p.

Scatchard, G., and Prentiss, S. S., 1933, The freezing points of aqueous solutions. IV. Potassium, sodium and lithium chlorides and bromides: Am. Chem. Soc Jour., v. 55, p. 4355-4362.

Scatchard, G., Rush, R. M., and Johnson, J. S., 1970, Osmotic and activity coefficients for binary mixtures of sodium chloride, sodium sulfate, magnesium sulfate, and magnesium chloride in water at 25°C. III. Treatment with the ions as components: Jour. Phys. Chemistry, v. 74, p. 3786-3796.

Scholz, B., Lüdemann, H. D., and Franck, E. U., 1972, Spectra of Cu (II)-complexes in aqueous solutions at high temperatures and pressures: Bunsengesell. für Phys. Chemie Ber., v. 76, p. 406-409.

Schumm, R. H., Wagman, D. D., Bailey, S. M., Evans, W. H., and Parker, V. B., 1973, Selected values of chemical thermodynamic properties. Table for the lanthamide (rare earth) elements (elements 62 through 76 in the standard order of arrangement): Natl. Bur. Standards Tech. Note 270-7, 78 p.

Setchenow, M., 1892, Action de l'acide carbonique sur les solutions des sels à acides forts: Ann. Chim. Phys., v. 25, p. 225-270.

Seward, T. M., 1973, Thio complexes of gold and the transport of gold in hydrothermal solutions: Geochim. et Cosmochim. Acta, v. 37, p. 379-399.

———— 1974, Determination of the first ionization constant of silicic acid from quartz solubility in borate buffer solutions to 350°C: Geochim. et Cosmochim. Acta, v. 38, p. 1651-1664.

———— 1976, The stability of chloride complexes of silver in hydrothermal solutions up to 350°C: Geochim. et Cosmochim. Acta, v. 40, p. 1329-1341.

———— 1977, Solubility of coexisting pyrite and pyrrhotite in the system NaHS-H_2S-NaCl-H_2O at elevated temperature and pressure, *in* Hodder, A. P. W., ed., Geochemistry 1977: Wellington, New Zealand, Dept. Sci. Ind. Research Bull. 218, p. 44-48.

———— in press, Metal complex formation in aqueous solutions at elevated temperatures and pressures, *in* Wickman, F., and Rickard, D., eds., Proceedings, Nobel Symposium on the Chemistry and Geochemistry of Solutions at High Temperatures and Pressures (Stockholm, Royal Swedish Acad. Sci.): New York, Pergamon Press.

Shin, C., and Criss, C. M., 1979, Standard enthalpies of formation of anhydrous and aqueous magnesium chloride at 298.15 K: Jour. Chem. Thermodynamics, v. 11, p. 663-666.

Sienko, M. J., and Plane, R. A., 1963, Physical Inorganic Chemistry: New York, W. A. Benjamin, Inc., 166 p.

Sillén, L. G., and Martell, A. E., 1964, Stability Constants of Metal-Ion Complexes: London, Chem. Soc., 754 p.

———— 1971, Stability Constants of Metal-Ion Complexes: Supplement No. 1: London, Chem. Soc., 865 p.

Silvester, L. F., and Pitzer, K. S., 1976, Thermodynamics of geothermal brines. I. Thermodynamic properties of vapor-saturated $NaCl_{(aq)}$ solutions from 0-300°C: Natl. Tech. Inf. Service, LBL-4456, UC-66, TID-4500-R64, 62 p.

———— 1977, Thermodynamics of electrolytes. 8. High-temperature properties, including enthalpy and heat capacity, with application to sodium chloride: Jour. Phys. Chemistry, v. 81, p. 1822-1828.

———— 1978, Thermodynamics of electrolytes. X. Enthalpy and the effect of temperature on the activity coefficients: Jour. Solution Chemistry, v. 7, p. 237-337.

Singh, D., and Bromley, L. A., 1973, Relative enthalpies of sea salt solutions at 0° to 75°C: Jour. Chem. Eng. Data, v. 18, p. 174-181.

Singh, P. P., McCurdy, K. G., Wooley, E. M., and Hepler, L. G., 1977, Heat capacities of aqueous perchloric acid and sodium perchlorate at 298°K: $\Delta C°_P$ of ionization of water: Jour. Solution Chemistry, v. 6, p. 327-330.

Singh, P. P., Spitzer, J. J., McKay, R. M., McCurdy, K. G., and Hepler, L. G., 1978, Apparent molar heat capacities and volumes of silver nitrate and silver perchlorate in aqueous solution at 298.15K: Thermochim. Acta, v. 24, p. 111-115.

Singh, P. P., Wooley, E. M., McCurdy, K. G., and Hepler, L. G., 1976, Heat capacities of aqueous electrolytes: eight 1:1 electrolytes and $C°_P$ for ionization of water at 290K: Canadian Jour. Chemistry, v. 54, p. 3315-3318.

Smith, R. E., and Martell, A. E., 1976, Critical Stability Constants, V. 4: Inorganic Complexes: New York, Plenum Press, 256 p.

Snipes, H. P., Manly, C., and Ensor, D. D., 1975, Heats of dilution of aqueous electrolytes: temperature dependence: Jour. Chem. Eng. Data, v. 20, p. 287-291.

Soldano, B. A., and Bien, P. B., 1966, Osmotic behavior of aqueous salt solutions at elevated temperatures, Part IV: Chem. Soc. [London] Jour. (A), p. 1825-1827.

Soldano, B. A., and Meek, M., 1963, Isopiestic vapour-pressure measurements of aqueous salt solutions at elevated temperatures. Part III.: Chem. Soc. [London] Jour., p. 4424-4426.

Soldano, B. A., and Patterson, C. S., 1962, Osmotic behavior of aqueous salt solutions at elevated temperatures. Part II: Chem. Soc. [London] Jour., p. 937-940.

Sourirajan, S., and Kennedy, G. C., 1962, The system H_2O-NaCl at elevated temperatures and pressures: Am. Jour. Sci., v. 260, p. 115-141.

Spillner, F., 1940, Hochgespannter Wasserdampf als Lösungsmittel: Chem. Fabrik, v. 13, p. 405-424.

Spitzer, J. J., 1978, Ionic radii and the distance of closest approach in the Debye-Hückel theory of electrolytes: Jour. Solution Chemistry, v. 7, p. 669-673.

Spitzer, J. J., Olofsson, I. V., Singh, P. P., and Hepler, L. G., 1979a, Apparent molar heat capacities and volumes of aqueous electrolytes at 298.15 K: $Ca(NO_3)_2$, $Co(NO_3)_2$, $Cu(NO_3)_2$, $Mg(NO_3)_2$, $Mn(NO_3)_2$, $Ni(NO_3)_2$, and $Zn(NO_3)_2$: Jour. Chem. Thermodynamics, v. 11, p. 233-238.

———— 1979b, Apparent molar heat capacities and volumes of aqueous electrolytes at 25°C: $NaIO_3$, $KMnO_4$, and $MnCl_2$: Thermochim. Acta, v. 28, p. 155-160.

Spitzer, J. J., Singh, P. P., McCurdy, K. G., and Hepler, L. G., 1978a, Apparent molar heat capacities and volumes of aqueous electrolytes: $CaCl_2$, $Cd(NO_3)_2$, $CaCl_2$, $Cu(ClO_4)_2$, $Mg(ClO_4)_2$, and $NiCl_2$: Jour. Solution Chemistry, v. 7, p. 81-86.

Spitzer, J. J., Singh, P. P., Olofsson, I. V., and Hepler, L. G., 1978b, Apparent molar heat capacities and volumes of aqueous electrolytes at 25°C: $Cd(ClO_4)_2$, $Ca(ClO_4)_2$, $Co(ClO_4)_2$, $Mn(ClO_4)_2$, $Ni(ClO_4)_2$, and $Zn(ClO_4)_2$: Jour. Solution Chemistry, v. 7, p. 623-629.

Stakhanova, M. S., Vasilev, V. A., and Epikhin, Yu. A., 1963, Activity coefficients of alkali metal chlorides in mixed aqueous solutions: Russian Jour. Phys. Chemistry, v. 37, p. 182-185.

Stephens, H. P., and Cobble, J. W., 1971, Thermodynamic properties of the aqueous sulfide and bisulfide ions and the second ionization constant of hydrogen sulfide over extended temperatures: Inorganic Chemistry, v. 10, p. 619-625.

Stokes, R. H., and Robinson, R. A., 1948, Ionic hydration and activity in electrolyte solutions: Am. Chem. Soc. Jour., v. 70, p. 1870-1878.

———— 1973, Solvation equilibria in very concentrated electrolyte solutions: Jour. Solution Chemistry, v. 2, p. 173-191.

Stoughton, R. W., and Lietzke, M. H., 1960, The solubility of silver sulfate in electrolyte solutions. Part 6. Heats and entropies of solution vs. temperature. Species present in HNO_3 and H_2SO_4 media: Jour. Phys. Chemistry, v. 64, p. 133-136.

———— 1965, Calculation of some thermodynamic properties of sea salt solutions at elevated temperatures from data on NaCl solutions: Jour. Chem. Eng. Data, v. 10, p. 254-260.

———— 1967, Thermodynamic properties of sea salt solutions: Jour. Chem. Eng. Data, v. 12, p. 101-104.

Stull, D. R., and Prophet, H., 1971, JANAF thermochemical tables, 2d ed: Natl. Bur. Standards, Natl. Standards Ref. Data Ser., NBS 37, 1141 p.

Sweeton, F. H., and Baes, C. F., Jr., 1970, The solubility of magnetite and hydrolysis of ferrous ion in aqueous solutions at elevated temperatures: Jour. Chem. Thermodynamics, v. 2, p. 479-500.

Sweeton, F. H., Mesmer, R. E., and Baes, C. F., Jr., 1973, A high-temperature flowing EMF cell: Jour. Physics E: Sci. Instruments, v. 6, p. 165-168.

———— 1974, Acidity measurements at elevated temperatures. VII. Dissociation of water: Jour. Solution Chemistry, v. 3, p. 191-214.

Swinnerton, A. C., and Owen, G. E., 1948, Conductivity of dilute water solutions near the critical temperature (an abstract): Am. Jour. Physics, v. 16, p. 123.

Tait, P. G., 1889, Report on some physical properties of fresh water and sea water, *in* Thompson, Sir Charles Wyville, Physics and Chemistry Series, v. 2, Report on the Scientific Results of the Voyage of HMS Challenger during the years 1873-1876: London, The Stationery Office, p. 1-76.

Takenouchi, S., and Kennedy, G. C,. 1964, The binary system H_2O-CO_2 at high temperatures and pressures: Am. Jour. Sci., v. 262, p. 1055-1074.

———— 1965, The solubility of carbon dioxide in NaCl solutions at high temperatures and pressures: Am. Jour. Sci., v. 263, p. 445-454.

Tammann, G., 1893, Über die Binnendrucke in Lösungen: Zeitschr. Phys. Chemie, v. 11, p. 676-693.

———— 1895, Über die Volumänderungen bei der Neutralisation verdünnter Lösungen: Zeitschr. Phys. Chemie, v. 16, p. 91-96.

Tanner, J. E., and Lamb, F. W., 1978, Specific heats of aqueous solutions of NaCl, NaBr, and KCl: Comparisons with related thermal properties: Jour. Solution Chemistry, v. 7, p. 303-316.

Templeton, C. C., 1960, Solubility of barium sulfate in sodium chloride solutions from 25° to 95°C: Jour. Chem. Eng. Data, v. 5, p. 514-516.

Templeton, C. C., and Rodgers, J. C., 1967, Solubility of anhydrite in several aqueous salt solutions between 250°C and 325°C: Jour. Chem. Eng. Data, v. 12, p. 536-547.

Tham, M. K., Gubbins, K. E., and Walker, R. D., Jr., 1967, Densities of potassium hydroxide solutions: Jour. Chem. Eng. Data, v. 12, p. 525-526.

Tödheide, K., 1966, Wässrige Lösungen bei hohen Drucken und Temperaturen: Zeitschr. für Electrochemie, v. 70, p. 1022-1030.

———— 1972, Water at high temperature, *in* Franks, F., ed., Water, v. 1: New York, Plenum Press, p. 463-514.

Tödheide, K., and Franck, E. U., 1963, Das Zweiphasengebiet und die kritische Kurve im System Kohlendioxid-Wasser bis zu Drucken von 3500 bar: Zeitschr. Phys. Chemie, v. 37, p. 387-401.

Towns, M. B., Greeley, R. S., and Lietzke, M. H., 1960, Electromotive force studies in aqueous solutions at elevated temperatures. III. The standard potential of the silver-silver bromide electrode and the mean ionic activity coefficient of hydrobromic acid: Chem. Soc. Jour., v. 1960, p. 1861-1863.

Tremaine, P. R., Chen, J. D., Wallace, G. J., and Boivin, W. A., 1981, Solubility of uranium (IV) oxide in alkaline aqueous solutions to 300°C: Jour. Solution Chemistry, v. 10, p. 221-230.

Tremaine, P. R., and Goldman, S., 1978, Calculation of Gibbs free energies of aqueous electrolytes to 350°C from an electrostatic model for ion hydration: Jour. Phys. Chemistry, v. 82, p. 2317-2321.

Tremaine, P. R., and Le Blanc, J. C., 1980, The solubility of magnetite and the hydrolysis and oxidation of Fe^{2+} in water to 300°C: Jour. Solution Chemistry, v. 9, p. 415-442.

Ueno, M., Nakahara, M., and Osugi, J., 1979, Effect of pressure on the conductivities of HCl and KCl in water at 0°C: Jour. Solution Chemistry, v. 8, p. 881-886.

Urusova, M. A., 1971, Some thermodynamic characteristics of water in alkali halide salt solutions at high temperatures: Akad. Nauk SSSR Izv. Ser. Khim., v. 8, p. 1613-1618.

———— 1974, Phase equilibrium and thermodynamic characteristics of solutions in the systems NaCl-H_2O and NaOH-H_2O at 350-550°C: Geochem. Internat., v. 11, p. 944-950.

Urusova, M. A., and Ravick, M. I., 1971, Vapour pressure and solubility in the sodium chloride-water system at 350° and 400°C: Russian Jour. Inorganic Chemistry, v. 16, p. 1534-1535.

Vasil'ev, V. P., and Grechina, N. K., 1964, Revnovesiia v vodnikh rastvorakh iodudnikh kompleksov kadmiia: Zhur. Neorg. Khim., v. 9, p. 647-653.

von Halban, H., and Eisenbrand, J., 1928, Zur kenntnis des Zustandes starker Elektrolyte in konzentrierter Lösüng. I. Die Nitrate: Zeitschr. Phys. Chemie, v. 132, p. 401-432.

Wagman, D. D., Evans, W. H., Halow, I., Parker, V. B., Bailey, S. M., and Schumm, R. H., 1968, Selected values of chemical thermodynamic properties. Tables for the first thirty-four elements in the standard order of arrangement: Natl. Bur. Standards Tech. Note 270-3, 264 p.

Wagman, D. D., Evans, W. H., Parker, V. B., Halow, I., Bailey, S. M., and Schumm, R. H., 1969, Selected values of chemical thermodynamic properties. Tables for elements 35 through 53 in the standard order of arrangement: Natl. Bur. Standards Tech. Note 270-4, 152 p.

Wakefield, Z. T., Luff, B. B., and Reed, R. B., 1972, Heat capacity and enthalpy of phosphoric acid: Jour. Chem. Eng. Data, v. 17, p. 420-423.

Walther, J. V., and Helgeson, H. C., 1977, Calculation of the thermodynamic properties of aqueous silica and the solubility of quartz and its polymorphs at high pressures and temperatures: Am. Jour. Sci., v. 277, p. 1315-1351.

———— 1979, Reply to Fournier's discussion of "Calculation of the thermodynamic properties of aqueous silica and the solubility of quartz and its polymorphs at high pressures and temperatures": Am. Jour. Sci., v. 279, p. 1078-1082.

———— 1980, Description and interpretation of metasomatic phase relations at high pressures and temperatures: I. Equilibrium activities of ionic species in nonideal mixtures of CO_2 and H_2O: Am. Jour. Sci., v. 280, p. 575-606.

Wang, D. P., and Millero, F. J., 1973, Precise representation of the PVT properties of water and seawater determined from sound speed: Jour. Geophys. Research, v. 78, p. 7122-7128.

Ward, G. K., and Millero, F. J., 1974a, Molal volume of aqueous boric acid-sodium chloride solutions: Jour. Solution Chemistry, v. 3, p. 431-444.

———— 1974b, The effect of pressure on the ionization of boric acid in aqueous solutions from molal-volume data: Jour. Solution Chemistry, v. 3, p. 417-430.

Whalley, E., 1966, Chemical reactions in solution under high pressure: Zeitschr. Elektrochemie, v. 70, p. 958-968.

Whitfield, M., 1972, Self-ionization of water in dilute sodium chloride solutions from 5-35°C and 1-2000 bars: Jour. Chem. Eng. Data, v. 17, p. 124-128.

Wicke, E., Eigen, M., and Ackermann, T., 1954, Über den Zustand des Protons (Hydroniumions) in wässriger Lösung: Zeitschr. Physik. Chemie, v. 1, p. 340-364.

Wood, J. R., 1972, ms, Prediction of mineral solubilities in concentrated brines: a thermodynamic approach: Ph.D. thesis, The Johns Hopkins Univ., Baltimore, Maryland.

———— 1975, Thermodynamics of brine-salt equilibria. I. The systems NaCl-KCl-$MgCl_2$-$CaCl_2$-H_2O and NaCl-Na_2SO_4-H_2O at 25°C: Geochim. et Cosmochim. Acta, v. 39, p. 1147-1163.

———— 1976, Thermodynamics of brine-salt equilibria. II. The system NaCl-KCl-H_2O from 0 to 200°C: Geochim. et Cosmochim. Acta, v. 40, p. 1211-1220.

Wright, J. M., Lindsay, W. T., and Druga, T. R., 1961, The behavior of electrolyte solutions at elevated temperatures as derived from conductance measurements: Washington, D. C., U. S. Atomic Energy Comm. WAPD-TM-204, 31 p.

Wu, Y.-C., 1970, Young's mixture rule and its significance: Jour. Phys. Chemistry, v. 74, p. 3781, 3786.

Wu, Y.-C., Rush, R. M., and Scatchard, G., 1968, Osmotic and activity coefficients for binary mixtures of sodium chloride, sodium sulfate, magnesium sulfate, and magnesium chloride in water at 25°. I. Isopiestic measurements on the four systems with common ions: Jour. Phys. Chemistry, v. 72, p. 4048-4053.

———— 1969, Osmotic and activity coefficients for binary mixtures of sodium chloride, sodium sulfate, magnesium sulfate, and magnesium chloride in water at 25°C. II. Isopiestic and electromotive force measurements on the two systems without common ions: Jour. Phys. Chemistry, v. 73, p. 2047-2053.

Wu, Y.-C., Smith, M. B., and Young, T. F., 1965, Heats of mixing of electrolytes having common ions: Jour. Phys. Chemistry, v. 69, p. 1868-1876.

Yeatts, L. B., and Marshall, W. L., 1967, Aqueous systems at high temperature. XVIII. Activity coefficient behavior of calcium hydroxide in aqueous sodium nitrate to the critical temperature of water: Jour. Phys. Chemistry, v. 71, p. 2641-2650.

———— 1969, Apparent invariance of activity coefficients of calcium sulfate at constant ionic strength and temperature in the system $CaSO_4$-Na_2SO_4-$NaNO_3$-H_2O to the critical temperature of water. Association equilibria: Jour. Phys. Chemistry, v. 73, p. 81-90.

———— 1972a, Electrical conductance and ionization behavior of sodium chloride in dioxane-water solutions at 300° and pressures to 4000 bars: Jour. Phys. Chemistry, v. 76, p. 1053-1062.

———— 1972b, Solubility of calcium sulfate dihydrate and association equilibria in several aqueous mixed electrolyte salt systems at 25°C: Jour. Chem. Eng. Data, v. 17, p. 163-168.

Young, T. F., 1951, Recent developments in the study of interactions between molecules and ions, and of equilibria in solutions: Rec. Chem. Progress, v. 12, p. 81-95.

Young, T. F., and Smith, M. B., 1954, Thermodynamic properties of mixtures of electrolytes in aqueous solutions: Jour. Phys. Chemistry, v. 58, p. 716-724.

Young, T. F., Wu, Y.-C., and Krawetz, A. A., 1957, Thermal effects on the interactions between ions of like charge: Faraday Soc. Disc., v. 24, p. 37-42.

Zarembo, V. I., and Fedorov, M. K., 1975, Density of NaCl solutions in the 25-350° range and pressures up to 100 kg/cm²: Zhur. Prikl. Khim., v. 9, p. 1949-1953.

Zisman, W. A., 1932, The effect of pressure on the electrical conductance of salt solutions in water: Physics Reviews, v. 39, p. 151-160.